2

CONF-9306172--

BNL - 48923(I)

15th Combustion Research Conference

Split Rock Resort and Conference Center

Lake Harmony, Pennsylvania

June 2 - 4, 1993

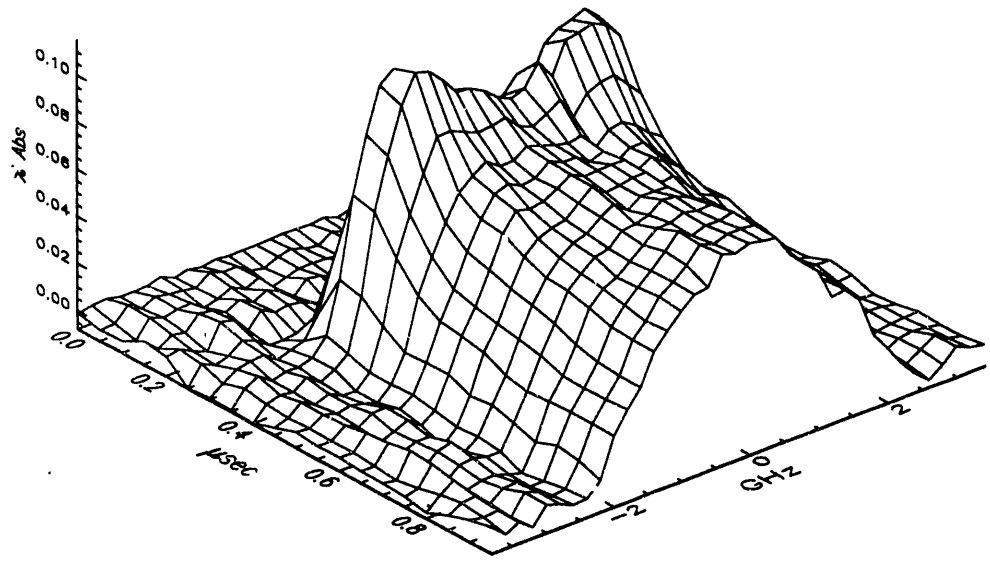

Sponsored by
Division of Chemical Sciences
Office of Basic Energy Sciences
U.S. Department of Energy
and
Chemistry Department
Brookhaven National Laboratory

Cover Figure

Transient absorption spectrum of the CN $X\ ^2\Sigma^+$ (v=0, J=69.5) fragment from C_2H_5SCN photodissociation at 193 nm. In this view, the probe laser propagates at the magic angle with respect to the dissociation polarization, thus the Doppler-broadened lineshapes are independent of the velocity anisotropy, and dependent only on the angular momentum polarization and the translational energy distribution.

15th Combustion Research Conference

Split Rock Resort and Conference Center

Lake Harmony, Pennsylvania

June 2 - 4, 1993

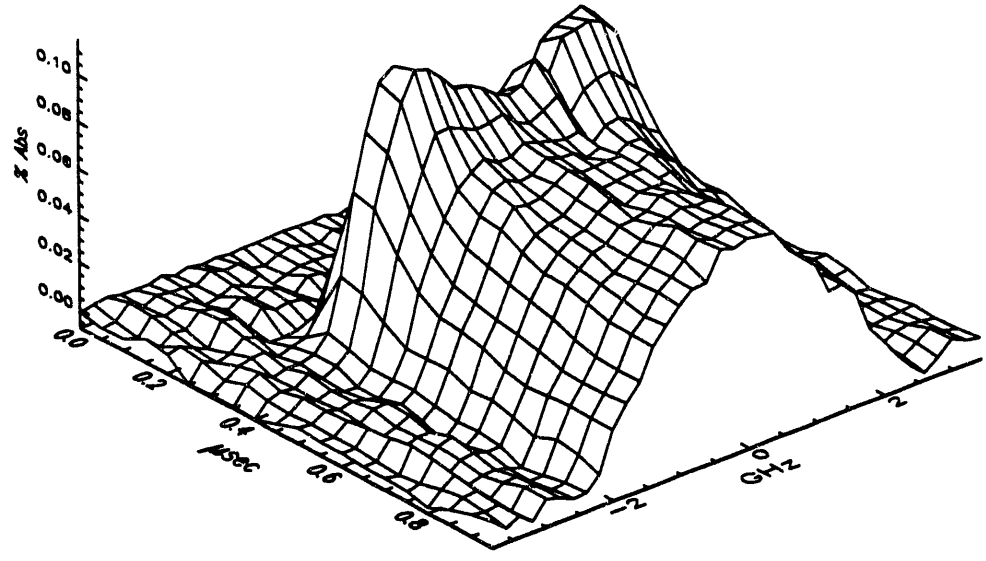

Sponsored by
Division of Chemical Sciences
Office of Basic Energy Sciences
U.S. Department of Energy
and
Chemistry Department
Brookhaven National Laboratory

Printed in the United States of America
Available from
National Technical Information Service
U.S. Department of Commerce
5285 Port Royal Road
Springfield, VA 22161

NTIS price codes:
Printed Copy: A17; Microfiche Copy: A01

FOREWORD

The Fifteenth Combustion Research Meeting, hosted this year by the Chemistry Department, Brookhaven National Laboratory, is being held from June 2 through June 4, 1993. As in the past, the purpose of this meeting is to foster collaboration, cooperation, and exchange of current research ideas among those grantees and contractors of the DOE Office of Basic Energy Sciences (BES) whose research is related to the understanding of combustion processes. This meeting affords a singular opportunity for the scientific community most directly involved with the chemistry and dynamics underlying combustion processes to contribute to the direction of the DOE basic research efforts related to combustion.

The BES program is not a combustion program. Rather, it is a basic research program with the long term objective of providing knowledge and concepts needed by scientists and engineers to model and optimize the performance of combustion-based devices to meet national goals of energy efficiency and environmental protection. The research efforts comprising this program cover a broad range of activities including:

Chemical Reaction Theory

Provision of accurate potential energy surfaces and calculation of dynamics on these surfaces to serve as a basis for developing and testing semi-empirical models for predicting, *with proven accuracy and reliability*, the effects of temperature and pressure on gas phase chemical reaction rates.

Development of efficient, accurate methods for calculating potential energy surfaces and for performing dynamics calculations.

Provision of potential energy surfaces and reactive and elastic scattering cross sections for prototypical systems.

Experimental Dynamics and Spectroscopy

Determination of the angular dependence of reaction cross sections as functions of collision energy and internal energy of prototypical reactants and products.

Characterization of molecular dissociation processes as functions of internal energy.

Development of molecular beam and spectroscopic techniques for providing such data.

Thermodynamics of Combustion Intermediates

Provision of bond dissociation energies of stable molecules and free radicals

Development of methods for measuring these quantities and assessing their accuracies.

Determination of the structure and relevant energy states of combustion intermediates.

Chemical Kinetics

Provision of reaction rates and branching ratios of reactions important in combustion, preferably at temperatures and pressures characteristic of combustion environments.

Development and demonstration of new methods for determining chemical reaction rates.

Provision and assessment of critical data for assessing the predictive accuracy of theories and models for the temperature and pressure dependence of combustion reaction rates.

Reaction Mechanisms

- Identification of critical paths in combustion systems through study and analysis of reaction subsystems such as pyrolysis and/or oxidation of classes of compounds.
- Development of methods for analyzing reaction mechanisms.
- Estimation of constituent reaction rates where these are not available by more direct means.
- Identification of key chemical reactions in combustion processes.

Combustion Diagnostics

- Development and evaluation of techniques for species identification and for measuring species concentrations in flames and combustion devices.
- Provision of reference data and models for the calibration of combustion diagnostic methods.
- Development and evaluation of techniques for measuring temperatures and velocities in combustion devices.

Fluid Dynamics and Chemically Reacting Flows

- Development and application of methods for characterizing species concentrations in flames as functions of time and position, and for characterizing turbulence structure in flames.
- Development of theories and computational techniques for characterizing turbulence in flames.
- Development of theories and computational methods for treating fluid dynamics and chemistry on comparable time scales.

This meeting brings together scientists who might not otherwise have occasion to communicate directly with each other. To this end, time that might have otherwise been assigned to additional presentations has been set aside for participants to discuss and plan work of mutual interest. To this end also, the extended abstracts are made available at the start of the meeting and serve in place of poster sessions. If the meeting accomplishes its objectives, its success will be due in large measure to the conscientious efforts of all the participants to engage in candid discussions of each other's work, to seek assistance from others with appropriate expertise, and to offer assistance to those encountering problems in the pursuit of their research.

This book of abstracts contains, in addition to the extended abstracts of all projects related to combustion and supported by the DOE Office of Basic Energy Sciences, the agenda for the meeting and the list of invitees. The abstracts, including those corresponding to this year's formal presentations, are in alphabetical order according to principal investigator or, if more than one, by the name of the first author on the abstract.

Special thanks are due to Ralph E. Weston and Nancy Sautkulis of the Department of Chemistry, Brookhaven National Laboratory, for the organization of this year's meeting.

William H. Kirchhoff
Fundamental Interactions Branch
Division of Chemical Sciences
Office of Basic Energy Sciences
U.S. Department of Energy

FIFTEENTH COMBUSTION RESEARCH CONFERENCE

Wednesday Morning Agenda ***Ralph E. Weston, Jr., Chair*** ***June 2, 1993***

8:30 am Opening Remarks, William H. Kirchhoff

8:45 am Plenary Lecture, Daniel Seery

9:45 am "Spectroscopy and Kinetics of Combustion Gases at High Temperatures", Ronald K. Hanson.....(138)

10:15 am *Break*

10:30 am "Kinetics Data Base for Combustion Modeling", Wing Tsang.....(316)

11:00 am "Chemical Kinetics and Combustion Modeling", James A. Miller.....(232)

11:30 am "Combustion Kinetics and Reaction Pathways", R. Bruce Klemm.....(185)

12:00 "Theoretical Studies of Nonadiabatic and Spin-Forbidden Processes: Investigations of the Reactions and Spectroscopy of Radical Species Relevant to Combustion Reactions and Diagnostics", David R. Yarkony.....(358)

Wednesday Evening Agenda ***Trevor J. Sears, Chair*** ***June 2, 1993***

7:30 pm "Spectroscopic and Dynamical Studies of Highly Energized Small Polyatomic Molecules", Robert W. Field.....(98)

8:00 pm "Spectroscopic Investigation of the Vibrational Quasi-Continuum Arising from Internal Rotation of a Methyl Group", Jon T. Hougen.....(153)

8:30 pm "The Attractive Quartet Potential Energy Surface for the $CH(a^4\Sigma^-)$ + CO Reaction: A Role for the a^4A'' State of the Ketenyl Radical in Combustion?", Henry F. Schaefer III.....(287)

9:00 pm *Break*

9:15 pm "Fundamental Spectroscopic Studies of Carbenes and Hydrocarbon Radicals", Carl Gottlieb.....(117)

9:45 pm "Applications of Laser-Induced Gratings to Spectroscopy and Dynamics", Eric A. Rohlfing.....(279)

Thursday Morning Agenda ***George Fisk, Chair*** ***June 3, 1993***

Thursday Evening Agenda ***Stephen R. Leone, Chair*** ***June 3, 1993***

Friday Morning Agenda ***Paul L. Houston, Chair*** ***June 4, 1993***

TABLE OF CONTENTS

ABSTRACTS

Analysis of Turbulent Reacting Flows

W. T. Ashurst, P. K. Barr & J. M. Card
Combustion Research Facility
Sandia National Laboratories
Livermore, California 94551-0969

Program Objective

Numerical simulations that treat one aspect of combustion in great detail, while treating other features more crudely, have been developed in order to highlight various aspects of combustion. This allows the full computer power to be devoted to simulating a single feature in each model, and simulates that feature well, rather than poorly representing all features. As an example, direct simulations of constant density Navier-Stokes turbulence have been used to determine premixed flame geometry. This recent work has shown that the most probable flame shape is that of a cylinder, caused by the tube-like shape of the most intense vorticity, and so this result implies that detailed flame-vortex interactions, which include chemistry and heat release, may be done in two-dimensional configurations. Currently, a four-step reduced chemical kinetic scheme is being used to estimate the effect of flame shape upon temperature and quenching behavior in a two-dimensional flame-vortex model.

Flame Propagation in Three-Dimensional Turbulence

Constant-density premixed flame propagation in three-dimensional Navier-Stokes turbulence has been simulated.[1] An advantage of this constant energy turbulence simulation is that the statistics of flame propagation are gathered in a statistically steady turbulent flow. A zero-thickness flame model with specified flame speed S_L has been used. A continuous scalar G evolves according to

$$\frac{\partial G}{\partial t} + \mathbf{u} \cdot \nabla G = S_L |\nabla G|$$

and because the flame is a passive scalar, the continuous scalar G contributes statistical information on flame propagation at each numerical grid point within the computational domain. Thus, a small system of only 64^3 grid points yields results comparable to larger systems in which a flame with finite thickness occupies only a small fraction of the total volume.

Comparison of flame curvature with experimental information, obtained in grid turbulence with the premixed flame stabilized near a wall, show that computed and measured curvature distributions agree, where each distribution is reduced by its own variance.[2] Further comparisons of flame curvature as a function of flame location within the turbulent flame zone are being done. Preliminary results indicate that the mean positive curvature (convex with respect to unburnt gas) does not vary with location, while the mean negative curvature increases with increasing distance from the front of the flame zone. Additional

features of the flame geometry will be examined in order to amend models of turbulent premixed flame zones.

Front Propagation Through Strong Turbulence

Direct simulations of turbulence have revealed the intense vorticity to be tube-like, with an apparent length of six diameters. The local swirling flow around the tube axis has several effects on flame propagation: 1) it produces the cylindrical flame shape described above; and 2) it enhances the flame advancement through the flow. The overall propagation rate is defined as the turbulent flame speed S_T, and its dependence upon the turbulent velocity flucations u' and the laminar flame speed S_L is required for engineering design purposes.

Simulations with the passive flame model in three- and two-dimensional flows have shown that flame propagation may be considered to have two components: 1) flame advancement within a swirling eddy; and 2) flame propagation between eddies. To simplify the concept, consider that the flow between eddies does not, on average, enhance the flame front propagation rate above the value of S_L. And, consider that within an eddy the flame front moves at speed $u' + S_L$. This structure of a flow composed of swirling eddies which are intermittently located in space yields an upper limit on the effective turbulent flame speed S_T. This limit occurs because only within an eddy does the flame front move at a speed larger than S_L, and so the time duration required for the flame moving at S_L to encounter the next eddy becomes the rate-limiting step as the turbulence becomes more intense, $u' >> S_L$.

From the passive flame simulations described above we obtain the result that $S_T/S_L = (1 + u'/S_L)/(a + bu'/S_L)$ where the coefficients a and b represent the eddy diameter and the spacing between eddies with values of $a \approx 1$ and $b < a$. This functional form exhibits a square-root behavior for S_T/S_L when $u' < S_L$, and appears to agree with some data correlations of turbulent flame speed.[1] Another interesting possibility is when the space between the eddies is actually occupied by eddies of a much smaller size, which might occur when the turbulence becomes stronger. If a new set of eddies at the smaller length scale did exist, then the above model could be repeated upon itself as a recursion relation. This recursion model is not completely formulated at this time, but simple conjectures lead to the overall behavior of S_T depending upon the levels of eddies within the flow and the swirling magnitude at each level. As a spectulation, such eddy-level concepts could explain the mixing transitions noted in experimental results by Dimotakis.[3]

Flame-Vortex Interaction

Previous simulations[4] of a vortex interacting with a diffusive flame sheet indicated the formation of a flame tongue with the possibility that the highest temperature occurs at the flame tip. Note, this diffusive flame structure does not have the propagation effect described above for the premixed flame, and because of the lack of a propagation mechanism, the diffusive flame zone is trapped in the neighborhood of the vortex. From the

three-dimensional turbulence simulations we infer that these intense vortex tubes have a long lifetime due to an extensional strain rate along the tube axis. This axial strain can maintain a constant vortical diameter, as in the Burgers' vortex solution where vorticity has a Gaussian radial distribution. The trapped diffusion flame lies outside the vortical region and the flame tip is formed at the radius corresponding to the maximum swirling velocity. The tip feature is a balance of the swirling convection and the diffusion of fuel and oxidizer. Simple model estimates[5] indicate that under most gaseous combustion conditions the flame tongue will not wrap completely around the vortex.

This work has been extended[6] to include a two-step reduced chemical-kinetic mechanism for a methane-air flame. An analytical treatment has been done by assuming that the flame tongue has a parabolic shape, and so the tip curvature and magnitude of diffusion at the tip are free parameters in this study. As before, the peak temperature occurs at the flame tip, suggesting that pollutant formation may be different at the tip. If the formation is greatly different than that created in the planar counterflow configuration, which is commonly used to represent a turbulent flamelet, then inclusion of flame tips in models of turbulent flow could be required. Numerical simulations that include more steps in a reduced kinetic model, and additionally include multi-component diffusion, have been initiated.

Future Research

Simulations of premixed flame propagation in three-dimensional turbulence will be done with inclusion of volume expansion due to chemical reaction. Considering the current agreement between experiment and simulations without heat release, then volume expansion effects upon the burnt gas vorticity may not be that important to the flame front dynamics. This apparent sucess of the constant density work could be related to the flame propagation, that is the flame moves into the unburnt vortical structure and leaves the burnt gas flow structure behind. Furthermore, the density ratio across the flame reduces the effect of the burnt gas vorticity upon the flame (motions in the dense gas will dominate those in the light gas). However, the burnt gas vorticity structures will be important for slow reactions behind the flame zone, such as the formation of water and carbon dioxide, in that these vortical structures will affect the mixing of post-flame gases.

The current turbulence simulations of premixed flame propagation, without heat release, provide strain rate conditions for further study of flame structure. It may be important that the most highly strained flames are in a swirling shear flow. In this swirling flow around a vortex tube, the strain rate along the tube axis is less than the strain rate created by the shear.[7] If the shear is close to cylindrical symmetry, then there may be no shear effect upon the flame structure. However, if the flame structure is not a stable one in this shearing motion, then the actual flame structure may exhibit transitions to other forms and, hence, create other pathways for pollutant formation. Another implication of the current work is that while it is appealing to use reduced chemical-kinetic schemes in

multi-dimensional flow problems, it is not certain that these reduced schemes will have the same dynamical behavior as more detailed chemical-kinetic models. Again, the current turbulence simulations can provide transient information for consideration by researchers interested in the detailed kinetic models of flame structure. Confirmation of the conditions under which the detailed kinetics may be replaced by reduced schemes is vital for reacting flow simulations.

References, (Including Recent DOE-Supported Publications)

1. Wm. T. Ashurst, "Flame Propagation Through Swirling Eddies, A Recursive Pattern," in press *Comb. Sci. & Tech.* (1993).
2. I. G. Shepherd & Wm. T. Ashurst, "Flame Front Geometry in Premixed Turbulent Flames," *Twenty-Fourth Symposium (International) on Combustion/The Combustion Institute* 485, (1992).
3. P. E. Dimotakis, "Some issues on turbulent mixing and turbulence," GALCIT Report FM93-1, California Institute of Technology.
4. Wm. T. Ashurst, "Vorticity Generation in a Nonpremixed Flame Sheet," *Numerical Combustion*, Lecture Notes in Physics, **351** (A. Dervieux and B. Larrouturou, Eds., Springer-Verlag, 1989).
5. Wm. T. Ashurst & F. A. Williams, *Twenty-Third Symposium (International) on Combustion/The Combustion Institute* 543 (1990).
6. J. M. Card, Wm. T. Ashurst & F. A. Williams, "Modification of Methane-Air Nonpremixed Flamelets by Vortical Interactions," in review.
7. Wm. T. Ashurst, "Constant-Density Markstein Flamelet in Navier-Stokes Turbulence," in review *Comb. Sci. & Tech.* (1992).
8. Wm. T. Ashurst & G. I. Sivashinsky, "On Flame Propagation Through Periodic Flow Fields," *Comb. Sci. & Tech.* **80**, 159 (1991).
9. A. R. Kerstein & Wm. T. Ashurst, "Propagation Rate of Growing Interfaces in Stirred Fluids," *Phys. Rev. Lett.* **68**, 934 (1992).
10. C. F. Edwards, N. R. Fornaciani, C. M. Dunsky, K. D. Marx and W. T. Ashurst, "Spatial Structure of A Confined Swirling Flow Using Planar Elastic Scatter Imaging and Laser Doppler Velocimetry," *Fuel*, in press (1993).

The Energetics and Dynamics of Free Radicals, Ions, and Clusters

Tomas Baer
Department of Chemistry
University of North Carolina
Chapel Hill, NC 27599-3290

PROGRAM SCOPE

The structure and energetics of free radicals, ions, and clusters are investigated by photoelectron photoion coincidence (PEPICO) and analyzed with *ab initio* molecular orbital methods and statistical theory RRKM calculations. The aim of the research is the collection of accurate structural and energetic data for free radicals, ions, and clusters. Equally important is the advancement of our fundamental understanding of ionization and dissociation processes. Among these is the effect of autoionization on the ion states produced by photoionization. The application of molecular orbital *ab initio* calculations is of central importance not only for the structural studies, but also because these calculations provide vibrational frequencies for the RRKM calculations. As a result, it is possible to carry out these rate calculations with only one adjustable parameter, namely the activation energy.

In the PEPICO experiment, molecules are prepared in a molecular beam so that their internal as well as translational energies are cooled to near 0 K. The coincidence condition between energy analyzed electrons and their corresponding ions insures that the ions are energy selected. The primary experimental information includes ionization and fragment ion appearance energies, and the ion time of flight (TOF) distributions. The latter are obtained by using the energy selected electron as a start signal and the ion as the stop signal. These types of experiments allow us to measure the ion dissociation rates in the 10^4 to 10^7 sec^{-1} range. Such ions are commonly referred to as metastable ions. In addition, the TOF peak widths are related to the release of translational energy in the ion dissociation process.

SUMMARY OF MAJOR RESULTS

Perhaps the most important advance during the past year has been in the field of cluster photoionization. We have developed an experimental method for differentiating similar mass cluster ions produced by the reactions:

$$(AB)_n + h\upsilon \rightarrow (AB)_n^+ + e^- \quad (1)$$

$$(Ab)_{n+m} + h\upsilon \rightarrow (AB)_n^+ + (AB)_m + e^- \quad (2)$$

This method is based on the kinetic energy of the ions measured by TOF. The release of kinetic energy is an essential part of all dissociation reactions. Because the initial velocity of the molecular beam in the direction of the ion extraction is extremely small, the parent time of flight (TOF) is exceedingly small. Thus any dissociation reaction, with its concomitant release of energy results in a much broader ion TOF peak. As little as 10 meV of translational energy can be measured by this approach.

Although it is now generally recognized that neutral clusters often dissociate upon

ionization, few studies have obtained unequivocal proof of this. Furthermore, the large electron energy in the electron impact ionization has been generally blamed for this cluster ion instability. Our results show that many cluster ions are unstable even when produced with photoionization at the very lowest photon energies possible. It is worth noting that when the cluster ions are produced by resonance enhanced multiphoton ionization (REMPI), this problem is considerably less prominent because in this two step process, the intermediate state can relax and provide more favorable Franck-Condon factors for producing the cluster ion.

The study of acetylene clusters has shown that neutral dimers and trimers cannot be ionized directly. All $C_4H_4^+$ and $C_6H_6^+$ signal comes from dissociative ionization of trimers and tetramers, respectively. From a statistical theory analysis of the kinetic energy release, it is possible to extract the final ion internal energy. This analysis demonstrates that the $C_4H_4^+$ and $C_6H_6^+$ ions are produced with 2 and 4 eV of vibrational energy respectively. This indicates massive rearrangement of the cluster ion structure upon ionization. In fact, the $C_4H_4^+$ and $C_6H_6^+$ ion structures are completely different from the neutral dimer and trimer structures. They are so different, that it makes no sense to speak of an ionization potential for these clusters. The cluster ions are simply unstable.

Molecular orbital *ab initio* calculations support the experiment. No stable dimer or trimer ion structure could be found. Geometry optimization always produced a stable ion with real chemical bonds in a structure that was totally different from the dimer and trimer neutrals.

Not all clusters ionize dissociatively. For instance, the acetone-Ar hetero dimer produces sharp TOF peaks which indicates that it is stable. On the other hand, the acetone dimer forms no stable dimer ions. Instead, we observe a broad monomer signal well below the monomer IP. How can this be? We propose the following mechanism:

$$(Ac)_2 + h\upsilon \rightarrow En^+ + Ac + e^-$$

where Ac = CH_3COCH_3 (acetone) and En = CH_2COHCH_3 (enol of acetone). The enol ion is about 1eV more stable than the acetone ion. The acetone ion evidently isomerizes to the more stable enol structure as the neutral acetone unit leaves.

The TOF peak width method has also been applied to the study of free radicals. One of the problems in a pyrolytic source is that a large assortment of stable molecules and free radicals are produced. When this mixture is ionized, it is sometimes difficult to distinguish an ion that is formed by direct ionization of its precursor, or if it is a product of a dissociative ionization from some unknown parent structure. The narrow peak widths in the TOF spectrum are clear signs that the AB^+ ion has come from the AB neutral.

Finally, a study of the butene ion dissociation has shed light on the role of rotational energy in such reactions. The butene ions were prepared in two ways: a) by photoionizing a cold sample in a molecular beam and b) by photoionizing a warm sample. The rates with low J's were measured and analyzed by RRKM calculations, including a version of the variational transition state theory (VTST). The measured rates for the warm sample which consisted of a distribution over the vibrational and rotational energies could then be analyzed with the previously determined cold rates. The suppression of the H loss channel versus the much looses CH_3 loss channel as the sample is heated is evidence for the rotational barrier in the former reaction path.

FUTURE PLANS

We plan to extend the study of cluster photoionization to determine what classes of clusters can be directly ionized. For instance, one might expect that non-polar, spherical molecules such as $(CH_4)_n$ clusters might have favorable Franck-Condon factors for ionization. Similarly, NO dimers are thought to ionize directly, but this has so far not been confirmed. Accurate *ab initio* calculations of ammonia dimers [Tachibana *et al* J.Phys.Chem. **95** 9647 (1991)] including barriers to rearrangement to $NH_4NH_2^+$ have been reported. From a knowledge of the neutral and ionic structures we will be able to calculate Franck-Condon factors (FCF) for dimer ionization and compare them to the experimental results. Because of the low FCF's at threshold, the ammonia dimer probably ionizes only dissociatively. On the other hand, the calculations also indicate that the mixed dimer, NH_3-H_2O, has a high barrier for rearrangement and formation of either the NH_4^+ + OH and the NH_2 + H_3^+ products. Thus, direct ionization of this neutral mixed dimer should be possible. In addition, we will be able to measure the barrier for isomerization followed by dissociation to H_3O^+ + NH_2.

The study of free radicals produced in a pyrolytic cell followed by supersonic expansion will be continued. Cooling of the free radicals has already been demonstrated by TOF mass spectrometry. The aim is to prepare t-butyl radicals in well characterized energy states and to measure the dissociation rate for CH_4 loss. The analysis of the dissociation rates using our calculated vibrationai frequencies will provide us with a good value for the ion heat of formation. This approach avoids the problem often encountered in ionization potential measurements which rely on good Franck-Condon factors for the 0-0 transition.

Finally, the role of rotations in unimolecular decay will be continued. The comparison of cold and warm data for reactions with loose and tight transition states can shed considerable light on this problem. The effect of rotations on the reaction rates is quite subtle and thus difficult to determine if all other parameters are not carefully controlled. The use of *ab initio* calculations which give vibrational frequencies and transition state moments of inertia are absolutely essential for the success of this study.

DOE SUPPORTED PUBLICATIONS FROM 1991-1993

J.S. Riley, T. Baer, and G.D. Marbury "Sequential ortho effects: Characterization on novel $[M-35]^+$ Fragment Ions in the Mass Spectra of 2-alkyl-4,6-Dinitrophenols", J. Am. Soc. Mass Spectrom. **2** 69 (1991)

K.M. Weitzel, J. Booze, and T. Baer, "Shifts in Photoionization Fragmentation Onsets; a Direct Measure of Cooling in a Supersonic Molecular Beam", Chem. Phys. **150** 263 (1991)

O. Dutuit, T. Baer, C. Metayer, and J. Lemaire, "Isotope effects in the dissociation of partially deuterated dimethyl ether (CH_3OCD_3) ions" Int. J. Mass Spectrom. Ion Proc. **110** 67 (1991)

T. Baer, K.M. Weitzel, and J. Booze, "Photoelectron Photoion Coincidence Studies of Ion Dissociation Dynamics" in *Vacuum Ultraviolet ionization and Dissociation of Molecules and Clusters*, World Scientific, Inc.C.Y. Ng, Ed. Pp 259-96 (1991).

T. Baer, The Measurement and Interpretation of Onset Energies", NATO ASI series C, # 347 249-65 (1991)

J.A. Booze, K.M. Weitzel, and T. Baer, "The Rates of HCl Loss from Energy Selected Ethylchloride Ions: A Case of Tunneling through an H-atom Transfer Barrier", J. Chem. Phys. **94** 3649-3656 (1991)

K.M. Weitzel, J.A. Booze, and T. Baer, "TPEPICO Study of the Ethane Loss from Energy Selected n-Pentane Ions Cooled in a Supersonic Expansion", Int. J. Mass Spectrom. Ion Proc. **107** 301-317 (1991)

K.M. Weitzel, J.A. Booze, and T. Baer, "The Metastable Formation of di-ethylchloronium Ions from Ethylchloride Dimers in a seeded Molecular Beam", Z. Phys. D. **18** 383-389 (1991)

J.Riley and T. Baer, "Dissociation Dynamics of Phenetole Cations by Photoelectron Photoion Coincidence" J. Am. Soc. Mass Spectrom. **2** 464-469 (1991)

J.A. Booze and T. Baer, "*Ab initio* Study of $C_3H_8O^+$ Ions", J. Phys. Chem. **96** 5710-5715 (1992)

J.A. Booze and T. Baer, "Dissociation dynamics of Energy Selected $CH_3CH_2CH_2OH^+$ and $CD_3CH_2CH_2OH^+$ ions", J. Phys. Chem. **96** 5715-5719 (1992)

J.A. Booze and T. Baer, "On the Determination of Cluster Properties by Ionization Techniques", J. Chem. Phys. **96** 5541-5543 (1992)

T. Baer, "Reactions of State Selected Ions Studied with Vacuum-UV Radiation, AIP Conf. Proc. **258** 3-17 (1992)

J.A. Booze and T. Baer "The Photoionization and Dissociation Dynamics of Energy Selected Acetylene Dimers, Trimers, and Tetramers", J. Chem. Phys. **98** 186-200 (1993)

J.R. Riley and T. Baer, "Unimolecular Decay of Energy Selected Dimethylformamide Cations: A combined molecular orbital and RRKM analysis", J. Phys. Chem. **97** 385-390 (1993)

T. Baer and J.A. Booze, "Long Lived Ion Complexes" in *Ion-Molecule Collision Complexes*, W. Hase Ed. JAI Press (1993)

T.H. Osterheld, T. Baer, and J.I. Brauman, "Infrared Multiple Photon Dissociation of Nitrobenzene Radical Cations. A Paradigm for Competitive Reactions" J. Am. Chem. Soc. in press (1993)

ENERGY TRANSFER PROPERTIES AND MECHANISMS

John R. Barker

Department of Atmospheric, Oceanic, and Space Sciences
Space Physics Research Laboratory
and Department of Chemistry
The University of Michigan
Ann Arbor, Michigan 48109-2143
[Internet: usergblg@um.cc.umich.edu]

Many chemical reaction systems are dominated by energy transfer. The principal motivation for this research is to characterize energy transfer processes in highly vibrationally excited molecules of moderate size, where individual states cannot be resolved. The over-all objective of this work is to develop accurate and practical models for describing and predicting energy transfer properties.

In previous work, we have used the infrared fluorescence technique to investigate energy transfer in azulene, benzene, benzene-d_6, toluene, and toluene-d_8. This work, which has used a single emission band (the C-H stretch modes near 3050 cm^{-1} or the C-D stretch near 2250 cm^{-1}), is capable of estimating the ensemble average excitation energy (the "bulk average energy", $\langle\langle E(t)\rangle\rangle$) as the excited species are being deactivated by collisions. The average energy in this "collisional energy cascade" is used to determine $\langle\langle \Delta E(t)\rangle\rangle$, the bulk average energy step size, which is a function of time and, hence, of the bulk average energy. In all cases investigated so far, the results show the same approximately linear energy dependence at low energy and there is a distinct tendency for $\langle\langle \Delta E\rangle\rangle$ to become less dependent on energy at higher internal energies.

The aim of the these experiments is to determine how the population distribution evolves during the deactivation process, because this is indicative of the collision step-size distribution (the "Holy Grail" of large molecule energy transfer studies). In particular, we want to measure not just the mean energy (the first moment), but the higher moments of the evolving distribution, as well.

We have now succeeded in carrying out the first experiments measuring the variance of the energy distribution (second central moment) for the benzene and benzene-d_6 systems, where a small fraction of the species are excited and are deactivated by the bulk of unexcited gas. This is the first time such detailed information has been obtained over essentially the entire collisional cascade. This was accomplished by a) the use of the time- and wavelength-resolved infrared emission spectrum of highly excited benzene and b) two-color IRF measurements of the fundamental and overtone emissions from the C-H (and C-D) stretch modes. The data analysis approach we have developed can be easily extended to other experimental techniques, including time and wavelength resolved ultraviolet

absorption, as long as suitable calibrations exist. This approach results in refined estimates of both the mean energy and the variance of the energy distribution, and it is superior to the one-color IRF technique we have used previously, because more data are used in the analysis.

The results are shown in Figure 1, which shows the width of the energy distribution as a function of the average energy during the collisional cascade. We have carried out Master Equation simulations of these systems and have found that the width of the distribution is much more sensitive to the assumed step size distribution than is the mean energy. Although the simple exponential model is a good approximation to the over-all behavior, a bi-exponential model (i.e.. including "supercollisions") is better.

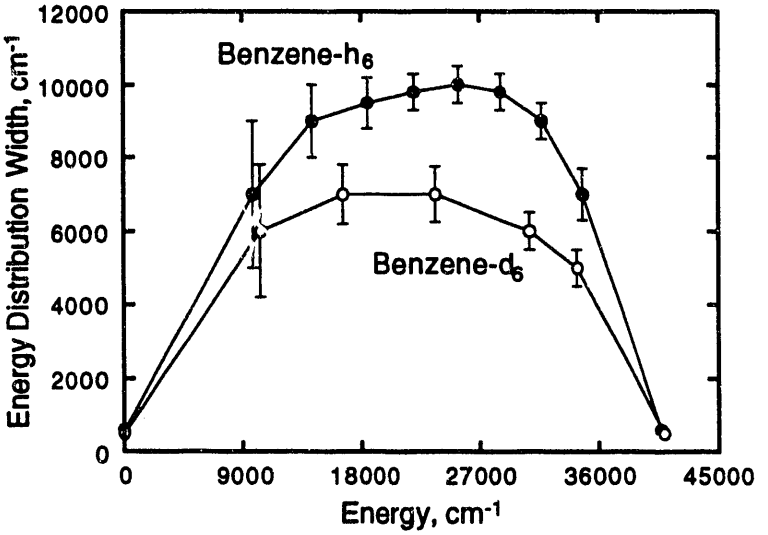

Figure 1. Widths of the time-dependent energy distributions during collisional cascades (initial excitation near 40,000 cm^{-1}).

We plan to pursue this line of experiments and extend the measurements to deactivation by weak colliders, such as the rare gases and small molecules (although the experimental difficulties will increase significantly). We will also investigate deactivation of toluene and toluene-d_8.

In a parallel effort, we have begun experiments using pump-probe techniques to measure the final state distributions of species involved in energy transfer collisions. The initial experiments have utilized REMPI probes of the collider, following excitation of benzene at 248 nm. We will also investigate fluorescence probes to determine their usefulness in such experiments.

II. Recent Publications Supported by DOE

Published or Accepted for Publication

"Vibrational Relaxation of Highly Excited Toluene," Beatriz M. Toselli, Jerrell D. Brenner, Murthy L. Yerram, William E. Chin, Keith D. King, and John R. Barker, J. Chem. Phys., **95**, 176 (1991).

"Polycyclic Aromatic Hydrocarbon Optical Properties and Contribution to the Acceleration of Stellar Outflows," Isabelle Cherchneff, John R. Barker, and Alexander G. G. M. Tielens, Astrophys. J., **377**, 541-552 (1991).

"Excitation of CO_2 by energy transfer from highly vibrationally excited benzene derivatives," Beatriz M. Toselli and John R. Barker, J. Chem. Phys., **95**, 8108 (1991).

"Infrared Emission Spectra of Benzene and Naphthalene: Implications for the Interstellar PAH Hypothesis," Jerrell D. Brenner and John R. Barker, Astrophys. J. (Letters), **388**, L39-L43 (1992).

"Isotope Effects in the Vibrational Deactivation of Large Molecules", Beatriz M. Toselli and John R. Barker, J. Chem. Phys., **97**, 1809-1817 (1992).

"Polycyclic Aromatic Hydrocarbons and Molecular Equilibria in Carbon Rich Stars," Isabelle Cherchneff, John R. Barker, and Alexander G. G. M. Tielens, Astrophys. J., **394**, 703-716 (1992).

"Radiative Recombination in the Electronic Ground State," John R. Barker, J. Phys. Chem., **96**, 7361-7367 (1992).

"Polycyclic Aromatic Hydrocarbon Formation in Carbon Rich Stellar Envelopes," Isabelle Cherchneff, John R. Barker, and Alexander G. G. M. Tielens, Astrophys. J., **410**, 269-287 (1992).

"Infrared Emission Studies of the Vibrational Deactivation of Benzene Derivatives," John R. Barker and Beatriz M. Toselli, Int. Rev. Phys. Chem., accepted for publication.

"Experimental Measurement of Energy Population Distributions in the Collisional Deactivation of Highly Vibrationally Excited Benzene and Benzene-d_6", Jerrell D. Brenner, Joseph P. Erinjeri, and John R. Barker, Chem. Phys. (Special issue on "Vibrational Energy Dynamics"), to be published.

"The Deactivation of Large Molecules," John R. Barker, Jerrell D. Brenner, and Beatriz M. Toselli, *Vibrational Energy Transfer Involving Large and Small Molecules*, Adv. Chem. Kinetics and Dyn., Vol. 2, to be published.

Turbulence-Chemistry Interactions in Reacting Flows

R. S. Barlow and C. D. Carter
Combustion Research Facility
Sandia National Laboratories
Livermore, California 94551

Interactions between turbulence and chemistry in nonpremixed flames are investigated through multiscalar measurements. Simultaneous point measurements of major species, NO, OH, temperature, and mixture fraction are obtained by combining spontaneous Raman scattering, Rayleigh scattering, and laser-induced fluorescence (LIF). NO and OH fluorescence signals are converted to quantitative concentrations by applying shot-to-shot corrections for local variations of the Boltzmann fraction and collisional quenching rate. These measurements of instantaneous thermochemical states in turbulent flames provide insights into the fundamental nature of turbulence-chemistry interactions. The measurements also constitute a unique data base for evaluation and refinement of turbulent combustion models.

Experimental work during the past year has focused on three areas: 1) investigation of the effects of differential molecular diffusion in turbulent combustion; 2) experiments on the effects of Halon CF_3Br, a fire retardant, on the structure of turbulent flames of CH_4 and $CO/H_2/N_2$; and 3) experiments on NO formation in turbulent hydrogen jet flames.

Differential Diffusion Effects in Turbulent Flames: Recent experimental and computational work has indicated that the degree of differential diffusion in a reacting flow can have a significant influence on the structure of the reaction zone and the relationships among species. In collaboration with the University of California, Berkeley, we have conducted an experimental investigation of differential diffusion in nonreacting and reacting flows over a wide range of conditions including laminar opposed flows and turbulent jets. A mixture of 36% H_2 and 64% CO_2 was used to match the density of air, while providing components in the fuel stream with widely differing molecular weights. Spontaneous Raman scattering was used to obtain point measurements of major species concentrations. Results in nonreacting laminar opposed flows are in good agreement with calculations and show that differential diffusion effects are independent of strain rate for this geometry. Data from nonreacting jet flows show that, on a conditionally averaged basis, the effects of differential diffusion disappear quickly as Reynolds number increases. Measurements in flames show strong effects of differential diffusion at all Reynolds numbers (up to 30,000). Current turbulent combustion models either neglect differential diffusion or assume that the degree of differential diffusion in turbulent flames is the same as in laminar flames. Experimental results showed that neither of these assumptions is correct for turbulent flames with intermediate Reynolds numbers.

Effects of CF_3Br on Turbulent Flames: We completed an extensive series of experiments to determine the effects of Halon CF_3Br, a fire retardant, on the chemical structure of flames. The experimental program included: i) measurements of the Raman spectra (and fluorescence interference spectra) in laminar premixed flames with CF_3Br; ii) additions to the Raman polychromator to include channels for CF_3Br, CF_2O, HBr, and HF, as well as the existing channels for all the major species in hydrocarbon flames; and iii) multiscalar measurements in laminar and turbulent nonpremixed flames. Fuels included CH_4 and $CO/H_2/N_2$ mixtures. Experiments covered a wide range of mixing conditions from laminar flames at low strain to turbulent flames near extinction. The resulting data base, which includes simultaneous measurements of temperature and thirteen species, will be useful in understanding the effects of flame retardants and other halogenated compounds on turbulent flame structure. These data will also serve as a baseline for investigations of

compounds to replace environmentally undesirable CF_3Br. This work was conducted in collaboration with Prof. A. R. Masri of Sydney University.

NO Formation in Turbulent Hydrogen Jet Flames: The capability to measure NO concentrations by laser-induced fluorescence was added to the multiscalar Raman/Rayleigh/LIF system. The NO fluorescence signals are converted to quantitative concentrations by applying corrections for shot-to-shot variations in the collisional quenching rate and Boltzmann fraction. These corrections are based on the simultaneous measurements of major species, OH, and temperature. The signal-to-noise ratio for the system is greater than 8:1 for [NO]=$2x10^{13}$ cm^{-3} (4 ppm in a 1550K flame). This new capability was applied to the study of NO formation in turbulent H_2-air jet flames. Multiscalar measurements were obtained in jet flames of H_2 and helium-diluted H_2 at several Reynolds numbers. All cases were chosen to match conditions for which gas-sampling probe measurements have been reported in the literature. Results in Fig. 1 show a gradual increase in NO levels with increasing streamwise distance. Figure 1 also shows that, at a given mixture fraction, the fluctuation in NO concentration decreases relative to the mean, as streamwise distance increases. This features of the NO measurements can be attributed to the streamwise evolution of reaction zone structure from thin, strained flamelets near the nozzle to broad diffuse regions near the flame tip. Favre average and conditional average results for NO versus mixture fraction are compared in Fig. 2. The Favre average is a density-weighted average, which yields results analogous to those from a gas-sampling probe. For the conditional average, data within a narrow interval of mixture fraction are averaged, independent of radial position in the flame. The present measurements show that the Favre averaging process causes a significant bias of the [NO] versus mixture fraction results, such that the peaks of the curves do not align with the stoichiometric value of the mixture fraction ($f_{stoic} = 0.0285$). The conditional average NO results give the correct relationship between NO and mixture fraction and show that the maximum NO concentrations consistently occur near the stoichiometric condition. This result resolves a controversy that has existed for ten years regarding the "rich shift" reported in some sampling-probe studies of NO formation in turbulent flames.

These laser-based measurements constitute a unique data base for evaluation of predictive models for NO formation in turbulent flames. In collaboration with computational groups at Berkeley and the University of Sydney, experimental results are being compared with predictions of two types of combustion models.

Plans: The multiscalar diagnostic system has unique capabilities to contribute to an improved understanding of the role of turbulence-chemistry interactions in NO formation in turbulent flames. This system will be used to investigate NO formation in nonpremixed turbulent jet flames of methane, $CO/H_2/N_2$, and methanol. Collaborations to compare experimental results with model predictions will continue. In addition to experiments on attached jet flames, which can be compared directly with predictions of state-of-the-art turbulent combustion models, we plan to carry out experiments on NO formation in bluff-body stabilized flames and lifted flames.

Two-photon CO LIF and O-atom LIF will be evaluated as potential single-shot, quantitative diagnostics in turbulent flames. Raman measurements of CO concentrations in methane flames are problematic, due to C_2 fluorescence interference, and improved accuracy in CO measurements would be very useful for investigations of turbulence-chemistry interactions in hydrocarbon flames. Quantitative O-atom LIF could be combined with the current multiscalar system to achieve instantaneous measurements of NO concentration and the thermal NO formation rate in turbulent flames.

The Raman/Rayleigh system for measurements of major species and temperature will be converted to use two Nd:YAG lasers rather than a flashlamp pumped dye laser. Improved accuracy, reliability, and productivity are expected.

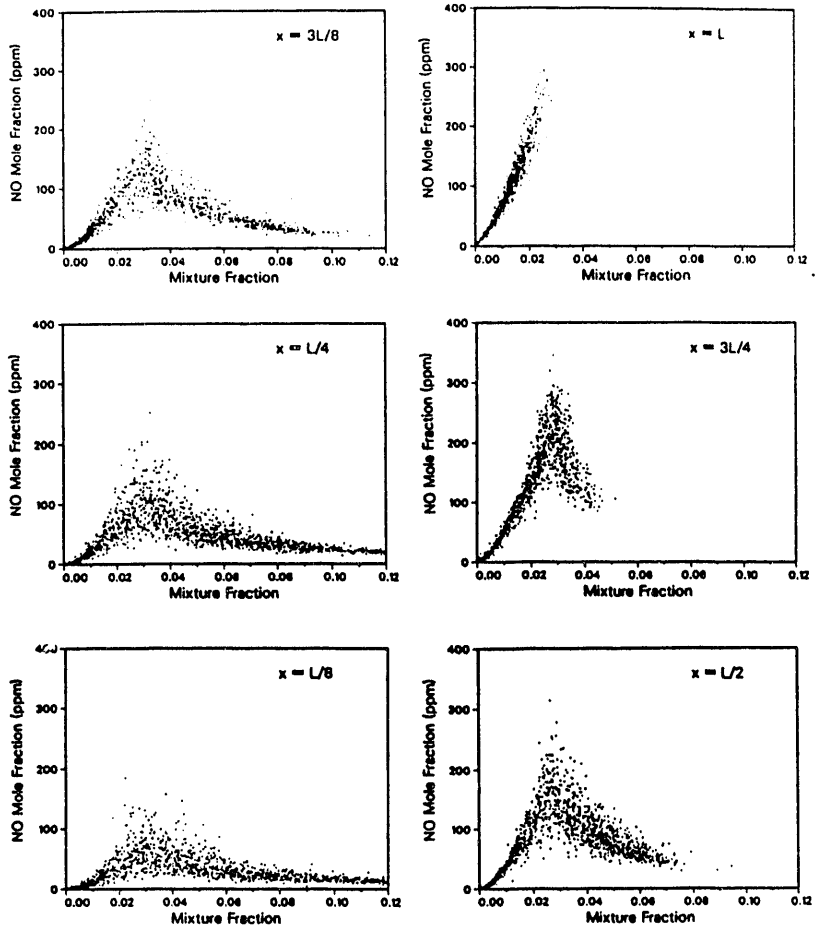

Figure 1. Scatter plots show a gradual increase in NO levels with increasing streamwise distance, x. Measurements were obtained in a hydrogen jet flame with a nozzle diameter of d=3.75 mm and a Reynolds number of 10,000. L is the visible flame length (L~180d).

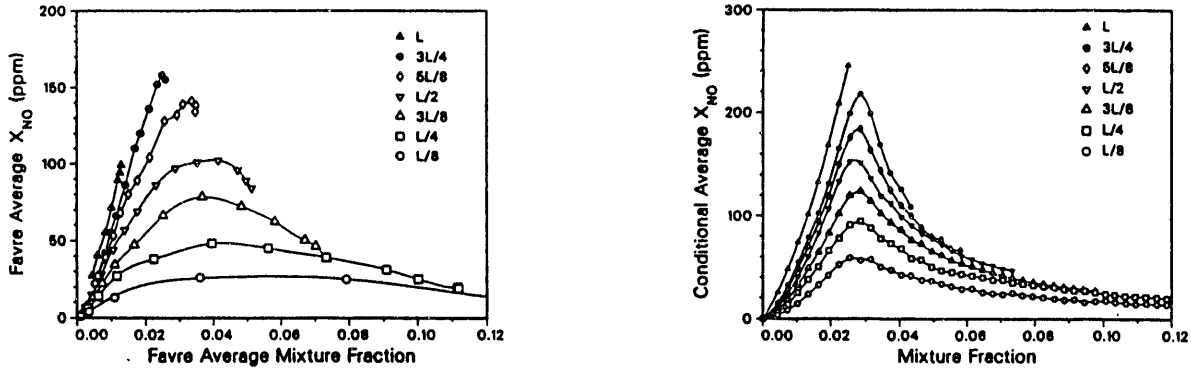

Fig. 2. Comparison of the Favre (density weighted) average and conditional average results for NO versus mixture fraction show that the Favre averaging process, which is inherent to gas-sampling probe measurements, can cause a significant bias in the relationship between NO and mixture fraction for measurements within turbulent flames.

Publications 1991-Present

R. S. Barlow, D. C. Fourguette, M. G. Mungal, and R. W. Dibble, "Experiments on the Structure of a Compressible Annular Reacting Shear Layer," *AIAA J.*, **30**, 2244-2251 (1992).

R. S. Barlow and J.-Y. Chen, "On Transient Flamelets and Their Relationship to Turbulent Nonpremixed Flames," *Twenty-Fourth Symposium (International) on Combustion* (The Combustion Institute, Pittsburgh, PA), pp. 231-237 (1992).

K. A. Buck, W. J. A. Dahm, R. W. Dibble, and R. S. Barlow, "Structure of Equilibrium Reaction Rate Fields in Turbulent Jet Diffusion Flames," *Twenty-Fourth Symposium (International) on Combustion* , The Combustion Institute, Pittsburgh, PA, pp. 295-301 (1992).

D. C. Fourguette, R. S. Barlow, M. G. Mungal, and R. W. Dibble, "Concentration Measurements in a Supersonic shear Layer," *AIAA J.*, in press (1993).

A. R. Masri, R. W. Dibble, R. S. Barlow, "Chemical Kinetic Effects in Nonpremixed Flames of H_2-CO_2 Fuel," *Combust. Flame*, **91**, 285-309 (1992).

A. R. Masri, D. W. Dibble, and R. S. Barlow, "Raman-Rayleigh Measurements in Bluff-Body Stabilized Flames of Hydrocarbon Fuels," *Twenty-Fourth Symposium (International) on Combustion* , The Combustion Institute, Pittsburgh, PA, pp. 317-322 (1992).

A. R. Masri, R. W. Dibble, and R. S. Barlow, "The Structure of Turbulent Nonpremixed Flames of Methanol over a Range of Mixing Rates," *Combust. Flame*, **89**: 167-185 (1992).

S. H. Stårner, R. W. Bilger, R. W. Dibble, and R. S. Barlow, "Piloted Diffusion Flames of $CO/CH_4/N_2$ and $CO/H_2/N_2$ Near Extinction," *Combust. Flame*, **83**: 63-74 (1991).

S. H. Stårner, R. W. Bilger, R. W. Dibble, and R. S. Barlow, "Measurements of Conserved Scalars in Turbulent Diffusion Flames," *Comb. Sci. Tech.* **86**: 223-236 (1992).

S. H. Stårner, R. W. Bilger, and R. S. Barlow, "Raman/LIF Measurements in a Lifted Hydrocarbon Jet Flame," *Eighth Symposium on Turbulent Shear Flows* Springer-Verlag, 1992.

S. H. Stårner, R. W. Bilger, R. W. Dibble, R. S. Barlow, D. C. Fourguette, and M. B. Long, "Joint Planar CH and OH LIF Imaging in Piloted Turbulent Jet Diffusion Flames Near Extinction," *Twenty-Fourth Symposium (International) on Combustion* , The Combustion Institute, Pittsburgh, PA, pp. 341-347 (1992)

COMBUSTION-RELATED STUDIES USING WEAKLY-BONDED COMPLEXES

Robert A. Beaudet
Department of Chemistry
University of Southern California
Los Angeles, CA 90089-0482
Tel: (213) 743-2997
FAX: (213) 743-7757

PROGRAM SCOPE:

Binary van der Waals complexes involving species of interest to combustion research are prepared in supersonic free-jet expansions, and their photochemical and photophysical properties are probed by using IR tunable diode laser (TDL) spectroscopy. In the first phase, geometries and other molecular properties are being determined from vibration-rotational spectra. In the second phase, these complexes will be used as precursors to study photoinitiated reactions in precursor geometry limited environments. Two complementary classes of binary complexes are being investigated. The first involves molecular oxygen and hydrogen containing constituents (e.g. O_2-HCN, O_2-HF, O_2-HCl, O_2-HBr, O_2-HI and O_2-hydrocarbons). These species are interesting candidates for study since upon photodissociating the hydride portion, the reaction of H and O_2 via the vibrationally excited $HO_2^{\dagger}$ intermediate can conceivably be studied, {*e.g.* BrH-O_2 + hν(193 nm) → Br-H-O_2 → Br + $HO_2^{\dagger}$ → Br + OH + O}. High resolution IR spectroscopy of such complexes have not been obtained previously and the structural information deriving from IR spectra is certainly very useful for better designing and understanding photoinitiated reactions that occur in these complexes.

The second thrust area is the study of a set of novel species involving oxygen *atoms* and small molecules such as HF, HCl, HBr, HI, HCN and simple hydrocarbons. An expansion gas is seeded with a precursor such as SO_2 and a second constituent. $O(^3P)$ is prepared by precursor photolysis just before the start of the supersonic expansion. Since the reactions of $O(^3P)$ and the above mentioned small molecules have significant activation energies, the complexes will be able to form and survive in the free-jet expansions, *e.g.*, the $O(^3P)$ + HCl reaction has an activation energy of 22 kJ/mol., which is considerably higher than the thermal collisional energy. Hence, the complex can be stabilized in the shallow van der Waals potential well just outside the activation barrier. Our initial objective is to study structural properties of these clusters by using laser IR spectroscopy. Once that proves successful, we will exploit vibrational excitation of the HX to promote the hydrogen exchange reaction of O + HX → OH + X occurring in these complexes. The nascent state distribution of the OH product can be probed with LIF. Experiments are also under way in which the nascent product state distribution of a photodissociation can be probed by using IR spectroscopy.

PROGRESS:

Rovibrational spectrum of DCl-O_2.

We have prepared the binary complex DCl-O_2 and observed its rovibrational spectrum by exciting the DCl stretching mode at 2089 cm^{-1}. Though the spectrum has not been completely analyzed and fitted, the complex is clearly linear. Essentially the spectrum consists of three overlapping P and R branches, one for each spin state. We have been waiting for another diode to cover the remainder of the spectrum before we can determine

the band center, the exact J values and fit the spin spin interaction constants. The values of the interaction constants, λ and μ appear to differ from molecular oxygen. The measured transitions are given in Table 1.

Line frequencies, spacings, and Δ_2 of the three branches of DCl-O_2.

Line position	Line spacing	Δ_2
2088.87616	0.10912	-0.00240
8.76704	0.10672	-0.00235
8.66032	0.10437	-0.00129
8.55595	0.10308	0.00010
8.45287	0.10318	0.00022
8.34969	0.10340	0.00196
8.24629	0.10536	0.00238
8.14093	0.10774	0.00211
8.03319	0.10985	0.00196
7.92334	0.11181	
7.81153		
2088.81320	0.11452	0.00086
8.69868	0.11538	0.00138
8.58330	0.11676	0.00009
8.46654	0.11685	0.00132
8.34969	0.11817	0.00062
8.23152	0.11879	0.00053
8.11273	0.11932	
7.99341		
2088.73506	0.11811	0.00276
8.61695	0.11535	-0.00406
8.5016	0.11941	0.00263
8.38219	0.11678	0.00205
8.26541	0.11473	-0.00276
8.15068	0.11749	-0.00172
8.03319	0.11921	
7.91398		

Units: cm^{-1}, Error: $\pm 0.0005\ cm^{-1}$

Vibrational State distribution in the OH + CO ⟶ CO_2 + H reaction

Very recently, we have used our pulse slit apparatus to investigate the vibrational state distribution of CO_2 produced from the following reaction:

$$OH + CO \longrightarrow CO_2 + H \qquad \Delta H = -24.9 \text{ kcal}$$

Nitric acid, carbon monoxide and a noble gas are flowed through the supersonic nozzle. The nitric acid is photolyzed with an excimer laser at 193 nm focused very close to the nozzle. The OH in the $\upsilon = 0$ and 1 states is produced efficiently by the following reaction.[1,2]

$$HNO_3 + h\upsilon \longrightarrow OH + NO_2$$

Subsequently, the OH reacts with the CO to form CO_2 and atomic hydrogen .[3] We observe the rovibrational spectrum of CO_2 in the 2350 cm^{-1} region. A sample of the experimental spectra is given in **Fig. 1.** We find a large number of intense hot bands of the bending mode, $(0,\upsilon_2,1) \rightarrow (0,\upsilon_2,0)$ and some of the stretching mode $(\upsilon_1,0,1) \longrightarrow (\upsilon_1,0,0)$ where υ_1 and υ_2 represent the number of quanta in the bending and stretching modes respectively. From this we can determine the CO_2 rovibrational state distribution directly by measuring the intensities of the infrared absorption of the hot bands. The observed S/N is about 100:1 for the most populated rovibrational states. On the basis of

these preliminary observations, we believe that we have developed an alternate technique to obtain the vibrational state distribution of products formed in simple bimolecular chemical reactions. Product state distributions of molecules such as CO_2 cannot be easily determined by other laser techniques such as LIF.

Thus, we can determine the CO_2 vibrational state distribution directly in the free expansion jet for this and other exothermic reactions with low entrance channel barriers The cooled expansion provides a cold environment with low rotational (~10K) and vibrational (~100k) background temperatures. Any additional population of the higher vibrational states will reflect the vibrational excitation of the products and suggest transition state geometries. Populated excited vibrational states of the bending mode suggest a bent transition state for this reaction. With simple classical harmonic oscillator approximations or quantum mechanical wavepacket calculations, the bond angle of the transition state can be estimated.

FUTURE WORK

At this time, we have only obtained preliminary results. We want to produce the OH from other precursors if possible, for example H_2O_2, to confirm that the NO_2 formed in the photolysis of the HNO_3 is not contributing to the reaction. Sufficient rotational lines for each vibrational state must be measured to verify the rotational temperatures and determine whether the rotational state distribution is relaxed. Because the vibrational hot bands are quite displaced from the corresponding ground state lines, intensity measurements must be done carefully. We will require several diodes to sufficiently cover the extensive CO_2 band.

Other reactions of interest to combustion can be studied in this way. We select for the first experiments reactions that produce a strong vibrational absorber in frequency regions where we either own or can purchase acceptable diodes. Thus, we will concentrate first on the NH + NO reaction. This has two exothermic channels, only one of which has been extensively studied.[4-7]

$$NH + NO \rightarrow HNNO^{\dagger} \rightarrow N_2 + OH \qquad \Delta H_0^{\circ} = -34{,}100\ cm^{-1} \quad (1a)$$

$$\rightarrow N_2O + H \qquad \Delta H_0^{\circ} = -12{,}320\ cm^{-1} \quad (1b)$$

The first reaction is the most exothermic and the easiest to study: OH is detected by LIF. To study the second channel, either N_2O or H atoms must be detected. Fueno *et al.*[8] has determined the N_2O yield in a static cell with a mass spectrometer: the channel producing N_2O accounts for about 70% of the NH reacted. NH was prepared in high yield by various ways, photolysis of HNCO or $CHBr_3/NO/Ar$[9] at 193 nm, or of NH_3 at 193 or 248 nm.

---

1. H. S. Johnson, S. G. Chang, and G. Whitten, *J. Phys. Chem.* **78**, 1 (1974).
2. J. Brunning, D.W. Derbyshire, I. W. M. Smith and M. D. Williams, *J. Chem. Soc., Faraday Trans.* 2, 1988, **84**, 105.
3. Cf. the following for an extensive set of references on this reaction: M. J. Frost, P. Sharkey, and I. W. M. Smith, *Farad. Discuss. Chem. Soc.* **91**, 305 (1991).
4. W. Hack and K. Rathman, *J. Phys. Chem.* **94**, 4155 (1990).
5. W. Hack and A. Wilms, Z. Phys. Chem. **93**, 3540 (1989).
6. T. Fueno, M. Fukuda, and K. Yokoyama, Chem. Phys. **124**, 265 (1988),
7. J. A. Harrison, A. R. Whyte, and L. F. Phillips, Chem. Phys. Lett. **129**,346 (1986).
8. Fueno, ibid.
9. K. Yamasaki, S. Okada, M. Koshi, and H. Matsui, J. Chem. Phys. **95**, 5087 (1991).

PUBLICATIONS RELATED TO COMBUSTION RESEARCH:

66. **Photoinitiated Reactions in Weakly-Bonded Complexes**, S.K. Shin, Y. Chen, S. Nicholaisen, S.W. Sharpe, R.A. Beaudet, and C. Wittig *Adv. Photochem.*. Vol. 16, 249 (1991).
67. **Photoinitiated Reactions in Weakly-Bonded Complexes: Entrance Channel Specificity**, Y. Chen, Y.P. Zeng, S.K. Shin, G. Hoffmann, D. Oh, S. Sharpe, R.A. Beaudet, and C. Wittig, *Advance Molecular Vibrational and Collision Dynamics*. 1B,187 J. M. Bowman and M. A. Ratner, ed., 1991.
68. **Infrared Absorption Spectroscopy of the CO-Ar Complex**, A. R. W. McKellar, Y. P. Zeng, S. W. Sharpe, C. Wittig, and R. A. Beaudet, J. Molec. Spectr. 153, 475 (1992)
69. **Infrared Absorption Spectroscopy of the Weakly Bonded CO-Cl_2 Complex**. S. Bunte, J. B. Miller, Z. S. Huang, J. E. Verdasco, C. Wittig, and R. A. Beaudet. J. Phys. Chem.,1992, 96, 4140.
70. **High Resolution Infrared Diode Laser Spectroscopy of the $SO(^3\Sigma^-)$ in a Secondary-Slit Supersonic Expansion.**, Z. S. Huang, J. E. Verdasco, C. Wittig, and R. A. Beaudet, Chem. Phys. Lett.
71. **Infrared Spectroscopy of CO_2-D(H)Br and its molecular structure**, Y. P. Zeng, S. W. Sharpe, S. K. Shin, C. Wittig, and R. A. Beaudet *Journal of Chemical Physics*. 97 5392 (1992)
1. **An *Ab Initio* Study of the Weakly Bonded CO-Cl_2Complex**, S. W. Bunte, C. F. Chabalowski, C. Wittig, and R. A. Beaudet, Jour. Phys. Chem. accepted.

The IR Spectrum of The CO_2 Following The Reaction of OH + CO -> CO_2 + H

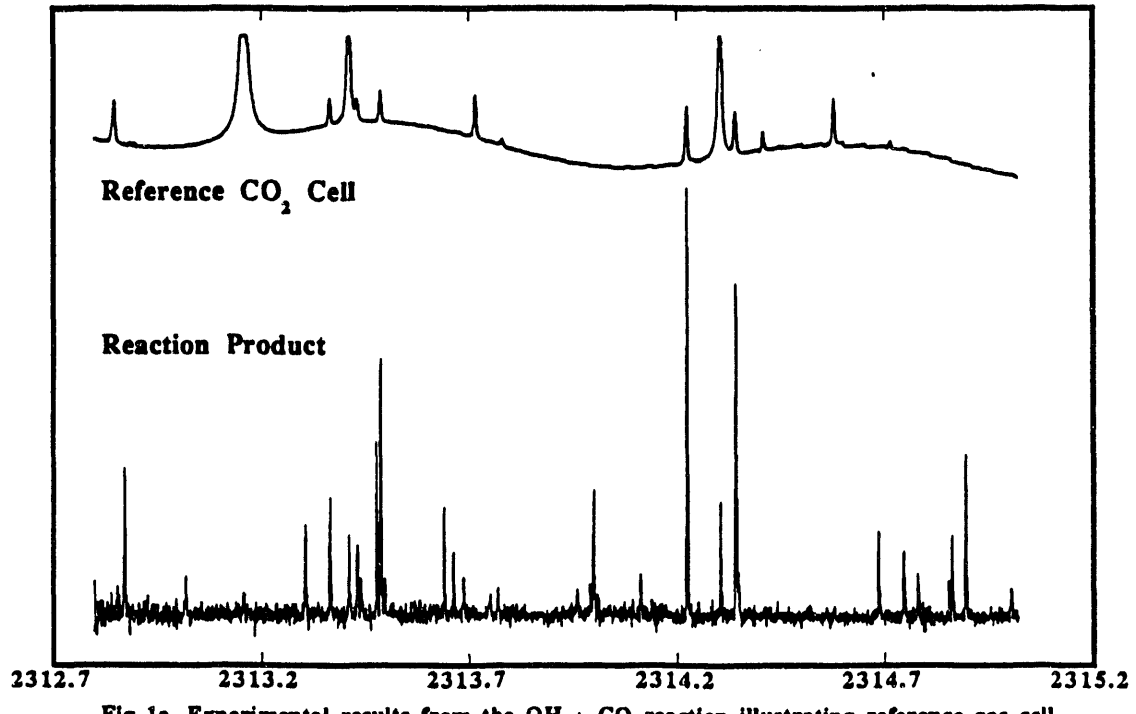

Fig 1a. Experimental results from the OH + CO reaction illustrating reference gas cell and observed spectrum of reaction product, CO_2.

Photoionization-Photoelectron Research

J. Berkowitz and B. Ruscic
Chemistry Division, Argonne National Laboratory (Bldg. 203)
9700 South Cass Avenue
Argonne, IL 60439-4843

The photoionization research program is aimed at understanding the basic processes of interaction of vacuum ultraviolet (VUV) light with atoms and molecules. This research provides valuable information on both thermochemistry and dynamics. Our recent studies include atoms, clusters, hydrides, sulfides and an important fluoride.

Recent Progress

I. Recent VUV-PIMS Studies of Transient Species

A. The combustion intermediates CH_2S and HCS

The transient species CH_2S and HCS were studied by photoionization mass spectrometry. They were prepared *in situ* from CH_3SH by sequential hydrogen abstraction with fluorine atoms. CH_2S was also prepared by pyrolysis CH_3SCl and CH_3SSCH_3. The photoion yield curve of CH_2S displays an abrupt threshold, and is similar in overall shape to that of the homolog CH_2O. The adiabatic ionization potential of CH_2S is found to be 9.376 ± 0.003 eV. Evidence has been found for nd and/or ns and np Rydberg states converging to the first excited state of CH_2S^+. In addition, the HCS^+ fragment from CH_2S has been determined to appear at ≤ 11.533 ± 0.021 eV at 0 K. In contrast to CH_2S, the photoion yield curve of HCS^+ from HCS displays a very broad Franck-Condon envelope, consistent with a transition from bent HCS to linear HCS^+. A Poisson fit to the experimental Franck-Condon factors indicates that the adiabatic ionization potential of HCS is ≤ 7.499 ± 0.005 eV, and perhaps as low as 7.412 ± 0.007 eV. The fragment curves at m/e = 46, 47, 48, and 49 from CH_3SSCH_3 have also been examined, and their relative shifts in energy determined. Together with measurements on CH_2S and HCS, and the previously reported ΔH^o_{f0} (CH_2SH^+) = 211.5 ± 2.0 kcal/mol (≤ 213.1 ± 0.2 kcal/mol), this is sufficient to establish ΔH^o_{f0} (CH_2S) = 28.3 ± 2.0 kcal/mol (≤ 29.9 ± 0.9 kcal/mol) and ΔH^o_{f0} (HCS) = 71.7 ± 2.0 kcal/mol (≤ 73.3 ± 1.0 kcal/mol, ≥ 69.7 ± 2.0 kcal/mol). These values are in very good agreement with recent *ab initio* calculations. The implications for various bond energies within the CH_nS system are also discussed.

B. The hydrides of antimony

Prior to the present study, very little was known experimentally regarding the bond energies D_0 (SbH), D_0 (H-SbH) and D_0 (H_2Sb-H). *Ab initio* calculations which have demonstrated accuracies of ± 2 kcal/mol for lighter hydrides are still too difficult for such heavy systems. We now have preliminary data on these bond energies, as well as ionization potentials for SbH and SbH_2. We shall compare our work with *ab initio* attempts incorporating relativistic effects (which have not yet demonstrated high accuracy), as well as a semiempirical prediction.

II. Antimony and Bismuth Atoms

The autoionization behavior in atoms is inherently a many-body process. Various *ab initio* methods have been applied to this problem, including RRPA, R-matrix and diagrammatic many-body perturbation theory (MBPT). Both the calculations and corresponding experiments become more difficult when applied to open-shell atoms, which are more prevalent than closed-shell atoms. Despite these complications, systematic behavior has been observed by us and rationalized for the halogen and chalcogen atoms. Previous work on the pnicogen (Group V) atoms from this laboratory has included N, P and As. We now have almost completed a study of Bi (generated by simple sublimation) and some data on Sb. For the latter, it has been necessary to employ successive H abstraction from SbH_3 as the source of Sb, since antimony sublimes as Sb_4.

III. The diatomic species Sb_2 and Bi_2

The photoion yield curves of Sb_2^+ (Sb_2) and Bi_2^+ (Bi_2) have been obtained, the former by subliming InSb, the latter by simple sublimation. In both cases, two autoionizing series (designated $p\sigma$ and $p\pi$) are observed, converging on the excited $^2\Sigma_g^+$ state. The ionization energy of the $^2\Sigma_g^+$ state in Sb_2 is lowered to 9.247 eV. The difference in quantum defects, $\delta p\pi - \delta p\sigma$, is shown to be related to the quadrupole moment of the molecular ion core of the $A^2\Sigma_g^+$ state in Pn_2^+ (Pn = pnicogen). The adiabatic ionization energies are also decreased from earlier values: AIP (Sb_2) $\leq$ 8.43 eV AIP (Bi_2) $\leq$ 7.34 eV. Although the uppermost occupied orbital is nominally a bonding $p\pi$ orbital, an analysis leads to the surprising conclusion that D_0 (Pn_2^+) $\gtrsim$ D_0 (Pn_2), where Pn = P, As, Sb and Bi).

IV. Photoionization of Group V trimers and tetramers

The photoionization of saturated antimony and bismuth vapors was investigated. In antimony, the dominant vapor species is Sb_4. Its photoion yield curve is similar to those of P_4 and As_4, displaying three autoionizing bands and an apparent adiabatic IP of 7.56 eV. The appearance potential of Sb_3^+ (Sb_4) occurs at $9.755^{+0.01}_{-0.04}$ eV, or $10.229^{+0.01}_{-0.04}$ eV at 0°K. This value, together with $\Delta H_{f_0}^0$ (Sb_3), yields IP (Sb_3) $\leq$ 6.61 eV. Bismuth vapor contains ~ 1% Bi_4 and even less Bi_3. The photoion yield curve of Bi_4^+, with an apparent adiabatic IP of 6.81 eV, also displays three autoionizing bands. An analysis of these bands, and comparison with the other Group V tetramers with T_d symmetry enables one to estimate vertical IP's of 9.0 eV for (a_1^{-1}), 7.5 and 8.9 eV for the spin-orbit split (t_2^{-1}), 7.0 and 7.4 eV for the Jahn-Teller split $(e)^{-1}$.

The photoion yield curve of Bi_3^+ has an adiabatic onset of $\leq$ 6.36 eV, corresponding to formation of Bi_3^+, $X\ ^1A_1$ in D_{3h} symmetry. An increase in slope at ~ 7.4 eV is identified with the configuration... $(1a_2'')\ (2e')^4\ (1e'')$, which may be an E' state. At ~ 8.8 eV, a pronounced increase in slope may indicate a higher excited state, fragmentation of Bi_4, or a near coincidence of the two. The directly or indirectly measured IP's of all Group V trimers are in fairly good agreement with ab initio calculations. The heats of formation of the neutral trimers can be rationalized by a simple model involving transferability of σ and π bond energies from the corresponding dimers and tetramers. The atomization energies of the trimer cations are significantly larger than for the corresponding neutrals, which may be related to the closed shell structure of the cations.

V. Three laws for D_0 (BiF)

BiF has been identified as an interesting candidate for developing a visible chemical laser in the blue-green spectral region. Its usefulness for this purpose is dependent upon its dissociation energy, about which there was considerable dispute. BiF and BiF_2 were prepared by vaporizing a Bi-BiF_3 mixture. Photoion yield curves were obtained, and thence AIP (BiF) = 8.658 ± 0.012 eV, AIP (BiF_2) = 8.05 ± 0.05 eV. The threshold for formation of Bi^+ from BiF occurs at 11.12_6 ± 0.05 eV, from which one deduces D_0 (BiF) ≤ 3.84 ± 0.05 eV. The equilibrium reaction, 2Bi(g) + BiF_3(g) → 3BiF(g), is examined by a second law and a third law treatment. From the second law, D_0 (BiF) = 3.76 ± 0.13 eV, and from the third law, D_0 (BiF) = 3.76 ± 0.13 eV, the latter error estimate allowing for uncertainty in the relative photoionization cross sections. The present results differ substantially from recent inferences placing D_0 (BiF) near 5 eV, and others which hover around 3 eV. From an analysis of the equilibrium reaction, Bi(g) + BiF_2(g) → 2BiF(g), it is concluded that D_0 (FBi-F) = 3.50 ± 0.15 eV, and D_0 (F_2Bi-F) = 4.5_1 ± 0.2 eV.

Future Plans

I. Short term

We plan to complete our studies of SbH_n and Sb. We intend to apply the chemical reaction method to the important combustion intermediates HCO, HO_2 and NCO.

II. Longer Term

We are in the process of assembling a VUV laser system. This apparatus should enable us to achieve still higher resolution in selected wavelength regions, particularly in the 90-105nm, region. Since the VUV laser is pulsed, it is well suited for the study of very short lived transient species, which are more readily generated by pulsed methods.

We also plan to use photoionization methods to prepare state-selected ions for the study of ion-molecule reactions of relevance in combustion and other chemical processes.

Work supported by the U.S. Department of Energy, Office of Basic Energy Sciences, Division of Chemical Sciences, under Contract W-31-109-ENG-38.

Publications of DOE Sponsored Research (1991-93)

Partial Cross Sections in the Photoionization of Open-Shell Atoms: Photoelectron Spectroscopy of Te. G. L. Goodman and J. Berkowitz, J. Chem. Phys. 94, 321-330 (1991).

Photoionization Mass Spectrometric Studies of Free Radicals
J. Berkowitz and B. Ruscic, in "Vacuum Ultraviolet Photoionization and Photodissociation of Molecules and Clusters", C.-Y. Ng, Ed., World Scientific, New Jersey (1991), p. 1-41

Photoionization Mass Spectrometric Study of Si_2H_6.
B. Ruscic and J. Berkowitz, J. Chem. Phys. 95, 2407-2415 (1991)

Photoionization Mass Spectrometric Studies of the Transient Species Si_2H_n (n= 2-5). B. Ruscic and J. Berkowitz, J. Chem. Phys. 95, 2416-2432 (1991)

Photoionization Mass Spectrometric Study of N_2H_2 and N_2H_3: N-H, N=N Bond Energies and Photon Affinity of N_2. B. Ruscic and J. Berkowitz, J. Chem. Phys. 95, 4378-4884 (1991)

Photoionization Mass Spectrometric Studies of the Isomeric Transient Species CD_2OH and CD_3O. B. Ruscic and J. Berkowitz, J. Chem. Phys. 95, 4033-4039 (1991)

Photoionization Mass Spectrometric Study of CH_3OF. B. Ruscic, E. H. Appleman and J. Berkowitz, J. Chem. Phys. 95, 7957-7961 (1991)

Vacuum Ultraviolet Photoionization Mass Spectrometric Study of C_{60} R. K. Yoo, B. Ruscic and J. Berkowitz, J. Chem. Phys. 96, 911-918 (1992)

Photoionization of As_2 and As_4: Implications for Group V Clusters R. K. Yoo, B. Ruscic and J. Berkowitz, J. Chem. Phys. 96, 6696-6709 (1992)

On s-like Window Resonances in Some Atoms and Homonuclear Diatomic Molecules J. Berkowitz, B. Ruscic and R. K. Yoo, Comments on Atomic and Molecular Physics 28, 95-121 (1992)

Three Laws for D_0 (BiF) R. K. Yoo, B. Ruscic and J. Berkowitz, Chem. Phys. 166, 215-227 (1992)

Photoionization Mas Spectrometric Studies of the Transient Species CH_2SH and CH_3S B. Ruscic and J. Berkowitz, J. Chem. Phys. 97, 1818-1823 (1992)

Photoionization Mass Spectrometry of CH_2S and HCS. B. Ruscic and J. Berkowitz, J. Chem. Phys. 98, 2568-2579 (1993)

Photoionization of Group V Trimers and Tetramers R. K. Yoo, B. Ruscic and J. Berkowitz, J. Electron Spectr. (accepted)

"Valence Ionization Processes in the VUV Region", J. Berkowitz, E. Rühl and H. Baumgärtel, Chapter for book entitled "VUV and Soft X-Ray Photoionization Studies", ed. by U. Becker and D. A. Shirley, in the Series "Physics of Atoms and Molecules",. (submitted)

"Photoion-Pair Formation", J. Berkowitz, Chapter for book entitled "VUV and Soft X-Ray Photoionization Studies", ed. by U. Becker and D. A. Shirley (submitted)

Three Methods to Measure RH Bond Bond Energies J. Berkowitz, G. B. Ellison and D. Gutman, Annual Revs. of Physical Chemistry (submitted)

Energy Partitioning in Elementary Chemical Processes

Richard Bersohn
Department of Chemistry
Columbia University
New York, NY 10027

In the past year research has centered on the decomposition of hot molecules, the reaction of ethynyl radicals with hydrogen molecules and the reaction of oxygen atoms with acetylene.

Decomposition of Hot Molecules

Our hot molecules are prepared by electronic excitation followed by rapid internal conversion and internal vibrational redistribution. Previous studies have been on the release of a hydrogen atom from the methyl group of methyl substituted benzenes and pyrazines and from the methylene group of cyclopentadiene and indene (benzocyclopentadiene). To interpret the results we postulate a vibrational temperature T_V which is the solution of the equation

$$h\nu + \sum_i \hbar\omega_i\{\exp(\hbar\omega_i/kT) - 1\}^{-1} = \sum_i \hbar\omega_i\{\exp(\hbar\omega_i/kT_V) - 1\}^{-1} \qquad (1)$$

In this equation ω_i are the vibrational frequencies, T is the initial temperature before absorption and $h\nu$ is the photon energy. The rate constants for release of a hydrogen atom fit equations of the form $k = A\exp(-E/kT_V)$ where E is the bond dissociation energy. The fluorescence excitation spectra of the released hydrogen atoms has a Gaussian shape from which a translational temperature, T_T can be extracted. The big surprise is that $T_T = T_V$ within about 10% for all systems measured. We have experimented with two new systems $C_6F_5CH_3$ (at the suggestion of J. Barker) and bisbenzene chromium. The vibrational temperature and dissociation rates of these two molecules and toluene are given in the following table.

Molecule	Photon Wavelength(nm)	$k(s^{-1})$	$T_V(K)$
toluene	193.3	3.1×10^6	2773
pentafluorotoluene	193.3	1.0×10^6	2565
bisbenzene chromium	279.0	0.7×10^6	1511
bisbenzene chromium	248.4	4.2×10^6	1621

Figs 1 and 2 on the next page show the rise and fall of H and Cr atom concentration. The fall reflects the fact that the atoms, once formed can migrate out of the beam of the probe laser. The pentafluorotoluene has a lower vibrational temperature for the same total internal energy than toluene because its vibration frequencies are softer and therefore the total energy is spread over more modes. Because of the lower temperature dissociation is slower. The two curves of Cr atom LIF signal vs. time show that the shorter the wavelength the faster is the dissociation. This latter molecule will be studied over a wider range of energies.

Reaction of Ethynyl Radicals with Hydrogen Molecules

The reactions

$C_2H + H_2 \rightarrow C_2H_2 + H$ $\quad H = -27$ kcal/mol (2)

$F + H_2 \rightarrow HF + H$ $\quad H = -33$ kcal/mol (3)

are remarkably parallel. C_2H is isoelectronic with the pseudohalogen CN and might therefore also be considered a pseudohalogen. The rate coefficients and energy disposal are given in the table below.

Reaction	$k(cm^3 molecule^{-1} s^{-1}$	$<E_T>$(kcal/mol)	$<f_T>$
$HCC + D_2$	$(2.3\pm0.4)\times10^{-11}$	7.8 ± 1.0	0.29
$DCC + H_2$	$(3.2\pm0.5)\times10^{-11}$	7.6 ± 0.7	0.28
$F + H_2$	2.6×10^{-11}[a]	12.9 ± 1.9[b]	0.37

a W.B.DeMore *et al.*, Jet Propulsion Laboratory Report 87-41, 1987
b S.Tasaki and R.Bersohn, unpublished work

These rate coefficients are two orders of magnitude faster than rate constants measured for thermalized ethynyl radicals. The nascent radicals, products of the photodissociation of either C_2D_2 or C_2H_2 may be more reactive because they are in excited vibrational states well mixed with the $A\ ^2\Pi$ state. Note that the majority of the exoergicity is released as internal energy in all three reactions.

Reaction of O atoms with Acetylene

Our effort is to find the effect of vibrational excitation on the branching ratio between the two exit channels, $CH_2 + CO$ and $H + HCCO$. By photodissociating NO_2 in the presence of an equimolar mixture of C_2H_2 and C_2D_2 we have found out that the yield of H atoms from C_2H_2 and D atoms from C_2D_2 is exactly the same. Apparatus is still under construction.

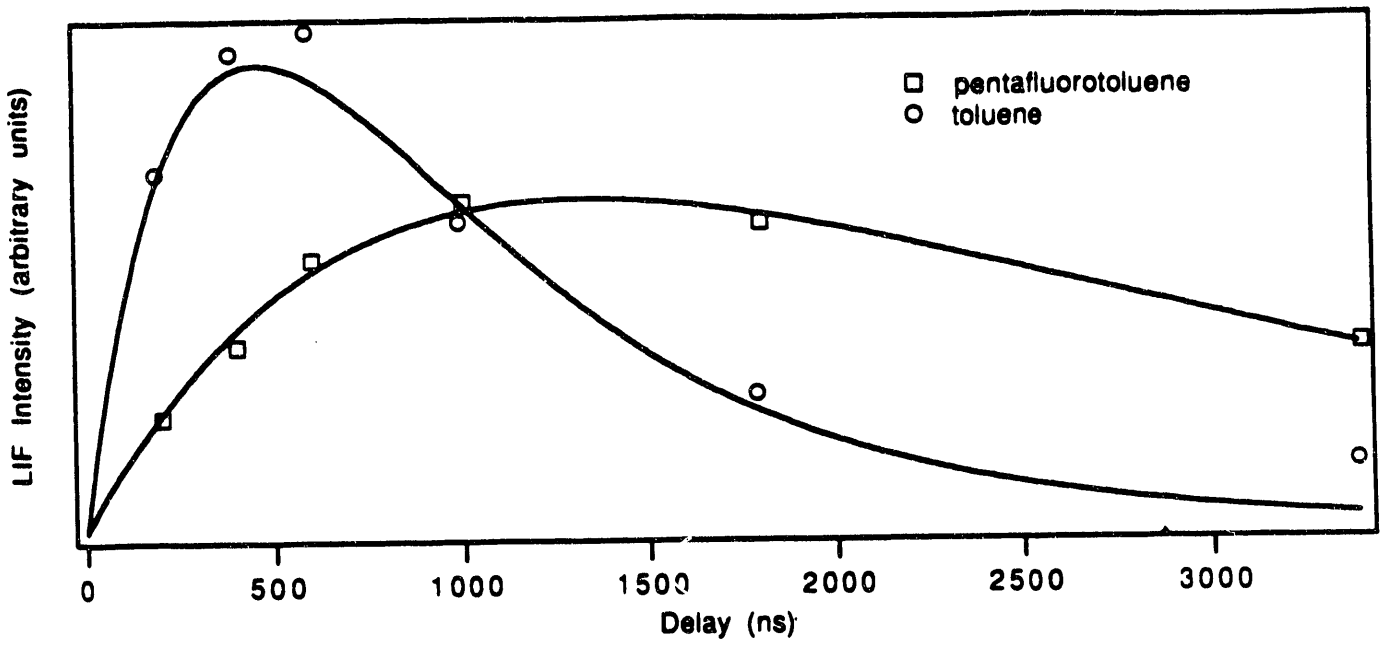

FIG. 1. Growth curves of H-atom signals from toluene and pentafluorotulene photolyzed at 193 nm.

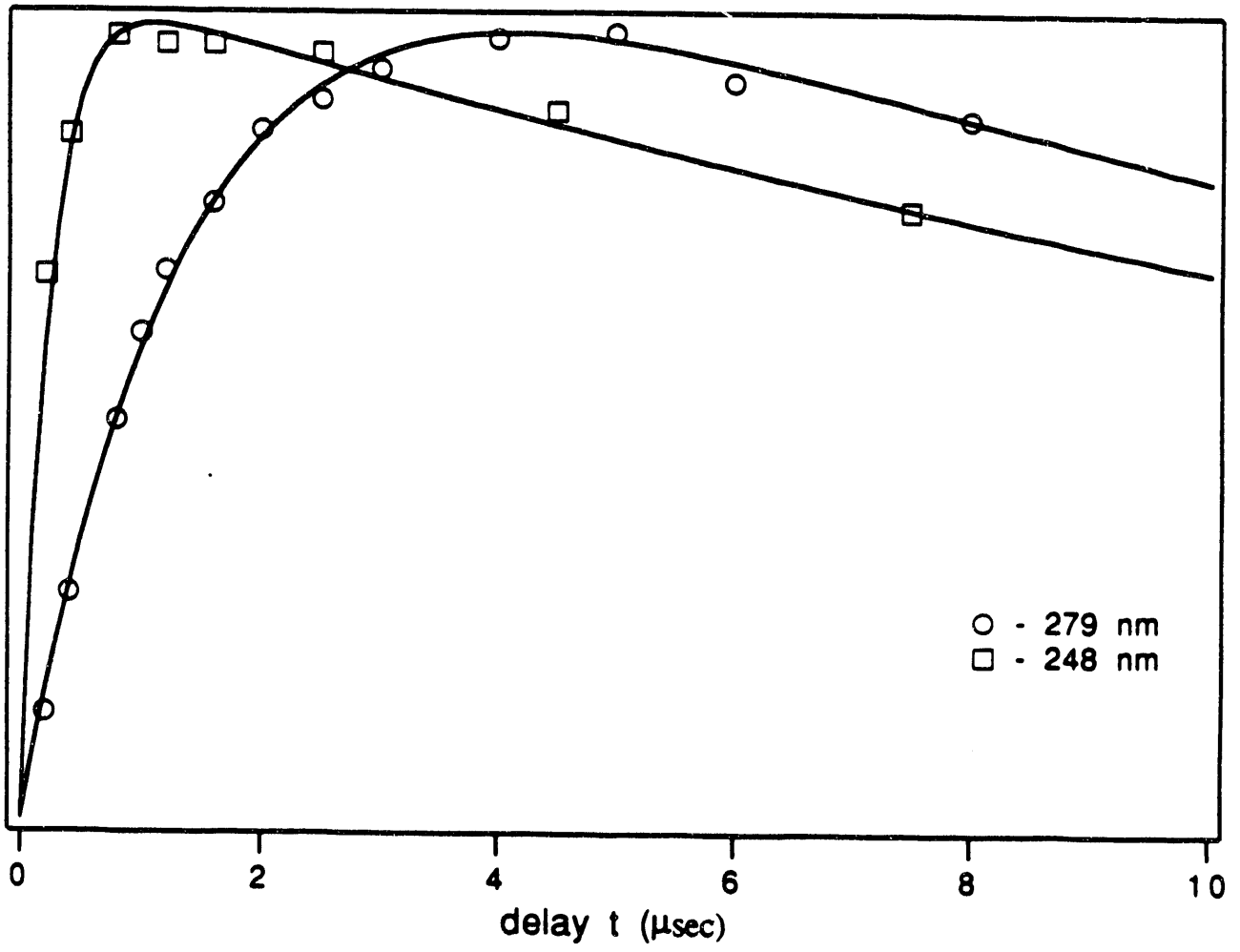

FIG. 2. Growth curves of Cr atom LIF signals from photodissociated $C_{12}H_{12}Cr$

Publications on Research Supported by the DOE in 1991-93

1. Unimolecular dissociation of cyclopentadiene and indene with W.Yi and A.Chattopadhyay, J.Chem.Phys. 94,5984(1991)
2. The photodissociation of acetylene with S.Satyapal, J.Phys.Chem. 95,8004(1991)
3. Temperatures of Fragments in Unimolecular Dissociations, chapter in Mode Selective Chemistry, J.Jortner et al. (eds.), Kluwer Academic Publishers, 1991
4. with A.Penner, A.Danon, E.W.Kuipers, S.Dagan, A.Amirav in H.Werner et al. Selective Reactions of Metal Activated Molecules,Vieweg,Braunschweig,1992,p.105
5. Reaction of Two-Photon-Excited Xenon and Krypton Atoms with Hydrogen Molecules with M.Kawasaki, Y.Matsumi, A.Chattopadhyay, N.Shafer, S.Satyapal, S.Tasaki, W.Yi, J.Phys.Chem. 96,7010(1992)
6. with B.Katz in J. A. Kaye, Isotope Effects in Gas-Phase Chemistry, ACS Symposium Series 502, 1992
7. Photodissociation of Chloroaromatic Compounds: Cl/Cl^* Ratios with S.Satyapal and S.Tasaki, Chem.Phys.Lett. 203,349(1993)
8. Dynamics of Photoionization and Photodissociation of Bisbenzene Chromium with A.Penner, A.Amirav and S.Tasaki J.Chem.Phys. in press

Theoretical Studies of Combustion Dynamics

Joel M. Bowman
Department of Chemistry
Emory University
Atlanta, GA 30322

The basic objectives of this program are to develop and apply theoretical techniques to fundamental dynamical processes of importance in gas-phase combustion. There are two major areas currently supported by this grant. One is reactive scattering of diatom-diatom systems, and the other is the dynamics of complex formation and decay based on L^2 methods. In all of these studies we focus on systems that are of interest experimentally, and for which potential energy surfaces based, at least in part, on *ab initio* calculations are available.

We extended our adiabatic/bend reduced dimensionality quantum theory to a calculation of mode selectivity in the reactions $H_2O(v_s v_b v_a) + H \rightleftharpoons OH(v) + H_2(v')$ $HOD(v_{OD} v_b v_{OH}) + H \rightleftharpoons OH(v) + HD(v')$, $OD(v)+H_2(v')$.These reactions in the forward directions have been recently studied experimentally by several groups.[1-3] In the case of the reaction with HOD striking mode specificity with respect to the product branching ratio was seen. We found similar specificity in our calculations of reaction probabilities for zero total angular momentum,[4] and more recently for rotationally averaged cross sections.[5] Selected results from these calculations are shown below. First, we plot the cross section for the reaction H+HOD(000) versus the total energy. As seen there is a slight preference to form OD over the OH.

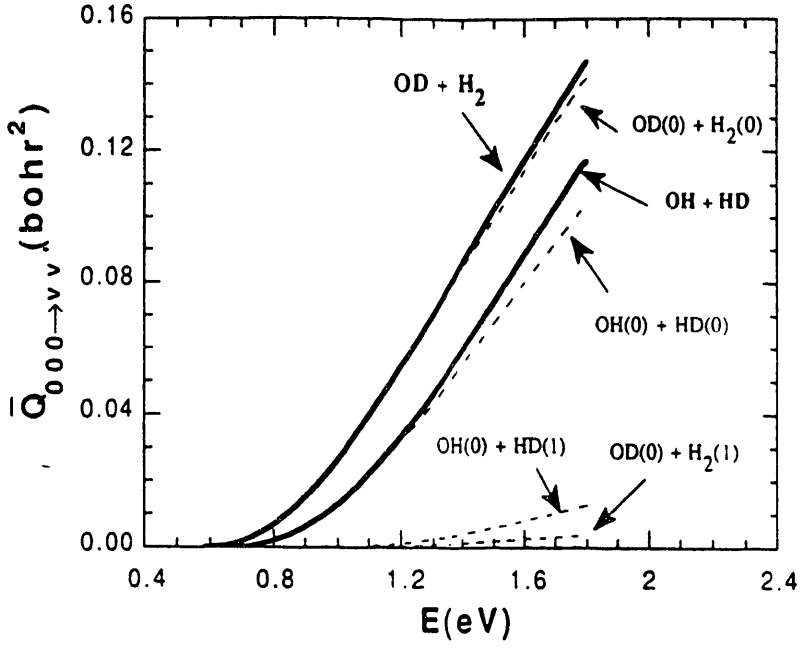

Fig. 1 Vibrational state-to-state, rotationally averaged cross sections for H + HOD(000) as a function of the total energy, measured with respect to the energy of non-rotating HOD(000). The solid curve labeled "OD + H_2" is the cross section summed over the vibrational states of OD and H_2. The solid curve labeled "OH + HD" is the cross section summed over the vibrational states of OH and HD.

Next, we plot the cross sections for the reaction with the OD stretch fundamental or the OH stretch fundamental in HOD excited.

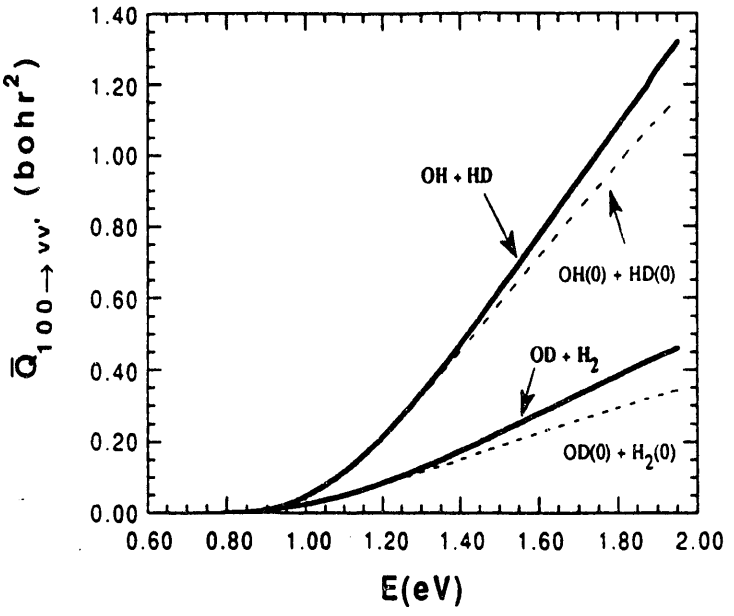

Sme as Fig. 1 but for H + HOD(100).

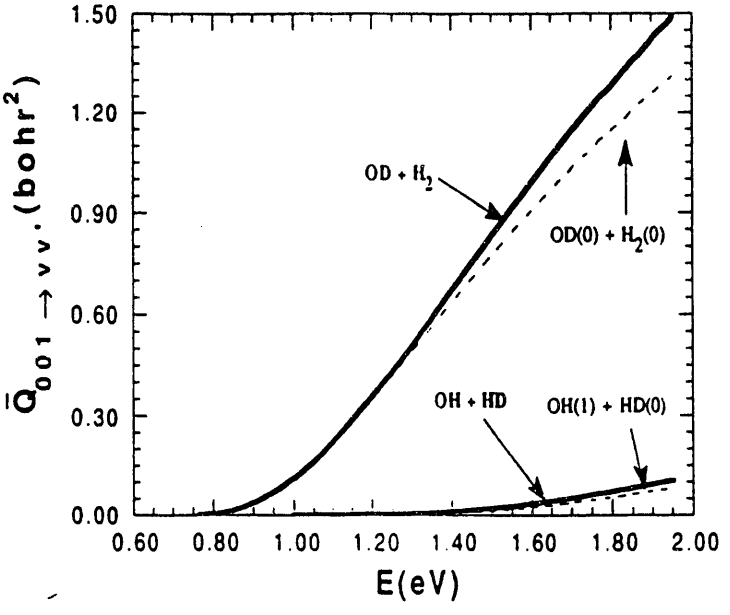

Same as Fig. 1 but for H + HOD(001).

As seen excitation of the OH local mode in HOD leads predominantly to the H_2 +OD products, whereas excitation of the OD local mode in HOD leads predominantly to the HD+OH products. These effects can be understood from the substantial OH (or OD) stretch character of the transition state normal mode corresponding to the imaginary

reaction path frequency. Thus, excitation of the OH (or OD) stretch greatly excites motion along the reaction coordinate.

These results are in a very good qualitative, and good quantitative accord with the experiments of Zare and co-workers.[2] We have also calculated cross sections for HOD(003) and for $H+H_2O$ with high overtones excited, and obtain results which are in very good accord with the experiments of Crim and co-workers.[1]

Our very recent work has focused on a simple Franck-Condon model of the reaction to obtain the rotational distributions of the OH (OD) and H_2 (HD) fragments. The results, although not quantitative, are in suprisingly good qualitative accord with experiment, which show cold rotational distributions.

We are continuing our collaboration with Dr. Al Wagner in comparisons of L^2 and scattering resonances for H+CO. In our most recent work, we found very good agreement for the positions of resonances for J = 1. While we do not find substantial K-asymmetry, we do see significant centrifugal effects, especially for highly excited bend states. We have made modifications of the *ab initio* potential to improve agreement with experiment.

We continue with calculations of all the bound states and also numerous quasibound of HO_2. As part of the overall goal to obtain the lifetimes and branching ratios to form the OH+O and $H+O_2$ products, we have nearly completed a rigorous variational transition state theory of these quantities. This is being done by using an exact density of states (resonances) $\rho(E)$, and a exact determination of the number of states open at the ith variational transition state $N_i^{\ddagger}(E)$, and then determining the microcanonical rate constant for a given product in the usual way, i.e.,

$$k_i(E) = \frac{N_i^{\ddagger}(E)}{2\pi\hbar\rho(E)}, \quad \text{where i = 1 corresponds to } O_2+H \text{ and i = 2 corresponds to OH+O.}$$

Similar calculations are being done for the $C+H_2$ CH_2 reaction, using a new, global *ab initio* potential due to Harding.

References

1. (a) A. Sinha, M. C. Hsiao, and F. F. Crim, J. Chem. Phys. **92**, 6333 (1990); (b) A. Sinha, M. C. Hsiao, and F. F. Crim, J. Chem. Phys. **94**, 4928 (1991); (c) F. F. Crim, M. C. Hsiao, J. L. Scott, A. Sinha and R. L. Vander Wal, Philos. Trans. R. Soc. London Ser. **A 332**, 259 (1990); (d) 5. M. C. Hsiao, A. Sinha and F. F. Crim, J. Phys. Chem. **95**, 8263 (1991).
2. (a) M. J. Bronikowski, W. R. Simpson, B. Girard, and R. N. Zare, J. Chem. Phys. **95**, 8647 (1991); ((b) D. E. Adelman, S. V. Filseth, and R. N. Zare, J. Chem. Phys., in press. c) M. J. Bronikowski, W. R. Simpson and R. N. Zare, J. Phys. Chem., to be published.
3. (a) K. Kessler and K. Kleinermanns, Chem. Phys. Lett. **190**, 145 (1992); (b) A. Jacobs, H. R. Volpp, and J. Wolfrum, Chem. Phys. Lett. **196**, 249 (1992).
4. J.M. Bowman and D-S. Wang, J. Chem. Phys. **96**, 7852 (1992).

PUBLICATIONS SUPPORTED BY THE DOE (1991-present)

A simple method to adjust potential energy surfaces: Application to HCO, J.M. Bowman and B. Gazdy, J. Chem. Phys. **94**, 816 (1991).

On "Effect of Rotational Quantum States (J=0, 1) on the Tunneling Reaction H_2+H " H+H_2 in Parahydrogen Solid at 4.2 K", J.M. Bowman, J. Phys. Chem. **95**, 4921 (1991).

Theoretical stabilization and scattering studies of resonances in the addition reaction H + CO ⇌ HCO, B. Gazdy, J.M. Bowman, S-W. Cho, and A.F. Wagner, J. Chem. Phys. **94**, 4192 (1991).

An L^2 stabilization study of bound states and resonances in HCO, B. Gazdy and J.M. Bowman, in Adv. Molec. Vibs. and Coll. Dynamics, eds. J.M. Bowman and M.A. Ratner, (JAI, Greenwich, 1991), pp. 105-137.

"Feature Article": Reduced dimensionality theory of quantum reactive scattering, J.M. Bowman, J. Phys. Chem. **95**, 4960 (1991).

Vibrational energies and wavefunctions of high energy localized and floppy states of HO_2, J. M. Bowman, Chem. Phys. Lett. **180**, 249 (1991).

The addition and dissociation reaction H + CO ⇌ HCO. 3. Implementation of isolated resonance RRKM theory with exact quantum studies for J=0, S-W. Cho, A.F. Wagner, B. Gazdy, and J.M. Bowman, J. Phys. Chem. **95**, 9897 (1991).

Time dependence of OH overtone relaxation in the hydroperoxyl radical, D. Chapman, J.M. Bowman, and B. Gazdy, J. Chem. Phys. **96**, 1919 (1992).

Theoretical studies of the reactivity and spectroscopy of H + CO ⇌ HCO. I. Stabilization and scattering studies of resonances for J=0 on the Harding ab initio surface, B. Gazdy, J.M. Bowman, S-W. Cho, and A.F. Wagner, J. Chem. Phys. **96**, 2799 (1992)

Isolated resonance decomposition of a multichannel S-matrix: A test from the scattering of H + CO ⇌ HCO, S-W. Cho, A.F. Wagner, B. Gazdy, and J.M. Bowman, J. Chem. Phys. **96**, 2812 (1992)

Reduced dimensionality quantum calculations of mode specificity in the OH+H_2 → H_2O reaction, D-S. Wang, and J.M. Bowman, J. Chem. Phys. **96** 8906 (1992).

Mode selectivity in reactions of H with HOD(100), HOD(001) and HOD(002), J.M. Bowman and D-S. Wang, J. Chem. Phys. **96**, 7852 (1992).

Variational calculations of bound and quasibound states of HCO(J=0 and 1) and comparison with experiment, J.M. Bowman and B. Gazdy, Chem. Phys. Lett. **200**, 311 (1992).

Quantum calculations of mode specificity in reactions of H with HOD and H_2O, D.Wang and J.M. Bowman, J. Chem. Phys. **98**, xxxx (1993).

An adiabatic-bend-Franck-Condon model for rotational distributions in the reaction H+H_2O and H+D_2O, D.Wang and J.M. Bowman, Chem. Phys. Lett., in press.

Combustion Chemistry

Nancy J. Brown
Lawrence Berkeley Laboratory, Berkeley , California 94720

Our research is concerned with the development and use of sensitivity analysis tools to probe the response of dependent variables to model input variables. Sensitivity analysis is important at all levels of combustion modeling. Our research in this area continues to be focused on elucidating the interrelationship between features in the underlying potential energy surface (obtained from ab initio quantum chemistry calculations) and their responses in the quantum dynamics, e.g., reactive transition probabilities, cross sections, and thermal rate coefficients. The goals of this research are: (i) to provide feedback information to quantum chemists in their potential surface refinement efforts, and (ii) to gain a better understanding of how various regions in the potential influence the dynamics. These investigations are carried out with the methodology of quantum functional sensitivity analysis (QFSA).

This past year, we have concluded the development of the QFSA techniques using the log-derivative Kohn variational method for scattering, and applied it to the collinear H + H_2 exchange reaction. Three papers have been published that describe this research. One paper was concerned with the development of a general description for calculating sensitivity coefficients independent of the scattering formalism employed in the calculations. Another described a methodology for predicting observables on a new or perturbed potential energy surface without re-calculating the dynamics. The third examined the sensitivity of the thermal rate coefficient to structure in the potential energy surface.

We have begun to investigate the same reaction in 3-D. The goal of this study is to use QFSA to investigate the H + H_2 reaction and its isotopic analogs to determine the level of chemical accuracy required in the PES to duplicate experimental results. This is important because the H_3 system plays a fundamental role in developing theories of chemical reactivity. Our initial effort has been concerned with collisions with the total angular momentum restricted to zero. Several regions of configuration space where the dynamics are highly sensitive to inaccuracies in the potential have been identified. These regions of importance vary with collision energy, but do not change dramatically as the previously studied collinear case. Near the reaction threshold, the dynamics are most sensitive to the saddle point region as expected. At higher energies ($\approx$1.0 to 1.5 eV), the inner core of the potential, where the dynamics "cuts the corner" in going from reactant to product arrangements, is most important for collinear geometries , and the outer corner, where the H_3 conformation is more compact than the transition state conformation, is most important for bent geometries. Surprisingly, the region of the potential traversed by the minimum energy path across the saddle point region has rather insignificant

sensitivities at these higher energies. There is an extraordinary amount of data generated in a 3-D sensitivity analysis of reactive scattering. We are currently using advanced visualization techniques for analysis.

Combustion modeling research is being performed to develop robust models of pollutant formation and destruction to use as design tools for future generation combustors. Our current modeling efforts have been in three areas: 1)examining the suitability of using isocyanic acid (HNCO) to reduce NO in the exhaust of engines burning natural gas; 2) modeling nitrogen chemistry in combustion involving premixed laminar flames burning natural gas that are in contact with a reactive heat transfer surface; and 3)adding chemistry to models of turbulent reacting flow.

A modeling study of the reduction of NOx by HNCO in exhausts typical of natural gas combustion in the presence of radical boosters (fuel) has been completed. Variables considered were the initial concentrations of NO, NO_2, CO, O_2, CH_4 , H_2, and HNCO as well as initial temperature. The NO reduction chemistry must be preceded by thermal ignition chemistry which generates radicals. The lowest temperature for which ignition occurs is the optimum temperature for reduction and defines the beginning of the temperature window. Reduction was not achieved for the "natural gas exhaust" for a reasonable residence time. Additional H_2 added to the exhaust mixture enhanced reduction, but the addition of CO and CH_4 did not.

Under some conditions the computed sensitivity coefficient for nitrogen species and temperature exhibited self-similarity (scaling). Self similarity occurs in dynamical systems where one or at most a few dependent variables dominate the physical behavior of the system. Four reaction paths were identified which controlled the fate of the NO: the conversion of NO to NO_2 via HO_2, the conversion of NO_2 to NO via reaction with H or O, the reduction of NO via NCO, and the reduction of NO from reactions with NH_i species. The relative importance of the four was determined by the initial conditions.

In order to predict pollutant formation and destruction in combustion systems with turbulent flow fields, the coupling between reactive and diffusive processes must be described properly. While fluid-mechanical turbulence models and detailed chemistry flame models are solvable on standard vector super computers, the combination of turbulent flow and detailed chemistry in the same model requires the next-generation of super computer: the massively parallel machine. With colleagues at Sandia National Laboratory, we have begun to use parallel computing to model pollutant formation in a H_2/Air turbulent diffusion flame. We have used a Probability Distribution Function (PDF) model that primarily involves Monte Carlo calculations and is thus highly amenable to efficient parallel implementation. The model was first implemented on a distributed network of 25 IBM RS6000 workstations. With our computer science colleagues at LBL and SNL, we have designed a new Parallel Object Oriented Environ-

ment and Toolkit (POET) whose purpose is to provide the user with a transparent link to the power of parallel distributed computing. POET is a high level object oriented framework that isolates the description of the physical model from the code that implements the parallel algorithm and flow. We are continuing to develop the toolkit and increase the level of detail in the chemical description of the flame. We are currently modeling a H_2/Air flame to determine NO concentrations using reduced schemes for the chemical mechanism. Principal component analysis is being used to obtain reduced mechanisms. Model/model and model/experiment comparisons are being made.

Publications

Brown, N.J., (1991), "Rate Coefficient Calculations for Combustion Modeling." Progress in Astronautics and Aeronautics 135, 37. Also LBL Report No. 27129.

Chang, J., Brown, N.J., D'Mello, M.D., Wyatt, R.E., and Rabitz, H., (1992), "Quantum Functional Sensitivity Analysis for the Collinear H + H_2 Reaction Rate Coefficient," J. Chem. Phys. 96, 3523-3530 Also LBL Report No. 31387.

Chang, J., Brown, N.J., and Rabitz, H. (1992), "Construction of Classical Sensitivity Maps for Rotationally Inelastic Collisions of H_2 with HD," J. Phys. Chem.96, 6890-6903. Also LBL Report No. 31750.

Chang, J., Brown, N.J., D'Mello, M.D., Wyatt, R.E., and Rabitz, H., (1992), "Quantum Functional Sensitivity Analysis within the Log-derivative Kohn Variational Method for Reactive Scattering," J. Chem. Phys.97, 6226-6239 Also LBL Report No. 32372

Chang, J., Brown, N.J., D'Mello, M.D., Wyatt, R.E., and Rabitz, H., (1992), "Predicting Observables on Different Potential energy Surfaces using Feature Sensitivity Analysis: Application to the Collinear H + H_2 Exchange Reaction," J. Chem. Phys. 97, 6240-6248. Also LBL Report No. 32373

Brown, N.J., and Garay, J., (1992). "Production of N_2O from the Reduction of NOx by HNCO." Extended Abstract for 5th International N_2O Workshop, Tsukuba, Japan.

Brown, N.J., and Garay, J., (1992). "The Reduction of NOx by HNCO." Western States Section/The Combustion Institute Paper 92-95. Also LBL Report No. 32950.

Koszykowski, M.L., Armstrong, R., Cline, R.E., Macfarlane, J., Brown, N.J., and Chen, J.Y., (1993). "The Advanced Combustion Modeling Environment (ACME)," 61-70, Computing at the Leading Edge: Research in the Energy Sciences, UCRL-TB-111084.

Chang, J. and Brown, N.J., (1993), "Quantum Functional Sensitivity Analysis for the 3-D (J=0) H + H_2 Reaction," Accepted for Publication in the Int. J. Quantum Chemistry.

Bond Selective Chemistry Beyond the Adiabatic Approximation

Principal Investigator: Laurie J. Butler
The James Franck Institute
The University of Chicago
5640 South Ellis Avenue
Chicago, IL 60637

I. Program Scope

One of the most important challenges in chemistry is to develop predictive ability for the branching between energetically allowed chemical reaction pathways. Such predictive capability, coupled with a fundamental understanding of the important molecular interactions, is essential to the development and utilization of new fuels and the design of efficient combustion processes. Existing transition state and exact quantum theories successfully predict the branching between available product channels for systems in which each reaction coordinate can be adequately described by different paths along a single adiabatic potential energy surface. In particular, unimolecular dissociation following thermal, infrared multiphoton, or overtone excitation in the ground state yields a branching between energetically allowed product channels which can be successfully predicted by the application of statistical theories, *i.e.* the weakest bond breaks. (The predictions are particularly good for competing reactions in which when there is no saddle point along the reaction coordinates, as in simple bond fission reactions.) The predicted lack of bond selectivity results from the assumption of rapid internal vibrational energy redistribution and the implicit use of a single adiabatic Born-Oppenheimer potential energy surface for the reaction. However, the adiabatic approximation is not valid for the reaction of a wide variety of energetic materials and organic fuels; coupling between the electronic states of the reacting species plays a key role in determining the selectivity of the chemical reactions induced. The work described below begun in the first year of our DOE funding investigates the central role played by coupling between electronic states in polyatomic molecules in determining the selective branching between energetically allowed fragmentation pathways in two key systems

II. Recent Progress

A. Selective C-Br bond fission in 1,3-bromoiodopropane: The intramolecular distance dependence of coupling between electronic configurations

The first experiments initiated this year under DOE funding used a state-of-the-art crossed laser-molecular beam apparatus to measure the branching between primary C-Br and C-I fission in 1,3-bromoiodopropane excited at 222 nm in the np(Br) -> σ^*(C-Br) absorption band. The photoexcitation promotes the molecule to an electronic state that has $(np_{Br})^1(\sigma^*_{C\text{-}Br})^1$ character in the Franck-Condon region, but is actually adiabatically bound because of an avoided electronic crossing with an $(np_I)^1(\sigma^*_{C\text{-}I})^1$ electronic configuration at stretched C-Br bond distances. If the two electronic configurations are strongly coupled at the avoided crossing the Born-Oppenheimer approximation will hold and the molecule would not dissociate at all. Conversely, if the off-diagonal potential coupling is very weak the adiabatic approximation will fail dramatically and the molecule will retain the np(Br) -> σ^*(C-Br) configuration through the avoided crossing and break selectively at the stronger C-Br bond, leaving the weaker C-I bond intact. For intermediate couplings between the two electronic configurations, the branching ratio between C-Br and C-I fission (resulting from crossing to the diabatic surface repulsive in the C-I bond) will evidence a reduction in branching to C-Br fission as the off-diagonal potential coupling increases. The experiments on 1,3-bromoiodopropane were proposed to test the distance and orientation dependence of this off-diagonal potential coupling that

inhibits the selective fission of the C-Br bond. In particular, the data provides a critical comparison with the branching previously observed by Y. T. Lee and coworkers for 1,2-C_2F_4BrI, which evidenced a 1:2 C-Br:C-I branching ratio upon excitation at 193 nm in the np(Br) -> σ^*(C-Br) absorption band.

The first experimental results this year showed that 1,3-bromoiodopropane does indeed cleave preferentially at the C-Br bond upon excitation at 222 nm. We measured the photofragment time-of-arrival spectra at m/e$^+$ = 79 (Br^+) and 127, (I^+) and at 42, ($C_3H_6^+$). (No significant signal at the parent ion of the C_3H_6I and C_3H_6Br photofragments were observable). The forward-convolution fit of the time-of-arrival spectra determined the distribution of energies imparted to relative product translation for each bond fission pathway; both distributions peaked at kinetic energies above 10 kcal/mole in translation as expected for dissociation on regions of surfaces which are repulsive in the bond that breaks. Integration of the signal at Br^+ and I^+ fit to the I atom and Br atom products yielded, after correction for ionization cross section and kinematic factors, a C-Br:C-I bond fission branching ratio of 1.47 to 1. This shows that in 1,3-bromoiodopropane, selective fission of the C-Br bond on the repulsive $(np_{Br})^1(\sigma^*_{C\text{-}Br})^1$ diabat, due to a dramatic failure of the Born-Oppenheimer approximation, dominates C-I fission. The experiments tested the hypothesis presented in our proposal to DOE that the increased distance between the orbitals on the C-Br chromophore from the C-I electronic orbitals would decrease the off-diagonal potential coupling matrix element between the two repulsive electronic configuration in 1,3-bromoiodopropane (with three CH_2 spacers between the atoms), and thus allow C-Br fission to dominate. Indeed, the results showed that the branching to C-Br fission was much more selective than that observed in 1,2-C_2F_4BrI (with two CF_2 spacers between the atoms). In order to test the intramolecular orientation dependence of the coupling, we need to analyze the angular distribution of the photofragments; this work is planned in the second year of the funding period.

In addition to the data on 1,3-bromoiodopropane, we also measured the time-of-flight spectra of the I and Br atom products from the photodissociation of IBr at 222 nm. We initiated this work to allow us to directly measure the relative ionization cross sections of I atoms and Br atoms in our apparatus to allow a better determination of the absolute C-Br:C-I bond fission branching ratios in 1,3-bromoiodopropane. (Mass-spectrometric determination of these branching ratios have traditionally relied on a semiempirical relationship which uses the atomic polarizability to estimate the ionization cross sections). Our data both accomplished this purpose and showed that the dissociation of IBr at 222 nm results exclusively in spin-orbit excited Br and I atom products. Photofragmentation upon excitation to the electronic state reached at 222 nm had not been previously measured, but we identified the analogous electronic state in I_2, which correlates to an asymptotic limit where both fragments are spin-orbit excited.

B. Testing adiabatic predictions for the C-S:S-H bond fission branching in CH_3SH

Our major theoretical progress in first year of the project focused on methyl mercaptan (CH_3SH), one of the major gaseous organosulfur pollutants produced in the combustion of oils and coals, a system which evidences preferential fission of the S-H bond over the weaker C-S bond upon photoexcitation in its first two ultraviolet absorption bands. Unlike other bond-selective processes which may be simply understood as the result of direct dissociation on a repulsive portion of a potential energy surface, the adiabatic excited electronic potential energy surface reached in the first absorption band has some Rydberg character in the Franck-Condon region and has two repulsive exit channels, one leading to S-H bond fission and one leading to C-S bond fission. Our first goal is to generate a theoretical prediction for the branching ratio between C-S and S-H bond fission upon excitation at a wide range of energies across the first absorption band, then measure the branching ratio in the lab. The work tests whether the observed

branching between bond fission pathways can be predicted within an adiabatic picture or whether the nonadiabatic coupling to the upper potential energy surface alters the dynamics and subsequent branching.

To accomplish the theoretical portion of the project, we have initiated two key collaborations, one with Prof. Karl Freed's group and one with Prof. John Light, also a DOE investigator. To generate a reliable theoretical prediction within the adiabatic approximation, we needed to calculate the lowest excited adiabatic electronic potential energy surface reached in the first absorption band. To accurately calculate excited electronic potential energy surfaces strikes fear in the heart of even the best *ab initio* electronic structure theorists, but using the effective valence shell Hamiltonian method developed by Freed and coworkers, my students have calculated several cross-sectional cuts along the ground and first two excited potential energy surfaces of methyl mercaptan. We are presently fitting an analytic potential function to these *ab initio* points to use in the collaborative exact scattering dynamics calculations.

Our primary experimental work on methyl mercaptan this year developed a method to vibrationally excite CH_3SH to several different vibrational levels in the ground electronic state prior to photoexcitation to the dissociative potential energy surface. We expect photodissociating vibrationally excited CH_3SH could alter the branching between S-H and C-S bond fission significantly, as the branching is controlled by the Franck-Condon overlap of the ground state vibrational wavefunction with the scattering wavefunctions in the C-S and S-H exit channels respectively. We needed to be able to excite not only the easily accessible C-H and S-H stretches, but also the C-S fundamental, the latter to enhance the branching to C-S bond fission. At only 700 cm^{-1}, the C-S stretching fundamental cannot be populated significantly with available tunable pulsed infrared lasers (for example, it is outside the tuning range of an optical parametric oscillator, and difference frequency lasers cannot provide enough population transfer), so we sought to populate this vibrational level with a stimulated Raman scheme. Using two laser beams, 532 nm from our Nd:Yag pump laser and the tunable output of our dye laser near 553 nm, we showed we could populate the C-S stretching fundamental by measuring a photoacoustic spectrum of the band. We also obtained photoacoustic spectra of the S-H, CH_3 symmetric stretch, and CH_3 asymmetric stretch fundamentals. If the ongoing theoretical calculations predict a marked change in the branching between the two dissociation channels upon photodissociating a molecule vibrationally excited in one of these modes, we can test the prediction experimentally using stimulated Raman to populate these vibrations in the parent molecule in the molecular beam.

C. Competition between bond fission channels and H_2 elimination in CH_3NH_2

The final project pursued in the first year of DOE support investigates the branching between energetically allowed photodissociation channels of CH_3NH_2 excited at 222 nm in the $n_N \rightarrow 3s$ absorption band. The work was motivated by a calculation of the first excited A" potential energy surface which showed that dissociation in the N-H and C-N coordinates occurs over barriers formed from avoided electronic crossings in each. Our experiments this year on this system measured the photofragment time-of-flight spectra in our crossed laser-molecular beam apparatus at several fragment masses. The data shows that at 222 nm four fragmentation pathways compete, N-H, C-H, and C-N bond fission and H_2 concerted elimination. Because this work on CH_3NH_2 was not proposed in our original grant application, the continuation of this work under DOE funding depends on DOE's interest and the availability of other funding sources.

III. Future Plans

The work in the second year of our project focuses on three systems in which the breakdown of the Born-Oppenheimer approximation can alter the expected branching

between chemical bond fission pathways. The following paragraphs detail the planned work on the preferential fission of the S-H bond over the S-C bond in methyl mercaptan, the competition between C-Br and C-I fission in 1,3-iodobromopropane, and the competition between bond fission channels and H_2 elimination in methyl amine.

Our experiments and collaborative calculations on CH_3SH in the coming year are designed to test whether the observed branching between bond fission pathways can be predicted within an adiabatic picture or whether the nonadiabatic coupling to the upper potential energy surface alters the dynamics and subsequent branching. The first crossed laser-molecular beam experiments planned in the second year of the project determine how the branching between S-H and C-S bond fission changes with excitation energy in the 230 nm absorption band. (We expect comparable signal to earlier successful work on this system at 222 nm. Doubling the output of our excimer-pumped dye laser in a BBO crystal can provide tunable high power pulsed light over the entire absorption band of interest.) Within an adiabatic picture, the branching between S-H and C-S bond fission is controlled by the Franck-Condon overlap of the ground vibrational wavefunction with the scattering wavefunctions in the C-S and S-H exit channels respectively at the photon energy used. We wish to compare the result to the predictions of scattering calculations on the adiabatic potential energy surface. Having calculated several crossections of the relevant surfaces using K. Freed's effective valence shell Hamiltonian method in the first year of the project, we can now pursue exact quantum scattering calculations on these surfaces in collaboration with Prof. J. Light, also a DOE investigator, in order to generate an adiabatic prediction for the change in branching ratio with excitation energy. We can also calculate the expected change in branching if a molecule with one quantum of vibrational energy in the C-S stretch or the S-H stretch is photodissociated. If the prediction shows a dramatic effect, we can follow the calculations with a double-resonance experiment, using stimulated Raman to populate these vibrational levels prior to photoexcitation (a population scheme tested in the first year of the project).

In the second year of the project we also plan to complete the experimental work on 1,3-iodobromopropane where excitation to an electronic state locally repulsive in the C-Br bond, but adiabatically bound, results in a competition between C-Br and C-I fission. Having measured the photofragment kinetic energy distributions upon excitation at 222 nm and calibrated the branching with photofragmentation experiments on IBr in the first year, we turn to determination of the angular distribution of photofragments. Measurement of the photofragment angular distributions can determine whether the off-diagonal potential coupling which inhibits the selective fission of the C-Br bond depends on the intramolecular orientation of the two bonds, as the two conformers would evidence different photofragment angular distributions. We expect this system will be ready for publication in the second year; it is most exciting as the selectivity depends on the total failure of the Born-Oppenheimer approximation (within this approximation the molecule would not dissociate at all, the photoexcitation is to an adiabatically bound surface!)

If sufficient resources and time can be allocated to a third project concurrent to the two described above, the final system planned for study in the second year is that of methyl amine. We have determined that upon excitation at 222 nm, four dissociation pathways compete, N-H, C-H, and C-N bond fission and H_2 elimination. As in CH_3SH, the production of fast H atoms dominates, but the excitation in CH_3NH_2 is to a region of a potential energy surface which is bonding in character in the N-H and C-N coordinates, so should be within the realm of the predictive capability of statistical transition state theories. The work planned for the second year includes photofragmentation of CH_3ND_2 to distinguish between the C-H and N-H fission pathways in the CNH_4^+ time-of-flight spectra and measurement of the resonance Raman spectrum excited at 222 nm to elucidate the early time dynamics that results in the diffuse structure in the absorption spectrum.

REACTION PRODUCT IMAGING

David W. Chandler
Sandia National Laboratories
Livermore, CA 94550

Over the past few years we have investigated the photochemistry of small molecules using the photofragment imaging technique[1,2]. Bond energies, spectroscopy of radicals, dissociation dynamics and branching ratios are examples of information obtained by this technique. Along with extending the technique to the study of bimolecular reactions, efforts to make the technique as quantitative as possible have been the focus of the research effort. To this end, we have measured the bond energy of the C-H bond in acetylene, the branching ratio of $I(^2P_{1/2})$ (I*) to $I(^2P_{3/2})$ (I) in the dissociation of HI, the energetics of CH_3Br, CD_3Br, C_2H_5Br and C_2H_5OBr dissociation, and the alignment of the CD_3 fragment from CD_3I photolysis. In an effort to extend the technique to bimolecular reactions, we have studied the reaction of H with HI forming H_2(v=0,1 J) + $I(^2P_{1/2}$ or $^2P_{3/2})$ and the reaction of $H + D_2 \rightarrow D + HD$.

One of the goals in the field of reaction dynamics is to be able to measure the angular distribution of products in a quantum-state-specific manner. As a step in this direction, we have reported the first application of ion imaging to a bimolecular reaction[3]. We study the $H + HI \rightarrow H_2 + I$ reaction in a neat supersonic molecular beam of HI. The supersonic expansion provides a reaction precursor possessing a very narrow thermal velocity distribution. By avoiding a thermally equilibrated HI source (eg. an effusive beam, or bulb), the center-of-mass collision energy spread has been substantially reduced. UV photolysis of HI generates both fast (~2.6 eV) and slow (~1.7 eV) H atoms with a difference in kinetic energy corresponding to the concomitant photolytic production of ground state I ($^2P_{3/2}$) and excited state I* ($^2P_{1/2}$), respectively. Moreover, it is energetically possible to form both ground state and electronically excited iodine atoms as abstraction reaction products along with the H_2. Hence, a total of four possible reaction pathways may be active in this system. The H_2 products are ionized by (2+1) resonance-enhanced multiphoton ionization (REMPI) before being imaged onto a position-sensitive detector. In this way we have measured the laboratory-frame velocity distribution of the state-selected reaction products.

Over the last year images of several quantum states of H_2 have been measured. Figure 1 shows images of v=0,J=17 and v=1,J=11 states along with the reconstructed images which represents the flux of products at a particular angle. The circles represent the three possible velocities of H_2 products obtainable with this experiemnt. The fastest H_2(v,J) detected corresponds to a fast H atom from HI reacting to produce a ground state I atom. The middle ring corresponds to either a fast H reacting to give an I* or a slow H atom reacting to give I. The smallest ring corresponds to slow H atoms reacting to give I* product in the reaction. As you can see for the H_2(v=0,J=17) quantum state no product is formed corresponding to slow H atoms reacting to form I* product but that this channel is clearly evident for the H_2(v=1,J=11) quantum state. One must conclude that either the slow H atoms do not react to form H_2 (v=0,J=17) and the two rings represent fast H atoms producing I and I* products or the slow channel reacts forming both H_2(v=1, J=11) and H_2(v=0, J=17) but the branching ratio in the reaction is very sensitive to the H_2 quantum state formed. These two quantum states differ by about 500 cm^{-1} in energy. The slow channel of the reaction at this photoysis wavelength is about the same energy as the fast channel when the reaction is induced by photolysis at 266 nm. Here the product distribution has been measured and H_2(v=0,J=17) is found to be a very minor product, the most reasonable conclusion is that the reaction produces substantial amounts of I* at both energies. This is the first direct observation of this reaction channel and its presence could help explain some of the discrepancies noted between the measured product internal state distribution and the calculated distributions (which do not take this channel into account).

We have measured[4] the differential cross section for the H + D_2 → HD + D reaction using a technique we call *Reaction Product Imaging* (RPI). In this experiment, a photolytically produced (266-nm photoylsis of HI) beam of H atoms crossed a beam of cold D_2 molecules. Product D-atoms were ionized at the intersection of the two particle beams and accelerated toward a position sensitive detector. The ion images appearing on the detector are two-dimensional projections of the three-dimensional velocity distribution of the D-atom products. The reaction was studied at nominal center-of-mass collision energies of 0.54 eV and 1.29 eV. At the low collision energy the measured differential cross section for D-atom production, summed over all final states of the HD(v, J) product, agrees well with recent quasiclassical trajectory calculations of Aoiz *et al.* while at the higher collision energy the agreement between the theoretical predictions and experimental results is less favorable. Figure 2 shows a schematic ofthe apparatus and Figure 3 the raw data and transformed distribution of D atom velocities from the 1.29eV collision of H + D_2. This work was done in collaboration with Theo Kitsopoulos (SNL), Dr. R. N. Zare (Stanford), Mark Buntine (Stanford), Ruth McKay (Stanford) and David Baldwin (SNL).

1. D.W. Chandler and P.L. Houston, J. Chem. Phys. 87, 1445 (1987).
2. D.P. Baldwin, M.A. Buntine and D.W. Chandler, J. Chem. Phys. 93, 6578 (1990); D.W. Chandler, J.W. Thoman, Jr., M.H.M. Janssen and D.H. Parker, Chem. Phys. Lett. 156, 151 (1989); D.W. Chandler, M.H.M. Janssen, S. Stolte, R.N. Strickland, J.W. Thoman, Jr. and D.H. Parker, J. Phys. Chem. 94, 4839 (1990);
3. M. A. Buntine, David P. Baldwin, Richard N. Zare and David W. Chandler, J. Chem. Phys. 94, 4672 (1991).
4. T. Kitsopoulos, M. A. Buntine, D. P. Baldwin, R. N. Zare and D. W. Chandler, Accepted Science (1993).

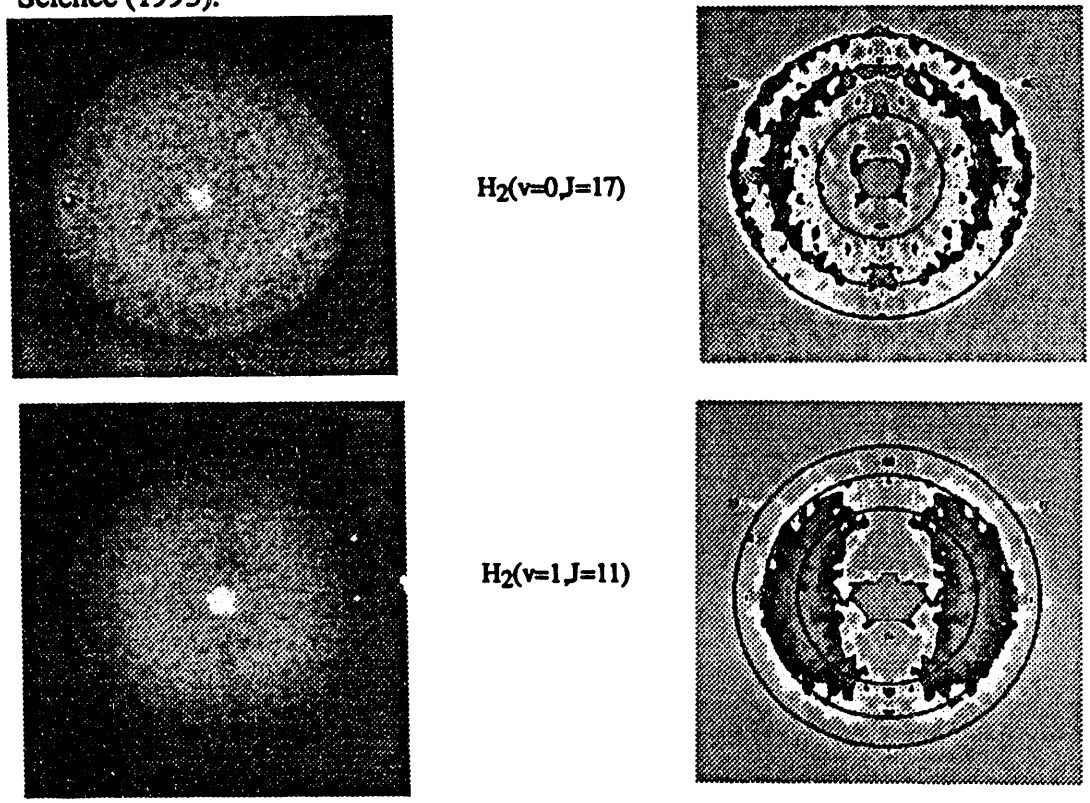

Fig. 1. Raw data and velocity distributions from ion image of H_2 (v=1, J=11) and H2(v=0,J=17) formed in the reaction H + HI → H_2 + I initiated in a beam of neat HI. Fast H atoms are formed by laser photolysis of HI, and the H_2 products are ionized before being projected onto a position-sensitive detector.

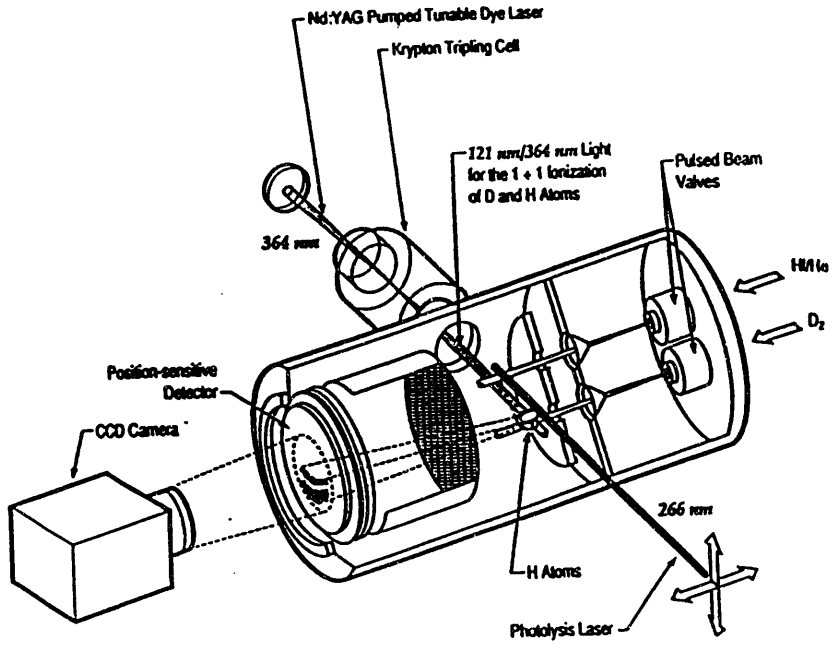

Figure 2. Scematic of apparatus used to obtain image of D atoms from H + D2 reaction.

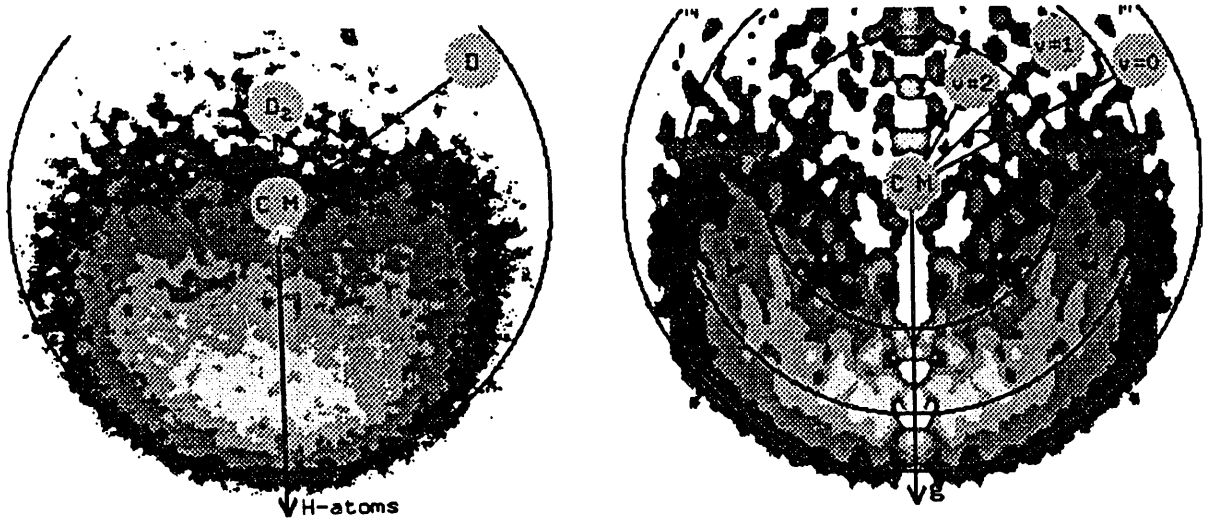

Fig 3. Image and reconstructed image of D atoms produced from the reaction H + D_2 → D + HD at a nominal center-of-mass collision energy of 1.29 eV. The open circles represent the calculated position of the scattered D-atoms corresponding to HD (v=0,1,2,J=0). The direction of the H-atom beam is indicated by the arrow, and the solid circles labeled D2 and CM, respectively.

Future Directions:

We plan on continuing to develop and utilize imaging techniques to study bimolecular reactions. We plan on developing the technique to a point where a single quantum state of a diatomic fragment of an atom-diatom reaction can be imaged. This will initially be done on the H+ D_2 reaction. We intend to extend this study to the system H +O_2 as well as develop sources for O atoms so that O atom reactions can be studied with this technique.

Publication 1991-93

Robin N. Strickland and David W. Chandler, "Reconstruction of Axisymmetric Image from its Blurred and Noisy Projection" Applied Optics **30**, 1811 (1991).

Maurice H. M. Janssen, David H. parker, Greg O. Sitz, Steven Stolte and David W. Chandler, "Rotational Alignment of the CD3 Fragment From the 266-nm Photodissociation of CD3I". J. Phys. Chem. **95**, 8007 (1991).

Mark A. Buntine, David P. Baldwin, R. N. Zare and David W. Chandler, " Application of Ion Imaging to Bimolecular Chemical Reactions: H + HI → H2 + I" J. Chem. Phys. **94**, 4672 (1991).

Wayne P. Hess, John W. Thoman Jr. and David W. Chandler "Photofragment Imaging: The 205-nm Photodissocaition of CH_3Br and CD_3Br" Chem. Phys. **163**, 277 (1992).

G. van den Hoek, J. W. Thoman Jr, D. W. Chandler and S. Stolte, "REMPI Spectroscopy of CF3I in the Bulk and in a Molecular Beam" Chem. Phys. Lett. **188**, 413 1992.

Mark A. Buntine, David P. Baldwin and David W. Chandler, "Photodissociation Dynamics of Doubly Excited States of Molecular Hydrogen" J. Chem. Phys. **96**, 5843 (1992).

Gerard Meijer and David W. Chandler " Degenerate Four Wave Mixing on Weak Transitions in the Gas-Phase Using a Tunable Excimer Laser" Chem. Phys. Lett. **192**, 1 (1992).

Gerard Meijer, Michel Versluis and David W. Chandler "Degenerate Four Wave Mixing Using a Tunable Excimer Laser to Detect Combustion Gases" Accepted to Applied Optics, 1992.

Mark A. Buntine, David W. Chandler and Carl C. Hayden " A two Color Laser-Induced Grating Technique for Gas-Phase Excited-State Spectroscopy" J. Chem. Phys. **97**, 1 (1992).

M. A. Buntine, D. P. Baldwin, R. N. Zare and D. W. Chandler "I/I* Branching Ratio for the Reaction H + HI = H_2(v=1, J=11)+ I/I* at 2.63 and 1.70 ev Collision Energies" Submitted to J. Chem. Phys. 1992.

T. A. Kitsopoulos, D. P Baldwin, M. A. Buntine, R. N. Zare and D. W. Chandler, "Reaction Product Imaging: The H + D_2 Reaction" Accepted Science 1993.

Direct Numerical Simulation of Turbulent Reacting Flows

Jacqueline H. Chen
Combustion Research Facility
Sandia National Laboratories
Livermore, California 94551-0969

Program Scope

The development of turbulent combustion models that reflect some of the most important characteristics of turbulent reacting flows requires knowledge about the behavior of key quantities in well defined combustion regimes. In turbulent flames, the coupling between the turbulence and the chemistry is so strong in certain regimes that it is very difficult to isolate the role played by one individual phenomenon. Direct numerical simulation (DNS) is an extremely useful tool to study in detail the turbulence-chemistry interactions in certain well defined regimes. Globally, non-premixed flames are controlled by two limiting cases: the fast chemistry limit , where the turbulent flame can be characterized by randomly distributed chemical equilibrium problems, and the slow chemistry limit, where the chemistry integrates in time the turbulent fluctuations. In between these two limits, finite-rate chemical effects are important and the turbulence interacts strongly with the chemical processes. This regime is important because industrial burners operate in regimes in which, locally the flame undergoes extinction, or is at least in some nonequilibrium condition. Furthermore, these nonequilibrium conditions strongly influence the production of pollutants.

To quantify the finite-rate chemistry effect, direct numerical simulations are performed to study the interaction between an initially laminar non-premixed flame and a three-dimensional field of homogeneous isotropic decaying turbulence. Emphasis is placed on the dynamics of extinction and on transient effects on the fine scale mixing process. Differential molecular diffusion among species is also examined with this approach, both for nonreacting and reacting situations. To address the problem of large-scale mixing and to examine the effects of mean shear, efforts are underway to perform large eddy simulations of round three-dimensional jets.

Recent Progress

Finite-Rate Chemistry Effects

Three-dimensional DNS of non-premixed flames have been performed using a compressible, variable density, variable viscosity higher-order finite difference code (Trouve 1991). In the simulations all of the turbulent scales of motion are resolved and the chemistry is modeled by a single-step Arrhenius reaction $A+B\text{---}> P$ and also by a two-step mechanism simulating radical production and consumption, $A+B\text{---}> I$ (first step), $A+I\text{---}> P$ (second step). The parameters of the reaction rate model are chosen to correspond to methane-air combustion. For the two-step mechanism the second step proceeds with an activation energy four times smaller than the first step and an enthalpy of reaction five times larger than the first step. The Taylor Reynolds number of the turbulence simulations is fifty and the Damkohler number, defined as the ratio of the large eddy turnover time to a chemical time given by the heat release, is varied between fast and slow chemistry limits to study finite rate effects on the flame structure. The flame thickness is chosen such that the reactive and turbulence length scales are of the same order of magnitude.

1. Single-step Chemistry Results

For intermediate values of the Damkohler number (between fast and slow chemistry) local extinction is observed when the scalar dissipation rate in the reaction zone exceeds a critical value. The flame is strained and extinguished by the vorticity and convection in the outer flow. The vorticity does not penetrate the flame except in locations where extinction is observed. Within the flame zone, dynamic viscosity increases due to temperature which has the effect of damping the turbulence. In the extinguished regions leakage of reactants from one side of the flame to the other occurs creating a partially premixed situation. A topic of current investigation is the role of reignition in locally extinguished flames. In the decaying turbulence configuration reignition was not observed; however, shearing the turbulence may provide conditions for which the partially premixed pockets will burn.

Overall, the response of the turbulent flame is bounded by the characteristics typical of a laminar flamelet. Namely, the scalar dissipation rate increases with reaction rate, until a critical value is reached at which extinction occurs. At early times in the simulation (one eddy turnover time) the maximum value of the reaction rate interpolated along the local flame surface normal vector, and plotted versus the inverse scalar dissipation rate, follows the usual laminar flamelet response . However, when the flame is undergoing full interaction with the turbulence, a deviation from the bounds indicated by the laminar flamelet is observed and is related to transient effects from the turbulence induced mixing. The reason for this deviation is due to the reaction rate being influenced by the local temperature as well as by the species mass fraction. It appears that turbulence enhanced mixing convects more species to the reaction zone than by a pure strained laminar flamelet. This observation suggests that even if the features of the turbulence are close to the flamelet regime, the dynamic information carried by the turbulence introduces some transient effects that certainly needs to be included in modeling to capture with accuracy finite-rate chemistry effects.

2. Two-step Chemistry Results

The structure of the reaction zone obtained with the two-step chemistry model in the case of slow chemistry is more complex than for the single-step chemistry case. The intermediate species, I, field contains a production-recombination zone on the oxidizer side of the domain and a diffusion zone on the fuel side. The two reaction zones are not entirely separated in physical and mixture fraction space. For the same value of the Damkohler number, the global contribution of the reaction to the energy source term is broader in mixture fraction space than the corresponding contribution in the single-step chemistry case. This event causes the flame to be less susceptible to extinction compared to a flame modeled with single-step chemistry suggesting that the modeling of extinction is strongly tied to the choice of the chemical scheme, in terms of the number of steps and the species involved.

Differential Diffusion Effects

With hydrogen and hydrocarbon flames, monotomic hydrogen and diatomic hydrogen atoms are present with heavier species that diffuse more slowly. It is well known that the laminar flame structure strongly depends on the larger diffusivity of the radical species which plays an important role in ignition processes and pollutant formation. Most turbulent combustion models assume that all of the species diffuse at the same rate, and hence, the conserved scalar approach can be used. In the present work,

DNS are performed and analyzed for unequal Schmidt number nonreacting and reacting cases to determine the extent to which unequal diffusivity effects persist in turbulent non-premixed flames.

In the nonreacting free-decaying turbulence simulations, a species C is added on the species A side with a Schmidt number of one-half, whereas Species A and B have a Schmidt number of unity. It is found that differential diffusion clearly shows up in scatter plots of the distribution of the ratio, R, of the mass fractions of species A and species C with respect to the mass fraction of species A. The turbulence causes a spread about the laminar response and as the mass fraction of A tends to zero, the ratio R also tends to zero. Similar results were reported in recent experiments at the Combustion Research Facility at Sandia.

In the reacting simulations, unequal Schmidt number effects are also present and cause the pdf of the curvature of a three-dimensional non-premixed flame to be skewed towards the less diffusive side. When all of the species have a Schmidt number of unity, the pdf of the curvature is symmetric (the flame surface exhibits both positive and negative curvature); however, when the Schmidt number of species A is changed to one-half (single-step chemistry), the probability of negative curvature increases corresponding to reaction zones that are curved into the B side. This observation is found to be correlated with the broader reaction zone found on this side in mixture fraction and in physical space. Similar trends have been reported in the case of premixed combustion.

Future Plans

Three-dimensional simulations of turbulent non-premixed flames including the effects of mean shear will be performed to study local extinction and reignition processes. The inclusion of complex chemistry in the DNS approach is currently underway using reduced chemical mechanisms for CO-H_2-N_2, CO_2-H_2-N_2,and H_2-O_2 combustion and efficient algorithms for evaluating the chemical kinetics source terms. Finally, large-eddy simulations of turbulent round jets with and without differential diffusion are being performed to enable direct comparison with experiments.

Publications

J. H. Chen, J. Lienau, W. Kollmann, "Numerical Simulation of Low Reynolds Number Turbulence in Round Jets", 1993, *Turbulent Shear Flows 9, (accepted).*

L. Vervisch, J. H. Chen, S. Mahalingam, and I. Puri, "Numerical Study of Finite Rate Chemistry Effects and Unequal Schmidt Numbers on Turbulent Non-premixed Flames", 1993, *Turbulent Shear Flows 9, (accepted).*

J. H. Chen, "The Effect of Compressibility on Conserved Scalar Entrainment in a Plane Free Shear Layer," 1992, *Turbulent Shear Flows 8, Springer Verlag,* editor R. Friedrich, pp. 297-311.

J. H. Chen, S. Mahalingam, I. Puri, and L. Vervisch, "Effect of Finite-Rate Chemistry and Unequal Schmidt Numbers on Turbulent Nonpremixed Flames Modeled with Single-step Chemistry", *Paper WSS/CI 92-52, Western States Section of the Combustion Institute Fall Meeting, Berkeley* (1992), *(in prep. for Combustion and Flame).*

J. H. Chen, S. Mahalingam, I. Puri, and L. Vervisch, "Structure of Turbulent Nonpremixed Flames Modeled with Two-step Chemistry", *Paper WSS/CI 92-51, Western States Section of the Combustion Institute Fall Meeting, Berkeley* (1992), *(in prep. for Combustion and Flame).*

R. Sondergaard, J. H. Chen, J. Soria, B. J. Cantwell, "Local Topology of Small Scale Motions in Turbulent Shear Flows", *Eighth Symp. on Turbulent Shear Flows* (1991).

J. H. Chen, "Differential Diffusion Statistics in Homogeneous Turbulence", *Fourth Intl. Conf. on Numerical Combustion, St. Petersburg, Fl.* (1991).

LASER SPECTROSCOPY OF HYDROCARBON RADICALS
DE-FG02-90ER14132

Peter Chen
Mallinckrodt Chemical Laboratory, Harvard University
Cambridge, Massachusetts 02138

We report the application of supersonic jet flash pyrolysis[1] to the clean, specific preparation of a wide range of radicals, biradicals, and carbenes in a skimmed molecular beam. We have prepared methyl[2] (CH_3), ethynyl[3] (C_2H), vinyl[3,4] (C_2H_3), three isomers[5,6] of C_3H_2, propargyl[7] (C_3H_3), allyl[8] (C_3H_5), cyclobutadiene[9] (*c*-C_4H_4), benzyne[10] (*ortho*-C_6H_4), α,3-dehydrotoluene[11] (*meta*-C_7H_6), dichlorocarbene[12] (CCl_2), and trichloromethyl radical[13] (CCl_3). Each species was produced cleanly and specifically, with little or no secondary reactions, by unimolecular thermal dissociation of appropriately designed and synthesized organic precursors.

Photoelectron spectra of the three isomeric C_3H_2 carbenes[5,6], *ortho*-benzyne[10] and the α,3-dehydrotoluene biradical[11], were used to establish adiabatic ionization potentials for use in thermochemical determinations. The thermochemistry of carbenes and biradical-like species was found to follow a semiquantitative valence-bond picture[14] in which the heat of formation of the carbene or biradical is reduced from an additivity estimate by the singlet-triplet splitting if the species has a singlet ground state. The triplet state is assigned to the "noninteracting biradical" of Benson additivity schemes.

Explicit modeling of the Franck-Condon envelope of the photoelectron spectra was used, along with chemical evidence, to identify the isomeric carbenes. For cyclopropenylidene, the simulated spectrum[15], using a geometry for $C_3H_2^{+\bullet}$ slightly adjusted from the optimized MP2/6-31G* structure, closely matched that obtained by experiment. Small variations in the bond lengths in the radical cation caused large, systematic changes in the simulated photoelectron spectrum. On this basis, we use the Franck-Condon modeling as a means to assign a geometry to this important ion. Franck-Condon modeling also allowed us to extract an adiabatic ionization potential[12] from the poorly resolved photoelectron spectrum of CCl_2. With $IP_{ad}[CCl_2] = 9.27 \pm 0.03$ eV, the heat of formation of the carbene was determined to be $\Delta H^0_{f,298}[CCl_2] = 51.0 \pm 2.0$ kcal/mol which is in good agreement with a recent negative ion collision-induced dissociation value of 52.1 ± 3.4 kcal/mol that used altogether independent auxiliary thermochemical data. Previous determinations by a range of methods had given values ranging from 39 to 59 kcal/mol. A fit of the photoelectron spectrum of cyclobutadiene[9] established that the Jahn-Teller distorted radical cation *c*-$C_4H_4^{+\bullet}$ is rectangular rather than rhomboidal. A better fit to model double-well potential surfaces is underway to extract tunneling splittings. The photoelectron spectrum[13] of CCl_3 was also obtained and fit to anharmonic potential function to determine the barrier to inversion of 525 ± 50 cm^{-1} and ionization potential of $IP_{ad}[CCl_3] = 7.95 \pm 0.04$ eV.

We have recently obtained the only rotationally-resolved electronic spectrum of allyl and allyl-d_5 radical by 1+1 resonant multiphoton ionization[8]. We have assigned all of the bands between 238 and 250 nm to transitions from the X^2A_2 ground state to three close-lying, coupled electronically excited states: B^2A_1, C^2B_1, and D^2B_2. Most interesting is the B state, which is nominally the *3s* Rydberg state. It is found to be nonplanar with a double-well potential along a b_1 coordinate. We have determined preliminary values for tunneling splittings. The nonplanarity is ascribed to strong vibronic coupling to the C state whose origin lies only 241 cm^{-1} higher in energy.

In collaboration with Dr. M.G. White at Brookhaven National Laboratory, the ZEKE-PFI photoelectron spectrum of CH_3 was obtained[2]. The spectrum is the first rotationally resolved photoelectron spectrum of a transient polyatomic radical, and shows unambiguous parallel band structure. A ZEKE-PFI detector has been constructed in one of the vacuum chambers in our laboratory. We have been able to obtain both resonant and nonresonant MPI ZEKE-PFI spectra of several test molecules.

Future plans include further application of resonant MPI spectroscopy to several isotopically substituted allyl radicals to better map the excited state double-well potential. Franck-Condon simulation methodology for fitting cation structures to the photoelectron spectra of radicals is also being tested as a way to determine bond lengths and angles for carbonium ions. ZEKE-PFI spectra of small alkyl radicals is also planned.

1 D.W. Kohn, H. Clauberg, P. Chen, *Rev. Sci. Instr.* **63**, 4003 (1992).

2 J.A. Blush, P. Chen, R.T. Wiedmann, M.G. White, *J. Chem. Phys.* **98**, 3557 (1993).

3 J.A. Blush, J. Park, P. Chen, *J. Am. Chem. Soc.* **111**, 8951 (1989).

4 J.A. Blush, P. Chen, *J. Phys. Chem.* **96**, 4138 (1992).

5 H. Clauberg, P. Chen, *J. Am. Chem. Soc.* **113**, 1445 (1991).

6 H. Clauberg, D.W. Minsek, P. Chen, *J. Am. Chem. Soc.* **114**, 99 (1992).

7 D.W. Minsek, P. Chen, *J. Phys. Chem.* **94**, 8399 (1990).

8 D.W. Minsek, J.A. Blush, P. Chen, *J. Phys. Chem.* **96**, 2025 (1992); J.A. Blush, D.W. Minsek, P. Chen, *J. Phys. Chem.* **96**, 10150 (1992).

9 D.W. Kohn, P. Chen, *J. Am. Chem. Soc.* in press; D.W. Kohn, P. Chen, *J. Phys. Chem.* in preparation.

10 X. Zhang, P. Chen, *J. Am. Chem. Soc.* **114**, 3147 (1992).

11 C.F. Logan, J.C. Ma, P. Chen, P.G. Wenthold, S.G. Wierschke, R.R. Squires, *J. Am. Chem. Soc.* in preparation.

12 D.W. Kohn, E.S.J. Robles, C.F. Logan, P. Chen, *J. Phys. Chem.* in press.

13 E.S.J. Robles, P. Chen, *J. Phys. Chem.* in preparation.

14 J.A. Blush, H. Clauberg, D.W. Kohn, D.W. Minsek, X. Zhang, P. Chen, *Acc. Chem. Res.* **25**, 385 (1992).

15 H. Clauberg, P. Chen, *J. Phys. Chem.* **96**, 5676 (1992).

LASER SPECTROSCOPY AND DYNAMICS OF TRANSIENT SPECIES

Dennis J. Clouthier
Department of Chemistry
University of Kentucky
Lexington, KY 40506-0055

The goal of this program is to study the vibrational and electronic spectra and excited state dynamics of a number of transient sulfur and oxygen species. A variety of supersonic jet techniques, as well as high resolution FT-IR and intracavity dye laser spectroscopy, have been applied to these studies.

1. Reactive Jet Spectroscopy of the FS_2 Free Radical

We have recently been exploring a new technique we call "reactive jet spectroscopy", in which exothermic chemical reactions within the throat of a supersonic jet are used to produce new transient intermediates. In the first of these experiments, we reacted F_2/argon mixtures with COS in hope of detecting the electronic spectrum of SF_2. We obtained a strong LIF spectrum in the 700 - 490 nm region with an extensive series of bands with an upper state interval of 495 cm^{-1}. However, the band types, vibrational intervals and degradation of the rotational structure prove that the spectrum is not that of SF_2. Further experiments have shown that the same spectrum can be obtained by the reaction of F_2 with COS, CS_2 or H_2S, so the carrier must have only fluorine and sulfur atoms. High resolution spectra were obtained with a ring laser, and the complex rotational structure shows clear evidence of J- and K_a-dependent spin splittings. On the basis of our own extensive *ab initio* calculations, the observed vibrational intervals, and a partial rotational analysis, we have concluded that the spectrum is the $\tilde{A}^2A' - \tilde{X}^2A''$ band system of the previously unknown FS_2 free radical.

The results of our *ab initio* studies are presented in Table 1, along with the experimental data. The predicted vibrational frequencies are in excellent agreement with those derived from

Table 1

A Comparison of *Ab Initio* Predictions and Experimental Results for the FS_2 Radical.

	UMP2/6-31G*	UMP2/6-311G (2d)	Expt.
ν_1'' [a]	748[b]	736	705
ν_2''	287	289	293
ν_3''	725	674	685
ν_1'	804	754	766
ν_2'	213	216	217
ν_3'	519	505	494
ΔE	12574	13285	14921

[a] ν_1 = SF stretch; ν_2 = bend; ν_3 = SS stretch.
[b] All quantities in cm^{-1}.

the spectra. The excitation energy is slightly underestimated, due to limitations of the unrestricted Hartree-Fock Moller-Plesset perturbation theory approach. However, experiment and theory agree that there is a strong blue shift in the first electronic transition of the XS_2 species when a more electronegative atom replaces hydrogen. Thus, the adiabatic excitation energies for HS_2, ClS_2 and FS_2 are calculated to be 6208, 11020 and 13285 cm^{-1}, while the experimental values for HS_2 and FS_2 are 7256 and 14921 cm^{-1}. The $\tilde{A}$ - $\tilde{X}$ band system of ClS_2 is unknown.

We have been able to record several bands of FS_2 at high resolution and the rotational analysis is in progress. When completed, these studies will provide the first data on the ground and excited state structure, rotational constants and spin constants of the FS_2 free radical.

2. Intersystem Crossing, Internal Conversion and Evidence for Rotation-Induced Vibrational Mixing in the Ground State of Thioformaldehyde

Last year, we reported studies of the S_1 - S_0 band system of thioformaldehyde at sub-Doppler resolution using intracavity dye laser spectroscopic techniques. The analysis of these data is now complete. A total of 360 upper state rotational levels in the 4^1 vibrational state have been studied. Ground state combination differences from the sub-Doppler spectra, combined with microwave and infrared data, have been used to improve the ground state constants of H_2CS. The excited state constants have been determined from a fit of 211 "unperturbed" transitions. Some of the upper state levels are found to be strongly perturbed by nearby triplet state levels and the perturbations have been shown to involve a vibronic spin-orbit mechanism with matrix elements of 0.05 - 0.15 cm^{-1}. At least 65% of the S_1 levels show evidence of small sub-Doppler perturbations due to interactions with high rovibronic levels of the ground state. The number of S_1 - S_0 perturbations is small at low J, but increases rapidly beyond J = 3 such that 40 - 80% of the observed S_1 levels of any given J are perturbed by ground state levels. Arguments based on the density of perturbing states show that K_a is not a good quantum number in the ground state, implying that there is rotation-induced mixing of the vibrational states. The distribution of perturbations shows that the ground state levels form an unevenly distributed background, in agreement with the conclusions from our previous photophysical studies.[1]

3. High Resolution FT-IR Spectroscopy of Formyl Chloride (HCOCl)

Formyl chloride is a transient molecule which readily decomposes to form HCl and CO. Although low resolution infrared spectra were studied many years ago,[2] high resolution studies have not been reported. We have been able to record spectra at 0.004 cm^{-1} resolution using a slow flow system of HCOCl produced by the reaction of formic acid vapor with PCl_5. The spectra are complicated because 5 of the 6 fundamentals are A/B hybrid bands and both the $HCO^{35}Cl$ and $HCO^{37}Cl$ isotopomers are fairly abundant (3:1). In order to eliminate as much congestion as possible, we have deconvoluted the spectra to give a resolution of about 0.003 cm^{-1}.

The ν_3 band (CH in-plane bend) at 1307.2 cm^{-1} has been completely assigned for $HCO^{35}Cl$ and $HCO^{37}Cl$ and found to be an A/B hybrid with a transition moment ratio of approximately 4:1. The ground state constants have been refined by simultaneous fitting of microwave data and IR combination differences. The excited state constants have been obtained from fitting assignments over a wide range of J and K_a values. The ν_3 band shows only a few minor perturbations due to interactions with the 5^16^1, 5^3 and 4^15^1 levels.

The ν_2 band (CO stretch) is a predominantly A-type band which shows evidence of perturbations in most of the upper state K-stacks. Sufficient numbers of unperturbed lines were identified to provide a reliable set of upper state constants. Most of the perturbations can be ascribed to Coriolis interactions with the rotational levels of the 3^15^1 state 23 cm^{-1} below 2^1. The perturbations are very similar in both isotopomers, so a detailed picture of the interactions between the various levels can be obtained.

We are currently engaged in further FT-IR studies of the spectra of HCOCl and DCOCl. We plan to record high resolution infrared spectra of sulfine (H_2CSO) this summer. Experiments are in progress to obtain the $\tilde{A}$ - $\tilde{X}$ bands of formic acid with rotational resolution and jet cooling. We are also constructing a time-of-flight mass spectrometer to be used in REMPI studies of nonfluorescent sulfur and oxygen containing transient molecules.

References

1. J. Dunlop and D. J. Clouthier, J. Chem. Phys. **93**, 6371 (1990).

2. I. C. Hisatsune and J. Heicklen, Can. J. Spectrosc. **18**, 77 (1973).

Publications 1991 - 1993.

1. D. J. Clouthier and J. Karolczak, "A Pyrolysis Jet Spectroscopic Study of the Rotationally Resolved Electronic Spectrum of Dichlorocarbene", J. Chem. Phys., **94**, 1 (1991).

2. J. R. Dunlop, J. Karolczak, D. J. Clouthier and S. C. Ross, "Pyrolysis Jet Spectroscopy: The S_1-S_0 Band System of Thioformaldehyde and the Excited State Bending Potential", J. Phys. Chem., **95**, 3045 (1991).

3. J. R. Dunlop, J. Karolczak, D. J. Clouthier and S. C. Ross, "Pyrolysis Jet Spectroscopy: Laser-Induced Phosphorescence of Thioformaldehyde and the Triplet Excited-State Bending Potential", J. Phys. Chem., **95**, 3063 (1991).

4. G. Huang, A. J. Merer and D. J. Clouthier, "Spectroscopy of VO: Hyperfine Parameters and Electron Configuration of the $B^4\Pi$ State", J. Mol. Spectrosc., **153**, 32 (1992).

5. D. J. Clouthier, G. Huang and A. J. Merer, "A Spectroscopic View of Internal Conversion in a Small Polyatomic Molecule: Sub-Doppler Intracavity Dye Laser Spectroscopy of Thioformaldehyde", J. Chem. Phys., **97**, 1630 (1992).

6. D. L. Joo, D. J. Clouthier, B. Lau and A. J. Merer, "An Analysis of the High-Resolution Infrared Spectrum of the ν_3 Band of Formyl Chloride", J. Mol. Spectrosc. submitted (1993).

7. D. L. Joo, D. J. Clouthier and A. J. Merer, "High-Resolution Infrared Spectroscopy of the ν_2 Band of Formyl Chloride: Rotational Analysis and Coriolis Interactions with $\nu_3 + \nu_5$", J. Mol. Spectrosc. submitted (1993).

8. D. J. Clouthier, G. Huang, A. G. Adam and A. J. Merer, "Sub-Doppler Intracavity Dye Laser Spectroscopy of Thioformaldehyde: Intersystem Crossing, Internal Conversion and Evidence for Rotation-Induced Vibrational Mixing in the Ground State", J. Chem. Phys. submitted (1993).

A SHOCK TUBE STUDY OF THE REACTIONS OF THE HYDROXYL RADICAL WITH COMBUSTION SPECIES

N. Cohen and J. B. Koffend
Space and Environment Technology Center
The Aerospace Corporation
P. O. Box 92957
Los Angeles, Calif. 90009-2957

DOE/SAN Grant FG03-87ER13812

The reactions of OH radicals with hydrocarbons have received a great deal of attention in recent years because of these processes are principal steps in the oxidation of organic fuels--whether occuring in combustion/propulsion systems, in the atmosphere, or elsewhere. Of the various radicals capable of attacking hydrocarbons, OH radicals are generally the most reactive. In the atmosphere, the combined effects of the OH radical's reactivity and concentration make it the single species that determines the atmospheric lifetime of an organic substance. In many combustion systems, the OH radical plays a similar rate-determining role in the kinetics of fuel oxidation.

The principal goals of the kineticist in the field of oxidation chemistry are (1) to measure as many elementary reaction rate coefficients as are conveniently studied in the laboratory; and (2) to develop theoretical and/or semiempirical tools for extrapolating from measured rate coefficients to unmeasured ones. The latter step is necessary because of the sheer number of reactions of possible interest. *Ab initio* theoretical studies provide the most refined nonexperimental procedures for the completion of part (2) of the above program, but again, the large number of reactions renders impractical detailed theoretical evaluation of every one. To this end, Benson and coworkers[1] developed the procedures of thermochemical kinetics: a collection of recipes and simple techniques for predicting reaction rate coefficients with reasonable accuracy. The method is most reliable when used simply to extrapolate rate coefficients from one temperature range to other temperatures, but a single temperature measurement can provide the basis for extrapolation. The procedure is further sharpened when applied to a family of homologous reactions for which a set of experimental measurements places more stringent constraints on the structural parameters of the activated complex that are required for the calculations. (It is assumed that the activated complexes for a homologous series of reactions are very similar to one another.) Studies of OH radicals with a series of alkanes have provided a wealth of experimental data that constitute an ideal test case for the application of thermochemical kinetics to predicting reaction rate coefficients.

To extend the semi-empirical techniques of Benson and coworkers, and to extend the database of reliable high temperature measurements of OH radicals with hydrocarbons and other fuels and their decomposition products, we undertook, with DOE support, a research program with both experimental and computational tasks. The experimental goal was to design a procedure for measuring, at combustion temperatures, the reaction rate coefficients of OH radicals with fuels and other species of importance in combustion or propulsion systems. The computational effort was intended to refine the semi-empirical transition-state-theory procedures for extrapolating rate coefficients of reactions of OH with combustion species of interest, for predicting rate coefficients for species not studied in the laboratory, and to examine the ability of the theory to predict rate coefficients for different pathways in the case the reagent possessed more than one nonequivalent H atoms.

These scientific goals can contribute to DOE's broad mission to improve the efficiency of combustion processes while minimizing undesirable effects including production of pollutants. Both aims require a detailed knowledge of the mechanisms of the combustion processes and the kinetics of each individual step. As noted above, OH radicals are a key species in oxidation and combustion of any fuel (or other molecule) containing abstractable H atoms--which includes all but the most exotic fuels. A series of measurements for a carefully selected array of species can provide the basis for a semi-empirical formulation to estimate rates for any

arbitrary molecule of interest--information that engineers, scientists, and other modelers will need in studying combustion problems, predicting fuel efficiency, or minimizing undesired pollutant products.

In the experimental portion of this program we have carried out shock tube measurements of the reactions of OH radicals with several species. The experiments were performed behind reflected shock waves in a stainless steel shock tube. The tube has a 10-m-long, 16.2-cm-diameter test section with a 3-m-long 7.5-cm-diameter driver section. OH radicals were produced in most cases by shock-heating t-butyl hydroperoxide (TBH) diluted in argon carrier gas. TBH dissociates rapidly at our temperatures (near 1200 K) to produce t-butoxy and OH radicals:

$$(CH_3)_3COOH \text{ --> } (CH_3)_3CO^{\bullet} + {}^{\bullet}OH \qquad k_a = 6.6 \times 10^7 \text{ sec}^{-1}$$

the t-butoxy radicals in turn very rapidly dissociate to give CH_3 radicals and acetone:

$$(CH_3)_3CO^{\bullet} \text{ --> } {}^{\bullet}CH_3 + CH_3COCH_3 \qquad k_b = ? \, 3 \times 10^{10} \text{ sec}^{-1}$$

The acetone then decomposes--but, unfortunately, not very fast on our time scale--to give $\cdot CH_3$ and $\cdot CH_3CO$ radicals:

$$CH_3COCH_3 \text{ --> } {}^{\bullet}CH_3CO + {}^{\bullet}CH_3 \qquad k_c = 40 \text{ sec}^{-1}$$

And the CH_3CO radicals will rapidly fall apart to give CH_3 and CO:

$$^{\bullet}CH_3CO \text{ --> } {}^{\bullet}CH_3 + CO \qquad k_d = ? \, 4 \times 10^{10} \text{ sec}^{-1}$$

The net result of four reactions is:

$$(CH_3)_3COOH \text{ --> } {}^{\bullet}OH + 3\,{}^{\bullet}CH_3 + CO$$

If the third reaction were sufficiently fast, then the analysis of the measurements would be considerably simplified, because we would then be looking at an instantaneously produced concentration of OH radicals, CH_3 radicals, and inert CO. The fact that this is not so forces us to model OH concentrations as a function of time and deduce reaction rates of the OH with added substrates by computer modeling.

Thin-film heat transfer gauges mounted in the tube wall signal the passage of the shock wave. The speed of the shock wave is calculated from the distance between the gauges and the time between the heat transfer gauge signals. From the shock speed, the pressure and temperature behind the reflected shock are calculated.

The shock tube, the gas-handling equipment, and the optical configuration were described in detail in Ref. 2; however, much of the electronics and hardware, not changed for over ten years, have been redesigned and modified extensively. The old gas handling system has been completely replaced using new components, including capacitance manometers for making more accurate and precise pressure measurements and gas mixtures. The antiquated system used to measure shock front velocities has been rebuilt replacing analog recording equipment with digital. Shock velocities accurate to better than ±0.3% can be obtained from the digitized data. Calibration experiments are now in progress to establish new system characteristics--in particular, the exponent ν defined in eq. (1) below:

$$\ln(I_o/I) = e_{eff} ([OH] \times l)^{\nu} \qquad (1)$$

where I is the light signal seen by a detector, l = optical path length and e_{eff} = effective extinction coefficient. e_{eff} and ν are functions of the gas temperature and pressure, the slit width, and the operating characteristics of the lamp.

The OH radical then undergo several reactions in the absence of any other reagents, and have a characteristic half-life. When another reagent is present, it too can react with the OH. The disappearance rate of OH as a function of the added reagent RH gives the reaction rate coefficient for the process, OH + RH --> products. The OH concentration behind the shock wave was monitored by uv absorption using OH resonance radiation at 309 nm, produced by a microwave discharge through a mixture of helium and water vapor flowing at 70 torr.

To date we have completed and published[2,3,4] shock tube measurements of the reactions of OH radicals with several species: H_2, CH_4, c-C_5H_{10}, i-C_4H_{10}, i-C_8H_{18}, neo-C_8H_{18}, 2,3-dimethylbutane, C_2H_2, C_2H_4,

C_3H_6, HCHO, CH_3COCH_3, CH_3OH, and C_2H_5OH. The results, all near 1200 K and 1 atm, are summarized below.

Reagent	Rate Coefficient (10^9 L/mol-s)
H_2	2.7
CH_4	2.6
C_2H_6	9.0
C_3H_8	16.0
i-C_4H_{10}	12.6
c-C_5H_{10}	28.0
neo-C_8H_{18}	18.0
i-C_8H_{18}	22.0
2,3-dimethylbutane	21.0
C_2H_2	0.28
C_2H_4	2.6
C_3H_6	9.6
HCHO	12.0
CH_3COCH_3	5.3
CH_3OH	5.2
C_2H_5OH	5.3

In addition, in a separate set of experiments, the reaction rate of OH with CH_3 radicals was measured.[5] This process is always occuring in our system because CH_3 radicals are produced in the decomposition of the TBH via reactions b, c, and d. Overall, three CH_3 radicals are produced for every OH radical in the pyrolysis of the TBH. In order to vary the ratio of [OH]:[CH_3], varying quantities of di-t-butyl-peroxide (TBP) were added to the TBH. Like TBH, TBP decomposes rapidly at the temperatures behind the reflected shock tube, but produces only CH_3 and CO:

$(CH_3)_3COOC(CH_3)_3$ --> 2 $(CH_3)_3CO^{\bullet}$	$k_e = 7 \times 10^8$ sec^{-1}
$(CH_3)_3CO^{\bullet}$ --> CH_3 + CH_3COCH_3	$k_f = ? 3 \times 10^{10}$ sec^{-1}
CH_3COCH_3 --> $^{\bullet}CH_3CO$ + $^{\bullet}CH_3$	$k_c = 40$ sec^{-1}
$^{\bullet}CH_3CO$ --> $^{\bullet}CH_3$ + CO	$k_d = ? 4 \times 10^{10}$ sec^{-1}

For a net overall reaction of:

$$(CH_3)_3COOC(CH_3)_3 \text{ --> } 4\ ^{\bullet}CH_3 + 2\ CO$$

Extraction of the OH + CH_3 reaction rate coefficient of 1.1×10^{11} L mol^{-1} s^{-1} required the utilization of a detailed computer model. Although we did not directly measure the products of the reaction, we believe that the primary mechanism for OH removal of CH_3 near 1200 K and 1 atm is by their combination to form CH_3OH.

The work on the hydrocarbons provided the incentive for revising an earlier model[6] used to carry out thermochemical transition state theory (TST) calculations for the reaction rate coefficients of OH with alkanes. In a careful review of the application of TST to OH + alkane reactions we concluded that there are good theoretical reasons for expecting different primary, secondary, or tertiary H atoms (distinguished on the basis of number of nearest neighboring C atoms) to have different rate parameters. If true, this invalidates the usual procedure of treating the total rate coefficient for OH + RH H abstraction processes as the sum of invariant primary, secondary, and tertiary rates multiplied by the respective number of such H atoms in the molecule. A separate question is whether there is really sufficient experimental evidence to justify distinguishing among different types of primary (or secondary, or tertiary) H atoms, or whether, given experimental and theoretical uncertainties, it is adequate to treat them all as equivalent. We have concluded that there are measurable and unambiguous differences among various primary H atom abstractions, and possibly among secondary atoms, but the database cannot as yet distinguish among tertiary H atoms.[7]

In the coming period we plan to continue our program of measuring reaction rates with selected hydrocarbons and oxygenated hydrocarbons, and extend it to halogenated hydrocarbons. We also plan to carry out some experiments designed to measure relative contributions from alternate channels (possibly by using

laser absorption spectroscopy) in the case of reactions with more than one pathway--e. g., OH + C_2H_5OH, CH_3CHO, CH_3CHCH_2, C_2H_4. An additional area of interest is the shock tube study of molecule-molecule reactions of importance in combustion, such as NH_3 + NO and NH_3 + NO_2.

References

1. S. W. Benson, *Thermochemical Kinetics,* 2nd edn. (Wiley, 1976) and references cited therein.
2. J. F. Bott and N. Cohen, *Int. J. Chem. Kinet.* **16**, 1557 (1984).
3. J. F. Bott and N. Cohen, *Int. J. Chem. Kinet.* **21**, 485 (1989).
4. J. F. Bott and N. Cohen, *Int. J. Chem. Kinet.* **23**, 1075 (1991).
5. J. F. Bott and N. Cohen, *Int. J. Chem. Kinet.* **23**, 1017 (1991).
6. N. Cohen, *Int. J. Chem. Kinet.* **14**, 1339 (1982); **15**, 503 (1983).
7. N. Cohen, *Int. J. Chem. Kinet.* **23**, 397 (1991).

Publications Related to this Grant

N. Cohen, "Are Reaction Rate Coefficients Additive? Revised Transition State Theory Calculations for OH + Alkane Reactions," *Int. J. Chem. Kinetics* **23**, 397 (1991).

N. Cohen, "The Use of Transition-State Theory to Extrapolate Rate Coefficients for Reactions of H Atoms with Alkanes," *Int. J. Chem. Kinetics* **23**, 683 (1991).

J. F. Bott and N. Cohen, "A Shock Tube Study of the Reaction of Methyl Radicals with Hydroxyl Radical," *Int. J. Chem. Kinetics* **23**, 1017 (1991).

J. F. Bott and N. Cohen, "A Shock Tube Study of the Reactions of the Hydroxyl Radical with Several Combustion Species," *Int. J. Chem. Kinetics* **23**, 1075 (1991).

N. Cohen and S. W. Benson, "The Thermochemistry of Alkanes and Cycloalkanes," Chapter 6 in *The Chemistry of Alkanes and Cycloalkanes*, R. Patai and Z. Rappoport, eds. (Wiley, 1992), pp. 215-287.

N. Cohen, "The Thermochemistry of Alkyl Free Radicals," ATR-91(7189)-1 (15 July 1991); submitted to *J. Phys. Chem.*

N. Cohen and S. W. Benson, "The Estimation of Heats of Formation of Organic Compounds," *Chem. Revs* (1993) [in press].

RESONANCE IONIZATION DETECTION OF COMBUSTION RADICALS

Terrill A. Cool

School of Applied and Engineering Physics

Cornell University, Ithaca, NY 14853

Fundamental research on the combustion of halogenated organic compounds with emphasis on reaction pathways leading to the formation of chlorinated aromatic compounds and the development of continuous emission monitoring methods will assist in DOE efforts in the management and disposal of hazardous chemical wastes. Selective laser ionization techniques are used in our laboratory for the measurement of concentration profiles of radical intermediates in the combustion of chlorinated hydrocarbon flames. A new ultrasensitive detection technique, made possible with the advent of tunable VUV laser sources, enables the selective near-threshold photoionization of *all* radical intermediates in premixed hydrocarbon and chlorinated hydrocarbon flames.

Three project objectives may be briefly summarized:

1. Measure concentration profiles of radical species in premixed hydrocarbon and chlorinated hydrocarbon flames for the development, refinement and verification of chemical kinetic flame modeling calculations.

2. Develop resonance ionization detection schemes for in situ monitoring of flame radical concentration profiles.

3. Perform resonance ionization spectroscopic studies of electronic states of combustion radicals to promote an improved understanding of the electronic structures of these species.

Most of our effort during the past year has centered on the *flame sampling laser ionization mass spectrometer* to be used for measurements of chlorinated hydrocarbon flame radical density profiles. A Spectra Physics GCR-6 Nd:YAG laser and an STI Ti/Sapphire laser are now in operation for the generation of VUV light by four-wave sum and difference frequency generation techniques with xenon and krypton nonlinear media. The apparatus has been tested and initial mass spectra for methane/oxygen and hydrogen/oxygen base flames have been recorded. These initial experiments were conducted with tripling of the third harmonic frequency of the Nd:YAG laser in a xenon cell to yield 118 nm (10.5 eV) photons for VUV photoionization mass spectrometry of reaction intermediates.

The base flames were seeded with trichloroethylene and vinyl chloride to demonstrate the feasibility of the technique. High quality mass spectra with a mass resolution of about 150 were demonstrated. Profile measurements of numerous radical intermediates and laser-induced photofragments were recorded. The sensitivity of the VUV photoionization method has enabled us to observe trace species such as COCl, the chloroformyl radical, which is of key importance in the combustion of chlorinated hydrocarbons, and yet has not been previously detected in laboratory flames. A glance at the reaction pathway diagram of Fig. 1 illustrates the role of COCl in the oxidation of trichloroethylene; COCl assumes a similar prominence in the oxidation of other chlorinated hydrocarbons. The exceptionally weak Cl-C bond (≈ 8 kcal/mole) of this radical makes ClCO of considerable chemical and spectroscopic interest.

Our experiments to date have only been performed with photons of a fixed 10.5 eV energy, rather than with energies tunable over the 7 to 11 eV range available when our tunable VUV system is completed. As a result we cannot conclusively determine whether the ClCO we detect is nascent within the flame zone or is formed as a result of the photofragmentation of $COCl_2$.

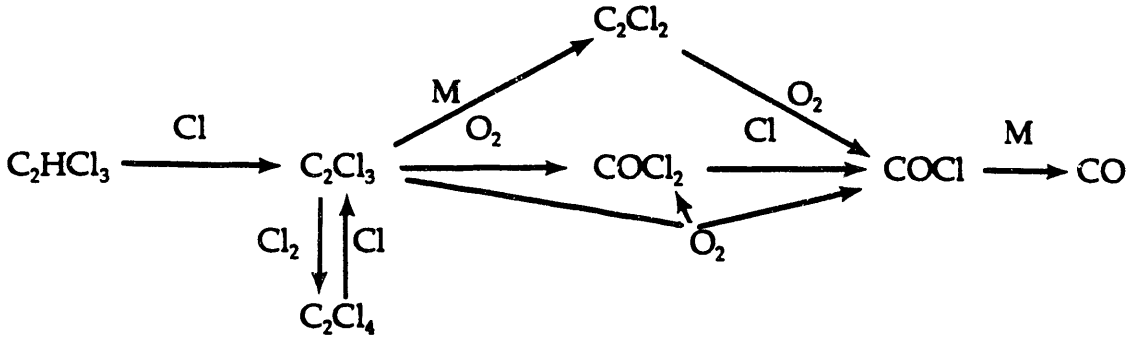

Figure 1: Major reaction pathways in the high temperature combustion of C_2Cl_3H

Publications of DOE sponsored research

T. A. Cool and P. M. Goodwin, "Observation of an Electronic State of C_2H Near 9 eV by Resonance Ionization Spectroscopy," J. Chem. Phys. 94, 6978 (1991).

X.-M. Song and T. A. Cool, "Resonance Ionization Spectroscopy of HCO and DCO: I. The 3*p* $^2\Pi$ Rydberg State", J. Chem. Phys. 96, 8664 (1992).

T. A. Cool and X.-M. Song, "Resonance Ionization Spectroscopy of HCO and DCO: II. The Hydrocarbon Flame Bands", J. Chem. Phys. 96, 8675 (1992).

THE PHOTODISSOCIATION AND REACTION DYNAMICS OF VIBRATIONALLY EXCITED MOLECULES

F.F. Crim

Department of Chemistry
University of Wisconsin-Madison
Madison, Wisconsin 53706

This research determines the nature of highly vibrationally excited molecules, their unimolecular reactions, and their photodissociation dynamics. The goal is to characterize vibrationally excited molecules and to exploit that understanding to discover and control their chemical pathways. Most recently we have used a combination of vibrational overtone excitation and laser induced fluorescence both to characterize vibrationally excited molecules and to study their photodissociation dynamics. We have also begun our first laser induced grating spectroscopy experiments designed to obtain the electronic absorption spectra of highly vibrationally excited molecules.

VIBRATIONALLY MEDIATED PHOTODISSOCIATION

We study the role of vibrational excitation in photodissociation dynamics by using a vibrational state preparation technique, such as vibrational overtone excitation, to create molecules with particular nuclear motions and then exciting some of those molecules to a dissociative electronic state. Because the vibrational excitation alters the dissociation dynamics in the excited state, both by providing access to different portions of the excited state surface and by altering the motion of the system on the surface, we usually refer to dissociation of these excited molecules as vibrationally mediated photodissociation.[1] We have studied vibrationally mediated photodissociation in a number of molecules, HOOH, $HONO_2$, t-BuOOH, and, most recently, H_2O and HOD. In the latter two molecules, we demonstrated the controlled breaking of a bond in vibrationally mediated photodissociation, determined the distribution of energy in the products, and obtained the electronic absorption spectrum of the vibrationally excited molecule.[1]

Hydroxylamine (NH_2OH) is an intriguing molecule for testing ideas that we have developed about vibrationally mediated photodissociation. It has a relatively weak H_2N-OH bond (256 kJ/mol) and two different types of bonds (N-H and O-N) that are likely candidates for vibrational overtone excitation. Our approach to exploring its vibrationally mediated photodissociation dynamics is to obtain its vibrational overtone absorption spectrum,[2] using photoacoustic spectroscopy, to study its single photon photodissociation, and to observe its vibrationally mediated photodissociation for excitation of both the O-H and N-H bonds.

The photoacoustic spectra of NH_2OH in the vicinity of the second ($3\nu_{OH}$), third ($4\nu_{OH}$), and fourth ($5\nu_{OH}$) overtones of the O-H stretching vibration illustrate an intriguing aspect of hydroxylamine. The spectra for the second and third overtone

vibrations have sharp, albeit congested, rotational structure, but the spectrum for the fourth overtone vibration has none. Simulating the spectra as those of an asymmetric top with predominantly an *a*-type rotational contour having a small *b* or *c*-type contribution reproduces the rotational structure quite well *provided* we assign a linewidth of 0.5 cm^{-1} in the case of $3\nu_{OH}$ and 1 cm^{-1} in the case of $4\nu_{OH}$. Both of these widths exceed the bandwidth of the dye laser and clearly reflect couplings within the molecule. The situation in both the experiment and simulation is dramatically different for $5\nu_{OH}$, where we must use a linewidth of 10 cm^{-1} to reproduce the spectrum. Although the fourth O-H stretching overtone region lies below the dissociation threshold for NH_2OH, the coupling apparently changes dramatically between $4\nu_{OH}$ and $5\nu_{OH}$. We are now probing the vibrationally mediated photodissociation dynamics for molecules excited in these different regions by measuring the distributions of the products among their quantum states.

We have also begun calculations based on *ab initio* potential energy surfaces to explore these vibrational dynamics. After obtaining a number of points on the potential energy surface, we have calculated the vibrational eigenvalues and used them to predict the evolution of excitation initially deposited in the O-H stretch. Fast decay from this state translates into a large linewidth in our spectra. In these first calculations, the states $3\nu_{OH}$ and $4\nu_{OH}$ live a very long time, consistent with their relatively narrow lines, while $5\nu_{OH}$ decays in a fraction of a picosecond, consistent with its broader lines. We believe that NH_2OH has interesting experimental behavior that will yield to good theoretical interpretation.

LASER INDUCED GRATING SPECTROSCOPY

The basic approach of a laser induced grating experiment is to form an interference pattern in a sample by crossing two identical excitation beams, obtained by splitting a single laser beam into two parts, and to probe it with another beam that diffracts from the resulting grating. The interfering excitation beams create a grating pattern with regions of excited state population separating regions with no excited molecules, corresponding to maxima and minima in the interference pattern. The probe beam diffracts from these regions if the excited state prepared by the excitation beam produces a different index of refraction or absorption coefficient at the probe wavelength than the ground state. This approach is well established for liquids and has been demonstrated in gases, but its application to detecting highly vibrationally excited states has just begun.

The simplest laser induced grating measurement we are performing creates a grating with the vibrational overtone excitation light and probes it with ultraviolet light in a transition to the electronically excited state. This corresponds to the first two steps in vibrationally mediated photodissociation, but diffraction of the probe beam, not the formation of a photofragment, signals the transition to the electronically excited state. Buntine *et al.* have pioneered this approach in highly vibrationally excited water vapor.[3] They excite the $|04\rangle^-$ state with interfering vibrational overtone excitation beams and probe the excited state by diffraction of 266-nm light, which makes a transition from the vibrationally excited state to the dissociative electronically excited state. The larger cross section for electronic excitation of the vibrationally

excited molecule compared to the ground vibrational state molecule at the selected wavelength produces the difference in index of refraction between the maxima and minima in the grating that diffracts the probe light. Varying the wavelength of the excitation laser produces the vibrational overtone excitation spectrum of water.

We have learned the details of laser induced grating spectroscopy with experiments on NO, using a two-photon excitation, and with experiments on water, using vibrational overtone excitation. We have the methodology well in hand, have reproduced the earlier measurements[3] of the vibrational overtone excitation spectrum of the $|04\rangle^-$, and are studying other vibrational states such as $|13\rangle^-$. The most intriguing possibility for this technique is obtaining the ultraviolet excitation spectrum out of different vibrational states. We have already shown that this spectrum has structure that reflects the nodal structure of the vibrationally excited state and the dissociating state.[4] Implementing laser induced grating spectroscopy will allow us to obtain these spectra easily and sharpen our comparison with detailed theoretical calculations.

1. F. F. Crim, Ann. Rev. Phys. Chem. (1993) (in press).

2. X. Luo, P. R. Fleming, T. A. Seckel, and T. R. Rizzo, J. Chem. Phys. **93**, 9194 (1990).

3. M. A. Buntine, D. W. Chandler, and C. C. Hayden, J. Chem. Phys. (to be submitted).

4. R. L. Vander Wal, J. L. Scott, and F. F. Crim, J. Chem. Phys. **94**, 1859 (1991).

PUBLICATIONS SINCE 1991 ACKNOWLEDGING DOE SUPPORT

State Resolved Photodissociation of Vibrationally Excited Water: Rotations, Stretching Vibrations, and Relative Cross Sections, R. L. Vander Wal, J. L. Scott, and F. F. Crim, J. Chem. Phys. **94**, 1859 (1991).

An Experimental and Theoretical Study of the Bond-Selected Photodissociation of HOD. R. L. Vander Wal, J. L. Scott, F. F. Crim, K. Weide, and R. Schinke, J. Chem. Phys. **94**, 3548 (1991).

The Effect of Bending Vibrations on Product Rotations in the Fully State-Resolved Photodissociation of the A-State of Water. R. Schinke, R. L. Vander Wal, J. L. Scott, and F. F. Crim, J. Chem. Phys. **94**, 283 (1991).

Controlling Bimolecular Reactions: Mode and Bond Selected Reaction of Water with Hydrogen Atoms. A. Sinha, M. C. Hsiao, and F. F. Crim, J. Chem. Phys. **94**, 4928 (1991).

Energy Disposal in the Vibrational State- and Bond-Selected Reaction of Water with Hydrogen Atoms. M. C. Hsiao, A. Sinha, and F. F. Crim, J. Phys. Chem. **95**, 8263 (1991).

Mode- and Bond-Selected Bimolecular Reaction of Water. F. F. Crim, A. Sinha, M. C. Hsiao, and J. D. Thoemke, in Mode Selective Chemistry, J. Jortner, *et al.* editors, (1991), pp. 217-225.

The Photodissociation of Water in the First Absorption Band: A Prototype for Dissociation on a Repulsive Potential Energy Surface. V. Engel, V. Staemmler, R. L. Vander Wal, F. F. Crim, R. J. Sension, B. Hudson, P. Andresen, S. Hennig, K. Weide, and R. Schinke, J. Phys. Chem. **96**, 3201 (1992).

Vibrationally Mediated Photodissociation: Exploring Excited State Surfaces and Controlling Decomposition Pathways. F. F. Crim, Ann. Rev. Phys. Chem. (1993) (in press).

INFRARED ABSORPTION SPECTROSCOPY AND CHEMICAL KINETICS OF FREE RADICALS

Robert F. Curl and Graham P. Glass
Department of Chemistry and Rice Quantum Institute
Rice University, Houston, TX 77251

This research is directed at the detection, monitoring, and study of the chemical kinetic behavior by infrared absorption spectroscopy of small free radical species thought to be important intermediates in combustion. During the last year, infrared kinetic spectroscopy using excimer laser flash photolysis and color-center laser probing has been employed to study the high resolution spectrum of HCCN, the rate constant of the reaction between ethynyl (C_2H) radical and H_2 in the temperature region between 295 and 875 K, and the recombination rate of propargyl (CH_2CCH) at room temperature.

THE CH STRETCH OF HCCN

HCCN was produced by 193 nm excimer laser photolysis of dibromoacetonitrile

$$HBr_2CCN + h\nu\ (193\ nm) \rightarrow HCCN + 2Br \qquad (1)$$

and the region of the CH stretching fundamental of the ground triplet state near 3250 cm^{-1} was probed with a tunable color center laser. The CH stretch fundamental, ν_1, was observed, assigned, and analyzed. In addition to the CH stretching fundamental, several hot bands associated with excitation of the CH stretch from excited states of the bending vibrations were observed and the two bands associated with the lowest energy bending fundamentals, $\nu_1+\nu_5-\nu_5$ and $\nu_1+\nu_4-\nu_4$, were analyzed. From measurements of the intensity of these hot bands relative to the fundamental, the energy of ν_5 and ν_4 have been found to be 187±20 cm^{-1} and 383±20 cm^{-1} respectively. The value found for ν_5, 187±20 cm^{-1}, which corresponds to the energy of the lowest excited state involving off-axis motion, is intermediate between that expected for a normal linear molecule and that expected for a bent molecule suggesting a very floppy HCX bending potential characteristic of a quasilinear molecule.

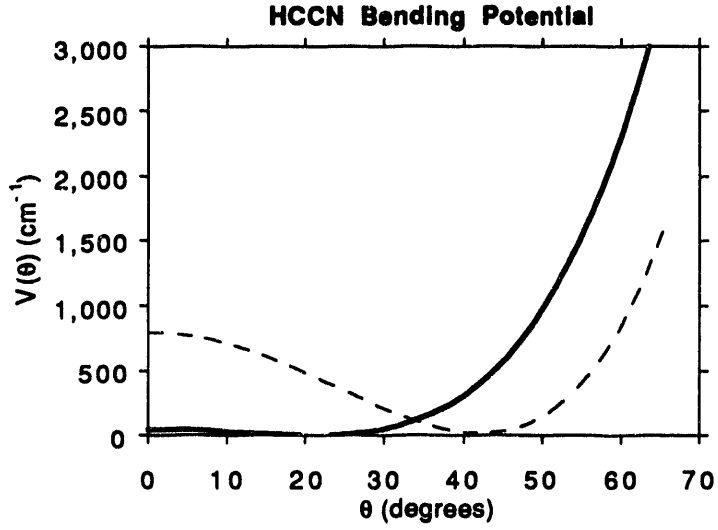

Figure 1. Potential function for the HCC angle agreeing with observed ν_5 energy. The molecule is linear when $\theta = 0$. The dashed curve is the *ab initio* (CCI) curve of Malmquist *et al.*

The bending vibrational energy levels of the ground electronic state of HCCN have been calculated for a range of possible bending potentials by Malmquist *et al* [1] who carried out an *ab initio* study of the triplet ground electronic state of HCCN. As with all other *ab initio* calculations of the structure of ground state HCCN, they found the equilibrium geometry of the molecule is bent. Because all previous

spectroscopic investigations of HCCN found the molecule to be linear, Malmquist *et al* provided the bending energy levels for a parametrically variable potential function capable of taking the bent *ab initio* potential all the way to linearity. The bending potential resulting from their parameterization that gives $\nu_5 \approx 190\ cm^{-1}$ is depicted above. This potential suggests that the HCC bond angle flops about linearity.

T DEPENDENCE OF THE RATE CONSTANT FOR THE REACTION BETWEEN CCH AND H_2

High temperature rate measurements on the reaction between C_2H and molecular hydrogen:

$$C_2H + H_2 \text{ ----> } H + C_2H_2 \qquad (2)$$

are crucial to a critical evaluation of the mechanism of acetylene pyrolysis,[2,3] which, of course, is an essential part of any more general hydrocarbon combustion mechanism. Since C_2H formation in such systems occurs primarily via the reverse of reaction (2), and since no experimental measurements of reaction (-2) exist, it is usual, when modelling either acetylene pyrolysis or combustion, to estimate the rate of reaction (-2) from the equilibrium constant, K_2, and the rate constant, k_2, for the forward reaction. Only one direct experimental investigation of the reaction between C_2H and H_2 at temperatures in excess of 300 K has been published.[4] This study suffers from two limitations: (1) It covered only a limited temperature range (298-438 K), and (2) only the ratio of k_2 to the rate of reaction of C_2H with acetylene, was measured. The only information concerning the rate of reaction (2) at combustion temperatures, comes from a TST calculation by Harding et al,[5] which utilized ab initio methods (POL-CI) for determining the properties of the potential energy surface in the saddle point region.

In our work, the rate of the reaction between C_2H and H_2 has been measured over the temperature range 295-855 K. The C_2H radical was produced by excimer laser photolysis of C_2H_2 at 193 nm, and its transient absorption was monitored throughout the reaction by using a tunable infrared color-center laser. The temperature dependence of the rate constant exhibited a non-Arrhenius form that could be well represented by the expression: $k = (9.44 \pm 0.50) \times 10^{-14}\ T^{0.9} \exp(-1003 \pm 40/T)\ cm^3 molecule^{-1} s^{-1}$. Figure 2 shows a comparison of our data with previous work.

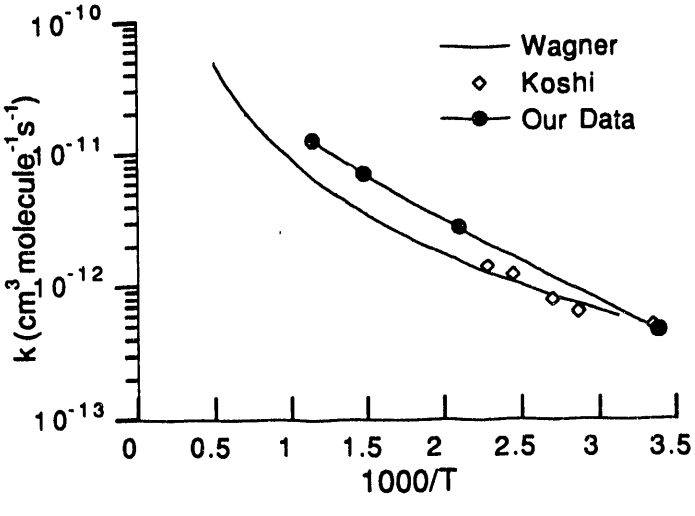

Fig. 2. The rate of the reaction, $C_2H + H_2$, as a function of temperature.

RECOMBINATION RATE OF PROPARGYL RADICAL

We reported last year an infrared kinetic spectroscopic investigation of the CH stretching fundamental of propargyl radical and described in our oral presentation preliminary measurements of the

propargyl recombination rate at room temperature. Propargyl is produced by flash photolysis of propargyl bromide or chloride.

$$CH_2X\text{-}C{\equiv}CH + h\nu \rightarrow X + CH_2\text{-}C{\equiv}CH \qquad (3)$$

with X=Br or Cl. Another possible photolysis channel may be

$$CH_2X\text{-}C{\equiv}CH + h\nu \rightarrow HX + CH\text{-}C{\equiv}CH \qquad (4)$$

The time decay of the propargyl signal follows second order kinetics suggesting that propargyl is reacting with itself or another photolyis product. When X=Br, the Br atom can be observed with the same apparatus using the magnetic-dipole-allowed fine structure transition of the bromine atom at 3685 cm^{-1}. As the Br absorption cross section is known, the infrared absorption cross-section of propargyl can be determined by comparing its intensity to that of Br using the stoichiometry of reaction (3). The Br atom signal exhibits first order decay, which is faster than the propargyl decay under the same conditions. These observations show that propargyl does not react with the precursor C_3H_3Br nor with Br. When X=Cl, it is possible to observe transitions of the HCl vibrational fundamental. Indeed these appear promptly upon photolysis indicating that (4) is actually taking place. However, quantitative measurements establish that the ratio of moles HCl to moles C_3H_3 is 0.14 ± .02. Thus (4) is a minor channel when X=Cl, and the observed second order decay of propargyl must be caused by the reaction of propargyl with itself probably via recombination. These observations permit the determination of this recombination rate by measurement of the decay of the C_3H_3 concentration with time after photolysis of propargyl chloride. The resulting rate constant is 1.8(4) x 10^{-10} cm^3 $molecule^{-1}$ s^{-1}.

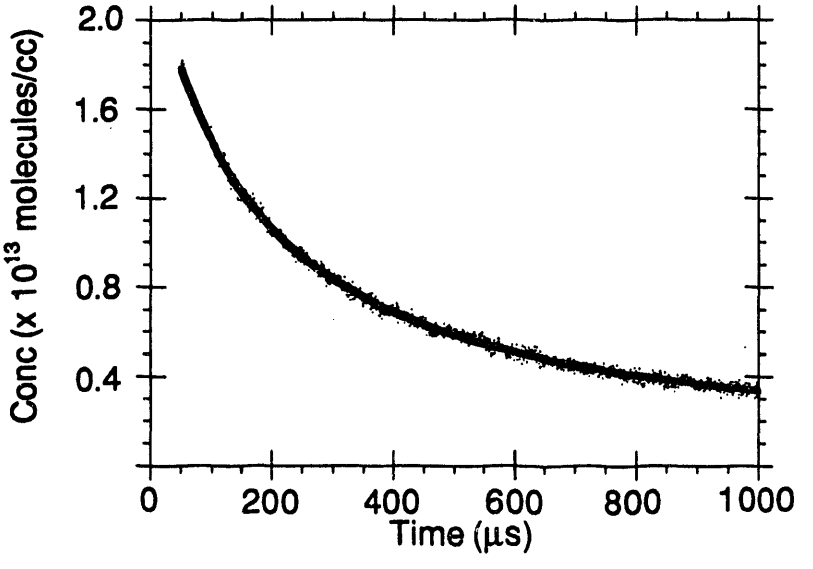

Fig. 3 Time decay of propargyl concentration fitted by second order kinetics expression.

---

[1]P. Malmquist, R. Lindh, B. O. Roos, and S. Ross, Theo. Chim. Acta 73 (1988) 155.
[2]J. H. Kiefer, and W. A. Von Drasek, Int. J. Chem. Kinetics, 22, 747 (1990).
[3]R. D. Kern, K. Xie, H. Chen, and J. H. Kiefer, 23rd Symposium (International) on Combustion (The Combustion Institute, Pittsburgh 1990) p. 69.
[4]M. Koshi, K. Fukuda, K. Kamiya, and H. Matsui, J. Phys. Chem., 96, 9839 (1992).
[5]L. B. Harding, G. C. Schatz, and R. A. Chiles, J. Chem. Phys., 76, 5172 (1982).

Publications 1991 to present

1. "The ν_1 fundamental of HCCN: Evidence for quasilinearity", C. L. Morter, S. K. Farhat, and R. F. Curl, Chem. Phys. Lett. (accepted).

2. "Rotationally Resolved Spectrum of the ν_1 CH Stretch of the Propargyl Radical (H_2CCCH)", C. L. Morter, C. Domingo, S. K. Farhat, E. Cartwright, G. P. Glass, and R. F. Curl, Chem. Phys. Lett. **195**, 316-321 (1992).

3. "Acetylene Combustion Reactions: Rate Constant Measurements of HCCO with O_2 and C_2H_2", K. K. Murray, K. G. Unfried, G. P. Glass, and R. F. Curl, Chem. Phys. Lett. **192**, 512-516 (1992).

4. "Infrared Flash Kinetic Spectroscopy of the Ketenyl Radical", K. G. Unfried, G. P. Glass, and R. F. Curl, Chem. Phys. Lett. **177**, 33-38 (1991).

SPECTROSCOPY AND REACTIONS OF VIBRATIONALLY EXCITED TRANSIENT MOLECULES

Hai-Lung Dai
Department of Chemistry
University of Pennsylvania
Philadelphia, PA 19104-6323

I. Program Scope

Spectroscopy, energy transfer and reactions of vibrationally excited transient molecules are studied through a combination of laser-based excitation techniques and efficient detection of emission from the energized molecules with frequency and time resolution. Specifically, a Time-resolved Fourier Transform Emission Spectroscopy technique has been developed for detecting dispersed laser-induced fluorescence in the IR, visible and UV regions. The structure and spectroscopy of the excited vibrational levels in the electronic ground state, as well as energy relaxation and reactions induced by specific vibronic excitations of a transient molecule can be characterized from time-resolved dispersed fluorescence in the visible and UV region. IR emissions from highly vibrational excited levels, on the other hand, reveal the pathways and rates of collision induced vibrational energy transfer.

II. Recent Progress

A. Fourier Transform Dispersed Fluorescence Spectroscopy: Highly Excited Vibrational Levels of Singlet Methylene

Recently we have reported the development of time-resolved Fourier transform emission spectroscopy (TR-FTES), a new technique for recording dispersed emission spectra in the visible or uv region of laser excited species with 50nsec and 0.25 cm^{-1} resolution. As a spectroscopic tool for excited vibrational levels, FTES has many advantages. The spectral range that can be obtained in a single experiment is very large (10^3-10^4 cm^{-1}). In comparison with grating spectrometers for dispersing fluorescence, the resolution is much higher. Fourier transform spectroscopic techniques give accurate absolute frequencies, without the need for external calibration. And the dispersed fluorescence spectra can be taken with real time resolution for the examination of collision processes that will change the nature of the excited rovibronic state.

All of these advantages make TR-FTES a uniquely superior technique for fast recording survey spectra of excited vibrational levels over wide spectral ranges, for species with short lifetimes and/or low concentrations. We have achieved a first demonstration of these advantages in a study of the high vibrational levels of CH_2 in the lowest singlet state. Spectra presented here will show that several previously unknown vibrational levels in the 5,000-7,500 cm^{-1} region, including the v_2=5 level, can be detected with excellent signal/noise

ratios for a sample with <10 mTorr CH_2 partial pressure within only 10^5 laser pulse operation. With the present laser repetition rate, these spectra of a few thousands wavenumber and ~1 cm^{-1} resolution take only *a couple of hours* of laser operation to obtain. This is at least an order of magnitude more efficient than previous methods using grating spectrometers.

The newly detected (1,2,0), (2,0,0), (0,5,0), and (1,3,0) vibrational levels, together with the (0, n=2-4,0) and (1,1,0) levels detected by us using the stimulated emission pumping technique and the fundamental levels previously determined by Moore and coworkers, allow the determination of a good portion of the singlet CH_2 potential energy surface. The barrier height to linearity of the $\tilde{a}^1A_1$ state has been recalculated with greater accuracy. *Ab initio* calculations have shown that the (0,5,0) level suffers severe Renner-Teller coupling with the $\tilde{b}$ state, which has also been confirmed by this FTES study.

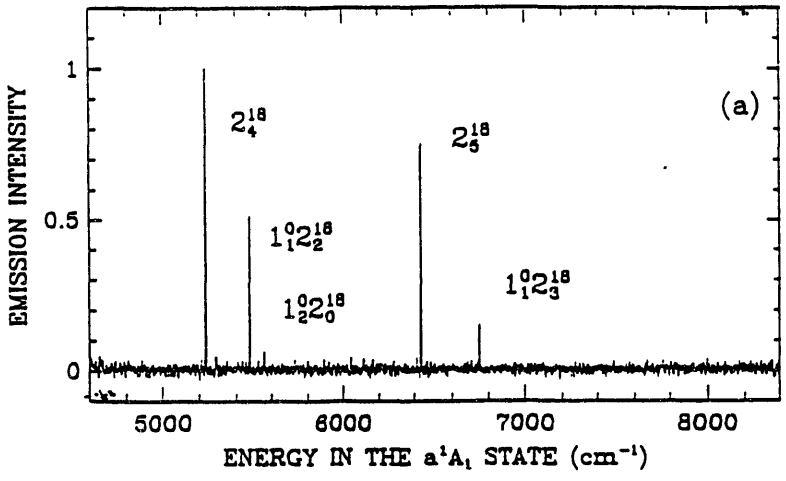

Fig 1: Fourier transform dispersed fluorescence spectra recorded after excitation of the CH_2 $\tilde{b}\ ^1B_1$ (0,18,0) $J_{K_aK_c}=0_{00}$ level. Five $\tilde{b}\rightarrow\tilde{a}$ vibrational bands can be seen and are labelled in the spectra. Each band consists of a single rotational transition, $0_{00}\rightarrow1_{10}$.

B. State-to State Rotational Energy Transfer and Reaction with Ketene of Highly Vibrationally Excited $\tilde{b}^1B_1$ CH_2

Dispersed fluorescence spectra from the CH_2 $\tilde{b}\ ^1B_1 \rightarrow \tilde{a}\ ^1A_1$ band were recorded with time-resolution by Fourier transform emission spectroscopy after pulsed excitation of a single rotational level of the $\tilde{b}^1B_1$ (0,16^0,0) state. Fluorescence observed from the initially excited level and from levels populated by rotational energy changing collisions with the bath gas (ketene) was used to deduce the state-to-state rate constants for rotational energy transfer and the state-resolved rate constants for total collisional removal of $\tilde{b}^1B_1$ CH_2. The observed propensity rules for rotational energy transfer — $\Delta J = \pm 2$, $\Delta K_a = 0$, and $\Delta K_c = \pm 2$ — are consistent with a quadrupole-dipole interaction between $\tilde{b}^1B_1$ (0,16^0,0) CH_2 and ketene. The existence of a quadrupole in the

intermolecular interaction suggests that the structure of CH_2 in the $\tilde{b}^1B_1$ $(0,16^0,0)$ state, averaged over the time of a collision, must be linear. The state-to-state rotational energy transfer rate constants range from approximately equal to the hard sphere gas kinetic rate to four times the gas kinetic rate, with the largest rate constants between rotational levels with the smallest energy gaps. Examination of fluorescence spectra recorded with polarization analysis shows that rotationally elastic ($\Delta J = 0$) M changing collisions are negligible. State-resolved rate constants for reactive collisions between $\tilde{b}^1B_1$ CH_2 and ketene were obtained by subtracting the rotational energy transfer contribution from the total rate constants for collisional removal of $\tilde{b}^1B_1$ CH_2 (obtained from a Stern-Volmer analysis). These rate constants vary from one to five times the hard sphere gas kinetic rate, and increase with rotational energy for the levels studied. Their magnitudes show that CH_2 is about two times as reactive in its $\tilde{b}^1B_1$ state than its $\tilde{a}^1A_1$ state.

III. Future Plans- Intramolecular Dynamics and Intermolecular Energy Transfer of Highly Excited Vibrational Levels Characterized by Time-Resolved IR Emission Spectra

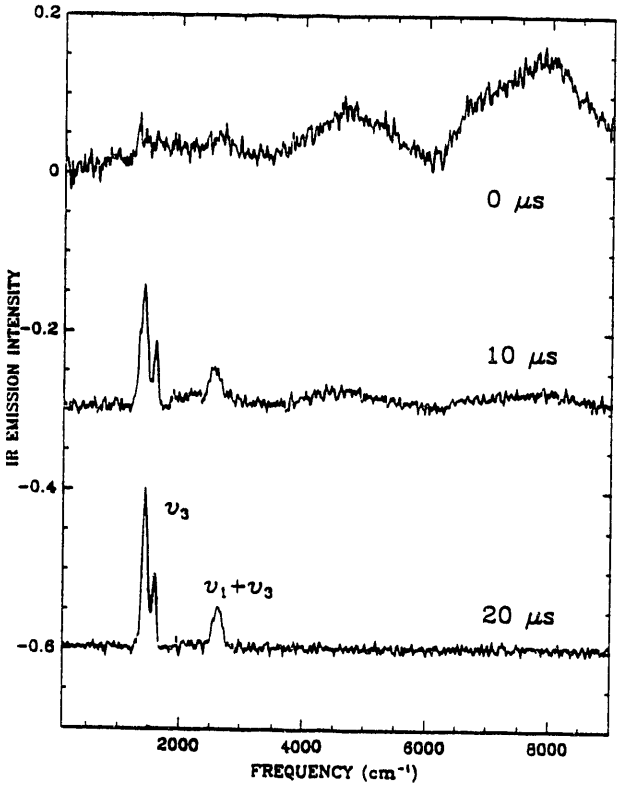

Figure 2 Time-resolved IR emission spectra from NO_2 (200mTorr) following the $\tilde{B}\leftarrow\tilde{X}$ excitation at 22,000 cm^{-1}.

Stimulated emission pumping or internal conversion followed by electronic excitation can be used to prepare molecules at highly excited vibrational levels with well defined energy. IR emission from these levels arises from vibrational transitions through harmonic oscillator selection rules and can be used to characterize their vibrational wavefunction. IVR in terms of coupling between the zeroth-order modes and isomerization reactions in terms of coupling between the zeroth-order structures can be probed. Furthermore, collisional relaxation of these highly excited levels can be monitored by detecting the IR emission from the subsequently populated lower vibrational levels. The figure shows that we have successfully recorded the IR emission spectra, in 50 ns time interval, from a 200 mTorr NO_2 gas following the $\tilde{B}\leftarrow\tilde{X}$ excitation

at 22,000 cm^{-1}, using the time-resolved FT emission spectroscopy. Congested IR emission spectrum at t=0 shows the complex vibrational characters of the vibrational levels at such high energy. Later-time emission shows a tremendous, but gradual, blue shift with time in the ν_3 peak position, indicating collision induced cascading of the excited vibrational levels.

IV. Publications from this project since 1991

The Chemical and Physical Properities of Vibration-Rotation Eigenstates of H_2CO (S_0) at 28,300 cm^{-1}

In "Advances in Molecular Vibrations" Ed. J. M. Bowman, (JAI press, Connecticut, 1991), pp.305-327, H. L. Dai

Vibrational Spectroscopy and Dynamics of Transient and Weakly Bound Molecules by Stimulated Emission Pumping

In "Advances in Multi-Photon Processes and Spectroscopy", Ed. S. H. Lin, (World Scientific, Teaneck New Jersey, 1991), Vol. 7, pp. 169-230, H. L. Dai

Time-resolved Fourier Transform Spectroscopy with $<10^{-7}$ Second Time- and 0.25 cm^{-1} Spectral Resolution in the Visible Region

Rev. Sci. Instr.,63, 3261-67 (1992)

G. Hartland, W. Xie, H. L. Dai, A. Simon, and M. J. Anderson

Strong Asymmetry Induced ΔK_a=3 Transitions in the CH_2 b $B_1 \rightarrow a A_1$ Spectrum: A Study by Fourier Transform Emission Spectroscopy

J. Chem. Phys. **97**, 7010-2 (1992)

Gregory V. Hartland, Wei Xie, Dong Qin, and Hai-Lung Dai

State-to State Rotational Energy Transfer and Reactions of Highly Vibrationally Excited b^1B_1 CH_2 with Ketene by Time-Resolved Fourier Emission Spectroscopy

J. Chem. Phys., in press

Gregory V. Hartland, Dong Qin, and Hai-Lung Dai

Fluoresence Excitation Spectrum of the $b^1B_1 \leftarrow \tilde{a} A_1 2_0^n$(n=18-23) Bands of CD_2

J. Mol. Spectr.., **158**, 162-9 (1993)

Wei Xie and Hai-Lung Dai

Fourier Transform Dispersed Fluorescence Spectroscopy: Observations of New Vibrational Levels in the 5,000-8,000cm^{-1} Region of $\tilde{a} A_1 CH_2$

J. Chem. Phys., **98**, 2469-72 (1993)

Gregory V. Hartland, Dong Qin, and Hai-Lung Dai

Highly Excited Vibrational Levels Studies by Time-Resolved Fourier Transform Emission Spectroscopy

SPIE Proc. Vol. 1856 (Int. Soc. Opt. Eng., Bellings, Washington, 1993), in press, G. V. Hartland, D. Qin, and H. L. Dai

Stimulated and Dispersed Emission Studies of the Excited Vibrational Levels of a Transient Molecule: Singlet Methylene, in "Molecular Dynamics and Spectroscopy by Stimulated Emission Pumping", ed.. H. L. Dai and R. W. Field, *Adv. Series in Physical Chemistry, (World Scientific, 1993).*

Gregory Hartland and Hai-Lung Dai

Intramolecular and Nonlinear Dynamics

Michael J. Davis

Chemistry Division
Argonne National Laboratory
Argonne, IL 60439

Research in this program focuses on three interconnected areas. The first involves the study of intramolecular dynamics, particularly of highly excited systems. The second area involves the use of nonlinear dynamics as a tool for the study of molecular dynamics and complex kinetics. The third area is the study of the classical/quantum correspondence for highly excited systems, particularly systems exhibiting classical chaos.

Recent Progress

Much of the recent progress involves the application of our hierarchical analysis of molecular spectra. The most important new aspect of this project has been the detailed mapping of energy transfer pathways present in highly excited molecular systems. Another important aspect of recent progress has been the further understanding of the eigenstates of dynamical systems in which the classical dynamics is strongly chaotic. Our past work concentrated on systems, which while they exhibited widespread chaos, could be understood by generating intramolecular bottlenecks. Eigenstates could be understood in terms of motion which was trapped within these bottlenecks. These more chaotic systems exhibit mixing which is closer to what is necessary to justify statistical theories of reactions in a rigorous manner, but still fall short, at least at the energies we have studied them, because the mixing occurs over a limited number of phase space regions. These regions are those defined by a demarcation based on the previously noted bottlenecks.

The figure summarizes some of our recent progress. It is divided into three sets of two rows, indicating three projects. The top two sets demonstrate the range of systems, extending from a model dynamical system in the top two rows to a fully three-dimensional study (J=0) of an $OHCl^-$ photodetachment spectrum done in collaboration with Koizumi and Schatz (middle two rows). The important feature of the top two rows is that a discernible and localized pattern emerges in the last plot of the top row and the first three plots of the second row, but the pattern is not present in the first four plots at lower energy (designated as "k" in the plots) or higher energy. These plots demonstrate a specific type of bottleneck to energy transfer which exists over only a narrow range of energy. Such processes point to the difficulty of assigning spectra of highly excited molecules over long energy ranges and point to the utility of our hierarchical analysis, which is a systematic approach to "divide and conquer" a spectrum. "Divide and conquer" refers to viewing a spectrum and intramolecular dynamics at all levels of resolution (i.e., time scales) and over all energy scales.

The results generated for the $OHCl^-$ photodetachment spectrum agree very favorably with those of Bradforth and Neumark, whose experimental spectrum shows very little structure. The hierarchical analysis of the theoretical spectrum of Koizumi and Schatz has demonstrated that initially the OHCl fragment shows stretching motion of the

H-atom with is mostly OH stretch. This is evident in the experimental spectrum when it is compared to the theoretical version. At longer times (not evident in the experimental spectrum), there is internal rotation, hindered rotation or bend motion (depending on where the wavefunctions are viewed in terms of the O-Cl distance). The fourth row of the figure shows internal OH rotation. These are plots of wavefunctions associated with the smoothed spectrum shown above them, with the numbers on the spectrum (1-4) corresponding to the states below it, moving from left to right. The coordinate system of these latter plots involve the O and Cl atoms being fixed (the O at the center and the Cl at the far right, center) and the H moving in the plane. At the O-Cl distance in the plot (5.91 au) the motion of the H in the plane involves rotation around the O-atom (internal OH rotation). The wavefunctions in the figure illustrate a sequence of internal rotor states of increasing angular momentum, with the number of angular nodes increasing from 7 to 10 in the plots.

The final two rows of plots in the figure demonstrate our work on energy transfer pathways. The demarcation of "quantum phase space" is indicated in the plot on the upper left of these two rows, and our methodology for generating pathways is indicated in the plot on the lower left. This plot shows a tree generated from the hierarchical analysis with a series of dots on its left half indicating a particular pathway. The series of plots moving from left to right in the bottom row show the energy transfer down this particular path (the first four dots on the tree, read from top to bottom). We can compare this energy transfer pathway to another one for a different spectrum of the same system, which is shown above it in the last four plots of this row (no tree is plotted for this case). The two spectra used to generate these plots result from similar initial condition (see the second plots in each row), but some of their energy transfer pathways can be quite different as indicated in the two rows of plots.

Future Plans

Several experimental and theoretical spectra will be studied using the hierarchical analysis. These include SEP spectra generated in Field's group and a theoretical model spectrum of HO_2 generated by Bowman and co-workers. It is expected that a detailed study of the energy transfer pathways in the vibrational dynamics of HO_2 will be undertaken. We also intend on studying Perry's model of IVR he uses to describe spectra obtained in his group. In addition we intend or initiating a detailed study with Gray on vibrational mixing caused by electronically nonadiabatic coupling. Another project will involve comparisons between the hierarchical analysis and the approach of Kellman and co-workers. A new project will be started involving the use of nonlinear dynamics to study complex chemical kinetics (with Skodje, Boulder).

Publications

M. J. Davis, R. S. MacKay, and A. Sannami, "Markov shifts in the Henon family", Physica D **52**, 171 (1991).

M. J. Davis, C. C. Martens, R. G. Littlejohn, and J. S. Pehling, "Classical dynamics and the nature of highly excited states", in *Advances in Molecular Vibrations*, J. M. Bowman, ed. (JAI Press, 1991).

M. J. Davis and R. T. Skodje, " Chemical reactions as problems in nonlinear dynamics: A review of statistical and adiabatic approximations from a phase space perspective", in *Intramolecular and Nonlinear Dynamics*, W. L. Hase, ed. (JAI Press, 1992)

M. J. Davis, "Smoothed eigenstates from molecular spectra", Chem. Phys. Lett. **192**, 479 (1992).

M. J. Davis, "Hierarchical analysis of molecular spectra", J. Chem. Phys. **98**, 2614 (1993).

M. J. Davis, "Trees from spectra: Generation, analysis, and energy transfer information", in *Molecular dynamics and spectroscopy by stimulated emission pumping*, H.-L. Dai and R. W. Field, eds. (submitted).

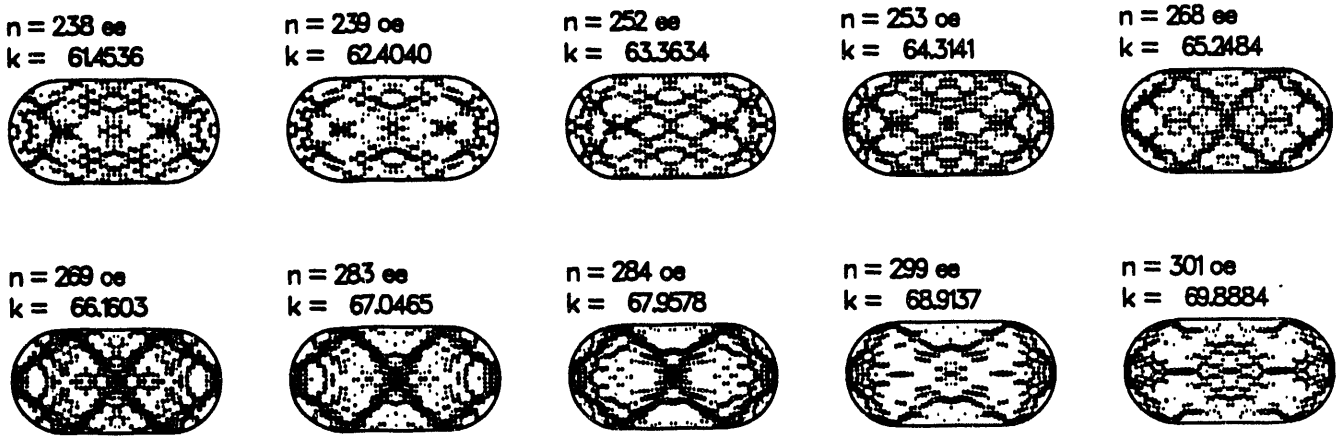
n = 238 ee
k = 61.4536
n = 239 oe
k = 62.4040
n = 252 ee
k = 63.3634
n = 253 oe
k = 64.3141
n = 268 ee
k = 65.2484
n = 269 oe
k = 66.1603
n = 283 ee
k = 67.0465
n = 284 oe
k = 67.9578
n = 299 ee
k = 68.9137
n = 301 oe
k = 69.8884

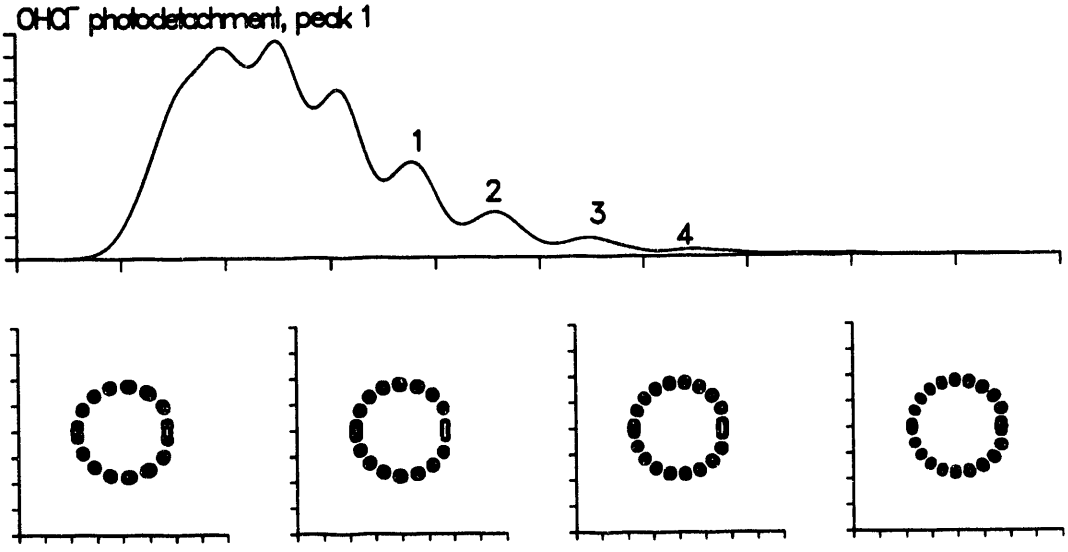
OHCl⁻ photodetachment, peak 1
1
2
3
4

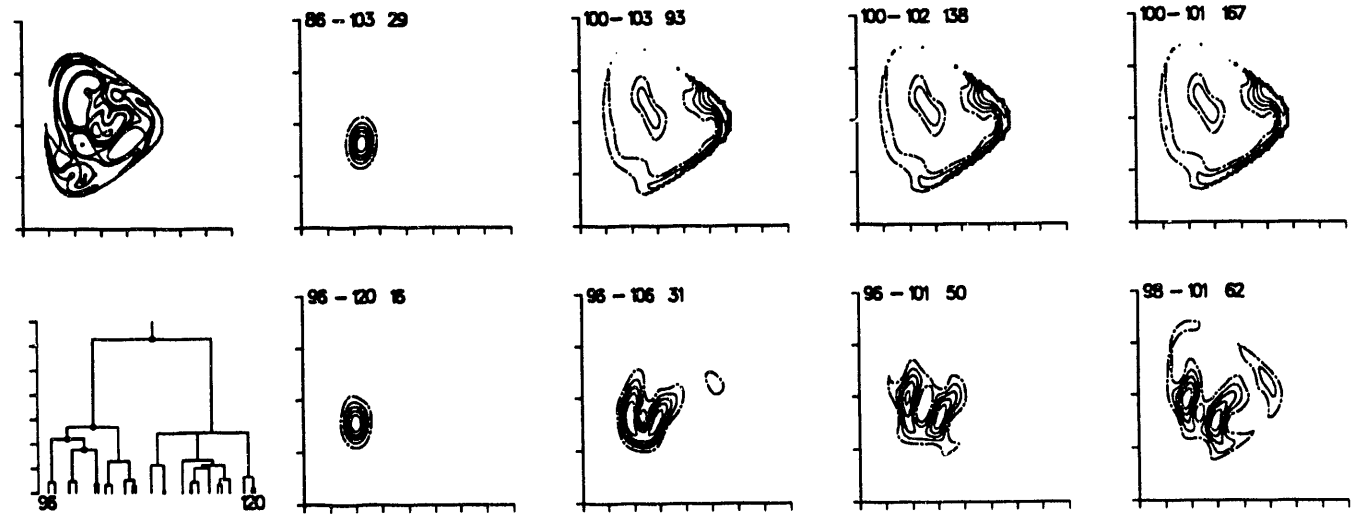
86 – 103 29
100 – 103 93
100 – 102 138
100 – 101 157
96 – 120 16
96 – 106 31
96 – 101 50
96 – 101 62
96
120

COMPREHENSIVE MECHANISMS FOR COMBUSTION CHEMISTRY: EXPERIMENT, MODELING, AND SENSITIVITY ANALYSIS

Frederick L. Dryer and Richard A. Yetter
Department of Mechanical and Aerospace Engineering
Princeton University, Princeton, New Jersey 08544-5263
Grant No. DE-FG02-86ER-13503

Program Scope

This research program is an integrated experimental/numerical effort to study pyrolysis and oxidation reactions and mechanisms for small-molecule hydrocarbon structures under conditions representative of combustion environments. The experimental aspects of the work are conducted in large diameter flow reactors, at pressures from one to twenty atmospheres, temperatures from 550 K to 1200 K, and with observed reaction times from 10^{-2} to 5 seconds. Gas sampling of stable reactant, intermediate, and product species concentrations provides not only substantial definition of the phenomenology of reaction mechanisms, but a significantly constrained set of kinetic information with negligible diffusive coupling. Analytical techniques used for detecting hydrocarbons and carbon oxides include gas chromatography (GC), and gas chromatography/Fourier Transform Infrared spectrometry (GC/FTIR) for off-line analyses. Non-Dispersive Infrared (NDIR) and FTIR methods are utilized for continuous on-line sample detection of light hydrocarbons, carbon oxides, oxygenated species, and water. Laser induced fluorescence and resonance absorption measurements of OH have also been performed in an atmospheric pressure flow reactor (APFR), and a variable pressure flow (VPFR) reactor is presently being instrumented to perform optical measurements of radicals and highly reactive molecular intermediates.

The numerical aspects of the work utilize zero and one-dimensional pre-mixed, detailed kinetic studies, including path, elemental gradient sensitivity, and feature sensitivity analyses. The program emphasizes the use of hierarchical mechanistic construction to understand and develop detailed kinetic mechanisms. Numerical studies are utilized for guiding experimental parameter selections, for interpreting observations, for extending the predictive range of mechanism constructs (by comparison with literature data from other kinetic experiments), and to study the effects of diffusive transport coupling on reaction behavior in flames. Modeling using well defined and validated mechanisms for the CO/H_2/Oxidant systems and perturbations of oxidation experiments by small amounts of additives are also used to derive absolute reaction rates and to investigate the compatibility of published elementary kinetic and thermochemical information.

Over the last two years, this program has: 1) Continued development of a comprehensive experimental data base for the $CO/H_2/O_2$ system; 2) Developed and continued refinement of a comprehensive kinetic mechanism for the $CO/H_2/O_2$ system; 3) Performed comprehensive mechanistic studies on formaldehyde oxidation, inclusive of APFR results and literature results from static reactors, shock tubes, and flames; 4) Performed a mechanistic study of APFR data on ethanol oxidation, including an estimation of the branching ratios for C_2H_5OH+X, X= OH, H and identification of elementary reactions needing additional study; 5) Completed and evaluated the first *insitu* optical diagnostic measurements of OH in the APFR; 6) Studied the uni-molecular decomposition rate for 1,3,5-Trioxane at temperatures from 700 to 800 K; 7) Demonstrated seeded perturbation experiments on the moist CO oxidation in flow reactors as a means to determine elementary rate constants for specific reactions; 8) Determined elementary rates for $CH_4+OH \rightarrow CH_3+H_2O$ at 1026 and 1140 K, and $C_3H_6+OH \rightarrow$ products at 1020 K; 9) Performed experimental studies of the H_2/O_2 reaction system at conditions between the extended-second and third explosion limits.

Recent Progress

Work in progress includes: 1) Experimental and mechanistic studies on the complex dependence of the moist CO oxidation rate on oxygen concentration; 2) Experimental and numerical studies on the H_2/O_2, and $CO/H_2/H_2O/O_2$ systems at pressures to 15 atm.; 3) Methanol oxidation studies to twenty atmospheres, with subsequent mechanistic studies inclusive of the previous APFR data, as well as literature results from shock tubes, static reactors and flames; 4) Extending prior OH resonance absorption techniques utilized in the APFR to the VPFR; 5) Developing a lamp-based resonance absorption approach to measure CH_3. These items are discussed in detail in the last progress report, and items 1-3 are briefly summarized here.

Studies in our laboratory [J. Roesler, R.A. Yetter, and F.L. Dryer, Combust. Sci. and Tech., 82, 87 (1992); 85, 1 (1992)], [1][1] show that oxygen addition has a counter-intuitive effect on the rate of moist CO oxidation, actually decreasing the rate below approximately 1040 K at atmospheric pressure (Fig. 1). The comprehensive model we developed earlier [11] qualitatively predicted this trend, but under-predicted the extent of inhibition. Using a new critically reviewed value for the rate of $HO_2+OH \rightarrow H_2O+O_2$[D.L. Baulch et al., J. Phys. Chem. Ref. Data, 21, 411 (1992)], the revised model was found to accurately predict the new inhibition data without affecting previous validation comparisons near atmospheric pressure. Full details are available elsewhere [1].

Experiments underway on both the H_2/O_2 and $CO/H_2O/O_2$ systems, extend earlier work [9] at conditions between the "extended" second and third H_2/O_2 explosion limits. Constant pressure, adiabatic H_2/O_2 experiments near the "extended" second limit show the transition from slow to fast reaction (from self-heating) as the system goes from nearly straight chain character to chain branching. Kinetically, this is due to the competition of the chain branching $H+O_2 \rightarrow O+OH$ and the terminating $H+O_2+M \rightarrow HO_2+M$ reactions. As the pressure is further increased, the $H+O_2+M \rightarrow HO_2+M$ reaction dominates the branching reaction so that the overall reaction rate is steady. The overall pressure dependence of the slow reaction is found to be proportional to $P^{0.56}$. Currently, the revised H_2/O_2 sub-set of the $CO/H_2/O_2$ mechanism offers a good description of the stoichiometric chemistry for the full pressure range studied. However, at fuel lean conditions where HO_2 and H_2O_2 chemistry is known to become more important, the model reaction rates are too fast relative to the experiment. Specific reactions most likely to be produce these discrepancies are presently being identified.

The effect of increased pressure on the $CO/H_2O/O_2$ system is also under study. At 1038 K, and between 3 and 6 atmospheres (Fig. 2), the effect of increasing pressure is to decrease the overall reaction rate (proportional to $P^{-0.5}$). The transition behavior resulting from crossing of the explosion limit is evident in Fig. 2. At higher pressures and for all stoichiometries, the model (with the revised HO_2+OH rate) is too fast relative to the data. Discrepancies are likely due to the increased importance of other reactions involving HO_2 which have similarly large uncertainties. Reaction flux and sensitivity analyses further suggest that inaccuracies in reaction rates for $CO+HO_2 \rightarrow CO_2+OH$ and $CO+O+M \rightarrow CO_2+M$, or in the pressure dependence of $CO+OH \rightarrow CO_2+H$ may also contribute to the noted dispcrepancies.

New experiments have been performed on methanol oxidation over a range of pressures from 1-20 atmospheres and temperatures from 1100-750 K, with the higher temperatures corresponding to the lower pressures. An equivalence ratio range from 0.4 to 2.5 was covered. Data for stoichiometric oxidation at 15 atmospheres are shown in Fig. 3. The solid lines are numerical predictions utilizing a newly developed mechanism initially based on our earlier atmospheric pressure work [T.S. Norton and F.L. Dryer, Int. J. Chem. Kin., 22, 219 (1990)]. The stable species detected by FTIR were methanol, formaldehyde, carbon monoxide, carbon dioxide, water and formic acid. In the rich oxidation experiments, 1,2-ethanediol (ethylene glycol) was detected following the depletion of oxygen. The absolute quantities of these species are still being determined, but preliminary estimates yield values in the 50-100 ppm range for each. The measured total carbon data for the experiments without inclusion of these species are constant to within ±5%. Hydrogen peroxide is expected in quantities of approximately 100-500 ppm; FTIR interferences from methanol, water and formaldehyde prevented its determination.

A small amount of carbon dioxide is detected at the first data point. Extrapolation of the first few points back to the time of injection does not yield a zero result (as is the result in the case of other species). This effect was much more pronounced in early experiments in which nearly 10% of the methanol was found to be converted to carbon dioxide by the first data point. After this initial amount was formed, the carbon dioxide mole fraction remained essentially constant until late in the reaction. This phenomenon was eventually shown to result from the presence of cupric oxide and cuprous oxides (both effective oxidation catalysts) resulting from anode/cathode erosion in an arc plasma gas heater similar to that used in the APFR [T.J. Held, Ph.D. Thesis, in progress; T.J. Held and F.L. Dryer, CSSCI/ESSCI Meeting, New Orleans, 1993] Similar catalytic effects have been noted in VPFR experiments on H_2/NO_2 mixtures [R.A. Yetter, N. Ilincic,

[1] Bracketed numbers refer to papers published under this grant (see below).

F.L. Dryer, M. Allen and J. Gaetto, 29th JANNAF Combustion Meeting, Hampton, VA, 1992]. This contamination and the resulting effects were reduced to the levels shown here in subsequent VPFR work by implementing a new electrical resistance gas heating method (utilized in the experiments shown here). Numerical modeling studies are presently in progress (Fig. 3) which encompass these new data as well as other static reactor, flow reactor, stirred reactor, shock tube and flame data in presently in the literature. Previous models do not account for the experimental indication that the fate of the hydroxymethyl (and perhaps also formyl) radical in the absence of oxygen is not solely decomposition. The elevated pressure (and thus concentration) and lower temperature relative to previous studies favors the possibility of some radical-radical reactions. The presence of formic acid and 1,2-ethanediol is an indication of some possible routes. The combination reaction of hydroperoxyl and hydroxymethyl radicals may yield an excited complex which could decompose, yielding formic acid, H and OH, or could rearrange and decompose, giving formic acid and water. 1,2-Ethanediol is an obvious hydroxymethyl recombination product.

Future Plans

Reaction systems of interest during the next year include those for pyrolysis and oxidation of simple oxygenates (especially, formaldehyde and acetaldehyde), and simple olefins (especially ethene). In addition to studying the H_2/O_2, $CO/H_2/O_2$ systems and perturbation of these systems by trace amounts of hydrocarbons, we hope to study H_2O_2 decomposition over similar pressure ranges. Our research emphasizes the extension of reaction kinetic studies on these small molecules to (higher) pressures and (lower) temperatures where the reaction of radicals with oxygen and the reactions involving RO_2 and HO_2 are important.

Publications and Theses, 1991 - Present

1. J.F. Roesler, R.A. Yetter, and F.L. Dryer, "On the Dependence of the Rate of CO Oxidation on O_2 Concentration", Comb. Sci. and Tech., Submitted, Jan. 1993.
2. S. Hochgreb and F.L. Dryer, "A Comprehensive Study on CH_2O Oxidation Kinetics", Combust. Flame, 91, 257 (1992).
3. R.A. Yetter and F.L. Dryer, "Inhibition of Moist Carbon Monoxide by Trace Amounts of Hydrocarbons", Twenty-Fourth International Symposium on Combustion, The Combustion Institute, Pittsburgh, PA, 1992. p. 757.
4. T.S. Norton and F.L. Dryer, "An Experimental and Modeling Study of Ethanol Oxidation Kinetics in an Atmospheric Pressure Flow Reactor", I.J. Chem. Kin., 24, 319 (1992).
5. S. Hochgreb and F.L. Dryer, "Decomposition of 1,3,5-Trioxane", J. Phys. Chem., 96, 295 (1992).
6. R.A. Yetter, F.L. Dryer, and D.M. Golden, "Combustion Kinetics for High Speed Chemically Reacting Flows", An invited Contribution to Major Research Topics in Combustion, ICASE/NASA Series, M.Y. Hussaini, A. Kumar and R.G. Voigt, eds., Springer-Verlag, NY, 1992. pp. 309.
7. S. Hochgreb, Ph.D. Thesis, Department of Mechanical and Aerospace Engineering, Princeton University, Princeton, NJ., April 1991. MAE 1910-T.
8. F.L. Dryer, "The Phenomenology of Modeling Combustion Chemistry", Part 1, Chapter 3, in Fossil Fuel Combustion - A Sourcebook, W. Bartok and A.F. Sarofim, eds., John Wiley and Sons Inc., NY, 1991.
9. M.L. Vermeersch, T.J. Held, Y. Stein, and F.L. Dryer, "Autoignition Chemistry of n-Butane in a Variable Pressure Flow Reactor:, SAE Transactions, 100, 645 (1991).
10. G.T. Linteris, R.A. Yetter, K. Brezinsky, and F.L. Dryer, "Hydroxyl Radical Concentration Measurements in Moist Carbon Monoxide Oxidation in a Chemical Kinetic Flow Reactor", Combust. and Flame, 86, 162 (1991).
11. R.A. Yetter, F.L. Dryer, and H. Rabitz, "A Comprehensive Reaction Mechanism for Carbon Monoxide/Hydrogen/Oxygen Kinetics", Comb. Sci. and Tech., 79, 97 (1991).
12. R.A. Yetter, F.L. Dryer, and H. Rabitz, "Flow Reaction Studies of Carbon Monoxide/Hydrogen/Oxygen Kinetics" , Comb. Sci. and Tech., 79, 129 (1991).
13. G.T. Linteris, K. Brezinsky, and F.L. Dryer, "A High Temperature 180 Degree Laser Induced Fluorescence Probe for Remote Trace Radical Concentration Measurements", Applied Optics Letters, 30, 381 (1991).

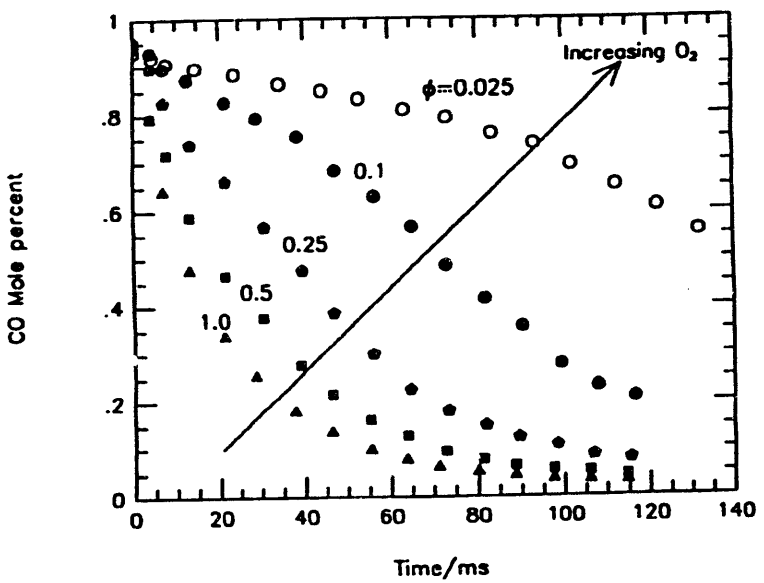

Figure 1: Effect of increasing oxygen concentration on the reaction rate of a moist CO reaction bath at 1 atm, 1000 K, 1% H_2O, 0.94% initial CO

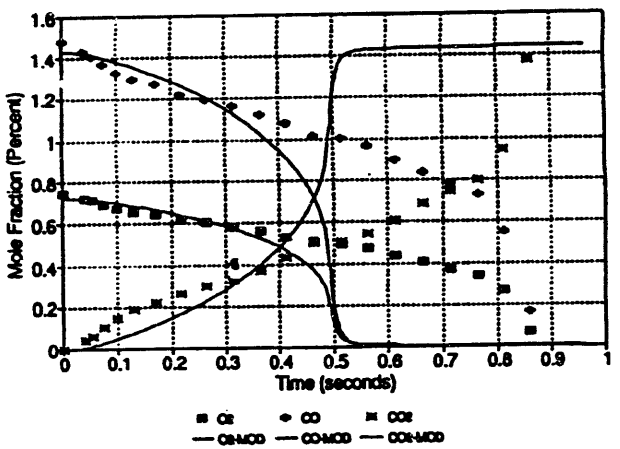

Figure 2: Moist CO oxidation at 6 atm, 1038 K, 0.78%

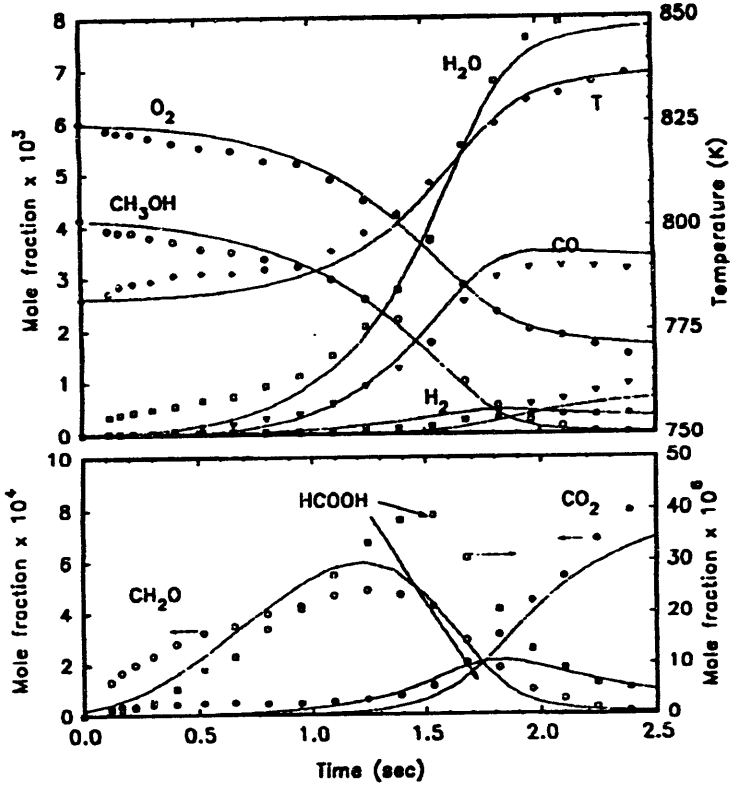

Figure 3: Methanol oxidation at 15 atm., 783K.

Kinetic Studies of Elementary Chemical Reactions

Joseph L. Durant, Jr.
Department 8353
Combustion Research Facility
Sandia National Laboratories
Livermore, CA

Our program concerning kinetic studies of elementary chemical reactions is presently focussed on understanding reactions of NHx species. To reach this goal we are pursuing experimental studies of reaction rate coefficients and product branching fractions, as well as using electronic structure calculations to calculate transition state properities and reaction rate calculations to relate these properties to predicted kinetic behavior. The synergy existing between the experimental and theoretical studies allow us to gain a deeper insight into more complex elementary reactions.

We have carried out a combined experimental and theoretical study of the reaction of NH(ND) ($^3\Sigma^-$) with NO aimed at understanding the product distribution from that reaction. The reaction was studied at room temperature using the discharge flow technique with mass spectrometric detection of the reaction products. Measured product branching fractions at room temperature for production of N_2O + H(D) were 0.87 ± 0.17 for ND ($^3\Sigma^-$) + NO and 0.84 ± 0.4 for NH ($^3\Sigma^-$) + NO (1 σ statistical errors). Stationary points on the HNNO potential energy surface were characterized using the Gaussian 2 *ab initio* method. The calculated energetics for the surface support the measured product

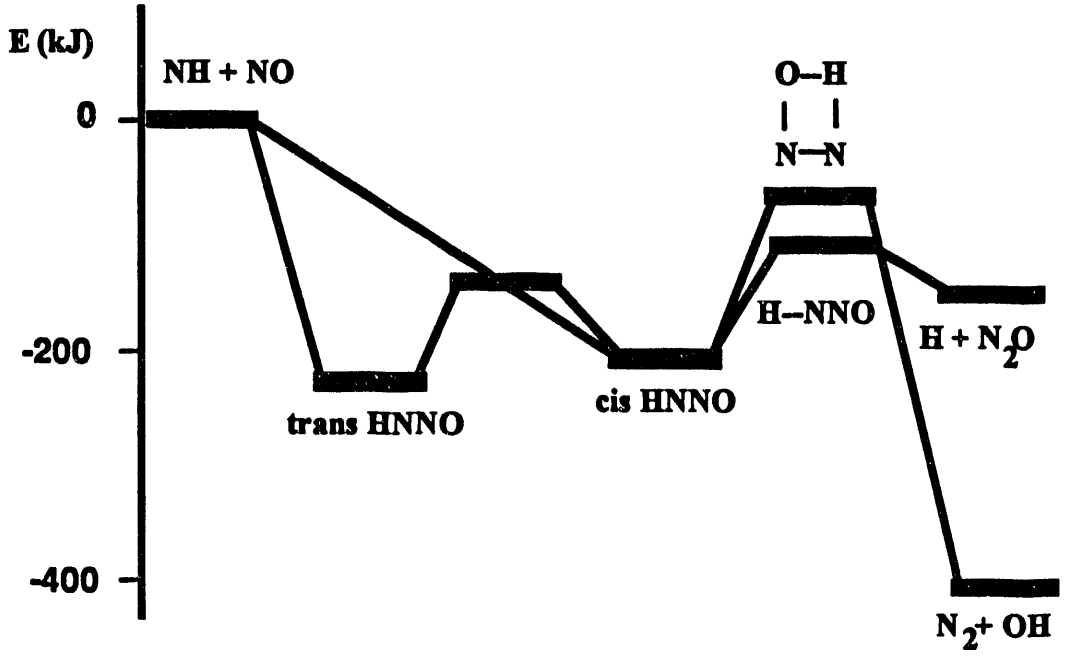

Figure 1: Schematic diagram of HNNO $^2A'$ potential energy surface.

branching fraction. The initial addition of NH ($^3\Sigma^-$) to NO produces both cis- and trans-HNNO. Barriers of 24 kcal/mole and 31 kcal/mole relative to cis-HNNO were located for dissociation of the cis isomer into H + N_2O and OH + N_2. The barrier to interconversion of the isomers was calculated to be approximately 18 kcal/mole, relative to the more stable trans-HNNO. The trans-HNNO was found to isomerize to the cis form before decomposing. The potential energy surface calculated explains the major features of the reaction.

Recently we have begun using discharge flow in conjunction with laser-photolysis/cwLIF to measure reaction rate coefficients of radical-atom and radical-radical reactions. We use discharge flow to produce the atom or radical which will be in excess, and then use laser-photolysis/cwLIF to produce and monitor the second radical species. We are now examining the reaction of NH_2 with O. Preliminary work has demonstrated the applicability of the method, and the high quality of NH_2-radical decay profiles possible.

The focus of our theoretical work recently has been the calculation of transition state properties using the Gaussian 2 (G2) methodology[G2] and a modification which we call G2Q. The ready availability of powerful workstations has given the experimentalist considerable computational horsepower. This, coupled with the easily implemented G2 methodology has made it possible for the non-specialist to calculate accurate heats of formation for many molecules. Pople and coworkers have performed extensive calculations to validate G2 for use on species at their equilibrium geometries, thus providing a realistic picture of the accuracy of the method.

We have quantified the performace of G2 for transition states by calculating properties for 9 transition states which have been thoroughly characterized. These transition states were either studied by use of CASSCF/MRCI methods, or by combination of

Table 1: Classical Barrier Heights (kcal/mole)

	G2	G2Q	literature
H+H_2 ($^2\Sigma$)	10.8	10.8	9.5
H+N_2 (^{2}A')	14.4	14.5	15.2
H+NO (^{3}A")	2.8	4.1	4.1
NH+O ($^5\Pi$)	5.3	5.4	5.5
NH+O ($^3\Pi$)	12.8	11.9	11.7
N+O_2 (^{2}A')	3.9	6.2	11.7; 6.6
H+F_2 ($^2\Sigma$)	1.8	2.8	2.1; 2.9[a]
O+H_2 ($^3\Pi$)	15.3	14.8	12.7; 14.7[a]
O+HCl (^{3}A")	10.6	10.4	8.5

a) energy does not include a multireference Davidson correction

experimental and theoretical results. Table 1 presents our results for calculation of the classical barrier heights for the 9 transition states studied. The G2 method performs well in predicting these energies (even for non-isogyric reactions), with an absolute average deviation of 1.5 kcal/mole. The G2 method uses MP2/6-31G* geometries and scaled HF/6-31G* frequencies. These methods have been documented to perform well for

equilibrium geometries. However, we find that the scaled HF frequencies perform very poorly in predicting transition state frequencies. The MP2 geometries are in less serious disagreement, but the predicted geometries, especially along the reaction coordinate, are still not as good as we desired. We investigated modifying the G2 method for use with transition states by using QCISD/6-311G** geometries and frequencies. The QCISD geometries and frequencies agree well with values from the literature, and this modified G2 procedure, which we call G2Q, offers improved performance in predicting transition state energies.

We have shown that G2 and G2Q work well for a broad class of transition states, including transition states on many excited-state surfaces and systems which have considerable spin contamination. With present-day workstations calculations on systems of three heavy atoms are tractable using G2Q and larger systems can be treated at the G2 level.

We are continuing our work on reactions of NHx species. Most exciting is the work using discharge flow/laser photolysis/cwLIF to study atom- and radical-radical reactions. We are continuing our work on the NH_2 + O system, both experimentally, using DF/LP/cwLIF to measure the reaction rate coefficient, and theoretically, using G2Q to study the potential energy surface.

Publications

J. A. Miller, J. V. Volponi, J. L. Durant, Jr., J. E. M. Goldsmith, G. A. Fisk and R. J. Kee, "The Structure and Reaction Mechanism of Rich, Non-Sooting C_2H_2/O_2/Ar Flames," Twenty-Third Symposium (International) on Combustion, 187 (1991).

J. L. Durant, Jr., "Anomalous Methoxy-Radical Yields in the Fluorine + Methanol → Products Reaction. I: Experimental," Journal of Physical Chemistry, **95**, 1070 (1991).

J. A. Gray, P. H. Paul and J. L. Durant, "Electronic Quenching Rates for NO($A^2\Sigma^+$) Measured in a Shock Tube", Chem. Phys. Lett., **190**, 226 (1992).

J. W. Thoman, Jr., J. A. Gray, J. L. Durant and P. H. Paul, "Collisional Electronic Quenching of NO($A^2\Sigma^+$) by N_2 from 200 to 4500 K", J. Chem. Phys., **97**, 8156 (1992).

J. L. Durant and C. M. Rohlfing, "Transition State Structures and Energetics Using Gaussian-2 Theory", J. Chem. Phys., in press.

LASER PHOTOELECTRON SPECTROSCOPY OF IONS

G. Barney Ellison
Department of Chemistry & Biochemistry
University of Colorado
Boulder, CO 80309-0215

Grant DE-FG02-87ER13695

During the last year we have (a) completed a review article that critically contrasts three methods to measure R-H bond energies, (b) finished a spectroscopic study of the phenylnitrene anion, and (c) successfully completed an overhaul of the light source of the photodetachment spectrometer. We have fabricated and installed an Ar III laser that provides us with approximate 100 W of 3.531 eV photons.

A. Many techniques[1] have been used to measure a huge number of bond dissociation energies and it is not our purpose to survey this massive field. Instead, we[2] have discussed three approaches that are commonly used to determine the R-H bond energies of *gas phase* polyatomic molecules: a) the study of radical kinetics, b) the use of negative ion thermochemical cycles, and c) photoionization mass spectroscopic techniques. It is essential to stress the *complementarity* of these three experimental methods; they are all inter-related. The goal of our essay was to dissect each of these methods in order to describe how the measurements are carried out, what the limitations are, and to demonstrate by direct comparison that all give the same bond energies. These three methods can be used on a large number of species (hundreds) and have an accuracy between ± 3 kcal/mol and ± 0.2 kcal/mol. The purpose of our article was to compare these three experiments with each other and to demonstrate by direct comparison that they achieve consistent results.

B. We have begun to study aromatic ions and the first[3] of our systems is the most famous organic nitrene, phenylnitrene. Our approach to the study of C_6H_5N is to scrutinize the photoelectron spectrum of the radical anion, $C_6H_5N^-$. The negative ion photoelectron spectra furnish us with a measure of the electron affinity of phenylnitrene; EA(C_6H_5N) is 1.45 ± 0.02 eV and EA(C_6D_5N) is 1.44 ± 0.02 eV. The photoelectron spectrum of $C_6H_5N^-$ is composed of an extensive Franck-Condon envelop which suggests that the electric charge is strongly delocalized over the radical anion. Besides detachment of the $C_6H_5N^-$ ion to the ground state of phenylnitrene, $\tilde{X}\,^3A_2$, our spectra also contain bands which belong to the singlet state of C_6H_5N, $\tilde{a}\,^1A_2$. The ΔE_{ST} is 18.0 ± 0.5 kcal/mol in excellent agreement with recent *ab initio* computations.[4]

The ground states of several nitrenes have been studied by EPR spectroscopy and all but aminonitrenes are known to be a triplets. Phenylnitrene can be written as a localized diradical with

a (p_x,p_y) pair of electrons triplet-coupled. Consequently the ground state of C_6H_5N is $\tilde{X}\,^3A_2$ and we can represent our negative ion photodetachment experiment as:

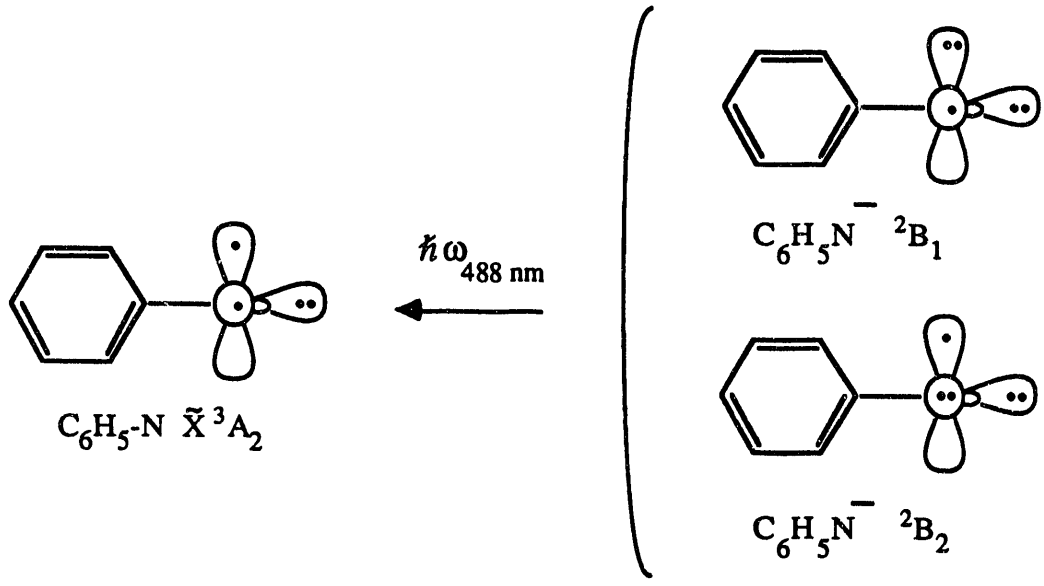

This suggests that we need to consider two different states for the $C_6H_5N^-$ ion. One of these, $^2B_2$, is a ($\sigma\pi^2$) species while the $^2B_1$ state is a ($\sigma^2\pi$) ion. The extensive Franck-Condon envelop in our spectra is a clear indication[5] that the ground state of the $C_6H_5N^-$ ion has a substantially different geometry than C_6H_5N. The extended Franck-Condon contour in our photodetachment spectra with excitation of ring-breathing modes implies that the ground state of the $C_6H_5N^-$ ion is $\tilde{X}\,^2B_2$ and that much of the charge is delocalized from the N atom onto the phenyl ring. This contrasts with the $\tilde{A}\,^2B_1$ ion which localizes the extra electron in the b_2, non-bonding orbital, on the N atom. Preliminary UHF calculations on both states of the $C_6H_5N^-$ ion in a 6-311++G** basis lead to the $^2B_2$ state being stabilized by about 10 kcal/mol below the $^2B_1$ state. Fig. 1 is a symbolic drawing which contrasts the electronic states of NH with those of C_6H_5N.

C. In our previous laser system, the photoelectron spectrometer was placed in the extended cavity of an Ar II ion laser (Spectra-Physics model 171-08). By using the multimode intracavity radiation working on a single line in the visible region (488 nm or 514.5 nm), we were able to achieve a circulating power of roughly 100 W with a beam waist of 0.2 mm. The most energetic line that we could access with our standard Ar II laser was the line at λ_o = 488.0 nm which generates 2.540 eV photons. We were thus limited to studying molecular ionic systems which are bound by 2.540 eV or less. In order to address these problems, we have fabricated a laser build-up

system which will generate over 100 W of UV laser light with a polarization that can be easily varied.

This new build-up cavity, see Fig. 2, is essentially a Fabry-Perot interferometer. When the cavity length supports an integral number of wavelengths one gets constructive interference. The length of the build-up cavity is defined by the length of our vacuum chamber housing the hemispherical analyzer. The cavity mirrors serve as the vacuum windows. The theoretical amplification of light is given by the expression

$$\frac{I_{CIR}}{I_{INC}} = \frac{2\left[(1 - R_1)(1 - R_2)\right]^{\frac{1}{2}}}{\left[1 - (R_1 R_2)^{\frac{1}{2}} \exp(-\delta)\right]^2}$$

where R_1, R_2 are the reflectivities of the mirrors and and δ is a loss factor. I_{CIR} is the circulating intensity inside the build-up cavity and I_{INC} is the incident intensity. The amplification of the above system is $I_{CIR}/I_{INC} \cong 350$. Simply stated, the intensity of useable laser radiation at $\lambda = 351.1$ nm (3.531 eV) could be as large as (1.0 W)•(350) or roughly 350 W. The actual working amplification factors are I_{CIR}/I_{INC} equal to 100—350, due to additional losses in the laser system. Taking into account these added losses, we are still able to generate over 100 W of circulating power of 351.1 nm light.

The optical system sketched in Fig. 2 is structured around the Coherent INNOVA 200-25/7 Ar III ion laser operating in the 330-364 nm region. The laser operates single frequency on the 351.1 nm line by using a solid etalon and prism. The light passes into an acousto-optic modulator, which serves to isolate the laser and build-up cavities. The AOM also modulates the laser light with a dither frequency from a frequency generator. This dither is used to generate an error signal used for correction of frequency drift of the laser and build-up cavities. Approximately 0.2% of the light is transmitted out of the build-up cavity and strikes a photodiode. The photodiode signal then enters a phase sensitive lock-in detector. The error function generated from the photodiode signal and the frequency generator is analyzed and the magnitude of the correction determined. This correction is carried out by a set of three servoamplifiers which drive a piezoelectric ceramic translator on the end mirror of the laser cavity, a piezoelectric translator on the entrance mirror of the build-up cavity, and the frequency shift of the AOM.

We have achieved a stable lock to the final build-up cavity. Initial test results of the system produced a stable amplification for extended periods of time (over one hour). Excellent mode

structure allowed us to adjust both the gain of the servo-amplifiers and the integration time constant for maximum amplification. By measuring the intensity of injected laser radiation as well as the intensity of the transmitted beam, we can esimate the actual build-up of power within the cavity.

DOE Publications/1991—1993

1. D.C. Cowles, M.J. Travers, J.L. Frueh, and G.B. Ellison, "Photoelectron Spectroscopy of CH_2N^-" J. Chem. Phys. **94**, 3517-3528 (1991); J. Chem. Phys. **95**, 3864 (1991).

2. M.J. Travers, D.C. Cowles, E.P. Clifford, and G.B. Ellison, "Photoelectron Spectroscopy of the Phenylnitrene Anion," J. Am. Chem. Soc. **114**, 8699-8701 (1992).

3. T.T. Dang, E.L. Motell, M.J. Travers, E.P. Clifford, G.B. Ellison, C.H. DePuy, and V.M. Bierbaum, "Experimental and Computational Studies of Deuterated Ethanols: Gas Phase Acidities, Electron Affinities, and Bond Dissociation Energies" Int. J. Mass Spectrom. Ion Processes **123**, 171-185 (1993).

4. J. Berkowitz, G.B. Ellison, and D. Gutman, "Three Methods to Measure RH Bond Energies," Annu. Rev. Phys. Chem. (submitted, 1993).

REFERENCES

1 Some of the "standard reviews" are: S.W. Benson, Chem. Rev. **78**, 23 (1978); D.F. McMillen and D.M. Golden, Ann. Rev. Phys. Chem. **33**, 493 (1982); J.B. Pedley, R.D. Naylor, and S.P. Kirby, *Thermochemical Data of Organic Compounds*, 2nd Ed. (Chapman and Hall, New York, 1986); D. Griller, J.M. Kanabus-Kaminska, and A. Maccoll, J. Mol. Structure (Theochem) **163**, 125 (1988).

2 J. Berkowitz, G.B. Ellison, and D. Gutman, "Three Methods to Measure RH Bond Energies," Annu. Rev. Phys. Chem. (submitted, 1993).

3 Michael J. Travers, Daniel C. Cowles, Eileen P. Clifford, and G. Barney Ellison, J. Amer. Chem. Soc. **114**, 8699 (1992).

4 S-J Kim, T.P. Hamilton, and H.F. Schaefer III, J. Amer. Chem. Soc. **114**, 5349 (1992); D.A. Hrovat, E.E. Waali, and W.T. Borden, J. Amer. Chem. Soc. **114**, 8700 (1992).

5 The charge delocalization onto the phenyl ring in $C_6H_5N^-$ is completely analogous to that previously found in the benzyl and phenoxide anions. For example, detachment of the $C_6H_5O^-$ ion is accompanied by excitation of ring breathing modes of the phenyl ring. See R.F. Gunion, M.K. Gilles, M.L. Polak, and W.C. Lineberger, Int. J. Mass Spectrom. Ion Proc.**117**, 601 (1992).

Nitrene States

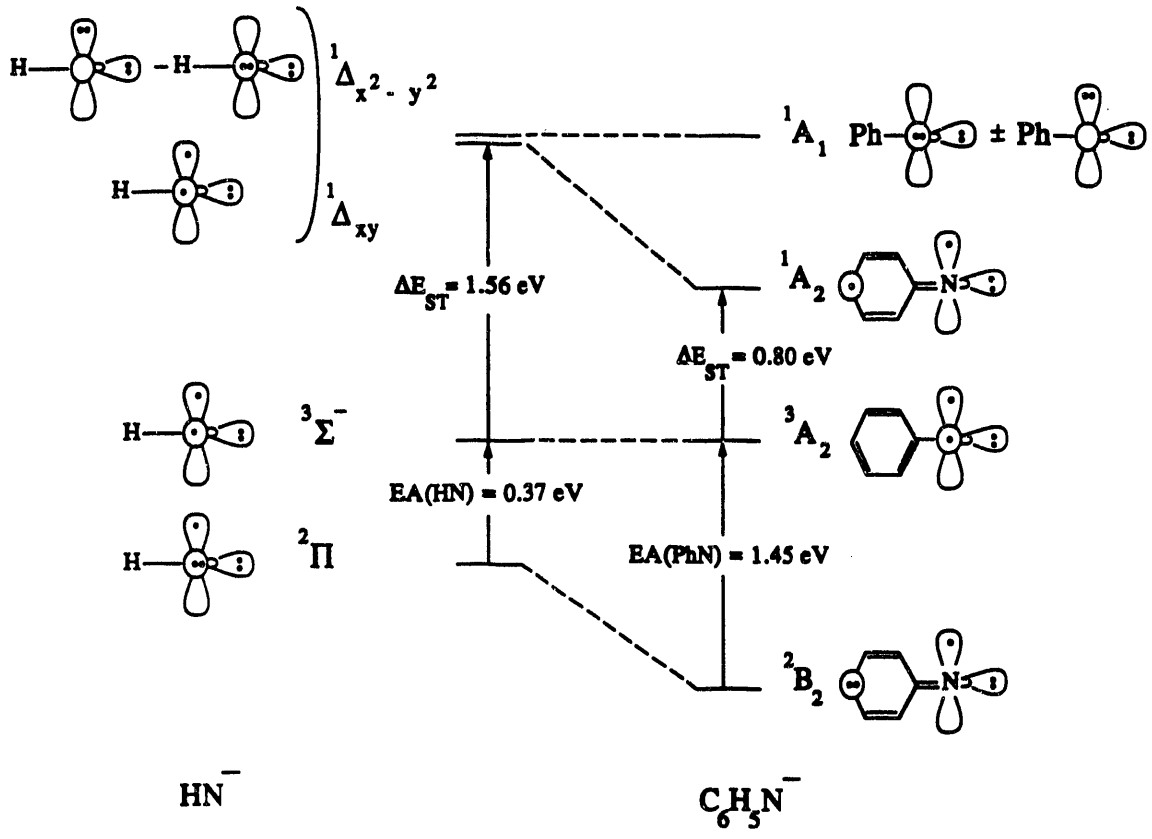

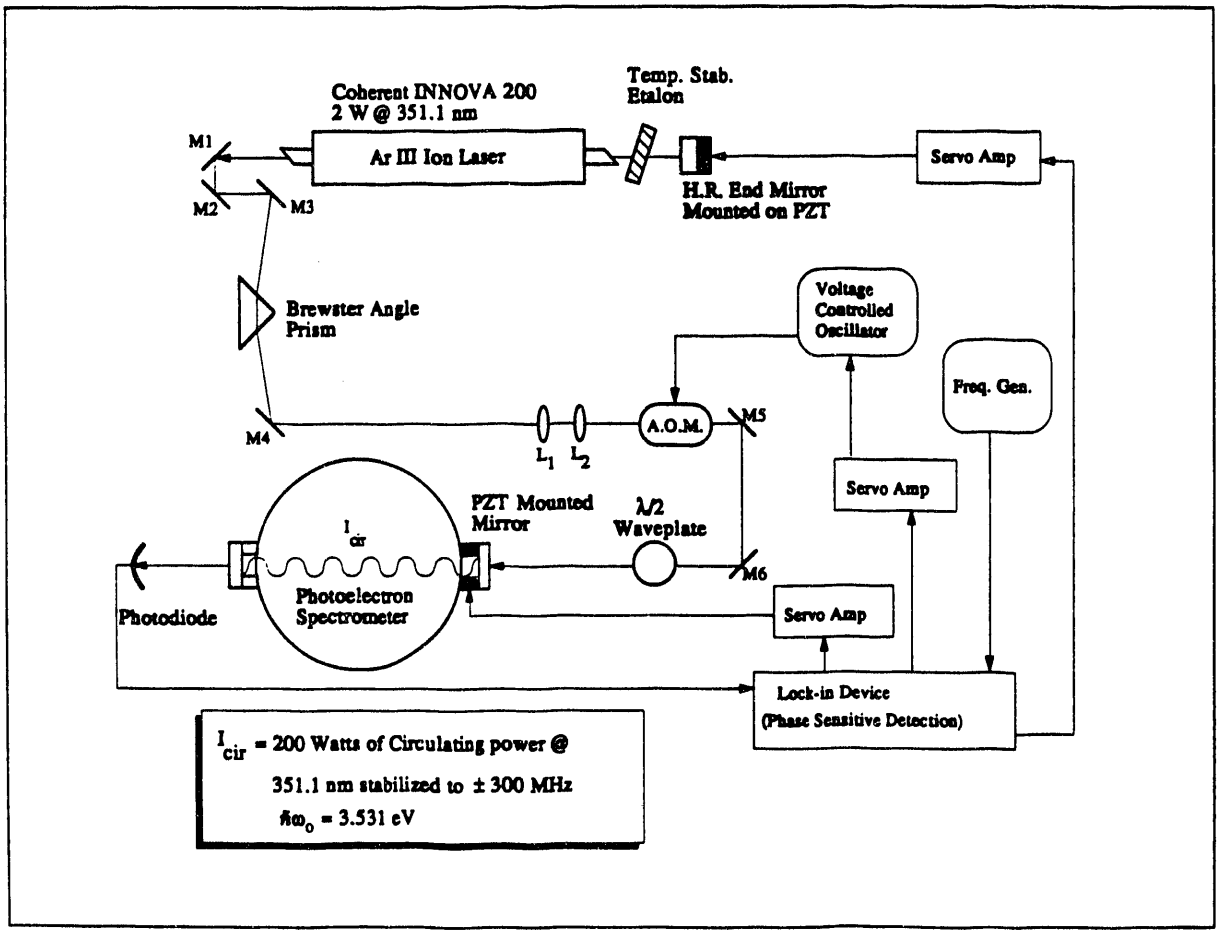

Low Energy Ion-Molecule Reactions

James M. Farrar
Department of Chemistry
University of Rochester
Rochester, NY 14627

Project Scope

This project is concerned with elucidating the dynamics of elementary ion-molecule reactions at collision energies near and below 1 eV. From measurements of the angular and energy distributions of the reaction products, we infer intimate details about the nature of collisions leading to chemical reaction, the geometries and lifetimes of intermediate complexes that govern the reaction dynamics, and the collision energy dependence of these dynamical features. We employ the crossed beam low energy mass spectrometry technology that we have developed over the last several years, and the focus of our current research is on proton transfer and hydrogen atom transfer reactions of the O^- ion with species such as HF, H_2O, and NH_3.

Recent Progress

Our work during the past year has focused on vibrational state resolved studies of the O^- + HF reaction, as well as the application of a classical inversion method to reactive and nonreactive collisions with the goal of extracting deflection functions for the scattering fluxes and opacity functions for chemical reaction.

The proton transfer reaction between O^- and HF

$$O^- + HF \rightarrow OH + F^- \qquad \Delta H^\circ = -0.48 \text{ eV}$$

has been examined by Hamilton *et al.*[1] in thermal energy flow tube studies by probing the OH (v'=0, 1) vibrational states with LIF. More recently, drift tube studies by Knutsen *et al.*[2] have yielded product state distributions over an expanded range of incident kinetic energies up to 0.23 eV, which showed that, relative to the thermal energy reference data, incremental translation appears to be partitioned preferentially into product vibration. Knutsen *et al.* have interpreted this observation as a consequence of the attractive well on the potential surface, estimated from *ab initio* calculations to be 1.94 eV relative to the reagents.[3] The principle drawback of product state distribution measurements such as these is their inability to provide definitive evidence for the participation of intermediate complexes. In the present study, we have examined the energy and angular distribution for the O^- + HF reaction at a collision energy approximately twice as large as the upper limit in the drift tube work, but still only one-fifth of the calculated $[OHF]^-$ well depth. With favorable kinematics, we are able to extract vibrational state populations for the nascent OH product, as well as to provide direct evidence for the participation of a transient complex in the proton transfer reaction.

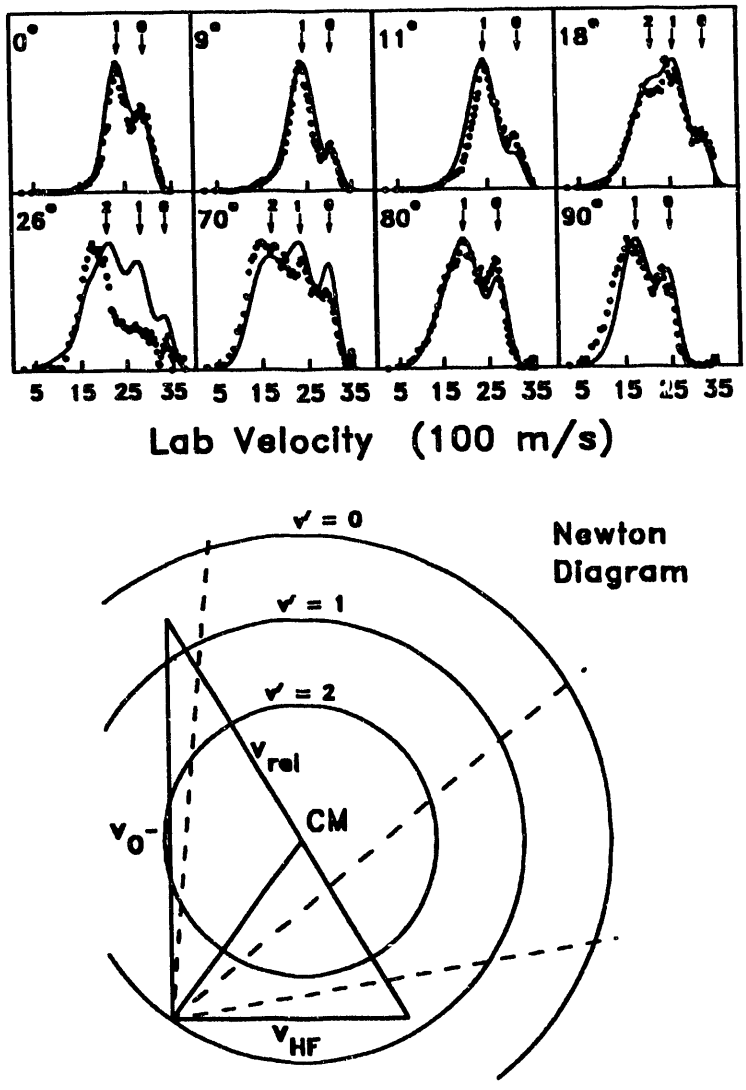

Figure 1: F^- fluxes for the O^- + HF system at E_{rel} = 0.42 eV.

system at a collision energy of 0.42 eV. The data show clear contributions from from OH in vibrational states v' = 0, 1, and 2. Kinematic analysis that includes parametric kinetic energy and angular distribution cross sections for each OH product vibrational state yields a cross section ratio of 0.54: 0.40: 0.06 for v'=0: v'=1: v'=2. This product state distribution is in qualitative agreement with phase space theory, although the measured distribution has more v'=1 and less v'=0 than predicted by the calculations. The complete product barycentric flux distribution is shown in Figure 2 and demonstrates forward-backward symmetry associated with the formation of a transient O^-·HF complex that lives several rotational periods. Although previous studies of this reaction have speculated that such a complex should mediate the dynamics, product state distributions appear to be dominated by the Heavy + Light-Heavy mass combination rather than the details of the potential surface. The present experiment is the first direct observation of the complex.

Recently, we have begin to apply a classical inversion technique to our reactive collision data. The method, based on work by Gilbert and collaborators,[4] requires that both reactive and non-reactive cross sections be measured. The cross sections are written in terms of deflection functions for reactive and non-reactive collisions as well as an opacity function for reaction. The latter quantity is particularly interesting in the context of proton transfer reactions. The O^- + H_2O system provides a particularly good illustration of the method. At the lowest collision energies, our data show two channels: a direct, rebound channel producing OH^- in the backward direction, as well as a collision complex channel yielding a symmetric forward-backward flux distribution. The opacity function analysis shows clearly that the rebound channel occurs with a narrow range of impact parameters out to about 1 Å, while collision complex formation is governed by a wider range of impact parameters out to about 3Å. With increasing energy, the collision complex components to the cross section attenuate and the formation of products by stripping reactions is governed by large impact parameters out to 3Å. At present, this model is based on angular distributions only, and one goal of our research for the next year will be to incorporate energy-dependent terms in the deflection functions such that we can include differential cross sections in energy in the analysis.

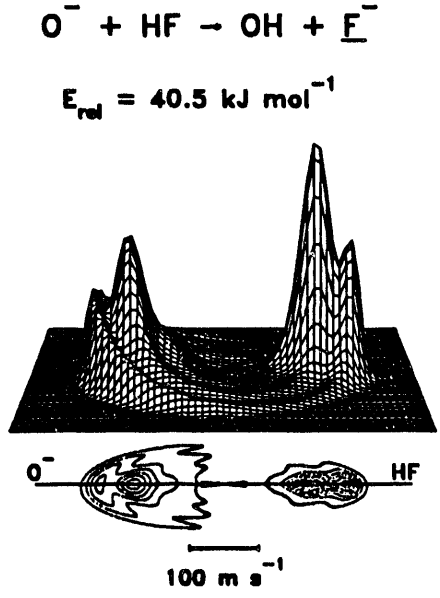

Figure 2: Barycentric flux distribution for F^- product

Future Plans

We will focus our efforts on further developments of the inversion method for reactive collisions. Experimentally, we will examine the behavior of the O^- + HF reaction at higher collision energies. We will also begin to look at isotope exchange reactions such as OD^- + NH_3 → OH^- + NH_2D. With the acquisition of a narrow bandwidth optical parametric oscillator, we also hope to explore proton transfer and isotope exchange reactions in which we excite overtones in reagents such as H_2O, NH_3, and HF to explore the role of the competition between selective vibrational excitation and translational energy.

References

1. C. E. Hamilton, M. A. Duncan, T. S. Zwier, J. C. Weisshaar, G. B. Ellison, V. M. Bierbaum, and S. R. Leone, *Chem. Phys. Lett.* **94**, 4 (1983).

2. K. Knutsen, V. M. Bierbaum, and S. R. Leone, *J. Chem. Phys.* **96**, 298 (1992).

3. S. E. Bradforth, D. W. Arnold, R. B. Metz, A. Weaver, and D. M. Neumark, *J. Phys. Chem.* **95**, 8066 (1991).

4. M. A. Collins and R. G. Gilbert, *Chem. Phys. Lett.* **41**, 108 (1976); S. M. McPhail and R. G. Gilbert, *Chem. Phys.* **34**, 319 (1978).

Publications

D. F. Varley, D. J. Levandier, and J. M. Farrar, "Dynamics of the Reaction of O^- with H_2O: Reactive and Nonreactive Decay of Collision Complexes," *J. Chem. Phys.* **96**, 8806 (1992).

D. J. Levandier, D. F. Varley, and J.M. Farrar, "Low Energy Ion-Molecule Reaction Dynamics: Complex and Direct Collisions of O^- with NH_3," *J. Chem. Phys.* **97**, 4008 (1992).

J. M. Farrar, "Crossed Beam Studies of Ion-Molecule Complexes: Collisions and Clusters", in *Advances in Classical Trajectory Methods*, Vol. 2, "Dynamics of Ion-Molecule Complexes", edited by W.L. Hase, JAI Press, 1993, p. 0000, in press.

D. J. Levandier, D. F. Varley, M. A. Carpenter, and J. M. Farrar, "A Crossed Beam Study of Ion-Molecule Proton Transfer Dynamics: Vibrational State-Resolved Products in the O^- + HF Reaction", *J. Chem. Phys.* **99**, XXXX (1993), accepted for publication.

Quantitative Degenerate Four-Wave Mixing Spectroscopy: Probes for Molecular Species

R. Farrow, D. Rakestraw, P. Paul, R. Lucht, P. Danehy†, E. Friedman-Hill and G. Germann

Combustion Research Facility
Sandia National Laboratories
Livermore, CA 94550

Program Scope

Resonant degenerate four-wave mixing (DFWM) is currently the subject of intensive investigation as a sensitive diagnostic tool for molecular species.[1] DFWM has the advantage of generating a coherent (beam-like) signal which results in null-background detection and provides excellent immunity to background-light interference. Since multiple one-photon resonances are involved in the signal generation process, the DFWM technique can allow sensitive detection of molecules via electronic, vibrational or rotational transitions. These properties combine to make DFWM a widely applicable diagnostic technique for the probing of molecular species.

We are conducting fundamental and applied investigations of DFWM for quantitative measurements of trace species in reacting gases. During the past year we have focused our efforts in two areas: (1) understanding the effects of collisional processes on the DFWM signal generation process, and (2) exploring the applicability of infrared DFWM to detect polyatomic molecules via rovibrational transitions.

Recent Progress

Although DFWM is a four-wave mixing process, it can also be viewed as a laser-induced grating technique. Three beams are input to the sample, historically referred to as the forward and backward pump beams and the probe beam. The probe beam and one of the pump beams interfere in the medium to form a field-intensity grating. If the laser is tuned to an allowed transition, an excited-state population grating is "written" in the medium, corresponding to a finite saturation of absorption in the fringes of the grating. The other pump beam diffracts from this saturation grating, generating the signal beam.

This simple picture yields insight into the effects of various processes affecting DFWM, such as saturation, electronic quenching, rotational energy transfer (RET), and thermal-grating formation. For example, increasing the laser intensity to the point of extreme saturation should result in reduced scattering efficiency, due to reduction of the contrast of the population grating. Collisions can lead to electronic quenching of the upper-state grating and to energy transfer out of both upper- and lower-state gratings, also reducing the strength of the gratings. In addition, thermal gratings can be formed as internal molecular energy is converted to translational energy (heat), and can be probed via the resulting perturbation of the index of refraction of buffer gases. To quantitatively interpret DFWM intensities, thermal-grating scattering must be distinguished from that of population gratings, as the mechanisms of forming and probing these two types of gratings have different dependencies on pressure, laser detuning and intensity, and absorption cross-section.

To investigate these effects in greater detail we are performing two-color, uv four-wave mixing measurements. A tunable laser provides probe and forward pump beams to initially generate a grating, and a second (independently tunable and delayable) laser provides a backward pump beam to probe the grating. The former is a single-mode pulsed laser, consisting of a pulse-amplified ring-dye laser which is frequency-doubled and mixed with the fundamental from an injection-seeded Nd:YAG laser. The latter is a grating-tuned pulsed laser with an intra-cavity etalon which is frequency-tripled. The outputs of both lasers are independently tunable near 226 nm, with programmable relative pulse timing, pulse energies up to 1 mJ, and respective bandwidths of ~0.004 cm^{-1} and ~0.05 cm^{-1}. We are investigating mixtures of NO with N_2 and/or CO_2 in a static cell, using total pressures from 50 to 1100 Torr and NO pressures typically below 50 mTorr. All beams have vertical polarizations and are collimated and apertured to diameters ranging from 2-3 mm.

---

†High-Temperature Gas Dynamics Laboratory, Department of Mechanical Engineering, Stanford University.

CO_2 and N_2 were selected as buffer gases for these studies because their respective quenching cross-sections for the *A* state of NO have a ratio of at least 1000:1,[2] while their collisional broadening coefficients are similar to within 3%. Thus, mixtures of CO_2 and N_2 can be prepared that provide an enormous variation in NO quench rate but which have the same NO line-broadening and nearly the same pressures. We have recently performed DFWM studies in such mixtures to investigate the effects of quenching on DFWM signal intensities. To briefly summarize the results, we found that for low (100 Torr) buffer-gas pressures and non-saturating laser intensities, DFWM signals decreased moderately (~50%) as the quenching rate increased by more than 10^3. For saturating laser intensities, the decrease was even milder (~15%). The decreases in both cases were in quantitative agreement with a two-level DFWM theory[3] and a detailed direct numerical simulation,[4] with the latter giving best agreement for strong saturation. The observed insensitivity to quench rate can be explained by the fact that quenching rates are additive with RET rates in determining the DFWM signal strength (both serve to depopulate the resonant NO levels), and the latter tends to mask the former. In contrast, laser-induced fluorescence (LIF) experiments are typically performed with broadband detection so that LIF signals are unaffected by RET but are nearly inversely proportional to quench rate.

Studies with higher buffer pressures of CO_2 (>200 Torr) revealed that thermal-grating (TG) processes were contributing significantly to the DFWM signal. For mixtures of N_2 and CO_2 near 300 Torr, the DFWM signal actually *increased* with increasing quenching (CO_2 mole fraction), by up to ~800%. At these higher pressures, population-grating contributions were diminished as a result of faster collisional dephasing and depopulation processes, while TG formation was enhanced by faster quenching and collision-aided heat release, by decreased thermal diffusion, and by the increased index of refraction. Figure 1 shows DFWM intensity measurements plotted against CO_2 pressure, for various backward pump-pulse delays relative to the probe/forward pump pulses. For a 2-ns delay, the signal initially decreases with increasing pressure, as expected for a population-grating mechanism.[3] At 200 Torr, the trend reverses and the signal begins increasing with buffer pressure, as result of TG scattering. With a 10-ns delay the laser pulses remain partially overlapped so that the population-grating signal is still observed, but the TG signal has increased slightly. With the pulses completely separated at a 22-ns delay, the population-grating signal can no longer be observed and TG scattering is completely isolated.

The distinctive temporal beats characteristic of TG scattering are illustrated in Fig. 2 in a backward-pump time-delay scan performed with 1000 Torr of CO_2. Similar beats have been observed in gas-phase, two-color FWM of methanol by Hayden *et al.*[5] and of OH in a flame by Williams *et al.*[6] The beats result from the excitation of standing acoustic waves by the sudden deposition of a heat grating; as the waves propagate through a fixed point in space the resulting pressure fluctuations modulate the DFWM scattering efficiency. The solid curve in Fig. 2 is a calculation of the transient spatial modulation of the index of refraction of CO_2 generated by a thermal grating, squared and convolved with a gaussian laser pulse shape. The calculation is based on a one-dimensional solution of the linearized hydrodynamics equations and makes use of known gas constants and the measured angle between the probe and pump beams (which determines the grating spacing).

The extension of DFWM into the infrared spectral region promises to allow application to a much larger variety of molecules through the use of infrared absorption. We have extended our previous investigations of diatomic molecules[7] to include several polyatomic species. We have demonstrated sensitive detection of methane and acetylene via the C-H asymmetric stretch modes near 3000 and 3300 cm^{-1} respectively. A portion of an infrared DFWM spectrum of methane is shown in Fig. 3. We use a single-longitudinal-mode optical parametric oscillator, OPO, with two stages of parametric amplification to generate our infrared light. The scanning bandwidth of the OPO is <0.007 cm^{-1} which allows sub-Doppler resolution to be obtained. The high spectral brightness of our source combined with the strong infrared absorption result in saturation broadening at low pressures for laser intensities greater than ~0.1 Mw/cm^2. The spectrum in Fig. 3 was obtained using a laser power of 1-2 μJ in ~4-mm diameter beams.

We are in the process of investigating the effects of collisions on the interpretation of infrared DFWM intensities. Initial results demonstrate that the lack of collisional quenching and the relatively long vibrational to translational energy transfer rates exclude substantial TG contributions to the signal intensities at pressures as high as 1 atmosphere. We also find that the observed collisional line shapes are in good agreement with the moving-absorber line-shape model.[3]

Future Plans

We will continue to study the importance of TG scattering relative to population-grating scattering in uv DFWM, using a two-laser configuration. Although not discussed above, TG contributions can be unambiguously distinguished by tuning the backward pump laser away from any absorptions; the remaining signal then arises solely from non-resonant scattering via the index-of-refraction grating. Preliminary results in flames indicate that TG scattering contributes less than 5% to DFWM signals from nascent flame NO, using 10-ns laser pulses. Using nearly the same two-laser setup, we have recently demonstrated the capability of probing the transfer of molecular orientation and alignment in rotationally inelastic collisions, by forming a pure polarization grating and probing the polarization coherence transferred to other rotational levels. Infrared DFWM experiments will continue to focus on the detection of polyatomic molecules. We will begin to examine the ability of DFWM to probe complex gas mixtures exhibiting substantial spectral congestion in the mid-infrared. We also plan to investigate high-temperature and high-pressure effects on DFWM by performing spectral measurements in an internally heated pressure vessel. We are concurrently developing a DFWM simulation and fitting code that incorporates current theoretical model and which will be made available to users.

References

1. R. L. Farrow and D. J. Rakestraw, *Science*, **257**, 1894 (1992).
2. J. A. Gray, P. H. Paul, and J. L. Durant., Chem. Phys. Letters **190**, 266-270 (1992).
3. R. L. Abrams, J. F. Lam, R. C. Lind, D. G. Steel, and P. F. Liao, "Phase Conjugation and High-Resolution Spectroscopy by Resonant Degenerate Four-Wave Mixing," in *Optical Phase Conjugation*, ed. R. A. Fisher (Academic Press, New York, 1983), p. 211.
4. R. P. Lucht, R. L. Farrow, and D. J. Rakestraw, "Saturation Effects in Gas-Phase Degenerate Four-Wave Mixing Spectroscopy: Nonperturbative Calculations", accepted *J. Opt. Soc. Am. B.* (1993).
5. M. A. Buntine, D. W. Chandler, and C. C. Hayden, in preparation.
6. S. Williams, J. W. Forsman, P. Paul, and L. A. Rahn, in preparation.
7. R. L. Vander Wal, B. E. Holmes, J. B Jeffries, P. M. Danehy, R. L. Farrow and D. J. Rakestraw, *Chem. Phys. Lett.*, **191**, 251 (1992).

BES-supported Publications, 1991-93

1. L. A. Rahn, R. L. Farrow and G. J. Rosasco, "Measurement of the self-broadening of the H_2 $Q(0\text{-}5)$ Raman transitions from 295 K to 1000 K," Phys. Rev. A **43**, 6075 (1991).
2. J. A. Gray and R. L. Farrow, "Predissociation lifetimes of OH $A\ ^2\Sigma^+$ ($v' = 3$) obtained from optical-optical double-resonance linewidth measurements," J. Chem. Phys. **95**, 7054 (1991).
3. D. J. Rakestraw, T. Dreier and L. R. Thorne, "Detection of NH radicals in flames using degenerate four-wave mixing", Proceedings of the *Twenty-Third International Symposium on Combustion*, 1901 (1991).
4. R. L. Vander Wal, B. E. Holmes, J. B Jeffries, P. M. Danehy, R. L. Farrow and D. J. Rakestraw, "Detection of HF using infrared degenerate four-wave mixing", *Chem. Phys. Lett.*, **191**, 251 (1992).
5. R. L. Farrow, Thomas Dreier and D. J. Rakestraw, "Investigation of the dependence of degenerate four-wave mixing intensities on transition dipole moment", *J. Opt. Soc. Am. B.*, **9**, 1770 (1992).
6. R. L. Vander Wal, R. L. Farrow and D. J. Rakestraw, "High-resolution investigation of degenerate four-wave mixing in the $\gamma(0,0)$ band of nitric oxide", *Proceedings of the Twenty-Fourth International Symposium on Combustion*, 1653 (1992).
7. R. L. Farrow and D. J. Rakestraw, "Detection of trace molecular species using degenerate four-wave mixing", *Science*, **257**, 1894 (1992).
8. R. P. Lucht, R. L. Farrow, and D. J. Rakestraw, "Saturation effects in gas-phase degenerate four-wave mixing spectroscopy: nonperturbative calculations", accepted *J. Opt. Soc. Am. B.* (1993).

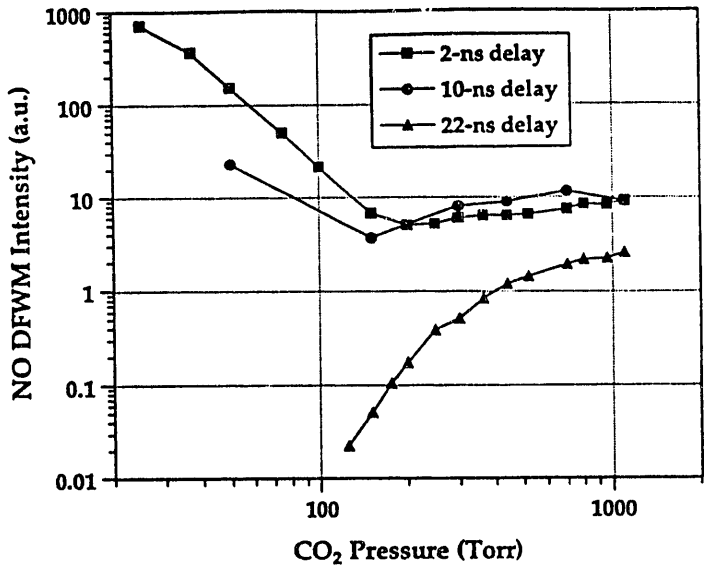

Figure 1.
DFWM line intensity measurements from trace quantities of NO in various pressures of CO_2, for three different time delays between the grating-forming laser pulses and the probing pulse.

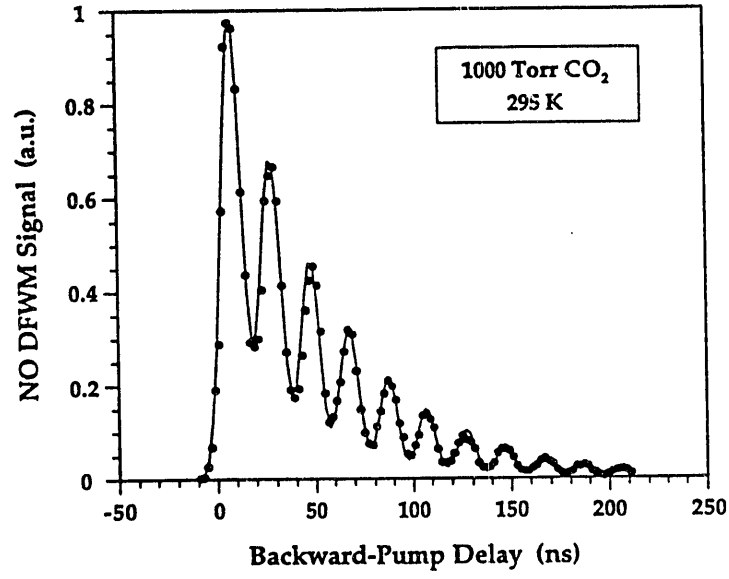

Figure 2.
DFWM intensity measurements from 40 mTorr of NO in 1000 Torr of CO_2, as a function of time delay between the grating-forming laser pulses and the probing pulse.

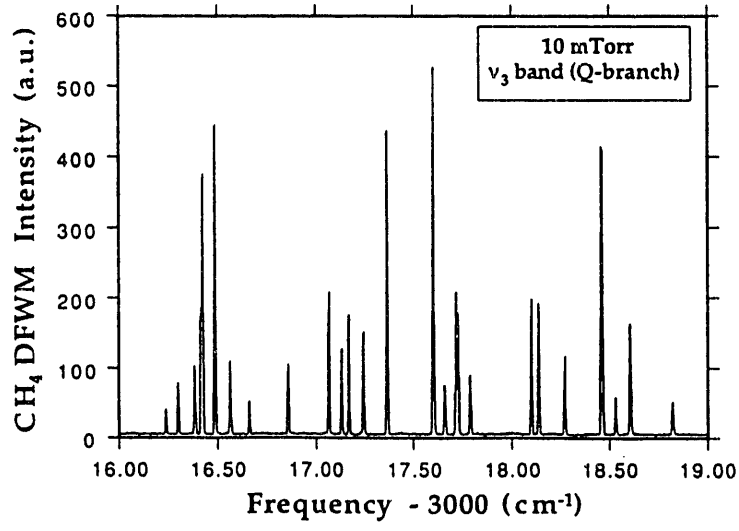

Figure 3.
Infrared DFWM spectrum of methane at 10 mTorr. Pump and probe energies of 1-2 mJ were used to avoid significant saturation effects.

Studies of ground-state dynamics in isolated species by ionization-detected stimulated Raman techniques

Peter M. Felker
Department of Chemistry and Biochemistry
University of California, Los Angeles, CA 90024-1569

PROGRAM SCOPE

Our objectives are two-fold. First, we aim to develop methods of nonlinear Raman spectroscopy for application in studies of sparse samples. Second we want to apply such methods to structural and dynamical studies of species (molecules, complexes, and clusters) in supersonic molecular beams. In the past year we have made progress in several areas. The first pertains to the application of mass-selective ionization-detected stimulated Raman spectroscopies (IDSRS) to the size-specific vibrational spectroscopy of solute-solvent$_n$ clusters. The second involves the application of IDSRS methods to studies of jet-cooled benzene clusters. The third pertains to the use of IDSRS methods in the study of *in*termolecular vibrational transitions in van der Waals complexes.

RECENT PROGRESS

IDSRS studies of solvent vibrational structure in benzene-$(N_2)_n$ clusters

We have shown that with mass-selective, ionization-loss stimulated Raman spectroscopy (ILSRS) it is possible to measure size-selective vibrational spectra of the solvent moieties in neutral solute-(solvent)$_n$ clusters. The relevant clusters are benzene-$(N_2)_n$, $n = 1 - 32$. The vibrational resonances characterized for these species were their N–N stretch resonances. We see clear signs in the spectra of both the filling-up and opening-up of solvent binding sites with increasing cluster size. As far as we know, these results are the first to incorporate subwavenumber resolution and a high degree of size-selectivity in the vibrational spectroscopy of solvent moieties in such clusters. The study opens up the possibility for many more detailed spectroscopic studies of solute-solvent and solvent-solvent interactions.

IDSRS studies of molecule-(rare gas)$_n$ clusters

Molecule-(rare gas)$_n$ clusters serve as very important model systems for the study of intermolecular interactions, many-body dynamics, predissociation processes, phase-transitions in finite-size systems, surface adsorption, and vibrational energy flow. Until recently the only vibrational spectroscopic studies of such species had been ones with fairly low species-specificity. With mass-selective ILSRS we have been successful in performing such studies with a high degree of species-specificity on carbazole-$(Ar)_n$ and benzene-$(Ar)_n$ clusters. Results on the latter system pertain to the nondegenerate, totally symmetric ring-breathing and C-H stretch fundamentals of benzene. As such, only a single peak should appear if the molecular beam sample has only a single type of cluster at any given cluster size. However, we observe in the size range from $n = 16$ to 21 two Raman bands for each of these fundamental. The results indicate the presence of two gross cluster types in this size range. These two types may differ in a structural sense or they may differ in a dynamical sense. The evidence available presently suggests a structural interpretation, namely that

we are observing the manifestations of the Ar solvent shell closing about the benzene moiety in the $n = 16$ to 21 size range. In any case, the IDSRS results on this system and on the carbazole-$(Ar)_n$ system are unprecented in regard to their combination of resolution and species-specificity in the vibrational spectroscopy of neutral solute-solvent$_n$ clusters.

IDSRS studies of benzene clusters

We have performed extensive mass-selective IDSRS studies pertaining to the intramolecular vibrations of benzene dimer isotopomers. We have been particularly interested in using such results to learn about the geometry of the species. Several important results bearing on this issue have been obtained. First, the IDSRS data are only consistent with a dimer in which the benzene moieties reside in inequivalent sites. Second, IDSRS evidence strongly indicates that one of the benzene sites ("site *b*") in the dimer is characterized by high symmetry (C_{3v} or higher) and the other ("site *a*") by lower symmetry. Third, the vibronic spectroscopy associated with the two sites is markedly different. The benzene in the site *b* exhibits marked van der Waals structure upon $S_1 \leftrightarrow S_0$ vibronic excitation. The site-*a* benzene moiety does not. Fourth, in the C–H stretch region the vibrational dynamics associated with site *a* is markedly different than that associated with site *b*. All of these results are consistent with a T-shaped dimer structure in which the stem of the T corresponds to site *a*, the top of the T corresponds to site *b*, and there is free internal rotation about the C_6 axis of the site-*b* moiety.

We have also obtained IDSRS results on benzene trimer isotopomers. Our results relating to geometry point to a symmetrical cyclic structure for the trimer. The evidence for this takes several forms: (a) the number of Raman resonances in the region of the ν_1 and ν_2 fundamentals, (b) the shifts of those resonances as a function of isotopic substitution, and (c) the intensities of the resonances as a function of isotopic substitution. Results pertaining to the vibrational dynamics of the trimer have also been obtained. In particular, we find that the trimer lives for nanoseconds or longer upon vibrational excitation to the ν_1 region (992 cm^{-1}). In the region of the ν_2 fundamental (3070 cm^{-1}) the trimer lives for at least as long as 8 ps, as determined by linewidth measurements on the Raman resonances.

Mass-selective IDSRS experiments have also been performed on higher clusters of benzene. From these results one qualitative conclusion that emerges is that the tetramer, pentamer, and hexamer have benzene sites that are inequivalent. We also find dynamical behavior for the tetramer that is consistent with that of the dimer and trimer, namely that vibrational excitation to the ν_1 region gives rise to long-lived excited vibrational states. A prominent ν_1 resonance for the tetramer has a resolution-limited linewidth of 0.05 cm^{-1}, indicating a lifetime of greater than 100 ps.

Studies of intermolecular vibrational transitions in weakly bound complexes

Very recently we have shown that mass-selective IDSRS methods can be successfully employed in the study of van der Waals - vdW - (i.e., intermolecular) transitions in weakly bound molecular complexes. Such studies have considerable potential in helping one to map out intermolecular potential energy surfaces. We have observed vdW resonances in two classes of species. In benzene-X (X = Ar, Kr, and N_2) we have found a single Raman band in the vdW region for each of the species. These bands are notable in several respects. First, they exhibit nontrivial rotational structure. Second, they have polarization

ratios consistent with nontotally symmetric Raman transitions. Third, their shifts upon perdeuteration of the benzene moiety are substantial (5 to 10%). Fourth, they all occur in the 30 to 38 cm^{-1} range. Finally, they all correlate with lower-frequency resonances in the first excited singlet states of the complexes. All in all, the evidence suggests that the observed Raman bands correspond to fundamentals of the degenerate vdW bending mode in the complexes.

Benzene dimer isotopomers comprise the second class of species for which we have observed vdW transitions. Three bands have been observed. One at very low frequency ($\sim$ 3 cm^{-1}), a second one at 9 to 10 cm^{-1}, and a third at 46 to 53 cm^{-1}. At present, our interpretation of these bands is quite tentative. However, plausible assignments, based on isotope effects, prior knowledge of benzene dimer, rotational band contours, etc., can be made. With such assignments we are encouraged that a considerable amount can be learned about the very important benzene–benzene intermolecular potential.

FUTURE PLANS

The area of size-selective vibrational spectroscopy on clusters is wide-open. We plan to continue our ILSRS studies of solute-(solvent)$_n$ clusters. Studies of particular interest to us are ones in which the Raman spectra of the ***solvent*** species are measured as a function of cluster size. Also wide open is the use of IDSRS methods in the characterization vdW transitions in molecular complexes. We plan on undertaking many studies in this area in the near future. The third area we plan to explore in the future relates to picosecond time-domain measurements of ground-state dynamics in complexes and clusters. Such studies will be employ picosecond pump-probe IDSRS methods. Of interest are the dynamics of processes such as vibrational relaxation, intermolecular vibrational energy flow, and evaporation in molecular clusters.

DOE-SPONSORED RESEARCH PAPERS 1991-1993

1. B. F. Henson, G. V. Hartland, V. A. Venturo, R. A. Hertz, and P. M. Felker: "Stimulated Raman spectroscopy in the ν_1 region of isotopically substituted benzene dimers: Evidence for symetrically inequivalent benzene moieties," Chem. Phys. Lett. **176** 91-98 (1991).

2. G. V. Hartland, P. W. Joireman, L. L. Connell, and P. M. Felker: "High-resolution Fourier transform-stimulated emission and molecular beam hole-burning spectroscopy with picosecond excitation sources: Theoretical and experimental results," J. Chem. Phys. **96** 179-197 (1992).

3. G. V. Hartland, B. F. Henson, V. A. Venturo, and P. M. Felker: "Ionization-loss stimulated Raman spectroscopy of jet-cooled hydrogen-bonded complexes containing phenols," J. Phys. Chem. **96** 1164-1173 (1992).

4. V. A. Venturo, P. M. Maxton, B. F. Henson, and P. M. Felker: "Size-selective Raman spectroscopy of carbazole-(Ar)$_n$ clusters at subwavenumber resolution,"

J. Chem. Phys. **96** 7855-7858 (1992).

5. B. F. Henson, G. V. Hartland, V. A. Venturo, P. M. Maxton, and P. M. Felker: "Stimulated Raman spectroscopy of complexes and clusters in supersonic molecular beams," Proc. Soc. Photo.-Opt. Instrum. Eng. **1638** xxx (1992).

6. P. M. Felker, B. F. Henson, V. A. Venturo, and G. V. Hartland: "Applications of nonlinear Raman spectroscopy to molecular beam studies," Proc. 13th Intl. Conf. on Raman Spectroscopy, edited by W. Kiefer, et al. (Wiley, Chichester, 1992), pp. 230-231.

7. B. F. Henson, G. V. Hartland, V. A. Venturo, and P. M. Felker: "Raman-vibronic double-resonance spectroscopy of benzene dimer isotopomers," J. Chem. Phys. **97** 2189-2208 (1992).

8. V. A. Venturo, P. M. Maxton, and P. M. Felker: "Size evolution of solvent vibrational structure in neutral solute-solvent$_n$ clusters: Benzene-$(N_2)_n$, $n = 1 - 32$," J. Phys. Chem. **96** 5234-5237 (1992).

9. V. A. Venturo, P. M. Maxton, and P. M. Felker: "Raman/ vibronic double-resonance spectroscopy of benzene-doped argon clusters," Chem. Phys. Lett. **198** 628-626 (1992).

10. B. F. Henson, V. A. Venturo, G. V. Hartland, and P. M. Felker: "Stimulated Raman spectroscopy of benzene trimer and higher clusters," J. Chem. Phys. **xxx** in press (1993).

11. P. M. Felker: "Applications of mass-selective ionization-loss stimulated Raman spectroscopy in studies of molecular complexes and clusters," in Molecular Dynamics and Spectroscopy by Stimulated Emission Pumping, edited by R. W. Field and H. L. Dai, (World Scientific), in press.

Spectroscopic and Dynamical Studies of Highly Energized Small Polyatomic Molecules (DOE DE-FG02-87ER13671)

Robert W. Field and Robert J. Silbey
Department of Chemistry
Massachusetts Institute of Technology
Cambridge, Massachusetts 02139

Information about large amplitude motions directly from real and computed spectra of acetylene.

Quantum mechanics encodes classical ball-and-spring motions and quantum tunneling effects into molecular vibration-rotation spectra in a fiendishly complicated way. Although laser chemists dream of exerting control over large amplitude motions (LAM) in polyatomic molecules, we still know remarkably little about extracting a picture of LAM, at chemically interesting levels of internal excitation, directly from information rich frequency-domain spectra.

Through our studies of the Stimulated Emission Pumping (SEP)[1-10] and Dispersed Fluorescence (DF)[11] spectra of acetylene, we have developed a generally applicable scheme for extracting information about LAM directly from spectra. The low resolution DF spectrum contains regular progressions of *feature states.*[11] These feature states are the early time localized, assignable *Franck-Condon bright states.*[9,10] When the DF spectrum contains insufficient information to assign securely all of the progression-forming feature states[11], the mystery states can be assigned by high resolution SEP detective work.[9,10] The rotational constants and vibrational fine structure of a low energy member of a mystery progression can both identify the mystery progression and the anharmonic or Coriolis mechanism by which it becomes bright at early time. The $\sim 10^3$:1 dynamic range of SEP enables us to identify and characterize all of the important "resonances" whereby energy flows at early time from Franck-Condon bright states into nominally dark states.

The early time dynamics (and the spectroscopic perturbations) is described by a multi-resonance "*superpolyad*" effective Hamiltonian Matrix model.[9,10,12] This model expresses each resonance in terms of a single adjustable parameter and utilizes harmonic oscillator matrix element *scaling rules*, both intra- and inter-superpolyad. The inter-superpolyad scaling provides a basis for predicting and modeling the incredibly complicated spectra and dynamics at higher E_{VIB} or at longer time (higher resolution). It is important to note that each superpolyad contains all of the most important early time dynamics, yet $\mathbf{H}^{eff}$ for each value of the superpolyad quantum number ($N=5v_1 + 3v_2 + 5v_3 + v_4 + v_5$) for C_2H_2 $\tilde{X}\ ^1\Sigma_g^+$, where $E_{VIB} = kN$, $k \approx 650\ cm^{-1}$)[10,12] contains a small fraction of the basis states in the $E_{VIB} = k(N \pm 1/2)$ region.

If one wishes to observe a particular LAM, such as 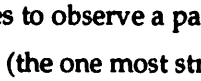 isomerization, then one wants to light up a specific member of a polyad (the one most strongly coupled to the isomerization path). Using IR-UV double resonance and/or perturbations (in either the $\tilde{A}$ or $\tilde{X}$-state) to populate selected vibrational levels of the $\tilde{A}\ ^1A_u$ state, we are able to Franck-Condon brighten the local bend, local CH stretch superpolyad components that most resemble the isomerization pathway.

We plan to record IR-UV DF and SEP spectra in the $E_{VIB} \approx 16{,}000\ cm^{-1}$ region of the acetylene↔vinylidene barrier maximum. The DF spectra will make use of a recently obtained intensified diode array detector. A change in the structure of a superpolyad is a sensitive detector of a change in topography of a potential surface (as would occur near the top of a barrier to isomerization). IR-SEP spectra will be more sensitive to isomerization resonances because of the improved contrast ratio of the Spectral Cross-Correlation diagnostic[7] and superior Franck-Condon access to the isomerization coordinate.

We are collaborating with R. Wyatt (Texas) in the calculation of acetylene SEP spectra, with M. Kellman (Oregon) in superpolyad and bifurcation analyses of SEP spectra, and with M. Davis (Argonne) in hierarchical analyses of DF and SEP spectra.

Fluorescence excitation and SEP studies of the HCO $\tilde{B}^2A'$-$\tilde{X}^2A'$ system.

We have recorded SEP spectra of the following $\tilde{X}$-state "resonances"[13] at energies well above the H-CO dissociation limit.

$(v_{CH}, v_{CO}, v_{BEND})$	E_{VIB}	A	B	Γ
(0,0,0)	0.00	24.3296	1.446	0.0
(0,3,2)	7643.7	28.4	1.408	0.95
(0,3,3)	8547.9	34.3	1.424	1.2
(0,4,0)	7428			0.7
(0,4,1)	8390.5	25.5	1.401	2.1
(0,4,3)	10432			2.0
(0,5,0)	9091.97	23.7	1.384	0.8
(0,5,1)	10153.1	25.9	1.34	2.3
(0,5,2)	11194.7		1.39	50
(0,6,0)	10836.1	23.6	1.371	1.8

These data (both energy levels and level widths) provide stringent tests of the best hybrid *ab initio* /experimental $\tilde{X}$-state potential surface.[14]

We are examining the Renner-Teller interaction between the $\tilde{X}^2A'$ and $\tilde{A}^2A''$ states (two components of a $^2\Pi$ state in the linear geometry)[15] at energies near the previously undetected lowest vibrational levels of the $\tilde{A}$-state. The HCO $\tilde{A}$-$\tilde{X}$ Renner-Teller interaction is unusual in that it is responsible for both level shifts and predissociation in the $\tilde{A}$-state. The lowest vibrational levels of the $\tilde{A}$-state will provide the most crucial information about the linear $^2\Pi$ state, the Renner-Teller interaction, and a global model for the resonance widths in the $\tilde{X}$-state.

Irregular K_a structure in the HCO $\tilde{B}^2A'$ state suggests that the $\tilde{B}$-state is perturbed by a quartet state.[13]. We hope to characterize this quartet state by Magnetic Rotation Spectroscopy (MRS) and lifetime selected fluorescence excitation spectroscopy.

We have initiated a collaboration with T. Sears (Brookhaven) on the study of HCO generated by photolysis of formic acid.

We expect to use the HCO $\tilde{A}$-$\tilde{X}$ and $\tilde{B}$-$\tilde{X}$ systems to demonstrate the sensitivity and selectivity of laser-MRS and Fourier Transform-MRS as applied to free radicals.

Spectroscopic techniques for the study of free radicals.

A step-scan Fourier Transform (FT) spectrometer is being set up for use with pulsed laser excitation and pulsed radical formation processes. The key problem is pulse-by-pulse intensity normalization.

We have demonstrated the selectivity, sensitivity, and resolution of MRS[16], Frequency Modulation enhanced MRS (FM-MRS)[17], sub-Doppler Sideband-OODR Zeeman (SOODRZ) spectroscopy[18], and Selective Detection by Magnetic Resonance - FM-MRS in cw studies of diatomic molecules. We are investigating the extension of these techniques to pulsed laser studies of polyatomic free radicals.

REFERENCES

1. C. Kittrell, E. Abramson, J.L. Kinsey, S. McDonald, D.E. Reisner, D. Katayama, and R.W. Field, J. Chem. Phys. 75, 2056-2059 (1981).

2. E. Abramson, R.W. Field, D. Imre, K.K. Innes, and J.L. Kinsey, J. Chem. Phys. 83, 453-465 (1985).

3. R. L. Sundberg, E. Abramson, J.L. Kinsey, and R.W. Field, J. Chem. Phys. 83, 466-475 (1985).

4. E. Abramson, R.W. Field, D. Imre, K.K. Innes, and J. L. Kinsey, J. Chem. Phys. 80, 2298-2300 (1984).

5. J.P. Pique, Y. Chen, R.W. Field and J.L. Kinsey, Phys. Rev. Letts. 58, 475-478 (1987).

6. J.P. Pique, Y.M. Engel, R.D. Levine, Y.Chen, R.W. Field, and J.L. Kinsey, J. Chem. Phys. 88, 5972-5974 (1988).

7. Y. Chen, D.M. Jonas, J.L. Kinsey, and R.W. Field, J. Chem. Phys. 91, 3976-3987 (1989).

8. Y. Chen, S.D. Halle, D.M. Jonas, J.L. Kinsey, and R.W. Field, J. Opt. Soc. Am. B 7, 1805-1815 (1990).

9. D.M. Jonas, S.A.B. Solina, B. Rajaram, R.J. Silbey, R.W. Field, K. Yamanouchi, and S. Tsuchiya, J. Chem. Phys., 97, 2813-2816 (1992).

10. D.M. Jonas, S.A.B. Solina, B. Rajaram, S.J. Cohen, R.J. Silbey, R.W. Field, K. Yamanouchi, and S. Tsuchiya, "Intramolecular Vibrational Relaxation in the SEP Spectrum of Acetylene," J. Chem. Phys.

11. K. Yamanouchi, N. Ikeda, S. Tsuchiya, D.M. Jonas, J.K. Lundberg, G.W. Adamson, and R.W. Field, J. Chem. Phys. 95, 6330-6342 (1991).

12. M.E. Kellman and G. Chen, J. Chem. Phys. 95, 8671 (1991).

13. X. Zhao, G.W. Adamson, and R.W. Field, J. Mol. Spectrosc. 00, 0000-0000 (1993).

14. J.M. Bowman, J.S. Bittman, and L.B. Harding, J. Chem. Phys. 85, 911 (1986).

15. R.N. Dixon, Chem. Phys. Lett. 190, 430 (1992) and J. Chem. Soc. Farad. Trans. 88, 2575 (1992).

16. M. Li and R.W. Field, J. Chem. Phys. 90, 2967-2970 (1989).

17. Michael C. McCarthy and Robert W. Field, J. Chem. Phys. 96, 7237-7244 (1992).

18. M.C. McCarthy and R.W. Field, "Frequency Modulation Enhanced Magnetic Rotation Spectroscopy of PdH, PdD, NiH, and CuH," J. Chem. Phys.

RECENT PUBLICATIONS

1. P. Dupré, R. Jost, M. Lombardi, P.G. Green, E. Abramson, and R.W. Field, "Anomalous Behavior of the Anticrossing Density as a Function of Excitation Energy in the C_2H_2 Molecule", Chem. Phys. 152, 293-318 (1991).

2. K. Yamanouchi, N. Ikeda, S. Tsuchiya, D.M. Jonas, J.K. Lundberg, G.W. Adamson, and R.W. Field, "Vibrationally Highly Excited Acetylene as Studied by Dispersed Fluorescence and Stimulated Emission Pumping Spectroscopy: Vibrational Assignment of Feature States", J. Chem. Phys. 95, 6330-6342 (1991).

3. J.K. Lundberg, R.W. Field, C.D. Sherrill, E.T. Seidl, Y. Xie, and H.F. Schaefer III, "Acetylene: Synergy Between Theory and Experiment," J. Chem. Phys. 00, 0000-0000 (1993).

4. D.M. Jonas, S.A.B. Solina, B. Rajaram, R.J. Silbey, R.W. Field, K. Yamanouchi, and S. Tsuchiya, "Intramolecular Vibrational Relaxation and Forbidden Transitions in the SEP Spectrum of Acetylene," J. Chem. Phys., 97, 2813-2816 (1992).

5. D.M. Jonas, S.A.B. Solina, B. Rajaram, S.J. Cohen, R.J. Silbey, R.W. Field, K. Yamanouchi, and S. Tsuchiya, "Intramolecular Vibrational Relaxation in the SEP Spectrum of Acetylene," J. Chem. Phys. 00, 0000-0000 (1993).

6. X. Zhao, G.W. Adamson, and R.W. Field, "The HCO $\tilde{B}^2A' \leftarrow \tilde{X}^2A'$ System: Fluorescence Excitation and Stimulated Emission Pumping Spectra", J. Mol. Spectrosc. 00, 0000-0000 (1993).

7. P. Dupré and Peter G. Green, "Determination of a Large Singlet~Triplet Coupling Matrix Element in the Acetylene Molecule," Chem. Phys. Lett. 000, 000-000 (1993).

Laser Studies of Chemical Reaction and Collision Processes

George Flynn, Department of Chemistry, Columbia University
New York, New York 10027

Our work has concentrated on several interrelated projects in the area of laser photochemistry and photophysics which impinge on a variety of questions in combustion chemistry and general chemical kinetics: (1) Infrared diode laser probes of the quenching of molecules with "chemically significant" amounts of energy in which the energy transfered to the quencher has, for the first time, been separated into its vibrational, rotational, and translational components; (2) Probes of quantum state distributions and velocity profiles for atomic fragments produced in photodissociation reactions.

The Diode Laser Probe Technique

The application of infrared diode lasers to study time-dependent dynamic events was developed in our laboratory under DOE sponsorship. This technique provides exceptionally useful information about a wide variety of dynamic molecular processes. The essence of the diode absorption method is the realization that **any** vibrational-rotational level of a small polyatomic molecule can be monitored through an absorption transition of the type:

$$CD_3F(v_1,v_2,v_3,v_4,v_5,v_6;\ J,K,V) + h\nu(\lambda=4.5\ \mu m) \rightarrow CD_3F(v_1,v_2,v_3,v_4+1,v_5,v_6;\ J+1,K,V)$$

where v_i is the quantum number for mode i, J is the total rotational angular momentum quantum number, K is the projection of the total angular momentum on the molecular axis, and V the velocity. The source of infrared light is a continuously tunable, spectrally pure, cw, low power diode laser. Because of the extremely high spectral resolution of the infrared diode probe, the recoil velocity of molecules created by an encounter with a high energy atom or molecule can also be monitored by using a very stable interferometer to time resolve the infrared absorption profile through the Doppler effect. We have used this technique to monitor CO_2, OCS, N_2O, CS_2, DCl, CO, CD_3F, and CF_3D.

Quenching of Molecules with "Chemically Significant" Amounts of Energy

The simplest model for unimolecular decomposition is the Lindemann-Hinschelwood mechanism in which a substrate S is excited by collisions to a level S^* with energy sufficient to cause break up of the substrate. For large molecules the time scale for decomposition of S^* is sufficiently long that further collisions with the bath molecules can cause deactivation of the excited substrate thus quenching the unimolecular decay process. While many studies of the quenching of such highly excited substrate molecules have been performed, until recently there was no technique which could be used to follow these processes with quantum state resolved detail on a single collision time scale. We have recently developed a technique for studying the deactivation of highly vibrationally excited donor molecules by small bath gas molecules on a single collision time scale using infrared diode laser probe techniques. By focussing on the bath states instead of the excited substrate S^*, we are able to completely resolve not only the vibrational excitation of the molecule but also, due to the extraordinary resolution of the diode probe method, the rotational excitation and translational recoil of these same vibrationally excited bath molecules.

In a typical experiment excited pyrazine molecules ($C_6H_4N_2^{(E)}$) are produced at energy E=40,640 cm^{-1} by an excimer laser,

$$C_6H_4N_2 + h\nu\ (248\ nm) \rightarrow C_6H_4N_2^{(E)}$$

Collisions with CO_2 cause translational, rotational and vibrational excitation of the first ν_3 stretching (00^01, 2349 cm^{-1}) vibrational state, and rotational, translational excitation in the ground vibrationless (00^00) level,

$$C_6H_4N_2^{(E)} + CO_2\ (00^00) \rightarrow C_6H_4N_2^{(E-\Delta E)} + CO_2\ (00^01, J, V)$$
$$C_6H_4N_2^{(E)} + CO_2\ (00^00) \rightarrow C_6H_4N_2^{(E-\Delta E)} + CO_2\ (00^00, J', V')$$

J, J' represent rotational angular momentum quantum numbers, and V,V' are the recoil velocities for the corresponding ro-vibrational states. A tunable diode laser operating cw at 4.5 μm is used to probe the P and/or R branch bands of the following transitions,

$$CO_2\ (00^01, J, V) + h\nu\ (4.3\ \mu m) \rightarrow CO_2\ (00^02, J\pm1, V)$$

$$CO_2\ (00^00, J', V') + h\nu\ (4.3\ \mu m) \rightarrow CO_2\ (00^01, J'\pm1, V')$$

Velocity recoils are measured by probing the nascent Doppler profiles for different spectral lines. The initially excited $C_6H_4N_2^{(E)}$ molecules can produce deexcited species, such as $C_6H_4N_2^{(E-\Delta E)}$, which are also able to excite CO_2. In our experiments, however, the CO_2 populations and Doppler velocity profiles are measured at such a short time after the initial dye laser excitation pump pulse and at such low sample pressures that these channels are minimized.

The interaction between excited $C_6H_4N_2^{(E)}$ and CO_2 leads to the excitation of translational, rotational and vibrational degrees of freedom of the CO_2 molecules. The rotational distribution for the vibrationally excited states can be approximated by a Boltzmann distribution, and the increase in rotational temperature (ΔT^R) between the nascent rotational temperature and ambient temperature was found to be $\Delta T^R_{001}<10K$.

The translational excitation of CO_2 molecules scattered into the 00^01 state, as well as the recoil velocity of $CO_2(00^00,J')$ rotationally excited ground state molecules produced by collisions with $C_6H_4N_2^{(E)}$, were measured. The nascent absorption line shapes can be well fitted to a Gaussian function. The width of the fitted Doppler profile provides a measure of the translational temperature of the nascent CO_2 molecules. The average increase in translational temperature for the individual excited 00^01 ro-vibrational states derived from these line broadening measurements is <20K. In dramatic contrast the linewidth of the ground vibrationless state, which corresponds to a translational temperature of 3000K for the J=70 level, is significantly broader than the room temperature ambient value, and substantially broader than the recoil linewidth for the excited vibrational level $CO_2(00^01)$. The probability for exciting the 00^01 vibrational state, sumed over all J levels, is 1% per gas kinetic collision.

The translational excitation of the ground state is clearly much more efficient than that of the vibrationally excited state $CO_2(00^01)$ in taking up energy from $C_6H_4N_2^{(E)}$). The small rotational and translational energy increase accompanying vibrational excitation is consistent with a long range, attractive force, vibrationally resonant energy transfer mechanism in which the gain of *vibrational* energy by the bath is closely matched by loss of *vibrational* energy by the donor $C_6H_4N_2^{(E)}$. On the other hand, the large translational energy increase of the vibrationless ground state is consistent with a short range, repulsive force mechanism in which internal vibrational energy of the $C_6H_4N_2^{(E)}$ is transferred non-resonantly to the translational and rotational degrees of freedom of the bath states. For the pyrazine/CO_2 collision system we also find that the linewidths of the ground vibrationless states increase with increasing J, suggesting a direct relationship between bath recoil and angular momentum as would be expected for a collision in which the available orbital angular momentum in the collision limits the overall rotational angular momentum of the quencher.

Photodissociation Dynamics for the ICl Molecule at 237 nm

The UV (237 nm) photodissociation of ICl molecules has been studied. The basic experimental approach can be described as follows. ICl molecules are photodissociated by a 237.808 nm polarized laser pulse, and the same laser pulse is used to ionize Cl atoms in the excited spin orbit state, $^2P_{1/2}$ (Cl*), via 2+1 REMPI. Cl^+ ions are detected with excellent time resolution using a TOF mass spectrometer:

$$ICl + h\nu\ (237.808\ nm) \rightarrow I + Cl/Cl^*$$

$$Cl^* + 3h\nu\ (237.808\ nm) \rightarrow Cl^+ + e^-$$

Similarly, for detecting chlorine atoms in the ground state, $Cl(^2P_{3/2})$, 236.284 nm or 237.732 nm laser wavelengths are used. The velocity distributions of chlorine atoms along the flight tube axis in each state and the branching ratio between these two states have been measured. The upper states corresponding to absorption at 237 nm have been determined from these studies.

From the ion current temporal profiles for $Cl(^2P_{3/2})$, it is obvious that the $Cl(^2P_{3/2})$ produced from ICl photodissociation at 237.732 nm is from a perpendicular type transition. This corresponds to a $\Delta\Omega=1$ transition for molecules in Hund's case (c). Since the ground state is $X^1\Sigma_{0+}$, the excited state must have $\Omega=1$. There are five states with $\Omega=1$, $A^3\Pi_1$, Z_1, $a(^3\pi_1)$, $b(^3\pi_1)$, and another as yet unobserved $\Omega=1$ state. Except for this last state, all of the others have been observed. The $a(^3\pi_1)$, $b(^3\pi_1)$ states are van der Waals states which have shallow minima at large ICl nuclear distance (r_e=4.01 Å and 4.15 Å for $a(^3\pi_1)$ and $b(^3\pi_1)$, respectively). The large differences in equilibrium internuclear distance between these states and the ground state leads to very small values for the Frank-Condon factors resulting in very small transition probabilities to these levels from the ground state. The contribution from these van der Waals states to absorption at 237 nm must, therefore, be very small. Thus, the most likely excited states for this perpendicular transition are the $A^3\Pi_1$ and Z_1 states. From the ion current temporal profiles for $Cl^*(^2P_{1/2})$, it is clear that Cl* atoms produced by ICl photodissociation at 237.808 nm are from a parallel type, $\Delta\Omega=0$, transition. There are two possible states, 0^+ and $B^3\Pi_{0+}$ which could give rise to such a parallel transition. At large internuclear distances, the adiabatic curve for the 0^+ state correlates with excited state chlorine atoms, and the $B^3\Pi_{0+}$ adiabatic curve correlates to ground state chlorine atoms. During the dissociation, the amount of excited state and ground state fragments produced by absorption of light can change when a potential curve crossing region is passed. Starting from the simple Landau-Zener model for a potential curve crossing, the calculated value of the crossing probability for ICl molecules dissociated at 237 nm in the present work is 1.0. This indicates that ICl molecules, which absorb 237.808 nm photons and are excited to the $B^3\Pi_{0+}$ state, will cross to the 0^+ state during dissociation, producing excited state chlorine atoms. On the other hand, if ICl is excited to the 0^+ state, during the dissociation it will pass through the crossing region to form the $B^3\Pi_{0+}$ state, producing chlorine atoms in the ground state. Since chlorine atoms in the excited state are observed corresponding to the parallel transition, this transition must be $X^1\Sigma^+ \rightarrow B^3\Pi_{0+}$.

Present and Future Experimental Program

Present and future efforts using the high resolution infrared absorption probe and REMPI techniques are being concentrated on quantum state and recoil velocity resolved studies of chemical reactions; on the energy dependence of the quantum state resolved vibration/rotation excitation cross sections in collisional encounters between highly vibrationally excited molecules and cold bath gases; and on the determination of final vibrational, rotational, and translational energy profiles for collisions involving molecular reorientation.

DOE Publications
(1991-1993)

1. Lei Zhu, Scott A. Hewitt, and George W. Flynn, "Quantum Interference Effects in the Collisional Excitation of the Fermi Doublet States of CO_2 by Hot Electrons and Hot H(D) Atoms", J. Chem. Phys. 94,4088(1991)
2. A. J. Sedlacek, R. E. Weston, Jr., and G. W. Flynn, "Interrogating the Vibrational Relaxation of Higly Excited Polyatomics with Time-Resolved Diode Laser Spectroscopy: C_6H_6, C_6D_6, and C_6F_6+CO_2", J. Chem. Phys. 94, 6483 (1991)
3. Liedong Zheng, James Chou, and George Flynn, "Relaxation of Molecules with Chemically Significant Amounts of Energy: Vibrational, Rotational and Translational Energy Recoil of an N_2O Bath Due to Collisions with NO_2(E=63.5 KCAL/MOLE)", J. Phys. Chem. 95, 6759(1991)
4. Jeunghee Park, Yongsik Lee, and George Flynn, "Tunable Diode Laser Probe of Chlorine Atoms Produced from the Photodissociation of a Number of Molecular Precursors", Chem. Phys. Lett. 186,441(1991)
5. Jeunghee Park, Yongsik Lee, John F. Hershberger, Jeanne M. Hossenlopp, and George W. Flynn, "Chemical Dynamics of the Reaction between Chlorine Atoms and Deuterated Cyclohexane", J. Am. Chem. Soc. 114, 58(1992)
6. Ralph E. Weston, Jr. and George W. Flynn, "Relaxation of Molecules with Chemically Significant Amounts of Energy: The Dawn of the Quantum State Resolved Era", Ann. Rev. Phys. Chem., 43, 559(1992)
7. C. K. Ni and G. W. Flynn, "Correlation between Molecular Recoil and Molecular Orientation in Collisions of Symmetric Top Molecules with Hot Hydrogen Atoms", Chem. Phys. Lett. 193, 69(1992)
8. G. E. Hall, J. T. Muckerman, J. M. Preses, R. E. Weston, Jr., and G. W. Flynn, "Time-Resolved FTIR Studies of the Photodissociation of Pyruvic Acid at 193 nm", Chem. Phys. Lett., 193, 77(1992)
9. Scott A. Hewitt, Lei Zhu, and George W. Flynn, "Diode Laser Probing of CO_2 and CO Vibrational Excitation Produced by Collisions with High Energy Electrons from 193 nm Excimer Laser Photolysis of Iodine", J. Chem. Phys.,97, 6397(1992)
10. J. M. Preses, G. E. Hall, J. T. Muckerman, T. J. Sears, R. E. Weston, Jr., C. Guyot, J. C. Hanson, G. W. Flynn, and H. J. Bernstein, "A Fourier-Transform Spectrophotometer for Time-Resolved Emission Measurements", Rev. Sci.. Inst., 64, 95(1993)
11. L. Zhu and G. W. Flynn, "Quantum State Resolved Studies of Rovibrational Excitation of N_2O and OCS Following Collisions with Low-Energy Electrons", J. Phys. Chem., 97, 881(1993)
12. Farooq A. Khan, Thomas G. Kreutz, George W. Flynn, and Ralph E. Weston, Jr., "Translationally and Rotationally Resolved Excitation of $CO_2(00^0 2)$ by Collisions with Hot Hydrogen Atoms", accepted for publication.
13. Chi-Kung Ni and George W. Flynn, "State and Velocity Distributions of Cl Atoms Produced in the Photodissociation of ICl at 237 nm", submitted for publication.
14. Amy S. Mullin, Jeunghee Park, James Z. Chou, George W. Flynn, and Ralph E. Weston, Jr., "Some Rotations Like It Hot: Selective Energy Partitioning in the State Resolved Dynamics of Collisions between CO_2 and Highly Vibrationally Excited Pyrazine", submitted for publication.
15. Ralph E. Weston, Jr., and George W. Flynn, "Diode Laser Studies of Collisional Energy Transfer", submitted for publication.
16. Lei Zhu, Thomas G. Kreutz, and George W. Flynn, "Diode Laser Probe of State-Specific Excitation of CO_2 following Collisions with $O(^1D)$: II. Electronic Quenching", in preparation

March 1993

HTP KINETICS STUDIES ON ISOLATED ELEMENTARY COMBUSTION REATIONS OVER WIDE TEMPERATURE RANGES

Arthur Fontijn, George Yaw Adusei,
Jasmina Hranisavlevic, and Parma N. Bajaj

High-Temperature Reaction Kinetics Laboratory
The Isermann Department of Chemical Engineering
Rensselaer Polytechnic Institute
Troy, NY 12180-3590

Program Scope

The goals of this project are to provide accurate data on the temperature dependence of the kinetics of elementary combustion reactions, (i) for use by combustion modelers, and (ii) to gain a better fundamental understanding of, and hence predictive ability for, the chemistry involved. Experimental measurements are made mainly by using the pseudo-static HTP (high-temperature photochemistry) technique.

While continuing rate coefficient measurements, further aspects of kinetics research are being explored. Thus, starting from the data obtained, a method for predicting the temperature dependence of rate coefficients of oxygen-atom olefin reactions above 500 K has been developed. It yields good agreement with experiment and confirms the underlying mechanistic assumptions. Mechanistic information of another sort, i.e. by product analysis, has recently become accessible with the inauguration of our heated flow tube mass spectrometer facility; early results are reported here. HTP experiments designed to lead to measurements of product channels by resonance fluorescence have started.

Recent Progress

O-Atom Reactions with Olefinic Compounds

A self- consistent mechanistic picture has emerged from our studies of the O-atom reactions with the C_4H_8 butene isomers, 1,3-butadiene, and three chlorinated ethylenes. The data on 1-butene and 1,3-butadiene have already been published.[1,2] A paper on comparison of the four butene reactions is in preparation[3] and the chlorinated ethylene results have been selected for presentation at the "Third International Congress on Toxic Combustion By-Products", this June, and will be submitted for the volume resulting from that meeting.

The work by Singleton and Cvetanovic[4] has shown that below 500 K the k(T) data for O-atom olefin reactions can be described by a simple TST expression for an electrophilic addition channel. Fig. 1 shows, for 1-butene, that this description breaks down progressively with increasing temperature. H-abstraction is a likely high-temperature second channel for this class of reactions. We have therefore developed a general method for estimating k(T) for abstraction of H by O atoms at various positions in hydrocarbons,[3] which builds on the Huie and Herron method[5] for alkanes.

Good agreement between the sums of these abstraction and addition rate coefficients and the experimental observations is obtained, Fig. 1. By contrast, for 1,3-butadiene abstraction is calculated to contribute negligibly in the 280-1015 K range investigated, which is confirmed by the experiments, Fig. 2.

The validity of this approach is further illustrated by the comparison of the O + chloro-ethylene reactions. It may be seen in Fig. 3 that at lower temperatures the rate coefficients for these increase at approximately the same rate, i.e. the four reactions shown have about the same activation energies there. The difference in absolute magnitudes, i.e. of the A factors, is in agreement with the rule that electrophilic addition proceeds preferentially at the least substituted carbon atom. However, above about 700 K the parallelism is not maintained for 1,2-$C_2H_2Cl_2$. The calculations show that at the temperatures investigated (up to about 1300 K) abstraction is only important for the reaction of this compound. Subtracting the calculated rate coefficients for this channel restores the parallelism with the other reactions. Our measurements are currently being extended to include trichloro-ethylene.

It follows that k(T) can now be predicted for further reactions for which no high-temperature observations have been made. All that is required is a rate coefficient measurement at a low temperature where addition dominates, and based on it a TST calculation for the rate coefficients of that channel. Addition of the calculated abstraction rate coefficients then should give the overall k(T) data. Extension of this approach to other series of homologous reactions would appear feasible. Experimental verification remains desirable, especially where further structural effects such as steric hindrance could be significant.

Further reactions

Figure 4 gives the results of our O + methylacetelyne measurements. At least over the temperature range investigated there is no evidence for deviation from Arrhenius behavior, in agreement with the Homann and Wellmann[6] results. The latter were obtained at 2.7 mbar in a fast-flow reactor with mass spectrometric monitoring of O atoms. By contrast the present work was performed at pressures from 120 to 660 mbar by the pseudo-static HTP method, where O atoms are monitored by resonance fluorescence. The agreement under such different conditions has strengthened the confidence in the data for this important combustion reaction. A manuscript will be prepared.

In the past year we have developed a method for studying Cl-atom reactions at elevated temperatures, i.e. the KrF excimer laser photolysis of NaCl. This was done in a modified HTP reactor, where the cooled reactant inlet is replaced by a salt evaporator.[7] We have now begun to study the Cl + H_2 → HCl + H reaction with this set-up. We recently completed a study of the reverse reaction[8] and like for it hope to double the temperature range of the available measurements. These reactions are of interest for modelling emissions of HCl, an undesirable combustion product. Also, as these are single-channel processes, measurements of the product atoms can be used as a means to help calibrate quantitative product measurements by resonance fluorescence. Such calibration would be necessary for mechanistic studies on multichannel reactions.

Another method for making mechanistic studies has recently become available to us, mass spectrometry. As a first study we are making product analyses for the O-atom benzene reaction, the rate coefficients for which we recently reported.[9] These first experiments were made at 405 K and concerned the phenoxy/phenol product ratio, observed as mass 93 over 94. The experiments, done in a He atmosphere at 4 to 16 mbar in a flow reactor, showed a sharp increase in this ratio with decreasing reaction time. This indicates phenol formation from phenoxy-H recombination. In further experiments we used HCl as an H-atom scavenger, which reacts much slower with O atoms. Upon HCl addition only mass 94 is significantly affected. The increases in the 93/94 ratio indicate that at most 25% of the phenol formed could have been from the decomposition of original O-atom benzene adduct. These bulk mechanistic results agree with the conclusions from a crossed molecular beams study.[10]

Plans

As this grant terminates May 31, 1993, there can be no plans for continuation under its aegis. However, in the above we have sketched the directions we want to follow in our research, if and when new support can be found.

References

1. T.Ko, G.Y. Adusei, and A. Fontijn, *J. Phys. Chem.* 95, 9366 (1991).
2. G.Y. Adusei and A. Fontijn, *J. Phys. Chem.* 97, 1406 (1993).
3. G.Y. Adusei and A. Fontijn, *J. Phys. Chem.*, to be submitted.
4. D.L. Singleton and R.J. Cvetanovic, *J. Am. Chem. Soc.* 98, 6812 (1976).
5. R.E. Huie and J.T. Herron, *Prog. React. Kinet.* 8, 1 (1975).
6. K.H. Homann and Ch. Wellmann, *Ber. Bunsenges. Phys. Chem.* 87, 527 (1983).
7. A. Fontijn and P.M. Futerko, in Gas-Phase Metal Reactions, A. Fontijn, Ed., North-Holland , Amsterdam, 1992, Chap. 6.
8. G.Y. Adusei and A. Fontijn, *J. Phys. Chem.* 97, 1409 (1993).
9. T. Ko, G.Y. Adusei, and A. Fontijn, *J. Phys. Chem.* 95, 8745 (1991).
10. S.J. Sibener, et al, *J. Chem. Phys.* 72, 4341 (1980).

Research Publications Resulting From This Grant, 1991-1993

T. Ko, G.Y. Adusei, and A. Fontijn, "Kinetics of the $O(^3P) + C_6H_6$ Reaction over a Wide Temperature Range", *J. Phys. Chem.*, 95, 8745-8748 (1991).

T. Ko, G.Y. Adusei, and A. Fontijn, "Kinetics of the Reactions between $O(^3P)$ and 1-Butene from 335 to 1110 K", *J. Phys. Chem.*, 95, 9366-9370 (1991).

G.Y. Adusei and A. Fontijn, "Kinetics of the Reactions between $O(^3P)$ Atoms and 1,3-Butadiene between 280 and 1015 K", *J. Phys. Chem.*, 97, 1406-1408 (1993).

G.Y. Adusei and A. Fontijn, "A High-Temperature Photochemistry Study of the H+HCl $\rightarrow$ H_2+Cl Reaction from 298 to 1192 K", *J. Phys. Chem.*, 97, 1409-1412 (1993).

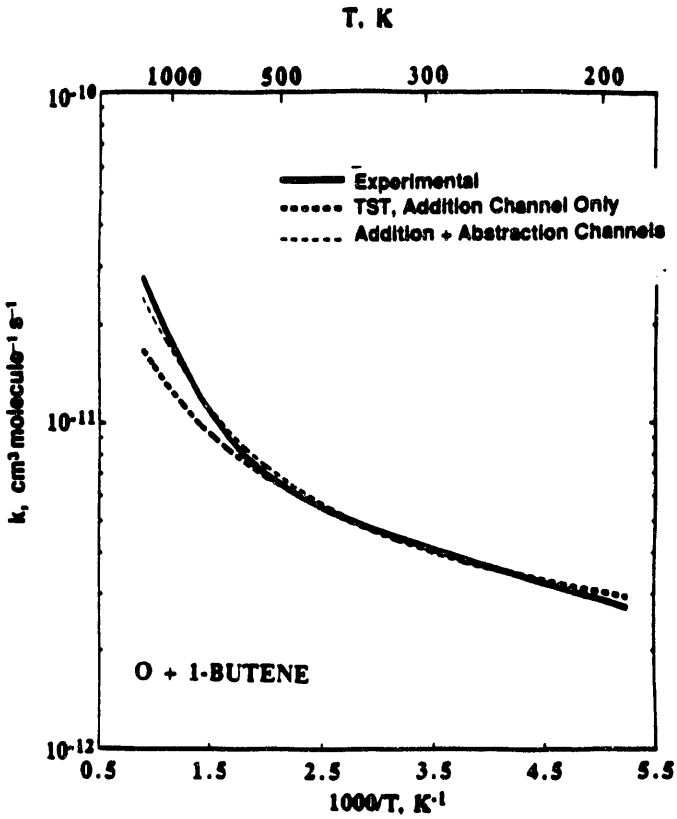

Fig. 1 Comparison of calculated rate coefficients with experimental best fit for the O + 1-butene reaction.

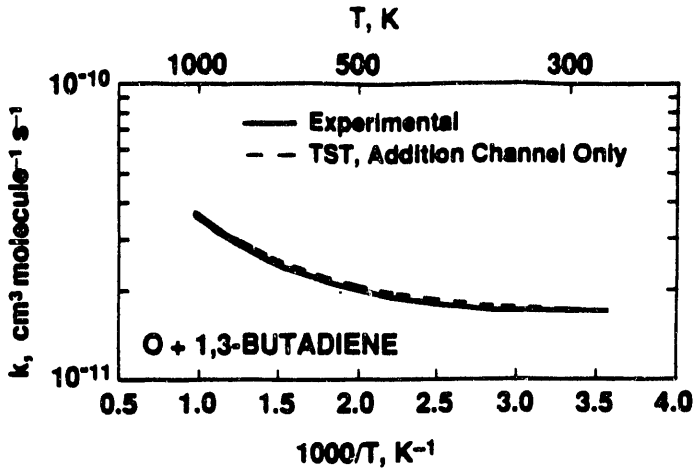

Fig. 2 Comparison of calculated rate coefficients with the experimental fit for the O + 1-butadiene reaction.

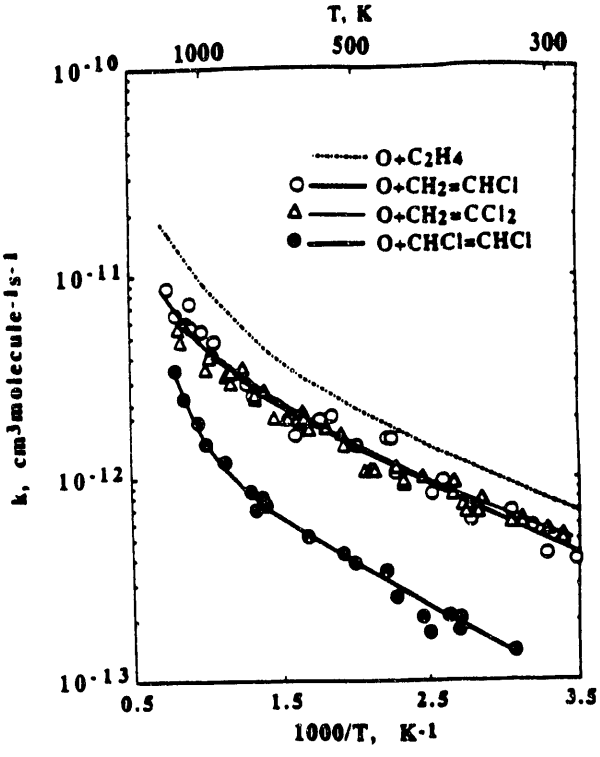

Fig. 3 Arrhenius plots for the O-atom reactions with ethylene and chloro-ethylenes.

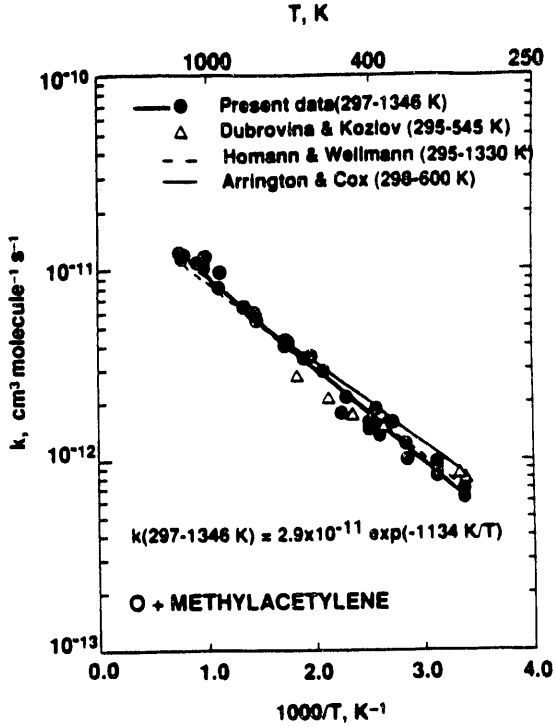

Fig. 4 Summary of rate coefficien data for the O + methylacetylene reaction

STATE-TO-STATE DYNAMICS OF MOLECULAR ENERGY TRANSFER

W. Ronald Gentry and Clayton F. Giese
Chemical Dynamics Laboratory
University of Minnesota
207 Pleasant St. SE
Minneapolis, MN 55455

PROGRAM SCOPE

The goal of this research program is to elucidate the elementary dynamical mechanisms of vibrational and rotational energy transfer between molecules, at a quantum-state resolved level of detail. Molecular beam techniques are used to isolate individual molecular collisions, and to control the kinetic energy of collision. Lasers are used both to prepare specific quantum states prior to collision by stimulated-emission pumping (SEP), and to measure the distribution of quantum states in the collision products by laser-induced fluorescence (LIF). The results are interpreted in terms of dynamical models, which may be cast in a classical, semiclassical or quantum mechanical framework, as appropriate.

RECENT PROGRESS

Under this DOE project to date, we have measured state-resolved integral cross sections as a function of kinetic energy for: (1) state- and mode-selective vibrational excitation of iodine, aniline, para-difluorobenzene and trans-glyoxal in collisions with various species, and (2) rotationally-resolved inelastic scattering of iodine, para-difluorobenzene and trans-glyoxal in collisions with helium, and (3) energy transfer from highly excited vibrational levels of $I_2(X^1\Sigma_g^+)$ prepared by SEP.[1-9] Experiments of types (1) and (2) were carried out with molecules initially in the ground vibrational state, with a rotational temperature of about 1 K, prepared in a pulsed supersonic expansion.[10] Our recent investigations of type (3) represent the first crossed-beam experiments to employ SEP for the preparation of highly excited vibrational levels of the ground electronic state

of a molecule. During the past year we have extended the range of systems under study to include the open-shell species NO($^2\Pi$), and the range of experiments to include measurements of differential as well as integral cross sections.[11]

Because of its open-shell electronic structure ($^2\Pi_{1/2}$ ground state) NO scattering is dynamically much more complicated than that of closed-shell molecules, even when the collision partner is a singlet atom. Collisions in such systems occur on two potential energy surfaces of A' and A'' symmetry, which are degenerate only in linear geometries or at long range.[12] The electronic interaction gives rise to two scattering channels, one of which is multiplet-conserving ($^2\Pi_{1/2} \rightarrow {}^2\Pi_{1/2}$), and the other multiplet-changing ($^2\Pi_{1/2} \rightarrow {}^2\Pi_{3/2}$). For molecules of Hund's case (a) (which is a good approximation for NO states of small angular momentum), multiplet-conserving collisions are governed by the average potential, while multiplet-changing collisions depend on the difference between the A' and A'' potentials.[13] The dynamical coupling becomes even more complicated for larger values of j, as the angular momentum coupling becomes intermediate between Hund's cases (a) and (b).

Our initial experiments were carried out on collisions of ground-state NO with Ar, and included both electronic channels:

$$NO(^2\Pi_{1/2}, v = 0, j = \tfrac{1}{2}) + Ar \rightarrow NO(^2\Pi_{1/2}, v = 0, j') + Ar$$

$$NO(^2\Pi_{1/2}, v = 0, j = \tfrac{1}{2}) + Ar \rightarrow NO(^2\Pi_{3/2}, v = 0, j') + Ar.$$

So far, fully rotationally state-resolved differential cross sections have been measured for three different collision energies, 117 cm^{-1}, 149 cm^{-1}, and 442 cm^{-1}. We have measured both the angular distributions of individual final rotational states j', and the distributions of j' at fixed values of c.m. scattering angle. Differential cross sections for the same system but at higher collision energies have also been measured by Houston and coworkers, who used an imaging technique.[14]

Qualitatively, the angular distributions for multiplet-conserving collisions show rotational rainbow features which shift to larger angles with increasing j'. The overall magnitude of the differential cross sections decrease with increasing j'. Rotational rainbow structure is also seen in the distributions of j' at constant c.m. scattering angle, and in some cases two maxima are seen clearly. The multiplet-changing differential cross

sections are about an order of magnitude smaller than the multiplet-conserving differential cross sections at 442 cm^{-1} collision energy.

Some of the most interesting features of the data are the differences observed in the apparent populations of final states j' when measured on different transitions. There are two possible causes of such effects—preferential population of one member of a Λ-doublet by collision, and preferential alignment (polarization) of the scattered molecules. For high rotational states, Q branch transitions have greater intensities for transition dipoles aligned parallel to j', while the P and R branches favor transition dipoles perpendicular to both j' and the internuclear axis. In principle, it should be possible to separate these effects by measuring the laser polarization dependence of the signals for the separate transitions, but this is difficult both experimentally, because the differences are small, and theoretically, because the rotational branches are mixed for the most accessible values of j'. Our preliminary experiments have shown that in fact *both* phenomena must be contributing to the effects observed.

Because of the complexity of the scattering dynamics in this system, rigorous comparisons with theory are needed to interpret the data. In our first paper[11] we compared our results with quantum scattering calculations carred out by Schinke and coworkers[15] in 1986, using a modified version of the potentials due to Nielsen, Parker and Pack.[16] Large discrepancies were seen, as might be expected for the relatively crude electron-gas potentials. This last summer, we have been collaborating with Millard Alexander of the University of Maryland, who carried out new *ab initio* calculations of the potentials using the Correlated Electron Pair (CEPA-1) method, and then performed quantum close-coupling calculations of the inelastic differential cross sections with the new potentials.[17] Preliminary comparisons indicate good qualitative agreement with virtually all our data, and semiquantitative agreement with most of it. Detailed analysis of the remaining discrepancies is currently being carried out.

FUTURE PLANS

Further work on the NO + Ar system is in progress. First, we are carrying out experiments at the higher collision energies used by Houston *et al.* in order to have a direct comparison with their results. Besides

providing independent confirmation of the results, these experiments will enable us to assess the relative advantages and disadvantages of the two quite different techniques. Second, we are continuing to pursue the question of preferential Λ-doublet population versus molecular alignment effects in the scattered products. At higher rotational states, e.g. $j' = 18.5$, the P, Q and R-branch transitions can all be separately resolved, making it possible to extract in a fairly straightforward fashion the degree of molecular alignment from measurements of the laser polarization dependence of the product LIF signals for each of the various transitions.

---

1. G. Hall, K Liu, M.J. McAuliffe, C.F. Giese, and W.R. Gentry, *J. Chem. Phys.* **78**, 5260 (1983).
2. K Liu, G. Hall, M.J. McAuliffe, C.F. Giese, and W.R. Gentry, *J. Chem. Phys.* **80**, 3494 (1984).
3. G. Hall, K Liu, M.J. McAuliffe, C.F. Giese, and W.R. Gentry, *J. Chem. Phys.* **81**, 5577 (1984).
4. G. Hall, C.F. Giese, and W.R. Gentry, *J. Chem. Phys.* **83**, 5343 (1985).
5. W.R. Gentry, in *Electronic and Atomic Collisions*, ed. by D.C. Lorents, W.E. Meyerhof and J.R. Peterson (Elsevier, Amsterdam, 1986), pp. 13-22.
6. G. Hall, K Liu, M.J. McAuliffe, C.F. Giese, and W.R. Gentry, *J. Chem. Phys.* **84**, 2624 (1986).
7. V.A. Shamamian, D.L. Catlett, Z. Ma, S. Jons, C.F. Giese and W.R. Gentry (unpublished).
8. Z. Ma, S. Jons, C. F. Giese and W. R. Gentry, *J. Chem. Phys.* **94**, 8608 (1991).
9. Z. Ma, S. Jons, C.F. Giese and W.R. Gentry (unpublished).
10. W. R. Gentry, Ch. 3 in *Atomic and Molecular Beam Methods*, ed. by G. Scoles (Oxford, New York, 1988).
11. S.D. Jons, J.E. Shirley, M.T. Vonk, C.F. Giese and W.R. Gentry, *J. Chem. Phys.* **97**, 7831 (1992).
12. S. Green and R.N. Zare, *Chem. Phys.* **7**, 62 (1975); R.N. Dixon and D. Field, *Proc. R. Soc. London Ser A.* **368**, 99 (1979); M.H. Alexander, *J. Chem. Phys.* **76**, 5974 (1982); M.H. Alexander and P.J. Dagdigian, *J. Chem. Phys.* **80**, 4325 (1984).
13. M.H. Alexander, *Chem. Phys.* **92**, 337 (1985).
14. A.G. Suits, L. S. Bontuyan, P.L. Houston and B. J. Whitaker, *J. Chem. Phys.* **96**, 8618 (1992); and additional work in press.
15. H. Joswig, P. Andresen and R. Schinke, *J. Chem. Phys.* **85**, 1904 (1986).
16. G.C. Nielsen, S.A. Parker and R.T. Pack, *J. Chem. Phys.* **66**, 1396 (1977).
17. M.H. Alexander, private communication (1993).

AROMATIC-RADICAL OXIDATION CHEMISTRY

I. Glassman and K. Brezinsky
Princeton University
Department of Mechanical and Aerospace Engineering
Princeton, N.J. 08544
Grant # DE-FG02-86ER13554

The research effort has focussed on discovering an explanation for the anomalously high CO_2 concentrations observed early in the reaction sequence of the oxidation of cyclopentadiene. To explain this observation, a number of plausible mechanisms have been developed which now await experimental verification. One experimental technique for verifying mechanisms, used successfully in previous DOE supported research, is to probe the reacting system by perturbing the radical concentrations. Two forms of chemical perturbation of the oxidation of cyclopentadiene were begun during this past year - the addition of NO_2 and CO to the reacting mixture.

The addition of NO_2 to the oxidation of benzene and toluene has been a very effective technique for probing the postulated mechanisms for these compounds. NO_2 through its reaction with H produces NO and OH. The NO is unreactive and the OH generally abstracts an H from a hydrocarbon source to form H_2O. Consequently, the reactive H atom which would ordinarily feed the radical pool growth through the branching reaction $H + O_2 \rightarrow OH + O$ is redirected toward a less influential pathway. The net effect is a decrease in O and H atom concentrations. The effect of such a decrease on the oxidation of benzene and toluene was dramatic. Those dramatic results have been reported previously in DOE annual reports and articles published in the archival literature.

A large reduction in O atom concentration should have a significant effect on the quantity of CO produced during the oxidation of cyclopentadiene. The CO is postulated to form by direct reaction of oxygen atom with cyclopentadienyl radical and through addition of O to acetylene. The importance of both of these paths would be reduced by the addition of NO_2. However, the production of CO_2 by the direct reaction between intermediates and O_2 would be unaffected. The addition of NO_2 should affect first the concentration of CO and therefore serve as a direct probe of postulated routes.

A different type of probing of the postulated sources of CO_2 at rich conditions would involve the addition of CO to the oxidation of cyclopentadiene. Although the postulated mechanism presumes as unimportant for sources of CO_2, the CO reactions with HO_2, O and OH, the relatively minor contributions of these reactions could be confirmed by accelerating their rates through an artificial augmentation of the CO levels.

IMPLEMENTATION and RESULTS

The perturbation of the oxidation by the addition of CO required only that CO be fed into the reacting stream through one of the four fuel injector tubes. No other experimental modifications were necessary. As expected from the postulated mechanisms, the addition of CO had no effect on the CO_2 concentrations or on the concentrations of any other species. This observation is consistent with the production of CO_2 being primarily the result of a process that does not involve CO as a precursor.

Quantitative measurements of NO_2/NO concentrations during the previously conducted toluene and benzene perturbation experiments were not made because it appeared that all the NO_2 within the flow reactor was converted to NO at the tip of the stainless steel sampling probe. To avoid this problem during the perturbation of the oxidation of cyclopentadiene a sequence of tests were conducted to examine the effect of experimental conditions on the delivery and measurement of NO_2/NO in the flow reactor.

A known concentration of NO_2 was passed through the chemiluminescent NO_2/NO analyzer to calibrate the analysis response. NO_2 was then introduced into the unheated nitrogen carrier stream by passing it through one of the quartz capillary fuel injector tubes. By this means, contact of the NO_2 with the stainless steel surface of the inlet section was avoided. The NOx analyzer indicated that NO_2 passed through the cold reactor unchanged. Oxygen was added to the nitrogen stream and no change in the NO_2 concentration was measured. This result was expected since at these temperatures NO_2 is thermally stable and will not react with oxygen. The flow reactor walls and carrier gas were heated to approximately 1000K in order to measure the effect that high temperature surfaces may have on NO_2 concentrations. No significant effect was observed. Therefore, from the results of these tests, it was concluded that NO_2 could be introduced into the hot flow reactor and accurately measured even in the presence of oxygen and stainless steel surfaces whose temperatures are kept well below 1200K.

The effect on the NO_2 measurement of the presence of cyclopentadiene was examined next by introducing the hydrocarbon into the hot nitrogen carrier gas through the other three quartz injector tubes. In the presence of the cyclopentadiene the NOx analyzer gave spurious readings. No NO_2 was detected and the NO concentration was much greater than the initial concentration of NO_2. Since at these temperatures NO can only be produced from the NO_2 some interference in the measurement by the cyclopentadiene was implied by the anomalously high NO concentration. The cyclopentadiene was able to enter the test chamber of the NO_2 analyzer and interfere with the measurement since a cold trap ordinarily used to capture heavy hydrocarbons and prevent them from reaching the on-line NOx, CO, CO_2 and O_2 meters was removed after it was found to trap out NO_2 as well. Hydrocarbon selective traps necessary to protect the meters and ensure accurate measurements are now being investigated.

Preliminary tests of the effect of NO_2 on the stoichiometric oxidation of cyclopentadiene were conducted even in the absence of reliable measurements of NO_2. The initial NO_2 and oxygen concentrations were set prior to the introduction of cyclopentadiene. After the hydrocarbon was added, samples were taken and the contents examined to determine the effect of the initial concentrations of NO_2 on the species profiles. No measurement of the change in concentration of NO_2 as a function of extent of reaction was possible because of the unresolved analysis problems mentioned above. Nevertheless, the results of these preliminary experiments have indicated that the ratio of the concentrations of CO and CO_2 is changed so that at stoichiometric conditions the ratio resembles that obtained during a leaner oxidation experiment. The NO_2 appears to reduce the amount of CO_2 produced. A very minor reduction in the CO concentration was noted. These preliminary observations were unexpected since as discussed above, the addition of NO_2 was predicted to reduce CO concentration without changing that of the CO_2. The investigation of these unexpected observations is currently in progress.

FUTURE RESEARCH

1) Resolution of the experimental problems associated with the NO_2 perturbation technique.

2) Perturbation of the oxidation of cyclopentadiene as a function of NO_2 concentration, stoichiometry, temperature and the presence of NO.

3) The perturbation of the oxidation of cyclopentadiene by the addition of cyclopentadienylidene diradical formed from the dissociation of diazocyclopentadiene. This perturbation experiment will test the role that direct reaction of the diradical with molecular oxygen to produce CO_2 plays in forming CO_2.

4) The oxidation of phenol. A first year graduate student has been added to the program in order to conduct these experiments. The experiments will link the attack on the aromatic ring with the oxidation chemistry of cyclopentadiene.

Publications Resulting From Program Since 1991

1)"A High Temperature 180 Degree Laser Induced Fluorescence Probe for Remote Trace Radical Concentration Measurements", Applied Optics 30, 381 (1991).

2) "High Temperature Oxidation Mechanics of Meta and Para Xylene", J.Phys. Chem. 95, 1626 (1991).

3) "A Kinetic Model for the Oxidation of Toluene Near 1200K". J. Phys. Chem. 96, 2151 (1992).

4) "A Flow Reactor Study of the Oxidation of 1,3-Cyclopentadiene", MSE Thesis, Princeton University, Robert Butler, 1992.

5) "Benzene/Toluene Oxidation Models: Studies Based on Flow Reactor and Laminar Flame Speed Data", Division of Fuel Chemistry, Preprint, ACS Symposium on Combustion Chemistry, National Meeting of the ACS, 1991.

6) "The Oxidation of Cyclopentadiene", Division of Petroleum Chemistry Preprints, 37, 1467.

Fundamental Spectroscopic Studies of Carbenes and Hydrocarbon Radicals

Carl A. Gottlieb and Patrick Thaddeus
Division of Applied Sciences
Harvard University
Cambridge, MA 02138

Highly reactive carbenes and carbon-chain radicals are studied at millimeter wavelengths by observing their rotational spectra. The purpose is to provide definitive spectroscopic identification, accurate spectroscopic constants in the lowest vibrational states, and reliable structures of the key intermediates in reactions leading to aromatic hydrocarbons and soot particles in combustion.

The Structures of the Cumulene Carbenes H_2CCC and H_2CCCC

Following our detection[1] of H_2CCC we measured the rotational spectra of its three isotopic species with a single ^{13}C, and D_2CCC, and determined all the bond lengths and the HCH angle, i.e., the substitution structure. In collaboration with Peter Botschwina (Göttingen) an equilibrium structure for H_2CCC was derived to an accuracy comparable to which the stable molecule ketene, H_2CCO, is known (i.e., bond lengths accurate to 0.001 Å and bond angle accurate to 0.2°) by converting the measured ground state rotational constants to equilibrium constants using vibration-rotation coupling constants calculated *ab initio*. Botschwina has just calculated *ab initio* a preliminary equilibrium structure of H_2CCCC, the next member of the cumulene carbene series which we have also detected.[2] The rotational spectrum of D_2CCCC has been measured; once the ^{13}C isotopic species are observed, an equilbrium structure of H_2CCCC will be derived by the same procedure used for H_2CCC.

The HCCCO Radical

We published a paper during the past year describing the millimeter-wave spectra of the propynonyl radical, HCCCO, and its deuterated counterpart DCCCO — the first detection of this fundamental radical, and a key radical in combustion formed[3] in three-body addition reactions of CCH with CO. Our measurements, in combination with the recent measurement[4] of the ν_2 mode of HCCCO in solid Ar, should facilitate assignment of the IR spectrum of free HCCCO.

A zero point (r_0) structure recently determined from the rotational constants of four of its isotopic species (HCCCO, DCCCO, $HCC^{13}CO$, and $HCCC^{18}O$) differs considerably from the theoretical structure;[5] the HCC angle is closer to 180° than the *ab initio* calculation of 139° and the two carbon-carbon distances are close to triple and single bonds, respectively, rather than double bonds as predicted. Consistent with the reaction mechanism of Lander *et al.*,[3] the two ^{13}C isotopic species with a single ^{13}C not adjacent to the O atom were not observed when ^{13}CO was the source of ^{13}C in the discharge. Experiments to measure the two remaining ^{13}C isotopic species of HCCCO, using $H^{13}CCH$ instead of ^{13}CO as the isotopic source, are in progress. They should allow us to determine a full substitution (r_s) structure and to estimate the electron density along the CCC chain from the ^{13}C hyperfine structure.

Three New Vibrationally Excited States of Cyclopropenylidene

The millimeter-wave rotational spectrum of cyclopropenylidene (c-C_3H_2), the three-membered carbene ring we detected in 1985, was measured (Fig. 1) in three new vibrationally excited states (two with *A* and one with *B* symmetry). Strong rotational transitions were also observed in the ν_3 state, previously detected in the infrared by Hirahara *et al.*,[6] and an accurate set of spectroscopic constants was determined for all four states. The three new states were assigned on the basis of relative intensities, comparison of the measured inertial defects with those derived from harmonic force constants calculated *ab initio* (A. D. McLean, personal communication), and by symmetry considerations.

Infrared spectroscopy is required to unravel further the vibrational structure of cyclopropenylidene (Fig. 2). All fundamental modes other than ν_5 are infrared active, although the small predicted infrared absorption coefficients for some may make detection difficult. The molecular constants that we have determined for the excited vibrational states in conjunction with those of the ground state should aid detection of the infrared active modes. Perhaps the best candidate for IR detection is ν_6 whose predicted infrared absorption coefficient[7] is only a factor of two less than that of ν_3.

Fig. 1

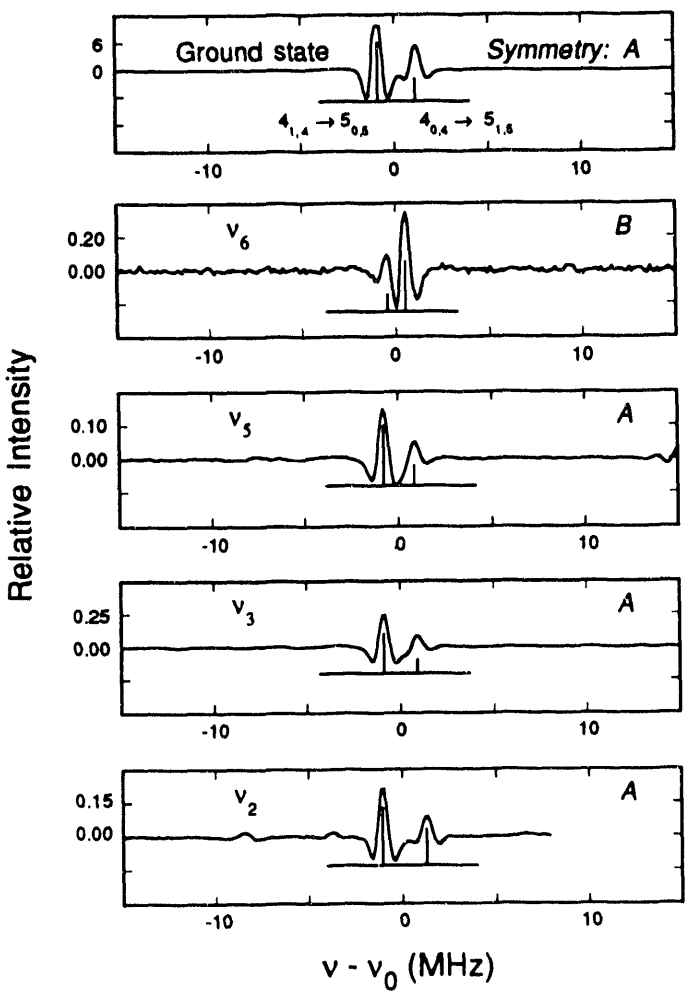

Fig. 2

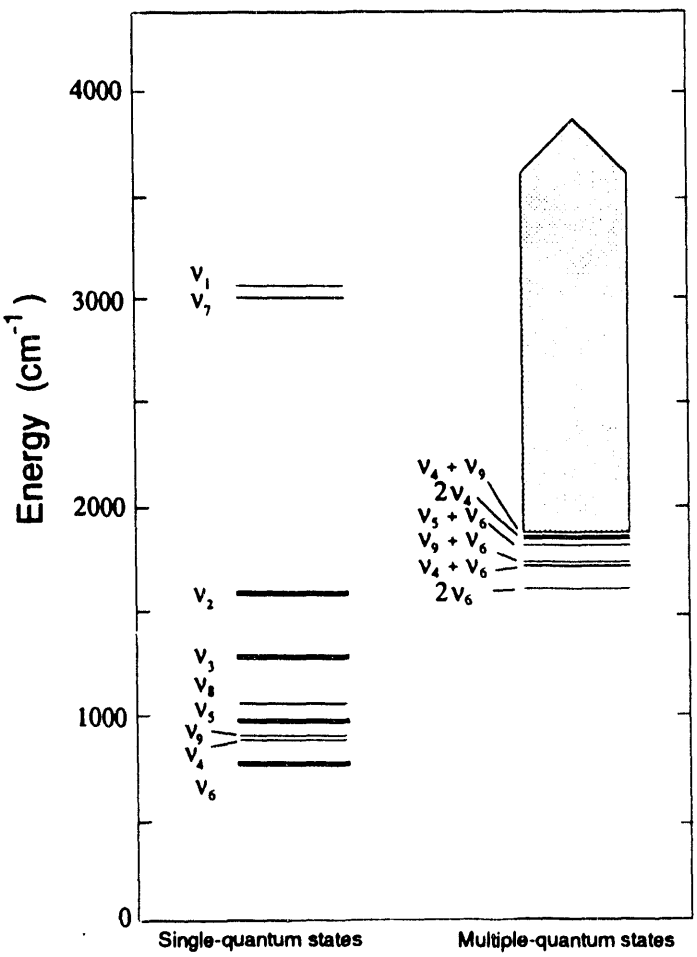

The HCCS Radical

The HCCS radical was detected in a discharge through CS_2 and C_2H_2. It previously was seen with low resolution in the optical region.[8,9] We determined for the first time the fine-structure and lambda doubling constants in the $^2\Pi$ ground state, and detected three isotopic species ($HC^{13}CS$, $HCC^{34}S$, and DCCS; the first two in natural abundance) which allowed a preliminary (r_0) structure to be derived. The suprisingly high concentration of HCCS in our source indicates that other small sulfur bearing radicals such as HCS, HCCCS, and HCCCCS may also be detectable with our current instrumentation.

Production of Radicals and Carbenes by H Atom Abstraction

An entirely new reactive molecule spectrometer with a cell specially designed for the production of hydrocarbon radicals and carbenes by H atom abstraction was constructed. Its design, based on the cell used for the detection of the HOCO radical by Radford *et al.*,[10] incorporates a faster pumping system and the same wide frequency sweeping capability, sensitive detection scheme, and data acquistion system used in our discharge spectrometer.

The known carbenes c-C_3H_2 and H_2CCC were observed by H atom abstraction from both allene and methyl acetylene, establishing that carbenes are produced with good concentration in reactions of either F or Cl atoms with molecules containing multiple C–C bonds. Experiments with D and ^{13}C labelled allene or methyl acetylene might help determine if c-C_3H_2 and H_2CCC are formed by isomerization of HCCCH (propargylene).

Future Plans

We will continue to search for new carbenes and radicals with a strong emphasis on three- and five-membered carbene rings. Our recent success in producing carbenes by H atom abstraction from molecules with multiple C–C bonds, leads us to believe that abstraction of two H atoms from methyl acetylene, methylenecyclopropene, and cyclopentadiene may yield in detectable concentrations, respectively, propargylene (HCCCH), cyclopropenylidene carbene (H_2C_3=C), and cyclopentadienylidene (C_5H_4). Searches will be made in low pressure dc discharges for the cumulene carbenes H_2C_5 and H_2C_6; the carbon-chain radicals C_7H and C_8H; and the ring-chain carbene C_5H_2.

References

1. J. M. Vrtilek, C. A. Gottlieb, E. W. Gottlieb, T. C. Killian, and P. Thaddeus, *Astrophys. J. Lett.*, **364**, L53 (1990).
2. T. C. Killian, J. M. Vrtilek, C. A. Gottlieb, E. W. Gottlieb, and P. Thaddeus, *Astrophys. J. Lett.*, **365**, L89 (1990).
3. D. R. Lander, K. G. Unfried, G. P. Glass, and R. F.Curl, *J. Phys. Chem.*, **94**, 7759 (1990).
4. Q. Jiang and W. R. M. Graham, *J. Chem. Phys.*, in press.
5. Z. A. Tomašić and G. E. Scuseria, *J. Phys. Chem.*, **95**, 6905 (1991).
6. Y. Hirahara, A. Masuda, and K. Kawaguchi, *J. Chem. Phys.*, **95**, 3975 (1991).
7. T. J. Lee, A. Bunge, and H. F. Schaefer III, *J. Am. Chem. Soc.*, **107**, 137 (1985).
8. S. L. N. G. Krishnamachari and D. A. Ramsay, *J. Mol. Spectrosc.*, **71**, 205 (1981).
9. B. Coquart, *Can. J. Phys.*, **63**, 1362 (1985).
10. H. E. Radford, W. Wei, and T. J. Sears, *J. Chem. Phys.*, **97**, 3989 (1992).

Publications

(a) Related Work

1. J. M. Vrtilek, C. A. Gottlieb, E. W. Gottlieb, T. C. Killian, and P. Thaddeus, "Laboratory Detection of Propadienylidene, H_2CCC," *Astrophys. J. Letters*, **364**, L53 (1990).

2. T. C. Killian, J. M. Vrtilek, C. A. Gottlieb, E. W. Gottlieb, and P. Thaddeus, "Laboratory Detection of a Second Carbon Chain Carbene, H_2CCCC," *Astrophys. J. Letters*, **365**, L89 (1990).

3. R. Mollaaghababa, C. A. Gottlieb, J. M. Vrtilek, and P. Thaddeus, "The Millimeter-Wave Spectrum of Highly Vibrationally Excited SiO," *Astrophys. J. Letters*, **368**, L19 (1991).

4. A. L. Cooksy, S. Drucker, J. Faeder, C. A. Gottlieb, and W. Klemperer, "High Resolution Spectrum of the $v = 1$ state of ArHCN," *J. Chem. Phys.*, **95**, 3017 (1991).

5. A. L. Cooksy, J. K. G. Watson, C. A. Gottlieb, and P. Thaddeus, "The Rotational Spectrum of the Carbon Chain Radical HCCCO," *Astrophys. J.*, **386**, L27 (1991).

6. J. M. Vrtilek, C. A. Gottlieb, E. W. Gottlieb, and P. Thaddeus, "Laboratory Measurement of the Rotational Spectrum of HCCS," *Astrophys. J.*, **398**, L73 (1992).

(b) DOE Supported

1. A. L. Cooksy, J. K. G. Watson, C. A. Gottlieb, and P. Thaddeus, "The Millimeter-Wave Spectra of the HCCCO and DCCCO Radicals," *J. Mol. Spectrosc.*, **153**, 610 (1992).

2. R. Mollaaghababa, C. A. Gottlieb, and P. Thaddeus, "Hyperfine Structure of the SiC Radical," *J. Chem. Phys.*, **98**, 968 (1993).

3. C. A. Gottlieb, T. C. Killian, P. Thaddeus, P. Botschwina, J. Flügge, and M. Oswald, "Structure of the Cumulene Carbene, H_2CCC," *J. Chem. Phys.*, **98**, 4478 (1993).

4. R. Mollaaghababa, C. A. Gottlieb, and P. Thaddeus, "Millimeter-Wave Spectrum of Vibrationaly Excited C_3H_2," *Journal of Chemical Physics*, submitted.

5. T. C. Killian and C. A. Gottlieb, "Millimeter-Wave Rotational Spectra of Vibrationaly Excited CCH and CCD," in preparation.

6. A. L. Cooksy, T. C. Killian, C. A. Gottlieb, and P. Thaddeus, "Millimeter-Wave Spectroscopy of Vibrationally Excited C_4H," in preparation.

Trace species detection: Spectroscopy and molecular energy transfer at high temperature

Jeffrey A. Gray
Combustion Research Facility
Sandia National Laboratories
Livermore, CA 94551-0969

Program Scope

Monitoring the concentration of trace species such as atomic and molecular free radicals is essential in forming predictive models of combustion processes. LIF-based techniques have the necessary sensitivity for concentration and temperature measurements but have limited accuracy due to collisional quenching in combustion applications. The goal of this program is to use spectroscopic and kinetic measurements to quantify non-radiative and collisional effects on LIF signals and to develop new background-free alternatives to LIF.

Roger Farrow and I have measured the natural linewidth of several OH A-X (3,0) rotational transitions to determine predissociation lifetimes in the upper state,[1] which were presumed to be short compared to quenching lifetimes, and as a result, we make quantitative predictions about the applicability of predissociation fluorescence methods at high pressures. Joe Durant, Phil Paul, Jay Thoman (Williams College), and I are investigating collisional energy transfer in the A-state of NO.[2,3] We derive new quenching rates which enable direct corrections to NO LIF quantum yields at high temperature. These quenching rates are now being used in studies of turbulence/chemistry interactions. In a related study, Roger Farrow, Joe Durant and I have measured the electric dipole moment μ of excited-state NO using Stark quantum-beat spectroscopy. μ is an essential input to our harpoon model which predicts quenching efficiencies for NO (A) by a variety of combustion-related species. John Goldsmith, Rick Trebino, and I are developing new coherent multiphoton techniques for measurements of atomic hydrogen concentration in laboratory flames to avoid the quenching problems associated with previous multiphoton LIF schemes.[4]

Recent Results

We continue to measure energy transfer rates for NO at high temperature using our shock-tube apparatus.[1-3] We excite the A-X (0,0) band of NO at ~ 226 nm behind incident and reflected shock waves and record time-resolved (0,3) fluorescence. Our double-diaphragm technique enables repeated rate measurements at reproducible temperatures between 1000 and 4500 K. We have now determined quenching rate coefficients (k_m) for N_2, O_2, CO_2, CO, NO, H_2O, H_2, H, O, N_2O, NO_2, CH_4, C_2H_6, C_2H_4, C_2H_2, NH_3, and Ar at high temperatures; these measurements have so far involved more than 1200 shock-tube runs. Quenching rates for the radical species H and O are determined from repeated measurements at various positions behind shock waves through chemically

reacting mixtures. Values for k_m at specific temperatures are normalized by the relative collision velocity to derive quenching cross sections ($\sigma_m \equiv k_m/\langle v \rangle$). Fig. 1 summarizes our measured quenching cross sections for NO $A^2\Sigma^+$.

Several models of the quenching process have also been investigated to understand and predict the temperature variations of cross sections. A charge-transfer (harpoon) model, which has frequently been applied to describe atomic collisions, appears to be most successful in comparison with our measurements.[5] Crossing radii (r_c) for covalent and ion-pair potential surfaces are calculated using the known ionization potential of NO $A^2\Sigma^+$, electron affinities for each collision partner, and standard Lennard-Jones coefficients. The harpoon model under predicts cross sections for a few species that have electronic band systems near or slightly red of the NO A-X (0,0) band. In these cases, quenching more likely occurs via a near-resonant electronic energy transfer mechanism.

The electric dipole moment μ of NO in its A state is an important input to the harpoon quenching model. In addition, this dipole moment has been the subject of some controversy with regard to electronic structure calculations of molecular Rydberg states. We have recently measured μ using Stark quantum-beat spectroscopy. The Stark effect in the $A^2\Sigma^+$ state of NO is greatly complicated by molecular hyperfine structure and results in our observation of a complex pattern of beat frequencies in electric fields between 0 and 20 kV/cm. Our analysis of these frequencies involved a multi-state perturbation treatment including electronic, rotational, fine, hyperfine, and Stark couplings between eigenstates. Fig. 2 shows our observed beat frequency measurements as a function of applied electric field. The solid curves represent the results of a non-linear least-squares fit to the data. Our final result, including an estimate of the polarizability correction, is $\mu = 1.08 \pm 0.04$ D. This result compares favorably with a prior measurement[6] of μ in v'=3 and suggests that theoretical values for μ are currently in error by up to 20%.

We have developed two new multiphoton schemes for the detection of atomic hydrogen in laboratory flames.[4] Two laser beams near 243 nm are crossed at a small angle through the flame to produce an interference pattern. Ground-state (n=1) H atoms are excited via two-photon absorption to n=2 in the regions of space where the lasers interact constructively. This *grating* of excited atoms then diffracts a third laser beam tuned to either 486 nm or 656 nm (n=2→4 or n=2→3 transition) to generate a coherent signal beam. This six-wave mixing process is as sensitive and quantitative as LIF and avoids problems such as interferences from overlapping spectral emission that can affect LIF. The effects of collisional quenching are further reduced using another technique which is based on purely coherent scattering; we have recently demonstrated quantitative detection of H in flames using such a technique and find that the signal scales as the dephasing time (1/linewidth) rather than the excited state lifetime. Dephasing rates in flames are expected to be less sensitive than quenching rates to variations in species composition.

Future Work

We plan to measure quenching rates for OH $A^2\Sigma^+$ by numerous flame species at high temperature using our shock tube. The rates will be useful in making direct corrections to LIF measurements of OH in flames. In addition, we shall test the applicability of a harpoon model to OH quenching and contrast the physical mechanisms with those successfully described for NO $A^2\Sigma^+$. We shall also incorporate a photolysis

source to create a wider variety of radicals in the shock tube, and the primary future direction shall be elementary rate kinetics.

We shall continue to apply non-linear optical diagnostic methods to detect trace species in low-pressure flames. Concentration profiles of these species shall be used in conjunction with profiles of stable species (acquired by microprobe mass spectrometry in the flame chemistry laboratory) to validate combustion chemistry mechanisms and models. We shall apply the two-photon coherence technique developed for atomic hydrogen to atomic oxygen in flames.

Flame chemistry models are typically validated by concentration measurements of reactants, products, or a few intermediates. Data are scarce for small polyatomic radicals because such species rarely fluoresce and often exhibit unstructured absorption spectra. For example, HO_2 has known discrete IR absorption bands and broad, unresolved UV absorption bands; neither of these band systems alone can provide the necessary sensitivity, selectivity or spatial resolution required of an optical diagnostic for flames. We shall apply two-color laser-induced grating spectroscopy, which makes use of double-resonance selectivity and "background-free" sensitivity, to record concentration profiles of HO_2 in low-pressure flames. These profiles will provide important tests of modeling the branching ratio for the crucial $H+O_2+M$ reactions in diffusion flames . A combination of molecular spectroscopy, diagnostics development and kinetic modeling will be required to advance the understanding of flame chemistry.

References

** 1. J. A. Gray and R. L. Farrow, J. Chem. Phys. **95**, 7054 (1991).

** 2. J. A. Gray, P. H. Paul and J. L. Durant, Chem. Phys. Lett. **190**, 266 (1992).

** 3. J. W. Thoman, Jr., J. A. Gray, J. L. Durant, Jr., and P. H. Paul, J. Chem. Phys. **97**, 8156 (1992).

** 4. J. A. Gray, J. E. M. Goldsmith, and R. Trebino, Opt. Lett. **18**, 444 (1993).

5. P. H. Paul, J. A. Gray, J. L. Durant, Jr., and J. W. Thoman, Jr., submitted to Appl. Phys B.

6. T. Bergeman and R. N. Zare, J. Chem. Phys. **61**, 4500 (1974).

** **BES-Supported Publications (1991-1993)**

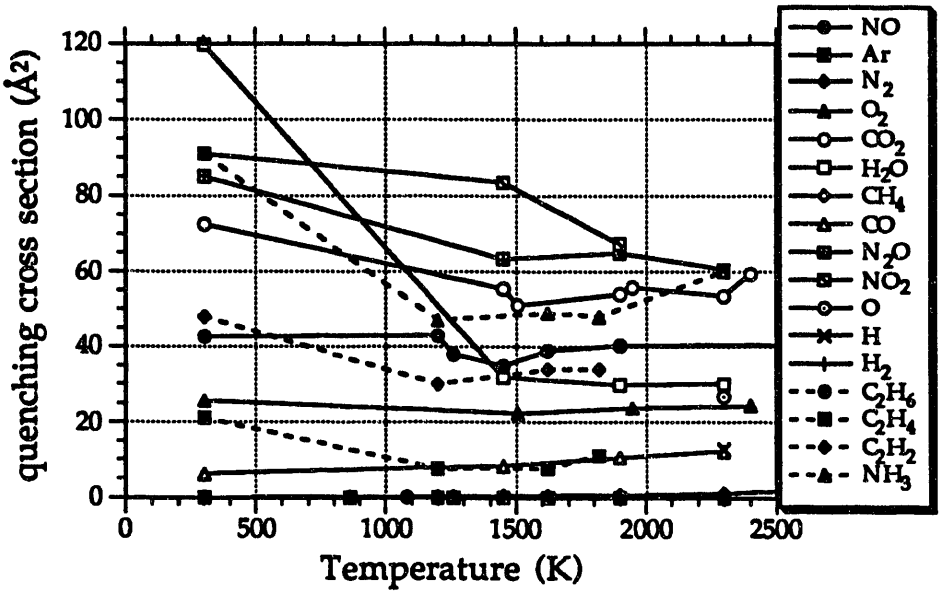

Fig. 1: Observed cross sections for collisional quenching of NO $A^2\Sigma^+$ by several combustion-related species (M) were obtained from LIF decay rates measured in shock-heated mixtures of Ar, M and NO. The temperature dependencies of σ_M are seen to vary dramatically.

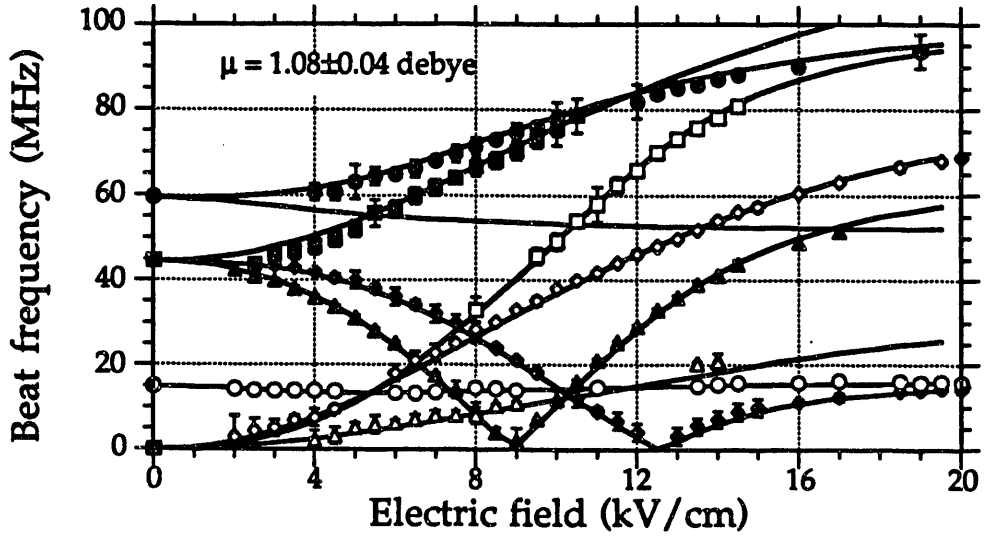

Fig. 2: Observed Stark quantum-beat frequencies from NO $A^2\Sigma^+$ v'=0, N'=1 J'=1.5 as a function of applied electric field. The solid lines represent predictions of a model Hamiltonian: hyperfine constants and the electric dipole moment μ are determined using a non-linear least squares fit.

CHEMICAL DYNAMICS IN THE GAS PHASE: TIME-DEPENDENT QUANTUM MECHANICS OF CHEMICAL REACTIONS

Stephen K. Gray
Theoretical Chemistry Group
Chemistry Division
Argonne National Laboratory
Argonne, IL 60439

I. GENERAL SCOPE

A major goal of this research is to obtain an understanding of the molecular reaction dynamics of three and four atom chemical reactions using numerically accurate quantum dynamics. This work involves: (i) the development and/or improvement of accurate quantum mechanical methods for the calculation and analysis of the properties of chemical reactions (e.g., rate constants and product distributions), and (ii) the determination of accurate dynamical results for selected chemical systems, which allow one to compare directly with experiment, determine the reliability of the underlying potential energy surfaces, and test the validity of approximate theories. My research emphasizes the use of recently developed time-dependent quantum mechanical methods, i.e. wave packet methods.

II. RECENT PROGRESS

A novel approach to solving the time-dependent Schrödinger equation was developed, and shown to be very efficient.[1] In this work I also presented an adaptation of a very old method of spectral analysis, known as Prony's method. This method allows one to accurately identify any resonances that may be influencing the quantum dynamics and yields, from short-time dynamics, accurate estimates of resonance positions and widths. I presented a detailed three-dimensional application to the decay of resonances in the formyl radical: HCO $\rightarrow$ H + CO.[1] My results compared favorably with results obtained by Gazdy, Bowman (Emory), Cho and Wagner (ANL) using a completely different theoretical approach. I also applied these ideas to a study of the fragmentation of ArI_2, further illustrating the general utility of my methods, and also demonstrating that there may be important intramolecular vibrational relaxation (IVR) effects in this system with potentially important consequences for real-time dynamics.[2]

My initial formyl radical study focused on the dynamics of resonances associated with the ground electronic state of HCO.[1] However, it is well known that the first excited electronic state, which has a linear equilibrium geometry, can be coupled to the ground electronic state through the Renner-Teller (RT) effect when there is overall rotation. Recently, Houston's group and Cornell has characterized the properties of many of what I term "RT resonances" in HCO. These states are obtained by exciting from the ground to excited electronic state such that there is also bending exctation present. Coupling to the lower electronic state through the RT effect leads to predissociation of HCO to produce H + CO products that correlate with the ground electronic state. This represents a rather formidable theoretical problem: it is necessary to describe a rotating triatomic system with two vibronically coupled potential energy surfaces. In collaboration with E. Goldfield (Cornell Theory Center) and L. Harding (ANL), I have been applying the accurate quantum dynamics methods noted above to RT-induced predissociation of HCO. Accurate *ab initio* calculations were performed by Harding to generate the upper electronic state potential surface, and the previously developed Bowman-Bittman-Harding (BBH) ground electronic state surface was employed. Considerable effort was also spent on developing a

realistic Hamiltonian model to describe this complicated electronically non-adiabatic process. Extensive wave packet calculations have been performed, and detailed comparisons of resonance energies, decay constants, and CO rotational product distributions with Houston's results have been made. Our results have allowed us to develop a mechanistic picture of the RT process, and have pointed to how the lower BBH surface may be in error, particularly near collinear geometries.

III. FUTURE PLANS

Electronically non-adiabatic processes, such as the RT effect outlined above, will be further explored. With respect to the RT effect in HCO, modifications to the upper and lower surfaces will be considered, and effects previously neglected (such as the role of CO vibration) will be included. This work will lead to a thorough understanding of the RT dynamics in this system, and to improved potential energy surfaces for HCO. Other systems with important vibronic coupling effects, including NO_2, will also be investigated (with M. Davis, ANL).

Four-atom chemical reactions will be studied. These systems are challenging and exciting in many ways. The addition of just a single atom essentially doubles the number of degrees of freedom present in relation to three-atom systems. Realistic studies of such systems will require state-of-the-art computational technology, possibly, e.g., massively parallel computers. Technical theoretical problems can also arise owing to the increased number of reaction pathways. In collaboration with F. Le Quéré, I have already shown how wave packet methods can deal with the multiple continua that can arise when two or more reaction channels are present in certain four-atom clusters .[3] The wave packet dynamics of the reaction $H + CO_2 \rightarrow OH + CO$ will be explored (with E. Goldfield). This important combustion reaction has also been the focus of interesting real-time experiments from both Zewail's and Wittig's groups. Models including up to four active degrees of freedom will be developed and studied. The role of "HOCO" resonances as intermediates will be elucidated. Studies of other interesting four-atom systems, including C_2H_2 (with E. Sibert, Wisconsin) are also planned.

IV. PUBLICATIONS

1. Stephen K. Gray, "Wave packet dynamics of resonance decay: An iterative equation approach with application to HCO $\rightarrow$ H + CO," J. Chem. Phys. **96**, 6543 (1992).

2. Stephen K. Gray, "Quantum dynamics of $ArI_2 \rightarrow Ar + I_2$," Chem. Phys. Lett. **197**, 86 (1992).

3. F. Le Quéré and S.K. Gray," Quantum dynamics of van der Waals clusters: Model results for He_2Cl_2 and Ne_2Cl_2 fragmentation," J. Chem. Phys., *in press* (1993).

Dynamics of Synchrotron VUV-Induced Intracluster Reactions

J. Robb Grover

Department of Chemistry, Brookhaven National Laboratory, Upton, NY 11973

Scope

Photoionization mass spectrometry (PIMS) using the tunable vacuum ultraviolet radiation available at the National Synchrotron Light Source is being exploited to study photoionization-induced reactions in small van der Waals mixed complexes. The information gained includes the observation and classification of reaction paths, the measurement of onsets, and the determination of relative yields of competing reactions. Additional information is obtained by comparison of the properties of different reacting systems. Special attention is given to finding unexpected features, and most of the reactions investigated to date display such features. However, understanding these reactions demands dynamical information, in addition to what is provided by PIMS. Therefore the program has been expanded to include the measurement of kinetic energy release distributions.

Progress

The measurement of ion kinetic energies is a mature field, and under ideal conditions very high precision can be achieved. However, severe experimental constraints preclude application to this program of most of the many methods that have been developed. Since signal rates are often low, $<10^{-1}$ sec^{-1}, it is particularly important to preserve as much signal strength as possible, so methods involving stringent source collimation cannot be used. Photoelectron-photoion-coincidence (PEPICO) methods might appear to be ideal, but the background of accidentals would be prohibitive, because the low signal rates are accompanied by much greater total ion production rates, typically $>10^{6}$ sec^{-1}. In addition the loss of intensity associated with selection of a given electron energy cannot be tolerated. Synchrotron light has insufficient resolution to permit the use of Doppler shifts. Another constraint is the size of the volume within which the product ions are generated as the photon beam crosses the molecular beam containing the target clusters. This volume cannot be reduced to less than 1 mm^3 without unacceptable loss of signal strength. Also, the wide divergence of the synchrotron radiation from its focus limits the physical geometry available to an apparatus.

Only retarding-potential methods have the necessary property of signal strength preservation, but suffer from difficulties in interpretation due to the addition of the molecular beam velocity to the product recoil velocities. However, a useful substitute for the retarding potential is provided by the use of a slit in a configuration in which the molecular beam velocity is combined with a transverse electric field. The molecular beam must be reasonably well velocity-focused, and its velocity must be comparable to or greater than the velocities being measured. As with conventional retarding potential methods, an integral signal is obtained, differentiation of which is required for recovery of the energy distribution.

Energy calibration of the apparatus utilized the free jet acceleration of argon in a series of argon-helium mixtures, in which the composition of the expanding gas was varied from Ar:He = 1:0 to 1:39, so that the laboratory energy of the argon increased from 0.063 to 0.518 eV. To understand the instrument's resolution, measurements were made of the kinetic energy release distribution of O^+ from the absorption of 640 Angstrom photons by CO_2 that had been accelerated to 0.477 eV by expansion of a 19:1 He:CO_2 mixture. These photons excite the 19.39 eV state $CO_2^+(\tilde{C}^2\Sigma_g^+)$, which then dissociates to the v=0 and v=1 vibrational states of the ground electronic state of CO by the emission of O^+ ions of 0.206 and 0.036 eV. After differentiation of the data and conversion to the center-of-mass system, two broad peaks were resolved at the correct energies, the relative intensities of which agreed with Eland's result.

Kinetic energy release distributions have been measured for intracluster reactions induced in the mixed-gas expansions of 1,3-C_4H_6/SO_2, C_6H_6/HCl, C_6H_5Cl/NH_3 and C_6H_6/O_2. Nearly all of the observed distributions can be adequately described as the sum of two evaporation-type spectra. The results for the system 1,3-C_4H_6/SO_2 are described first. For $(C_4H_6{\cdot}SO_2)+$, a photon energy of 1300 Angstroms, near threshold for production from the dimer 1,3-$C_4H_6{\cdot}SO_2$, gives an effective translational temperature of 50 K, which is essentially the same as the rotational temperature calculated for the nozzle beam. This is quantitatively verified by the analogous near-threshold measurements of the kinetic energy distribution of 1,3-$C_4H_6^+$ in the same expansion, which also gives 50 K. At 600 Angstroms and 800 Torr, where most of the $(C_4H_6{\cdot}SO_2)^+$ is produced from trimers and larger complexes, the 50 K component still appears, but with only small intensity. This spectrum is dominated by a component whose average energy is 0.14 eV. Since the average energy deposited in the parent complex ion (mainly one or the other of the two heterotrimers) is about 6 eV, it is clear that most, if not all, of the normal modes of the heterotrimer (52 on average) are involved in the ejection or "evaporation" of the $(C_4H_6{\cdot}SO_2)^+$. Examination at 600 Angstroms of the formation of the monomer ion $C_4H_6^+$ reveals a similar story; the low-temperature component still gives the beam temperature, and the high-temperature component is consistent with the involvement of most of the normal

modes of the clusters from which the $C_4H_6^+$ ions are emitted. The high-temperature component grows systematically stronger as the nozzle pressure is increased, in tandem with the growing proportion of clusters in the beam. The results for the intracluster reaction product $C_4H_6SO^+$ stand in sharp contrast to the foregoing. There is no low-temperature component corresponding to the beam temperature, and the spectrum is dominated by a component whose effective temperature far exceeds that of the $(C_4H_6{\cdot}SO_2)^+$ produced under the same conditions. Since $C_4H_6SO^+$ is produced by a mechanism involving at least two steps, emission of an oxygen atom followed by detachment of one or more "solvent" molecules, further conclusions must depend on modeling calculations. It is clear, however, that the oxygen atom carries away considerable energy, and that $C_4H_6SO^+$ is not produced by a statistical process.

The results for the system C_6H_6/O_2 are similar in many ways to those just described. Here also, at 700 Angstroms, one sees growth of a higher-energy component of $C_6H_6^+$ ions as the nozzle pressure rises, indicating that they are "evaporated" from excited clusters. An unusual feature, however, is that the kinetic energy release distribution of $(C_6H_6{\cdot}O_2)^+$ shows no higher-energy component that can be ascribed to production from larger clusters. This provides independent confirmation of our earlier report that the ion $(C_6H_6{\cdot}O_2)^+$ is formed only from the parent dimer $C_6H_6{\cdot}O_2$, and not from larger clusters, in contrast to what is found in essentially all other systems. The kinetic energy release of the intracluster reaction product $C_6H_6O^+$ is far in excess of what would be expected for a statistical mechanism, which is only to be expected, since its onset is fully 4.9 eV higher than its thermochemical threshold.

The production of $C_6H_6Cl^+$ from C_6H_6/HCl complexes contrasts with the above, because its kinetic energy release distribution is nearly the same as for the higher-temperature component of the distribution for $(C_6H_6{\cdot}HCl)^+$. Partly this is because the mass of the ejected hydrogen atom is so small that it contributes very little recoil to the much more massive residual ion, and partly because the separation of the hydrogen atom drains a large fraction of the excitation energy from the (trimer) parent ion.

The C_6H_5Cl/NH_3 system displays features sharply different from all of the others described above. The kinetic energy release distribution of $C_6H_5Cl^+$ shows no higher-energy component arising from its production from clusters, even at nozzle pressures such that many clusters are known to be present in the beam. Evidently this is because all of the heterocomplex ions decay by another pathway. There are two intracluster reaction products: aniline ion, $C_6H_5NH_2^+$, and anilinium ion, $C_6H_5NH_3^+$. The onset of anilinium ion corresponds to its adiabatic appearance potential, unlike nearly every other intracluster reaction product we have studied. Furthermore, its kinetic energy release distribution is

consistent with the involvement of most or all of the normal modes of its parent dimer ion $(C_6H_5Cl{\cdot}NH_3)^+$, which indicates that it is produced mainly in statistical or nearly statistical processes. This is also unlike the other intracluster reaction products described above, but consistent with the adiabaticity of its onset. On the other hand, $C_6H_5NH_2^+$ conforms to the usual pattern. Its onset is far above its thermochemical threshold (by 1.2 eV), it is produced much more efficiently from trimers than from dimers, and its kinetic energy release is markedly higher than that of $C_6H_5NH_3^+$, consistent with substantial participation by nonstatistical processes.

Publications 1991-1993

Cluster Beam Analysis via Photoionization, J.R. Grover, W.J. Herron, M.T. Coolbaugh, W.R. Peifer and J.F. Garvey, *J. Phys. Chem.* **95**, 6473-6481 (1991)

Complexes of Oxygen with Benzene and Hexafluorobenzene, J.R. Grover, G. Hagenow and E.A. Walters, *J. Chem. Phys.* **97**, 628-642 (1992)

Cluster Beam Analysis via Photoionization: Thiophene Seeded in Helium and Argon and Bromotrifluoromethane plus Methanol Seeded in Argon, E.A. Walters, J.R. Grover, J.T. Clay, P. Cid-Aguero, and M.V. Willcox, *J. Phys. Chem.* **96**, 7236-7243 (1992)

STUDIES OF COMBUSTION KINETICS AND MECHANISMS

David Gutman, Department of Chemistry
Catholic University of America, Washington, D. C. 20064

RESEARCH OBJECTIVES

The objective of the current research is to gain new quantitative knowledge of the kinetics and mechanisms of the reactions of polyatomic free radicals which are important in hydrocarbon combustion processses. The special facility designed and built for these studies (which includes a heatable tubular reactor coupled to a photoionization mass spectrometer) is continually being improved. Where possible, these experimental studies are coupled with theoretical ones, sometimes conducted in collaboration with others, to obtain an improved understanding of the factors determining reactivity.

COMPLETED STUDIES

1. WEAK COLLISION EFFECTS IN THE REACTION CH_3CO <====> CH_3 + CO, A. Bencsura, V. D. Knyazev, I. R. Slagle, and D. Gutman

(Ber. Bunsenges. Phys. Chem. 1992, 96, 1338)

ABSTRACT

Rate constants for the unimolecular decomposition of CH_3CO have been obtained as a function of temperature (420-500 K) and helium density (3-18x10^{16} atom cm^{-3}), conditions which are in the second order region of the fall-off curve. An Arrhenius expression for the low-pressure limit unimolecular rate constant was obtained from the results, $k_1^o(He) = (6.7\pm1.8)x10^{-9}exp[(-6921\pm126\ K)/T]$ cm^3 $molecule^{-1}$ s^{-1}. Using a Master Equation formalism to calculate values of k_1, a set of the two energy parameters needed in the calculations, E_o and $<\Delta E>_{down}$ (including its temperature dependence), was found that is within the range of expected values (including a temperature dependence in the case of $<\Delta E>_{down}$), which, when incorporated into the Master Equation, provides calculated rate constants which agree well with the measured ones. They are $E_o = 65.3\pm4.0$ kJ mol^{-1} and $<\Delta E>_{down} = 65.6 + 0.271T$ cm^{-1} (the latter, a parameterized expression, is valid only in the temperature range of this study). A transition state model for the unimolecular decomposition of CH_3CO was produced which provides high-pressure limit rate constants for this reaction ($k_1^\infty(CH_3CO \text{ ---> } CH_3 + CO) = 2.50x10^{13}exp(-8244\ K/T)$ s^{-1} and $k_{-1}^\infty(CH_3 + CO \text{ ---> } CH_3CO) = 7.64x10^{-13}exp(-3073\ K/T)$ cm^3 $molecule^{-1}s^{-1}$) and k(E) values for solving the Master Equation for reaction conditions that are in the fall-off region. Fall-off behavior of k_1 and k_{-1} reported by others for several different bath gases was reproduced within the uncertainty limits of the experimental results using the Master Equation formalism incorporating the transition state model, the energy parameter E_o given above, and reasonable values for $<\Delta E>_{down}$ for the different bath gases used. This Master Equation formalism and transition state model should provide unimolecular rate constants for reaction (1,-1) in the fall-

off region for additional bath gases using reasonable estimates of $<\Delta E>_{down}$ (e.g., values obtained for this energy-transfer parameter for collisions between other polyatomic radicals and the bath gases of interest).

2. **KINETICS OF THE UNIMOLECULAR DECOMPOSITION OF iso-C_3H_7: WEAK COLLISION EFFECTS IN HELIUM, ARGON, AND NITROGEN**, P.W. Seakins, S.H. Robertson, M.J. Pilling, I.R. Slagle, G.W. Gmurczyk, Á. Bencsura, D. Gutman, W.Tsang

(J. Phys. Chem., Accepted for Publication, 1993)

ABSTRACT

Rate constants for the unimolecular decomposition of iso-C_3H_7 have been determined by laser flash photolysis coupled with photoionisation mass spectrometry, over the temperature range 720-910K. The reaction was studied in He, at densities of 3 - 30 x 10^{16} atom cm^{-3}. More limited measurements were made for Ar and N_2. The reaction is in the fall-off region under all conditions studied. Three methods of data analysis were employed: (i) A transition state model was constructed by reference to literature values of dissociation and association limiting high pressure rate constants over the temperature range 177 - 910K. The model gives $k_1^\infty = 6.51 \times 10^7\ T^{1.83} \exp(-17793/T)\ s^{-1}$ and $k_{-1}^\infty = 9.47 \times 10^{-15}\ T^{1.16} \exp(-440/T)\ cm^3\ molecule^{-1}\ s^{-1}$ for dissociation and association respectively. The model was incorporated into a modified strong collision model and the data fitted using $\langle\Delta E\rangle_{down}$ as a variable parameter, giving 136 cm^{-1} (He), 130 cm^{-1} (Ar) and 129 cm^{-1} (N_2). (ii) A Troe analysis, using the transition state model to determine both k_1^∞ and S_T and employing k_1^0 as the variable parameter, is consistent with $\langle\Delta E\rangle_{down}$ = 200 cm^{-1} for He. (iii) Finally, the microcanonical rate constants for dissociation were calculated by inverse Laplace transformation of the association rate constants of Harris and Pitts and incorporated in a Master Equation analysis with $\langle\Delta E\rangle_{down}$ and ΔH_0^0 as the variable parameters. The analysis gives $\langle\Delta E\rangle_{down}$ = 210 cm^{-1} for He and $\Delta H_{f,298}^0$ (iso-C_3H_7) = 21.0 kcal mol^{-1}.

3. **KINETICS OF THE THERMAL DECOMPOSITION OF THE n-PROPYL RADICAL, Ákos Bencsura, Vadim D. Knyazev, Shi-Ben Xing, Irene R. Slagle and David Gutman**

(24th Symp. [Int.] Combust., 1992, 24, 629)

ABSTRACT

The kinetics of the unimolecular decomposition of the n-propyl radical has been investigated. Experimentally, the decomposition was monitored in time-resolved experiments by using a heatable flow reactor coupled to a photoionization mass spectrometer. The radicals were produced by pulsed excimer laser photolysis of 4-heptanone. Unimolecular rate constants were determined as a function of bath gas (He, Ar, and N_2), temperature (12 temperatures between 620 and 730K), and bath gas density (6 densities between 3 and 30x10^{16} molecule cm^{-3} for He

and 3 densities between 3 and $12x10^{16}$ molecule cm^{-3} for Ar and N_2). The rate constants are in the fall-off region under the conditions of these experiments. The data were fit using a Master Equation analysis. The average step-sizes down (the adjusted parameter in the analysis) were: 220 (He), 267 (N_2) and 261 (Ar) cm^{-1}. The unimolecular rate constants were parameterized for the temperature range 300 - 1000K and 0.001 to 10 atmospheres using a modified Lindemann-Hinshelwood expression.

4. **KINETICS AND THERMOCHEMISTRY OF THE OXIDATION OF UNSATURATED RADICALS: $C_4H_5 + O_2$**, Irene R. Slagle, Ákos Bencsura, Shi-Ben Xing, and David Gutman

(24th Symp. [Int.] Combust., 1993, 24, 653)

ABSTRACT

The kinetics and mechanism of the reaction of C_4H_5 (methylpropargyl radical) with O_2 were investigated from 296 to 900K in a tubular reactor coupled to a photoionization mass spectrometer. At room temperature the reaction proceeds by a simple pressure-dependent addition reaction. Between 369 and 409K the equilibrium $C_4H_5 + O_2 \rightleftharpoons C_4H_5O_2$ was clearly observable and equilibrium constants were measured as a function of temperature. These measurements yielded the values of $\Delta H°_{298}$ (-78 ± 3 kJ mol^{-1}) and $\Delta S°_{298}$ (-122 ± 9 J mol^{-1} K^{-1}). Above 600K the rate of reaction of methylpropargyl with O_2 is independent of density and increases with temperature with a phenomenological rate constant equal to $6.9x10^{-14}exp(-10.5$ kJ $mol^{-1}/RT)$ cm^3 $molecule^{-1}$ s^{-1}. A mechanism of the $C_4H_5 + O_2$ reaction is proposed which involves initial formation of a $C_4H_5O_2$ adduct. At temperatures above 600K, decomposition of the chemically activated adduct competes with redissociation to $C_4H_5 + O_2$. The role of elementary reactions between unsaturated radicals and molecular oxygen in combustion processes is briefly reviewed.

FUTURE STUDIES

During the next year the studies of the unimolecular decomposition of free radicals will continue. Additional investigations of the kinetics and mechanisms of the reactions of unsaturated polyatomic free radicals with molecular oxygen will be initiated. Finally, we shall begin a new set of experiments designed to investigate the chemical kinetics of cross combination reactions involving methyl radicals, $CH_3 + R$.

PUBLICATIONS (1991-Present)

1. I. R. Slagle, G. W. Gmurczyk, L. Batt, and D. Gutman, 23rd Symposium (International) on Combustion; The Combustion Institute, 1991, 23, 115, "Kinetics of the Reaction between Oxygen Atoms and Propargyl Radicals".
2. I. R. Slagle, L. Batt, G. W. Gmurczyk, D. Gutman, and W. Tsang, J. Phys. Chem.

1991, 95, 7732. "The Unimolecular Decomposition of the Neopentyl Radical".

3. A. Bencsura, V. D. Knyazev, S.-B. Xing, I. R. Slagle, and D. Gutman; 24th Symposium (International) on Combustion; The Combustion Institute 1992, 24, 629, "Kinetics of the Thermal Decompositon of the n-Propyl Radical".
4. I. R. Slagle, A. Bencsura, S.-B. Xing, and D. Gutman; Symposium (International) on Combustion; The Combustion Institute 1992, 24, 629, "Kinetics and Thermochemistry of the Oxidation of Unsaturated Radicals: $C_4H_5 + O_2$".
5. A. Bencsura, V. D. Knyazev, I. R. Slagle, and D. Gutman; Ber. Bunsenges. Phys. Chem. 1992, 96, 1338, "Weak Collision Effects in the Reaction $CH_3CO <====> CH_3 + CO$".
6. P. W. Seakins, S. H. Robertson, M. J. Pilling, I. R. Slagle, G. W. Gmurczyk, A Bencsura, D. Gutman, and W. Tsang, 1993, J. Phys. Chem. (Accepted for publication). "Kinetics of the Unimolecular Decomposition of iso-C_3H_7: Weak Collision Effects in Helium, Argon, and Nitrogen"
7. Y. Feng, J. T. Niiranen, A. Bencsura, V. D. Knyasev, and W. Tsang; J. Phys. Chem., 1993, 97, 871, Kinetics of the Unimolecular Decomposition of C_2H_5.

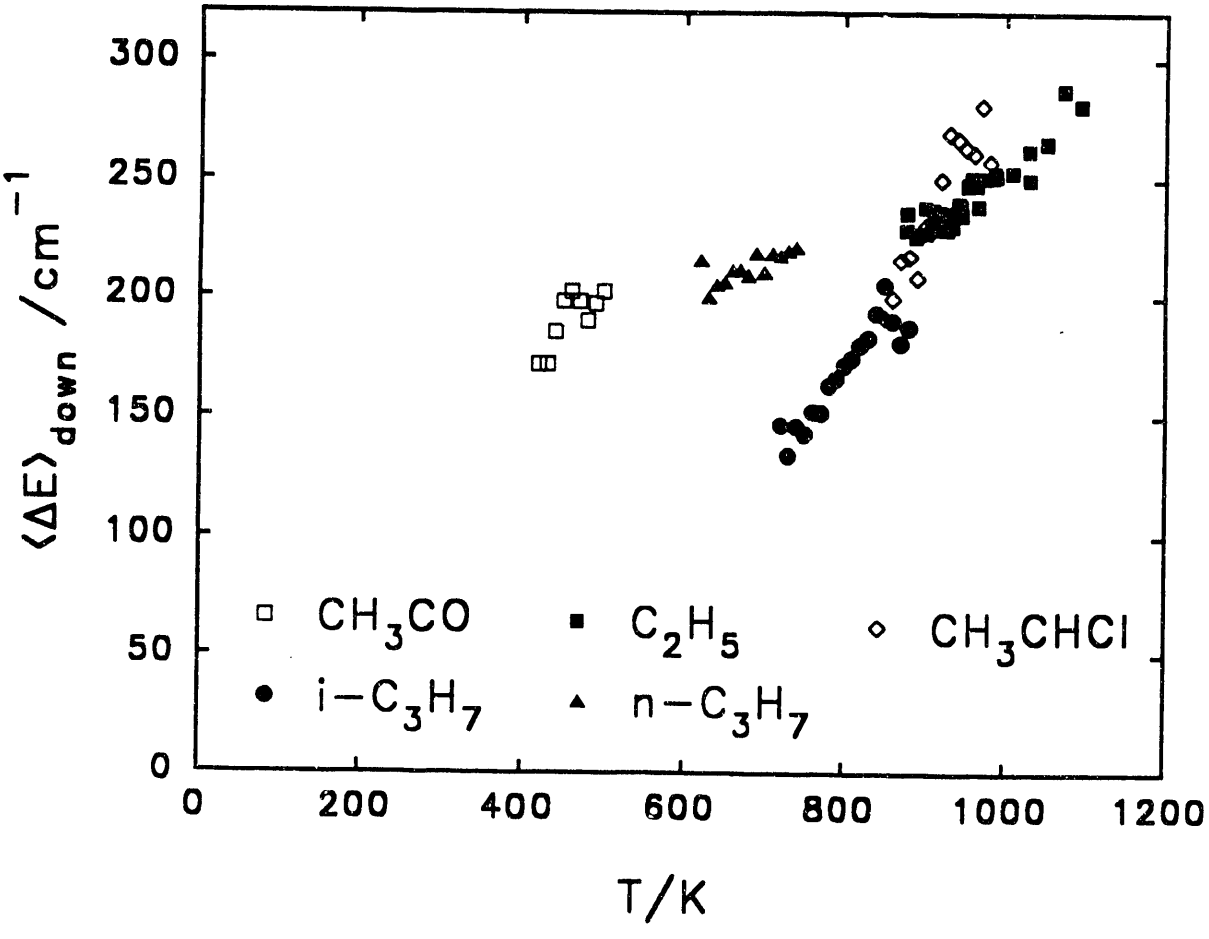

Summary of delta E down determinations for free radicals vs. T in helium bath gas. CH_3CHCl determinations are unpublished results. Points are averages of determinations obtained at each temperature.

High-Resolution Spectroscopic Probes of Collisions and Half-Collisions

Gregory E. Hall

Chemistry Department, Brookhaven National Laboratory, Upton, NY 11973

Project Scope

Research in this program explores the dynamics of gas phase collisions and photodissociation by high-resolution laser spectroscopy. Simultaneous state and velocity detection frequently permits a determination of scalar or vector correlations among products. The correlated product distributions are always more informative, and often easier to interpret than the uncorrelated product state distributions.

Recent Progress

We have recently built an apparatus to record transient absorption spectra with 50 ns time resolution and 20 MHz frequency resolution using a single-frequency Ti:sapphire laser. With multi-pass beam paths, nascent CN photofragments can be detected using the strong $A \leftarrow X$ band transitions. The Doppler-broadened shapes of single rotational lines depend on two angles which can be controlled by adjusting the polarization of pump and probe lasers. The analysis of the lineshapes is similar to that required for LIF vector correlation analysis, but simpler, as only one photon is involved in the detection stage. We discuss as examples the 193 nm dissociation of NCCN and C_2H_5SCN.

Cyanogen (NCCN) has a vibrationally structured absorption spectrum at 193 nm, assigned to vibronically allowed bands of a $^1\Delta_u \leftarrow {}^1\Sigma_g^+$ transition. Previous work by McDonald has shown the fragmentation to be isotropic and the CN state distributions to be well described by phase space theory with an available energy for fragments of 4800 cm^{-1}. Accurate Doppler-broadened lineshapes allow a more stringent test of the energy partitioning: the speed distribution of a spectroscopically selected fragment is related to the internal energy distribution of the undetected coincident fragment. The lineshape measurements thus allow a view of the two-dimensional joint distribution of photofragment pairs: $P(J_1;J_2)$, rather than the marginalized distribution $P(J)=\Sigma_{J2}\, P(J_1;J_2)$.

We confirm that the lineshapes are independent of probe direction or polarization, but find J-dependent differences in the Q- and R-branch CN lineshapes that indicate a tendency for J and v, the CN angular momentum and recoil velocity vectors, to be increasingly perpendicular at higher J magnitudes. Weighted sums of Q- and R- branch lineshapes can be differentiated to give the laboratory speed distributions, which can then be compared to the phase space theory predictions for each measured rotational state. High rotational states are observed to recoil significantly faster than predicted by phase space theory, while low rotational states recoil somewhat more slowly. We interpret this as evidence that high-J, low-J pairs are more likely and high-J, high-J pairs are less likely than expected, based on energy and angular momentum conservation constraints included in the phase space theory. This is fully consistent with the observed $\mathbf{v} \perp \mathbf{J}$ correlation, which can be expressed in the phase space theory as a reduced rotational degeneracy for some combinations of product states.

Photodissociation of alkyl thiocyanates (RSNC) and alkyl isothiocyanates (RNCS) was extensively studied in this group three years ago; R+NCS and RS+CN dissociation channels were characterized by LIF of NCS, CN and RS fragments. The chemical branching, evidence for excited state isomerization, and composite CN product distributions made this family of molecules a tempting target for analysis of vector correlations. We have so far characterized the CN channel from C_2H_5SCN dissociated at 193 nm. The CN (X, v=0) here is produced in a composite rotational distribution, with a sharp peak at $N=70\pm15$ and a broad distribution at lower J.

A "double magic angle" geometry exists for transient absorption that permits laboratory speed distributions to be calculated from combined R and Q branch measurements. The measured speed distribution implies that the C_2H_5S radical coincident with the most likely CN state (N=69,v=0) has only about 20% of the total available energy, despite having most of the total product degrees of freedom. From this speed distribution, three nearly orthogonal lineshape functions can be generated which serve as a basis for fitting any transition in any geometry for the same probed CN rotational state. The fit coefficients in a series of geometries and rotational branches provide an overdetermined set of linear equations for five low-order bipolar moments of the v and J angular distribution, as originally described by Dixon in the context of Doppler-resolved chemiluminescence. The only approximation in the analysis is the assumption that the bipolar moments are independent of velocity. By following the initial stages of collisional relaxation, we see that this approximation becomes poor after a few hundred nanoseconds, but is good at earlier times for the high-J lines. Time-dependent absorption lineshapes for an R- and Q-branch line probing the same quantum state of CN (v=0,J=69.5) are shown in the figures for one of six polarization combinations used. In this single magic-angle geometry, the velocity anisotropy has no influence on the lineshapes, which do, however, depend on higher moments of the v and J angular distribution, as well as the velocity relaxation. The measured bipolar moments for nascent high-J CN indicate a prompt dissociation from a mixed parallel and perpendicular transition. The low excited singlet states are analogous to the states of linear NCS^-, which will be a $^1\Sigma^-$ and a $^1\Delta$ state. The latter will be split into a Renner pair: A′ and A″. The velocity distribution is mostly parallel, while the perpendicular component is characterized by an A″ type transition, based on the measured

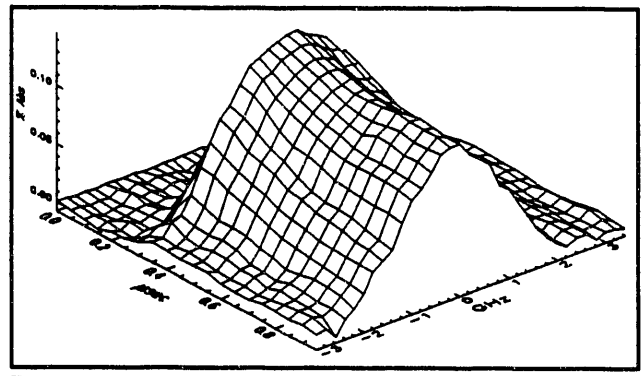

Transient absorption signal for CN photofragments from C_2H_5SCN at 193 nm. $R_1(69.5)$ line in the (2,0) band of the $A \leftarrow X$ transition. .

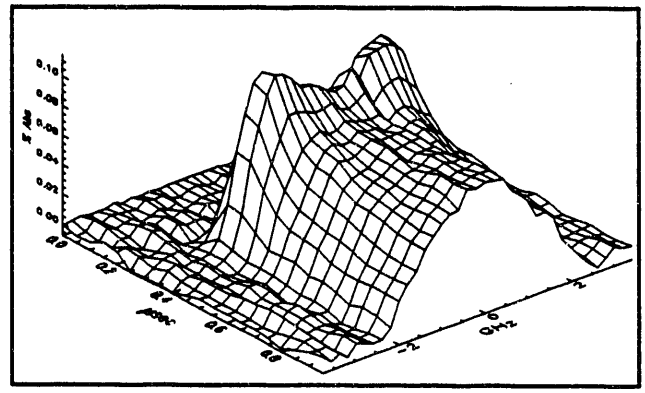

Same as above, but $Q_1(69.5)$ line. The probe beam is at 54.7° to the photolysis polarization, and polarized in the plane containing the photolysis E vector.

$\beta_0^2(22)$ moment. The v,J correlation is near its limiting perpendicular value, excluding any torsional excitation in the exit channel. The low J CN (X,v=0) states have a composite lineshape, including both fast and slow fragments. The slower CN radicals evidently arise from another pathway where the C_2H_5S can accept a more statistical fraction of the total energy.

The CN photofragment studies will continue with HNCS, where CN elimination evidently follows isomerization in the excited state. The detailed characterization of microscopic channels in these complex systems displaying chemical branching is particularly attractive for systems small enough to attract serious theoretical attention.

Work has continued on the application of Doppler-resolved laser-induced fluorescence (LIF) lineshape analysis to characterize vector properties of reactive and inelastic collisions. We have primarily studied the reaction H + O_2 → OH + O, a chain-branching step of central importance to many combustion systems. The characterization of the detailed dynamics of high collision energy reactions provides an experimental check on the potentials and calculations that offer hope for understanding and predicting thermal rate constants. Our technique consists of preparing fast H atoms by dissociation of H-containing precursor molecules with a pulse of polarized ultraviolet light. Following a short delay to allow reaction with low pressure, thermal O_2, the nascent OH products are analyzed by LIF. From the Doppler lineshapes observed in different pump-probe geometries and polarizations, information on the scattering angle distribution (differential cross section) and angular momentum polarization is obtained for selected OH quantum states.

Recent Publications

Photodissociation of acetone at 193 nm: Rotational- and vibrational-state distributions of methyl fragments by diode laser absorption/gain spectroscopy.
G.E. Hall, D. Vanden Bout, and T.J. Sears.
J. Chem. Phys. **94,** 4182-88 (1991).

Time-Resolved FTIR Studies of the Photodissociation of Pyruvic Acid at 193 nm
G.E. Hall, J.T. Muckerman, J.M. Preses, R.E. Weston, Jr., and G.W. Flynn.
Chem. Phys. Lett. **193,** 77-83 (1992).

The S(D)+N_2 Quenching Process: Determination of the Branching Ratios of Triplet Fine Structure Products
G.C. McBane, I. Burak, G.E. Hall, and P.L. Houston.
J. Phys. Chem. **96,** 753-55 (1992).

A Fourier-Transform Spectrophotometer for Time-Resolved Emission Measurements
J.M. Preses, G.E. Hall, J.T. Muckerman, T.J. Sears, R.E. Weston, Jr.,C. Guyot, J.C. Hanson, G.W. Flynn, and H.J. Bernstein.
Rev. Sci. Instrum. **64,** 95-102 (1993).

Laser Induced Fluorescence Spectroscopy of the Jet-Cooled HNCN Radical
M. Wu, G.E. Hall and T.J. Sears.
J. Chem. Soc., Faraday Trans. **89,** 615-22 (1993).

SPECTROSCOPY AND KINETICS OF COMBUSTION GASES AT HIGH TEMPERATURES

Ronald K. Hanson and C. T. Bowman
High Temperature Gasdynamics Laboratory
Department of Mechanical Engineering
Stanford University
Stanford, CA 94305-3032

Program Scope

This program involves two complementary activities: (1) development and application of cw ring dye laser absorption methods for sensitive detection of radical species and measurement of fundamental spectroscopic parameters at high temperatures; and (2) shock tube studies of reaction kinetics relevant to combustion. Species currently under investigation in the spectroscopic portion of the research include NO and CH_3; this has necessitated the continued development of a unique intracavity frequency-doubling system for a cw ring dye laser which operates at wavelengths in the range 210-230 nm. Shock tube studies of reaction kinetics currently are focussed on reactions involving CH_3 radicals.

Recent Progress

Work during the current reporting period has been focussed on the following activities:

UV Ring Dye Laser Development We have continued to improve the performance of our cw UV ring dye laser. The system currently utilizes a high-power (7 W, all-lines UV) argon ion laser to pump a Coherent 699 ring dye laser which has been modified to incorporate an angle-tuned, intracavity-mounted, BBO frequency doubler. Output power levels in excess of 1 mW are obtainable; wavelength coverage is from 209-230 nm through use of two separate BBO crystals cut at different phase-matching angles. Although the alignment procedure for the laser is demanding (and tedious) to achieve stable, single-mode output, this laser provides important scientific capability. In particular, the rapid-tunability of single-mode output allows measurement of fully-resolved lineshapes of UV-active species in shock-heated flows, which is our approach for generating a wide range of gas temperatures; and the high brightness of the laser in a narrow spectral region allows much-improved detection sensitivity (relative to broadband arc or resonance lamp sources) for absorption measurements of species which absorb in the UV.

Broadening and Shift Parameters for NO We have previously reported measurements of fully resolved absorption lineshapes of NO gamma-band (0,0) transitions near 225 nm for NO dilute in either N_2 or Ar. These lineshape data, obtained over a temperature range of 295-2800 K and best-fit with Voigt profiles, yielded values for the collision-broadening and -shift parameters for a variety of rotational quantum numbers (see the paper by Chang et. al in the Publications Section). Interestingly, the broadening parameters obtained for NO in N_2 and Ar are about 5 times those found in past work with OH, and the ratio of the shift and broadening parameters (about 1/3) is also significantly larger for NO than for OH. These observations motivated further work to measure the broadening and shift parameters for NO perturbed by H_2O, O_2 and NO itself, owing both to the significance of these species in combustion environments and to the possibility of enhanced broadening and shift coefficients relative to those for N_2 and Ar.

The room temperature measurements are now complete and have been submitted for publication. A summary of our findings is provided in Table 1 of this abstract. The important observations are: (1) the broadening and shift coefficients are remarkably similar for four of the five perturbing species studied (Ar, O_2, NO, and N_2), with the H_2O coefficient being about 40% larger; (2) there is very little J-dependence in the results for the range of rotational quantum numbers studied; and (3) the ratio of the broadening and shift coefficients ($2\gamma/\delta$) is $-3.25 + 0.1$ for all the perturbers except H_2O which gives a value of -3.85. The next phase of research involves measurement of these parameters over a wide range of temperature to investigate their temperature dependence. A theoretical effort is also in progress to develop a lineshape theory compatible with our experimental observations.

Methyl Absorption Coefficient After mapping out the absorption coefficient of CH_3 between 215 and 225 nm, an optimum absorption wavelength of 216.615 nm was selected for use in kinetics studies. The absorption coefficient was measured over a range of temperature (1350–2450 K) using five separate sources of methyl as a check for consistency. The magnitude of the absorption coefficient is similar to the UV absorption coefficient of OH, allowing detection of ppm levels of methyl over a path length of 10 cm at typical shock tube conditions. Details of our findings have been submitted for publication.

Methyl Kinetics Our initial application of the CH_3 absorption diagnostic has been ethane decomposition. In these experiments, shock wave heating of ethane, dilute (50–500 ppm C_2H_6) in Ar or N_2, was used to drive the reaction, and detection of CH_3 was used to monitor reaction progress. Experiments were conducted over a modest range of pressure (0.6 to 4.4 atm) and temperature (1350–2110 K) to allow investigation of both pressure and temperature dependencies of the rate coefficient. A summary of the results and a comparison with the recommended expression of Wagner and Wardlaw is shown in Fig. 1. For clarity, we have scaled all our data to one pressure, namely 1 atm, and have shown both the high-pressure limit and 1-atm rate coefficient due to Wagner and Wardlaw. In brief, our data are in excellent agreement with Wagner and Wardlaw below 1500 K but fall increasingly below their recommendation at higher temperatures. Further work is in progress, both to consider the theoretical implication of our measured temperature dependence and to extend the pressure range of the measurements.

Future Plans

Research during the coming year will include the following activities:

1. Continued work to improve the power level and stability of the UV ring dye laser.

2. Continued study of absorption lineshapes of NO, including determination of collision-broadening and collision-shift coefficients for H_2O, O_2, and NO collision partners at elevated temperatures. This will include experimental measurements in static cell, flame and shock tube environments, and development of improved theories for NO lineshapes.

3. Continued study of methyl reactions, including the reactions of CH_3 with O_2, NO, H_2, OH and CH_3 itself.

4. New work to investigate sensitive, quantitative detection of HO_2 using cw laser absorption near 220 nm.

Publications (1991 - 1993)

1. D. F. Davidson, A. Y. Chang, M. D. DiRosa and R. K. Hanson, "Development of a CW Laser Absorption Diagnostics for CH_3," paper WSS/CI 91-20 at WSS/CI Spring Meeting, Boulder, CO, March 18-19, 1991.

2. A. Y. Chang, M. D. DiRosa and R. K. Hanson, "Temperature Dependence of Collision Broadening and Shift in the NO A←X (0,0) Band in the Presence of Argon and Nitrogen," J. Quant. Spectrosc. Radiat. Transfer **47**, 375-390 (1992).

3. D. F. Davidson, A. I. Chang, M. D. DiRosa and R. K. Hanson, "A CW Laser Absorption Diagnostic for Methyl Radicals, J. Quant. Spectrosc. and Radiat. Transfer, in press.

4. D. F. Davidson, M. D. DiRosa, R. K. Hanson and C. T. Bowman, "A Study of Ethane Decomposition in a Shock Tube using Laser Absorption of CH_3," Int. J. Chem. Kinetics, submitted 3/1/93.

5. M. D. DiRosa and R. K. Hanson, "Collision Broadening and Shift of NO γ(0,0) Absorption Lines by H_2O, O_2 and NO at 295 K," J. Mol. Spectrosc., submitted 3/31/93.

Table 1. Collision broadening and shift coefficients for NO A←X (0,0) at 295 K.[†]

Perturber	J" - 1/2	2γ ($cm^{-1}atm^{-1}$)	δ ($cm^{-1}atm^{-1}$)	$2\gamma/\delta$
Ar	3, 13, 26	0.503	-0.159	-3.16
O_2	3, 7, 13, 18, 26	0.527	-0.160	-3.31
NO	20, 26, 33	0.551	-0.168	-3.22
N_2	3, 13, 26	0.583	-0.180	-3.24
H_2O	3, 7, 11, 13, 18	0.787	-0.210	-3.85

[†]Entries of 2γ and δ for each perturber are J"-averaged. Dependence on J" is minimal.

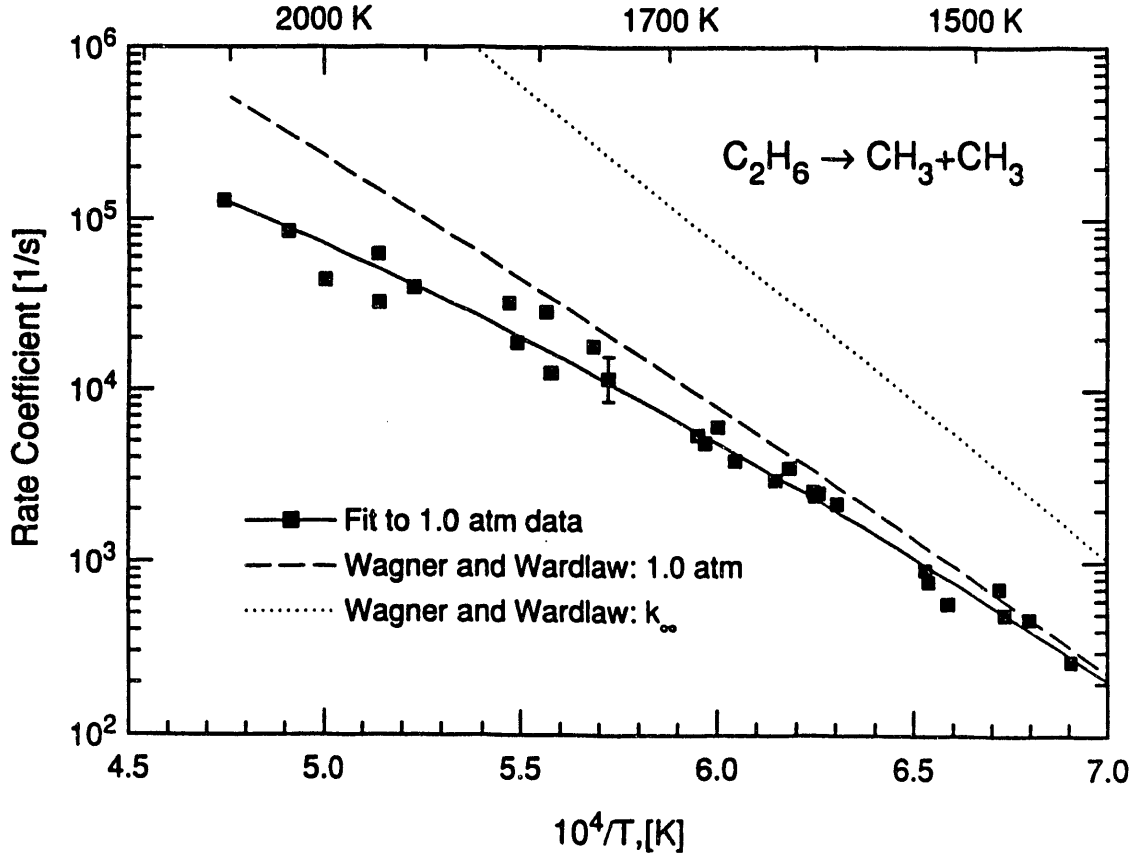

Fig. 1. Shock tube measurements of C_2H_6 decomposition rate coefficient and comparison with Wagner and Wardlaw recommendation.

Theoretical Studies of Potential Energy Surfaces*

Lawrence B. Harding

Chemistry Division
Argonne National Laboratory
Argonne, IL 60439

The goal of this program is to calculate accurate potential energy surfaces (PES) for both reactive and nonreactive systems. To do this the electronic Schrodinger equation must be solved. Our approach to this problem starts with multiconfiguration self-consistent field (MCSCF) reference wavefunctions. These reference wavefunctions are designed to be sufficiently flexible to accurately describe changes in electronic structure over a broad range of geometries. Electron correlation effects are included via multireference, singles and doubles configuration interaction (MRSDCI) calculations. With this approach, we are able to provide useful predictions of the energetics for a broad range of systems.

Reactive Potential Surfaces for $C(^1D)+H_2$. Potential surfaces for both linear and C2v approaches of $C(^1D) + H_2$ have been examined with large basis set (polarized triple-zeta), MRSDCI calculations employing a full valence CAS reference wavefunction. The calculations show no barrier to C_{2v} insertion on the $^1A_1$ surface. The calculations also predict a crossing between the $^1B_1$ and $^1A_2$ surfaces at an energy well below that of the $C(^1D) + H_2$ asymptote, giving a second, zero barrier route for insertion. These results are in accord with recent experiments by Reisler et al (1992) who found little or no Λ-doublet preference in the $CH(^2\Pi)$ product.

Collinear abstraction pathways have also been characterized for the $^1\Pi$, $^1\Delta$ and $^1\Sigma^+$ surfaces, all of which correlate with the $C(^1D) + H_2$ asymptote. Abstractions on the $^1\Delta$ and $^1\Sigma^+$ surfaces are predicted to be significantly endothermic, leading to excited states of CH with no barrier to the reverse reactions. Abstraction on the $^1\Pi$ surface is calculated to be 6.0 kcal/mole exothermic (including zero point), in good agreement with experiment, 6.0 kcal/mole. The predicted barrier to colinear abstraction is 13.0 kcal/mole. The later process has recently been invoked (Gericke et al, 1993) to explain a change in the dynamics of the $C(^1D) + H_2$ reaction for H_2 (v=1).

Ar + $O(^3P)$ Interaction Potentials. This year an extensive series of calculations on the $^3\Pi$ and $^3\Sigma^+$ potential curves of Ar-O have been completed. The calculations employed three different basis sets, polarized double-zeta, polarized triple-zeta, and polarized quadruple-zeta. All of these valence basis sets were augmented by the addition of diffuse functions to improve the description of the long-range interaction. The largest basis set employed then consists of (6s,5p,4d,3f,2g) contracted Gaussians on the oxygen and (7s,6p,4d,3f,2g) functions on the argon. With each of these basis sets interaction potentials were characterized using an RHF+1+2 wavefunction. The effects of corrections for both higher-order excitations and basis set superposition errors have also been examined. Higher order excitations are found to increase the binding energies by ~50% for all basis sets. Counterpoise corrections appear to slow the convergence of the interaction potential with respect to increases in the size of the basis set. The best calculations predict binding energies of 62 and 36 cm^{-1} for the $^3\Pi$ and $^3\Sigma^+$ states respectively. The calculations also predict a crossing between these two potential curves at ~4.2. Å. These calculations are now being used in collaboration with Schatz to aid in the interpretation of crossed-molecular beam scattering experiments of Liu.

CX_3-Y Dissociation Potentials. Potential curves for the bond cleavage reactions, CH_3-H, CH_3-F, CH_3-Cl, CF_3-H, CCl_3-H and CCl_3-Cl have been characterized using high level ab initio calculations. The smaller species were examined using both polarized double-zeta and polarized triple-zeta basis sets while for the larger species only polarized double-zeta calculations were feasible. The small molecule triple-zeta results have been used to scale the large molecule double-zeta results. For CH_3-F, calculations were carried out for all singlet states correlating with the CH_3+F ground state asymptote for both the C_{3v} reaction path and for planar approaches. The differences between the planar and nonplanar pathways give the barriers to methyl rotation relative to the incoming halogen as a function of the C-F distance. The planar calculations predict the existence of surface crossings between the three singlet surfaces correlating with $F(^2P)$. It is planned to use these potential surfaces to model the dissociation dynamics of CX_3-Y molecules.

H_3CO Decomposition Pathways. The reaction of atomic oxygen with methyl radicals has usually been assumed to proceed via addition, forming methoxy radical, followed by CH bond cleavage forming formaldehyde and atomic hydrogen. However recent measurements by Leone et al have suggested that carbon monoxide is also a product of this reaction. In an attempt to understand the mechanism for production of carbon monoxide an extensive search was made for alternative pathways for decomposition of methoxy radical. Particular reactions examined include,

$$
\begin{array}{llllll}
CH_3O & \rightarrow & H + H_2CO & & & (1) \\
 & \rightarrow & H_2 + HCO & \rightarrow & H_2 + H + CO & (2) \\
 & \rightarrow & H_2COH & \rightarrow & H + H_2CO & (3) \\
 & & & \rightarrow & H_2 + HCO \rightarrow H_2 + H + CO & (4) \\
 & & & \rightarrow & H_2 + HOC \rightarrow H_2 + H + CO & (5)
\end{array}
$$

The initial search was performed with a polarized double-zeta basis set and an RHF+1+2 wavefunction. The relative energies of the minima and transition states located in this way were then re-evaluated with a polarized triple-zeta basis set. Of reactions (2)-(5), the only one with a transition state energy close enough to (1) to be competitive is reaction (3) which leads to the same products. No transition states for either the direct (1,1) elimination of H_2 from CH_3O, reaction (2), or the (1,2) elimination of H_2 from H_2COH, reaction (4), could be located. A relatively low energy pathway for the (1,1) elimination of H_2 from CH_3O was located with the constraint that the CH bond lengths to the departing hydrogens be kept equal. However, when this constraint was relaxed the geometry collapsed to the transition state for loss of atomic hydrogen. A transition state for the (1,1) elimination of H_2 from H_2COH was found, reaction (5), however it is predicted to lie more than 50 kcal/mole above the barrier to reaction (1). These results then provide no explanation for the observation of carbon monoxide as a direct product.

Intermediates in the Reaction of C_2H+O_2. Calculations aimed a characterizing possible intermediates in the reaction of C_2H with O_2 are now in progress. The calculations predict no barrier to the addition of O_2 and C_2H, forming a planar peroxy radical, HC_2O_2 ($^2A''$). This addition is predicted to be 42 kcal/mole exothermic. Other energetically accessible intermediates include an excited state of the peroxy radical, $^2A'$, calculated to lie 14 kcal/mole above the ground state, and two ring structures, a three membered ring and a four membered ring predicted to lie 2 and 16 kcal/mole above the peroxy radical, respectively. Several OCCHO structures have also been examined, all are predicted to lie > 50 kcal/mole below the peroxy radical.

*Work performed under the auspices of the Office of Basic Energy Sciences, Division of Chemical Sciences, U.S. Department of Energy, under Contract W-31-109-Eng-38.

PUBLICATIONS:

Ab Initio Examination of the Electronic Excitation Spectrum of CCH
A.G. Koures and L. B. Harding, *J. Phys. Chem.* **94**, 1035-1040 (1991).

Theoretical Studies of the Hydrogen Peroxide Potential Surface. 2. An Ab Initio, Long-Range, $OH(^2\Pi) + OH(^2\Pi)$ Potential
L. B. Harding, *J. Phys. Chem.* **95**, 8653-8660(1991).

REMPI Mass Spectrum of the OH Radical in the Gas Phase
R. Forster, H. Hippler, K. Hoyermann, G. Rhode and L. B. Harding,
Chem. Phys. Letts. **183**, 465-470(1991).

Isotope Effects in Addition Reactions of Importance in Combustion: Theoretical Studies of the Reactions $CH+H_2 \leftrightarrow CH_3 \leftrightarrow CH_2+H$
A.F. Wagner and L. B. Harding,
ACS Symposium Series 502, J.A. Kaye, Ed., 48-63(1992).

The Homogeneous Pyrolysis of Acetylene II: The High Temperature Radical Chain Mechanism
J.H. Kiefer, S.S. Sidhu, R.D. Kern, K. Xie, H. Chen, and L.B. Harding,
Combust. Sci Tech., **82**, 101-130(1992).

A Quasiclassical Trajectory Study of OH Rotational Excitation in OH+CO Collisions using Ab Initio Potential Surfaces
K. Kudla, A.G. Koures, L.B. Harding and G.C. Schatz,
J. Chem. Phys. **96**, 7465-7473(1992).

Theoretical Studies of the Reactions $H+CH \leftrightarrow C+H_2$ and $C+H_2 \leftrightarrow CH_2$ Using Ab Initio Global Ground State Potential Surface for CH_2
L. B. Harding, R. Guadagnini and G.C. Schatz,
J. Chem. Phys., (submitted).

Femtosecond Laser Studies of Ultrafast Intramolecular Processes

Carl Hayden
Combustion Research Facility
Sandia National Laboratories
Livermore, CA 94551-0969

Program Scope

The goal of this research is to better understand the detailed mechanisms of chemical reactions by observing, directly in time, the dynamics of fundamental chemical processes. In this work femtosecond laser pulses are used to initiate chemical processes and follow the progress of these processes in time. We are currently studying ultrafast internal conversion and subsequent intramolecular relaxation in unsaturated hydrocarbons. In addition, we are developing nonlinear optical techniques to prepare and monitor the time evolution of specific vibrational motions in ground electronic state molecules.

Recent Progress

(1) Ultrafast Internal Conversion Studies

Ultrafast internal conversion offers a unique opportunity to generate vibrationally excited molecules on a 100 fsec time scale and to study their time evolution at excitation energies well above potential barriers to isomerization and dissociation. Spectroscopic studies[1,2] have provided much information on the initially excited electronic states involved in internal conversion. However, information on dynamics from these spectroscopic studies does not extend beyond the time scale for electronic dephasing, which in some cases can be less than 10 fsec. For molecules that undergo internal conversion much faster than any relevant fluorescence times there is very little experimental information on the processes occuring after the initial electronic dephasing time. With femtosecond lasers we are now able to follow these processes in time and observe subsequent steps, such as, evolution through intermediate electronic states, isomerization and vibrational energy redistribution.

The femtosecond pulses needed for these experiments are produced by a laser system that we have developed over the past several years. Low power pulses are generated by a colliding-pulse mode-locked dye laser operating at 628 nm. These 300 pJ pulses are amplified to 100 μJ in a multi-pass dye amplifier. A portion of the amplified pulse is focussed into a thin quartz window to generate a broad band continuum. The desired bandwidth filtered from this continuum is further amplified to produce a high energy, tunable output. For the current experiments, this laser system generates 300 μJ pulses tunable around 750 nm with a pulse length of about 60 fsec. These pulses are doubled and then mixed with the fundamental to produce up to 10 μJ at 250 nm in pulses of less than 200 fsec. An additional continuum source and amplifier chain provides another synchronized and tunable femtosecond pulse output needed for multiple wavelength excite-probe measurements.

We have chosen the molecule 1,3,5-hexatriene for our first studies of ultrafast internal conversion. Previous spectroscopic studies have been interpreted to show that internal conversion in this molecule occurs in about 50 fsec. We have been studying this process using femtosecond photoionization of the excited state molecules. In these experiments a femtosecond pulse at 250 nm excites the 0-0 band of the S_2 state in 1,3,5-hexatriene (mixture of cis and trans isomers). A second femtosecond pulse at 350 nm ionizes the excited molecules and the ion yield is measured as a function of time delay between the excitation and ionization pulses. The results are shown in Fig. 1. A spike of ion production is observed at zero delay when the pulses overlap in time. This shows that the initial internal conversion process is very fast, within our time resolution of ~150 fsec. The ionizing pulse at 350 nm can excite the molecule only about 0.3 eV over the ionization threshold, so only low lying vibrational levels of the ion can be produced. As the excited state neutral rapidly evolves, its wave function ceases to overlap favorably with low ion levels and thus there is significant ion yield only when the excitation and probe pulses overlap.

To probe the internal conversion process further in time the ionization step must access higher vibrational levels of the ion. We do this by focusing the 350 nm pulse gently to enhance the multiphoton ionization probability. The result of scanning the focused 350 nm pulse in time relative to the 250 nm excitation pulse is shown in Fig. 2. The molecule is now seen to evolve for more than 1 picosecond. The multiphoton ionization also produces fragment ions. By using a mass spectrometer to observe the yield of a fragment ion we can distinguish multi-photon from single photon ionization because single photon ionization does not supply sufficient energy for fragmentation. The time delay scan for production of four-carbon fragments is also shown in Fig. 2. The production of fragment ions is delayed relative to the parent ion yield. This delay can be explained by recognizing that the parent ion yield contains both single and multiphoton ionization contributions. The initially excited neutral ionizes efficiently at the one photon level to give parent ions, but at the intensities used, fragment ions are not produced until the neutral evolves enough that its wavefunction overlaps favorably with higher ion levels and multiphoton ionization becomes efficient. Thus, the fragment ion delay curve traces the time evolution of the product of the internal conversion. We have measured all of the observed fragment ions and they have the same time delay curves, indicating that a single process in the neutral is being observed. These experiments set a lower limit of about 1.5 picoseconds on the time needed for the vibrational energy distribution to become statistical.

(2) Three-Color Femtosecond CARS Experiments

We are also developing the capability to coherently excite specific vibrational motions in molecules using femtosecond stimulated Raman pumping and then probe the time evolution of these motions. To coherently excite a vibration, two time-coincident femtosecond pulses are tuned so that their frequency difference corresponds to a Raman mode of the molecule. A third, time-delayed femtosecond pulse at a unique wavelength probes the resulting sample polarization by coherent anti-Stokes Raman scattering. The results obtained exciting the 992 cm^{-1} symmetric ring-breathing motion in benzene are shown in Fig. 3. The excitation pulses are at 700 and 750 nm while the probe pulse is at 375 nm. The anti-Stokes signal is detected around 350 nm. The large peak in the data at

zero time delay is due to nonresonant processes, but by using a time-delayed probe at a unique wavelength the resonant contribution is clearly distinguishable. The motion excited is nearly a vibrational eigenstate so the slow decay is due primarily to inhomogeneous effects such as the excitation of a broad rotational distribution. In Fig. 4 the results are shown for a similar experiment where several Raman modes around 1200 cm^{-1} are excited in 1,3,5-hexatriene. In this floppy molecule the intramolecular dephasing of the motion is clearly observed as the time scale for the decay is more than a factor of 10 shorter than in benzene. Beating between the different modes excited is also observed. This technique now allows us to specifically excite and monitor the time evolution of any Raman active motion in a molecule.

Future Plans

We have recently installed a photoelectron spectrometer that will more completely characterize the intermediates observed in internal conversion processes. Using this apparatus we have taken single-pulse photoelectron spectra of internally converting molecules and will soon be measuring photoelectron spectra as a function of delay between excitation and ionization laser pulses. We are also studying other molecules showing rapid internal conversion, such as 1,3-cyclohexadiene. In initial work on this molecule we have seen strong evidence for opening of the ring within ~200 fsec after excitation. Work on this and other molecules will continue.

Future work on femtosecond stimulated Raman excitation will be directed toward exciting higher energy vibrational motions in molecules by using resonant intermediate electronic states. This is a promising method for efficiently exciting vibrational overtones on a femtosecond time scale. We also plan to apply other detection methods, such as multiphoton ionization, that can detect subsequent time evolution of the vibrational excitation in addition to the coherence decay of the initially excited motion.

References

1. A. B. Myers and K. S. Pranata, J. Phys. Chem., **93**, 5079 (1989).
2. D. G. Leopold, R. D. Pendley, J. L. Roebber, R. J. Hemley, V. Vaida, J. Chem. Phys., **81**, 4218 (1984).

Publications, 1991-Present

R. Trebino and C.C. Hayden, "Anti-Resonant-Ring Transient Spectroscopy," Opt. Lett. **16**, 493 (1991).

A.M. Levine, E. Ozizmir, R. Trebino, C. C. Hayden, and A. Johnson, "New Developments in Autocorrelation Measurements of Ultrashort Pulses," *Laser Spectroscopy X*, eds. M. Ducloy, E. Giacobino, and G. Camy, p. 384 (1992).

M. A. Buntine, D. W. Chandler, and C. C. Hayden, "A Two-Color Laser-Induced Grating Technique for Gas-Phase Excited-State Spectroscopy," J. Chem. Phys., **97**, 707 (1992).

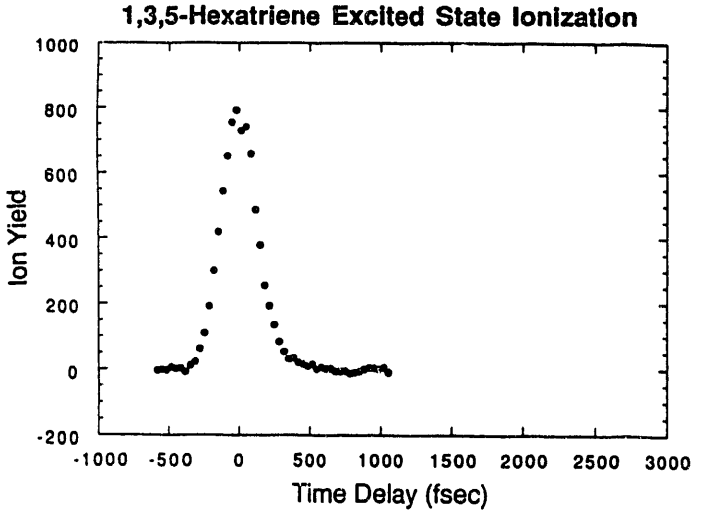

Fig. 1
Ion yield as a function of time delay between the 250 nm excitation pulse and a 350 nm ionization pulse.

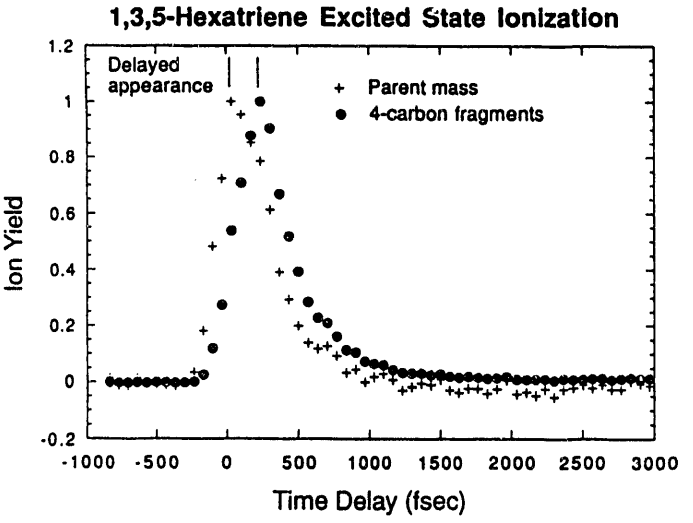

Fig. 2
Ion yield as a function of delay between 250 nm excitation pulse and a focused 350 nm pulse. Data are shown for parent ion detection and 4-carbon fragment ion detection. The fragment ion curve monitors the time evolution of the internal conversion product.

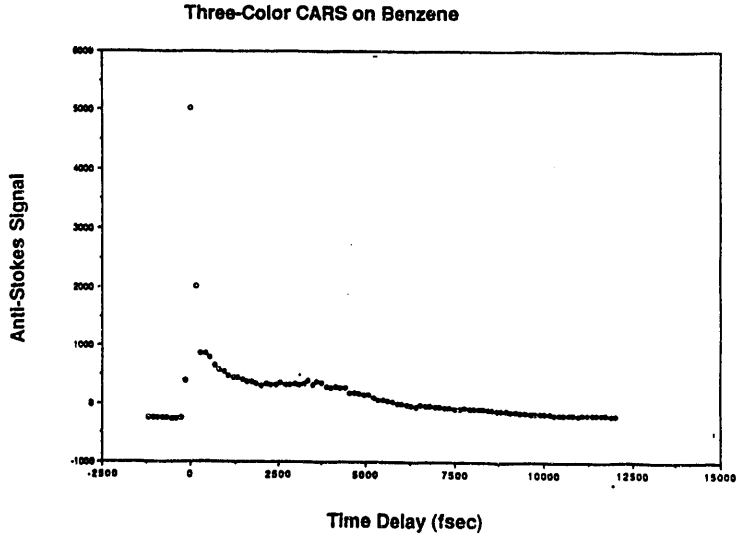

Fig. 3
Coherent anti-Stokes signal as a function of delay from the excitation pulses exciting the 992 cm^{-1} Raman mode in benzene. The spike at zero delay is due to nonresonant contributions to the four-wave mixing process.

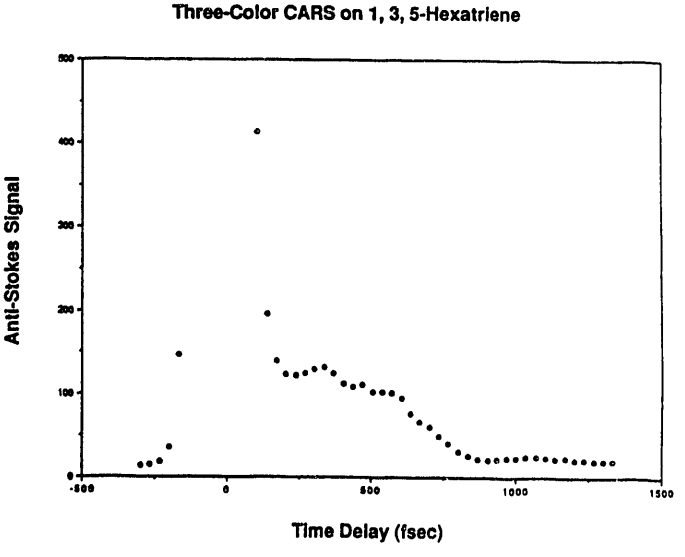

Fig. 4
Coherent anti-Stokes signal as a function of delay from the excitation pulses exciting Raman modes around 1200 cm^{-1} in 1,3,5-hexatriene. Note the change in time scale from the previous figure.

Elementary Reaction Rate Measurements at High Temperatures by Tunable-Laser Flash-Absorption

Jan P. Hessler

Gas Phase Chemical Dynamics Group
Chemistry Division
Argonne National Laboratory
9700 South Cass Avenue
Argonne, Illinois 60439

The major objective of this program is to measure thermal rate coefficients and branching ratios of elementary reactions. To perform these measurements, we have constructed an ultrahigh-purity shock tube to generate temperatures between 1000 and 5500 K. The tunable-laser flash-absorption technique is used to measure the rate of change of the concentration of species which absorb below 50,000 cm^{-1} *e.g.*: OH, CH, and CH_3. This technique is being extended into the vacuum-ultraviolet spectral region where we can measure atomic species *e.g.*: H, D, C, O, and N; and diatomic species *e.g.*: O_2, CO, and OH.

Correlation Analysis In a kinetic experiment that uses linear optical techniques, *e.g.* optical absorption, the magnitude of the observed signal always depends upon the product of the strength of the interaction between the light field and the absorbing species and the concentration of this species. For measurements of unstable species, such as radicals, kineticists have always had the fundamental problem that the concentration of the radical depends upon the kinetic behavior of the chemical systems used to produce the radical, which is not always known. Therefore, one encounters cyclic arguments where concentrations and kinetic behavior are inferred from previous measurements of the strength of the optical interaction which, of course, have been inferred from an assumed knowledge of the kinetic behavior of the radical. To help identify situations where the strength of the optical interaction may be measured without interference from the kinetics of the chemical system we have applied the ideas developed in correlation analysis[1] and derived reduced sensitivity coefficients for a given species with respect to the strength of the optical interaction, *i.e.* the absorption cross section. This approach allows us to directly compare the sensitivity with respect to a given reaction rate coefficient with the sensitivity with respect to the optical absorption cross section. In the future, we will extend these ideas to include techniques which depend upon a bulk parameter such as the density gradient measured by schlieren techniques, and non-linear optical techniques such as degenerate four-wave mixing. We have prepared a report which describes the codes needed to perform both a standard correlation analysis and one involving absorption cross sections. Contact the author for a copy of the codes and report.

A numerical problem frequently encountered in the least-squares analysis of experimental kinetic data stems from the fact that the condition number of the curvature matrix, *i.e.* the ratio of the largest-to-smallest diagonal elements, may be as high as 10^{70}. Such large values make accurate evaluation of rate coefficients almost impossible. To drastically reduce the condition number we have reformulated least-squares analysis to produce a dimensionless curvature matrix. This reformulation produces condition numbers that are generally less than 10^3. Additional advantages of this approach are that the relative

importance of different rate coefficients and physical parameters may be determined before the fitting procedure is initiated and, after the fit is complete, the correlation between the *best-fit* parameters may be described by a simple vector.

Methyl Chemistry At combustion temperatures there are two main channels for the reaction of methyl radicals with molecular oxygen

$$CH_3 + O_2 \rightarrow H_3COO^* \begin{cases} \rightarrow H_3CO + O \rightarrow H_2CO + O + H & \text{(Channel A)} \\ \rightarrow H_2COOH \rightarrow H_2CO + OH & \text{(Channel B)} \end{cases}$$

The reactions of channel A are endothermic whereas channel B is exothermic. The energy difference between these two channels is just the dissociation energy of hydroxyl, $D_0^0/k = 50970$ K. Because of this large energy difference, the branching ratio between these channels will control the ignition rate of hydrocarbon/oxygen mixtures.

Last year, we showed that in very lean mixtures, $[O_2]_0/[C_2H_6N_2]_0 > 4000$, the hydroxyl radical may be monitored to measure the rate of channel B without interference from the methyl-methyl recombination reactions or other hydrocarbon reactions and presented preliminary measurements of the rate coefficient for channel B. A more detailed examination of our results has shown that under the conditions of our initial experiments the rates of formation of hydroxyl and of vibrational relaxation of O_2 are comparable. Therefore, we have to measure the rate coefficient in the transition region between the shock front and the establishment of thermodynamic equilibrium. To accomplish this we have devised, or perhaps reinvented[2], a reaction mechanism which accurately mimics the vibrational relaxation of molecular oxygen, the reactions with the unrelaxed oxygen, and the temperature, pressure, and density changes in the transition region. Briefly, the approach is to add to the mechanism a rigid-rotor molecule of O_2 as an unrelaxed species. Vibrational relaxation may then be introduced by the reaction

$$O_2(\text{rigid-rotor}) + M \rightarrow O_2(\text{equilibrium}) + M$$

where a different rate expression is supplied for each collision partner. Important reactions within the transition region, such as with methyl, are written as

$O_2(\text{rigid-rotor}) + CH_3 \rightarrow H_2CO + OH$ with the rate coefficient $k_{\text{rigid-rotor}}$ and

$O_2(\text{equilibrium}) + CH_3 \leftrightarrow H_2CO + OH$ with the rate coefficient k_{equil}.

The specific heat, entropy, and enthalpy of the rigid-rotor molecule are determined by subtracting the vibrational contribution from the standard thermodynamic expressions.

To experimentally alter the rate of vibrational relaxation of O_2 we have performed experiments with both argon and a mixture of argon and helium as the buffer gas. From the experiments with argon plus helium we are able to extract a rate coefficient at equilibrium

$$k_{equil}(T) = 4.2 \times 10^{-13}\exp\{-4500/T(K)\}\ cm^3s^{-1}.$$

With the above rate coefficient held fixed, the rate coefficient for the reaction between methyl and O_2(rigid-rotor) is determined from experiments with only the argon buffer gas. This rate is

$$k_{rigid\text{-}rotor}(T) = 5.1 \times 10^{-14}\exp\{-2600/T(K)\}\ cm^3s^{-1}.$$

Physically we may identify the rate coefficient for the rigid-rotor as the rate coefficient for the reaction with $O_2(\nu = 0)$. We may then use the two measured rate coefficient to estimate the rate coefficient for $O_2(\nu = 1)$. We obtain $k[O_2(\nu=1)]/k[O_2(\nu=0)] \approx 7$. The results for the two measured rate coefficients and for the estimate of $k[O_2(\nu=1)]$ are shown in the figure. Our results for the rate coefficient at equilibrium compare favorably with the results of Saito et. al.[3], Fraatz[4], Zellner[5]. Also, they are only 30% below the recent work of Lissianski and Gardiner[6]. To our knowledge, this is the first observation of level-specific bimolecular rate coefficients in a shock tube experiment and for this type of reaction.

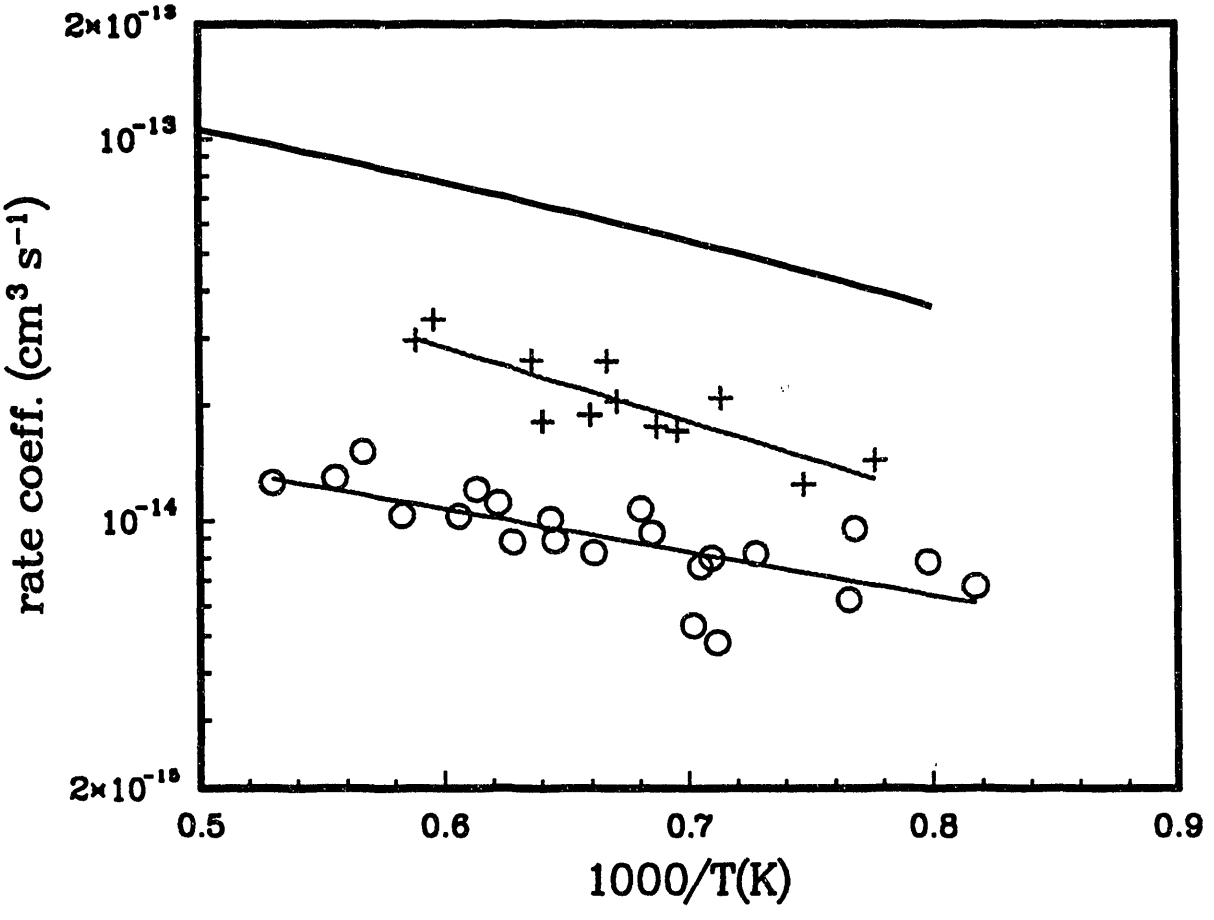

Figure 1. Rate coefficients for $CH_3 + O_2$(equilibrium) and $CH_3 + O_2$(rigid-rotor) $\rightarrow H_2CO + OH$. Data for O_2(rigid-rotor) is given by the symbol O and for O_2(equilibrium) by the symbol +. The solid line is the estimate of $k[O_2(\nu=1)]$.

This work is supported by the United States Department of Energy, Office of Basic Energy Sciences, under contract W-31-109-ENG-38.

Publications Supported by this Program, 1991-93

"Rate coefficient for the reaction H + O_2 → OH + O; Results at high temperatures, 2000 TO 5300 K," H. Du and J. P. Hessler, *J. Chem. Phys.* **96**, 1077-92 (1992).

"Correlation analysis of complex kinetic systems: A new scheme for utilizing sensitivity coefficients," J. P. Hessler, P. J. Ogren, *J. Chem. Phys.* **97**, 6249-58 (1992).

References

1. J. P. Hessler and P. J. Ogren, *J. Chem. Phys.* **97**, 6249-58 (1992).

2. J. H. Kiefer has informed us that this method is quite old. However, we have not been able to locate a published description of the method.

3. K. Saito, R. Ito, T. Kakumoto, and A. Imamura, *J. Phys. Chem.* **90**, 1422-27 (1986).

4. W. Fraatz, PhD Dissertation, Göttingen, 1990.

5. R. Zellner, in *Kinetics and mechanisms of elementary chemical processes of importance in combustion*, coordinated by R. A. Cox, Commission of the European Communities, 1990, pp. 165-177.

6. V. Lissianski and W. C. Gardiner, Jr., private communication, 7 Jan 1993.

Spectroscopic Investigation of the Vibrational Quasi-Continuum Arising from Internal Rotation of a Methyl Group

Jon T. Hougen, Molecular Physics Division, NIST, Gaithersburg, MD 20899

The goal of this project is to use spectroscopic techniques to investigate in detail phenomena involving the vibrational quasi-continuum in a simple physical system. Acetaldehyde was chosen for the study because: (i) methyl groups have been suggested to be important promotors of intramolecular vibrational relaxation, (ii) the internal rotation of a methyl group is an easily describable large-amplitude motion, which should retain its simple character even at high levels of excitation, and (iii) the aldehyde carbonyl group offers the possibility of both vibrational and electronic probing.

The present investigation of the ground electronic state has three parts: **(1)** understanding the "isolated" internal-rotation motion below, at, and above the top of the torsional barrier, **(2)** understanding in detail traditional (bond stretching and bending) vibrational fundamental and overtone states, and **(3)** understanding interactions involving states with multiquantum excitations of at least one of these two kinds of motion. Activities during the two and one-half years of this project will be grouped under the three headings of this paragraph.

(1) The internal-rotor manifold

A global fit has been carried out[1] on data consisting of (i) almost all a-type lines from torsional states with $v_t = 0$, 1 and 2 found in the broad-band submillimeter pure rotation spectrum of acetaldehyde recorded at room temperature in Nizhny Novgorod, Russia (measurement precision ~1 MHz), (ii) some 250 $v_t = 0$ and 1 a and b-type microwave lines near 300 GHz[2] (measurement precision ~50 kHz), and (iii) about 400 lines from the far-infrared $v_t = 2 \leftarrow 1$ a,b-hybrid hot band. While we still hope to add some b-type $v_t = 2$ microwave lines to this fit to improve the experimental precision of $\Delta K \neq 0$ energy intervals, it must be said that for the purposes of this project, all torsion-rotation levels below the top of the internal rotation barrier are now understood, both experimentally and theoretically. (To our surprise, the existing theoretical model[3] seems adequate for this understanding.)

We are now turning our attention to torsion-rotation levels just above the barrier. In particular, the A and E components of $v_t = 3$ and the A component of $v_t = 4$ all lie above the barrier, but below the first small-amplitude vibrational fundamental, so we expect these to be understandable within the framework of a pure torsion-rotation model. However, levels above the barrier fall in a regime where essentially no quantitative comparison of experiment and theory exists for any molecule. Preliminary calculations show that the $v_t = 3$ and 4 A states exhibit a strong Coriolis-like interaction (as the energy levels try to reorganize at the top of the barrier). We are exploring the usefulness of rotational energy surfaces[4] and other techniques for describing these levels. Experimentally, we believe we can get $\Delta K=0$, $\Delta J\neq 0$ energy level differences from the Nizhny Novgorod spectrum, but we do not yet

know which type of data (infrared hot bands, infrared combination bands, microwave spectra, double resonance studies, etc.) can provide $\Delta K \neq 0$ energy differences.

The theoretical paper, "in preparation" last year, is now nearly finished. This paper attempts to clarify some existing confusion associated with the K_a,K_c rotational quantum numbers, forbidden "c-type" transitions, and matrix elements of the dipole moment operator in a molecule exhibiting internal rotation, by discussing intensity questions in terms of the competition between internal rotation effects and asymmetric-rotor K-type doubling effects for control of the the "good quantum numbers" in the final eigenfunctions, and in terms of extended group theory[5]. The paper was delayed to permit inclusion of a description of the new version of the Brussels global fit program, which which now gives intensity predictions incorporating these theoretical results. Such intensity predictions will almost certainly be necessary to make sense of observed transitions involving torsion-rotation levels in the unstudied quantum mechanical regime above the barrier.

(2) The traditional vibrational manifold
(3) Interactions between internal rotation and ordinary vibrations

Significant progress has been made in studies of the traditional vibrational manifold and its interactions with quasi-continuum precursor states, but events did not unfold exactly as anticipated in last year's report.

The 920 cm^{-1} band was recorded at NIST using a CO_2 side-band laser and supersonic cooling. On the basis of the old Shimanouchi tables[6], this band was expected to be a CH_3 rocking fundamental, though low-resolution liquid and solid phase data from the same era[7] assigned it to a combination band. Later ab initio calculations[8] supported the combination band assignment, but challanged a higher-frequency mode reassignment of Ref. 7. As a result, contrary to expectations for such a small and apparently well-studied molecule, the location of some vibrational fundamentals is not completely settled. The NIST high-resolution work shows conclusively that the 920 cm^{-1} band is a combination band involving one quantum of the torsion. Further, on the basis of the torsional splittings observed in the NIST spectrum, the 20 cm^{-1} Fermi resonance interaction deduced in Ref. 7 seems to be correct, but we have recorded the presumed Fermi resonance partner (the C-C stretch at 867 cm^{-1}) to verify this explanation. Since Fermi resonance is often invoked in IVR explanations, it is important to this project to understand this large Δv(torsion) = 1 Fermi resonance in detail.

Analysis is nearing completion of the room-temperature Bruker FTIR spectrum of the 763 cm^{-1} fundamental recorded in Brussels by M. Herman. This band appears to show some evidence of small perturbations, which can only come from interaction with a combination level involving two quanta of the torsion, or with a pure torsional state lying well above the torsional barrier. Either of these explanations will be interesting from the point of view of torsion-induced mechanisms for driving IVR processes at higher energies, but it is still too early to tell what the actual situation is.

S. Belov and A. Andrews used a slit-nozzle diode laser spectrometer at NIST to record the C=O stretching fundamental. These

measurements were carried out against the advice of the PI, who thought (in the company of some others) that this band would be heavily fragmented by interaction with the bath states, and therefore would be unanalyzable at the present time. Contrary to such thinking, the present low-temperature spectrum seems relatively simple and uncluttered. Even though no assignments exist at present, it is tempting to conclude from the apparent simplicity of the spectrum, that strong interaction of the C=O stretch with the bath states will not be turned on until (i) the methyl group begins to rotate, or (ii) the whole molecule begins to rotate at high angular velocity. It is important from the point of view of understanding IVR processes to determine to what extent either or both of these speculations is correct, and we plan to continue work in the C=O stretching region.

Because of the frequency coincidence with the color center laser, Andrews, Pate and Fraser have also recorded the C=O overtone. Here preliminary assignments have already been made which indicate moderate fragmentation from interactions with the bath states even in the cold (several kelvin) spectrum.

A Fourier transform spectrum of the lowest fundamental of acetaldehyde at 509 cm^{-1}, which is essentially degenerate with a pure torsion free rotor E state with m = 7, has been recorded in Germany, and is being analyzed by Drs. S. Urban and P. Pracna (Phys. Chem. Institute in Prague), in collaboration with Dr. K. Yamada in Cologne. The present status of this work is not known at the time of this writing.

Work on the small-amplitude fundamentals will continue during the coming year, always with the goal of qualitative understanding and quantitive descriptions for interactions with the surrounding quasi-continuum precursor states. (It should be added here that Fraser, Pate and Andrews at NIST, though not funded by this project, are also quite interested in interactions with these bath states, and this rather outstanding team has investigated a number of other internal rotor molecules. The results and experience they are accumulating contribute directly to the design and interpretation of experiments in the present project.)

---

[1]S. P. Belov, M. Yu. Tretyakov, I. Kleiner and J. T. Hougen, J. Mol. Spectrosc. in press.
[2]W. L. Barclay, Jr., M. A. Anderson, L. M. Ziurys, I. Kleiner and J. T. Hougen, Ap. J. Supplement, in press.
[3]W. Liang, J. G. Baker, E. Herbst, R. A. Booker and F. C. DeLucia, J. Mol. Spectrosc. **120**, 298-310 (1986).
[4]W. G. Harter and C. W. Patterson, J. Chem. Phys. **80**, 4241-4261 (1984).
[5]J. T. Hougen and B. J. DeKoven, J. Mol. Spectrosc. **98**, 375-391 (1983).
[6]T. Shimanouchi, "Tables of Molecular Vibrational Frequencies, Consolidated Volume I," NSRDS-NBS 39, 1972.
[7]H. Hollenstein and Hs. H. Günthard, Spectrochim. Acta, **27A**, 2027-2060 (1971).
[8]K. B. Wiberg, V. Walters and S. D. Colson, J. Phys. Chem. **88**, 4723-4728 (1984).

Publication of DoE sponsored research:

"The Ground Torsional State of Acetaldehyde"
I. Kleiner, J. T. Hougen, R. D. Suenram, F. J. Lovas and M. Godefroid, J. Mol. Spectrosc. **148**, 38-49 (1991).

"The Ground and First Torsional States of Acetaldehyde"
I. Kleiner, J. T. Hougen, R. D. Suenram, F. J. Lovas and M. Godefroid, J. Mol. Spectrosc. **153**, 578-586 (1992).

"The Second Torsional State of Acetaldehyde"
S. P. Belov, M. Yu. Tretyakov, I. Kleiner and J. T. Hougen, J. Mol. Spectrosc. in press.

"The Laboratory Spectrum of Acetaldehyde at 1 mm (230-325 GHz)"
W. L. Barclay, Jr., M. A. Anderson, L. M. Ziurys, I. Kleiner and J. T. Hougen, Ap. J. Supplement, in press.

"Electric-Resonance Optothermal Spectrum of the 920 cm^{-1} $\nu_{14} + \nu_{15}$ Torsional Combination Band of Acetaldehyde"
S. Belov, G. T. Fraser, J. Ortigoso, B. H. Pate and M. Yu. Tretyakov, Chem. Phys. Lett. in press.

"Selection Rules and Intensity Calculations for a C_s Asymmetric Top Molecule Containing a Methyl Group Internal Rotor"
I. Kleiner, J. T. Hougen and M. Godefroid, in preparation.

DOE/ER/13934-1

STUDIES OF COMBUSTION REACTIONS AT THE STATE-RESOLVED DIFFERENTIAL CROSS SECTION LEVEL

P. L. Houston, A. G. Suits, L. S. Bontuyan, and B. J. Whitaker

Department of Chemistry
Cornell University
Ithaca, NY 14853-1301

Program Scope

State-resolved differential reaction cross sections provide perhaps the most detailed information about the mechanism of a chemical reaction, but heretofore they have been extremely difficult to measure. This program explores a new technique for obtaining differential cross sections with product state resolution. The three-dimensional velocity distribution of state-selected reaction products is determined by ionizing the appropriate product, waiting for a delay while it recoils along the trajectory imparted by the reaction, and finally projecting the spatial distribution of ions onto a two dimensional screen using a pulsed electric field. Knowledge of the arrival time allows the ion position to be converted to a velocity, and the density of velocity projections can be inverted mathematically to provide the three-dimensional velocity distribution for the selected product. The main apparatus has been constructed and tested using photodissociations. We report here the first test results using crossed beams to investigate collisions between Ar and NO. Future research will both develop further the new technique and employ it to investigate methyl radical, formyl radical, and hydrogen atom reactions which are important in combustion processes. We intend specifically to characterize the reactions of CH_3 with H_2 and H_2CO; of HCO with O_2; and of H with CH_4, CO_2, and O_2.

Recent Progress

State-to-state differential cross sections for inelastic collisions of NO with Ar have been measured in a crossed-beam experiment using time-of-flight ion imaging. Rotational rainbow peaks are observed in the angular distributions, and these move to backward scattering angles with increasing final rotational level. The images are analyzed using a Monte Carlo forward convolution program that accounts for the transformation from the center-of-mass differential cross sections to the experimental image. The results are interpreted using a simple two-dimensional hard ellipse model to provide quantitative insight into the anisotropy of the potential energy surface. Rotational rainbow peaks appear in the angular distributions, and these move to backward scattering angles with increasing j'. A simple 2-dimensional hard ellipse model provides quantitative insight into the anisotropy of the potential energy surface: a value of 0.32 Å was obtained for the difference between the semi-major and semi-minor axes. For NO ($j' = 18.5$), two rainbow peaks are observed. These double rainbows are predicted for heteronuclear molecules, but have not previously been directly observed in the angular distributions. The 2-D analysis is used to obtain the

eccentricity of the hard ellipse potential from the positions of the two rainbow peaks. At 0.18 eV collision energy, a value of 0.06 Å was obtained for δ, the eccentricity of the ellipse. Finally, the angular distributions for the spin-orbit conserving collisions and spin-orbit changing collisions are remarkably similar, though they were thought to involve two different potential energy surfaces. An alternative mechanism is proposed to account for the spin-orbit changing collisions through non-Born-Oppenheimer spin-rotation coupling. The experiment represents an extension of the ion-imaging technique to a genuine crossed-beam configuration. This new experimental method is general and versatile: it may be used wherever REMPI techniques are applicable, and quantum state resolved angular distributions are obtained for all scattering angles simultaneously.

The program has advanced significantly in the past six months in that we have developed and tested an H atom beam source. We have succeeded recently in generating a well-defined beam of H atoms from photodissociation of H_2S, itself entrained in a molecular beam. Figure 1 displays the position contours of the H atom pulsed beam at the time when a probe laser operating on the Lyman-α transition ionizes the atoms. The arrow on the figure shows the origin of the H atoms, the point at which a 193 laser dissociated a beam of H_2S. The beam has a well defined velocity and width, and is intense enough so that we anticipate good signal to noise for the H + O_2 reaction.

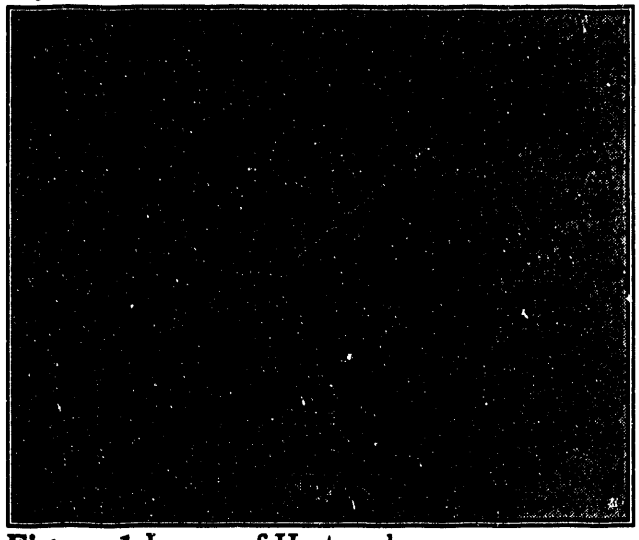

Figure 1 Image of H atom beam.

Future Plans

The next step is to cross this source with another beam of O_2, positioned to intersect the H atom beam at the H atom location shown in the figure. We will then attempt first to detect the O atom product by 2+1 resonance enhanced multiphoton ionization near 226 nm. Attempts will also be made to monitor the OH product through its multiphoton ionization transitions. Simultaneously, we will test a methyl radical source based on photodissociation of methyl iodide.

Publications Acknowledging DOE Support

1. D. B. Moss, K. A. Trentelman, and P. L. Houston, "193 Photodissociation Dynamics of Nitromethane," J. Chem. Phys. **96**, 237-247 (1992).

2. A. G. Suits, L. S. Bontuyan, P. L. Houston, and B. J. Whitaker, "Differential Cross Sections for State-Selected Products by Direct Imaging: Ar + NO," J. Chem. Phys. **96**, 8618-8620 (1992).

3. L. S. Bontuyan, A. G. Suits, P. L. Houston, and B. J. Whitaker, "State-resolved Differential Cross Sections for Crossed-beam Ar-NO Inelastic Scattering by Direct Imaging," J. Phys. Chem., submitted.

AROMATICS OXIDATION AND SOOT FORMATION IN FLAMES

J. B. Howard, C. J. Pope, R.A. Shandross and T. Yadav

Department of Chemical Engineering
Massachusetts Institute of Technology
Cambridge, Massachusetts 02139

SCOPE

This project is concerned with the kinetics and mechanisms of aromatics oxidation and soot and fullerenes formation in flames. The scope includes detailed measurements of profiles of stable and radical species concentrations in low-pressure one-dimensional premixed flames. Intermediate species identifications and mole fractions, fluxes, and net reaction rates calculated from the measured profiles are used to test postulated reaction mechanisms. Particular objectives are to identify and to determine or confirm rate constants for the main benzene oxidation reactions in flames, and to characterize fullerenes and their formation mechanisms and kinetics.

RECENT PROGRESS

Stable and radical species profiles in the aromatics oxidation study were measured using molecular beam sampling with on-line mass spectrometry. A trace additive technique was used in which benzene in low concentration is studied in a well-characterized hydrogen-oxygen-argon flame. In an effort to identify and measure the concentration of species expected to be important primary or secondary products of benzene oxidation, phenoxy and cyclopentadienyl radicals to not appear to be present at the detection limit of the equipment. Phenyl radical is present in sufficient concentrations to permit measurement of its concentration profile. Comparison of the phenyl data against predictions from an early model indicate that either phenyl is not a dominant intermediate in benzene destruction or the phenyl destruction pathway was inadequately modeled. Also measurable are phenol and cyclopentadiene, the relative concentrations of which in a rich H_2-O_2 flame compared to a rich benzene-O_2 flame indicate that benzene destruction may differ significantly between these two systems. Several commonly used H_2-O_2 combustion models failed to predict well the O_2 concentration profile in the rich H_2-O_2-trace benzene flame, possibly indicating inadequate description of the O-atom chemistry.

The rate of soot formation measured by conventional optical techniques was found to support the hypotheses that particle inception occurs through reactive coagulation of high molecular weight PAH in competition with destruction by OH attack, and that the subsequent growth of the soot mass occurs through addition reactions of PAH and C_2H_2 with the soot particles. Soot structure indicated by high resolution electron microscopy of collected samples has the appearance of small particles within the roughly spherical units or spherules comprising the soot agglomerates. This structure would be consistent with the growth mechanism inferred from gas phase species if the small internal particles represent reactive coagulation of heavy PAH, and the larger spherules represent coagulation of the smaller particles in parallel with mass deposition from PAH and C_2H_2.

During the previous year, fullerenes C_{60} and C_{70} in substantial quantities were found in the flames being studied. The fullerenes were recovered, purified and spectroscopically identified. The yields of C_{60} and C_{70} have now been determined over ranges of conditions in low-pressure premixed flames of benzene and oxygen. Similar flames with acetylene as fuel were found to produce fullerenes but in smaller yields than benzene flames. The largest observed yields of C_{60}+C_{70} from benzene-O_2 flames are 20% of the soot produced and 0.5% of the carbon fed. The largest rate of production of C_{60}+C_{70} was observed at a pressure of 69 torr, a C/O ratio of 0.989 and a dilution of 25% helium. Several striking differences between fullerenes formation in flames and in graphite vaporization systems include an ability to vary the C_{70}/C_{60} ratio from 0.26 to 8.8 (cf., 0.02 to 0.18 for graphite vaporization) by adjustment of flame conditions, and production of several apparent adducts involving fullerenes C_{60}, C_{70}, $C_{60}O$ and $C_{70}O$, which undergo facile dissociation to the fullerene cage and a hydrocarbon moiety. A $C_{60}C_5H_6$ adduct was isolated and found to be identical to the Diels-Alder adduct of C_{60} and cyclopentadiene. Fullerenes formation in flames is a molecular weight growth process analogous to the formation of PAH and soot but involving curved and hence strained structures. A kinetically plausible mechanism of the formation of C_{60} and C_{70} fullerenes in flames has been constructed based on the types of reactions already used in describing PAH and soot growth, but including intramolecular rearrangements and other reactions needed to describe the evolution of the unique structural features of the fullerenes.

FUTURE PLANS

In the aromatics oxidation work, further investigation into the presence of C_6H_7 in the rich H_2-O_2-trace benzene flame will be performed. Measurements will be made closer to the burner in a leaner flame, to see if the large predicted quantities of C_6H_7 can be found. The remaining important species (H, OH, H_2O, CO_2, C_2H_2, mass 16, and possibly others) will be measured, and the flame will be further probed for other early aromatics destruction intermediates.

Formal reaction path and sensitivity analyses will be done using reactions from the various mechanisms available, to elucidate the major pathways of benzene oxidation in the rich H_2-O_2 flame. Mechanisms proposed by Chevalier and Warnatz and Emdee, Brezinsky and Glassman will be used as starting points in the analysis. Improvements in the benzene oxidation chemistry resulting from modeling the rich H_2-O_2-trace benzene flame will be tested on the equivalence ratio 1.8 benzene-O_2 flame of Bittner and H_2-O_2-trace benzene flame of Jackson and Laurendeau.

In the study of soot formation a series of soot samples collected through the zones of soot inception and growth will be subjected to high resolution electron microscopy. The objective will be to gain further insight into the mechanistic interpretation of the internal structure of the particles.

The research on fullerenes will be enhanced by the acquisition through an instrumentation grant of a LC/MS instrument with ionization capabilities especially suited for fullerenes. The previous LC/MS analyses of samples from the project have been of major importance, but were performed by collaborators in Canada (see the three listed publications by Anacleto et al.). The in-house availability of the LC/MS will allow more extensive and rapid identification of new fullerenes and curved PAH of interest as fullerene precursors.

PUBLICATIONS FROM THIS PROJECT (1991, 1992 and 1993)

Howard, J.B.: "Radical Sites as Active Sites in Carbon Addition and Oxidation Reactions at High Temperatures", *Fundamental Issues in Control of Carbon Gasification Reactivity*, J. Lahaye and P. Ehrburger, Eds., pp. 377-382, Kluwer Academic Publishers, 1991.

Howard J.B.: "Carbon Addition and Oxidation Reactions in Heterogeneous Combustion and Soot Formation", *Twenty-Third Symposium (International) on Combustion*, The Combustion Institute, Pittsburgh, 1107-1127 (1991).

Shandross, R.A., Longwell, J.P. and Howard, J.B.: "Noncatalytic Thermocouple Coating for Low-Pressure Flames", *Combustion and Flame*, **85**, 282-284 (1991).

Howard, J.B., McKinnon, J.T., Makarovsky, Y., Lafleur, A.L., and Johnson, M.E.: "Fullerenes C_{60} and C_{70} in Flames", *Nature*, **352**, 139-141 (1991).

Anacleto, J.F., Pereault, H., Boyd, R.K., Pleasance, S., Quilliam, M.A., Sim, P.G., Howard, J.B., Makarovsky, Y., and Lafleur, A.L.: "C_{60} and C_{70} Fullerene Isomers Generated in Flames. Detection and Verification by Liquid/Mass Spectrometry Analyses", *Rapid Communications in Mass Spectrometry*, **6**, 214-220 (1992).

PUBLICATIONS (1991, 1992 and 1993) (cont'd)

Howard, J.B., McKinnon, J.T., Johnson, M.E. Makarovsky, Y., and Lafleur, A.L.: "Production of C_{60} and C_{70} Fullerenes in Benzene-Oxygen Flames", *J. Phys. Chem.*, **96**, 6657-6662 (1992).

Howard, J.B., Lafleur, A.L., Makarovsky, Y., Mitra, S., Pope, C.J., and Yadav, T.: "Fullerenes Synthesis in Combustion", *Carbon*, **30**, 1183-1201 (1992).

Mitra, S., Pope, C.J., Gleason, K.K., Makarovsky, Y., Lafleur, A.L., and Howard, J.B.: "Synthesis of Fullerenes (C_{60} and C_{70}) by Combustion of Hydrocarbons in a Flat Flame Burner, *Mat. Res. Soc. Symp. Proc.*, **270**, 149-154 (1992).

Anacleto, J.F., Boyd, R.K., Pleasance, S., Quilliam, M.A., Howard, J.B., Lafleur, A.L., and Makarovsky, Y.: "Analysis of Minor Constituents in Fullerene Soots by LC-MS using a Heated Pneumatic Nebuliser. Interface with Atmospheric Pressure Chemical Ionization, *Canad. J. Chem.*, **70**, 2558-2568 (1992).

McKinnon, J.T. and Howard, J.B.: "The Roles of PAH and Acetylene in Soot Nucleation and Growth", *Twenty-Fourth Symposium (International) on Combustion*, The Combustion Institute, Pittsburgh, 965-971 (1992).

Howard, J.B.: "Fullerenes Formation in Flames", *Twenty-Fourth Symposium (International) on Combustion*, The Combustion Institute, Pittsburgh, 933-946 (1992).

Rotello, V.M., Howard, J.B., Yadav, T., Conn, M.M., Viani, E., Giovane, L.M., and Lafleur, A.L.: "Isolation of Fullerene Products from Flames: Structure and Synthesis of the C_{60}-Cyclopentadiene Adduct", *Tetrahedron Letters* (in press).

Anacleto, J.F., Quilliam, M.A., Boyd, R.K., Howard, J.B., Lafleur, A.L., and Yadav, T.: "Charge-Transfer Ionspray LC-MS Analyses of Fullerenes and Related Compounds from Flame-Generated Materials", *Rapid Communications in Mass Spectrometry* (in press).

IONIZATION PROBES OF MOLECULAR STRUCTURE AND CHEMISTRY

Philip M. Johnson
Department of Chemistry
State University of New York, Stony Brook, NY 11794

PROGRAM SCOPE

Various photoionization processes provide very sensitive probes for the detection and understanding of the spectra of molecules relevant to combustion processes. The detection of ionization can be selective by using resonant multiphoton ionization or by exploiting the fact that different molecules have different sets of ionization potentials. Therefore the structure and dynamics of individual molecules can be studies even in a mixed sample. We are continuing to develop methods for the selective spectroscopic detection of molecules by ionization, and to use these methods for the study of some molecules of combustion interest.

MASS ANALYZED THRESHOLD IONIZATION SPECTROSCOPY

Techniques have recently been developed to obtain the spectra of ions by exploiting the fact that very high Rydberg states converging on each ionic state can be very long lived. By time delays or small electric fields, the ions or electrons resulting from field ionization of these high Rydbergs can be separated from the charged particles resulting from direct photoionization. Scanning an excitation energy across the ionization continuum (with one or more photons) and looking for the signature provided by the high Rydberg states therefore produces a high resolution spectrum of the ion. When electrons are detected, a time delay separation is used and the method is called ZEKE. We have introduced the technique of providing mass resolution to the threshold ionization spectrum by separating the photoions from the field produced ions in a small electric field. We call this mass analyzed threshold ionization spectroscopy (MATI).

Recently we have been working on the improvement of the MATI apparatus, particularly with respect to its mass resolution. In order to have good spectral resolution in the optical spectrum, it is necessary in general to use a very low field ionization voltage. This very low voltage necessary in the source region of the machine presents a very great challenge to the design. To that end we have designed and built a much more sophisticated spectrometer which has space focussing and velocity focussing for the ions in a tandem geometry. With this we have substantially improved the mass resolution of the MATI technique to a very usable form. It is now possible to get mass resolution greater than 60 with an extraction field of less than one volt/cm. The mass resolution improves dramatically with increasing extraction voltage but optical resolution suffers. Further development is under way aimed toward enabling MATI to be used at higher temperatures, possibly even ambient, where thermal velocities are significant with respect to those provided by the low voltages of the source. We are also exploring the

possibilities of creating an apparatus in which MATI could be done with a continuous light source such as a VUV lamp or a synchrotron.

We have continued our study of the vibrational structure of diazines, particularly pyrazine, exploring the capabilities of ab initio force field calculations in understanding the threshold ionization spectra. MP2/6-31G* calculations of the vibrational frequencies of the neutral ground, S_1, and the ionic ground state have been compared with the experimental values, finding that certain vibrations of S_1 and the ion which engage in extensive vibronic coupling are not properly determined by the calculated force field. Most vibrational frequencies are accurately reproduced, however. Variations in the complexity of the threshold ionization spectra with the level of S_1 excitation indicate that internal vibrational relaxation is taking place at a very low energy in that state, possible involving vibronic interactions and mixing with the triplet manifold.

AUTOIONIZATION OF CARBON DIOXIDE

In (3+1) resonance enhanced multiphoton ionization photoelectron spectra of CO_2, photoionization competes with dissociation. In addition to direct photoionization, autoionization is possible through accidental resonances embedded in the continuum at the four-photon level. Photoabsorption from these long-lived autoionizing states leads to resonance enhanced above threshold absorption (REATA). REATA produces photoelectron terminations on the $\tilde{C}$ state of CO_2^+. Previous experiments did not indicate whether the dissociation occurred at the three-photon level or four-photon level. REMPI-PES of CO_2 via several Rydberg states have been collected at a number of laser intensities, and it was found that the photoelectron spectra terminating on each individual ionic state do not change over the range of experimentally available laser intensities. This indicates that the dissociation of CO_2 occurs at the four-photon level. The long vibrational progressions in the PES indicate that the dominant ionization process is autoionization rather than direct ionization. Relative intensities of the $\tilde{X}$ and $\tilde{C}$ state components of the PES do change with intensity, confirming the $\tilde{C}$ state assignment and its five-photon mechanism.

DOE PUBLICATIONS

P. M. Johnson and M. Wu, "Autoionization structure and rotational contours in the multiphoton ionization spectrum of carbon dioxide," J. Chem. Phys. **94**, 868 (1991).

P. M. Johnson, "Resonance ionization spectra as a reflection of excited state dynamics," Inst. Phys. Conf. Ser. No. 114: Section 4 [RIS 90], IOP Publishing Ltd, 145 (1991).

L. Zhu and P. M. Johnson, "Mass analyzed threshold ionization spectroscopy," J. Chem. Phys. **94**, 5769 (1991).

M. Wu, D. P. Taylor and P. M. Johnson, "Resonance enhanced multiphoton ionization-photoelectron spectra of CO_2 (I): Photoabsorption above the ionization potential," J. Chem. Phys. **94**, 7596 (1991).

M. Wu, D. P. Taylor and P. M. Johnson, "Resonance enhanced multiphoton ionization-photoelectron spectra of CO_2 (II): Competition between photoionization and dissociation," J. Chem. Phys. **95**, 761 (1991).

S. Hillenbrand, L. Zhu, and P. M. Johnson, "The pulsed field ionization spectrum and lifetimes of the states at the S_1 origin of pyrazine," J. Chem. Phys. **95**, 2237 (1991).

T. Sears, W. Fawzy and P. Johnson, "Transient diode laser absorption spectroscopy of the ν_2 fundamental of trans-HOCO and DOCO," J. Chem. Phys. **97**, 3996 (1992).

D. Taylor and P. Johnson, "Resonance enhanced multiphoton ionization photoelectron spectra of CO_2 III. Autoionization dominates direct ionization," J. Chem. Phys. **98**, 1810 (1993).

L. Zhu and P. Johnson, "Vibrations of pyrazine and its ion as studied by threshold ionization spectroscopy," J. Chem. Phys., to be published.

P. Johnson and L. Zhu, "Mass analyzed threshold ionization: structural information for a mass spectrum and mass information for ionic spectroscopy," Intl. J. of Mass Spectrom. Ion Phys., to be published.

M. Yen, P. Johnson, and M. White, "The VUV photodissociation of the chlorofluorocarbons: Photolysis of CF_3Cl, CF_2Cl_2 and $CFCl_3$ at 187 nm, 125 nm and 118 nm," J. Chem. Phys., to be published.

PHOTOCHEMISTRY OF MATERIALS IN THE STRATOSPHERE

Principal Investigator: Harold S. Johnston
Chemical Sciences Division
Lawrence Berkeley

Mailing address: Department of Chemistry
University of California
Berkeley, CA 94720

Program scope

This research is concerned with global change in the atmosphere, including photochemical modeling and, in the past, experimental gas-phase photochemistry involving molecular dynamics and laboratory study of atmospheric chemical reactions. The experimental work on this project concluded in August 1991, but there is a back-log of several journal articles to be written and submitted for publication. The theoretical work involves photochemical modeling in collaboration with Lawrence Livermore National Laboratory (LLNL) and advising the Upper Atmosphere Research Program on Atmospheric Effects of Stratospheric Aircraft, National Aeronautics and Space Administration (NASA).

Recent Progress

The photodissociation of NO_3 was studied using the method of molecular beam photofragmentation translational spectroscopy (ref. 12 below). The existence of two photodissociation channels was confirmed under collision-free conditions. The observed quantum yield for the concerted 3-center rearrangement resulting in $NO(^2\Pi)$ and $O_2(^3\Sigma_g^-, {}^1\Delta)$ was 0.70±0.10 at 588 nm and decreased sharply at wavelengths shorter than 587 nm, falling to less than 0.001 at 583 nm. The observed quantum yield for the product channel, NO_2 + O, increased at wavelengths below 587 nm to 0.99. From these observed spectroscopic results, the zero-temperature dissociation energy, $D_0(O\text{-}NO_2)$, is 48.69±0.25 kcal/mol, which when combined with the enthalpies of formation of $O(^3P_2)$ and $NO_2(^2A_1)$ yields $\Delta_f H^o_0$ = 18.87±0.33 kcal/mol and $\Delta_f H^o_{298}$ = 17.62±0.33 kcal/mol. From the wavelength dependence and translational energy distribution for the O_2 + NO products, the potential energy barrier for $NO_3(^2A'_2) \rightarrow NO(^2\Pi) + O_2(^3\Sigma_g^-, {}^1\Delta)$ was found be 47.3±0.8 kcal/mol. The present results are more precise than, but in good agreement with, previous results by F. Magnotta (Geophys. Res. Lett. **7**, 769, 1980) and D. Neumark et al. (J. Chem. Phys., **94**, 1740, 1991).

Another laboratory (private communication) has confirmed the proposal (ref.10 below) that nitrosyl sulfuric acid rapidly converts inactive HCl to photochemically active ClNO at stratospheric temperatures.

Future Plans

From considerations of thermochemistry and room temperature rates, it appears probable that several additional heterogeneous reactions are important in stratospheric photochemistry. To explore these possibilities, this project is collaborating with CSD investigators at Berkeley and with others at Livermore and elsewhere.

Acknowledgment

This work was supported by the Director, Office of Energy Research, Office of Basic Energy Sciences, Chemical Sciences Division of the U. S. Department of Energy under Contract No. DE-AC03-76SF00098.

References to Publications of DOE Sponsored Research (1991-1993)

1. Harold S. Johnston, "M. J. Prather, and R. T. Watson, "The Atmospheric Effects of Stratospheric Aircraft," NASA Reference Publication 1250, January 1991, 28 pages, LBL-31860.

2. Joel D. Burley, "Part I. Kinetic Energy Dependencies of Selected Ion-Molecule Reactions. Part II. Photochemistry of (FSO3)2, FSO3, and FNO." Ph. D. Dissertation, University of California, Berkeley, California, July 1991, LBL-31027.

3. Kenneth O. Patten, "Collisional Energy Transfer from Excited Nitrogen Dioxide," Ph. D. Dissertation, University of California, Berkeley, California, 244 pages, May 1991, LBL-30599.

4. Charles E. Miller, "The Photodissociation of R-NO_2 Molecules" Ph. D. Dissertation, University of California, Berkeley, California, April 1991, LBL-30540.

5. Wade N. Sisk, Charles E. Miller and Harold S. Johnston "Spectroscopy of Nitrogen Dioxide Fluorescence III. Internal Energy Distributions of fluorescent NO_2 after Photolysis of Jet-Cooled N_2O_4," accepted for publication in Journal of Physical Chemistry, LBL-31551.

6. Charles E. Miller and Harold S. Johnston, "Spectroscopy of Nitrogen Dioxide Fluorescence IV. Variable Wavelength Photo-dissociation of $ClNO_2$ and $HONO_2$, accepted for publication in Journal of Physical Chemistry, LBL-31552.

7. Bongsoo Kim, Philip L. Hunter, and H. S. Johnston, "NO_3 Radical Studied by Laser Induced Fluorescence," J. Chem. Phys., **96**, 4057 (1992). LBL-30869.

8. Joel D. Burley and H. S. Johnston, "Photoabsorption Cross Sections of $(FSO_3)_2$ and FSO_3," J. Photochem. Photobiol. A: Chem. **66**, 141 (1992). LBL-31547.

9. Joel D. Burley and H. S. Johnston, "Ionic Mechanisms for Heterogeneous Stratospheric Reactions and Ultraviolet Photoabsorption Cross Sections for NO_2^+, HNO_3, and NO_3^- in Sulfuric Acid," Geophys. Research Letters **19**, 1359 (1992). LBL-31660.

10. Joel D. Burley and H. S. Johnston, "Nitrosyl Sulfuric Acid and Stratospheric Aerosols," Geophys. Research Letters **19**, 1363 (1992). LBL-32177.

11. H. S. Johnston, "Atmospheric Ozone," Annual Rev. Phys. Chem. **43**, 1 (1992). LBL-33576.

12. H. Floyd Davis, Bongsoo Kim, H. S. Johnston, an d Yuan T. Lee, "Dissociation Energy and Photochemistry of NO_3," J. Phys. Chem. **97**, 2172, 1993), LBL-33113.

DYNAMICAL ANALYSIS OF HIGHLY EXCITED MOLECULAR SPECTRA.

Michael E. Kellman
Department of Chemistry, University of Oregon, Eugene, OR 97403.

PROGRAM SCOPE:

The goal of this program is new methods for analysis of spectra and dynamics of highly excited vibrational states of molecules. In these systems, strong mode coupling and anharmonicity give rise to complicated classical dynamics, and make the simple normal modes analysis unsatisfactory. New methods of spectral analysis, pattern recognition, and assignment are sought using techniques of nonlinear dynamics including bifurcation theory, phase space classification, and quantization of phase space structures. The emphasis is chaotic systems and systems with many degrees of freedom.

RECENT PROGRESS AND FUTURE PLANS:

The goal of earlier work was a method to extract dynamical information about molecules from analysis of fits of their spectra with spectroscopic fitting Hamiltonians. This led to a systematic analysis using nonlinear dynamics tools such as bifurcation theory. The result was an essentially complete classification of the spectroscopic fitting Hamiltonian for two coupled modes, and application of this analysis to assignment of spectra in terms of new quantum numbers appropriate to the underlying dynamics of the quantum states [L. Xiao and M.E. Kellman, J. Chem. Phys. 93, 5805 (1990); J. Chem. Phys. 93, 5821 (1990)].

Two further major steps, far more challenging than earlier work, are needed in this project for achievement of the desired framework for analyzing highly excited spectra. The first problem is classification of the quantum spectra of chaotic systems. The second problem is phase space classification of systems with many degrees of freedom, and using this to classify the quantum spectrum.

I. CLASSIFICATION AND PATTERN RECOGNITION IN SPECTRA OF CHAOTIC SYSTEMS

Recent Progress

The basic problem is quantization of the phase space structure elucidated by bifurcation analysis of chaotic molecular systems. This is necessary to achieve a rigorous quantum number assignment based on phase space structure. Our earlier work on assignment of systems such as the normal-local modes transition, or a single Fermi resonance in coupled C-H bend and stretch, made use of the fact that a good fit can be obtained with a single resonance coupling. This is implicitly based on the notion that the true dynamics in these systems, which sometimes undoubtedly contain a degree of chaos, is well-approximated by the remnants of invariant tori. We are trying to put this idea on a rigorous basis, on the basis of mathematical work of Mather and others which shows that the remnants of tori are Cantor sets ("cantori"). We are attempting to apply this work to the assignment problem by semiclassically quantizing cantori, including the determination of wave functions.

Future Plans

An important case which cannot be handled by the classification methods developed to date which is of relevance to molecular spectroscopy is chaotic systems where the primary resonance coupling, e.g. the coupling between local modes which gives rise to the symmetric-antisymmetric stretch splitting, is very large. For example, for very large coupling between Morse oscillators, there is a series of resonances between normal modes; these resonances fall outside our local-normal two-zone classification of the catastrophe map of the Darling-Dennison Hamiltonian. There are significant cases in spectroscopy where this is probably very important, for example, in CO_2 and CS_2. We plan to investigate extension of the use of fitting Hamiltonians and their attendant bifurcation analysis to these cases.

II. BIFURCATIONS AND CLASSIFICATION OF SYSTEMS WITH MANY DEGREES OF FREEDOM

Recent Progress

All of the discussion so far, both of our past work on single resonance Hamiltonians and work in progress on chaotic systems, has been for two degree-of-freedom systems. Independent of the problems that arise from the presence of chaos in these systems, it is evident that a successful approach to highly excited spectra has to confront directly the problem of many interacting degrees of freedom. This divides naturally into two parts. The first is the problem of identifying the dimensions of phase space actually affected by bifurcations. A very important by-product is the identification of approximate constants of motion associated with the unbifurcated degrees of freedom. These are associated with energy transfer pathways and "superpolyad" quantum numbers which are proving useful to other groups in accounting for some of the main features of complex spectra, in particular, fits of acetylene absorption spectra and hierarchies of splittings in dispersed fluorescence and SEP spectra. A solution to this problem has been presented with a theory [M.E. Kellman, J. Chem. Phys. 93, 6630 (1990)] of approximate constants of motion derived from spectral fitting Hamiltonians with multiple Fermi resonances. The formalism reduces to methods of vector algebra and leads to a simple "resonance vector" method which is quite easy to apply. The constants of motion correspond to "superpolyad" and other quantum numbers very useful for assigning complex spectra. In ongoing studies we have been analyzing these quantum numbers in fits of experimental and simulated spectra of C_2H_2 currently under investigation in several laboratories. The resonance vector analysis has been applied by Field and coworkers to dispersed fluorescence and SEP spectra of acetylene in a model including vibrational angular momentum and vibrational l-resonance. They find that the superpolyad number is very useful for organizing information about energy transfer pathways, including the observation of hierarchies of time scales for the energy flow.

The second problem is the classification of the structure of the bifurcated degrees of freedom. The superpolyad quantum number permits a simplification similar to that in the two-mode system, in that it makes it possible to solve analytically for the large-scale bifurcation structure for spectroscopic fitting Hamiltonians of chaotic many-degree-of-freedom systems. An important feature of the single resonance Hamiltonians used in our earlier work is that they yield a simple and exhaustive classification of the bifurcated phase space structure of the fitting Hamiltonian, thereby leading to a set of quantum numbers appropriate to the classical dynamics

underlying a given spectrum. For the single resonance Hamiltonian, it is possible to achieve this classification analytically, without numerical solution of Hamilton's equations. This capability for the single resonance Hamiltonian to find an analytical classification affords great insight into the molecular dynamics underlying the assignment. For chaotic two degree-of-freedom systems, the hope is that this classification will carry over to most physically important situations. This will happen if the *large-scale bifurcation structure* of the chaotic Hamiltonian is essentially that given by the single resonance approximate Hamiltonian. That this expectation may often be reasonable is indicated by our finding [J.M. Standard and M.E. Kellman, unpublished] that wave functions of coupled stretches in ozone calculated on a potential surface are essentially similar to those of the single resonance fitting Hamiltonian, with the same local/normal dichotomy suitable for spectral assignment.

Insofar as possible, it is desirable that the analysis of the many degree-of-freedom problem incorporate and generalize the property of the single resonance Hamiltonian that it gives an analytic solution to the large-scale bifurcation structure and spectral assignment. At first this might appear unlikely, because the multidimensional Hamiltonian is likely to have more than one resonance, hence be chaotic. For example, a fit of the spectrum of all three vibrational modes of water requires not only a stretch-stretch coupling, but also a 2:1 Fermi resonance between the symmetric stretch and the bend. However, for the single-resonance Hamiltonian it is not the lack of chaos *per se* that allows an analytic classification. Rather, the key factor is the existence of a conserved global action (polyad number). The integrability of the single-resonance Hamiltonian that confines trajectories to invariant tori is merely a by-product of this extra constant of motion. The crucial feature of the Hamiltonian for classifying phase space is therefore not that all the trajectories be integrable, but only that the large-scale bifurcation structure be analytically solvable. Furthermore, this analytic solvability as a consequence of the polyad number extends to many degree-of-freedom chaotic systems. The basic idea is that the large-scale bifurcation structure is defined by the *lowest-order periodic orbits* and their bifurcations. If the superpolyad number is a constant of motion, it can be shown that the lowest-order periodic orbits can be solved analytically, even for a multidimensional chaotic system.

Future Plans

This is the basic result needed to find the lowest period orbits and their bifurcations, i.e., the sought-after large-scale bifurcation structure. The mapping out of this structure for systems with three and more degrees of freedom is presently being carried out with the aim of a classification analogous to the catastrophe map for two degree of freedom systems. The starting point is the construction of bifurcation diagrams for individual molecules based on the fits of their experimental spectra. The accompanying figure shows the bifurcation diagrams recently obtained[1] for H_2O and H_2S. It is evident that these diagrams are complex and that different information is obtained for each molecule. In future work we plan to investigate (1) recognition of spectral hallmarks of these bifurcations, and (2) systematic mapping out of the complete bifurcation structure of three-mode systems, analogous to our earlier "catastrophe map" classification of two-mode systems. In connection with (1), we plan a comparison of our dynamical bifurcation analysis with Davis' hierarchical tree analysis.

1. Zimin Lu and M.E. Kellman, "Bifurcation analysis of three-mode vibrational Hamiltonian for spectra of triatomics", manuscript in preparation.

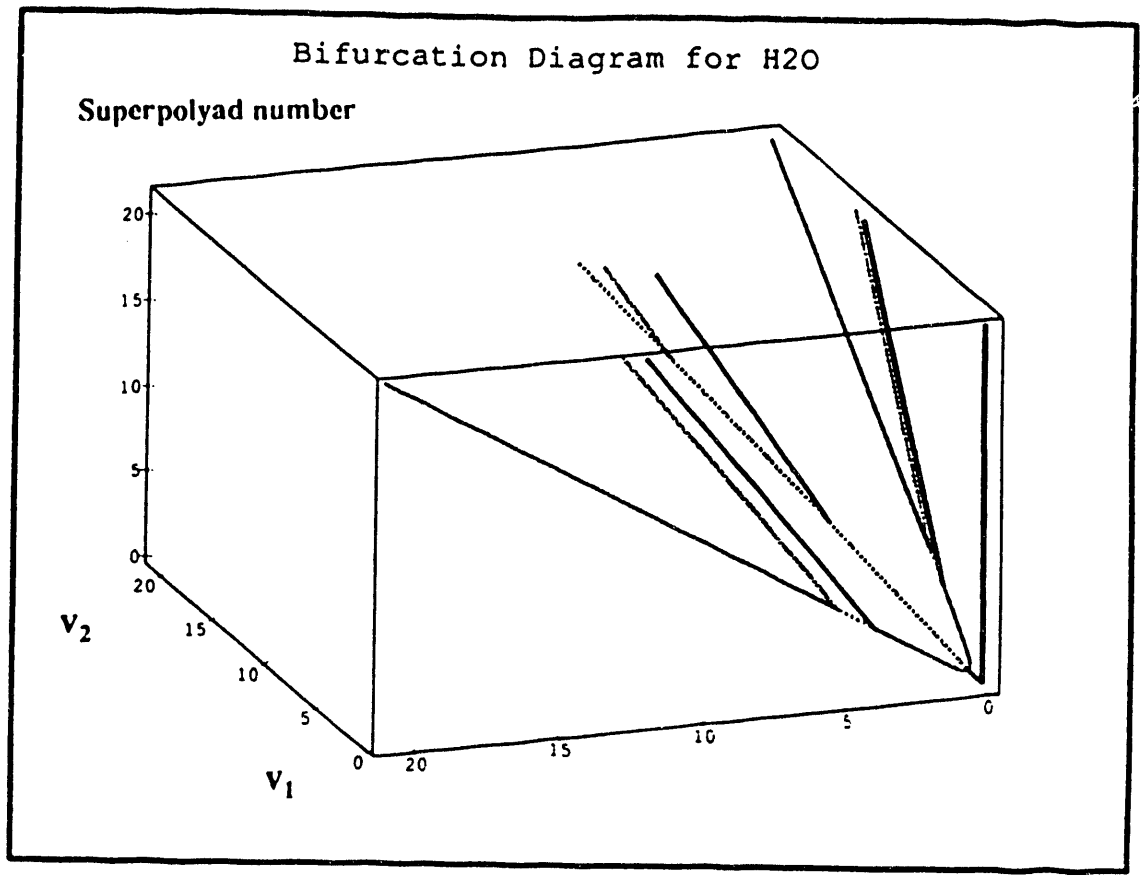

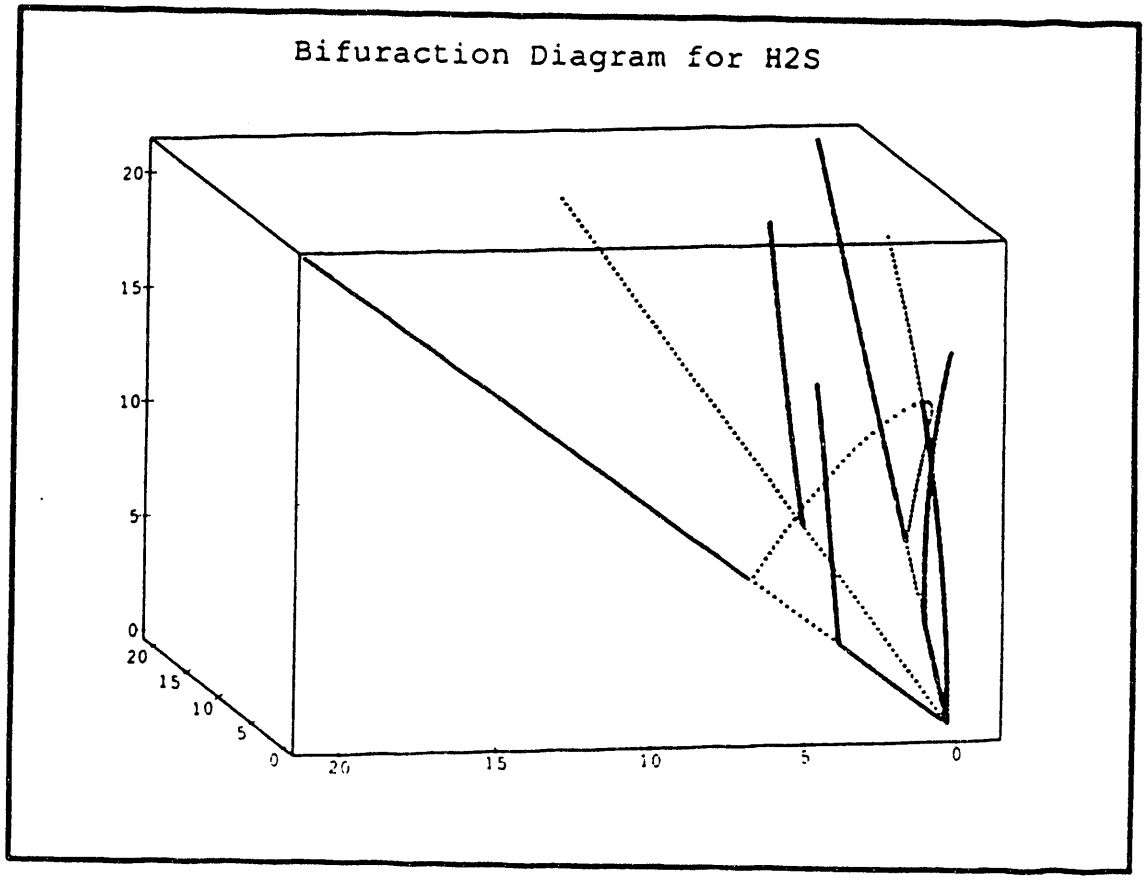

Bifurcation diagrams from fits of three-mode experimental spectra of H_2O and H_2S including local stretches 1 and 2 and bending mode. Axes are the number of quanta v_1 and v_2 in the local stretch modes, and the superpolyad number $N = (v_1 + v_2 + v_b/2)$.

TOLUENE PYROLYSIS STUDIES AND HIGH TEMPERATURE REACTIONS OF PROPARGYL CHLORIDE

R. D. Kern, H. Chen and Z. Qin
Department of Chemistry
University of New Orleans
New Orleans, LA 70148

Program Scope

The main focus of our program is to investigate the thermal decompositions of fuels that play an important role in the pre-particle soot formation process. It has been demonstrated that the condition of maximum soot yield is established when the reaction conditions of temperature and pressure are sufficient to establish a radical pool to support the production of polyaromatic hydrocarbon species and the subsequent formation of soot particles. However, elevated temperatures result in lower soot yields which are attributed to thermolyses of aromatic ring structures and result in the bell-shaped dependence of soot yield on temperature. We have selected several acyclic hydrocarbons to evaluate the chemical thermodynamic and kinetic effects attendant to benzene formation. To assess the thermal stability of the aromatic ring, we have studied the pyrolyses of benzene, toluene, ethylbenzene, chlorobenzene and pyridine. Time-of-flight mass spectrometry (TOF) is employed to analyze the reaction zone behind reflected shock waves. Reaction time histories of the reactants, products, and intermediates are constructed and mechanisms are formulated to model the experimental data. Our TOF work is often performed in collaboration with Professor John Kiefer and his use of laser schlieren densitometry (LS) to measure density gradients resulting from the heats of various reactions involved in a particular pyrolytic system. The two techniques, TOF and LS, provide independent and complementary information about ring formation and ring rupture reactions.

Recent Progress

Although the thermal decomposition of toluene has been investigated by a variety of shock tube techniques over a wide range of temperature, total reaction pressure and initial reactant concentration (see listing in Table I), there remain several unresolved questions about the mechanism and disagreements in the experimental data.

Table I: Summary of shock zone reaction conditions

Technique	Temp (K)	Total Press (atm)	$[C_7H_8]_o$ (mol cm^{-3})	Ref.
UVAS	1450-1900	1.3-36.3	$(0.1\text{-}1.0) \times 10^{-8}$	1
TOF	1590-2145	0.3-0.5	$(4.36\text{-}4.92) \times 10^{-8}$	2
LS	1400-2300	0.13-1.3	$(1.1\text{-}27) \times 10^{-8}$	2
ARAS	1410-1730	3	$(1\text{-}5) \times 10^{-10}$	3
ARAS	1450-1790	0.4	$(0.03\text{-}0.6) \times 10^{-10}$	4
ARAS	1380-1700	1.5-7.8	$(0.3\text{-}4.7) \times 10^{-10}$	5
SPST	1100-2700	4-8	$(0.48\text{-}48.0) \times 10^{-8}$	6

One of the disagreements involves the independent measurement of H atom production in toluene pyrolysis using atomic resonance absorption spectroscopy (ARAS) by Skinner[3,4] and by Just[5]. An example is displayed in Figure 1: the solid circles represent data[5] at 1545 K; the solid line is due to model calculations using the rate constants from ref. 4. The results are general; i.e., the rate data from Skinner[3,4] are consistently lower than those of Just[5].

Figure 1

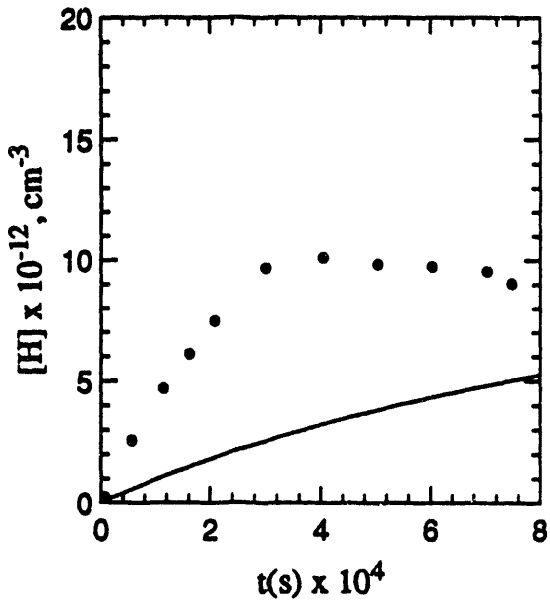

Figure 2

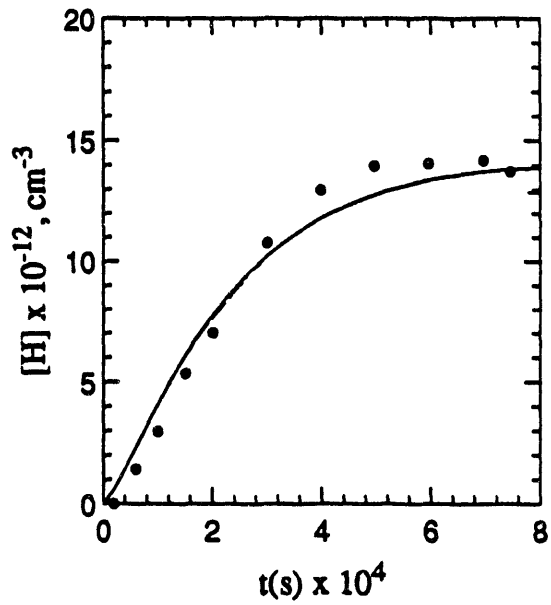

Other key questions concern the relative importance of two channels in the initial step

$$C_7H_8 \rightarrow C_7H_7 + H \quad (1)$$
$$\rightarrow C_6H_5 + CH_3 \quad (2)$$

and the subsequent rates of benzyl and phenyl radical decomposition.

$$C_7H_7 \rightarrow C_5H_5 + C_2H_2 \quad (3)$$
$$\rightarrow C_3H_3 + C_4H_4 \quad (4)$$
$$C_6H_5 \rightarrow C_4H_3 + C_2H_2 \quad (5)$$
$$C_4H_3 \rightarrow C_4H_2 + H \quad (6)$$

A 28-step mechanism was formulated[7] which includes pressure dependent rate constant expressions for the two initiation steps. RRKM calculations show that (1) and (2) are comparable in rates in the range 1400–1600 K, but that (2) is dominant at higher temperatures due to the irreversibility of the phenyl radical decomposition channels, (5) and (6). The dominance of reaction (2) is consistent with the appearance of CH_4 as a product recorded in the single pulse shock tube (SPST)[6] and TOF[2] experiments. The proposed mechanism[7] models successfully the LS[2], TOF[2], and ARAS[5] reaction profiles (see Figure 2), but not the data of refs. 1, 4, 5.

Propargyl radical has been shown to be an efficient precursor to benzene formation and as a consequence an effective promoter of soot formation in the pyrolyses of allene[8,9], 1,2 butadiene[10] and in rich acetylene flames[11]. However, in mixtures of propargyl chloride dilute in neon, benzene is not detected as an expected product of reactions involving C_3H_3 radicals. Moreover, in mixtures of C_3H_3Cl containing H_2, benzene is readily observed. Experiments on a 3% C_3H_3Cl – 5% D_2 – 92% Ne mixture revealed a constant temporal HCl/DCl product ratio that is approximately equal to 5. If C-Cl bond fission is the major initiating reaction, the HCl/DCl ration would be < 1 due to the reaction of $Cl + D_2 \rightarrow DCl + D$. Therefore it is proposed that the major channel for C_3H_3Cl dissociation yields HCl and singlet cyclopropenylidene.

$$C_3H_3Cl + M \rightarrow C_3H_2 + HCl + M \quad (83\%)$$
$$C_3H_3Cl + M \rightarrow C_3H_3 + Cl + M \quad (17\%)$$

In the presence of H_2, C_3H_2 reacts exothermically to form the thermally excited adduct $C_3H_4^*$ which readily isomerizes to either allene or propyne as predicted by a bimolecular-QRRK calculation[12]. The calculation reveals that formation of allene and propryne account for 97% of the product distribution.

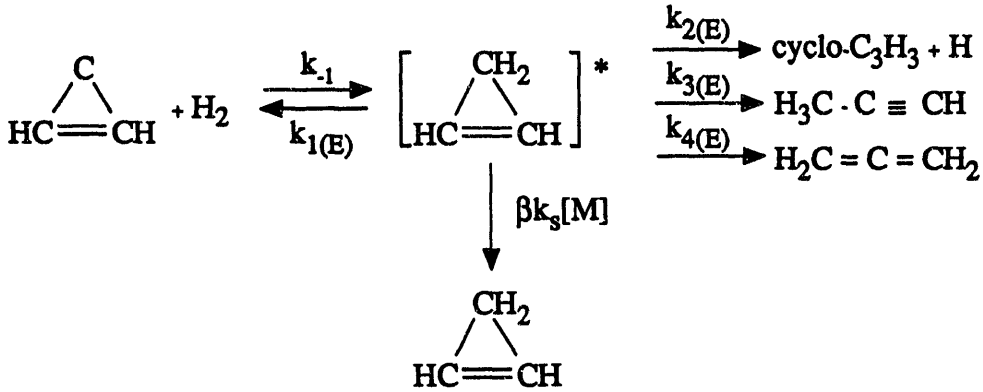

Subsequent reactions in the mechanism lead to benzene formation. Benzene production is also recorded in mixtures of C_3H_3Cl + allene, C_3H_3Cl + propyne, $C_3H_3Cl + C_2H_2$ and $C_3H_3Cl + C_2H_4$. Computer simulation of the data utilizing a 36 step mechanism yields satisfactory agreement between the calculated and experimental results.

Supplemental DOE funds were used to purchase a high speed real time digitizer, interface and microcomputer to process the TOF data. We have caputured single shot TOF experiments on the ditigitzer at sampling rates of 1 ns intervals during 1 ms observation periods. A vendor-recommended software package is proving unsatisfactory and a program has been written to transfer the TOF data from the digitizer to the microcomputer.

Future Plans

We will be testing our new data processing system by studying the thermolyses of ethylene and cyclopentadiene.

References

1. L. D. Brouwer, W. Müller-Markgraf and J. Troe, J. Phys. Chem. 92, 4905 (1988).
2. K. M. Pamidimukkala, R. D. Kern, M. R. Patel, H. C. Wei and J. H. Kiefer, J. Phys. Chem. 91, 2148 (1987).
3. V. S. Rao and G. B. Skinner, J. Phys. Chem. 88, 4362 (1984).
4. V. S. Rao and G. B. Skinner, J. Phys. Chem. 93, 1864 (1989).
5. M. Braun-Unkhoff, P. Frank and Th. Just, 22nd Symposium (Int.) on Combustion, 1988, p. 1053.
6. M. B. Colket and D. J. Seery, Poster paper PS55 presented at 20th Symposium (Int.) on Combustion, Ann Arbor, Michigan, 1984.
7. same as ref. 6 listed below under ***Publications***.
8. C. H. Wu and R. D. Kern, J. Phys. Chem. 91, 6291 (1987).
9. M. Frenklach, S. Taki, M. B. Durgarasad, R. A. Matula, Combust. Flame 54, 81 (1983).
10. R. D. Kern, H. J. Singh and C. H. Wu, Int. J. Chem. Kinet. 20, 731 (1988).
11. J. A. Miller and C. F. Melius, Combust. Flame, in press.
12. A. M. Dean, J. Phys. Chem. 89, 4600 (1985).

Publications During 1991-93 of DOE Sponsored Research

1. R. D. Kern, and K. Xie, "Shock Tube Studies of Gas Phase Reactions Preceding the Pre-Particle Soot Formation Process", Prog. in Energy and Combust. Sci. 17, 191-210 (1991).

2. R. D. Kern, K. Xie, H. Chen, and J. H. Kiefer, "High Temperature Pyrolyses of Acetylene and Diacetylene Behind Reflected Shock Waves", Twenty Third Symposium (International) on Combustion, The Combustion Institute, Pittsburgh, PA, 1991, p. 69-75.

3. J. H. Kiefer, S. S. Sidhu, R. D. Kern, K. Xie, H. Chen, and L. B. Harding, "The Homogeneous Pyrolysis of Acetylene II: The High Temperature Radical Chain Mechanism", Combust. Sci. and Tech. 82, 101-30 (1992).

4. R. D. Kern, K. Xie, and H. Chen, "A Shock Tube Study of Chlorobenzene Pyrolysis", Combust. Sci. and Tech. 85, 77-86 (1992).

5. R. D. Kern, K. Xie, H. Chen, S. S. Sidhu, and J. H. Kiefer, "The Reaction of C_4H_2 and H_2 Behind Reflected Shock Waves", 18th Symposium (International) on Shock Waves, Springer-Verlanger, Berlin, Germany, 1992, p. 729-34.

6. R. D. Kern, H. Chen, H. J. Singh, K. Xie, J. H. Kiefer, and S. S. Sidhu, "Thermal Dissociation Studies of Toluene at High Temperatures", Proceedings of the 6th Toyota Conference on Turbulence and Molecular Processes in Combustion, T. Takeno (Ed.), Elsevier, Amsterdam, in press.

7. R. D. Kern, H. Chen, Z. Qin, and K. Xie, "Reactions of C_3H_3Cl with H_2, C_3H_4, C_2H_2 and C_2H_4 Behind Reflected Shock Waves", 19th International Symposium on Shock Waves, 1993, accepted.

Stochastic Models for Turbulent Reacting Flows

Alan Kerstein
Combustion Research Facility
Sandia National Laboratories
Livermore, CA 94551-0969

The goal of this program is to develop and apply stochastic models of various processes occurring within turbulent reacting flows in order to identify the fundamental mechanisms governing these flows, to support experimental studies of these flows, and to further the development of comprehensive turbulent reacting flow models.

The rates and mechanisms of chemical reactions in turbulent flow are governed by a minimum of three distinct physical processes: convection, molecular mixing, and chemical kinetics. Although other processes such as radiative heat transfer play a key role in many combustion applications, the focus of this project is on the three aforementioned processes and their interactions. None of these processes, generic to all reacting flows, is represented in a fully adequate manner in existing computational models of turbulent reacting flow. The scope and reliability of existing models is therefore limited, and improvements in this regard would have both scientific and technological benefits.

In many instances, the treatment of molecular mixing is the key limitation to improvements in model performance. In the simplest formulations applied to combustion problems, there is no explicit treatment of molecular mixing because large-scale entrainment is the rate-determining process. Though adequate in many instances for determination of the overall burning rate, this approach omits the interplay between temperature fluctuations and chemical variations that influences thermal NO production, soot formation, and other important chemical processes in flames.

The methodology for modeling turbulent mixing that has been developed by the P.I. is denoted the "linear-eddy" approach [1,2]. As its name implies, this approach is designed to capture the relevant physics through a representation of turbulent mixing involving one spatial dimension. In this representation, molecular diffusion can be treated in a physically sound manner by fully resolving the concentration field computationally and by implementing Fick's law (or its appropriate multispecies generalization) directly. In applications to chemically reacting flows, the chemical-kinetic mechanism (complete or reduced, as appropriate) is implemented within each resolved cell of the computational domain.

The limitation to one spatial dimension renders the computation affordable for Reynolds numbers (Re) at which laboratory experiments are performed. In many such experiments, the overall flow structure is simple enough for linear eddy, formulated as a stand-alone model, to capture salient features of the spatial development of the mixing process. For more complicated configurations, the approach that will be adopted in future applications is to formulate linear eddy as subgrid model separately implemented within each cell of a large-eddy or other comparable simulation, with appropriate communication between the linear-eddy simulations. Though costly, this approach is well suited to massively parallel computer architectures. Preliminary demonstrations of the feasibility of this approach have been performed.

The key to the effectiveness of the model is the formulation of a suitable one-dimensional representation of turbulent stirring. Specializing to an incompressible fluid (though

compressible cases can also be treated), continuity is obeyed in one dimension only by the trivial flow consisting of a spatially constant velocity at any instant. To represent convective stirring in one dimension, it is therefore necessary to allow discontinuous fluid motions.

In the linear-eddy approach, convective stirring is simulated by means of a stochastic process, rather than by solving a fluid-mechanical equation. This process consists of a random sequence of events, each involving an instantaneous spatial rearrangement of a portion of the scalar field. Rearrangement events are the linear-eddy analogs of turbulent eddies. The linear extent of the scalar field that is rearranged during a given event represents the eddy size. The model incorporates inertial-range scaling through the adoption of an eddy-size distribution function with appropriate power-law behavior and with upper and lower cutoffs representing the integral and Kolmogorov scales, respectively.

Each rearrangement event is a "triplet map," specially formulated to emulate the action of a single eddy. The selected portion of the concentration field is replaced by three images of itself, each compressed by a factor of three. The central image is spatially inverted. The latter step assures that discontinuities will not be introduced.

Qualitatively, the triplet map captures the action of compressive strain. Quantitatively, the triplet map has the following features: (1) A spatially homogeneous, statistically stationary sequence of triplet-map events induces exponential growth of material-surface area. (2) Based on the foregoing specification of the eddy-size distribution, the growth rate scales as the local rate of strain.

Operationally, the linear-eddy model is implemented as a Monte Carlo simulation. Molecular processes evolve in a conventional manner based on deterministic finite-difference solution of the governing equations. This deterministic evolution is punctuated by instantaneous, randomly occurring rearrangement events. The model has natural analogs of the Reynolds, Schmidt and Damkohler numbers, allowing parameters governing the rearrangement process to be expressed in terms of physical quantities.

Analysis of this formulation and comparison of computed results to measurements demonstrate that many intuitive notions based on continuum flow carry over, quantitatively as well as qualitatively, to the linear-eddy framework. For instance, the linear-eddy analog of eddy duration ("turnover time") is the time between successive events of a given size at a given locality.

For spatially developing mixing configurations with either localized or extended scalar sources, linear-eddy simulations capture the phenomenology of macromixing as well as micromixing, and the interplay between the two. This interplay is most evident in multistream mixing problems. Linear-eddy simulations reproduce, with quantitative accuracy, detailed mixing measurements by Warhaft in a three-stream configuration, and Damkohler-number effects observed by Bilger in a two-stream configuration [3].

In future work, the advantages of the linear-eddy modeling approach for computation of turbulent reacting flows with multistep chemistry will be exploited by applying the model to several experimental configurations of current interest. The model will be used to interpret chlorocarbon chemistry measurements being performed in a turbulent plug flow apparatus at MIT, and mixing measurements being performed at the University of Arizona in an incinerator simulator. For the latter application, comparison to cold-flow mixing measurements will serve to validate the model formulation. Further computations will be performed to extrapolate the results to actual incinerator conditions. The linear-eddy modeling approach is the first yet proposed that has the potentiality to provide reliable extrapolations of this sort.

Another topic that will be addressed in future work is differential molecular diffusion. When fluid containing species of unequal molecular diffusivities is entrained into a background fluid, the different species may experience different effective dilution rates and therefore can separate. The dependence of this differential molecular diffusion effect on turbulence intensity as characterized by Re is not well understood experimentally or theoretically. In this regard, the P.I. recently obtained a novel result by analyzing this problem from the viewpoint of scaling laws governing the power spectrum of a diffusive scalar in turbulence. It was deduced that the commonly used measure of differential molecular diffusion should scale as $Re^{-1/4}$, a slower falloff than has previously been proposed. This implies an unanticipated persistence of the effect at the high Re values corresponding to combustors and reactors of technological interest. Confirmatory computations using the linear-eddy model are planned.

Another topic addressed in this program is turbulent premixed flame propagation. Both the geometry [4] and the propagation rate [5] of turbulent flames have been considered.

The mechanism determining the premixed burning velocity in a turbulent medium is generally considered to be best understood in the weak-turbulence limit $u' << S$, where u' is the rms velocity fluctuation and S is the laminar flame speed. In this limit, the dependence $(U / S) - 1 \sim (u'/S)^2$ has been derived, where the turbulent burning velocity U is operationally defined as S times the surface area of the wrinkled flame per unit projected transverse area.

This standard result is based on consideration of the effect of one cycle of an oscillatory perturbation of the front, corresponding to forward propagation of the front for a streamwise distance equal to one wavelength of the perturbing field. During the present project, the cumulative effect of many such perturbations over a streamwise distance of many wavelengths has been analyzed. It was found that over this longer distance, corresponding to a heretofore unrecognized "slow" time-scale governing the propagation process, the cumulative effect of the perturbations is a buildup of flame-front fluctuations until a balance is eventually reached between fluctuation generation and decay mechanisms.

The method of analysis is a variant of the "nonequilibrium Flory theory" of Hentschel and Family [Phys. Rev. Lett. **66**, 1982 (1991)]. Interface evolution is characterized by a stochastic differential equation. The growth rate of fluctuations induced by the stochastic forcing term is estimated using random-walk theory, and this rate is compared to the decay term to obtain a balance condition, and thus to estimate the fluctuation amplitude, transient relaxation time, and other relevant properties. The scaling corresponding to this balance is $(U / S) - 1 \sim (u'/S)^{4/3}$. Numerical flow simulations confirm this prediction.

A recent research initiative involved the development and application of a novel concept, denoted conditional similarity, for the mechanistic interpretation of turbulent mixing measurements.

It is proposed that similarity scaling of image data from turbulent shear flows should be based not on the time-averaged flow centroid, vorticity spread, etc. but on instantaneous values deduced from individual images. The motivation is that flow microstructure is more sensitive to large-scale properties at the given instant than to an average that includes conditions far removed in time. On this basis, a conditional similarity concept was formulated that suggests a new data reduction approach. Using this approach, conditional similarity hypotheses, which generalize conventional similarity hypotheses, can be tested. An initial application to mixing measurements performed at Sandia by Bob Schefer demonstrated the utility of the approach. Additional applications are planned.

1. A. R. Kerstein, "Linear-Eddy Modeling of Turbulent Transport. Part 4. Structure of Diffusion Flames," *Combustion Science and Technology* **81**, 75 (1992).

2. A. R. Kerstein, "Linear-Eddy Modeling of Turbulent Transport. Part 5. Geometry of Scalar Interfaces," *Physics of Fluids A* **3**, 1110 (1991).

3. A. R. Kerstein, "Linear-Eddy Modeling of Turbulent Transport. Part 7. Finite-Rate Chemistry and Multi-Stream Mixing," *Journal of Fluid Mechanics* **240**, 289 (1992).

4. A. R. Kerstein, "Fractal Dimension of Propagating Interfaces in Turbulence," *Physical Review A* **44**, 3633 (1991).

5. A. R. Kerstein and W. T. Ashurst, "Propagation Rate of Growing Interfaces in Stirred Fluids," *Physical Review Letters* **68**, 934 (1992).

KINETICS OF COMBUSTION RELATED PROCESSES AT HIGH TEMPERATURES

John H. Kiefer
Department of Chemical Engineering
University of Illinois at Chicago
Chicago, Illinois 60680

This past year has seen an excursion into perhalomethane dissociation using the laser-schlieren (LS) technique, with work on CCl_4 already published (see below) and on CF_3Cl under analysis. However, our emphasis has again been on the study of relaxation and dissociation of large molecules using the converging/diverging nozzle method to generate very weak (low pressure) shock waves.

Vibrational Relaxation in Large Molecules

We have now observed relaxation in norbornene (C_7H_{10}), norbornadiene (C_7H_{10}), benzene, cyclopropane, cubane (C_8H_8) quadricyclane (C_7H_8), and CF_3Cl. In all but cubane, where we had an inadequate sample, we have been able to observe relaxation over a wide range of temperature. With the exception of cubane and quadricyclane, whose exothermic isomerization causes severe flow instabilities (incipient detonation), our measurements cover 400-1200 K. The most surprising result is that, of all these species, only norbornene shows a single relaxation time. Contrary to conventional wisdom[1,2], which has multiple relaxation a rare occurrence, we see double relaxation in all other species we have examined (see Figure 3). This suggests two conclusions. First, the resolution of our method is as good or better than ultrasonic techniques. For double relaxation it may actually be superior because small deviations from exponential decay are easily discerned. Second, the "series" model of rate controlling energy transfer though the lowest-frequency mode is far from being generally applicable, at least for large molecules dilute in krypton. We are continuing to investigate this phenomenon in other molecules and over a wider range of mixture composition.

Dissociation Rates and Incubation Times in Norbornene.

Norbornene (C_7H_{10}, bicyclo [2,2,1] hept-2-ene) dissociates to ethylene and cyclopentadiene via a retro-Diels-Alder reaction. The thermochemistry of this process is well known, and its rate has been reliably determined at low temperatures[3,4]. The products of this process are stable, on the LS microsecond timescale, up to 1400-1500K. In fact, we see no evidence of any parallel dissociation or isomerization channel, nor of any secondary reactions, to 1500 K.

In norbornene we are able to resolve both vibrational relaxation (500-1300 K) and dissociation (900-1500 K). Over a somewhat narrower range, 900-1300 K, both relaxation and dissociation can be seen in the same experiment. From such experiments, and from a modeling of other, higher pressure dissociation experiments, we have derived the incubation times and steady-state reaction rate constants of figures 1 and 2. Incubation can

be observed in this molecule in large part because the relaxation process is only weakly dependent on T ($P\tau \alpha T^{0.6}$). The incubation time to relaxation time ratios of figure 2 drop somewhat more rapidly ~T^{-2}. The dissociation rate constants of figure 3 show very strong and sudden unimolecular falloff, but this is well reproduced by the simple RRKM calculation also shown. We are preparing a complete description of this work for publication.

Unimolecular Dissociation of C_2H_2 (with A.F. Wagner)

We are currently extending our analysis of the effect of restricted internal rotation of the H-atoms on the rate of low-pressure-limit dissociation of small unsaturated hydrides (see the HCN paper below) to C_2H_2. A semi-classical, excluded volume approach would seem able to deal with the H-H interaction in this dihydride, but there are some unusual features of the potential which still present problems.

Future Plans

Our plans include the completion of our work on allene/propyne pyrolysis incorporating a LS study of 1,2-butadiene decomposition, the decomposition of other perhalomethanes, CF_3Br, CF_3I, CF_4, along with further study of relaxation and relaxation dissociation coupling in large molecules.

References

1. T.L. Cottrell and J.C. McCoubrey, "Molecular Energy Transfer in Gases", Butterworths, London (1961).
2. B. Stevens, "Collisional Activation in Gases", Pergamon, NY (1967).
3. B.C. Roquite, J. Chem. Phys. 69, 1351 (1965).
4. W.C. Herndon, W.B. Cooper, Jr. , and M. J. Chambers, J. Phys. Chem. 68, 2016 (1964).

Publications 1991 -

"Rate of the Retro-Diels-Alder Dissociation of 1,2,3,6-Tetrahydropyridine over a Wide Temperature Range", S.S. Sidhu, J.H. Kiefer, A. Lifshitz, C. Tamburu, J.A. Walker, and W. Tsang, Int. J. Chem. Kinet. 23, 215 (1991).

"Thermal Isomerization of Cyclopropanecarbonitrile. The Use of Multiple Chemical Thermometers in Single Pulse Shock Tube Experiments", A. Lifshitz, I. Shweiky, J.H. Kiefer, and S.S. Sidhu, Proc. 18th Symposium (Int'l) on Shock Waves, Springer-Verlag, Berlin, 1992, p. 825.

"The Reaction of C_4H_2 and H_2 Behind Reflected Shock Waves", R.D. Kern, K. Xie, H. Chen, and J.H. Kiefer, Proc. 18th Symposium (Int'l) on Shock Waves, Springer-Verlag, Berlin, 1992, p. 729.

"The Homogeneous Pyrolysis of Acetylene II: The High Temperature Radical Chain Mechanism", J.H. Kiefer, S.S. Sidhu, R.D. Kern, K. Xie, H. Chen, and L.B. Harding, Combust. Sci. and Tech. 82, 101 (1992).

"Rate of CH_4 Dissociation over 2800-4300 K: The Low-Pressure-Limit Rate Constant", J.H. Kiefer and S.S. Kumaran, J. Phys. Chem. 97, 414 (1993).

"The Importance of Hindered Rotations and other Anharmonic Effects in the Thermal Dissociation of Small Unsaturated Molecules: Application to HCN", A.F. Wagner, J.H. Kiefer, and S.S. Kumaran, 24th Symposium (Int'l) on Combustion, Sydney, 1992, pg. 613.

"The Formaldehyde Decomposition Chain Mechanism", E.A. Irdam, J.H. Kiefer, L.B. Harding and A.F. Wagner, Int. J. Chem. Kinet., in press.

"Thermal Dissociation Studies of Toluene at High Temperatures", R.D. Kern, H. Chen, H.J. Singh, K. Xie, J.H. Kiefer and S.S. Sidhu, Proc. 6th Toyota Conference on Turbulence and Molecular Processes in Combustion, T. Takeno, Ed. To be published by Elsevier.

"The Thermal Decomposition of Carbon Tetrachloride", J.V. Michael, K.P. Lim, S.S. Kumaran and J.H. Kiefer, J. Phys. Chem. 97, 1914 (1993).

"Comment: Radical Processes in the Pyrolysis of Acetylene", J.H. Kiefer, Int. J. Chem. Kinet. 25, 215 (1993).

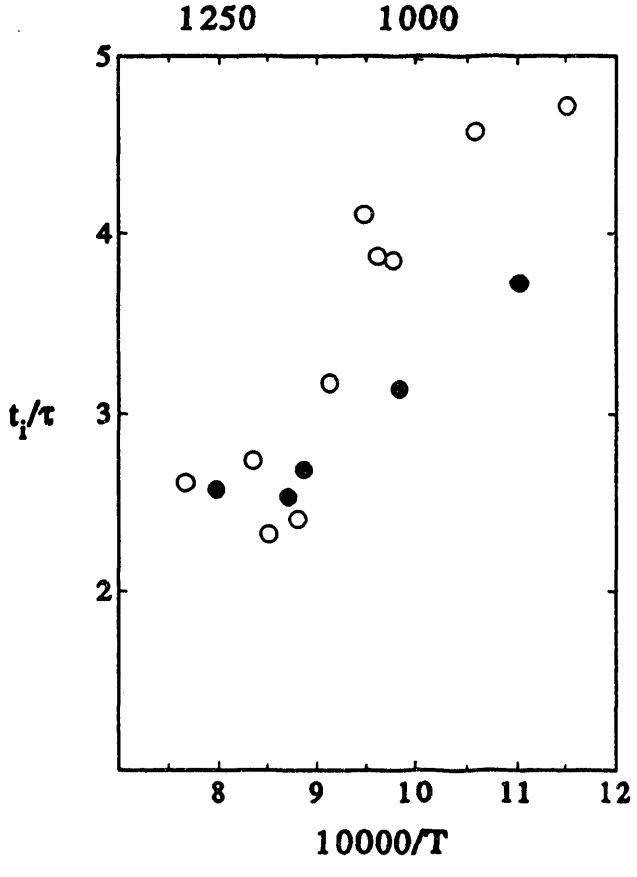

Figure 1: Unimolecular incubation times for norbornene (NB)/Kr mixtures expressed as t_i/τ, where τ is the observed vibrational relaxation time. Here (●) are 0.5% NB/Kr and (O) 2.0% NB.

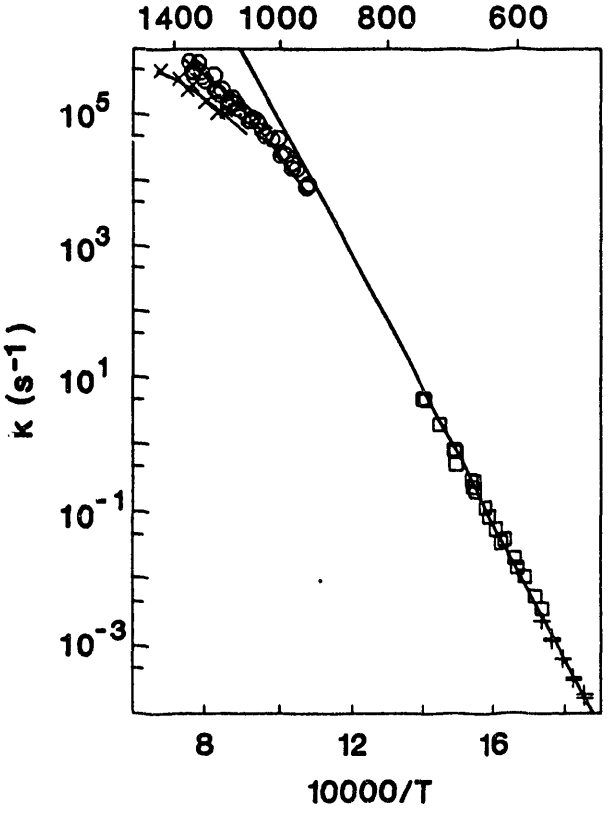

Figure 2: Dissociation rate constants in NB-Kr, (O) mean pressure of 350 torr, (X) 150 torr. (□) are the data of ref. 4 and (+) those of ref. 3. The lines show the results of RRKM calculations, the long diagonal line being k_∞.

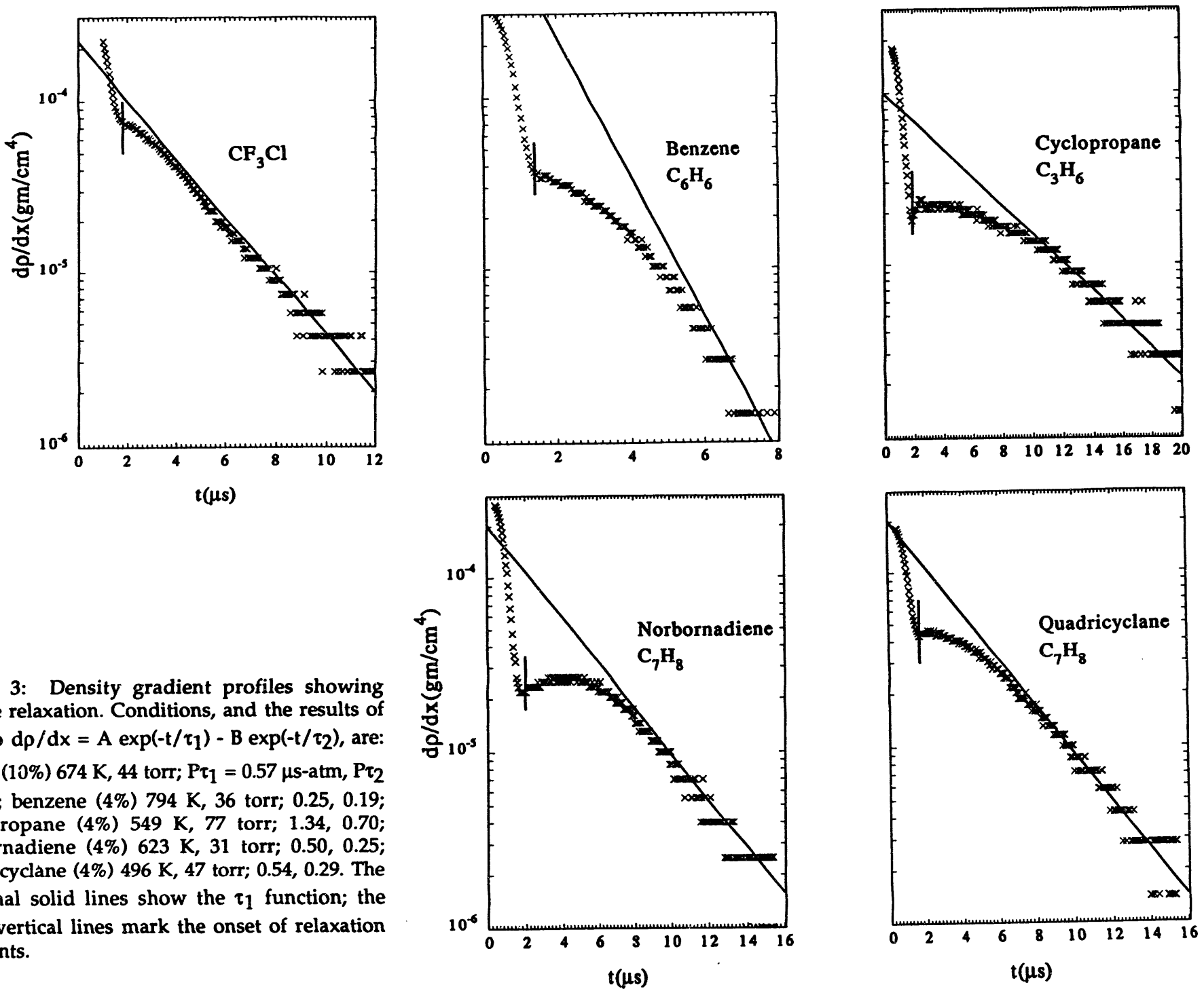

Figure 3: Density gradient profiles showing double relaxation. Conditions, and the results of a fit to $d\rho/dx = A \exp(-t/\tau_1) - B \exp(-t/\tau_2)$, are: CF_3Cl (10%) 674 K, 44 torr; $P\tau_1$ = 0.57 μs-atm, $P\tau_2$ = 0.23; benzene (4%) 794 K, 36 torr; 0.25, 0.19; cyclopropane (4%) 549 K, 77 torr; 1.34, 0.70; norbornadiene (4%) 623 K, 31 torr; 0.50, 0.25; quadricyclane (4%) 496 K, 47 torr; 0.54, 0.29. The diagonal solid lines show the τ_1 function; the short vertical lines mark the onset of relaxation gradients.

COMBUSTION KINETICS AND REACTION PATHWAYS

R. Bruce Klemm and James W. Sutherland
Combustion Kinetics Group/Bldg. 815
Department of Applied Science
Brookhaven National Laboratory
Upton, NY 11973

PROGRAM SCOPE: This project is focused on the fundamental chemistry of combustion. The overall objectives are to determine rate constants for elementary reactions and to elucidate the pathways of multichannel reactions. A multitechnique approach that features three independent experiments provides unique capabilities in performing reliable kinetic measurements over an exceptionally wide range in temperature, 300 to 2500K. Recent kinetic work has focused on experimental studies and theoretical calculations of the methane dissociation system ($CH_4 + Ar \rightarrow CH_3 + H + Ar$ and $H + CH_4 \rightarrow CH_3 + H_2$). Additionally, a discharge flow-photoionization mass spectrometer (DF-PIMS) experiment is used to determine branching fractions for multichannel reactions and to measure ionization thresholds of free radicals. Thus, these photoionization experiments generate data that are relevant to both reaction pathways studies (reaction dynamics) and fundamental thermochemical research. Two distinct advantages of performing PIMS with high intensity, tunable vacuum ultraviolet light at the National Synchrotron Light Source are high detection sensitivity and exceptional selectivity in monitoring radical species.

RATE CONSTANT FOR $O(^3P) + C_2H_6$ (400K to 1500K): In the present study, rate constants for the $O + C_2H_6$ reaction were measured using three independent methods: (i) discharge flow-resonance fluorescence ($453 < T < 1048K$); (ii) flash photolysis-resonance fluorescence ($416 < T < 520K$); and (iii) flash photolysis-shock tube ($728 < T < 1489K$). There is excellent agreement among the three individual data sets obtained by these independent techniques in the overlapping ranges of temperature. The data were fit by a simple Arrhenius equation; and the mean deviation of experimental points from this fit was $\pm 11.1\%$ at the one sigma level. However, slight curvature in the plot was evident at the highest temperatures and an improved fit was obtained by using a three parameter expression:

$$k(T) = 1.45 \times 10^{-13} T^{0.957} \exp(-3340\ K/T)\ cm^3\ molecule^{-1}\ s^{-1}$$

The mean deviation of the experimental points from this fit is $\pm 9.6\%$. Great care was exercised in this work to document the extent of secondary reaction complications, particularly at low temperatures (e.g. due to the reaction of O-atoms with ethyl radicals). This work has also extended (to higher temperatures) the range for the directly measured rate constant value by nearly 300 degrees (K). Additionally, the present kinetic results for the reaction of $O(^3P)$ with ethane do not display the extreme non-Arrhenius behavior of those reported by Fontijn and co-workers, i.e. it was not necessary to invoke a large tunnelling effect for this particular reaction. Indeed, the present results are in reasonably good agreement with a simple TST calculation reported by Golden and co-workers that does not incorporate a tunnelling correction.

RATE CONSTANT FOR $O(^3P)$ + 1-C_4H_8: The rate constant for the reaction of ground-state atomic oxygen with 1-C_4H_8 was measured by the FP-ST technique over the temperature range 780K to about 1400K. At temperatures above 1400K the results suggested that the kinetic system was no longer simple and that reliable kinetic data were not obtainable. The data (780K - 1400K) were combined with data obtained previously in this laboratory by the FP-RF and DF-RF techniques over the temperature range 294K - 871K. The combined results ($294K < T < 1400K$) were in reasonable agreement with the recent data of Fontijn et al. that were obtained over the more limited temperature range of 335K to 1110K using their high-temperature photochemistry (HTP) technique.

The combined data from the three independent techniques (FP-RF, DF-RF and FP-ST) employed in the present study were best fit to a sum-of-exponentials expression:

$$k(T) = 1.4 \times 10^{-11} \exp(-375K/T) + 6.8 \times 10^{-10} \exp(-3800K/T) \text{ cm}^3 \text{ molecule}^{-1} \text{ s}^{-1}$$

These results are consistent with the onset of a second reaction channel due to H-atom abstraction at high temperatures, $T > 1000K$.

PHOTOIONIZATION STUDIES: REACTION PATHWAYS AND PHOTOIONIZATION THRESHOLDS: The objectives of this experimental project are to investigate pathways for multichannel elementary reactions and to obtain photoionization spectra and ionization energies for important combustion-related radical species. The independent DF-PIMS apparatus was specifically designed to be operated on the U-11 beam line at the NSLS to utilize the intense and tunable VUV radiation available there.

The reaction of N-atoms with ethyl radicals may be important in "prompt" NO_x mechanisms and it has been implicated as a complicating feature in flow tube studies of "active nitrogen" reactions. The thermodynamically accessible channels for the N + C_2H_5 reaction are given below along with the corresponding ΔH in kcal/mol:

N + C_2H_5	→ H_2CN + $\underline{CH_3}$	[-56]
	→ $H(CH_3)CN$ + H	[-55]
	→ $\underline{C_2H_4}$ + NH	[-39]
	→ HCN + CH_3 + H	[-23]
	→ CH_3CN + 2H	[-19]
	→ CH_3CN + H_2	[-123]
	→ HCN + CH_4	[-124]
	→ CH_3CHNH	[-139]
	→ cyc-C_2H_4NH	[-111]

The H_2CN + CH_3 channel and the NH + C_2H_4 channel were previously found in this laboratory to be major product pathways. By using perdeuterated ethane to generate C_2D_5, via F atom abstraction, it was possible to isolate the underlined products by mass. In the present study a quantitative branching fraction for the NH + C_2H_4 channel was determined to be 0.6 ± 0.2. The other major channel, H_2CN + CH_3, presumably accounts for most of the remainder (0.4).

In addition, photoionization spectra and ionization thresholds for BrO and HOBr were obtained using DF-PIMS at the NSLS. BrO and HOBr were generated in the flow tube by reacting O-atoms and OH-radicals, respectively, with Br_2. Spectra for both were measured over the wavelength range, 106-122 nm. For BrO, a threshold at 10.46 ($\pm$ 0.02) eV was obtained. This value is slightly larger than one (10.29 eV) determined using photoelectron spectroscopy. However, in the PES study it appears that signal due to direct ionization of BrO was obscured by that from Br_2^+ and $O_2^+(^1\Delta)$. A directly measured photoionization threshold for HOBr (10.62 $\pm$ 0.02eV) has apparently not been reported previously.

METHANE DISSOCIATION REVISITED: Last year, the kinetic study of (i) the reaction of CH_3 radicals with H_2 and (ii) the thermal dissociation of methane was reported at the Combustion Symposium. In that work, primary product H-atoms were monitored directly using the atomic resonance absorption detection technique with a detection sensitivity of about $5x10^{10}$ atoms cm^{-3}. For the reaction of $CH_3 + H_2$, experiments were performed using either acetone or ethane to generate CH_3 radicals rapidly by thermal dissociation in argon. Results from this study agree well with those for the $CH_3 + H_2$ reaction that were computed using $k_2 = k_2 / K_2$ (where k_2 is the rate constant for the $H+CH_4 \rightarrow CH_3 + H_2$ reaction and K_2 is the equilibrium constant) as reported in an earlier study from this laboratory. The discrepancy between these results and those (for k_2) reported by Roth and Just therefore remained. Similarly, for the methane dissociation study, the results for $k_1°$ were also in good agreement with previous results reported from this laboratory.

Further work during the past year, has focused on checking H-atom calibration measurements and performing additional methane dissociation experiments. All calibration and kinetic results to date have confirmed our previous measurements and therefore the discrepancy between this project's results and those of the older studies remains. Also during the past year, three new shock tube studies on methane dissociation have been reported. A laser schlieren study (Univ. of Chicago), at temperatures of 2800-4400K, provided values for $k_1°$ (using an RRKM extrapolation procedure) that were about 50% larger than those of Roth and Just at 2000K. The second study (Stanford University), in which the $[CH_3]$ was monitored with a detection sensitivity of about $1x10^{13}$ radicals cm^{-3}, gave $k_1°$ values (1800-2300K) that were within the experimental uncertainty of those of Roth and Just. however, their results were consistently smaller over their entire temperature range. While both of these studies employed kinetic modeling to derive $k_1°$ data, the Stanford Univ. work was much less sensitive than the Univ. of Chicago work to variation of rate constants for other reactions in the mechanism (i.e. the CH_3 detection study was considerably more direct than the laser schlieren work). Finally, a third study (DLR/Stuttgart) was reported as a Poster at the Combustion Symposium last year in Sydney. In that investigation, H-atoms were generated thermally (via $C_2H_5I \rightarrow C_2H_5 + I$, $C_2H_5 \rightarrow C_2H_4 + H$) and rate constant values for $H + CH_4 \rightarrow CH_3 + H_2$ were measured directly. At temperatures above 1700K, the effect of methane dissociation was observable in non-zero baselines for [H] at long reaction times. In this study, the [H] data were analyzed using non-linear fitting methods and values for $k_1°$ and k_2 ($H + CH_4$) that agreed with Roth and Just were reported. However, we performed an analysis of some of their data (DLR) using a linearized fitting procedure (i.e. closed form solution) and derived $k_1°$ and k_2 values that are considerably smaller than those reported. Indeed, the re-analyzed k_2 values (for three runs) were about one-half of theirs (or only about 30% larger than our published results) and the re-analyzed $k_1°$ values (for two runs) were less than one-half of theirs (or about 80% larger than our published results).

FUTURE PLANS: High temperature kinetic studies that utilize the unique capabilities of this project will continue on the reaction of $O(^3P)$ atoms with selected alkanes and alkenes, e.g. propane and isobutene. Where appropriate (e.g. O-atom + olefin reactions), the kinetic work will be augmented by reaction pathways studies using DF-PIMS. In addition, studies on the thermal decomposition of C_2H_6 may be initiated together with appropriate kinetic modelling studies. DF-PIMS studies will also continue to emphasize thermochemical measurements (ionization energies and enthalpies) for a wide variety of radical species that can be generated cleanly in the discharge flow reactor. A potentially significant error in the values of the rate constant for CH_4 dissociation reported by other workers has been identified as the result of studies in this laboratory. This discrepancy, which has important practical and theoretical consequences, has not been satisfactorily resolved as yet, despite significant contributions from this and several other laboratories. Therefore, the kinetic study of methane dissociation will continue but greater emphasis will be placed on critical evaluations and theoretical calculations. In particular, modification (smaller step sizes) of the "Unimol" code to perform RRKM/master equation calculations may be required to obtain internally consistent results for the CH_4 system.

RECENT PUBLICATIONS:

1. Rabinowitz, M. J., Sutherland, J. W., Patterson, P. M., and Klemm, R. B. Direct rate constant measurements for $H+CH_4 \rightarrow CH_3+H_2$, 897-1792K, using the FP-ST technique. J. Phys. Chem. 95, 675-81 (1991).
2. Sutherland, J. W., Patterson, P. M., Klemm, R. B. Rate constants for the reaction $0(^3P) + H_20 \leftrightarrow OH+OH$, over the temperature range 1053K to 2033K using two direct techniques. Proc. Twenty-third Int'l. Sympos. on Combustion, The Combustion Institute, Pittsburgh, 1990, pp. 51-7 (1991).
3. Nesbitt, F. L., Marston, G., Stief, L. J., Wickramaaratchi, M. A., Tao, W., and Klemm, R. B. Measurement of the photoionization spectra and ionization threshold of the H_2CN and D_2CN radicals. J. Phys. Chem. 95, 7613-7 (1991).
4. Yarwood, G., Sutherland, J. W., Wickramaaratchi, M. A., and Klemm, R. B. Direct rate constant measurement for the reaction $0+N0+Ar \rightarrow N0_2+Ar$, 300K to 1341K. J. Phys. Chem. 95, 8771-5 (1991).
5. Tao, W., Klemm, R. B., Nesbitt, F. L., and Stief, L. J. A discharge-flow photoionization mass spectrometric study of hydroxymethyl radicals (H_2COH and H_2COD): photoionization spectrum and ionization energy. J. Phys. Chem., 96, 104-7 (1992).
6. Klemm, R. B., Sutherland, J. W., Rabinowitz, M. J., Patterson, P. M., Quartemont, J. M., and Tao, W. Shock tube kinetic study of methane dissociation: $1726K<T<2134K$. J. Phys. Chem. 96, 1786-93 (1992).

OTHER PUBLICATIONS:

1. Klemm, R. B., Sutherland, J. W., and Tao, W. Shock tube kinetic study of the $CH_3 + H_2 \leftrightarrow H + CH_4$ reaction and the methane dissociation reaction. Twenty-fourth Int's. Sympos. on Combustion, July, 1992, Poster Paper #52.
2. Klemm, R. B., Sutherland, J. W., Patterson, P. M., and Tanzawa, T. Direct rate constant measurements for the reaction $O(^3P)$ with ethane: $416K<T<1489K$. Twenty-fourth Int'l. Sympos. on Combustion, July, 1992, Poster Paper #53.

Studies in Combustion Dynamics

M. L. Koszykowski
Combustion Research Facility
Sandia National Laboratories
Livermore, CA 94551

The goal of this program is to develop a fundamental understanding and a quantitative predictive capability in combustion modeling. A large part of the understanding of the chemistry of combustion processes comes from "chemical kinetic modeling." However, successful modeling is not an isolated activity. It necessarily involves the integration of methods and results from several diverse disciplines and activities including theoretical chemistry, elementary reaction kinetics, fluid mechanics and computational science. Recently we have developed and utilized new tools for parallel processing to implement the first numerical model of a turbulent diffusion flame including a "full" chemical mechanism.

Turbulent Flame Modeling:

Presently, one of the most important problems in turbulent combustion modeling is correctly approximating the coupling between reactive and diffusive processes on the smallest scales. Future progress in combustor design is very promising if modeling capabilities are further extended so that detail at a finer level of structure can be predicted. To be sufficiently accurate to be used as design tools, these models and their corresponding computational codes must include both chemistry, fluid mechanics, and their interactions over a broad range of time and length scales.

While fluid-mechanical turbulence models and detailed-chemistry flame models in simple flows are solvable on standard vector supercomputers, the combination of turbulent flow and detailed chemistry in the same model requires the next generation supercomputer: the massively parallel machine. We have investigated a probability density function (PDF) code for a jet flame diffusion problem. The PDF algorithm involves mostly Monte Carlo calculations and is highly amenable to an efficient parallel implementation. A toolkit approach is used to partition the algorithmic portions of the code (e.g. equation solver, Monte Carlo simulation) from the application specific code.

Parallel Architecture:

Existing tools for parallel software development generally fall into two categories: 1) high-level tools and compilers that hide the parallelization details, making them easy to use but also hiding the pitfalls that lead to bottlenecks; or, 2) low-level tools for message passing that create scalable code, but require detailed knowledge of algorithms and software that are difficult for the non-systems programmer to use. The purpose of our approach, that of a toolkit, is to allow a physical scientist to create an integrated and scalable application code that transparently accesses parallel computing resources and avoids the traditional pitfalls associated with parallel computing. The toolkit is a high-level object-oriented framework for parallel computing that is designed for direct integration of existing application codes. It is written in C++ in an extensible manner that guarantees scalable code.

Chemically Reacting Flow Problem

We have investigated a turbulent diffusion flame that consists of a cylindrical jet which injects a fuel into a coflowing air stream and is ignited. The model is composed of three parts: the turbulent motion model, the chemical reaction model and the coupling between

chemical reactions and turbulence. The downstream exhaust is computed using an advancing grid beginning from the inlet and advancing downstream until chemical activity is complete. Symmetry allows this problem to be modeled using a one dimensional grid that effectively represents a radial slice of the cylindrical nozzle. The model is based on the probability density function (PDF) approximation.

The algorithm is a piecewise Monte Carlo method in which the Monte-Carlo aspect of the problem comes from the transport (or mixing) of particles to and from nearest-neighbor cells. This mixing is a result of fluid-mechanical turbulence and Fickian diffusion. The chemistry that accounts for most of the computation, is local to each cell in which particles from one node cell are required to communicate with only the right and left neighbor cells.

The toolkit implementation builds upon a piecewise Monte Carlo (PMC) object. The first step is to spatially-domain decompose the linear grid. The PMC object then exploits the nearest-neighbor dependence of the physics of this problem and defines three types of cells: left boundary, right boundary, and interior. The data necessary to compute an interior cell is the cell itself and its right and left neighbors. We define a callback around this called Inside. It receives three objects called *Data Racks* that hold all of the data relevant to the cell and its neighbors. The callback will recover the data necessary to do its computation by sending messages to the Data Racks and, once the computation is accomplished, the callback will send a message updating the relevant data in the Data Racks. The two leftmost cell's Data Racks will be sent to another callback (LBndry) to handle the left boundary condition. The rightmost two cell's Data Racks will be sent to a third callback (RBndry) to handle the right boundary condition. These three routines are sufficient to accomplish the PDF calculation.

The PMC object takes care of processor-to-processor communication such as updating the ghost nodes (nodes that are overlap processors) and returning the results to a host processor. Independent callback routines fill out stubs on the PMC object to provide the physics particular to the PDF problem.

Results

The entire one-dimensional grid of cells plus boundary conditions for the two cells on left and right ends of the grid compose the Monte Carlo portion of the problem and accounts for 99.3% of the computer time, even with minimal chemistry. At the appropriate time, statistics computed from the particles distributed over the cells contribute to an update of the flow field, either as an iteration converging on a steady state or as a time step in a nonsteady problem. The addition of realistic chemistry increases the computation required by 10 to 100 fold.

Through our toolkit, the power necessary to compute PDF chemically reacting flow problems with realistic chemistry on massively parallel and distributed systems has been provided. Moreover, by encapsulating the PMC algorithm in an autonomous object and thus insulating the specific physics of a PDF problem from the algorithm, we produce reusable code that can be used on other chemically reacting flow problems. Ultimately, the update of the flow field will require an equation solver; however, in this early implementation we anticipate avoiding this issue by solving the entire flow field on every processor. Since this step requires little computation and the communication of very few averaged numbers to each processor, it is expected that the lack of salability in this step will have little impact on the speed-up necessary for this application.

The results, shown in figure 1, are in excellent agreement with experiment. In the coming year we will make detailed predictions of species concentration profiles and compare with experiment, as well examining the effects of the molecular diffusion approximation on the coupling of the chemistry with the fluid mechanics.

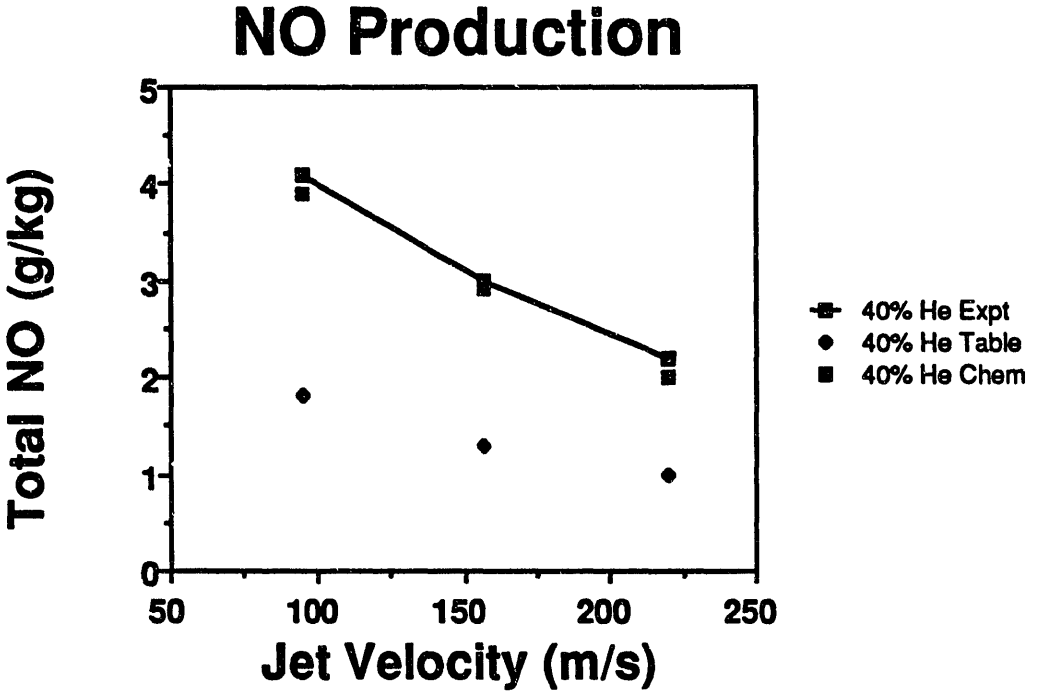

Figure 1 shows our prediction for total NO formation in a turbulent diffusion flame including a complete H_2-AIR chemical mechanism. Also included are the experimental measurements and previous results using a reduced mechanism and a look-up table for the chemical calculations.

Publications:

J. F. Macfarlane, R. C. Armstrong, R. E. Cline and M. L. Koszykowski, "Application of Parallel Object-Oriented Environment and Toolkit (POET) to Combustion Problems", Proc. of IEEE International Conference on System Sciences, January 5, 1993.

M. L. Koszykowski, R. C. Armstrong, R. E. Cline Jr., J. F. Macfarlane, J. Y. Chen, and N. J. Brown, "ACME - the Advanced Combustion Modeling Environment", Computing at the Leading Edge: Research in the Energy Sciences, February 1993.

M. L. Koszykowski, J. F. Macfarlane, and R. C. Armstrong "Achieving Full Chemistry in Combustion Models Using POET" Proc. of the 1993 High Performance Computing Synposium - Grand Challange Applications, Arlington Virginia, March 29, 1993.

W. A. Glauser, M. L. Koszykowski, W. A. Lester, and Brian L. Hammond, "Random Walk Approach to Mapping Nodal Regions of N-Body Wavefunctions. I. Ground State Hartree-Folk Wavefunctions for First Row Atoms," J. Chem. Phys., 98, 12, 1992.

W. A. Glauser and M. L. Koszykowski, "Anomalous Methoxy Yields In the Fluorine + Methanol Reaction. 2. Theory," J. Phys. Chem., 95, 10705, 1991.

W. A. Glauser and M. L. Koszykowski, "Vibrational Dispersion Interactions in Van der Waals Complexes: Effect upon Stability and Infrared Spectra," J. Phys. Chem., 95, 8507, 1991.

LASER SOURCES AND TECHNIQUES FOR SPECTROSCOPY AND DYNAMICS

Andrew H. Kung

Chemical Sciences Division
Lawrence Berkeley Laboratory
Berkeley, California, 94720

Project Scope

This program focuses on the development of novel laser and spectroscopic techniques in the IR, UV, and VUV regions for studying combustion related molecular dynamics at the microscopic level. Laser spectroscopic techniques have proven to be extremely powerful in the investigation of molecular processes which require very high sensitivity and selectivity. Our approach is to use quantum electronic and non-linear optical techniques to extend the spectral coverage and to enhance the optical power of ultrahigh resolution laser sources so as to obtain and analyze photoionization, fluorescence, and photoelectron spectra of jet-cooled free radicals and of reaction products resulting from unimolecular and bimolecular dissociations. New spectroscopic techniques are developed with these sources for the detection of optically thin and often short-lived species. Recent activities center on regenerative amplification of high resolution solid-state lasers, development of tunable high power mid-IR lasers and short-pulse UV/VUV tunable lasers, and development of a multipurpose high-order suppressor crossed molecular beam apparatus for use with synchrotron radiation sources. This program also provides scientific and technical support within the Chemical Sciences Division to the development of LBL's Combustion Dynamics Initiative.

Recent progress

1. Regenerative Amplification of Single Frequency Optical Parametric Oscillators We have demonstrated for the first time an extremely broadly tunable all solid-state single-frequency source based on an optical parametric oscillator (OPO) regenerative amplifier arrangement. The source combines the virtues of an OPO with those of a solid-state laser amplifier to provide high power jitter-free pulsed radiation that is near-diffraction limited, rapidly and broadly tunable, and very narrowband. The work is motivated by the desire to have a solid state device that would have excellent frequency control, and can easily be time-synchronized to other laser pulses. To achieve this, we started with a commercial single-frequency OPO that is tunable from 700 nm to 1000 nm and injected its 2-nsec long pulses into a Ti:Al_2O_3 ring cavity. Optics in the cavity were arranged to operate in the regenerative amplifier mode. Pulse injection and extraction were achieved by polarization coupling using two Pockels cells and a polarizer. A half-wave Fresnel Rhomb served to spoil lasing in the absence of an injected pulse. This regenerative arrangement has the advantage of being extremely broadband. It relaxes the need for longitudinal and transverse mode-matching. Timing and frequency are controlled by the OPO, while output power and spatial filtering are provided by the Ti:Al_2O_3 resonator. The amplifier output was nearly TEM_{00}. Pulse energy was measured from 840 nm. to 910 nm. With injection of a 0.5 mJ pulse from the OPO, the output energy ranged from 40 mJ at 840 nm. to 20 mJ at 920 nm.. The slow fall-off in wavelength dependence is significant because stand-alone Ti:Al_2O_3 lasers and linear amplifiers become inefficient at 910-920 nm and beyond. This device thus results in a much broader tuning range. The output photon efficiency was 20% to 24%. Improvements to the cavity should increase this efficiency since depletion of the Ti:Al_2O_3 fluorescence was observed to reach 60%. Addition of a power amplifier will boost the output energy to more than 100 mJ.

2. Tunable High Power IR Laser Development The purpose of this task is to develop a high resolution, high power, mid-infrared laser source. The goal is to make available a tunable infrared laser that is suitable to use in research on multiphoton excitation and dissociation experiments. It has been commonly recognized that understanding the photodissociation dynamics and reactivity of hydrocarbon free-radicals are essential for understanding the combustion processes of fossil fuels. Infrared multiple-photon absorption will imitate the combustion process in the excitation of reactive species. IR-UV pump and probe will allow the study of mode selectivity in photodissociation. In both cases, an intense IR laser is required. The preliminary specifications of the IR laser are as follows: tuning range, 3 to 10 microns, pulse energy 10 to 100 mJ, wavelength stability 1 in 10^4, and transform-limited resolution.

Three approaches were evaluated for this development, all involving non-linear optical techniques to convert fixed frequency or tunable high power visible or near-IR lasers to the mid-IR: difference frequency mixing, optical parametric oscillation (OPO), and Raman shifting. It was clear that a fourth approach, direct lasing, is not feasible because no suitable material is available.

Crystal materials that are transparent in the mid-IR generally have low optical damage thresholds. This investigation therefore focuses on using Raman shifting in gases as the wavelength conversion stage. Gases can be replenished easily if needed. Previous studies have shown that good conversion can be achieved in a multi-pass Raman cell of H_2 and its isomers. Furthermore, the monochromaticity and spatial quality of the input can be preserved. Our calculation shows that a 20 pass Raman cell operating with 10 atm. of H_2 will be required to obtain powerful IR radiation down to 8 microns. Generation at 10 μm becomes problematic due to decreasing Raman gain and inception of H_2 dimer absorption.

For a preliminary study, we have constructed a high pressure Raman cell using second order Stokes in H_2 to produce IR in the region of 2 to 4 μm. The cell was tested for 600 psia operation. It was placed in a cavity of two 1" diameter concave copper mirrors that are separated by ~2m to effect multiple passing of a pump laser beam. We have chosen an external mirror arrangement because it simplifies the initial multipass alignment procedure. Successful second Stokes generation has been obtained with this cell using a Ti:sapphire based pump laser. In this preliminary study, 0.5 mJ of 3 μm radiation has been produced using 10 mJ of incident pump energy. With optimization of the Raman process and use of full power from the OPO regenerative amplifier system that is being developed for this project, we should meet the goal of obtaining >10 mJ in the 3 μm region.

3. Multipurpose high order suppressor and crossed molecular beam apparatus Studies on high-order suppression of undulator light have shown that a combination of reflection filtering and rare gas filtering will provide a spectral purity of better than 1/100,000 for the energy range of 5-30 eV. The reflection filters cut off photons with energy higher than 30 eV and the rare gas filter then serves to absorb unwanted orders from the undulator emission. We have finished the engineering design of a gas filter. The filter employs an active length of 10 cm and is for use with a maximum gas pressure of 30 Torr. It is embedded in a multipurpose triply differentially pumped chamber that features a flexible design. By placing a rare gas tube in the center of the chamber the machine will serve as a high-order suppressor. Alternatively, when a rotating pulsed molecular beam source is placed in the center of the chamber, it can be used as a photodissociation apparatus.

Future Plans

Development of the regenerative amplifier continues with measurements to determine the full tuning range of the device. A booster amplifier is being incorporated to increase the device output energy by a factor of ten. With this pulse energy, the device will be suitable for use as the front-end of the tunable IR system.

Investigation in using high order Raman shifting to generate high power tunable IR is in progress. We are optimizing the use of the external cavity multipass cell to generate 2 to 4 μm radiation. This will provide us with a preliminary IR source to study the spectroscopy and mode-selective dissociation dynamics of hydrocarbon free-radicals. In order to reach the ultimate goal of making 5-8 μm mid-IR radiation, we are designing a multipass cell with internal mirrors for third order Raman shifting. A large number of passes is necessary to reach threshold for Raman conversion since the Raman gain falls off significantly as the IR wavelength gets longer. In addition to H_2, we are also investigating using HD and D_2 as the medium for efficient conversion.

Development of the multipurpose chamber is proceeding with the design of a versatile rotating source chamber that fits into the main chamber of the high-order suppressor. When mounted at the top of the main chamber, the source chamber supplies rare gases for high-order suppression of undulator radiation. This source chamber can also be utilized to produce free radicals by photolysis in front of a pulsed nozzle or by pyrolysis in a nozzle attached to the chamber. As another option, two such chambers can be fitted to the main chamber to form a crossed-beam machine for studying scattering experiments.

Recent Publications:

A.H. Kung, Regenerative Amplification of a Single-Frequency Optical Parametric Oscillator, Opt. Lett., (submitted).

E.F. Cromwell, D.J. Liu, M.J.J. Vrakking, A.H. Kung, and Y.T. Lee, Dynamics of H_2 Elimination from Cyclohexadiene, J. Chem. Phys. **95**, 297-307 (1991).

A.H. Kung and Y.T. Lee, Spectroscopy and Reaction Dynamics Using Ultrahigh Resolution VUV Lasers, in **Vacuum Ultraviolet Photoionization and Photodissociation of Molecules and Clusters**, C.Y. Ng, editor, World Scientific Publishing Company, Singapore (1991), pp.487-502.

Dynamics and Structure of Stretched Flames

Chung K. Law
Department of Mechanical and Aerospace Engineering
Princeton University, Princeton, NJ 08544

Program Scope

The program aims to gain fundamental understanding on the structure, geometry, and dynamics of laminar premixed flames, and relate these understanding to the practical issues of flame extinction and stabilization. The underlying fundamental interest here is the recent recognition that the response of premixed flames can be profoundly affected by flame stretch, as manifested by flow nonuniformity, flame curvature, and flame/flow unsteadiness. As such, many of the existing understanding on the behavior of premixed flames need to be qualitatively revised. The research program consists of three major thrusts: (1) Detailed experimental and computational mapping of the structure of aerodynamically-strained planar flames, with emphasis on the effects of heat loss, nonequidiffusion, and finite residence time on the flame thickness, extent of incomplete reaction, and the state of extinction. (2) Analytical study of the geometry and dynamics of stretch-affected wrinkled flame sheets in simple configurations, as exemplified by the Bunsen flame and the spatially-periodic flame, with emphasis on the effects of nonlinear stretch, the phenomena of flame cusping, smoothing, and tip opening, and their implications on the structure and burning rate of turbulent flames. (3) Stabilization and blowoff of two-dimensional inverted premixed and diffusion flames, with emphasis on understanding the controlling mechanisms of flame stabilization and determining the criteria governing flame blowoff. The research is synergistically conducted through the use of laser-based diagnostics, computational simulation of the flame structure with detailed chemistry and transport, and mathematical analysis of the flame dynamics.

Recent Progress

Useful contributions have been made in understanding the structure of laminar premixed and diffusion flames, with emphasis on the influence of aerodynamics and chemical kinetics. Highlights of some of these accomplishments are briefly discussed in the following.

Effects of Curvature on Diffusion Flame Extinction

Although considerable understanding has been gained on the properties of stretched premixed flames, studies on stretched diffusion flames have been limited to effects of aerodynamic straining on the planar counterflow flames. Since flames in practical situations are seldom planar, as in the case of the laminar flamelets in turbulent diffusion flames, it is of interest to study the effects of curvature on the burning intensity of diffusion flames. In this study we adopted the tip of the Burke-Schumann flame as a representative curved flame. An asymptotic analysis of the flame structure in the tip region showed that increasing the flame curvature facilitated near-complete reaction and thereby enhanced the burning intensity. Consequently, for unity Lewis number flames, increasing the flow velocity reduced the flame radius and thereby tended to inhibit tip opening; Lewis number (Le) is defined as the ratio of the thermal diffusivity of the mixture to the mass diffusivity between the deficient reactant and the inert in the mixture. Experimental results using near unity Le acetylene/air flames agreed with the predicted flame geometry and its inability to achieve tip opening. Tip opening, however, could be achieved by using a sub-unity Le fuel stream of hydrogen and carbon dioxide, which caused a general lowering of the flame temperature in the entire flame tip region. Further experimentation then confirmed the theoretical result that negative stretch, in the form of compressive flame curvature, promoted burning and thereby retarded extinction.

Dual Extinction States of Radiation-Affected Flames

Existing understanding of flame extinction is based on the concept of the Damköhler number, Da, defined as the ratio of the characteristic flow time to a characteristic reaction time in the flame. Thus for a steadily-burning flame, decreasing Da reduces the available time for reaction and thereby promotes extinction. The viability of this concept has been extensively demonstrated both theoretically and experimentally. Such an understanding, however, is based on a conservative system in that in the reaction-sheet limit the flame temperature is the adiabatic flame temperature. A combustion system is nevertheless inherently nonadiabatic due to radiative loss from the flame as well as the hot surfaces which may be present in the system.

The subtlety here is that radiative heat loss is a volumetric process and its loss rate frequently increases with increasing system dimension and thereby the flow time. Thus while increasing the system Da allows more time for chemical reaction to proceed, it also leads to more heat loss and therefore reduces the flame temperature. With sufficient reduction in the flame temperature, extinction can conceivably also occur even with the increase in the time available for reaction.

Combining the above considerations, we have theoretically demonstrated that burning can exist only for a range in Da, bounded by a kinetically-controlled Da on the lower limit and a loss-controlled Da on the upper limit. When these two limits coincide, steady burning is not possible.

Theory of Fundamental Flammability Limits

While "flammability limit" has a long and prominent history in the description of combustion phenomena, a clear and unique fundamental definition, which will also allow for its unambiguous theoretical and experimental determination, has yet to be identified. As a consequence, the term "flammability limit" has been widely and loosely applied to diverse situations of unsustainable combustion, many of which represent only limits of flame extinction. Clearly, if flammability limit is indeed a useful fundamental concept, then a combustible fuel/oxidizer system can have only a lean limit and a rich limit, which occur at two distinct concentrations. As such, these two flammability limits should be unique physico-chemical properties of a combustible system, independent of such external influences as conductive and convective heat loss, aerodynamic straining, gravity-related phenomena, etc.

In view of the above considerations, the configuration based on which flammability limit can be usefully defined is the state at which steady propagation of the one-dimensional, planar premixed flame in the doubly-infinite domain fails to be possible. The two omnipresent, system-independent processes which could cause extinction of such a flame are radiative loss and the chain branching and termination reactions in the chemical reaction mechanism. While radiative loss is an obvious extinction mechanism, extinction due to chain reactions can be anticipated from the following consideration. That is, as the flammability limit is approached, the continuous reduction of the flame temperature weakens the temperature-sensitive branching reaction relative to the termination reaction which is in general less temperature sensitive. This causes a slowdown in the overall reaction rate. Eventually the flame can be so weakened that it is extinguished by system perturbations which are invariably present.

In this study the flammability limits of many mixtures were first experimentally determined by measuring the extinction limits of stretched, counterflow flames and extrapolating the results to zero stretch. Extensive determinations were conducted for the lean and rich limits for mixtures of methane, ethane, ethylene, acetylene, and propane with air, and for the effects of dilution, inert substitution, and chemical additives. In the theoretical investigation, the one-dimensional planar flame propagation was first simulated with detailed chemistry and transport, but without radiative heat loss. The sensitivity of the dominant chain termination reaction to the dominant chain branching reaction was continuously monitored as the concentration of the

deficient reactant was reduced. Extinction was assumed to occur when the normalized sensitivity reached unity. The predicted values agreed well with the experimental data. Furthermore, a study of the characteristics of the chain mechanisms for different mixtures also explained some well-known anomalies concerning flammability limits.

In a follow-up investigation, radiative heat loss was included, and the characteristic extinction turning point was obtained. A particularly significant result from this study was that, at the state of the heat-loss induced turning point, the normalized sensitivity of the chain reactions also assumed the unity value. This therefore provides a unified interpretation of the flammability limits based on both the physical process of heat loss and the chemical process of chain termination. That is, as the flammability limit is approached, the overall reaction is weakened due to the increased importance of the chain termination reaction. The heat release rate is eventually reduced to such an extent that radiative heat loss becomes important and leads to flame extinction.

Flame Stabilization and Blowoff

Two contributions were made in this endeavor. First, we have provided a comprehensive review on the fundamental physico-chemical mechanisms governing the structure and stabilization of premixed and diffusion flames in subsonic and supersonic flows. Specific topics discussed included the ignition of combustibles in homogeneous and diffusive media, the extinction of premixed and diffusion flames through reactant leakage, heat loss, and aerodynamic stretching, the stabilization and liftoff of burner-stabilized and rim-stabilized flames, and the various proposed mechanisms for the stabilization and blowout of jet diffusion flames. The fundamental similarities and differences between the various critical phenomena are indicated, and potential research topics suggested.

The second project basically started our research endeavor on the understanding of flame stabilization and blowoff. To appreciate the approach we have undertaken, we first note that the mechanism with which a Bunsen flame is stabilized at the burner rim is generally considered to be well established. The concept is based on the existence of a dynamic balance between the local flow velocity and flame velocity at a certain point on the flame surface, and the ability of the flame to adjust its velocity, and thereby the location of stabilization, through heat loss to the rim. Blowoff occurs when such a balance cannot be achieved everywhere over the flame surface. This mechanism has served as the fundamental concept in flame stabilization in other situations.

In the stabilization mechanism just described, heat loss to the burner rim is the only factor that can modify the flame speed. However, recent studies on the general structure and response of laminar flames have conclusively demonstrated that the burning intensity of the flame can also be significantly modified by the extent of flow nonuniformity, flame wrinkling and unequal molecular diffusivity of the system. The presence of these additional factors offers enhanced flexibility for the flame to achieve stabilization, and significantly enriches the phenomena of flame stabilization and blowoff.

Perhaps the most intriguing question to ask then is whether flame stabilization can be achieved in the absence of heat loss, through the modification of the flame burning intensity by other factors. To explore this possibility, an inverted flame experiment was conducted. Here a thin rod was placed coaxially in a uniform flow of combustible mixture. If the flow velocity was not large, upon ignition an inverted (Bunsen) flame could be established downstream of the trailing edge of the rod. With continuous increase in the flow velocity, the flame would recede from the rod and would be eventually blown off. The extent of heat loss from the flame base to the stabilizing rod was determined by measuring the temperature in the stabilizing region between the flame base and the rod by using both thermocouples and laser Raman spectroscopy.

The results showed that when the flame base was moderately away from the rod, the amount of heat transfer to the rod was essentially negligible. This therefore demonstrated that

flame stabilization could be accomplished through flame stretch and nonequidiffusion effects, in the absence of heat loss. A theory was subsequently formulated based on the dynamic balance between the local flame and flow velocities. The results showed that such a balance could indeed be accomplished.

Future Plans

During the course of this program, we have come to recognize the versatility of studying the response of premixed flames in complex flow fields by treating the flame as a hydrodynamic interface, whose local rates of propagation are affected by the local hydrodynamic states of flow nonuniformity, flame curvature, and flame/flow unsteadiness. For the proposed program we shall therefore focus our study on the dynamics of laminar premixed flames. The study will have the following three major thrusts: (1) The response of a planar flame to aerodynamic straining will be studied in the counterflow configuration. The issues to be addressed are the structure and thickness of the flame when subjected to varying stretch, the effects of heat loss and nonequidiffusion, and the mechanisms of extinction. (2) The behavior of wrinkled flames in simple flow fields which are of relevance to the modeling of turbulent flames through the concept of laminar flamelets. Specifically, we shall study the geometry and the tip opening phenomenon of the Bunsen flame to identify the influence of flame curvature, and the response of the flamelets in spatially-periodic flow fields. (3) Continuation of the present effort in flame stabilization in order to obtain a unified description of the mechanisms of flame stabilization and blowoff.

Journal and Major Publications Resulting from Present Program

1. "Structure and Extinction of Diffusion Flames with Flame Radiation," by B.H. Chao, C.K. Law and J.S. T'ien, *Twenty-Third Symposium (International) on Combustion,* The Combustion Institute, Pittsburgh, PA, pp. 523-531 (1991).
2. "On the Opening of Burke-Schumann Flame Tip and the Effects of Curvature on Diffusion Flame Extinction," by H.G. Im, C.K. Law and R.L. Axelbaum, *Twenty-Third Symposium (International) on Combustion,* The Combustion Institute, Pittsburgh, PA, pp. 551-558 (1991).
3. "A Kinetic Criterion of Flammability Limits: The C-H-O-Inert System," by C.K. Law and F.N. Egolfopoulos, *Twenty-Third Symposium (International) on Combustion,* The Combustion Institute, Pittsburgh, PA, pp. 413-421 (1991).
4. "On Closure in Activation Energy Asymptotics of Premixed Flames," by C.K. Law, B.H. Chao and A. Umemura, *Combustion Science and Technology*, Vol. 88, pp. 59-88 (1992).
5. "Mechanisms of Flame Stabilization in Subsonic and Supersonic Flows," by C.K. Law, *Major Research Topics in Combustion* (Eds.: M.Y. Hussaini, A. Kumar and R.G. Voigt), Springer-Verlag, New York, pp. 201-236 (1992).
6. "On Adiabatic Stabilization of Inverted Flames," by C.J. Sung, C.K. Law and A. Umemura, *Twenty-Fourth Symposium (International) on Combustion*, The Combustion Institute, Pittsburgh, PA, pp. 205-212 (1992).
7. "A Unified Chain-Thermal Theory of Fundamental Flammability Limits," by C.K. Law and F.N. Egolfopoulos, *Twenty-Fourth Symposium (International) on Combustion*, The Combustion Institute, Pittsburgh, PA, pp. 137-144 (1992).
8. "Asymptotic Theory of Flame Extinction with Surface Radiation," by B.H. Chao and C.K. Law, *Combustion and Flame*, Vol. 92, pp. 1-24 (1993).

Molecular Beam Studies of Reaction Dynamics

Yuan T. Lee
Chemical Sciences Division
Lawrence Berkeley Laboratory
Berkeley, California 94720

Scope of Project

The major thrust of this research project is to elucidate detailed dynamics of simple elementary reactions that are theoretically important and to unravel the mechanism of complex chemical reactions or photochemical processes that play important roles in many macroscopic processes. Molecular beams of reactants are used to study individual reactive encounters between molecules or to monitor photodissociation events in a collision-free environment. Most of the information is derived from measurement of the product fragment energy, angular, and state distributions. Recent activities are centered on the mechanisms of elementary chemical reactions involving oxygen atoms with unsaturated hydrocarbons, the dynamics of endothermic substitution reactions, the dependence of the chemical reactivity of electronically excited atoms on the alignment of excited orbitals, the primary photochemical processes of polyatomic molecules, intramolecular energy transfer of chemically activated and locally excited molecules, the energetics of free radicals that are important to combustion processes, the infrared-absorption spectra of carbonium ions and hydrated hydronium ions, and bond-selective photodissociation through electric excitation.

Current Research and Recent Results

A. Primary Dissociation Processes

1. IR spectroscopy of ionic complexes of CH_5^+. Ionic complexes of CH_5^+ have been investigated using infrared spectroscopy based upon vibrational predissociation. We studied $CH_5^+(H_2)$ and $CH_5^+(CH_4)_n$(n = 1,2,3) in the frequency region from 2650 - 4150 cm^{-1} with 0.2 cm^{-1} resolution. In the IR spectra of $CH_5^+(H_2)$, the vibrational bands of the CH_5^+ group have been observed for the first time. They appeared as one broad feature which may indicate the floppy nature of CH_5^+. Also, the H-H stretching band of H_2 in $CH_5^+(H_2)$ appeared as a rotationally resolved feature with line splitting and two anomalously intense peaks. Now we continue to study these features using a higher resolution IR laser in order to get information on the structure and intramolecular dynamics of CH_5^+ as well as $CH_5^+(H_2)$. In the IR spectra of $CH_5^+(CH_4)_n$(n = 1,2,3), a trend in the frequency shifts and changes in intensity of the C-H stretching bands was found as the size of complexes increases from n = 1 to 3. From the trend we were able to get information on the solvation structure and dynamics of CH_5^+ with CH_4.

2. VUV Photochemistry of Small Molecules. Using a new high power VUV excimer laser operating at 157 nm, the photochemistry of CO_2, SO_2, SiH_4, CH_3Cl, CH_3Br and CH_2BrCl was studied via the photofragmentation translational spectroscopy technique.

In CO_2 photolysis an interesting spin-forbidden process was observed, leading to CO + $O(^3P)$ products. The electronic branching ratio $O(^3P)/O(^1D)$ was found to be 0.06. The vibrational branching ratio for the CO(v) + $O(^1D)$ was found to be [CO(v=0)]/[CO(v=1)] = 1.3. In the photolysis of SO_2, a channel leading to S + O_2 products was observed, as well as the expected SO + O channel. The molecules CH_3X (X= Br, Cl) were shown to eliminate H, X and HX upon irradiation at 157nm. In addition, the molecule CH_2BrCl was found to eliminate molecular BrCl.

The photochemistry of SiH_4 is interesting and relevant to the microelectronics industry (i.e. laser chemical vapor deposition of silicon thin films). It was previously thought that SiH_4 decomposes through H atom elimination to form the SiH_3 radical. We have shown, however, that molecular H_2 elimination, forming the $SiH_2(^1A_1)$ diradical is a major channel, thus altering our view of silane photochemistry.

3. Photodissociation Dynamics of ClO_2. The photochemical decomposition of the symmetric chlorine dioxide radical (ClO_2) in the atmosphere is of potential importance in the balance of global ozone. However, there has been considerable uncertainty regarding the excited state dynamics of this molecule. Two chemically distinct photodissociation pathways are thermodynamically possible upon electronic excitation at wavelengths shorter than 496nm:

$$OClO \rightarrow ClO(^2\Pi) + O(^3P) \quad (1)$$

$$\rightarrow Cl(^2P) + O_2(^3\Sigma_g^-, {}^1\Delta_g) \quad (2)$$

Although it has generally been believed that channel (1) dominates, there has been considerable controversy regarding the possible existence of channel (2) since it leads to catalytic decomposition of ozone in the atmosphere. Although a number of groups have attempted to determine Cl atom quantum yields and identify the electronic state(s) of the O_2 molecule, the results have been largely inconclusive. We have studied the dynamics of these processes using photofragment translational energy spectroscopy with a tunable excitation laser and have clearly observed both fragment partners for both channels.

Although the Cl + O_2 channel is relatively minor (<5%), we find that both electronic states of O_2 are formed in the dissociation process with comparable yields. The Cl + O_2 channel results from a concerted unimolecular decomposition with a large fraction of the excess energy channeled into relative translational motion.

The ClO_2 ($A^2A_2 \leftarrow X^2B_1$) absorption spectrum possesses a well defined progression primarily resulting from excitation to the (ν_1,0,0),(ν_1,1,0),(ν_1,0,2), and (ν_1,1,2) levels of the excited electronic state. It is thus possible to prepare the electronically excited molecule in various well defined vibrational levels. We observe a considerable degree of state specificity in the photodissociation dynamics. Excitation of the symmetric bending or symmetric stretching modes of OClO (A^2A_2) leads to Cl + O_2 with a quantum yield of several percent. However, excitation of an asymmetric stretching mode at nearly the same energy leads to <0.4% yield of Cl + O_2. Such mode specificity in branching ratios for chemically distinct products is extremely unusual.

B. Reaction Dynamics

1. Ozone Reactions with Br, Cl Atoms. BrO and ClO radical species play very important roles in the catalytic destruction cycles of ozone in stratosphere. To further understand the mechanisms of these two important reactions, we have carried out the crossed molecular beams studies on these two systems.

Cl + $O_3 \rightarrow$ ClO + O_2 (ΔH° = -39.0 kcal/mole) has been studied at four different collision energies from 6 kcal/mole to 32 kcal/mole. The Cl atomic beam is generated by thermal dissociation of Cl_2 in a high temperature graphite nozzle source. The ClO product angular distribution and time-of-flight (TOF) distribution have been measured at each collision energy. In general, our results show that there is a large translational energy release in products and product ClO is scattered in a wide range of angles. With collision energy increased, ClO lab angular distributions peak more in the forward direction with respect to Cl atom. In the center-of-mass (CM) frame, the translational energy release is large and accounts for 40-60% of the total available energy. Furthermore, the translational energy release is coupled with the center-of-mass angle, the kinetic energy release at the small CM angle is larger than that at the large CM angle. With the increase of the collision energy, the fraction of the total energy channeled into translation is increased and the difference between the fast and slow kinetic energy releases becomes larger as well. The center-of-mass angular distribution is predominantly sideways peaked and moves to more forward direction with the increase of the collision energy. The reaction Cl + O_3 is a direct reaction and the Cl atom is likely to attack the ozone molecule in the coplanar approach. The varied approaches of the Cl atom toward the ozone molecule would lead to a wide range of scattering angles and also the different types of kinetic energy releases.

The semi-empirical calculation by Murrell and co-worker suggested that the ClO product would be mostly forward scattered with respect to the Cl atom when Cl approaches the ozone molecule in a collinear pathway. The translational energy release in the products was predicted to be ~ 50% of the total available energy. Our results

qualitatively agree those from the semi-empirical calculation, however, an *ab initio* calculation on Cl + O_3 system is going to be very helpful.

Br + O_3 → BrO + O_2 (ΔH° = -30.8 kcal/mole) has been investigated at five different collision energies from 5 kcal/mole to 26 kcal/mole. BrO product angular distribution and TOF distribution have been measured at each collision energy. The results from Br + O_3 reaction are very similar to those of Cl + O_3 reaction. There is again a large translational energy release in products peaking away from zero and that product BrO is scattered in a large range of angles. With collision energy increased, BrO lab angular distributions peak more forward with respect to Br atom. Preliminary analysis for this reaction at 18 kcal/mole collision energy shows that the product kinetic energy release is in the range of 35%-50% of the total available energy and it is also dependent on the CM scattering angle. The BrO center-of-mass angular distribution peaks at 65° in the CM frame. It seems that both Br + O_3 reaction and Cl + O_3 reaction are involved with very similar mechanisms.

Ozone reactions with I atom and NO molecule (I + O_3 → IO + O_2 and NO + O_3 → NO_2 + O_2) are also important in atmospheric chemistry and will be carried out accordingly.

2. D + H_2 → DH(v,J) + H Reactive Scattering. Over the past few years we have set up a new crossed molecular beam machine to study rotationally state-resolved differential cross sections for the hydrogen exchange reaction D + H_2 --> DH(v,J) + H. A beam of D atoms is generated by laser photolysis of DI and crossed with a pulsed molecular H_2 beam. DH reaction products are state-specifically ionized a few centimeters downstream from the crossing point using Doppler-free (2+1) Resonance-Enhanced Multi-Photon Ionization (REMPI), and imaged onto a position-sensitive detector. By varying the time delay between the D-atom generation and the DH detection, we can map out the angular distribution of a specific ro-vibrational DH product state.

In the past year we have observed the first state-resolved DH^+ signal which depended on both the operation of the DI and H_2 pulsed jets as well as the operation of both the DI photolysis laser and the DH detection laser, as required for D + H_2 reactive signal. A surprising observation in the experiments has been the occurrence of abundant DH formation believed to be result from collisions of D atoms produced in the DI photolysis volume, with various metal surfaces in the experiment, such as the differential wall between the DI chamber and the H_2 chamber. This source of DH background was not observed in the earlier D + H_2 experiments carried out about five years ago in this group on one of the universal crossed molecular beam machines. Some progress has been made towards reducing this DH background.

The conditions under which the DI and H_2 pulsed molecular beams need to be operated have been tested in detail. For the DI pulsed jet we have determined the optimum pressure and timing conditions that ensure the generation of an intense D-atom beam with a narrow velocity and angular distribution. A range of different H_2 source configurations have allowed us to deplete up to 70% of the D atom beam intensity.

The success of our new D + H_2 experiment relies to a large extent on the detection sensitivity for DH molecules that can be achieved. Using Doppler-free (2+1) REMPI with a counterpropagating ultra-violet laser beam arrangement, we have achieved a detection sensitivity for molecular hydrogen better than 10^4 molecules/cc/quantum state. With this detection sensitivity we anticipate differential cross section measurements with countrates of several ions per lasershot.

3. Cl Atom Reaction with NO_2 Molecule. The endothermic reaction Cl + NO_2 → ClO + NO (ΔH° = 8.6 kcal/mole) is the reaction to connect NO_x and ClO_x groups in atmospheric chemistry. Because $ClNO_2$ is a stable molecule, a collision long-lived complex is expected to form in this reaction. By the unique feature of the crossed molecular beam experiment, collision energies could be adjusted to probe the energy dependence of reaction probability in this endothermic reaction. Threshold region could be well studied by lowing collision energy.

We have studied this reaction at three different collision energies from 2 kcal/mole above the threshold to 15 kcal/mole above the threshold. The ClO product CM angular distributions have the forward-backward type symmetry which clearly confirms that Cl + NO_2 reaction proceeds through a long-lived complex. With the increase of the

collision energy, the forward component in the CM angular distribution is also increased which might demonstrate the transition from a long-lived complex mechanism to a direct reaction with the shortening of the complex lifetime.

Future Plans

A. Primary Dissociation Processes

1. Primary Dissociation of Hydrocarbons by IR Multiphoton Excitation. With the proposed development of a high power IR laser covering 2-5μ, it will be possible to deposit a large amount of energy by multiphoton excitation through C-H or O-H stretching vibration. Primary dissociation of larger hydrocarbons containing 6-10 carbon atoms will be investigated. Of special interest will be the dissociation of various isomers.

2. Investigation of Energy Flow from High Frequency Modes to Low Frequency Modes in Unimolecular Decomposition. The relative efficiencies of energy flow among high frequency modes and low frequency modes can be examined if a molecule can be found which contains two weak chemical bonds of comparable bond dissociation energies and one of the dissociating bonds is coupled strongly to high frequency modes and the other to low frequency modes. $CH_3CH_2OH^+$ satisfies these conditions. This molecule has two dissociation channels forming $CH_3CHOH^+ + H$, and $CH_2OH^+ + CH_3$. These two channels of either H atom or CH_3 radical removal from the central C atom are competitive and require about 20 kcal/mol of energy. If O-H stretching vibration is excited by a direct overtone excitation beyond the dissociation energy level, the branching ratio measured as a function of excitation energy will reveal the nature of energy flow from the high frequency O-H stretching mode. If the energy is indeed first distributed among high frequency modes before flowing into low frequency modes, one would expect a C-H bond rupture to dominate, contrary to the results expected from a statistical theory.

Comparison of the results of this experiment with those of another experiment in which $CH_3CH_2OH^+$ is deposited with the same amount of internal excitation with different initial conditions will be very revealing. We intend to pursue this by selecting the internal energy of $CH_3CH_2OH^+$ by using the ion-electron coincidence technique.

3. H and H_2 Elimination from Hydrocarbon Free Radicals Excited by UV Photons. Understanding the energetics and decomposition pathways of hydrocarbon free radicals is crucial to describing combustion processes. Despite their importance, the dissociation of these species has not been studied extensively using molecular beams. Under the collisionless conditions of the molecular beam elucidation of the primary processes that are a result of the intrinsic dynamics of the dissociation is feasible. The development of molecular beam sources that can generate a high number density of these transient species should allow their detailed study using the technique of photofragment translational spectroscopy. The loss H and H_2 are the major dissociative pathways of simple hydrocarbon free radicals and, therefore, the recent modification of one crossed laser-molecular beam machine to allow detection of the H and H_2 photofragments is an important improvement. The advent of H and H_2 detection to our photodissociation apparatus should not only facilitate the study of these radicals but also allow unambiguous determination of the product branching ratios. Since H and H_2 elimination are the *only* energetically accessible channels, reinvestigation of methyl radical photodissociation at 193 nm is planned as the first system. Propargyl (C_3H_3) radical is one of the simplest conjugated free radicals and is postulated to be important in the formation of aromatic compounds, such as benzene, in flames. The photodissociation of propargyl radical is, therefore, important in understanding the properties of combustion intermediates. Ethyl radical and vinyl radical will also be investigated to determined their dissociative properties.

B. Reaction Dynamics

1. Reaction of CH_3 with Unsaturated Hydrocarbons. Radical addition to unsaturated bonds is the primary mechanism in most chain polymerizations and is also important in the formation of soot in combustion processes. The recent development of a novel molecular beam source, capable of generating an intense number density of methyl radicals, presents the possibility of studying the dynamics of reactions involving CH_3 and unsaturated hydrocarbons. Although the H atom addition to ethylene is more rapid than to acetylene the trend is reversed for

CH_3 addition. This has been attributed to a larger pre-exponential factor for the $CH_3 + C_2H_2$ reaction, offsetting the increase in the activation energy. Ab initio calculations agree qualitatively with these findings and suggest a late activation barrier to both of these reactions. Clearly these important reactions need to be examined under crossed molecular beams conditions to experimentally determine the thermodynamics and activation barriers.

2. Reaction of $O(^1D)$ with Methane and Ethane. The dissociation of O_3 in the throat of a pulse molecular beam source using He as a carried gas is an excellent way to produce an intense pulsed $O(^1D)$ beam. The reactions of $O(^1D)$ with methane and ethane will form highly vibrationally excited methanol and ethanol as reaction intermediates. These intermediates will dissociate by eliminating OH, H, H_2 or H_2O. The highly vibrationally excited methanol and ethanol are also reaction intermediates of the reactions of CH_3 and C_2H_5 with OH. Radical-radical reactions are extremely difficult to pursue in a crossed molecular beams experiment. However, in these cases, the same reaction intermediates can be prepared by the insertion of $O(^1D)$ into C-H bond. When a high power IR laser becomes available it is also possible to investigate the dissociation of methanol and ethanols by the IRMPD approach.

3. Heterogeneous Reaction of Atoms with Solid Surface and Chemisorbed Molecules. In the scattering of H atom with LiF, surprisingly, the formation of HF products were observed. With our new beam surface apparatus, we intend to carry our systematic investigation of reactions of solids with gaseous atoms and radicals. Three types of reactions will be pursued: (1) Reactions of Cl, O and H with graphite; (2) reactions of chemisorbed C_2H_4 on Pt with various atoms; and (3) reaction and decomposition of CH_4 on a metal oxide surface with or without continuous exposure to a stream of O_2 for the understanding of catalytic oxidation of CH_4.

4. Pulse Pyrolysis of Organometallic Transition Metals for Crossed Molecular Beam Studies of Transition Metal Atoms. Because of extremely low vapor pressures, the production of an atomic beam of transition metal from the vapor is extremely difficult. The laser ablation was often used for the production of cold transition metal clusters. However, the intensity is rather limited for carrying out a crossed molecular beams experiment.

A possible alternative way of producing an intensive transition metal atom beam is by the pyrolysis of organometallic compounds during the pulsed supersonic expansion. The heated tube for pulsed beam expansion has to be of sufficient temperature to induce complete dissociation, and even if some of the transition metal atoms are condensed on the heater inner surface during the expansion, it should re-evaporate during the off cycle. A pulsed beam source capable of operating at 3000°C will be needed for this purpose.

Publications

1. A.G. Suits, P. de Pujo, O. Sublemontier, J.-P. Visticot, J. Berlande, T. Gustravsson, J.-M. Mestdagh, P. Meynadier, and Y.T. Lee, The Dynamics of Electronically Inelastic Collisions from 3-Dimensional Doppler Measurements. Phys. Rev. Lett. **67**, 3070-3073 (1991). LBL-30900
2. Albert Stolow, Barbara A. Balko, Evan F. Cromwell, Jingsong Zhang, and Yuan T. Lee, The Dynamics of H_2 Elimination from Ethylene. J. Photochem. Photobiol. **62**, 285-300 (1992). LBL-31009
3. Arthur G. Suits, Hongtao Hou, H. Floyd Davis, and Yuan T. Lee, Reaction Dynamics from Orbital Alignment Dependence and Angular Distributions of Ions Produced in Collision of $Ba(^1P)$ with NO_2 and O_3. J. Chem. Phys. **96**, 2777-2785 (1992). LBL-31260
4. Xingsheng Zhao, Gilbert M. Nathanson, and Yuan T. Lee, Modeling Simulation of Secondary Processes in Photofragment-Translational Spectroscopy. Acta Physico-Chimica Sinica **8**, 70-81 (1992).
5. Anne-Marie Schmoltner, Deon S. Anex, and Yuan T. Lee, IR Multiphoton Dissociation of Anisole: Production and Dissociation of Phenoxy Radical. J. Phys. Chem. **96**, 1236-1240 (1992). LBL-30788
6. H. Floyd Davis, Arthur G. Suits, and Yuan T. Lee, Reactions of Barium Atoms with Triatomic Oxidants. 1: Ba + NO_2. J. Chem. Phys. **96**, 6710-6726 (1992). LBL-31492
7. Marcus J.J. Vrakking, Allan Bracker, and Yuan T. Lee, Comment on Two-Photon Spectroscopy of N_2: Multiphoton Ionization, Laser-Induced Fluorescence, and Direct Absorption via the $a''^1\Sigma_{g^+}$ State. J. Chem. Phys. **96**, 7195-7196 (1992). LBL-31486
8. B.A. Balko, J. Zhang, and Y.T. Lee, Photodissociation of Ethylene at 193 nm. J. Chem. Phys. **97**, 935-942 (1992). LBL-31102

9. Michael H. Covinsky, Arthur G. Suits, H. Floyd Davis, and Yuan T. Lee, The Reaction Dynamics of Sodium with Ozone. J. Chem. Phys. **97**, 2515-2521 (1992). LBL-30555
10. H. Floyd Davis and Yuan T. Lee, Dynamics and Mode Specificity in OClO Photodissociation. J. Phys. Chem. **96**, 5681-5684 (1992). LBL-32189
11. H. Floyd Davis, Arthur G. Suits, and Yuan T. Lee, Reaction Dynamics of Ground State and Electronically Excited Barium Atoms, in **Gas Phase Metal Reactions**, A. Fontijn, ed., Elsevier (1992), pp.319-347. LBL-32009
12. Evan F. Cromwell, Albert Stolow, Marcus J.J. Vrakking, and Yuan T. Lee, Dynamics of Ethylene Photodissociation from Ro-Vibrational and Translational Energy Distributions of H_2 Products. J. Chem. Phys. **97**, 4029-4040 (1992). LBL-32292
13. A.G. Suits, P. de Pujo, O. Sublemontier, J.-P. Visticot, J. Berlande, T. Gustravsson, J.-M. Mestdagh, P. Meynadier, and Y.T. Lee, The Dynamics of Electronic to Vibrational,Rotational and Translational Energy Transfer in Collision of $Ba(^1P_1)$ with Diatomic Molecules. J. Chem. Phys. **97**, 4094-4103 (1992). LBL-32441
14. R.E. Continetti and Yuan T. Lee, Molecular Beam Studies and Hot Atom Chemistry. Handbook of Hot Atom Chemistry, eds., J.P. Adloff, P.O. Gaspar, A.G. Maddock, M. Immamura, T. Matsuura, H. Sano, and K. Yoshihara, Kodansha Ltd. Publishers, Tokyo, Japan (1992) pp.133-155. LBL-29314

SUBMITTED ONLY

1. A.M. Schmoltner, S.Y. Huang, R.J. Brudzynski, P.M. Chu, and Y.T. Lee, Crossed Molecular Beam Study of the Reaction of $O(^3P)$ + Allene. J. Chem. Phys. (submitted) (1992). LBL-27917
2. Doo Wan Boo, John M. Price, and Y.T. Lee, Infrared Spectroscopy of $CH_{5^+}(H_2)$. J. Chem. Phys. (submitted) (1992). LBL-32503
3. Marcus J.J. Vrakking, Yuan T. Lee, Richard D. Gilbert, and Mark S. Child, Resonance-Enhanced One- and Two-Photon Ionization of Water Molecule: Preliminary Analysis by Multichannel Quantum Defect Theory. J. Chem. Phys. (submitted) (1992). LBL-32590
4. L.I. Yeh, Y.T. Lee, and J.T. Hougen, Vibration-Rotation Spectroscopy of the Hydrated Hydronium Ions $H_5O_2^+$ and $H_9O_4^+$. J. Chem. Phys. (submitted) (1992). LBL-32591
5. Albert Stolow and Yuan T. Lee, Photodissociation Dynamics of CO_2 at 157.6 nm by Photofragment-Translational Spectroscopy. J. Chem. Phys. (submitted) (1992). LBL-32651
6. Marcus J.J. Vrakking, Allan S. Bracker, Toshinori Suzuki, and Yuan T. Lee, Ultra-Sensitive Detection of Hydrogen Molecules by (2+1) REMPI. Rev. Sci. Instrum. (in press) (1993). LBL-32881
7. H. Floyd Davis, Bongsoo Kim, Harold S. Johnston, and Yuan T. Lee, The Dissociation Energy and Photochemistry of NO_3. J. Phys. Chem. (in press) (1993).

TIME-RESOLVED FTIR EMISSION STUDIES OF LASER PHOTOFRAGMENTATION AND RADICAL REACTIONS

Stephen R. Leone
Joint Institute for Laboratory Astrophysics and
Department of Chemistry and Biochemistry
University of Colorado
Boulder, Colorado 80309-0440
(303) 492-5128 SRL@JILA.COLORADO.EDU

Time-resolved Fourier transform infrared emission experiments are used to study photofragmentation processes, single collision reactions, energy transfer events, and laser-initiated radical-radical reactions. The apparatus unites a commercial FTIR spectrometer with a high repetition rate excimer laser. Fringes of the He:Ne reference laser are used for the time synchronization of the FTIR as the mirror sweeps. The zero crossings of these fringes are also used to trigger the variable repetition rate laser with a chosen delay time. Following a short delay after the laser pulse, the analog-to-digital converter samples the signal on the infrared detector. Thus emissions from the excited fragments of the photolysis event are recorded with the FTIR at specific time delays after the laser pulse. We also utilize the capability to multiplex time delays after the laser pulse to obtain several sequential time-resolved spectra at once.

A number of technical improvements to the apparatus have been developed over the past year. The variation in the blackbody emission has always been a problem, requiring the subtraction of two spectra (with and without the laser excitation), which have customarily been taken at rather different times. Small variations in the positions of detection elements can lead to large errors during the subtraction. A dual boxcar arrangement has been developed to acquire the blackbody background level of emission before the laser pulse and to subtract this level from the signal + blackbody emission after the laser pulse. This results in a reliable, real time subtraction of the background blackbody flux. One of the largest sources of noise in the experiment is the pulse to pulse fluctuations of the laser. In addition, we have found that the laser amplitude varies in a systematic way following the start of each mirror sweep, giving rise to a monotonic decrease in the laser pulse energy over the course of the mirror sweep. A fast electronic subtraction network has been designed and is being constructed in the shop to normalize the output of the FTIR detector with a signal proportional to the total fluorescence emission intensity. Finally, the phase correction around the zero path difference center burst has also been a continuing source of problems in the time-resolved software mode, because the software only permits data to be taken on the positive side of the center burst. Installation of a small optical flat to phase shift the trigger initiated by the white light source (McWhirter and Sievers, Appl. Spectrosc. 45, 1391 (1991)) allows the infrared interferogram to be taken on both sides of the center burst, and thus our phase correction is now done accurately for every spectrum.

The most recent studies have focused specifically on collision processes, such as single collision energy transfer, reaction dynamics, and radical-radical reactions. We employ the FTIR technique in the study of single collision energy transfer processes using translationally fast H atoms, as well as radical-radical reactions, e.g. $CH_3 + O$, $CF_3 + H(D)$, and $Cl + C_2H_5$. The fast atoms permit unique high energy regions of certain transition states of combustion species to be probed for the first time. A few examples of the results of this work are given below.

Initially, we probed the vibrational and rotational excitation and alignment dynamics in a single collision experiment of 2.2 eV (in the center of mass) H atoms colliding with H_2O. The fast H atoms are produced by photolysis of H_2S and these atoms collide with H_2O in a jet. The water molecules are excited in many vibrational modes by the 2.2 eV H atom, including the symmetric and antisymmetric stretch and two quanta of the bend. In the antisymmetric stretch, there is a dramatic propensity to produce primarily motion about the K_c inertial axis, which is the axis perpendicular to the plane of the water molecule. This K_c motion strictly defines the collision geometry that leads to the antisymmetric stretch excitation. From the observed direction of the rotational angular momentum, the collision that produces the excitation must be constrained to occur approximately in the plane of the water molecule. Two new theoretical studies have confirmed the origin of the high degree of alignment in the collisions of $H + H_2O$. Theoretical work by both George Schatz and David Clary, and their associates, shows that the planar transition state that leads to the reaction to form $OH + H_2$ plays an important role in this dynamics.

Another transition state for $H + H_2O$ may also exist; that is the pyramidal $[H_3O]$ species. The pyramidal state will lead to possible exchange reactions, which can be probed by isotopic substitution, e.g. $H + D_2O \rightarrow D + HOD$. The barrier to this exchange is thought to be quite high; however, the energy of a 2.2 eV H atom is sufficient to probe this surface. In a first series of experiments, we have observed the result of collisions between H (2.2 eV) and D_2O with the FTIR. A strong emission is observed from the D_2O antisymmetric stretch, but in addition, a weak region of emission is directly assignable to the OH stretch of HOD. Further theoretical work was necessary in our group to assign the lines of the HOD species and to characterize the spectrum. The assignment has been completed and new experiments are underway to probe the rotational dynamics resulting from these two different dynamical pathways in $H + D_2O$ collisions.

Experiments continue to be carried out on radical-radical reactions. Previously we characterized the CO(v) product from the $CH_3 + O$ reaction. In a collaboration with Larry Harding, he has calculated all the possible transition states deriving from the CH_3O and CH_2OH species. Thus far the calculations do not find pathways that are favorable to produce CO(v), for example by elimination of H_2 from CH_2OH followed by decomposition of HOC. The pathways do exist, but they are sufficiently high in energy that other pathways might typically be more favored.

The group of Dave Gutman will attempt new studies on this reaction to probe the quantum yields of various products, which will hopefully provide additional insight into this reaction.

The reaction of Cl + C_2H_5 has been studied with a complete analysis of the HCl(v) product distribution as well as the rate coefficient. The excimer laser is used to form an initial high density of Cl atoms and a smaller density of ethyl radicals simultaneously from a variety of precursors. We have studied the time evolution of the HCl product from the addition-elimination process: Cl + $C_2H_5 \rightarrow [C_2H_5Cl] \rightarrow C_2H_4$ + HCl(v). By using two lasers and suitable time delays, we are able to demonstrate that the vibrationally excited HCl is formed by the interaction of Cl with ethyl radicals. Sequences of time-resolved FTIR emission spectra have been acquired, and the risetime of the v=4 state was analyzed to obtain the reaction rate constant for the radical-radical process. The estimated result is $3.0 \pm 1.0 \times 10^{-10}$ cm^3 $molecule^{-1}$ s^{-1}, in good agreement with a previous determination of Kaiser, Rimai, and Wallington (J. Phys. Chem. 93, 4094 (1989)), but in strong contrast to the much slower value of Dobis and Benson (J. Am. Chem. Soc. 112, 1023 (1990), 113, 6377 (1991)). The monotonically decreasing HCl vibrational distribution is characteristic of an addition elimination reaction (v=1/2/3/4 = 0.39±0.04/0.29±0.03/0.22±0.02/0.10±0.02).

Vibrational distributions and the branching ratios between HF and DF for the radical-radical reaction between CF_3CH_2 + D are also in the process of being analyzed. An approximately 3:1 ratio of HF(v) to DF(v) product gives strong indication of the addition-elimination mechanism in this case.

Another future set of studies involves the detailed spectra of the methyl radical, which is being studied following photodissociation of acetone with 193 nm light. The methyl radical shows a number of hot bands in emission, and the project involves a characterization of these higher vibrational bands. We are interested in assigning spectral features and dynamical populations of bands that contain one quanta of the antisymmetric stretch together with one quantum of the out of plane bending vibration. We have also observed a combination band which is in the right frequency range to be due to simultaneous excitation of the antisymmetric stretch and the in plane bending vibration. There is little information of the in-plane bending vibration, and work is continuing on this problem.

List of Publications Supported by this Contract

S. R. Leone, 1991-1993

E. L. Woodbridge, M. N. R. Ashfold, and S. R. Leone, "Photodissociation of ammonia at 193.3 nm: Rovibrational state distribution of the $NH_2(A^2A_1)$ fragment," J. Chem. Phys. 94, 4195 (1991).

C. M. Lovejoy, L. Goldfarb, and S. R. Leone, "Preferential in-plane rotational excitation of H_2O (001) by translational-to-vibrational transfer from 2.2 eV H atoms," J. Chem. Phys. 96, 7180 (1992).

P. W. Seakins and S. R. Leone, "A laser flash photolysis/time resolved FTIR emission study of a new channel in the reaction of CH_3 + O: The production of CO(v)," J. Phys. Chem. 96, 4478 (1992).

P. W. Seakins, E. L. Woodbridge, and S. R. Leone, "A laser flash photolysis, time-resolved Fourier transform infrared emission study of the reaction Cl + $C_2H_5 \rightarrow$ HCl(v) + C_2H_4," J. Phys. Chem. (in press).

SPECTROSCOPY AND REACTION DYNAMICS OF COLLISION COMPLEXES CONTAINING HYDROXYL RADICALS

Marsha I. Lester
Department of Chemistry
University of Pennsylvania
Philadelphia, PA 19104-6323

The DOE supported work in this laboratory has focused on the spectroscopic characterization of the interaction potential between an argon atom and a hydroxyl radical in the ground X $^2\Pi$ and excited A $^2\Sigma^+$ electronic states. The OH-Ar system has proven to be a test case for examining the interaction potential in an open-shell system since it is amenable to experimental investigation and theoretically tractable from first principles.[1] Experimental identification of the bound states supported by the Ar + OH (X $^2\Pi$) and Ar + OH (A $^2\Sigma^+$) potentials makes it feasible to derive realistic potential energy surfaces for these systems. The experimentally derived intermolecular potentials provide a rigorous test of *ab initio* theory and a basis for understanding the dramatically different collision dynamics taking place on the ground and excited electronic state surfaces.

Electronic Spectroscopy Probe of the OH (A $^2\Sigma^+$) + Ar Potential

Previously unobserved intermolecular levels supported by the OH A $^2\Sigma^+$ + Ar potential energy surface have been characterized by laser-induced fluorescence measurements in the OH A-X 0-0 spectral region. The intensities of electronic transitions to these levels are significantly weaker than those of the transitions previously reported. Spectral hole-burning experiments have been conducted to verify that these newly identified features are, in fact, due to excitation of OH-Ar (X $^2\Pi$) from its lowest intermolecular level. Among the newly identified features are transitions to the lowest vibrational level $v_s = 0, v_b = 0$, the excited intermolecular bending level with two quanta of intermolecular stretch $v_s = 2, v_b = 1$, and intermolecular vibrational levels with two quanta of bending excitation ($v_b = 2$).

A comparison of the observed intermolecular levels with the bound states computed for a semi-empirical potential proposed by Bowman *et al.*[2,3] indicated that the potential could be refined to improve the agreement with experimental results. The potential parameters have been adjusted to increase the potential anisotropy by ~2% and the steepness of the radial potential in the O-H-Ar well region by ~3%. The bound states supported by the adjusted potential have been calculated taking into account the electron spin angular momentum of the OH radical.[4] The calculated vibrational energies and rotor constants reproduce to within 1% the rovibrational structure observed experimentally. Neither the semi-empirical potential nor our adjustments to that potential provide a good representation of the intermolecular potential at energies close to the dissociation limit. A theoretical simulation of the OH-Ar electronic excitation spectrum based on the adjusted intermolecular potential yields an intensity pattern which is consistent with experimental results.

The variation of the adjusted potential with OH--Ar separation (R) at fixed angles (θ) is shown in Fig. 1. The adjusted potential exhibits a minimum at a linear O-H--Ar configuration (θ = 0°) with an equilibrium bondlength of 2.8 Å and a well depth of 1061.6 cm^{-1}.

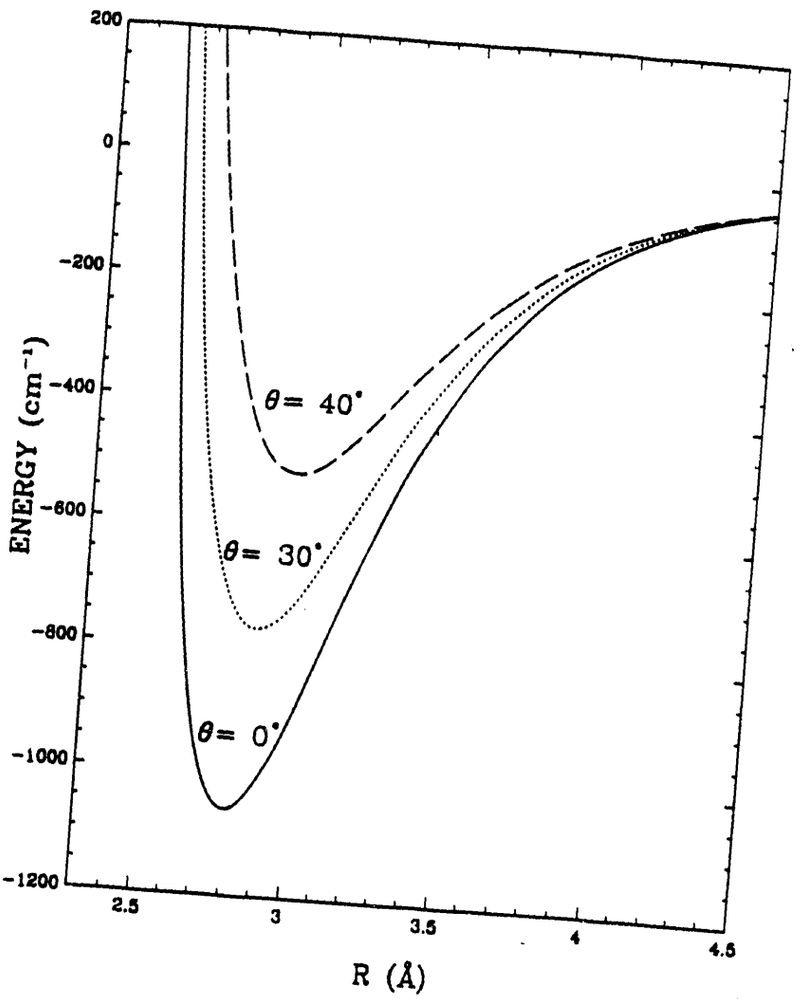

Fig. 1. OH ($A\ ^2\Sigma^+$) + Ar potential in the region of the O-H-Ar well.

Rotational Predissociation of OH-Ar ($A\ ^2\Sigma^+$)

Metastable levels of electronically excited OH-Ar ($A\ ^2\Sigma^+$) which lie as much as 350 cm^{-1} above the first dissociation limit have also been detected by laser-induced fluorescence measurements.[5] A series of OH-Ar features have been identified starting at the OH $A\ ^2\Sigma^+$ (v=0, j=0.5) + Ar dissociation limit and extending beyond the j=4.5 threshold. A similar pattern of features is observed above the OH $A\ ^2\Sigma^+$ (v=1, j=0.5) + Ar asymptote. Hole-burning experiments have confirmed that these fluorescence excitation features are due to transitions originating from the lowest intermolecular level of OH-Ar ($X\ ^2\Pi$). These metastable levels contain internal rotational excitation of OH and a total energy which exceeds the intermolecular binding energy. The excess energy amounts to as much as 50% of the binding energy. Complexes prepared in these levels may predissociate by converting excess OH rotational excitation into relative translational energy of the fragments.

Some of these OH-Ar features exhibit sharp rotational structure with linewidths on the order of 0.1 cm^{-1}, the laser bandwidth, while other features are significantly broadened. The linebroadening indicates that internal rotational predissociation is occurring on a 50 ps timescale or faster. The predissociation lifetimes of the metastable levels correlating with OH $A\ ^2\Sigma^+$ (v=0) are substantially shorter than the corresponding features associated with OH $A\ ^2\Sigma^+$ (v=1). The linewidths do not appear to vary systematically with excess energy above the dissociation thresholds.

The internal state distributions of the OH A $^2\Sigma^+$ photofragments produced upon rotational predissociation of OH-Ar (A $^2\Sigma^+$) have been evaluated for many of the metastable levels. In these experiments, a second tunable dye laser is introduced to stimulate downward transitions on OH A $^2\Sigma^+$ - X $^2\Pi$ transitions. When this laser is resonant with a transition originating from an OH A $^2\Sigma^+$ rovibrational level populated in the predissociation process, the spontaneous fluorescence emanating from the OH A $^2\Sigma^+$ photofragments is depleted. The resultant fluorescence depletion spectrum yields the nascent rotational-vibrational distribution of the OH A $^2\Sigma^+$ fragments. Initial results indicate a high degree of selectivity in the OH A $^2\Sigma^+$ product rotational distribution.

Rotational predissociation is induced by the anisotropy of the interaction potential which couples states with different OH angular momenta. Therefore, experimental measurements of rotational predissociation will enable characterization of the short-range anisotropy of the OH A $^2\Sigma^+$ + Ar potential. Towards this end, the energies and wavefunctions of the predissociative levels derived from an *ab initio* potential[1] for OH A $^2\Sigma^+$ + Ar are being computed variationally for comparison with experimental results. A flux projection technique[6] is used to identify the predissociative states as well as to determine their lifetimes.[7] The predissociation dynamics of these metastable levels will also yield new insight into rotationally inelastic collisions between Ar and OH A $^2\Sigma^+$ (v=0, 1) at energies from 0 to 350 cm^{-1}.

Future Plans

Future experiments will examine the intermolecular interactions of hydroxyl radicals on reactive potential energy surfaces, specifically between hydroxyl radicals and molecular hydrogen. The OH and H_2 molecules will be aggregated in a binary complex that is stabilized in a shallow well below the activation barrier to reaction. The OH-H_2 complexes will be excited in the vicinity of the OH A $^2\Sigma^+$ - X $^2\Pi$ transition to probe the intermolecular vibrational levels supported by the OH A $^2\Sigma^+$ + H_2 potential. The intermolecular stretching and bending levels will access a range of distances and orientations, providing a global picture of the intermolecular potential energy surface. Both laser-induced fluorescence and direct absorption methods will be utilized to locate crossings in the intermolecular potential energy surfaces which are responsible for collision-induced quenching.

References

1. A. Degli-Esposti and H.-J. Werner, *J. Chem. Phys.* **93**, 3351 (1990).

2. J. M. Bowman, B. Gazdy, P. Schafer, and M. C. Heaven, *J. Phys. Chem.* **94**, 2226 (1990); **94**, 8858E (1990).

3. Y. Guan and J. T. Muckerman, *J. Phys. Chem.* **95**, 8293 (1991).

4. C. Chakravarty, D. C. Clary, A. Degli-Esposti, and H.-J. Werner, *J. Chem. Phys.* **93**, 3367 (1990).

5. R. W. Randall, L. C. Giancarlo, and M. I. Lester, work in progress.

6. S. E. Choi and J. C. Light, *J. Chem. Phys.* **92**, 2129 (1990).

7. S. E. Choi and M. I. Lester, work in progress.

DOE Supported Publications
1991 - 1993

1. M. T. Berry, M. R. Brustein, M. I. Lester, C. Chakravarty, and D. C. Clary, "Stimulated Emission Pumping of van der Waals Vibrations in the Ground Electronic State of OH-Ar", *Chem. Phys. Lett.* **178**, 301-310 (1991).

2. W. H. Green, Jr. and M. I. Lester, "A Perturbation Theory Guide to Open-Shell Complexes: OH-Ar ($X\ ^2\Pi$)", *J. Chem. Phys.* **96**, 2573-2584 (1992).

3. M. T. Berry, R. A. Loomis, L. C. Giancarlo, and M. I. Lester, "Stimulated Emission Pumping of Intermolecular Vibrations in OH-Ar ($X\ ^2\Pi$)", *J. Chem. Phys.* **96**, 7890-7903 (1992).

4. M. I. Lester, R. A. Loomis, L. C. Giancarlo, M. T. Berry, C. Chakravarty, and D. C. Clary, "Refinement of the OH $A\ ^2\Sigma^+$ (v=0) + Ar Intermolecular Potential Energy Surface", *J. Chem. Phys.* **98**, xxxx (1993).

5. M. I. Lester, W. H. Green, Jr., C. Chakravarty, and D. C. Clary, "Stimulated Emission Pumping as a Probe of the OH ($X\ ^2\Pi$) + Ar Intermolecular Potential Energy Surface", to appear in *Molecular Dynamics and Spectroscopy by Stimulated Emission Pumping*, H.-L. Dai and R. W. Field, Eds. (World Scientific, 1993).

6. M. I. Lester, S. E. Choi, and R. W. Randall, "Intermolecular Vibrations and Predissociative Resonances in Open-Shell Complexes", to appear in SPIE Proceedings on Laser Techniques for State-Selected and State-to-State Chemistry, C.-Y. Ng, Ed. (1993).

Theoretical Studies of Molecular Interactions

William A. Lester, Jr.

Chemical Sciences Division, Lawrence Berkeley
Laboratory and Department of Chemistry
University of California, Berkeley, California 94720

Scope of Project

This research program is directed at extending fundamental knowledge of atoms and molecules including their electronic structure, mutual interaction, collision dynamics, and interaction with radiation. The approach combines the use *ab initio* methods--Hartree-Fock (HF) multiconfiguration HF, configuration interaction, and the recently developed quantum Monte Carlo (QMC)--to describe electronic structure, intermolecular interactions, and other properties, with various methods of characterizing inelastic and reaction collision processes, and photodissociation dynamics. Present activity is focused on the development and application of the QMC method, surface catalyzed reactions, and reorientation cross sections.

Recent Progress

Correlated Sampling of Monte Carlo Derivatives with Iterative-Fixed Sampling

A correlated sampling method for determining the energy and other property derivatives by finite difference has been implemented within variational Monte Carlo. Determination of derivatives takes place over a fixed sample of electronic coordinates, so it is possible to distinguish small energy or other property differences accurately. Using finite differences avoids the evaluation of complicated derivative expressions and can be applied directly to Green's function Monte Carlo methods without the need for derivatives of the Green's function. The algorithm can be used to evaluate derivatives with respect to any parameters in the Hamiltonian or in the trial function. It has been applied to H_2 and Li_2 for their energy derivatives with respect to nuclear coordinates. Results are in agreement with experimental data.

Random-Walk Approach to Mapping Nodal Regions of N-Body Wave functions: Ground-State Hartree-Fock Wave functions for Li-C

Despite the widespread acceptance of the relevance of the nodes of one-body electronic wave function (atomic and molecular orbitals) in determining chemical properties, relatively little is known about the corresponding nodes of many-body wave functions. As an alternative to

mapping the nodal surfaces presents in the ground states of many-electron systems, we have focused instead on the structural domains implied by these surfaces. In the spirit of Monte Carlo techniques, the nodal hypervolumes of a series of atomic N-body Hartree-Fock level electronic wave functions have been mapped using a random-walk simulation in 3N dimensional configuration space. The basic structural elements of the domain of atomic or molecular wave functions are identified as nodal regions (continuous volumes of the same sign) and permutational cells (identical building blocks). Our algorithm determines both the relationships among nodal regions or cells (topology) as well as the geometric properties within each structural domain. Our results indicate that ground-state Hartree-Fock wave functions generally consist of four equivalent nodal regions (two positive and two negative), each constructed from one or more permutational cells. We have developed an operational method to distinguish otherwise identical permutational cells.

A Quantum-Mechanical Model of Heterogeneous Catalysis

A quantum-mechanical model for heterogeneous catalytic reactions has been developed based on the reaction Hamiltonian method developed by the authors.[1,2] It has been shown that the presence of the surface leads to additional channels of reaction. These are found to dominated the exponential smallness of the reaction probability of the direct channel producing large reaction probabilities for surface-catalyzed reactions. The dependence of catalytic reaction probability on reactant dissociation energy and vibrational frequencies, and the leakage of the electronic wave function out of the surface is described by the approach.

[1]V. Z. Kresin and W. A. Lester, Jr., Chem. Phys. **90**, 335 (1984).
[2]C. E. Dateo, V. Z. Kresin, M. Dupuis, and W. A. Lester, Jr., J. Chem. Phys. **86**, 2639 (1987).

Future Plans

Quantum Monte Carlo Study of the Energetics of CH-Containing Systems

Hydrocarbons provide a plethora of interesting chemical questions. To make possible QMC studies of the most interesting issues, the subject effort continues which draws on the broad range of recently developed QMC methodologies. Systems being studies in the present effort are CH, C_2H, and C_2H_2, as well as C_2. The primary effort uses the fixed-node short-time approximation QMC approach with optimized trial functions.

Reorientation Cross Sections of $He(^1S) + H_2(B\ ^1\Sigma_u^+)$

Reorientation cross sections are being computed for the $He(^1S) + H_2(B\ ^1\Sigma_u^+)$ system using a potential energy surface and following

a model previously introduced for rovibrational energy transfer. The model consists of restricting the scattering solely to the excited state potential energy surface and the use of the coupled-channel method. This study has been undertaken to complement experiments of C. B. Moore and collaborators.

DOE Supported Publications 1991-93

1. A. C. Pavao, M. Braga, C. A. Taft, B. L. Hammond, and W. A. Lester, Jr., "Theoretical Study of the CO Interaction with 3d Metal Surface," Phys. Rev. B 43, 6962 (1991).

2. P. Pernot and W. A. Lester, Jr., "Quantum Time-Dependent Treatment of Molecular Collisions: Scattering of He by $He(^1S) + H_2(B\ ^1\Sigma_u^+)$," Comput. Phys. Comm. 63, 259 (1991).

3. P. Pernot and W. A. Lester, Jr., "Multidimensional Wave-Packet Analysis: Splitting Method for Time-Resolved Property Determination," Int. J. Quan. Chem. 40, 577 (1991).

4. A. C. Pavao, M. Braga, C. A. Taft, B. L. Hammond, and W. A. Lester, Jr., "Theoretical Study of the CO Interaction with the Fe(100) Surface," Phys. Rev. B 44, 1910 (1991).

5. B. L. Hammond, M. M. Soto, R. N. Barnett, and W. A. Lester, Jr., "On Quantum Monte Carlo for the Electronic Structure of Molecules," Molec. Struct. (Theochem) 234, 525 (1991).

6. R. N. Barnett, P. J. Reynolds, and W. A. Lester, Jr., "Monte Carlo Algorithms for Expectation Values of Coordinate Operators," J. Comput. Phys. 96, 258 (1991).

7. R. N. Barnett, P. J. Reynolds, and W. A. Lester, Jr., "Computation of Transition Dipole Moments by Monte Carlo," J. Chem. Phys. 96, 2141 (1992).

8 Z. Sun, R. N. Barnett, and W. A. Lester, Jr., "Optimization of a Multideterminant Wave Function for Quantum Monte Carlo," J. Chem. Phys. 96, 2422 (1992).

9. J. S. Francisco, Y. Zhao, W. A. Lester, Jr., and I. H. Williams, "Theoretical Studies of the Structure and Thermochemistry of FO_2 Radical: Comparison of Moller-Plesset Perturbation, Complete-Active-Space Self-Consistent-Field, and Quadratic Configuration Interactions Methods," J. Chem. Phys. 96, 2861 (1992).

10. R. N. Barnett, P. J. Reynolds, and W. A. Lester, Jr., "Monte Carlo Determination of the Oscillator Strength and Excited State Lifetime for the Li $2^2S \rightarrow 2^2P$ Transition," Int. J. Quantum Chem. 42, 837 (1992).

11. Z. Sun, R. N. Barnett, and W. A. Lester, Jr., "Quantum and Variational Monte Carlo Interaction Potentials for $Li_2(X\,^1\Sigma_g^+)$," Chem. Phys. Letters 195, 365 (1992).

12. V. Z. Kresin and W. A. Lester, Jr., "A Quantum Mechanical Model of Heterogeneous Catalysis," Chem. Phys. Letters 197, 1 (1992).

13. Z. Sun, W. A. Lester, Jr., and B. L. Hammond, "Correlated Sampling of Monte Carlo Derivatives with Iterative-Fixed Sampling," J. Chem. Phys. 97, 7585 (1992).

14. W. A. Glauser, W. R. Brown, W. A. Lester, Jr., D. Bressanini, B. L. Hammond, and M. L. Kosykowski, "Random-Walk Approach to Mapping Nodal Regions of N-body Wave functions: Ground-state Hartree-Fock Wave functions for Li-C," J. Chem. Phys. 97, 9200 (1992).

15. J. W. de M. Carneiro, P. R. Seidl, J. G. R. Tostes, Ca. A. Taft, B. L. Hammond, M. M. Soto, and W. A. Lester, Jr., "The Effects of One Pairs on Charge Distribution in the Tetracyclic Norbornyl Derivatives," Chem. Phys. Lett. 202, 278 (1993).

ABSTRACT

Quantum Dynamics of Fast Chemical Reactions
DE-FG02-87ER13679

John C. Light
James Franck Institute and
Department of Chemistry
University of Chicago
Chicago IL 60637

The aims of this research are to explore, develop, and apply theoretical methods for the evaluation of the dynamics of gas phase collision processes, primarily chemical reactions. The primary theoretical tools developed for this work have been quantum scattering theory, both in time dependent and time independent forms. Over the past several years, we have developed and applied methods for the direct quantum evaluation of thermal rate constants, applying these to the evaluation of the hydrogen isotopic exchange reactions,[1,2] applied wave packet propagation techniques to the dissociation of Rydberg H_3^*, incorporated optical potentials into the evaluation of thermal rate constants,[4] evaluated the use of optical potentials for state-to-state reaction probability evaluations,[5] and, most recently, have developed quantum approaches for electronically non-adiabatic reactions which may be applied to simplify calculations of reactive, but electronically adiabatic systems.[6] Evaluation of the thermal rate constants and the dissociation of H_3^* were reported last year, and have now been published. We thus focus on activities since that time.

Although we intend to continue the evaluation of thermal rate constants via the thermal flux-flux correlation method introduced by Miller,[7] using a representation in the Discrete Variable Representation (DVR)[8,9] and sequential diagonalization/truncation to evaluate the eigenvalues and eigenfunctions of the Hamiltonian in the transition state region,[10] we hope first to incorporate substantial improvements. In particular since the other systems of interest such as the (OOH), (HOCO), (HCO) and even (HOH) systems are substantially heavier and have much higher density of states than the H_3 isotopic systems, substantial improvements are required before such studies can be carried out easily. We want, in addition, to have methods of evaluation of state-to-state rate constants and cross sections which can be applied to these more complex systems.

The use of optical potentials (imaginary absorbing potentials) in quantum scattering calculations for chemical reactions was pioneered by Neuhauser, Baer and co-workers.[11] Their use holds the potential for substantially reducing the coordinate range over which the accurate solutions of the Schrodinger equation is required, particularly for methods such as the flux-flux correlation function method which rely on a "partitioning" into reactive and non-reactive components of a thermal wave packet. We tested this idea on the collinear $H + H_2$ reaction and found that with suitable choice of range and optical potential we could, in fact, reduce the computation required in order to achieve accurate rate constants.[4] In addition, the use of optical potentials permits the time integrals required in the

autocorrelation method for k(T) to be evaluated to the proper $t \rightarrow \infty$ limit which improves the robustness of calculation. Innovations required for the approach to be useful require the tailoring of the optical potential to the temperature range of interest and the addition of the optical potential to the sequential diagonalization procedure only in the latter stages.

A second use of the optical potentials was also investigated for state-to-state reactive scattering. The formal properties of optical potentials are such that a number of rather simple, but different, looking expressions for the S-matrix are formally correct.[5] We investigated both the accuracy and efficiency of several of these expressions, again using the collinear H + H_2 exchange reaction as the test case. We developed a new procedure for fitting the S-matrix from the wave function (evaluated in the interaction and near asymptotic region only using the optical potential) which includes estimates of possible errors due to inadequacies of the optical potential. In addition the problem of most treatments, that at each energy matrix elements of potential between the initial state and the internal L^2 basis are required, is eliminated, although with some small loss in accuracy. Although these developments are encouraging, an alternative method developed under an NSF grant to look at resonances lifetimes can be adapted to reactive scattering and appears far superior.[12] This Finite Region Wave Function (FRSW) method will not be described here, but it requires only the evaluation of the full real Green's function in a finite discrete spectral representation, and requires no energy dependent integrals for the evaluation of the K-matrix or S-matrix, just the summation over the spectral representation. This approach is related to the Kohn variational log derivative method presented by Manolopoulos and Wyatt[13] a few years ago, but not used since. We intend to incorporate this method in the non-adiabatic reactive scattering calculations to be discussed next.

A major problem in reactive scattering on a single adiabatic electronic energy surface is the fact that the different coordinate systems are required to describe the nuclear motions of reactants and products efficiently. Neither coordinate system may be optimal for representing the strong interaction region. Resolutions of this problem to date require the use of non-orthogonal coordinate systems or energy dependent projections onto functions in the appropriate asymptotic coordinates. One project in our recent proposal was to finesse this problem by defining separate orthogonal reactant and product diabatic electronic potential energy surfaces, with appropriate coupling at each point to yield the desired ground adiabatic electronic potential surface. Because of the orthogonality of the electronic surfaces, different nuclear coordinate systems and bases may be used for each, the Hamiltonians for reactants and products can first be diagonalized separately, and finally the coupling between electronic surfaces can be introduced and the full Hamiltonian diagonalized to yield the spectral representation of the full Green's function. Now the surface projections of the asymptotic reactant and product nuclear states can be performed separately and simply using appropriate coordinates for each. Using the FRSW method, no energy dependent integrals are required in order to evaluate the K-matrix or S-matrix, only evaluation of the asymptotic translational functions on a surface.

This approach is being implemented, and results for the 1-D Eckhart barrier are shown below.[6] In Figure 1 the two diabatic surfaces, the interaction, and the desired resulting adiabatic Eckhart barrier are shown. In Figure 2 we compare the results of the two surfaces "non-adiabatic" approach with the analytic results for the one surface adiabatic problem. Agreement is sufficiently good to warrant the extension of the approach to collinear and 3-dimensional systems, which is in progress. Obviously the approach can also be used for systems in which electronically non-adiabatic transitions can occur.

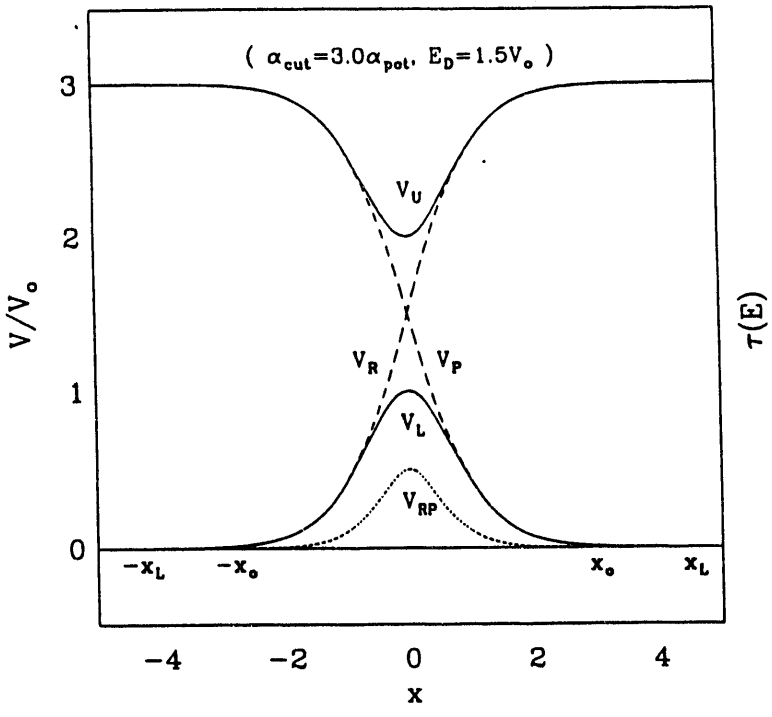

Fig. 1: V_L is the (adiabatic) Eckhart barrier; V_R, V_P, and V_{RP} are the reactant, product, and coupling potentials which yield V_L, V_U.

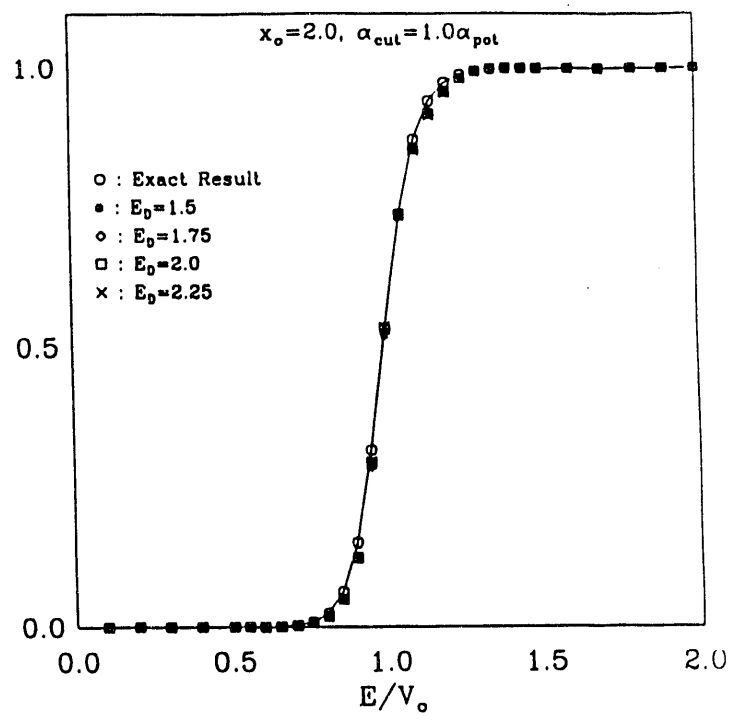

Fig. 2: Transmission probability as a function of E for $2E_D = V_L + V_U$ compared with analytic result for V_D alone.

Finally, we have investigated the comparative efficiency of time dependent wave packet methods and time independent L^2 diagonalization methods for state-to-state reactive scattering. Even though one time dependent calculation for a given initial state nominally gives a column of the S-matrix at many energies, the propagation time and the time involved in extracting the final state information seem to be substantially larger than the time required for evaluation at many energies by diagonalization of an L^2 basis and then extracting the S-matrix using the Kohn variational approach or, probably even better, by the FRSW method.[12] The conclusions of these studies are that the generation of the full real discrete Green's function in the non-adiabatic approach, together with the extraction of the K-matrix via the FRSW or Kohn variational log derivative methods will provide an approach which is substantially superior to those in current use (at least this is our expectation). Utilization of these and related techniques should also be possible for the evaluation of microcanonical or thermal rate constants, and should permit the larger and heavier systems of substantial combustion interest to be studied.

References

1) T.J. Park and J.C. Light, J. Chem. Phys. **94**, 2946 (1991).
2) Tae Jun Park and J.C. Light, J. Chem. Phys. **96**, 8853 (1992).
3) Jeffrey L. Krause, Anne, E. Orel, Kenneth C. Kulander and John C. Light, J. Chem. Phys. **96**, 4283 (1992).
4) D. Brown and J.C. Light, J. Chem. Phys. **97**, 5465 (1992).
5) Time-Independent Reactive Scattering with Absorbing Potentials, D. Neuhauser and J.C. Light, J. Chem. Phys., (submitted).
6) S. Shin and J.C. Light, in progress.
7) W.H. Miller, S.D. Schwartz and J.W. Tromp, J. Chem. Phys. **79**, 4889 (1983); W.H. Miller, J. Chem. Phys. **61**, 1823 (1974).
8) J.V. Lill, G.A. Parker and J.C. Light, Chem. Phys. Lett. **89**, 483 (1982).
9) Discrete Variable Representations in Quantum Dynamics, John C. Light, Proceedings of NATO ARW 019/92 in *Time Dependent Quantum Molecular Dynamics: Experiments and Theory*, J. Broeckhove, ed., (PLenum, NY 1992) (in press).
10) Quantum Dynamics of Small Systems Using Discrete Variable Representations, J.C. Light, R.M. Whitnell, T.J. Park and S.E. Choi, in *Supercomputer Algorithms for Reactive Dynamics and Kinetics of Small Molecules*, A. Lagana, Ed., NATO ASI Series C, Vol. 277 (Kluwer, Dortdrecht, 1989) pp. 187-214.
11) D. Neuhauser and M. Baer, J. Chem. Phys. **90**, 4351 (1989); ibid, **92**, 3419 (1990); D. Neuhauser, J. Chem. Phys. **95**, 4927 (1991).
12) Finite Range Scattering Wave Function Method for Scattering and Resonance Lifetime, Hyo Weon Jang and John C. Light, J. Chem. Phys. (submitted).
13) D.E. Manolopoulos and R.E. Wyatt, Chem. Phys. Lett. **152**, 23 (1988); ibid, **159**, 123 (1988); D.E. Manolopoulos, M.D'Mello and R.E. Wyatt, J. Chem. Phys. **91**, 6096 (1989); ibid. **93**, 403 (1990).

Publications Under DOE Grant (1991-1993)

1. Quantum Thermal Rate Constants for the Exchange Reactions of Hydrogen Isotopes: D + H_2, T.J. Park and J.C. Light, J. Chem. Phys. **94**, 2946 (1991).
2. Quantum Mechanical Calculations of the Dissociation of H_2, Rydberg States, Jeffrey L. Krause, Anne E. Orel, Kenneth C. Kulander and John C. Light, J. Chem. Phys. **96**, 4283 (1992).
3. Quantum Calculation of Thermal Rate Constants for H + D_2 Reaction, Tae Jun Park and J.C. Light, J. Chem. Phys. **96**, 8853 (1992).
4. Discrete Variable Representations in Quantum Dynamics, John C. Light, Proceedings of NATO ARW 019/92 in *Time Dependent Quantum Molecular Dynamics: Experiments and Theory*, J. Broeckhove, ed., (PLenum, NY 1992) (in press).
5. Evaluation of Thermal Rate Constants in the Eigenbasis of a Hamiltonian with an Optical Potential, D. Brown and J.C. Light, J. Chem. Phys. **97**, 5465 (1992).
6. Finite Range Scattering Wave Function Method for Scattering and Resonance Lifetimes, Hyo Weon Jang and John C. Light, J. Chem. Phys. (in press).

Kinetics and Mechanisms of Reactions Involving Small Aromatic Reactive Intermediates

M. C. Lin
Department of Chemistry
Emory University
Atlanta, GA 30322

I. Program Scope

Small aromatic radicals such as C_6H_5, C_6H_5O and C_6H_4 are key prototype species of their homologs. C_6H_5 and its oxidation product, C_6H_5O are believed to be important intermediates which play a pivotal role in hydrocarbon combustion, particularly with regard to soot formation.[1]

Despite their fundamental importance, experimental data on the reaction mechanisms and reactivities of these species are very limited. For C_6H_5, most kinetic data except its reactions with NO and NO_2, were obtained by relative rate measurements.[2-4] For C_6H_5O, we have earlier measured its fragmentation reaction producing C_5H_5 + CO in shock waves.[5] For C_6H_4, the only rate constant measured in the gas phase is its recombination rate at room temperature by Porter and Steinfeld.[6]

We have proposed to investigate systematically the kinetics and mechanisms of this important class of molecules using two parallel laser diagnostic techniques--laser resonance absorption (LRA) and resonance enhanced multiphoton ionization mass spectrometry (REMPI/MS). In the past two years, our study has been focused on the development of a new multipass adsorption technique[7,8]--the "cavity-ring-down" technique for kinetic applications. The preliminary results of this study appear to be quite good and the sensitivity of the technique is at least comparable to that of the laser-induced fluorescence method.[9,10]

II. Recent Progress

A. C_6H_5 Kinetic Measurements by the LRA Method

(1) The "cavity-ring-down" method

For the kinetic study, two lasers were employed sequentially. The first (KrF) laser operating at 248 nm was used for the production of the C_6H_5 radical. The photolysis laser was introduced into the system through three quartz ports perpendicular to the axis of the flow-tube reactor. The second tunable pulsed laser was introduced into the system to probe the radical along the axis of the flow reactor, which was vacuum-sealed with a pair of custom-made, highly reflective mirrors .

Similar to O'Keefe's spectroscopic studies,[7,8] our kinetic measurements were carried out by determining the photon lifetime of the probing pulse injected into the cavity through one of the mirrors. The photon decay time measured with a photomultiplier behind the second mirror can be described by the equation,[9]

$$-d\Phi/dt = \Phi\,(\alpha c l/nL + 1/t_c^{o}) \qquad (1)$$

where Φ is the number of photons injected into the cavity, t_c^o is the photon decay time in the absence of absorbing species (whose presence shortens the decay time), l is the length of the absorbing medium, L is the cavity length formed by the two mirrors, n is the index of refraction of the absorbing medium, c is the velocity of light and α is the absorption coefficient. Integration of eq. (1) gives rise to

$$\Phi = \Phi_o \exp(-t/t_c) \qquad (2)$$

where $$1/t_c = \alpha cl/nL + 1/t_c^o \text{ or } 1/t_c - 1/t_c^o = \alpha cl/nL \qquad (3)$$

In eq. (3), the absorption coefficient α, which is the product of the extinction coefficient (ε) and the concentration of the absorbing species of interest, $[A]_{t'}$, at t' after the firing of the photodissociation laser. The photolysis laser generates an initial concentration of the absorbing species, $[A]_o$, which decays exponentially in the presence of an excess amount of a molecular reactant. Thus, eq. (3) can be written as

$$1/t_c - 1/t_c^o = (cl\varepsilon/nL)\, A_o \exp(-k^I t')$$

or $$\ln(1/t_c - 1/t_c^o) = B - k^I t' \qquad (4)$$

where $B = \ln(cl\varepsilon [A]_o/nL)$ and k^I is the pseudo-first-order decay constant of the reactive species (C_6H_5). The slope of a plot of k^I vs. molecular reagent concentration gives the second order rate constant, k^{II}. In Table I we summarize the second-order rate constants measured at room temperature for several selected C_6H_5 reactions.

Some of the reactions studied here have been investigated recently by Preidel and Zellner[11] at low temperatures using the conventional multipass absorption technique and by Stein and coworkers[3,4] using the relative rate method for temperatures above 1000 K (see Table I).

(2) Temperature-dependence studies

The effects of temperature on five reactions have been studied at temperatures between 297 and 520 K. These reactions include NO, C_2H_2, i - C_4H_{10}, c -C_5H_{10} and c -C_6H_{12}. The Arrhenius parameters for these reactions are summarized in Table II. The activation energies of the five reactions vary from -0.7 kcal/mole for the association of C_6H_5 with NO to 5.7 kcal/mole for the abstraction of the H atom from i-C_4H_{10}. For the latter process, the result of Trotman-Dickenson and coworkers[2] agrees reasonably well with the present result given in Table II.

(B) Surface Photochemistry of C_6H_5NO and REMPI Characterization of Desorbed Photofragments

In order to characterize the REMPI spectroscopy of the phenyl radical, we have investigated the production of the radical from the photo-fragmentation of C_6H_5NO adsorbed on z-cut single crystal quartz and single crystal sapphire (1120) surfaces. The photo-fragmentation patterns of C_6H_5NO on these two surfaces at 193 and 248

nm are similar. The appearance sequence of fragment ions in the detector (mass spectrometer) is approximately: $NO^+ < C_4H_2^+ < C_6H_4^+ < C_4H_3^+ < C_6H_5^+ \equiv C_6H_6^+ \equiv C_6H_5NO^+$. This suggests that there is a significant photo-fragmentation of C_6H_5NO and that C_6H_4, which is likely a precursor of C_4H_2, was produced in the reaction.

Since NO was the first to arrive at the mass spectrometer, it can be cleanly ionized by by (1+1) REMPI via the $A^2\Sigma^+$ state without complication. Such an analysis carried out at 90 μsec and 180 μsec after photoinitiation gave rise to a rotational temperature of 550 K and 430 K, respectively. The final result from this study will be soon submitted for report and publication.

III. Future Plans

Our major emphasis next year will be on kinetic measurements for phenyl reactions with prototype alkanes, alkenes, alkynes and small aromatic molecules over a wide range of temperature and pressure accessible with the present technique. The measured kinetic data will be interpreted in terms of statistical theories.

VI. References

1. I. Glassman, Combustion, 2nd Ed., Academic Press, 1987.
2. J. A. Kerr and S. J. Moss, Handbook of Bimolecular Reactions, CRC Press, Boca Raton, FL., 1981.
3. A. Fahr, W. G. Mallard and S. E. Stein, 21st Symp. (Int.) on Combustion, p. 825, 1986.
4. A. Fahr and S. E. Stein, 22nd Symp. (Int.) on Combustion, p. 1023, 1988.
5. C.-Y. Lin and M. C. Lin, J. Phys. Chem. 90, 425 (1986).
6. G. Porter and J. Steinfeld, J. Chem. Soc., (A) 877 (1968).
7. A. O'Keefe and D. A. G. Deacon, Rev. Sci. Instrum., 59, 2544 (1988).
8. A. O'Keefe, J. J. Scherer, A. L. Cooksy, J. Heath and R. I. Saykally, Chem. Phys. Lett. 172, 214 (1990).
9. T. Yu and M. C. Lin, J. Am. Chem. Soc., accepted.
10. M. C. Lin and T. Yu, Int. J. Chem. Kinet., submitted.
11. M. Preidel and R. Zellner, Ber. Bunsenges. Phys. Chem. 93, 1417 (1989).

DOE (1991-present) Publications:

1. "Effects of NO on the thermal decomposition of CH_3ONO: overall kinetics and rate constants for the HNO + HNO and HNO + 2NO reactions," Y. He and M. C. Lin, Int. J. Chem. Kinet., **24**, 743 (1992).

2. "Kinetics of phenyl radical reactions studied by the cavity-ring-down method," T. Yu and M. C. Lin, J. Am. Chem. Soc., accepted.

3. "Kinetics of C_6H_5 reaction with HBr," M. C. Lin and T. Yu, Int. J. Chem. Kinet., submitted.

Table I. Rate Constants (in Units of cm^3/s) for C_6H_5 Reactions with Selected Molecules at Room Temperature (297 K).

Reactant	This Study	Preidel and Zellner[a]	Fahr and Stein[b]
HBr	$(4.1 \pm 1.5) \times 10^{-11}$	—	—
CH_2O	1.2×10^{-14}	—	—
O_2	2.78×10^{-15}	$\leq 10^{-17}$	—
C_2H_2	$(1.34 \pm 0.52) \times 10^{-15}$	$\leq 8 \times 10^{-16}$	(2.4×10^{-16})
C_2H_4	$(8.95 \pm 4.13) \times 10^{-16}$	$\leq 8 \times 10^{-17}$	(1.1×10^{-16})
C_6H_6	—	$\leq 3 \times 10^{-15}$	(2.9×10^{-18})
NO	$(3.5 \pm 0.5) \times 10^{-11}$	1.1×10^{-11}	—
NO_2	—	8.2×10^{-12}	—
i-C_4H_{10}	$(6.67 \pm 3.7) \times 10^{-17}$		
c-C_5H_{10}	$(4.97 \pm 1.0) \times 10^{-15}$		
c-C_6H_{12}	$(1.11 \pm 0.21) \times 10^{-14}$		

a. Preidel and Zellner (ref. 11).
b. Fahr and Stein (ref. 4); extrapolated from data obtained above 1000 K.

Table II. Arrhenius Parameters for Selected C_6H_5 Reactions Measured in this Study

Reactant	$10^{11} \times A$ (cm^3/s)	E_a (kcal/mole)
NO	7.41	-0.70
C_2H_2	0.19	3.22
i-C_4H_{10}	5.88	5.66
c-C_5H_{10}	2.75	4.07
c-C_6H_{12}	2.81	3.39

Abstract for 1993 DOE Combustion Research Meeting
Lake Harmony, Pennsylvania June 2-4, 1993

Crossed-Beam Studies of the Dynamics of Radical Reactions

Kopin Liu
Chemistry Division
Argonne National Laboratory

Scope

The objective of this program is to characterize the detailed dynamics of elementary radical reactions and to provide a better understanding of radical reactivity in general. The radical beam is typically generated by a laser photolysis method. After colliding with the reacting molecule in a crossed-beam apparatus, the reaction product state distribution is interrogated by laser spectroscopic techniques. Several radicals of combustion significance, such as O, CH, OH, CN and NCO have been successfully generated and their collisional behavior at the state-to-state integral cross section level of detail has been studied in this manner. During the past year, the detection system has been converted from LIF to REMPI schemes, and the emphasis of this program shifted to investigate the *product angular distributions*. Both inelastic and reactive processes have been studied.

Recent Results

(A) Collision-induced fine-structure transitions of $O(^3P_2)$ --> $O(^3P_{1,0})$

(1) by H_2 and He. The title processes were interrogated by the (2+1)-REMPI technique, and the translational energy dependences of the state-resolved integral cross sections were studied. Excellent agreements with recent theoretical calculations were found. The results also provided strong support for the validity of the Ω-conserving approximation at the state-to-state integral cross section level of detail for these systems.

(2) by Ar. In this case the angular distributions of scattered products $O(^3P_{1,0})$ were investigated by Doppler-shift technique. By exploiting the polarization of the probe laser, the m_j-dependent angular distributions were deduced from the Doppler profiles. In the language of vector correlation, such a m_j-resolved differential cross section corresponds to a three-vector, $(\mathbf{k},\mathbf{k}',\mathbf{j}')$, correlation study. Despite low resolution, the data clearly indicated that all three $(j, |m_j|)$ angular distributions exhibit oscillatory behaviors; and that these distributions are fairly sensitive to the potential energy curves involved. Collaborations with L. Harding and G. Schatz are in progress with the hope to provide a conceptual understanding of these results.

(B) Product angular and translational distributions in radical reactions

The experiments were conducted by measuring the Doppler profiles of D-atom from a chemical reaction. The (1+1)-REMPI detection scheme was employed here. A simple vuv generation scheme was adapted, which yielded ~ 30x higher conversion efficiency than the usual pure Kr-frquency tripling cell.

(1) $CN+D_2$ -->$DCN+D$ ($\Delta H_0 = -21.63$ kcal/mole). The reaction threshold was found to be ~ 2.5 kcal/mole, which is significantly lower than the value of 4.1 kcal/mole

deduced from the thermal rate constant data. Product translational energy and angular distributions for this reaction were obtained at four different collision energies, ranging from 4 to 7.5 kcal/mole. It was found that the products were mainly backward-scattered and DCN was highly excited internally, in accord with the expectation for a collinear, direct reaction with an early barrier. However, the collision energy dependences of product angular distributions reveal more sideway-to-forward components at higher energies, opposite to the conventional anticipation.

(2) $O(^1D)+D_2 \rightarrow OD+D$ ($\Delta H_0 = -42.96$ kcal/mole). The reaction cross section was found to be nearly independent of collision energy, ranging from 0.75 to 6 kcal/mole, and the Doppler profiles at five collision energies were examined. Again, the product OD are highly excited. But, the angular distributions change from nearly isotropic to forward-backward peaking with increasing collision energies. The variation of the shape of angular distributions with collision energies in this case is believed to provide the information about how the total angular momentum of reaction disposes into the product orbital and rotational angular momenta. To further investigate this system, the reaction with HD is planned.

Publications (1991 - 1993)

A crossed-beam study of the state-resolved integral cross sections for the inelastic scattering of $OH(X^2\Pi)$ with CO and N_2.
D. M. Sonnenfroh, R. G. Macdonald and K. Liu, J. Chem. Phys. 94, 6508-6518 (1991).

Inelastic scattering of $NCO(X^2\Pi)$ + He: prototypical rotational state state distributions for Hund's case(a) radicals?
R. G. Macdonald and K. Liu, J. Phys. Chem., 95, 9630-9633 (1991)

State-to-state collision dynamics of molecular free radicals
R. G. Macdonald and K. Liu, Optical Methods for Time- and State-Resolved Chemistry, SPIE Proceedings Series, Vol. 1638, C.-Y. Ng, Editor, 1992, pp. 416-422

The dynamical Renner-Teller effect II: rotational inelastic scattering of $NCO(X^2\Pi,00^10)$ + He
R. G. Macdonald and K. Liu, J. Chem. Phys. 97, 978-990 (1992)

The dynamical Renner-Teller effect III: rovibronic energy transfer pathways in the $NCO(X^2\Pi)$ + He system
R. G. Macdonald and K. Liu, J. Chem. Phys. 98, 3716-3725 (1993)

Transverse Flow Reactor Studies of the Dynamics of Radical Reactions

R.G. Macdonald
Chemistry Division
Argonne National Laboratory
Argonne IL 60439

Background

Radical-radical reactions are important in many areas of chemistry, especially in combustion chemistry; however, little state-specific information of any description is available for this class of chemical reactions. Our knowledge of the detailed molecular motions of polyatomic systems (more than three atoms) leading to chemical change is not very extensive. This is especially true for the interactions of two radical species. There are many potential energy surfaces (PES) correlating to reactants and/or products. The interplay between these multiple PESs may complicate the dynamics of these reactions. Generally at least one PES has a deep potential minimum leading to a stable adduct; however, there is often the opportunity for the formation of other product channels. Ultimately, the interactions among these various PESs are reflected in the final product state distributions among the various product channels. It is to provide information on this area of chemical dynamics, that a new apparatus has been constructed. The unique feature of this apparatus is a transverse flow reactor in which an atom or radical of known concentration will be produced in a continuous microwave discharge flow system. The other radical will be produced by pulsed laser photolysis of an appropriate precursor molecule. The time dependence of individual quantum states of products and/or reactants will be followed by rapid infrared laser absorption spectrophotometry.(IRLAS).

As an initial test of this new apparatus the dynamics of the $H + O_2 \rightarrow OH + O$ reaction will be studied. Although this reaction has been extensively studied, a complete product state distribution by a single experimental technique has not been carried out. In this initial experiment translationally hot H atoms will be created by photolysis of HBr/HCl. and state specific detection of individual OH(v,J) states probed by IRLAS.

Publications 1991-93

1. A crossed-beam study of the state-resolved integral cross sections for the inelastic scattering of $OH(X^2\Pi)$ with CO and N_2.
D. M. Sonnenfroh, R. G. Macdonald and K. Liu, J. Chem. Phys. 94, 6508 (1991).

2. Inelastic scattering of $NCO(X^2\Pi)$ + He: Prototypical rotational state distributions for Hund's case (a) radicals.
R. G. Macdonald and K. Liu, J. Phys. Chem. 95, 9630 (1991).

3. State-to-state collision dynamics of molecular free radicals.
R. G. Macdonald and K. Liu, SPIE Proc. (1992).

4. The dynamical Renner-Teller effect II: Rotationally inelastic scattering of NCO($X^2\Pi$, 00^10) + He.
R. G. Macdonald and K. Liu, J. Chem. Phys. 97, 978 (1992).

5. The dynamical Renner-Teller effect III: Rovibronic energy transfer pathways in the NCO($X^2\Pi$, 00^10) + He system.
R. G. Macdonald and K. Liu, J. Chem. Phys. 98, 3716 (1993).

FLASH PHOTOLYSIS-SHOCK TUBE STUDIES

Joe V. Michael

Gas Phase Chemical Dynamics Group
Chemistry Division
Argonne National Laboratory
Argonne, IL 60439

Even though this project in the past has concentrated on the measurement of thermal bimolecular reactions of atomic species with stable molecules by the flash or laser photolysis-shock tube (FP- or LP-ST) method using atomic resonance absorption spectrometry (ARAS) as the diagnostic technique,[1] during the past year we have concentrated on studies of the thermal decompositions of selected chlorocarbon molecules. These studies are necessary if the degradation of chlorine containing organic molecules by incineration are to be understood at the molecular level. Clearly, destruction of these molecules will not only involve abstraction reactions, when possible, but also thermal decomposition followed by secondary reactions of the initially formed atoms and radicals. Studies on the thermal decomposition of CH_3Cl are complete, and the curve-of-growth for Cl-atom atomic resonance absorption has been determined.[2] The new thermal decomposition studies are similar to those already reported for CH_3Cl.

In the first study, rate constants for the reaction,

$$CCl_4 + Ar \rightarrow CCl_3 + Cl + Ar, \qquad (1)$$

have been measured in reflected shock waves over the temperature range, 1084-1733 K. This study was complicated by the subsequent decomposition of CCl_3-radicals giving additional Cl-atoms. At sufficiently long times at least two atoms are released for every one molecule dissociated. Hence, rate constant determinations were made using initial rates of formation. Three loading pressures were used in this study, and a slight pressure dependence was noted. The second-order rate constant for the lowest loading pressure (giving P_5 = 235 Torr) is given by,

$$k_1 = 4.27 \times 10^{-8} \exp(-23528\ K/T)\ cm^3\ molecule^{-1}\ s^{-1}, \qquad (2)$$

over the temperature range. These data have been combined with laser schlieren density gradient measurements at higher temperatures by Kiefer and Kumaran. The two sets of results are in excellent agreement over the region of temperature overlap. Troe's theory of unimolecular reaction rates has been used to explain the combined results. The theoretical analysis suggests a value for ΔE_{down} of 1170 cm^{-1}. This work has been published.[3]

In the second study, rate constants for the reaction,

$$CF_3Cl + Kr \rightarrow CF_3 + Cl + Kr, \qquad (3)$$

have been measured in incident shock waves over the temperature range, 1521-2173 K. Since secondary reactions of Cl-atoms are not possible with CF_3Cl, there are fewer complications than with CH_3Cl, and therefore this study serves as a check of the earlier Cl-

atom curve-of-growth determination. Experiments were carried out with three different loading pressures, and a definite pressure dependence was observed suggesting that the reaction was near the low pressure limit. The second-order rate constant is given by,

$$k_3 = 3.26 \times 10^{-8} \exp(-31782\ K/T)\ cm^3\ molecule^{-1}\ s^{-1}, \quad (4)$$

to within ±10% at the two standard deviation level over the temperature range. The semi-empirical version of Troe's theory of unimolecular rates suggests a ΔE_{down} value of 638 cm^{-1}.

In the third study, rate constants for the reaction,

$$COCl_2 + Kr \rightarrow COCl + Cl + Kr, \quad (5)$$

have been measured over the temperature range, 1401-1967 K, in incident shock waves. Again, three loading pressures were used, and the reaction was shown to be near the low pressure limit. In this case, the initially formed radical, COCl, decomposes rapidly giving a second Cl-atom, and the temporal behavior of this subsequent process was so fast that it could not be isolated. The second-order rate constant is given by,

$$k_5 = 1.84 \times 10^{-8} \exp(-29145\ K/T)\ cm^3\ molecule^{-1}\ s^{-1}, \quad (6)$$

to within ±9% at the two standard deviation level over the temperature range.

In the fourth study, rate constants for the reaction,

$$CH_2Cl_2 + Kr \rightarrow \text{products} \quad (7)$$

are currently being investigated. The main products appear to be from molecular elimination, giving CHCl + HCl, rather than the simple bond breaking process, CH_2Cl + Cl. The first set of products account for about two-thirds of the reaction over the temperature range of ~1500-2000 K.

Additional atom with molecule reaction studies (e. g. Cl + H_2, hydrocarbons, etc.) and, also thermal decomposition investigations (e. g. $CHCl_3 \rightarrow$ products), are in the planning stage at the present time. The reactions that will be studied will either be of theoretical interest to chemical kinetics or be of practical interest in hydrocarbon combustion.

This work was supported by the U. S. Department of Energy, Office of Basic Energy Sciences, Division of Chemical Sciences, under Contract No. W-31-109-ENG-38.

References

1. J. V. Michael, J. Chem. Phys. **90**, 189 (1989).
2. K. P. Lim and J. V. Michael, J. Chem. Phys. **98**, 3919 (1993).
3. J. V. Michael, K. P. Lim, S. S. Kumaran, and J. H. Kiefer, J. Phys. Chem. **97**, 1914 (1993).

Publications from DOE Sponsored Work from 1991-93.

Rate Constants (296 to 1700 K) for the Reactions, $C_2H + C_2H_2 \rightarrow C_4H_2 + H$ and $C_2D + C_2D_2 \rightarrow C_4D_2 + D$, K. S. Shin and J. V. Michael, J. Phys. Chem. **95**, 5864 (1991).

Rate Constants for the Reactions, $H + O_2 \rightarrow OH + O$ and $D + O_2 \rightarrow OD + O$, over the Temperature Range, 1085 to 2278 K by the Laser Photolysis-Shock Tube Technique, K. S. Shin and J. V. Michael, J. Chem. Phys. **95**, 262 (1991).

Thermal Rate Constant Measurements by the Flash or Laser Photolysis-Shock Tube Method: Results for the Oxidations of H_2 and D_2, J. V. Michael, Preprint, 202nd American Chemical Society, Symposium on Combustion Chemistry, Fuel Chemistry Division **36**, 1563 (1991).

The Measurement of Thermal Bimolecular Rate Constants by the Flash Photolysis-Shock Tube (FP-ST) Technique: Comparison of Experiment to Theory, J. V. Michael, in *Advances in Chemical Kinetics and Dynamics*, J. R. Barker, editor, JAI Press, New York, Vol. 1, 1992, pp. 47-112.

Measurement of Thermal Rate Constants by Flash or Laser Photolysis in Shock Tubes: Oxidations of H_2 and D_2, J. V. Michael, Prog. Energy Combust. Sci. **18**, 327 (1992).

Isotope Effects at High Temperatures Studied by the Flash or Laser Photolysis Shock Tube Technique, J. V. Michael, in *Isotope Effects in Gas Phase Chemistry*, J. A. Kaye, editor, American Chemical Society, Washington, 1992, pp. 80-93.

A Kinetics Study of the $O(^3P) + CH_3Cl$ Reaction over the 556-1485 K Range by the HTP and LP-ST Techniques, T. Ko, A. Fontijn, K. P. Lim, and J. V. Michael, Twenty-Fourth International Symposium on Combustion (1991) **24**, 735 (1992).

Rate Constants for the N_2O Reaction System: Thermal Decomposition of N_2O; $N + NO \rightarrow N_2 + O$; and Implications for $O + N_2 \rightarrow NO + N$, J. V. Michael and K. P. Lim, J. Chem. Phys. **97**, 3228 (1992).

The Thermal Decomposition of CH_3Cl using the Cl-atom Absorption Method and the Bimolecular Rate Constant for $O + CH_3$ (1609-2002 K) with a Pyrolysis Photolysis-Shock Tube Technique, K. P. Lim and J. V. Michael, J. Chem. Phys. **98**, 3919 (1993).

Thermal Decomposition of Carbon Tetrachloride, J. V. Michael, K. P. Lim, S. S. Kumaran, and J. H. Kiefer, J. Phys. Chem. **97**, 1914 (1993).

Shock Tube Techniques in Chemical Kinetics, J. V. Michael and K. P. Lim, Annu. Rev. Phys. Chem., in press.

Chemical Kinetics and Combustion Modeling

James A. Miller
Combustion Research Facility
Sandia National Laboratories
Livermore, CA 94551-0969

The goal of this program is to gain qualitative insight into how pollutants are formed in combustion systems and to develop quantitative mathematical models to predict their formation rates. The approach is an integrated one, combining low-pressure flame experiments, chemical kinetics modeling, theory, and kinetics experiments to gain as clear a picture as possible of the process in question. Our efforts are focused on problems involved with the nitrogen chemistry of combustion systems and on the formation of soot and PAH in flames.

Recent Progress

Growth of higher hydrocarbons in rich acetylene flames and ring formation (with Carl F. Melius and Joanne V. Volponi). Two factors have had a major influence on the modeling of rich acetylene flames in the past few years. First, the establishment of the heat of formation of C_2H at $\Delta H_f \approx 135$kcal/mole results in the abstraction reactions,

$$OH+C_2H_2 \rightleftarrows C_2H+H_2O$$

$$H+C_2H_2 \rightleftarrows C_2H+H_2,$$

being too endothermic to be dominant acetylene removal steps. Consequently, even in sooting flames, acetylene principally reacts with oxygen atoms. Secondly, the reaction of acetylene with oxygen atoms primarily produces HCCO+H, rather than $^3CH_2$+CO (the branching fraction is probably about 0.7). In rich flames the dominant chain carrier is H atom, and the reaction of H with HCCO produces singlet methylene,

$$H+HCCO \rightleftarrows {}^1CH_2+CO.$$

Singlet methylene plays a major role in initiating the growth of all the higher hydrocarbons. Most notably, $^1CH_2$ reacts very rapidly with acetylene to produce propargyl radicals,

$${}^1CH_2+C_2H_2 \rightleftarrows C_3H_3+H.$$

Progargyl is resonantly stabilized and does not react very rapidly with stable molecules. It thus attains fairly high concentrations in flames. We have shown that the reaction of propargyl with itself, probably producing C_6H_5 (phenyl)+H, is the most likely cyclization step in acetylene flames. Such a cyclization step was suggested previously by Kern and co-workers in shock tube studies of allene and 1,3 butadiene pyrolyses.

An extensive set of BAC-MP4 electronic structure calculations shows low-lying reaction paths to benzene (and phenyl+H) from two propargyl radicals whether the radicals are brought together head-to-head, tail-to-tail, or head-to-tail. Comparison of the BAC-MP4 predictions with experiments on the pyrolysis of linear C_6H_6 compounds is generally quite

good, as it is with C_3H_4 and C_4H_4 compounds, where similar rearrangement mechanisms are operative.

In our most recent work we have studied $C_2H_2/O_2/Ar$ and $H_2/O_2/Ar$ flames, to which we have added allene in an attempt to perturb these flames, which we have characterized in the past, in such a way as to focus attention on the C_3 hydrocarbon chemistry. The agreement of the model predictions with the experiments is quite good. Most notably the model correctly predicts both the magnitude and the early peak of the benzene profile in the $C_2H_2/O_2/Ar$-C_3H_4 flame. No benzene is detected in this flame without the allene.

Quantifying the Non-RRKM effect in the $H+O_2 \rightleftarrows OH+O$ reaction (with M. L. Kozsykowski and B. C. Garrett):

In 1986 I suggested from studying classical trajectories that this reaction exhibited pronounced non-RRKM behavior. However, two factors called this conclusion into question. The potential energy surface used in the calculations (the Melius-Blint potential) has some potentially serious flaws, and the value of the thermal rate coefficient at high temperature was uncertain. The latter made justification of the validity of the predictions by comparison with experiment difficult. However, the situation has now been remedied. The Varandas DMBE IV potential removes the obvious flaws in the Melius-Blint potential, and experiments at Stanford, Argonne, and Brookhaven have established the thermal rate coefficient to high accuracy to temperatures above 5000K. Quasi-classical trajectories on both potential energy surfaces are in excellent agreement with experiment. Utilizing a combination of microcanonical variational transition-state theory and classical trajectories we have quantified the non-RRKM effect in two different ways. The effect on the thermal rate coefficient is roughly a factor of two.

The reactions of NH with NO and O_2 (with Carl F. Melius):

Utilizing BAC-MP4 potential energy parameters and statistical methods we have calculated the branching fraction for the reaction of NH with NO and the thermal rate coefficient and product distribution for the $NH+O_2$ reaction. The predictions are in good agreement with a variety of experimental results. We discuss the sensitivity of the predictions to potential-energy parameters and to alternative mechanisms.

Future Directions

We shall continue to pursue research problems that will allow us to gain more insight into the formation and growth of aromatic compounds in flames of aliphatic fuels. Currently, we are completing our work with allene as a flame additive, after which we shall utilize 1, 3 butadiene in the same way. In addition, we are continuing our work on nitrogen chemistry. We have recently initiated a project with Bob Perry (Technor) to investigate the feasibility of using sodium hydroxide as an additive for N_2O removal in stationary diesels, primarily to be used in conjunction with RAPRENO$_x$.

PUBLICATIONS

1. J. A. Miller, J. V. Volponi, J. L. Durant, J. E. M. Goldsmith, G. A. Fisk, and R. J. Kee, "The Structure and Reaction Mechanism of Rich, Non-Sooting $C_2H_2/O_2/Ar$ Flames," *Twenty-Third Symposium (International) on Combustion*, pp. 187-194 (1991)

2. J. E. M. Goldsmith, J. A. Miller, R. J. M. Anderson, and L. R. Williams, "Multiphoton-Excited Fluorescence Measurements of Absolute Concentration Profiles of Atomic Hydrogen in Low-Pressure Flames" *Twenty-Third Symposium (International) on Combustion*, pp. 1821-1827 (1991)

3. J. A. Miller and C. F. Melius, "Kinetic and Thermodynamic Issues in the Formation of Aromatic Compounds in Flames of Aliphatic Fuels", *Combustion and Flame* **91**, 21-39 (1992)

4. J. A. Miller and C. T. Bowman, "Kinetic Modeling of the Reduction of Nitric Oxide in Combustion Products by Isocyanic Acid," *International Journal of Chemical Kinetics* **23**, 289-313 (1991)

5. J. A. Miller and C. F. Melius,"A Theoretical Analysis of the Reaction Between Hydrogen Atoms and Isocyanic Acid," *International Journal of Chemical Kinetics* 24, 421-432 (1992)

6. G. Dixon-Lewis, V. Giovangigli, R. J. Kee, J. A. Miller, B. Rogg, M. D. Smooke, G. Stahl, and J. Warnatz,"Numerical Modelling of the Structure and Properties of Tubular Strained Laminar Premixed Flames," *Progress in Aeronautics and Astronautics,* Vol. 131, pp. 125-144 (1991)

7. H. K. Moffatt, P. Glarborg, R. J. Kee, J. F. Grcar, and J. A. Miller, "Surface PSR: A Fortran Program for Modeling Well-Stirred Reactors with Gas and Surface Reactions," SAND 91-8001 (1991)

8. J. A. Miller and C. F. Melius, "The Reactions of Imidogen with Nitric Oxide and Molecular Oxygen," *Twenty-Fourth Symposium (International) on Combustion*, pp. 719-726 (1992)

9 P. Glarborg, K. Dam-Johansen, J. A. Miller, and R. J. Kee, "Modeling the Thermal De-NO_x Process in Flow Reactors: Nitrous Oxide Formation and Surface Effects," *International Journal of Chemical Kinetics* , in press (1993)

10. C. F. Melius, J. A. Miller, and E. M. Evleth, "Unimolecular Reaction Mechanisms Involving C_3H_4, C_4H_4, and C_6H_6 Hydrocarbon Species," *Twenty-Fourth Symposium (International) on Combustion*, pp. 621-628 (1992)

Reaction Dynamics in Polyatomic Molecular Systems

William H. Miller

Department of Chemistry, University of California, and
Chemical Sciences Division, Lawrence Berkeley Laboratory
Berkeley, California 94720

Program Scope

The goal of this program is the development of theoretical methods and models for describing the dynamics of chemical reactions, with specific interest for application to polyatomic molecular systems of special interest and relevance. There is interest in developing the most rigorous possible theoretical approaches and also in more approximate treatments that are more readily applicable to complex systems.

Recent Progress

1. Tunneling in Classical Trajectory Simulations

There are many approximate and reasonably satisfactory ways to include tunneling effects — which are most important when describing the motion of hydrogen atoms — in transition state-type theories for reaction rate constants. More generally, though, one would like to be able to include such effects directly within a classical trajectory simulation in order to be able to describe more general dynamical phenomena than just transmission through a reaction barrier. There are well-known "rigorous" semiclassical theories for doing this, but they are difficult to apply routinely within a standard trajectory simulation.

Makri and Miller developed an approach several years ago that had many of the desirable features one desires; it has the character of the "surface hopping" model that Tully and Preston devised to treat electronically non-adiabatic transitions from one potential energy surface (i.e., electronic state) to another, except that it describes tunneling from one classically allowed region of space to another (all on the same potential energy surface).

Most recently Keshavamurthy and Miller have been able to eliminate the most undesirable feature of the Makri *et al.* model, namely the necessity choosing an *ad hoc tunneling direction.* This recent development utilizes the *action variables* assorted with the transition state region and yields a prescription that specifies both *when* a tunneling transition should be considered and *with what probability* it should take place, all by a completely *local* prescription that is monitored along each classical trajectory. Test applications of this model show that it is even more accurate that the previous one, an unexpected bonus. Work is now in progress applying this approach to real chemical systems.

2. Anharmonicity in Transition State Theory

Several years ago it was shown how *ab initio* quantum chemistry calculations of the cubic and quartic anharmonicity about a transition state (i.e., saddle point on a potential energy surface) could be incorporated very efficiently in a semiclassical version of transition state theory (based on the "good" action variables associated with the transition state). Two recent developments have taken place that are based on this.

First, it has been shown how the random matrix/transition state model for the probability distribution of state-specific unimolecular decay rates can be expressed quantitatively in terms of the anharmonic transmission probabilities. This has been used to describe the dependence of the probability distributions on total angular momentum for the $H_2CO \rightarrow H_2CO$ unimolecular

reaction.

Second, it has been shown how the reaction rate can be expressed in a much more convenient transition state-looking form, namely,

$$k(T) = \frac{kT}{h}\frac{Q^{\ddagger}}{Q_r}\,, \tag{1}$$

where the "partition function of the activated complex", $Q^{\ddagger}$, is given by

$$Q^{\ddagger} = \int_{-\infty}^{\infty} d\theta\, \frac{1}{2}\, \mathrm{sech}^2\theta\, Q^{\ddagger}(\theta)\,, \tag{2}$$

where

$$Q^{\ddagger}(\theta) = \sum_{n_1, n_2 \cdots n_{F-1}=0} e^{-\beta E_{n_1 \cdots n_{F-1}}(\theta)}\,, \tag{3}$$

with

$$E_{n_1 \cdots n_{F-1}}(\theta) = V_0 + \sum_{k=1}^{F} \hbar\omega_k (n_k + \tfrac{1}{2}) + \sum_{k<k'=1}^{F} x_{k,k'} (n_k + \tfrac{1}{2})(n_{k'} + \tfrac{1}{2}) \tag{4}$$

and

$$(n_F + \tfrac{1}{2}) \equiv i\theta/\pi\,. \tag{5}$$

Here Eq. (4) looks like a standard energy-level formula for F-vibrational degrees of freedom (rotation is omitted in this simplified presentation), except that the "quantum number" for the reaction coordinate — mode F, for which the frequency ω_f is imaginary — is replaced by the tunneling action θ as indicated by Eq. (5). Eqs. (1) - (5) provide a very general way to include anharmonic effects uniformly in *all* the degrees of freedom of the transition state.

3. Rigorous Reaction Rate Theory

Seideman and Miller have shown that the cumulative reaction probability N(E) for a chemical reaction (the Boltzman average of which gives the thermal rate construct *exactly*) can be expressed as

$$N(E) = 4\mathrm{tr}[\varepsilon_r \bullet \mathbf{G}(E)^* \bullet \varepsilon_p \bullet \mathbf{G}(E)] \tag{6}$$

where ε_r and ε_p are absorbing potentials in the reactant and product absorbing regions, respectively, and the Green's function is

$$\mathbf{G}(E) = (E - \mathbf{H} + i\varepsilon)^{-1} \tag{7}$$

where

$$\varepsilon = \varepsilon_r + \varepsilon_p\,. \tag{8}$$

Applications of this approach to several reactions of interest one in progress, as well as further theoretical developments that significantly improve the efficiency by which this expression can be evaluated.

Future Plans

Current and future work on all of the topics described above are mentioned in the discussions there.

1991 - 1993 (to date) DOE Publications

1. W. H. Miller and J. Z. H. Zhang, How to Observe the Elusive Resonances in H or D + H_2 $\rightarrow$ H_2 or HD + H Reactive Scattering, J. Phys. Chem. **95**, 12 (1991), LBL-29939.

2. W. H. Miller, Some New Approaches to Semiclassical and Quantum Transition State Theory, Ber. Bunsenges Phys. Chem. **95**, 389 (1991), LBL-29938.

3. W. H. Miller and T. Seideman, Transition State Theory , Siegert Eigenstates, and Quantum Mechanical Reaction Rates, J. Chem. Phys. **95**, 1768 (1991), LBL-30639.

4. W. H. Miller, Quantum Mechanical Scattering for Chemical Reactions, in Methods in Computational Molecular Physics, ed. S. WIlson and G. H. F. Diercksen, Plenum, NY, 1992, pp. 519-533, LBL-31627.

5. Y. T. Chang, C. Minichino, and W. H. Miller, Classical Trajectory Studies of the Molecular Dissociation Dynamics of Formaldehyde: $H_2CO \rightarrow H_2 + CO$, J. Chem. Phys.**96**, 4341 (1992), LBL-31623.

6. W. H. Miller, Reaction Dynamics in Polyatomic Molecular Systems: Some Approaches for Constructing Potential Energy Surfaces and Incorporating Quantum Effects in Classical Trajectory Simulations, in Molecular Aspects of Biotechnology: Computational Models and Theories, ed. J. Bertran, Kluwer Academic Pub., pp. 193-235 (1992), LBL-31626.

7. W. H. Miller, S-Matrix Version of the Kohn Variational Principle for Quantum Scattering Theory of Chemical Reactions, in Advances in Molecular Vibrations and Collision Dynamics: Quantum Reactive Scattering, Vol. IIA, ed. J. M. Bowman, JAI Press, Greenwich, 1992, LBL-31625.

8. T. Seideman and W. H. Miller, Calculation of the Cumulative Reaction Probability via a Discrete Variable Representation with Absorbing Boundary Conditions, J. Chem. Phys. **96**, 4412 (1992), LBL-31624.

9. Y. T. Chang, C. Minichino, and W. H. Miller, Classical Trajectory Studies of the Molecular Dissociation Dynamics of Formaldehyde: $H_2CO \rightarrow H_2 + CO$," J. Chem. Phys. **96**, 4341 (1992), LBL-31623.

10. T. Seideman and W. H. Miller, Calculation of the Cumulative Reaction Probability via a Discrete Variable Representation with Absorbing Boundary Conditions, J. Chem. Phys. **96**, 4412 (1992), LBL-31624.

11. T. Seideman and W. H. Miller, Quantum Mechanical Reaction Probabilities via a Discrete Variable Representation-Absorbing Boundary Condition Green's Function, J. Chem. Phys. **97**, 2499 (1992), LBL-32180.

12. M. J. Cohen, N. C. Handy, R. Hernandez, and W. H. Miller, Cumulative Reaction Probabilities for $H+H_2 \rightarrow H_2+H$ from a Knowledge of the Anharmonic Force Field, Chem. Phys. Lett. **192**, 407 (1992), LBL-33537.

13. T. D. Sewell, D. L. Thompson, D. Gezelter, and W. H. Miller, Some Problems of Correcting the Zero-Point Energy Problem in Classical Trajectories, Chem. Phys. Lett. **193**, 512 (1992), LBL-33537.

14. W. H. Miller and T. Seideman, Cumulative and State-to-State Reaction Probabilities via a Discrete Variable Representation — Absorbing Boundary Condition Green's Function, in Time Dependent Quantum Molecular Dynamics: Experiments and Theory, ed. J. Broeckhove and L. Lathouwers, Plenum, N.Y., 1992, pp. 267-277, LBL-32181.

15. W. H. Miller, Beyond Transition State Theory — A Rigorous Quantum Theory of Chemical Reaction Rates, Accts. Chem. Res. in press, LBL-33326.

16. S. Keshavamurthy and W. H. Miller, A Semiclassical Model to Incorporate Multidimensional Tunneling in Classical Trajectory Simulations Using Locally Conserved Actions," Chem. Phys. Lett. in press, LBL-33344.

17. S. M. Auerbach and W. H. Miller, Quantum Mechanical Reaction Probabilities with a Power Series Green's Function, J. Chem. Phys. in press, LBL-33325.

18. R. Hernandez, W. H. Miller, C. B. Moore, and W. F. Polik, A Random Matrix/Transition State Theory for the Probability Distribution of State-Specific Unimolecular Decay Rates: Generalization to Include Total Angular Momentum Conservation and Other Dynamical Symmetries, J. Chem. Phys. (submitted), LBL-33750.

Q-Branch Raman Scattering and Modern Kinetic Theory

Louis Monchick (P.I.)

The Johns Hopkins University
The Applied Physics Laboratory
Milton S. Eisenhower Research Center
Johns Hopkins Road
Laurel, Maryland 20723-6099

ABSTRACT

At the moment of writing, this program is just about to start. Consequently, I can only report on the scope of the program and some related results that will be used to support the program. The program is an extension of previous APL work whose general aim was to calculate[1,2] line shapes of nearly resonant isolated line transitions with solutions of a popular quantum kinetic equation - the Waldmann-Snider equation[3] - using well known advanced solution techniques developed for the classical Boltzmann equation. The advanced techniques explored have been a BGK type approximation, which we[4] have termed the Generalized Hess Method (GHM), and conversion of the collision operator to a block diagonal matrix[5] of symmetric collision kernels which then can be approximated by discrete ordinate methods. The latter method, which we have termed the collision kernel method (CC), is capable of the highest accuracy and has been used quite successfully for Q-branch raman scattering.[1] The GHM method, not quite as accurate, is applicable over a wider range of pressures and has proven quite useful.[2]

In the new program, we propose extending these techniques to processes involving off-energy-shell-scattering events. This is motivated by the fact that theories based solely by on-energy-shell scattering do not obey detailed balance[6,7] when applied to radiative transitions. A quantum kinetic equation that does can be derived by projection operator techniques[6] or from the BBGKY hierarchy.[8] The collision operator turns out to be the Fano collision operator which is rather more awkward to handle than the Waldmann-Snider collision operator because it entails a convolution over the frequency of the transition.

The first task of the new project is the formulation of the GHM method for the Fano operator and progress of this stage will be reported at the coming meeting. Formal results should be available incorporating the Fano collision operator, finite radiator concentrations and half-integral rotational quantum numbers.

References

[1] R. Blackmore, S. Green and L. Monchick, *J. Chem. Phys.* **91**, 3846 (1989).

[2] J. Schaefer and L. Monchick, *Astron. Astrophys.* **265**, 859 (1992).

[3] L. Waldmann, *Z. Naturforsch. Teil A* **12**, 660 (1957); **13**, 609 (1958); R. F. Snider, *J. Chem. Phys.* **32**, 1051 (1960).

[4] L. Monchick and L. W. Hunter, *J. Chem. Phys.* **85**, 713 (1986).

[5] R. Blackmore, *J. Chem. Phys* **86**, 4188 (1987).

[6] J. Albers and J. M. Deutch, *Chem. Phys* **1**, 89 (1973).

[7] L. Monchick, *J. Chem. Phys.* **95**, 5047 (1991).

[8] L. Monchick, unpublished.

Photochemical Reaction Dynamics

C. Bradley Moore

Materials and Chemical Sciences Division of the Lawrence Berkeley Laboratory and Department of Chemistry, University of California, Berkeley, California 94720

The purpose of the program is to develop a fundamental understanding of unimolecular and bimolecular reaction dynamics with applications in combustion and energy systems. Recently completed and on-going work is abstracted below.

I. Structures in the Energy Dependence of the Rate Constant for Ketene Isomerization

Edward R. Lovejoy and C. Bradley Moore

The isomerization of highly vibrationally excited and rotationally cold ketene has been investigated by monitoring the ^{12}CO and ^{13}CO dissociation products following laser excitation of jet-cooled $^{12}CH_2{}^{13}CO$, $^{13}CH_2{}^{12}CO$, and $^{12}CD_2{}^{13}CO$. The rate constants for the reactions $^{12}CH_2{}^{13}CO \leftrightarrow {}^{13}CH_2{}^{12}CO$ and $^{12}CD_2{}^{13}CO \leftrightarrow {}^{13}CD_2{}^{12}CO$ are reported as a function of energy with a resolution of 1 cm^{-1}. The rate constants exhibit pronounced peaks as a function of energy near the reaction threshold, Fig. 1. This structure is attributed to quasistable motion along the reaction coordinate in the vicinity of the isomerization transition state.

II. Organometallic CO Substitution Kinetics in Liquid Xe by Fast Time-Resolved IR Spectroscopy

Bruce H. Weiller, Eric P. Wasserman, C. Bradley Moore and Robert G. Bergman

The reaction of Cp*Rh(CO)Xe(Cp*=C_5Me_5) with CO was studied using time-resolved IR spectroscopy of liquid rare gas solutions. IR spectra for Cp*Rh(CO)Xe were obtained using pulsed UV laser photolysis of $Cp^*Rh(CO)_2$ in liquid Xe and a rapid-scan FTIR spectrometer with 0.09 s time resolution. Assignment to the Xe complex was confirmed from the similarity of the spectra and lifetime of the complex when a mixture of Xe in liquid Kr was used. The reaction of Cp*Rh(CO)Xe with added CO is very fast and the rate constant was measured by fast time-resolved IR spectroscopy to be $(5.7 \pm 0.6) \times 10^5$ to $(1.9 \pm 0.2) \times 106$ $M^{-1}s^{-1}$ over the temperature range 202 to 242 K. The kinetics are consistent with an associative substitution mechanism with activation parameters for the bimolecular rate constant of log(A) =- 8.8 ± 0.3 ($\Delta S^{\ddagger}$ = -20 ± 1 cal/mol K) and E_a = 2.8 ± 0.3 kcal/mol ($\Delta H^{\ddagger}$ = 2.4 ± 0.3 kcal/mol).

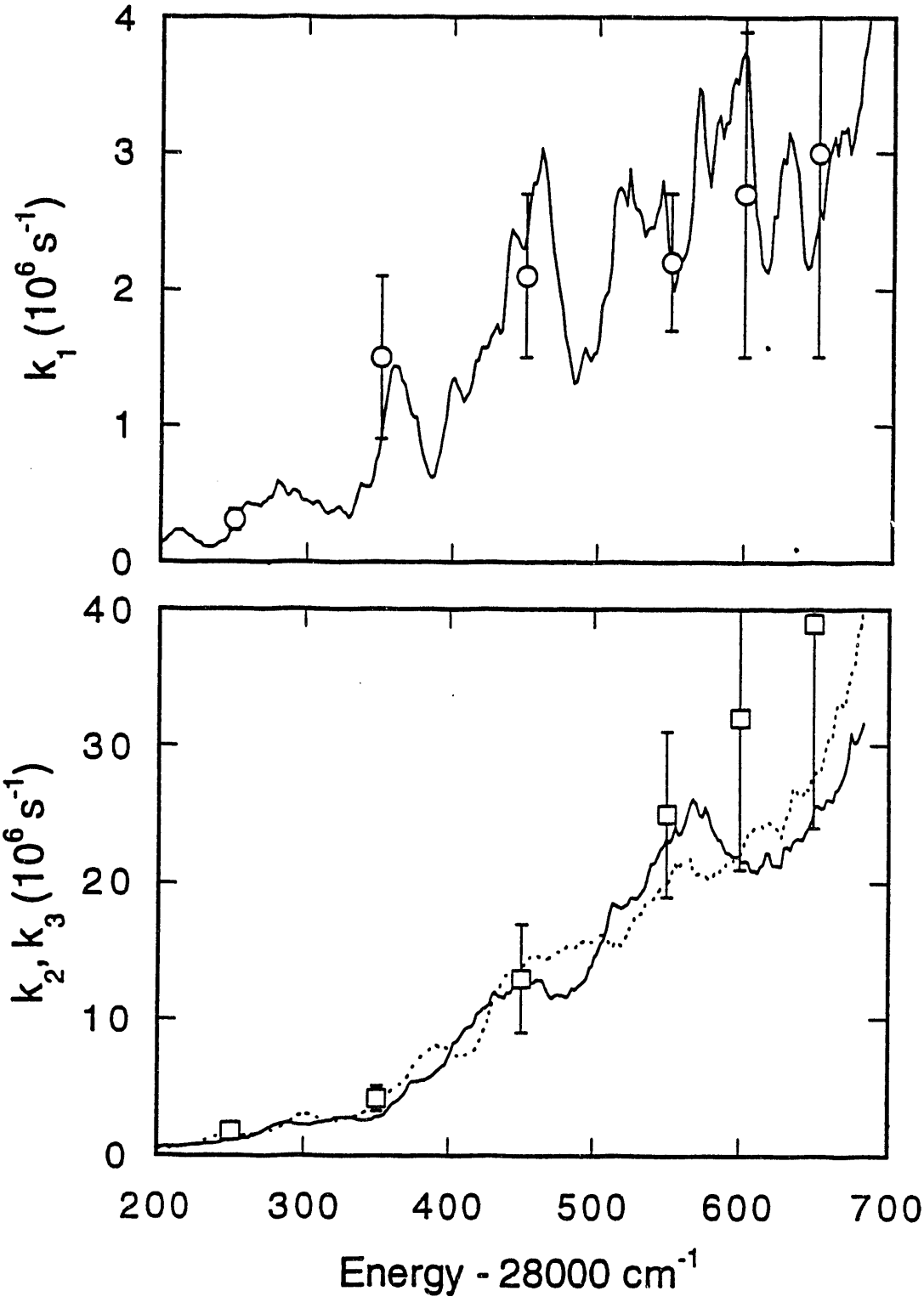

Fig. 1. Isomerization (k_1) and decomposition rate constants for $^{12}CH_2{}^{13}CO$ (k_2, solid line) and $^{13}CH_2{}^{12}CO$ (k_3, dotted line) derived from PHOFEX data of the ^{12}CO and ^{13}CO products based on mechanism. The points are experimental values of k_1 and k_3 from measurements of the temporal evolution of the CO products. The error bars are 95% confidence intervals for precision.

III. Transition States and Rate Constants for Unimolecular Reactions

William H. Green, Jr., C. Bradley Moore, and William F. Polik

This review concentrates on the interpretation of recent experiments performed near reaction thresholds and on the potential surfaces and dynamical models necessary for their interpretation. The first section addresses reactions with barriers. First tunneling and the structure in *k(E,J)* caused by the discrete nature of the level count *W(E,J)* are discussed. Then the stepped structure revealed in the dissociation of ketene over a small barrier to triplet methylene and carbon monoxide is described. The quantum statistics of the dissociation rates for formaldehyde are described, along with their quantitative interpretation derived from the *ab initio* PES. The following section on bond breaking without barriers concentrates on the dissociation of ketene to singlet methylene and carbon monoxide and of NCNO to NC and NO. These and other data provide stringent tests for PST, variational RRKM, and other theoretical models. In the final section, some limitations of the energy randomization hypothesis of statistical unimolecular reaction rate theories are discussed.

IV. Work in Progress

Unimolecular reaction studies on triplet ketene are being initiated with full rotational state resolution in the initial excitation. An IR optical parametric oscillator is being set up to select a single excited rovibrational state which will then be further excited to the reaction threshold by a UV laser pulse. The carbon atom isotopic exchange reaction rate resonances will also need to be studied with complete rotational resolution.

The B-state of hydrogen is being produced by tunable vacuum UV laser excitation. Experiments are being set up using a monochromator to disperse fluorescence and study collision-induced vibration-rotation energy transfers as a function of initial quantum state. Future studies are planned using a second vacuum UV laser to probe the velocity distribution of H-atom fragments from collision-induced electronic curve crossing. William Lester's group is carrying out *ab initio* theoretical work on these systems.

Energy transfer and chemical reaction rates are being studied for triplet CH_2 radicals. A diode laser infrared flash kinetic spectrometer is being used to study the reaction with O_2 in order to identify product states and intermediates. Reaction rates for radical-radical reactions are being measured. Infrared and ultraviolet spectra of intermediates in organometallic photochemistry in gas and liquid phase are being studied jointly with R. G. Bergman. Emphasis is on CH activation chemistry. Studies of CH activation systems in liquid Kr and Xe are proceeding well.

V. Publications

1. S. K. Kim, Y. S. Choi, C. D. Pibel, Q.-K. Zheng and C. B. Moore, "Determination of the Singlet/Triplet Branching Ratio in the Photodissociation of Ketene," *J. Chem. Phys.* **94**, 1954 (1991).

2. E. R. Lovejoy, S. K. Kim, R. A. Alvarez and C. B. Moore, "Kinetics of Intramolecular Carbon Atom Exchange in Ketene," *J. Chem. Phys.* **95**, 4081 (1991).

3. E. P. Wasserman, C. B. Moore and R. G. Bergman, "Gas-Phase Rates of Alkane C-H Oxidative Addition to a Transient CpRh(CO) Complex," *Science* **255**, 315 (1992).

4. E. R. Lovejoy, S. K. Kim and C. B. Moore, "Observation of Transition State Vibrational Thresholds in the Rate of Dissociation of Ketene," *Science* **256**, 1489 (1992).

5. W. H. Green, Jr., C. B. Moore and W. F. Polik, "Transition States and Rate Constants for Unimolecular Reactions," *Ann. Rev. Phys. Chem.* **43**, 591 (1992).

6. E. R. Lovejoy and C. Bradley Moore, "Structures in the Energy Dependence of the Rate Constant for Ketene Isomerization," *J. Chem. Phys.* (in press).

7. B. H. Weiller, E. P. Wasserman, C. B. Moore, and R. G. Bergman, "Organometallic CO Substitution Kinetics in Liquid Xe by Fast Time-Resolved IR Spectroscopy," *J. Chem. Soc.* (in press).

8. R. Hernandez, W. H. Miller, C. B. Moore, and W. F. Polik, "A Random Matrix/Transition State Theory for the Probability Distribution of State-Specific Unimolecular Decay Rates: Generalization to Include Total Angular Momentum Conservation and Other Dynamical Symmetries," *J. Chem. Phys.* (in press).

Theoretical Aspects of Gas-Phase Molecular Dynamics

James T. Muckerman

Chemistry Department, Brookhaven National Laboratory, Upton, NY 11973

Project Scope

Research in this program is focused on the development and application of time-dependent quantum mechanical and semiclassical methods for treating inelastic and reactive molecular collisions, and the photochemistry and photophysics of atoms and molecules in laser fields. Particular emphasis is placed on the development and application of grid methods based on discrete variable representations, on time-propagation methods, and, in systems with more that a few degrees of freedom, on the combined use of quantal wavepackets and classical trajectories.

Recent Progress

The construction of analytic discrete variable representations (DVRs), using projection operators expressed in terms of appropriate basis sets and corresponding sets of Gaussian quadrature points and weights, has allowed us to investigate a variety of one- and multi-dimensional quantal problems having either time-dependent or time-independent Hamiltonians. An example of a time-independent application is our recent study of the vibrational levels of the electronically excited van der Waals radical complex Ar–OH($A\ ^2\Sigma^+$). In that work a proposed potential energy function of Bowman *et al.* was used to predict new band systems. An example of a time-dependent system is the suppression of ionization of the hydrogen atom $3d$ Rydberg state in intense YAG (1064 nm) and Ti:Sapphire (780 nm) laser fields. This work, being carried out in collaboration with T. Uzer (Georgia Inst. of Tech.), will be discussed in some detail in the following paragraph.

Our full-dimensionality studies of H($3d$) in linearly polarized laser fields are made possible by a novel analytic DVR based on Sturmian functions (*i.e.*, exponentially damped generalized Laguerre polynomials). This DVR permits the numerical (unequally spaced) grid to extend to large values of the radial coordinate without requiring a prohibitive number of grid points. The goals of the work are to test the methodology and to identify the regimes of laser frequency, intensity, and pulse duration which stabilize the atom with respect to ionization. Results to date have demonstrated the stabilization phenomenon in the general range of laser frequency and peak electric field strength suggested by the Shakeshaft criterion, which is based on the relative sizes of the ponderomotive and photon energies. Stabilization is expected to occur when the ponderomotive energy exceeds the photon energy. Studies involving the low-lying $3d$ Rydberg state allow *standard* IR lasers to operate in the "intense field" regime (5 to 133×10^{12} W/cm^2), and only two photons are required for ionization. Ionization is also slow for Rydberg states, thereby allowing for a finite pulse rise time without completely ionizing the atoms before the stabilization condition is achieved. Figure 1 shows the probability density of the electron in the initial $3d_0$ state and at a time during a YAG laser pulse at which stabilization has occurred. These calculations were carried out on a direct-product DVR grid based on 64 Sturmian functions (extending to 242 a.u.) and 22 Legendre polynomials (for m=0).

We have also combined the use of analytic DVRs with a representation of the time-propagation operator based on the recursive Lanczos method for eigenvalue problems. We have developed an estimator for the error which allows us to control the accuracy of the wavepacket propagation. This new approach, which also employs a first-order Magnus approximation for time-dependent Hamiltonians, has proved to be more stable, more accurate and far more efficient than our previous methodology.

The greater efficiency of our wavepacket code has permitted us to undertake a study of the optimal control of five-color multiphoton infrared dissociation of HF. In collaboration with H. Rabitz (Princeton Univ.) we have used optimal control theory to find the set of infrared laser frequencies and time centers of five identically

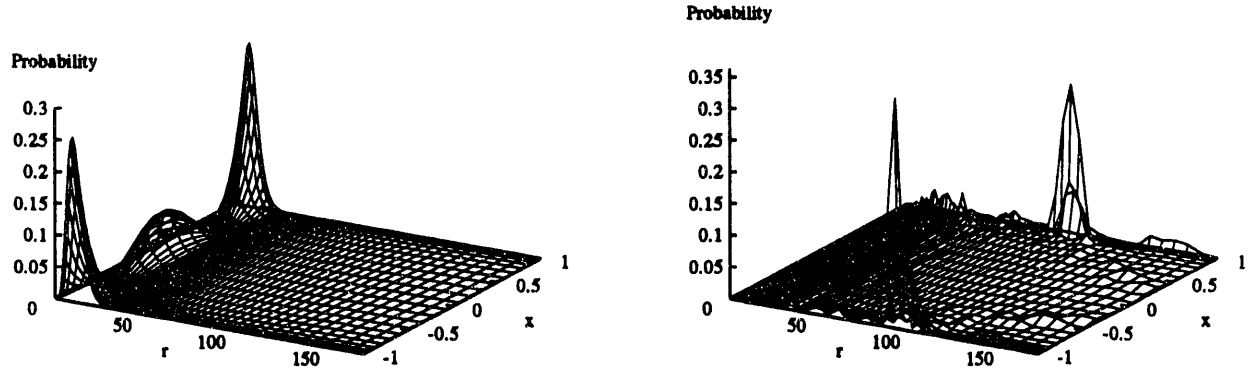

Fig. 1. Probability density of hydrogen atom wavepacket on DVR grid before and during a 1064 nm laser pulse with peak intensity of 1.33×10^{14} W/cm^2. The panel on the left shows the initial $3d_0$ Rydberg state, while that on the right shows the transient state after 10 optical cycles of the rising laser pulse. The radial coordinate is in atomic units of length. The angular coordinate is $x = \cos\theta$, where θ is the angle between the position vector of the electron and the electric field vector of the laser.

shaped (and partially overlapping) Gaussian pulses of subpicosecond duration (FWHM = 0.85 ps) which maximizes the dissociation yield of ground-state HF molecules. We have carried out these calculations in their full dimensionality (assuming the linear polarization of all lasers to be aligned) using accurate potential energy and dipole moment functions. The wavepacket was represented by a 165-point plane wave DVR in the radial coordinate and a 16-point DVR based on Legendre polynomials in the angular coordinate. An eight-vector Lanczos time propagator with a first-order Magnus approximation was used with a time step of 0.33 fs. A smooth optical potential was employed to absorb dissociating waves, and the simplex method was used for determining the optimal values of the pulse timings and carrier frequencies. The optimal pulse sequence was found to dissociate 47% of the ground-state HF molecules.

We have analyzed the dynamics of the HF molecule in the optimal pulse to determine mechanistic information. We find that, contrary to the suggestion of Chelkowski *et al.*, the optimal pulse is not "chirped" to the red, *i.e.*, the carrier frequencies of the five pulses do *not* decrease from earliest to lastest in the firing sequence in order to maintain a $\Delta v=1$ resonance as the population of the HF molecule is moved up the anharmonic vibrational ladder. In fact, the HF molecule cannot climb the vibrational ladder solely with $\Delta v=1$ transitions because the dipole matrix element, $< v,j|\mu|v+1,j+1 >$, vanishes at approximately $v=12$, and is quite small between $v=11$ and $v=13$. In this range, however, the $\Delta v=2$ dipole matrix element is quite large (see Fig. 2). Our results indicate that $\Delta v > 0$ transitions are quite important in the dissociation dynamics. The success of Chelkowski *et al.* with a chirped pulse appears to depend critically on their unphysical assumption of a constant dipole derivative (*i.e.*, linear model for the dipole moment function).

Another area of active research involves the use of adiabatic invariance in the semiclassical preparation of initial states and analysis of final states in quasiclassical trajectory calculations of chemical reactions involving polyatomic reactants and/or products. In collaboration with J.J. Valentini (Columbia Univ.) we are studing the hot-atom reaction $H + CD_4 \rightarrow HD + CD_3$ using adiabatic invariance to prepare selected vibrational states of the CD_4 reactant molecule. The purpose of this work is to explain the unusual positive correlation between vibrational and rotational energy in the product HD molecule observed in the Valentini group's experimental studies of the reaction.

Future applications of our DVR and wavepacket propagation methods will focus on such processes as the OH overtone-induced dissociation of H_2O_2 and on the dynamics of reactions such as $O + H_2 \rightarrow OH + H$. The latter type of study will employ a combined wavepacket/trajectory approach in hyperspherical coordinates in

which the overall rotations of the system will be treated classically. New efforts in analytic DVR development will include an attempt to represent the spherical harmonics on a fixed grid.

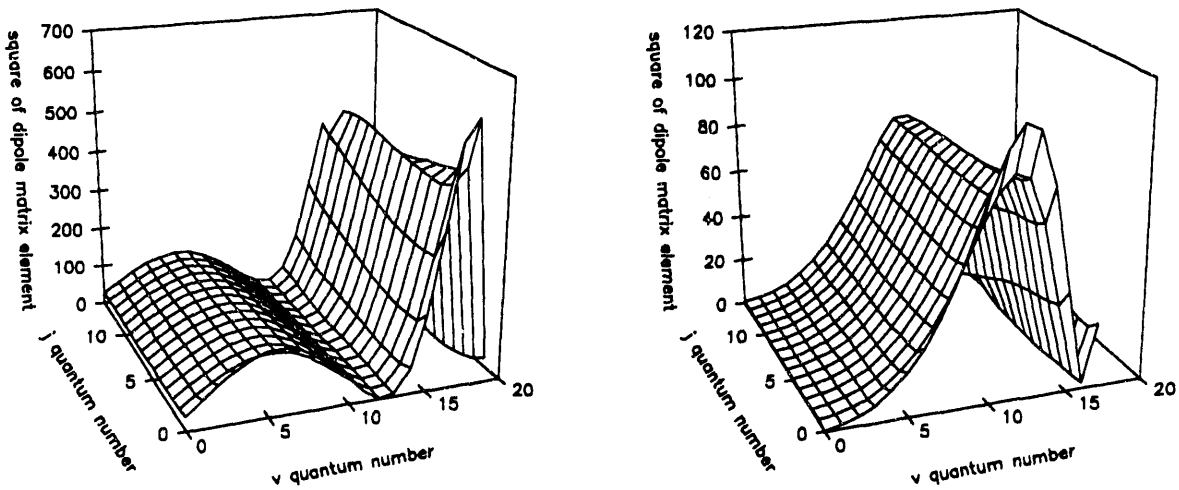

Fig. 2. The square of the dipole matrix element as a function of v and j. The left panel corresponds to $\Delta v=1$ transitions, $\langle v,j|\mu|v+1,j+1\rangle$ for various v and j. Note the node at v=12. The right panel corresonds to $\Delta v=2$ transitions for which the square of the dipole matrix element is large in the vicinity of v=12.

Publications

Calculation of the vibrational levels of the electronically excited Ar–OH($A\ ^2\Sigma^+$) using a proposed potential energy surface and analytic discrete variable representations

Y. Guan and J.T. Muckerman

J. Phys. Chem. **95**, 8293-8299 (1991)

Time-resolved FTIR studies of the photodissociation of pyruvic acid at 193 nm

G.E. Hall, J.T. Muckerman, J.M. Preses, R.E. Weston Jr. and G.W. Flynn

Chem. Phys. Lett. **193**, 77-83 (1992)

An analytic discrete variable representation for the Coulomb problem

R.V. Weaver, J.T. Muckerman and T. Uzer

In *Time-Dependent Quantum Molecular Dynamics: Experiments and Theory*, L. Lathouvers, ed., Plenem Press, in press

Quantum dynamics of predesorption: A three-dimensional study

Y. Guan, J.T. Muckerman and T. Uzer

J. Chem. Phys. (submitted)

A Fourier-transform spectrophotometer for time-resolved emission measurements using a 100-point transient digitizer

J.M. Preses, G.E. Hall, J.T. Muckerman, T.J. Sears, R.E. Weston Jr., C. Guyot, J.C. Hanson, G.W. Flynn and H.J. Bernstein

Rev. Sci. Instrum. **64**, 95-102 (1993)

Studies of the quantum dynamics of Rydberg electrons in superintense laser fields using discrete variable representations

J.T. Muckerman, R.V. Weaver, T.A.B. Kennedy and T. Uzer

Grid Methods in Atomic and Molecular Quantum Calculations, C. Leforestier, ed., Kluwer Academic Publ., in press

FAST BEAM STUDIES OF FREE RADICAL PHOTODISSOCIATION

Daniel M. Neumark

Department of Chemistry, University of California, Berkeley, CA 94720
and
Chemical Sciences Division, Lawrence Berkeley Laboratory, Berkeley, CA 94720

We have developed a novel technique for studying the photodissociation spectroscopy and dynamics of free radicals. In our experiment, radicals are generated by laser photodetachment of a fast (6-8 keV) mass-selected negative ion beam. The resulting radicals are photodissociated with a second laser, and the photofragments are collected and detected with high efficiency using a microchannel plate detector. The overall process is :

$$ABC^- \xrightarrow{h\nu_1} ABC + e^- \xrightarrow{h\nu_2} A+BC,\ AB+C$$

Two types of fragment detection schemes are used. To map out the photodissociation cross section of the radical, the photodissociation laser $h\nu_2$ is scanned and the total photofragment yield is measured as a function of ν_2. This is a spectroscopy experiment which tells us at which frequencies the radical undergoes photodissociation. We also perform photodissociation dynamics using a photofragment coincidence detection scheme based on the two-particle position and time sensing detector developed by Los.[1] In these experiments, $h\nu_2$ is fixed, and we determine the photofragment masses, kinetic energy release, and scattering angle (relative to the laser polarization) for each photodissociation event. From this we construct photofragment kinetic energy and angular distributions for each product channel.

Thus far, photodissociation dynamics experiments using this detector have been carried out for O_2, N_3, and CH_2NO_2. In the O_2 experiment, we excite the $B^3\Sigma^-(v'=7) \leftarrow X^3\Sigma^-(v''=4)$ transition in the Schumann-Runge band. The O_2 B state predissociates to form two $O(^3P_J)$ atoms. Our photofragment kinetic energy resolution is sufficiently high to resolve the different combinations of fine structure (J) levels for the two O atoms, yielding a correlated fine structure distribution from which we learn about the nature of the repulsive states responsible for the predissociation of the B state.

In the N_3 experiments, we excite the predissociating $B^2\Sigma^+$ state of N_3 and measure the N + N_2 energy and angular distributions. We find that the v=0 level of the B state undergoes significant predissociation to both the spin-forbidden $N(^4S) + N_2$ channel and the spin-allowed $N(^2D) + N_2$ and $N(^2P) + N_2$ channels. However, the spin-forbidden channel is largely quenched from predissociation of the ν_2=1 bend-excited level of the B state. This mode-specific effect is attributed to an increase in the rate of spin-allowed dissociation due to bend excitation in the B state. We also find that the N_2 product is highly rotationally excited, implying that bent geometries play a significant role in the dissociation of N_3.

The CH_2NO_2 experiments were motivated by the extensive work by several investigators on the analogous closed-shell molecule, nitromethane (CH_3NO_2). Photolysis of nitromethane near 193 nm primarily results in C-N bond fission to form $CH_3 + NO_2$. In contrast, we find the excitation of CH_2NO_2 from 240-270 nm results in two channels: $CH_2NO + O$ (N-O bond fission) and $CH_2O + NO$ (rearrangement/elimination). The C-N bond fission channel is not observed. The kinetic energy distributions for the two observed channels are quite different; the bond fission channel peaks near zero kinetic energy, while the NO elimination channel peaks well away from

---

[1] D. P. de Bruijn and J. Los, Rev. Sci. Instrum. 53, 1020 (1982).

zero, consistent with a sizeable barrier. The overall dynamics can be qualitatively explained, but a more detailed understanding of the excited states of CH_2NO_2 would certainly be useful.

1991 - 1993 (to date) DOE Publications

1. R. E. Continetti, D. R. Cyr, and D. M. Neumark, "Fast Beam Studies of N_3 Photodissociation," Chem. Phys. Lett. 182, 406 (1991); LBL-31879.

2. R. B. Metz and D. M. Neumark, "Adiabatic Three-Dimensional Simulations of the IHI^-, $BrHI^-$ and $BrHBr^-$ Photoelectron Spectra," J. Chem. Phys. 97, 962 (1992); LBL-31880.

3. D. R. Cyr, R. E. Continetti, R. B. Metz, D. L. Osborn, and D. M. Neumark, "Fast Beam Studies of NCO Free Radical Photodissociation," J. Chem. Phys. 97, 4937 (1992); LBL-32365.

4. D. J. Leahy, D. R. Cyr, D. L. Osborn, and D. M. Neumark, "Fast-Beam Studies of Free Radical Photodissociation: the CH_2NO_2 Radical," SPIE International Symposium on Advanced Electronic and Optoelectronic Materials, (1993); LBL-33418.

5. R. E. Continetti, D. R. Cyr, D. L. Osborn, and D. M. Neumark, "Photodissociation Dynamics of the N_3 Radical," J. Chem. Phys., submitted; LBL-33584.

Vacuum Ultraviolet Photoionization and Photodissociation of Polyatomic Molecules and Radicals

C. Y. Ng

Ames Laboratory, USDOE and Department of Chemistry
Iowa State University, Ames, Iowa 50011

I. Photodissociation of Radicals

In the past decade, tremendous progress has been made in understanding the photodissociation (PD) dynamics of triatomic molecules. However, the PD study of radicals, especially polyatomic radicals, has remained essentially an unexplored research area. Detailed state-to-state PD cross sections for radicals in the UV and VUV provide challenges not only for dynamical calculations, but also for *ab initio* quantum chemical studies. We have developed a laser based pump-probe apparatus for the measurement of absolute PD cross sections of radicals. The successful applications of this apparatus for the measurement of absolute PD cross sections for CH_3S and HS are summarized below.

(1) Our recent PD studies of CH_3SSCH_3 and CH_3SCH_3 suggest that the CH_3S photofragment can further dissociate by the absorption of a second 193 nm photon to produce S predominantly in the ^1D state. In order to examine this suggestion, we have measured directly the nascent electronic state distributions of $S(^3P_{2,1,0}; {}^1D_2)$ atoms formed in the 193 nm PD of CH_3SCH_3 according to reactions (1) and (2). In this experiment, the 2+1 resonance-enhanced multiphoton ionization (REMPI) schemes are used to detect $S(^3P_{2,1,0}; {}^1D_2)$.

$$CH_3SCH_3 + h\nu\ (193\ nm) \xrightarrow{\sigma_1} CH_3 + SCH_3 \qquad (1)$$

$$SCH_3 + h\nu\ (193\ nm) \xrightarrow{\sigma_2} S(^3P_{2,1,0}; {}^1D) + CH_3 \qquad (2)$$

The S^+ signal resulting from the 2+1 REMPI is directly proportional to the number density of S. i.e., [S]. Since σ_1 is known, the absolute cross sections for the formation of $S(^3P_{2,1,0}; {}^1D)$ from CH_3S can be determined by calibrating to the S^+ signals due to the formation of $S(^3P_{2,1,0}; {}^1D)$ from CS_2.

$$CS_2 + h\nu\ (193nm) \rightarrow CS(v) + S(^3P_{2,1,0}; {}^1D_2) \qquad (3)$$

The absolute cross section for process (3) is known. The branching ratio for $S(^3P)/S(^1D)$ (=2.78) and the fine-structure distribution of $S(^3P_{2,1,0})$ resulting from the 193 nm PD of CS_2 have also been measured previously by the VUV laser-induced fluorescence and TOF mass spectrometric methods.

Using the procedures outlined above and the rate equation model, we have obtained an estimate of $1x10^{-18}$ cm^2 for σ_2. The branching ratio for $S(^3P)/S(^1D)$ due to process (2) is found to be 0.15/0.85, while the fine-structure distribution observed for $S(^3P_{2,1,0})$ is determined to be $^3P_2 : {}^3P_1 : {}^3P_0 = 0.59\pm0.02 : 0.32\pm0.02 : 0.09\pm0.04$, which is close to the statistical distribution of 5/9 : 3/9 : 1/9.

In order to rationalize the experimental observations, we have also examined the *ab initio* multi-configuration-self-consistence-field potential energy surfaces of CH_3S along the CH_3-S dissociation

coordinate in C_{3v} symmetry. For the 193 nm PD of $CH_3S(\tilde{X})$, the measured fine-structure distribution for $S(^3P_{2,1,0})$ is in accord with the predissociation of $CH_3S(\tilde{C}^2A_2)$ via the $CH_3S(\tilde{B}^2A_2)$ state. Predissociation of $CH_3S(\tilde{C}^2A_2)$ via the repulsive $CH_3S(\tilde{E}^2E)$ surface is most likely responsible for the efficient production of $S(^1D)$ in the 193 nm PD of $CH_3S(\tilde{X})$. For vibrationally excited $CH_3S(\tilde{X})$, a viable mechanism for the dominant production of $S(^1D)$ may involve direct dissociation via the $CH_3S(\tilde{E}^2E)$ state formed in the 193 nm photoexcitation.

(2) Based on the previous experiments and on energetic considerations, the scheme for the formation of $S(^3P_{2,1,0}; {}^1D)$ from the 193 nm PD of H_2S may involve processes (4)-(6).

$$H_2S + h\nu\ (193\ nm) \xrightarrow{\sigma_4} H + HS \qquad (4)$$

$$HS + h\nu\ (193\ nm) \xrightarrow{\sigma_5} H + S(^3P_{2,1,0}; {}^1D_2) \qquad (5)$$

$$H_2S + h\nu\ (193\ nm) \xrightarrow{\sigma_6} H_2 + S(^3P_{2,1,0}; {}^1D_2) \qquad (6)$$

By examining the PD power dependence of S^+, we have determined unambiguously the values for σ_4, σ_5, and σ_6 to be 6.5×10^{-18}, 1.1×10^{-18}, and 0.3×10^{-18} cm^2. The branching ratio $S(^3P)/S(^1D)$ = 0.87/0.13 observed for process (5) supports the direct PD mechanism for HS at 193 nm via the excited repulsive $HS(^2\Sigma^-, {}^2\Delta)$ potential energy surfaces. The fine-structure distribution $S(^3P_2) : S(^3P_1) : S(^3P_0)$ = 0.68 : 0.24 : 0.08 for process (5) is consistent with this conclusion.

II. Comparison of Experimental and Theoretical Ionization Energies and Electron Affinities

Because of the existence of many stable isomers for polyatomic radicals, results observed in photoionization (PI) and photodetachment experiments require theoretical interpretations. To complement our experimental studies on organosulfur chemistry, we have begun to perform *ab initio* calculations at the Gaussian-2 (G2) level of theory. Using the G2 theoretical procedure, we have examined the molecular structures and total energies for CH_2SH, CH_2S^-, CH_3S^-, CH_2SH^-, CH_3SH^-, CH_3^+, and CH_3SH^+. Combined with the results of previous G2 calculations, this calculation yields predictions for the adiabatic ionization energies (IEs) of CH_3 (9.79 eV), CH_2SH (7.41 eV), and CH_3SH (9.55 eV), which are in accord with the experimental IEs of 9.84 eV for CH_3, 7.536±0.003 eV for CH_2SH, and 9.440 eV for CH_3SH. The G2 values for the adiabatic electron affinities (EA) of CH_2S, CH_2SH to *trans*-$CH_2SH^-(C_s; {}^1A')$, CH_2SH to *cis*-$CH_2SH^-(C_s; {}^1A')$, and CH_3S are 0.38, 0.52, 0.61, and 1.86 eV, respectively. The EA(G2)'s of CH_2S and CH_3S also agree with the respective experimental values of 0.465±0.023, and 1.861±0.004 eV. We find that CH_3SH^- is unstable with respect to the electron detachment channel $CH_3SH + e^-$.

The G2 theory is targeted to provide accurate absolute total energies; hence G2 calculations of polyatomic species require the computing capacity of a supercomputer, which is still not easily accessible to individual laboratories. Because of the significantly less demand in computational capacity for density functional (DF) calculations compared to G2 calculations, DF is an attractive theoretical method, if it can provide reliable predictions for molecular energies, especially for larger neutral and ionic molecular species. Using the DF method, we have obtained predictions of IEs and EAs for CH_3S and CH_2SH. These calculations were carried out on a standard workstation. Table I compares the DF predictions with the experimental and G2 results. As shown in the table, E_o(DF) values are significantly higher than the corresponding G2 results. However, the relative ΔE_o(DF) and ΔE_o(G2) values, which can be determined in PI and photodetachment threshold measurements are surprisingly close, with absolute deviations $|\Delta E(G2) - \Delta E_o(DF)| \leq 0.212$ eV (average absolute deviation = 0.106 eV).

Table I. Energetics of $CH_3S^+(^3A_2)$, $CH_2SH^+(^1A')$, $CH_3S(^2A')$, $CH_2SH(^2A)$, $CH_3S^-(^1A_1)$ and $CH_2SH^-(^1A')$ at 0 K.[a,b]

Species	E_o(DF) (hartree)	ΔE_o(DF) (eV)	$\lvert\Delta E(G2)-\Delta E_o(DF)\rvert$ (eV)	ΔE_o(Expt) (eV)
$CH_3S^+(C_{3v};^3A_2)$	-435.96000 [-437.17155]	9.15_3 $[9.23_9]$	0.086	9.225±0.014 9.262±0.005
$CH_2SH^+(C_s;^1A')$	-436.01325 [-437.22405]	7.70_4 $[7.81_1]$	0.107	7.57 7.66 7.81
$CH_2SH(C_1;^2A)$	-436.28967 [-437.49660]	0.18_2 $[0.39_4]$	0.212	0.16 0.24 0.39
$CH_3S(C_s;^2A')$	-436.29637 [-437.51108]	0.000 [0.000]	0.000 0.000	0.00
trans-$CH_2SH^-(C_s;^1A')$	-436.30349 [-437.51645]	-0.19_4 $[-0.14_6]$	0.048	...
cis-$CH_2SH^-(C_s;^1A')$	-436.30782 [-437.51941]	-0.31_2 $[-0.22_7]$	0.085	...
$CH_3S^-(C_{3v};^1A_1)$	-436.36134 [-437.57963]	-1.76_8 $[-1.86_5]$	0.097	-1.861±0.004 -1.871±0.012

a) S.-W. Chiu, W.-K. Li, W.-B. Tzeng, and C. Y. Ng, *J. Chem. Phys.* 97, 6557 (1992); and references therein.

b) E_o represents the electronic energy plus the zero-point vibrational energy. ΔE_o values are energies relative to that for $CH_3S(^2A')$. E_o(G2) and ΔE_o(G2) are given in square brackets.

Publications of DOE sponsored research (1991-93)

1. S. Nourbakhsh, K. Norwood, H.-M. Yin, C.-L. Liao, and C. Y. Ng, "Vacuum Ultraviolet Photodissociation and Photoionization Studies of CH_3SCH_3 and SCH_3", *J. Chem. Phys.* 95, 5014-5023 (1991).

2. S. Nourbakhsh, K. Norwood, H.-M. Yin, C.-L. Liao, and C.Y. Ng, "Vacuum Ultraviolet Photodissociation and Photoionization Studies of CH_3SH and SH", *J. Chem. Phys.* 95, 946-954 (1991).
3. S. Nourbakhsh, H.-M. Yin, C.-L. Liao, and C. Y. Ng, "A 193 nm Laser Photofragmentation Time-of-Flight Mass Spectrometric Study of CH_3CH_2SH", *Chem. Phys. Lett.* 183, 348-352 (1991).
4. S. Nourbakhsh, K. Norwood, G.-Z. He,* and C. Y. Ng, "Photoionization Study of Supersonically Cooled Polyatomic Radicals: Heat of Formation of CH_3S^+", *J. Am. Chem. Soc.*, (Communication) 113, 6311-6312 (1991).
5. K. Norwood, S Nourbakhsh, G.-Z. He, and C. Y. Ng, "Photoionization Study of Supersonically Cooled CS Formed in the Excimer Laser Photodissociation of CS_2". *Chem. Phys. Lett.* 184, 147 (1991).
6. K. Norwood and C. Y. Ng, "Observation of Autoionizing Rydberg Series Converging to $SO_3^+(^2E',^2A_1')$", *J. Chem. Phys.* 95, 5553-5555 (1991).
7. K. Norwood, A Ali, and C. Y. Ng, "A Photoelectron-Photoion Study of H_2O and $(H_2O)_2$, *J. Chem. Phys.* 95, 8029-8037 (1991).
8. C. Y. Ng, "Molecular Beam Photoionization and Photoelectron-Photoion Coincidence Studies of High Temperature Molecules, Clusters, and Radicals", in *Vacuum Ultraviolet photoionization and Photodissociation of Molecules and Clusters*, edited by C. Y. Ng (World Scientific, Singapore, 1991), p. 169-257.
9. C. Y. Ng, editor, *Vacuum Ultraviolet Photoionization and Photodissociation of Molecules and Clusters* (World Scientific, Singapore, 1991), 572 pages.
10. S. Nourbakhsh, H.-M. Yin, C.-L. Liao, and C. Y. Ng, "A 193 nm Laser Photofragmentation Time-of-Flight Mass Spectrometric Study of C_6H_5SH and $C_6H_5SCH_3$", *Chem. Phys. Lett.* 190, 469-475 (1992).
11. C. Y. Ng and M. Baer, editors, *State-Selected and State-to-State Ion-Molecule Reaction Dynamics I: Experiment and II: Theory* (Wiley, New York, 1992), *Adv. Chem. Phys.* Vol. 82, 1280 pages.
12. C. Y. Ng, S.-W. Chiu, and W.-K. Li, "An *ab initio* Molecular Orbital Study of the Methylthio and Mercaptomethy Radicals", *J. Chem. Res.* 230 (1992).
13. C.-L. Liao, C.-W. Hsu, and C. Y. Ng, "Dynamics of S production in the 193nm Photodissociation of CH_3SSCH_3, CH_3SCH_3, CH_3SH, and H_2S", *Optical Methods for Time- and State-Resolved Selective Chemistry*, C. Y. Ng, Editor, Proc.SPIE 1638, p. 245-253 (1992).
14. C. Y. Ng, editor, *Optical Methods for Time- and State-Selected Chemistry*, Proc. SPIE 1638, (1992), 466 pages.
15. C.-W. Hsu, C.-L. Liao, Z.-X. Ma, P. J. H. Tjossem, and C. Y. Ng, "A study of the $S(^3P_{2,1,0};^1D)$ Production in the Photodissociation of CH_3S at 193 nm, *J. Chem. Phys.* 97, 6283-6290 (1992).
16. C.-W. Hsu, C.-L. Liao, Z.-X. Ma, P. J. H. Tjossem, and C. Y. Ng, "A Study of the $S(^3P_{2,1,0};^1D_2)$ Production in the 193nm Photodissociation of HS and H_2S", *Chem. Phys. Lett.* 199, 78 (1992).
17. S.-W. Chiu, W.-K. Li, Wen-Bih Tzeng, and C. Y. Ng, "A Gaussian-2 *Ab Initio* Study of CH_3^+, CH_3SH^+, CH_2SH, CH_2S^-, CH_3S^-, CH_2SH^-, and CH_3SH^-", *J. Chem. Phys.* 97, 6557-6568(1992).
18. D. P. Chong and C. Y. Ng, "Prediction of Adiabatic Ionization Energies and Electron Affinities for CH_3S and CH_2SH By Density Functional Method", *J. Chem. Phys.* 98, 759-760 (1993).
19. C. Y. Ng, editor, *Laser Techniques for State-Selected and State-to-State Chemistry*, Proc. SPIE, 1858 (1993), in press.
20. C. Y. Ng, T. Baer, and I. Powis, editors, *Cluster Ions* (Wiley, London, 1993), *Current Topics in Ion Chem. and Phys.* Vol. 1, in press.

Quantitative Imaging of Turbulent and Reacting Flows

Phillip H. Paul
Combustion Research Facility
Sandia National Laboratories
Livermore, CA 94551-0969

Program Scope

Quantitative digital imaging, using planar laser light scattering techniques is being developed for the analysis of turbulent and reacting flows. Quantitative image data, implying both a direct relation to flowfield variables as well as sufficient signal and spatial dynamic range, can be readily processed to yield two-dimensional distributions of flowfield scalars and in turn two-dimensional images of gradients and turbulence scales. Much of the development of imaging techniques to date has concentrated on understanding the requisite molecular spectroscopy and collision dynamics to be able to determine how flowfield variable information is encoded into the measured signal. From this standpoint the image is seen as a collection of single point measurements. Our present effort is aimed at realizing necessary improvements in signal and spatial dynamic range, signal-to-noise ratio and spatial resolution in the imaging system as well as developing excitation/detection strategies which provide for a quantitative measure of particular flowfield scalars.

The standard camera used for the study is an intensified CCD array operated in a conventional video format. The design of the system was based on detailed modeling of signal and image transfer properties of fast UV imaging lenses, image intensifiers and CCD detector arrays. While this system is suitable for direct scalar imaging, derived quantities (e.g. temperature or velocity images) require an exceptionally wide dynamic range imaging detector. To apply these diagnostics to reacting flows also requires a very fast shuttered camera. We have developed and successfully tested a new type of gated low-light level detector. This system relies on fast switching of a proximity focused image-diode which is direct fiber-optic coupled to a cooled CCD array. Tests on this new detector show significant improvements in detection limit, dynamic range and spatial resolution as compared to microchannel plate intensified arrays.

For applications in reacting flows we have chosen planar laser-induced fluorescence (PLIF) imaging as our primary diagnostic tool. PLIF is a species specific diagnostic which provides relatively high signal levels and access to most radical species of interest. To be able to develop experimental strategies which provide PLIF images of particular flowfield scalars requires a consideration of collisional quenching effects. We have completed an effort to model collisional quenching of OH $A^2\Sigma$ and NO $A^2\Sigma$. The purpose of this work is to provide a physical framework to consolidate experimental quenching cross-section measurements and then provide sets of correlations which can be used to design experiments or extrapolate to typical flowfield conditions. The quenching model is based on the combination of classical collision-complex formation and a curve-crossing or `harpoon' mechanism with the crossing probability based on a Landua-Zener formalism. The model has been used successfully to match NO quenching measurements made in our laboratory (see abstract by J. A. Gray et al.) and has been successfully tested against literature values for OH quenching.

Recent Progress

We have completed a detailed study of the flow in the near-field of a non-reacting round jet. This flow displays a very 2-D shear-layer like character which makes it of particular interest as a basis for comparison to direct numerical simulation results. Here we have used PLIF imaging of NO to obtain very high quality images of the conserved scalar fields. The use of trace NO in nitrogen provides both superior signal levels and a unity Schmidt number

experiment. Image data sets have been recorded over the range of $800 < Re_\delta < 80{,}000$ (a Reynolds number based on the mixing layer thickness at mid image). Probability density functions (PDFs) for mixed fluid as a function of position across the layer display a distinct non-marching character for pre-transition values of Re_δ , at higher values of Re_δ the PDF displays a marching component on the low speed side of the layer. Evidence for a marching component on the high speed side of the layer is found for $Re_\delta > 40{,}000$. At the highest Reynolds numbers, it is no longer possible to fully resolve the finest flowfield structure. There is then an ambiguity in the meaning of the measured signal: for a resolution element containing equal portions of jet and ambient fluid, the same signal will be recorded if the two fluids are fully segregated or if they are fully mixed at a molecular scale. To investigate the process of mixing at the finest scales in highly turbulent flows we have developed the `cold-chemistry' approach. We take advantage of the low cross-section for quenching of NO by N_2 and the high cross-section for quenching by O_2, < 0.0074 and 25 $Å^2$ respectively. By using PLIF of NO to image an NO seeded N_2 jet mixing into ambient air, the weighting imposed by the quenching provides a signal which can be directly interpreted as that fraction of the resolution element which contains pure unmixed fluid. Using this method we have confirmed and quantified the behavior of the PDFs for the incompressible shear layer and have extended the work to a study of the compressible layer. We find that the amount of mixed fluid is a weak function of compressibility, for convective Mach numbers in the range 0.3 to 1.2, and observe a scalar mixing PDF with a strong marching character.

The shear layer work was extended to a study of the near-field of a reacting H_2 - air non-premixed jet using simultaneous PLIF imaging of OH and trace acetone seeded into the jet fluid. The experiment makes use of a single laser to pump an isolated transition in the OH $A \leftarrow X$ system which coincides with the broad continuum characterizing the acetone $\tilde{A} \leftarrow X$ system. The resulting images are spectrally differentiated onto separate cameras using a bandpass filter for the OH and a longpass filter for the acetone. The OH image marks the reaction zone and the acetone provides a convenient flow tracer for the unmixed fuel, thermally decomposing well prior to the reaction zone. Image data sets have been recorded for both reacting and non-reacting conditions over the range $1000 < Re_d < 100{,}000$ (a Reynolds number based on nozzle diameter) and for a range of fuel dilutions with nitrogen or helium. These data provide strong quantitative evidence that the effect of the heat release associated with the reaction is to greatly stabilize or even laminarize the local turbulence. This laminarization suppresses both the largest and smallest scales of the turbulence. The heat release reduces the density of the ambient fluid thus damping the instability (the central mode) that drives the non-reacting shear layer. The flame appears to act as a boundary condition for a mixing layer (likely associated with one of the outer modes) that is formed between the high-speed jet fluid and the hot products produced in the flame zone. This reaction zone is not subjected to large scale fluid motions and appears as a simple strained laminar flame. The reaction zone is unbroken except at the highest Reynolds number where evidence for local extinction is found. This suggests that the flame is positioned so as to consume all of the entrained oxidizer. The present results have important implications for the far field structure of jet flames, that are in addition to the decrease in the Reynolds number associated with increased temperature. The stabilization of the turbulence near the flame zone may inhibit the large-scale motions that are responsible for entrainement in non-reacting jets. The ability of the continuous flame zone to exclude oxygen from the jet core may significantly alter the production or destruction of NO_x transported in the jet fluid.

The image-diode intensified CCD array has been used to study the details of mixing at the finest turbulence scales in the far field of a non-reacting round jet. Compared to our standard system, this new camera yields a significant advantage in spatial resolution, an improvement in the signal-to-noise ratio and signal dynamic range, and a reduction in the system fixed-pattern noise. High quality images with a realized spatial resolution of better than 100 microns were obtained using PLIF imaging of trace NO in N_2. Scalar dissipation images obtained by spatially differentiating these data reveal mixing zones that are composed of numerous fine filaments. This structure is previously unreported and is strikingly different

from that found in turbulent high Schmidt number flows (e.g. water). These experiments are being rerun with a new design for the sheet forming optics which should improve the spatial resolution by an additional factor of two while maintaining the image quality.

Future Work

We are developing a new camera to provide temporally resolved PLIF imaging. The camera is based on very high-speed readout of a CCD array and is intensified with a HOT-MCP tube. The system is designed to provide 3,500 frame-per-second imaging to memory with the capacity to continuously record up to one seconds worth of image data. Initial testing will be with a doubled diode-pumped slab-YAG laser (up to 10 kHz pulse rate) to perform planar Mie scattering imaging. We are presently investigating alternative laser technologies (e.g. larger diode-pumped YAG system or waveguide excimers) to be able to extend the system to PLIF imaging.

We are testing a new excitation/detection scheme for PLIF imaging of the CH radical. In hydrocarbon flames CH provides a unique means to study flame-front topology. Previous methods have provided relatively poor signal levels forcing a sacrifice in spatial resolution which has then limited the use of CH imaging to only slightly turbulent flows. Test of excitation/detection strategies for PLIF imaging for formaldehyde are also in progress. Imaging results of suitable quality have been obtained of the nascent formaldehyde produced in a methanol flame. Formaldehyde also promises to be an excellent flow tracer and possibly useful as a conserved scalar for reacting systems, surviving to higher temperatures than acetone and providing a near unit Schmidt number. PLIF imaging of nascent NO in flames is strongly compromised by a very high collisional quenching rate. As a remedy, we have successfully amplified the laser used for NO measurements (an excimer pumped dye laser doubled in BBO at near 225 nm) in an KrCl excimer medium. The substantial increase available pump energy should provide a significant improvement in NO imaging capability.

Publications related to this work

1. P. H. Paul, N. T. Clemens and D. B. Makel, `Planar laser-induced fluorescence imaging of OH in the exhaust of a bi-propellant thruster,' in Proc. NASA Langley Measurement Conf. (NASA, 1992), pp. 387-401.
2. J. W. Thoman, J. A. Gray, J. L. Durant and P. H. Paul, `Collisional electronic quenching of NO $A^2\Sigma^+$ by N2 from 300 to 4500K,' J. Chem. Phys. **97**, 8156 (1992).
3. N. T. Clemens and P. H. Paul, 'Scalar measurements in compressible axisymmetric mixing layers,' AIAA 31st Aerospace Sciences Conf. (submitted Phys. Fluids, Mar. 1993), AIAA-93-0220.
4. P. H. Paul `A model for the temperature-dependent collisional quenching of OH $A^2\Sigma^+$,' (submitted to JSQRT, Mar, 1993).
5. P. H. Paul, J. A. Gray, J. L. Durant and J. W. Thoman, `Collisional quenching correction for laser-induced fluorescence measurements of NO $A^2\Sigma^+$,' (submitted to AIAA J., Mar. 1993).
6. P. H. Paul, J. A. Gray, J. L. Durant and J. W. Thoman, `A model for collisional electronic quenching of NO $A^2\Sigma^+$,' (Appl. Phys. B, accepted Mar. 1993).
7. P. H. Paul and N. T. Clemens, 'Subresolution measurements of mixed fluid using electronic quenching of NO $A^2\Sigma^+$,' Opt. Lett.s **18**, 161 (1993).
8. P. H. Paul and N. T. Clemens, 'Planar laser-induced fluorescence imaging of lifted H2-air flames,' AIAA 31st Aerospace Sciences Conf. (submitted AIAA J., Feb. 1993), AIAA-93-0800.

Molecular Eigenstate Spectroscopy: Application to the Intramolecular Dynamics of Some Polyatomic Molecules in the 3000 to 7000 cm^{-1} Region

David S. Perry, Principal Investigator
University of Akron, Akron OH 44325-3601

I. Introduction

Intramolecular vibrational redistribution (IVR) appears to be a universal property of polyatomic molecules in energy regions where the vibrational density of states is greater than about 5 to 30 states per cm^{-1}. Interest in IVR stems from its central importance to the spectroscopy, photochemistry, and reaction kinetics of these molecules.

A bright state, φ_1, which in our case may be a C-H stretching vibration, carries the oscillator strength from the ground state. This bright state may mix with bath rotational-vibrational levels to form a clump of molecular eigenstates, each of which carries a portion of the oscillator strength from the ground state. In our work we explicitly resolve transitions to each of these molecular eigenstates. Detailed information about the nature of IVR is contained in the frequencies and intensities of the observed discrete transitions.

The primary goal of this research is to probe the coupling mechanisms by which IVR takes place. The most fundamental distinction to be made is between anharmonic coupling which is independent of molecular rotation and rotationally-mediated coupling. Of the rotationally-mediated mechanisms, Coriolis coupling is generally assumed to be stronger than centrifugal coupling. Coriolis interactions may be further classified as x, y, or z according to the axis about which the coupling rotation occurs. Each of these mechanisms obeys different symmetry restrictions and therefore each leaves its characteristic signature on fully resolved molecular spectra.

We are also interested in the rate at which IVR takes place. Our measurements are strictly in the frequency domain but information is obtained about the decay of the zero order state, φ_1, which could be prepared in a hypothetical experiment as a coherent excitation of the clump of molecular eigenstates. As the coherent superposition dephases, the energy would flow from the initially prepared mode into nearby overtones and combinations of lower frequency vibrational modes. The decay of the initially prepared mode is related to a pure sequence infrared absorption spectrum by a Fourier transform.

II. Direct Infrared Absorption in a Free Jet

The sample gases were cooled to about 5 K in a pulsed slit-jet expansion. The high resolution absorption spectrum of the jet was recorded by monitoring the transmitted intensity of an F-center laser beam. Spectra of the asymmetric methyl C-H stretch bands of 1-butyne[1] and ethanol[2] were recorded at about 0.001 cm^{-1} resolution. Both of these molecules exhibited intermediate case IVR with each zero-order line being fragmented into a clump of transition to molecular eigenstates.

Even though the spectra excited the same chromophore in each molecule, the spectra

were startlingly different for the two molecules. For 1-butyne, the measures of IVR (*see section V below*) were independent of J and show only a slight dependence on K_a. Therefore the coupling mechanism is dominantly anharmonic with some contribution from z-axis Coriolis interactions. For ethanol, there is evidence for anharmonic coupling at J=0, but the number of coupled levels increase rapidly with both J and K_a which indicates the presence of x/y and z-type Coriolis couplings respectively. It can be seen then that in both molecules more than one coupling mechanism is present although the relative strengths are qualitatively different. In Section V below, we describe the methodology that we have developed for estimating the relative strength of each mechanism when multiple coupling mechanisms are present.

The lifetimes for the decay of C-H stretching vibrations in 1-butyne and ethanol have been determined. The IVR lifetime in 1-butyne is 270 ps for both the methyl C-H and the acetylenic C-H vibrations. When the methyl C-H of ethanol is excited, the lifetime is shorter and decreases rapidly with K_a (116, 58, and 32 ps for K_a=0, 1, and 2). In these cases, we see that the IVR rate depends not on the identity of the chromophore but on the identity of the molecule and that fast IVR is associated with a Coriolis coupling mechanism.

III. Infrared Double Resonance

An infrared double resonance (IRDR) technique capable of recording molecular eigenstate spectra as a probe of IVR in polyatomic molecules has been developed. The IRDR technique has the following properties:

(i) All good quantum numbers can be assigned through the use of two high resolution laser beams. The assignment ambiguities which are unavoidable in single resonance experiments are removed. In fact by the nature of the experiment, most features are fully assigned at the moment they are recorded which relieves the necessity of tedious assignments by ground state combination differences and opens the door to the study of much more complex spectra.

(ii) The equipment can be operated in a saturation mode (Fig. 1) in which the pump and probe frequencies are the same, or in two double resonance modes (Fig. 2).

(iii) Through the use of two photons, vibrations can be accessed which are completely dark to single resonance spectroscopy, *e.g.* , the $\nu_1+\nu_6$ band of propyne (Fig.2).

(iv) The molecules are cooled in a free jet.

(v) The resolution is in the range 5 to 25 MHz.

(vi) High signal-to-noise (600:1) has been obtained in the propyne $2\nu_1$ region.

Our results[3,4] on the ν_6 , $\nu_1+\nu_6$, and $2\nu_1$ bands of propyne span the range of energy where IVR is turning on. The qualitative behavior, multiple perturbing states and indications of z-axis Coriolis interactions, is consistent for the three bands. The extent of mixing increases monotonically with vibrational energy. The $2\nu_1$ spectra reveal explicitly a two-stage IVR coupling mechanism, first anharmonic coupling to a relatively sparse tier of dark states which are in turn coupled to a denser tier by a z-axis Coriolis effect.[†]

[†] A. McIlroy, D. J. Nesbitt, E. R. Th. Kerstel, B. H. Pate, K. K. Lehmann, and G. Scoles, unpublished manuscript.

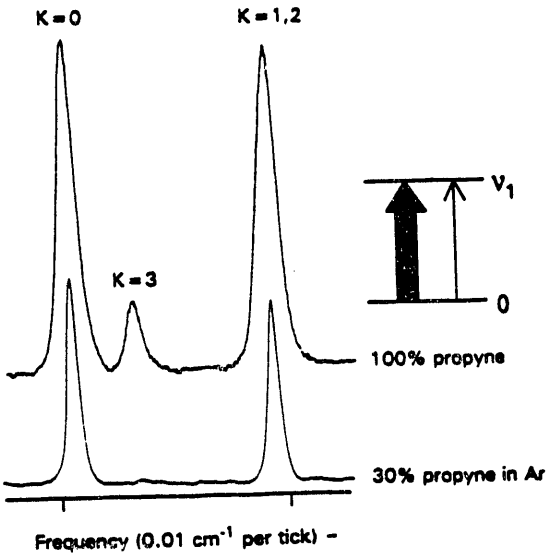

Fig. 1. Saturation spectrum of the R3 region of the propyne v_1 band.

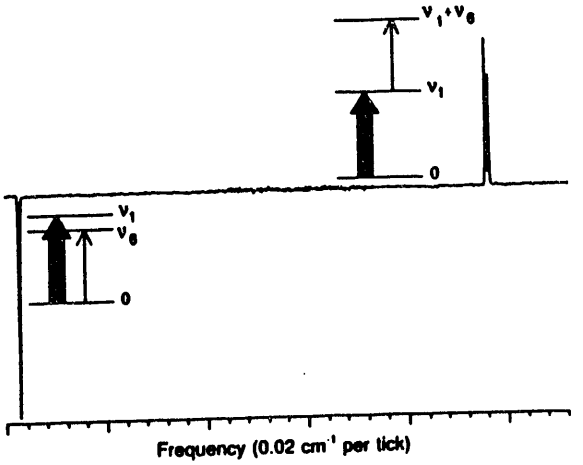

Fig. 2. Propyne spectrum illustrating two double resonance modes. The pump frequency (thick arrow) is held fixed while the probe frequency (thin arrow) is scanned.

IV. Microwave-Infrared Double Resonance

Microwave-infrared double resonance spectra have been recorded for a few rotational levels in the O-H stretch band of ethanol.[5] The experiment was done at the National Institute for Standards and Technology in collaboration with Brooks Pate and Jerry Fraser and was supported by this grant only through the stipend of the student, Greg Bethardy. This double resonance technique used optothermal detection with electrostatic focusing. The O-H IVR lifetime at 25 ps is extremely rapid, even faster than the average 59 ps for the methyl C-H stretch in the same molecule.

V. Random Matrix Simulation of Molecular Eigenstate Spectra

As the density of states increases with energy or with molecular size and flexibility, a single bright state is fragmented into an increasing number of closely spaced eigenstates. It quickly becomes impossible to identify the zero-order character of each dark state which is perturbing the bright state. The difficulty comes, in part, from our inability to calculate the energies of the zero-order dark states with sufficient precision, and, more fundamentally, from the fact that *the zero-order dark states are likely to be extensively mixed among themselves*. We are compelled, therefore, to devise a statistical treatment of the high resolution spectra in order to deal with our ignorance of the vibrational character of each

interacting bath state.

We have developed a methodology[6,7] based on a class of random matrix ensembles called the Gaussian-Poisson Ensembles. We assume that there is sufficient mixing *among the bath states* to validate a statistical treatment. Our methodology is capable of simulating infrared spectra exhibiting intermediate case and also those in the sparse limit where only one or two perturbing levels are observed. By varying the parameters defining the ensemble to fit the observed spectra, we are able to extract useful mechanistic information from the experimental data.

Since a statistical method cannot be expected to reproduce the individual line positions and intensities of an experimental spectrum, certain statistical measures of IVR are selected to serve as the interface for the comparison of experiment and theory. They are (i) the dilution factor, (ii) the interaction width, and (iii) the density of coupled levels.

The first step in simulating a spectrum is to select the model parameters which will define an ensemble of random matrices. We have used the RMS anharmonic coupling and Coriolis couplings (each of x, y, and z types). Separate parameters are used for the bright-bath interaction and for the bath-bath interaction. The second step is to select a matrix from the ensemble by choosing individual matrix elements from the appropriate distributions. This matrix is diagonalized to create a synthetic spectrum. Many matrices (64 to 512) are selected from the same ensemble and diagonalized to obtain a representative sampling of the ensemble. Ensemble average values of the measures of IVR, their distributions, and their dependence on the rotational quantum numbers are then compared to the experimental values. The model parameters are then varied until the agreement with experiment is satisfactory. In this way, we were able to obtain RMS anharmonic, Coriolis z-type, and Coriolis x/y-type matrix elements for the bright-bath coupling in 1-butyne and in ethanol. By matching the experimental density of states some information is also available about the Coriolis bath-bath coupling matrix elements.

VI. Future Plans

The infrared double resonance technique will be applied to the 6000 cm^{-1} region of propyne, methanol, and methyl amine. In propyne, advantage will be taken of accidental resonances to study vibrations such as $\nu_1+\nu_3+2\nu_9$ which are not simple C-H stretches but contain significant amplitude in other coordinates. Methanol and methylamine have low-barrier 3-fold symmetric potentials for internal rotation which might enhance the IVR rate relative to 1-butyne where the barrier is higher. These molecules will allow a direct comparison of C-H, O-H, and N-H stretches.

VIII. Papers Citing DOE Support

1. G. A. Bethardy and D. S. Perry, J. Chem. Phys., **98**, xxxx (1993).
2. G. A. Bethardy and D. S. Perry, in preparation.
3. Jungsug Go and D. S. Perry, J. Chem. Phys. **97**, 6994 (1992).
4. Jungsug Go, T. J. Cronin, and D. S. Perry, Chem. Phys., to be published.
5. G. A. Bethardy, G. T. Fraser, B. H. Pate, and D. S. Perry, in preparation.
6. D. S. Perry, J. Chem. Phys., **98**, xxxx (1993).
7. J. Go and D. S. Perry, in preparation.

REACTION AND DIFFUSION IN TURBULENT COMBUSTION

S.B. Pope
Mechanical and Aerospace Engineering
Ithaca, NY 14853

1. INTRODUCTION

The motivation for this project is the need to obtain a better quantitative understanding of the technologically-important phenomenon of turbulent combustion. In nearly all applications in which fuel is burned—for example, fossil-fuel power plants, furnaces, gas-turbines and internal-combustion engines—the combustion takes place in a turbulent flow. Designers continually demand more quantitative information about this phenomenon—in the form of turbulent combustion models—so that they can design equipment with increased efficiency and decreased environmental impact.

For some time the PI has been developing a class of turbulent combustion models known as PDF methods (see Pope 1985). These methods have the important virtue that both convection and reaction can be treated without turbulence-modelling assumptions. However, a mixing model is required to account for the effects of molecular diffusion. Currently, the available mixing models are known to have some significant defects. The major motivation of the project is to seek a better understanding of molecular diffusion in turbulent reactive flows, and hence to develop a better mixing model.

The primary approach adopted is the use of Direct Numerical Simulations (DNS) to study turbulent non-premixed combustion. In DNS, the fluid mechanical and thermochemical conservation equations are solved by an accurate numerical method, without any averaging or turbulence modelling. In principle, then, DNS could be used to study a turbulent diffusion flame, for example. In practice, however, computational limitations severely restrict the flows that can be simulated.

For non-reacting flows, DNS is restricted to simple geometries and moderate Reynolds number. For reacting flows there are severe restrictions on the thermochemistry. Indeed, DNS is a misnomer since simplifying assumptions are made about the chemical kinetics and molecular transport processes. It is completely out of the question to account for the 50 species and 200 reactions that typically occur in a turbulent flame.

What then is the use of DNS for turbulent combustion? Our approach is to use DNS to study very simple turbulent reactive flows, that contain qualitatively the same phenomena as real flames. Based on the insights and information gained, statistical models will be developed and tested. These models are then applicable to the turbulent flames of practical importance.

2. DIRECT NUMERICAL SIMULATIONS

We consider the simplest possible thermochemistry that allows the study of finite-rate kinetic effects in non-premixed combustion. Accordingly, the density is taken to be constant, and the molecular diffusivities are taken to be equal and constant. The mixing is then completely characterized by the mixture fraction ξ. A one-step *reversible* reaction is considered, with Y being the reaction progress variable.

We have carefully developed a simple thermochemical model in terms of ξ and Y which is suitable for DNS, and yet retains as much of the essential ingredients as possible. At equilibrium, Y adopts the value $Y_e(\xi)$. This function Y_e is defined by the stoichiometric mixture fraction ξ_s and by the equilibrium constant K. It is normalized to have a maximum value of unity.

Rather than the reaction progress variable, we consider its perturbation from equilibrium

$$y \equiv Y_e(\xi) - Y. \tag{1}$$

Then, the reaction rate is of the form:

$$S(\xi, y) = f(y)g(\xi)/\tau_c, \tag{2}$$

where f and g are normalized functions, and τ_c is the specified reaction time scale.

The parameters in the thermochemical model can be chosen to encompass a broad range of conditions—slow or fast reactions, high or low activation energy, small or large equilibrium broadening etc. An important parameter (which can be controlled) is the characteristic width of the reaction zone in mixture fraction space, $\Delta\xi_r$.

In DNS, it is very important to understand the demands of numerical resolution, not only to ensure accurate simulations, but also so that the broadest parameter range can be investigated. The three most important non-dimensional parameters are the Reynolds number R_λ, the Damkohler number Da, and $\xi'/\Delta\xi_r$—the ratio of the r.m.s. to the reaction zone thickness (in mixture fraction space).

Using numerical forcing, we study stationary homogeneous isotropic turbulence. The use of forcing not only facilitates the analysis and interpretation of the results, but it also allows higher Reynolds numbers to be obtained compared to the case of decaying turbulence. For non-reacting flows, the resolution issues are well understood: on a $(128)^3$ grid $R_\lambda \approx 90$ can be obtained.

In practice, the resolution requirements connected with the Damkohler number are simple to satisfy. The requirement is that the time step Δt be small compared to the reaction time scale τ_c. Other considerations already limit Δt to be small compared to the Kolmogorov time scale τ_η. Hence the fast-chemistry limit ($\tau_c/\tau_\eta < 1$) can be approached without penalty.

The resolution requirement connected to the parameter $\xi'/\Delta\xi_r$, on the other hand, is extremely restrictive. Considerable time has been spent in understanding and quantifying the requirement.

Some preliminary results are described in Section 4. But first, the theory with which they can be compared is presented.

3. THEORY

The first question being studied is the stability of the combustion system. Consider simulations with fixed values of R_λ and $\xi'/\Delta\xi_r$, but different values of Da. For very large Da, the composition is very close to equilibrium, and hence y is everywhere close to zero. For zero Da, on the other hand, there is no combustion and y increases with time. There is, therefore, a critical value of Da, above which stable combustion takes place and the composition field is statstically stationary. Below this critical value extinction occurs.

The evolution equation for y is

$$\frac{Dy}{Dt} = \Gamma\nabla^2 y - \frac{1}{2}\chi Y_e''(\xi) - S(\xi, y), \tag{3}$$

where

$$\chi \equiv 2\Gamma\nabla\xi \cdot \nabla\xi, \tag{4}$$

is the scalar dissipation. Note that Y_e'' is negative, and so the term in χ in Eq. (3) is positive. In view of the statistical homogeneity of the fields, the mean of Eq. (3) is

$$\frac{d\langle y\rangle}{dt} = -\frac{1}{2}\langle\chi Y_e''(\xi)\rangle - \langle S(\xi, y)\rangle. \tag{5}$$

For stable combustion $d\langle y\rangle/dt$ is zero, and hence the two terms on the right-hand side balance.

4. RESULTS

A convenient way to explore stability in DNS, is to perform a long simulation in which, starting from a large value, Da is slowly decreased (on a time scale that is greater than all relevant physical and chemical time scales). Thus a quasi-stationary state exists until the critical value of Da is reached. Figure 1 shows results from such a simulation, for $R_\lambda = 18$, $\xi'/\Delta\xi = 1$ and an initial Damkohler number of $Da_0 = 667$. It may be seen from Fig. 1(b) that the volume average of y, $[y]$, rises slowly as Da decreases (i.e. Da/Da_0 increases), until $\log(Da_0/Da)$ equals 3 (i.e. $Da \approx 0.67$), but then there is a sudden rise which corresponds to extinction.

Figure 1(c) shows the volume average of the two terms on the right of Eq. 15. (The solid line is $[S]$, the dashed line is $\left[-\frac{1}{2}\chi Y_e''(\xi)\right]$.) For large Damkohler numbers, the two quantities are very close to each other, confirming the quasi-stationarity. But beyond the critical Damkohler number they diverge—as extinction begins. This divergence is more precisely quantified on Fig. 1(d), which shows

$$\varepsilon_S \equiv [S]/\left[-\frac{1}{2}\chi Y_e''(\xi)\right] - 1. \tag{6}$$

Extinction occurs when ε_S drops significantly below zero.

Many other statistics have been examined. For example Fig. 1(a) shows the probability of local extinction, defined as

$$P_T \equiv \text{ Prob } \{y > 2y_{\max} | \xi_S - \Delta\xi_r < \xi < \xi_S + \Delta\xi_r\}, \tag{7}$$

where $y_{\max}$ is the value of y at which the reaction rate $S(\xi, y)$ is maximum.

Predictions of the critical value of Da have been obtained from flamelet theory (Peters 1984), from QEDR theory (Bilger 1988), and from the conditional moment closure (Bilger 1993), and a lower bound is obtained from Eq. (5).

5. FUTURE PLANS

DNS studies of stability are continuing, and the results are being related to the theoretical predictions mentioned above. Several near-critical values of Da will be selected for more

detailed study. For these cases the structure and the statistics of the composition fields will be examined in detail.

6. REFERENCES

Bilger, R.W. (1993) Phys. Fluids A **5**, 436.

Bilger, R.W. (1988) Twenty-second Symp. (Int'l.) on Combust. The Combustion Institute, p. 475.

Peters, N. (1984) Prog. Energy Combust. Sci. **10**, 319.

Pope, S.B. (1985) Prog. Energy Combust. Sci. **11**, 119.

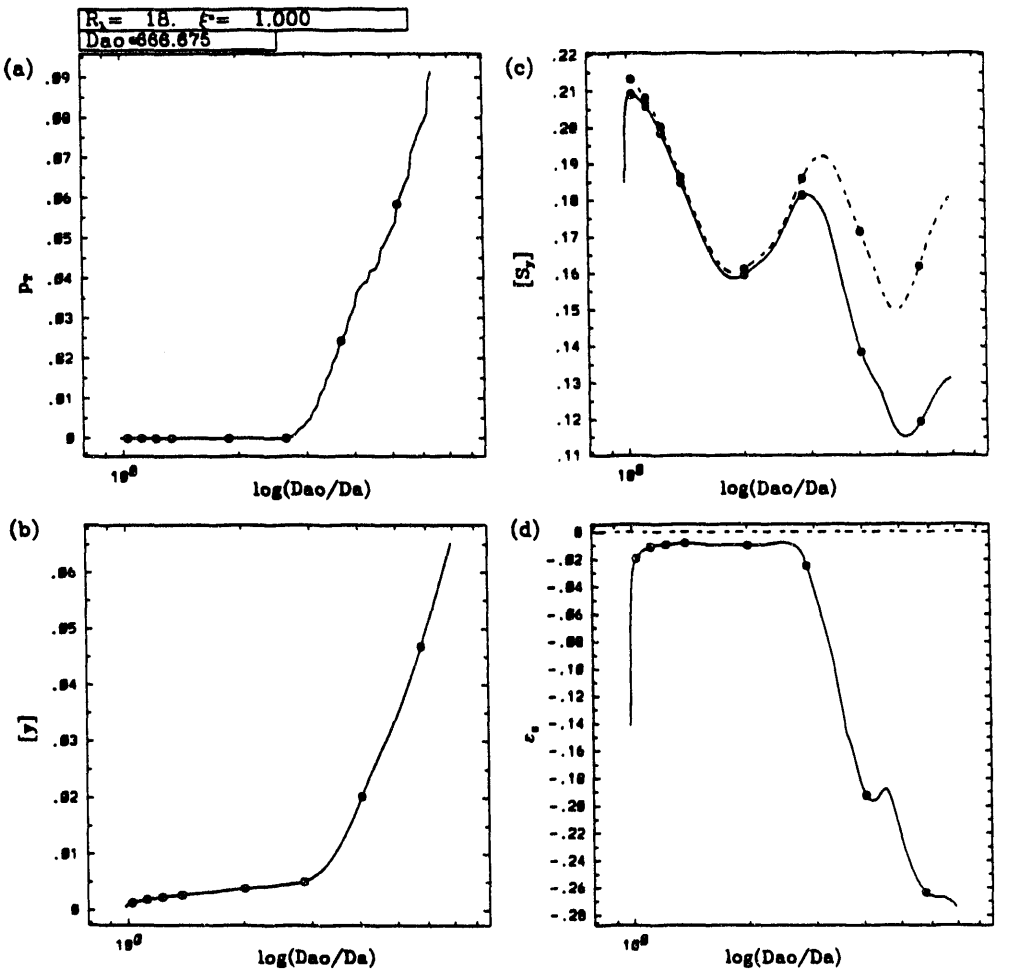

Fig. 1: Results from DNS with $R_\lambda = 18$, $\xi'/\Delta\xi_r = 1$, and quasi-statistically decreasing Da, with $Da_0 = 667$.

(a) Probability of local extinction (Eq. 7)

(b) Mean of y

(c) Means of S and $-\frac{1}{2}\chi Y_e''$

(d) ε_S defined by Eq. (6)

ANALYSIS OF FORWARD AND INVERSE PROBLEMS IN CHEMICAL DYNAMICS AND SPECTROSCOPY

by

Herschel Rabitz
Department of Chemistry
Princeton University
Princeton, NJ 08544

PROGRAM SCOPE:

The overall scope of this research concerns the development and application of forward and inverse analysis tools for problems in chemical dynamics and chemical kinetics. The chemical dynamics work is specifically associated with relating features in potential surfaces and resultant dynamical behavior. The analogous inverse research aims to provide stable algorithms for extracting potential surfaces from laboratory data. In the case of chemical kinetics, the focus is on the development of systematic means to reduce the complexity of chemical kinetic models. Recent progress in these directions is summarized below.

RECENT PROGRESS:

A. Forward Analysis

This research is focused on identifying the key features in potential surfaces with regard to their impact on cross sections and kinetic rate constants. Processes involving inelasticity, electronic curve crossing, and chemical reactivity are being studied. In order to explore rotationally inelastic dynamics, the prototypical He + H_2 system has been treated. In this case, a singular value decomposition of the sensitivity matrix, provided a quantitative assessment of the amount and type of physical information available in the potential and corresponding laboratory data. This same analysis is being extended to chemical reactivity for the H + H_2 system. A fully three-dimensional forward analysis of the F + H_2 reactive system has also been undertaken. This study revealed that subtle correlated features in both the entrance and exit channels of the potential, as well as near the barrier, are of importance.

B. Inverse Analysis

The inverse analysis techniques being explored explicitly rely on the forward tools discussed above. In particular, an algorithm is being pursued for the extraction of potential surfaces from quality laboratory data, without the imposition of *a priori* potential forms. In order to stabilize the algorithm, the criteria is introduced that the resultant potential be smooth to a required order of differentiability. In addition, any further rigorous information, such as asymptotic forms, can be similarly included. The analogous techniques of so-called Backus-Gilbert-Snider have been successfully employed by other researchers for allied inversion problems in the geophysical sciences, astrophysical sciences, and in the optical sciences. We are specifically utilizing differential cross section data and spectral line data for purposes of inversion. Most recently, the technique has been applied to electronic curve crossing, for extracting the coupling term between the potential surfaces. Computations are under way to illustrate the method for inelastic and reactive dynamics.

C. Chemical Kinetics Model Reduction

A serious problem in executing combustion models is the complexity of the chemical mechanisms involving many steps and species. Early approximations, such as the steady state approach, and the introduction of sensitivity analysis, suggests that such models may be significantly reduced in complexity and still yield viable results. This aspect of our research concerns the development of systematic means to reduce the complexity of chemical kinetic mechanisms. Thus far, the primary focus has been on the introduction of linear projective transformations of the chemical species to yield models of reduced complexity. An explicit algorithm has been set up to find the transformations to meet this goal. Such linear transformations have a degree of utility, but the most significant progress will be made by the introduction of nonlinear transformations. Research to introduce such nonlinear transformations is under way. In a parallel vein, we are also pursuing the use of multiple time scale analysis to provide an algorithm for model reduction based on separating the fast and slow kinetic processes. This latter work also makes a firm connection with the earlier steady state approaches. Application of these tools to combustion models is under way.

FUTURE PLANS

In the area of forward dynamical analysis, our research will increasingly focus on chemical reactivity. In a similar vein, the inverse work will treat inelastic date while moving towards treating chemical reactivity. Various aspects of this work are in collaboration with Nancy Brown. The work on chemical kinetics model reduction will continue to focus on the use of nonlinear species transformations for mechanism simplification. Treatments based on identifying the natural slow and fast time scales will also be pursued for reduction purposes. Finally, a collaborative study has been undertaken with Jim Muckerman, to design laser pulses for the manipulation of molecular dynamics.

REFERENCES TO DOE-SPONSORED RESEARCH

1. Factorization of Certain Evolution Operators Using Lie Operator Algebra: Convergence Theorems, M. Demiralp and H. Rabitz, *J. Math. Chem.*, **6**, 193 (1991).

2. Factorization of Certain Evolution Operators Using Lie Algebra: Formulation of the Method, M. Demiralp and H. Rabitz, *J. Math. Chem.*, **6**, 165 (1991).

3. Inversion of Gas-surface Scattering Data for Potential Determination Using Functional Sensitivity Analysis: I. A Case Study for the He-Xe/C(0001) Potential, T-S. Ho and H. Rabitz, *J. Chem. Phys.*, **94**, 2305 (1991).

4. A Comprehensive Reaction Mechanism for Carbon Monoxide/Hydrogen/Oxygen Kinetics, R.A. Yetter, F.L. Dryer, and H. Rabitz, *Comb. Sci. and Tech.*, **79**, 97 (1991).

5. Flow Reactor Studies of Carbon Monoxide/Hydrogen/Oxygen Kinetics, R.A. Yetter, F.L. Dryer, and H. Rabitz, *Comb. Sci. and Tech.*, **79**, 129 (1991).

6. The Rotation-Vibration Potential of He-H_2 and Its Connection with Physical Phenomena, M.J. Smith and H. Rabitz, *J. Chem. Phys.*, **94**, 7114 (1991).

7. Quantum Functional Sensitivity Analysis Within the Log-derivative Kohn Variational Method for Reactive Scattering, J. Chang, N. Brown, M. D'Mello, R.E. Wyatt, and H. Rabitz, *J. Chem. Phys.*, **97**, 6226 (1992).

8. Inversion of gas-surface scattering data for potential determination using functional sensitivity analysis: II. Extraction of the full interaction potential from low energy diffraction data, T-S. Ho and H. Rabitz, *J. Chem. Phys.*, **96**, 7092 (1992).

9. Regularized Inversion of Diatomic Vibration-rotation Spectral Data: A Functional Sensitivity Analysis Approach, H. Heo, T-S. Ho, K.K. Lehmann, and H. Rabitz, *J. Chem. Phys.*, **97**, 852 (1992).

10. Construction of Classical Functional Sensitivity Maps for Rotationally Inelastic Collisions of H_2 with HD, J. Chang, N.J. Brown, and H. Rabitz, *J. Phys. Chem.*, **96**, 6890 (1992).

11. A Strategy to Derive New Internal Coordinates by Partitioning the Internal Configuration Space According to Invariance Properties, J.P. Leroy, R. Wallace, and H. Rabitz, *J. Math. Chem.*, **11**, 365 (1992).

12. A method for inverting curvilinear transformations of relevance in the quantum mechanical Hamiltonian describing *n*-body systems, J.P. Leroy, R. Wallace, and H. Rabitz, *Chem. Phys.*, **165**, 89 (1992).

13. Parametric Sensitivity Analysis and Self-Similarity in Thermal Explosion Theory, S. Vajda and H. Rabitz, *Chem. Eng. Sci.*, **47**, 1063 (1992).

14. Quantum functional sensitivity analysis for the collinear H + H_2 reaction rate coefficient, J. Chang, N.J. Brown, M. D'Mello, R.E. Wyatt, and H. Rabitz, *J. Chem. Phys.*, **96**, 3523 (1992).

15. Predicting Observables on Different Potential Energy Surfaces Using Feature Sensitivity Analysis: Application to the Collinear H + H_2 Exchange Reaction, J. Chang, N. Brown, M. D'Mello, R.E. Wyatt, and H. Rabitz, *J. Chem. Phys.*, **97**, 6240 (1992).

16. On the Role of Potential Features in Fine-Structure Transitions with Application to $H^+ + F(^2P_{1/2}) \rightarrow H^+ + F(^2P_{3/2})$, D.A. Padmavathi, M.K. Mishra, and H. Rabitz, *Chem. Phys.*, in press.

17. On The Role of Potential Structure in the Collisional Excitation of Metastable $O(^1D)$ Atoms, D.A. Padmavathi, M.K. Mishra, and H. Rabitz, *Phys. Rev. A*, in press.

18. Generalized Parametric Sensitivity: Application to a CSTR, S. Vajda and H. Rabitz, *Chem. Eng. Sci.*, in press.

High-Resolution Inverse Raman and Resonant-Wave-Mixing Spectroscopy

Principal Investigator: Larry A. Rahn, Combustion Research Facility, Sandia National Laboratories, Livermore, CA 94551-0969

Program Scope: These research activities consist of high-resolution inverse Raman spectroscopy (IRS) and resonant wave-mixing spectroscopy to support the development of nonlinear-optical techniques for temperature and concentration measurements in combustion research. Objectives of this work include development of spectral models of important molecular species needed to perform coherent anti-Stokes Raman spectroscopy (CARS) measurements and the investigation of new nonlinear-optical processes as potential diagnostic techniques. Some of the techniques being investigated include frequency-degenerate and nearly frequency-degenerate resonant four-wave-mixing (DFWM and NDFWM), and resonant multi-wave mixing (RMWM).

Recent progress:

Thermal Grating Contributions to Resonant-Wave-Mixing Spectra of Flame OH

Larry A. Rahn, Michael S. Brown,* Jon W. Forsman, and Skip Williams+

Thermal grating signals arise in DFWM experiments when an optical intensity grating is formed and the resulting optical excitation relaxes to thermal energy. These periodic variations in gas temperature (the "thermal grating") give rise, after acoustic relaxation, to a density grating and an associated index grating. An optical signal that is coherent with the DFWM signal is generated when one of the pump beams scatters from the index grating. Because the thermal grating is formed by quenching collisions and relaxes by diffusion, it is enhanced at higher pressures. This trend is opposite that for the usual DFWM signal. The thermal grating signal also has a lower dependence on the transition moment and exhibits a different lineshape than that for DFWM. These and other unique features of thermal grating signals must be properly accounted for in quantitative spectral models for DFWM measurements.

Three techniques, DFWM, NDFWM, and two-color laser-induced-grating spectroscopy (TCLIGS), are used to investigate and confirm the importance of the thermal grating mechanism to resonant-wave-mixing signals in flames. The polarization characteristics of DFWM measurements on OH $A^2\Sigma^+ \rightarrow X^2\Pi$ transitions show disagreement with perturbation theory calculations for a two-level system consistent with the formation of thermal gratings. NDFWM spectra show narrow features at line center that fit theoretical lineshapes having significant contributions from both thermal gratings and multi-level open-system effects. These experiments also allow us to determine the relative strength and phase of the thermal grating signal. Finally, recent TCLIGS experiments using a time-delayed grating-probe beam indicate the excitation of acoustic oscillations in the flame by the transient excitation of a thermal grating. The DFWM experiments and theory are discussed in further detail below.

Polarization properties of $\chi^{(3)}$ for DFWM: Larry A. Rahn and Michael S. Brown*

The DFWM experiments reported here used the output of a frequency-doubled pulse-amplified cw dye laser operating near 615 nm. A geometry employing nearly counter-propagating pump beams in a three-dimensional phase-matching arrangement was used. The beams crossed in an interaction volume 5 mm above a 60-mm diameter flat-flame burner operated with gas flows of 4.8 l/min. of H_2 and 3.0 l/min. of O_2. At this location in the flame, the OH temperature and concentration were ~1450 K and ~2 x 10^{15} cm^{-3}, respectively. For the measurements reported here, the peak laser-beam intensities were held as low as possible to avoid saturation effects. In all cases the intensities were equal to or below ~ 70 kW/cm^2 [$\cong$ 0.1 I_{sat} for $R_1(9)$] The DFWM polarization intensity ratio measurements were performed at line center by rotating the polarizations of the lasers using half-wave plates while the signal was analyzed with a fixed polarizer to reduce scattered light. The signal was averaged for 1000 laser shots for each measurement and corrected

for scattered light when necessary. DFWM polarization intensity ratio measurements are plotted (symbols) in Fig. 1 versus the ground-state total angular momentum, J, for a number of transitions involving $\Delta J = 0$ and ± 1. We take the polarization subscripts of $\chi_{1234}^{(3)}$ to be that of the signal, (1), backward pump, (2), forward pump, (3), and probe beam, (4). The transitions arise from the R_1, R_{21}, Q_1, Q_{21}, and P_1 branches. The plotted intensities are normalized to the signal intensity with all polarizations parallel. Theoretical calculations, described below, assuming a closed, two-level system are plotted as lines in Fig. 1. Note that, in all cases, when the forward pump and probe beams are of the same polarization, the normalized signal significantly exceeds the theory.

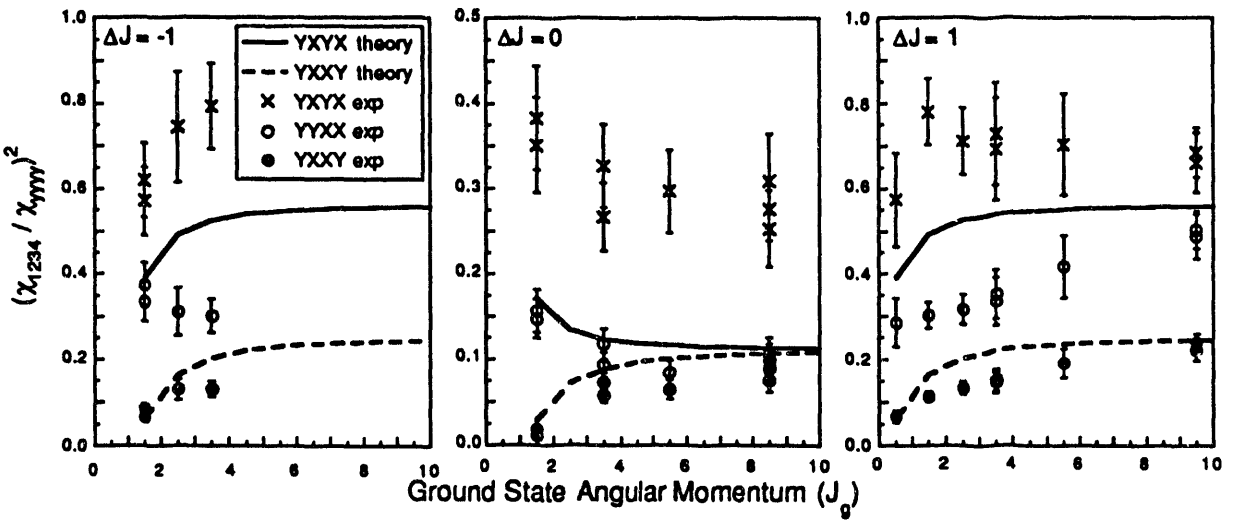

Fig. 1 The polarization characteristics of DFWM signals from OH in an H_2-O_2 flame. The plotted points are ratios of the line-center DFWM signal intensity normalized to the intensity with all polarizations parallel. The data are grouped by the net change in angular momentum (J) involved in the one-photon transition. Note the different vertical scale for the $\Delta J = 0$ transitions. The lines are theoretical ratios based on perturbation theory and a two-level approximation.

Comparisons to theoretical depolarization ratios, such as those in Fig. 1, can provide insight into the mechanisms contributing to the DFWM signal. In the collinear-beam approximation, analytical lineshapes that include Doppler effects can be derived in terms of the complex error function from the perturbation-theory analysis. We use a very general perturbation-theory treatment of $\chi^{(3)}$ for resonant four-wave mixing in molecular gases developed for application to resonance CARS measurements.[1] Recently, detailed formulae for resonance CARS linestrengths have been reported by Attal-Trétout, *et al.*[2] This treatment includes simplified expressions for the polarization dependence and is easily applied to DFWM. We assume here that only one ground state, having total angular momentum J_g is coupled to one excited state, J_n, by a one-photon transition of frequency ω_0. Accounting for the two time orderings of the counter-propagating pump-beam interactions and assuming three-dimensional phase matching, we find the following form for the DFWM susceptibility:

$$\chi_{1234}^{(3)} \propto I_{1234}\left[G_{\Delta k}^{g}(\Delta,\gamma_{gn},\gamma_g) + G_{2k}^{n}(\Delta,\gamma_{gn},\gamma_n)\right] + I_{1324}\left[G_{\Delta k}^{n}(\Delta,\gamma_{gn},\gamma_n) + G_{2k}^{g}(\Delta,\gamma_{gn},\gamma_g)\right], \quad (1)$$

where the subscripts and superscripts of the lineshape functions, G, refer to the k-vector and state in which the two-photon population gratings are formed. The Δk grating is formed by the two-photon interaction between the forward pump and probe beams while the 2k grating is formed by the backward pump interacting with the probe beam. The arguments of G refer to the laser detuning from resonance, ($\Delta = \omega_0 - \omega_1$), the dephasing rate for the one-photon transition, (γ_{gn}), and the population relaxation rates, (γ_g, γ_n). It should be noted that, due to level degeneracies, the

populations and the associated relaxation rates are tensor quantities, including scalar, alignment, and orientational components. The four-photon linestrength arises from the sequence of four electric-dipole interactions with the molecule. Its dependence on rotational quantum numbers and the alignment, ϕ_i, of the (linear) electric vector polarizations is given by[2]

$$I_{1234}(J_g,J_n) = \sum_k \begin{Bmatrix} J_g & J_g & k \\ 1 & 1 & J_n \end{Bmatrix}^2 \left\{ \begin{pmatrix} k & 1 & 1 \\ 0 & -1 & 1 \end{pmatrix}^2 [\cos(\phi_3-\phi_4+\phi_2-\phi_1) + (-1)^k \cos(\phi_3-\phi_4-\phi_2+\phi_1)] + \begin{pmatrix} k & 1 & 1 \\ -2 & 1 & 1 \end{pmatrix}^2 [\cos(\phi_3-\phi_4+\phi_2-\phi_1)] \right\}. \quad (2)$$

Here, the quantities in curly brackets and large parenthesis are 6j and 3j symbols, respectively. We find from Eq. (2) that

$$I_{1234}(J, J+1) = I_{1324}(J+1, J), \text{ and } I_{1234}(J, J+1) > I_{1324}(J+1, J), \quad (3)$$

and

$$I_{1234}(J, J) = I_{1324}(J, J). \quad (4)$$

We observe from Eq. 3 that the $\Delta J \neq 0$. linestrength factors, I_{1234} and I_{1324}, for the two pump beam time orders are not equivalent. As can be observed from Eq. 1, these two time orderings correspond to Δk population gratings in the ground (1234) and excited (1324) states. For $\Delta J = 0$. transitions, the linestrength factors are equal (Eq. 4) after the equally-weighted sum over k in Eq. 2. When $\gamma_g = \gamma_n$ or $G_{\Delta k} = G_{2k}$, the line strengths in Eq. (1) can be factored, ($I_{1234} + I_{1324}$), and the lineshape expressions in Eq. 1 can be combined into a form equivalent to that reported by Abrams and Lind.[3] In these cases, we find that, when the two pump beams are orthogonally polarized, the signal is predicted to be equal for either polarization of the probe beam, ($\chi_{yyxx}^{(3)} = \chi_{xyxy}^{(3)}$). These tensor elements are also equal when $J_g = J_n$ unless different tensor components (the summation index, k, in Eq. 2) of the population relax at different rates. In the backward geometry, when there is significant Doppler broadening, we expect $G_{\Delta k} \neq G_{2k}$ since the 2k grating will wash out and the signal will be dominated by $G_{\Delta k}$. In the experiment described here, for example, the Doppler width is about twice the one-photon dephasing rate[4] and $G_{\Delta k} \cong 20\ G_{2k}$. If the two-level approximation is valid, however, we would expect that $\gamma_g = \gamma_n$ since population leaving the excited level must return to the initial state, filling in the ground-state grating. The theoretical predictions shown in Fig. 1 have been calculated assuming that $\gamma_g = \gamma_n$. Deviations from these predictions provide clues to the nature of the failure of the two-level approximation. Note that the experimental ratios in Fig. 1 deviate from the theory such that $\chi_{yyxx} > \chi_{xyxy}$ for all transitions, including $\Delta J = \pm 1$, and $\Delta J = 0$.

The perturbation-theory results imply that the observed inequality of the components $\chi_{yyxx}^{(3)}$ and $\chi_{xyxy}^{(3)}$ can then be traced to $\gamma_g \neq \gamma_n$, different relaxation rates for the tensor components of population gratings, or to intensity-grating effects not described by the usual expressions for $\chi^{(3)}$. For example, an open-system effect that leaves a long-lived ground-state grating will exhibit $\chi_{yyxx}^{(3)} > \chi_{xyxy}^{(3)}$ for $\Delta J = 1$ and $\chi_{yyxx}^{(3)} < \chi_{xyxy}^{(3)}$ for $\Delta J = -1$ transitions. The observed deviations, however, are nearly the same for these two cases. The case for $\Delta J = 0$ transitions is particularly interesting, since the theory requires *both* open-system ($\gamma_g \neq \gamma_n$) *and* strong elastic orientational relaxation effects to explain the observations. This possibility has been investigated using NDFWM measurements of population lifetimes for different laser polarizations and found to be small and limited to low-J transitions in this flame. The only mechanism, then, consistent with the deviations observed in Fig. 1 is scattering due to an intensity-grating effect such as a thermal grating. A thermal grating would, in fact, contribute only when the forward-pump and probe polarizations are parallel, as is observed. The presence of thermal gratings has also been recently confirmed by NDFWM lineshape analysis and by two-color laser-induced-grating spectra.

* Molecular Physics Lab., PS 061, SRI International, 333 Ravenswood Ave., Palo Alto, CA 94025.

+ Chemistry Department, Stanford University, Stanford, CA 94305-5080

REFERENCES

1) S. A. J. Druet and J. P. E. Taran, Progr. Quantum Electron. **7**, 1 (1981).
2) Brigitte Attal-Trétout, Pascal Monot, and Klaus Müller-Dethlefs, Molec. Phys. **73**, 1257 (1991).
3) R. L. Abrams, J. F. Lam, R. C. Lind, D. G. Steel and P. F. Liao, in *Optical Phase Conjugation*, R. A. Fisher ed. (Academic Press Inc., New York, 1983).
4) Michael S. Brown , Larry A. Rahn and Thomas Dreier, Opt. Lett. **17**, 76 (1992).

Future Plans

The NDFWM lineshape experiments on OH will continue with emphasis on developing quantitative models for thermal grating effects, multilevel population relaxation effects, and orientational relaxation effects. This work will include measurements in the a variable-pressure flame and a microwave-discharge OH source. Pressure and collision-partner studies in the flame will help elucidate the nature of the population grating effects and will allow the development of a complete model for the mechanisms, intensities, and line shapes for DFWM. Measurements will be made on predissociative states of OH or O_2 to confirm the polarization and linestrength characteristics of systems in which only ground-state population gratings are formed. Also, cross-population (one pump beam at a different resonance frequency) studies will be made in an attempt to separate excited and ground-state lifetime measurements.

The discovery of thermal grating contributions to DFWM has motivated the investigation of thermal gratings for diagnostic measurements. Thermal grating spectra are easily modeled since they are just the square of the absorption spectrum, but offer the spatial resolution and background rejection of coherent techniques. Scattering from acoustic waves excited by transient thermal gratings may allow the measurement of ultrasound speed and therefore temperature. These methods will be investigated in laboratory flames with the possible extension to the internally-heated pressure vessel.

Recent inverse Raman (IRS) experiments have extended the H_2-Ar lineshape and shift studies to 1270 K and J-states beyond J = 1. This effort will continue in addition to measurements on the H_2-Ne system. Analysis of these results will provide insight into the fundamental H_2 speed-dependent inhomogeneous lineshape. IRS studies of collisional broadening of the O_2 Q branch will be initiated in a new internally-heated pressure vessel. We will also initiate a program to measure pure-rotational S-branch broadening coefficients for H_2 and O_2. The semiclassical line-broadening calculations in collaboration with J. P. Looney (NIST) will be continued using his implementation of the theory of J. Bonamy and D. Robert.

L. A. Rahn: BES-Supported Research Publications 1991-93

Robert P. Lucht, Rick Trebino, and L. A. Rahn, "Resonant Multiwave Mixing Spectra of Gas-Phase Sodium: Nonperturbative Calculations, "Phys. Rev. A., **45**, 8209 (1992).

L. A. Rahn, Michael S. Brown and Thomas Dreier, "High-Resolution Degenerate Four-Wave-Mixing Spectral Profiles of OH," Opt. Lett. **17**, 76 (1992).

L. A. Rahn, R. L. Farrow, and G. J. Rosasco, "Measurement of the Self-Broadening of the H_2 Q(0-5) Transitions from 295 to 1000 K," Phys. Rev. A **43**, 6075 (1991).

Reactions of Carbon Atoms in Pulsed Molecular Beams

Hanna Reisler
Department of Chemistry, University of Southern California
Los Angeles, CA 90089-0482

Program Scope

This research program consists of a broad scope of experiments designed to unravel the chemistry of atomic carbon in its two spin states, ^3P and ^1D, by using well-controlled initial conditions and state-resolved detection of products. Prerequisite to the proposed studies (and the reason why so little is known about carbon atom reactions), is the development of clean sources of carbon atoms. Therefore, in parallel with the studies of its chemistry and reaction dynamics, we continuously explore new, state-specific and efficient ways of producing atomic carbon. In our current program, $C(^3P)$ is produced via laser ablation of graphite, and three areas of study are being pursued: (i) exothermic reactions with small inorganic molecules (e.g., O_2, N_2O, NO_2) that can proceed via multiple pathways; (ii) the influence of vibrational and translational energy on endothermic reactions involving H-containing reactants that yield CH products (e.g., H_2O, H_2CO); (iii) reactions of $C(^3P)$ with free radicals (e.g., HCO, CH_3O). In addition, we plan to develop a source of $C(^1D)$ atoms by exploiting the pyrolysis of diazotetrazole and its salts in the ablation source. Another important goal involves collaboration with theoreticians in order to obtain relevant potential energy surfaces, rationalize the experimental results and predict the roles of translational and vibrational energies.

Recent Progress

— *$C(^3P) + N_2O$ reaction:* We have generated energy distributions in both the CN and NO products using *free ablation* as the $C(^3P)$ source, i.e., at relative collision energy 0.9 ± 0.4 eV. We find that the CN vibrational distribution is inverted, peaking at v=3 and extending to at least v=7. The $NO(X^2\Pi)$ vibrational distribution is much colder than the $CN(X^2\Sigma^+)$ distribution, peaking at v=0. This is not surprising, since NO is the 'old bond', which usually exhibits much less vibrational excitation than the 'new bond', CN. Since some energy flow does occur during the reaction, it suggests that although the reaction possesses 'direct' character, it proceeds through an intermediate CNNO complex which dissociates to products on a short time-scale with respect to energy redistribution in the complex. The CN and NO v=0 rotational distributions are 'hot' and not Boltzmann-like suggesting that a bent CNNO intermediate is involved producing a large exit-channel torque. The reaction was studied using free jets of carbon and N_2O beams, without control of the kinetic energy of the reactants. Also, because of the undefined geometry in the interaction region, flux-to-density transformations were difficult to achieve, and accurate energy distributions were not ob-

tained. Therefore, the experimental arrangement was upgraded as described below. The upgrade is now complete, and at present the reaction is being studied as a function of the translational energy of the carbon atoms.

— *Upgrading of pulsed-beam machine*: The laser-ablation crossed-beam machine built for the studies of carbon atom reactions is general and can be used for state-to-state studies of reactions of other atoms produced by ablation. It includes capabilities for controlling the translational energy of the reactants via aerodynamic acceleration, and their vibrational energy via tunable IR laser excitation. The original apparatus consisted of two differentially pumped sections — a reaction chamber and an ablation chamber containing the carbon source. The octagonal stainless steel reaction chamber was designed for maximum experimental flexibility, allowing for multiple laser-detection geometries. In the current configuration, the probe laser beam propagates in a direction orthogonal to the photomultiplier tube axis and is oriented at 45° to the axes of the atomic and molecular beams. Recently, the following modifications were introduced to enable work with skimmed, seeded beams:

- A pulsed-nozzle with opening times < 40 μs was added to the carbon source and side ablation was introduced, so that a skimmed seeded carbon beam, whose translational energy is controlled by changing the carrier gas combination, could be used.

- A third differentially pumped chamber was added (6" diffusion pumps) as a source chamber for the molecular reactant beam in order to reduce the pressure in the reaction chamber and minimize relaxation.

- Skimmers were added to both beams in order to define the interaction region for flux-to-density transformation.

- The ablation laser was changed to a Nd:YAG laser with gaussian optics operating on the 4th harmonic (266 nm). This modification was crucial for the elimination of higher C_n clusters which are more prevalent in seeded beams.

— *Detection of Atomic Carbon:* $C(^3P)$ produced by the ablation was detected directly via two-photon LIF to enable us to optimize its production. Atomic carbon was excited in the $3^3P \leftarrow 2^3P$ transition by two-photon LIF near 280 nm, and vuv fluorescence was detected with a solar blind photomultiplier. The distribution of the spin-multiplets was statistical and no $C(^1D)$ was detected (Fig. 1). C_2 and C_3 were routinely detected by one-photon LIF. We found that the concentrations of the C_n species depend crucially on the shape, focal point, intensity and wavelength of the ablation laser beam, and with proper ablation conditions atomic carbon can become the predominant species.

With the above improvements, good signals of products have been detected with only small interference from higher clusters. An example is

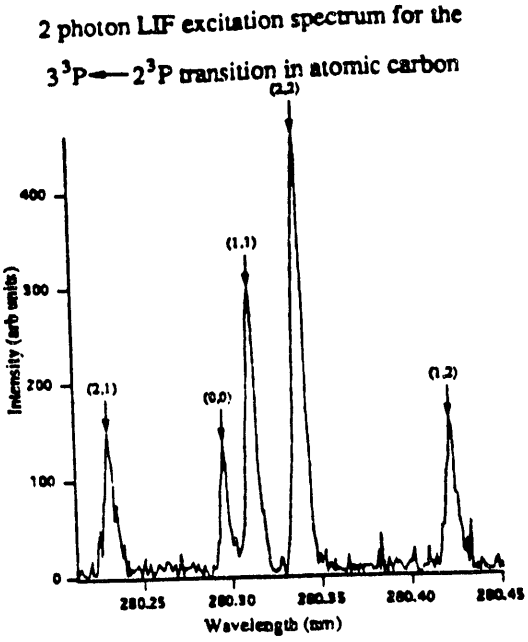

shown in Fig. 2, where the CN signal obtained in the $C(^3P) + N_2O$ reaction using a seeded beam of carbon in He is shown. In the figure we show the (0,0) transition of the CN(B← X) system.

Fig. 1: $C(^3P)$ detection

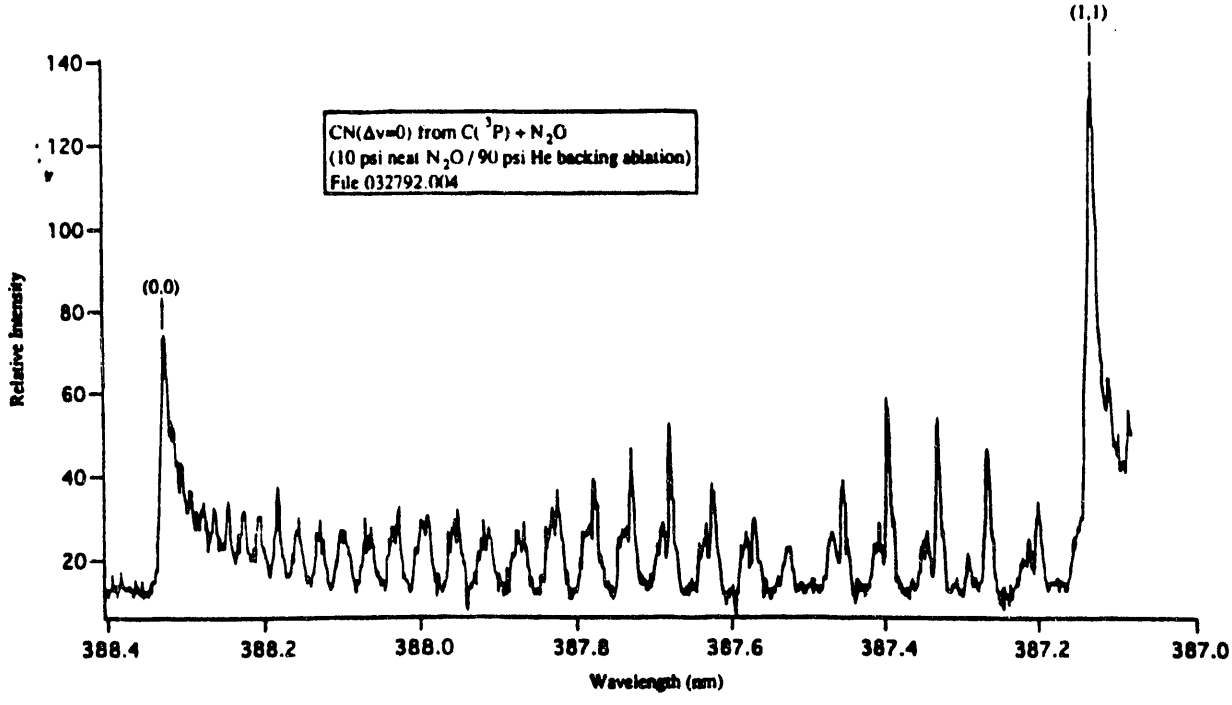

Fig. 2: CN v=0 LIF signal from the $C(^3P) + N_2O$ reaction

Future Plans

We will continue to study the prototypical $C(^3P) + N_2O$ system which can proceed via several exothermic pathways. We will determine the effect of the relative kinetic energy, observe as many primary product channels as possible, identify correlations among products, and attempt to determine the geometry of the CNNO intermediate and to induce spin-forbidden channels (e.g., by clustering N_2O with Xe).

We will study endothermic reactions of $C(^3P)$ with H-containing molecules, emphasizing the influence of reactant vibrational and translational energy. In contrast to reactions of $C(^3P)$ with oxidants, which are usually exothermic, many of its reactions with hydrocarbons and other H-containing molecules are endothermic. This is so because the CH product has a relatively weak bond (D_0 = 81 kcal mol^{-1}). Thus, these reactions provide opportunities for studying the importance of kinetic and vibrational energy in enhancing reactivity, and can yield information on activation barriers. Transitions involving CH, OH and NH stretches are often strong and localized, and their overtones can be efficiently excited. Moreover, in abstraction reactions yielding CH, the excited bonds are directly correlated with the reaction coordinate. The vibrational excitation will be achieved using an IR OPO recently constructed in our lab. High overtone excitation will be achieved using either intense tunable dye lasers or a narrow bandwidth Ti:Sapphire laser that we plan to purchase this summer.

We have also begun preparations for the study of reactions of atomic carbon with radicals, and are now constructing a pulsed pyrolysis source based on the design of Prof. Peter Chen [Rev. Sci. Inst., 63, 4003 (1992)]. With this source we will initially study the reaction of atomic carbon with HCO.

Publications in 1991-1993:

1. *The reactions of $C(^1D)$ with H_2 and HCl: Product state excitations, Λ-doublet propensities and branching ratios*, D.C. Scott, J. de Juan, D.C. Robie, D.M. Schwarz-Lavi and H. Reisler, J. Phys. Chem., **96**, 2509 (1992).

2. *Identification of the 278.2 nm peak of the CCl $A^2\Delta$-$X^2\Pi$ system as the (0,0) P_1 bandhead*, D.C. Robie, J. de Juan and H. Reisler, J. Molec. Spectrosc., **150**, 296 (1991).

3. *A crossed beam study of the reaction $C(^3P)+N_2O$: Energy partitioning between the NO and CN products* , S.A. Reid, F. Winterbottom, D.C. Scott, J. de Juan and H. Reisler, Chem. Phys. Lett., **189**, 430 (1992).

Spectroscopic Probes of Vibrationally Excited Molecules at Chemically Significant Energies

Thomas R. Rizzo

Department of Chemistry
University of Rochester
Rochester, NY 14627

This project involves the application of multiple-resonance spectroscopic techniques for investigating energy transfer and dissociation the dynamics of highly vibrationally excited molecules. Two major goals of this work are: 1) to provide information on potential energy surfaces of combustion related molecules at chemically significant energies, and 2) to test theoretical modes of unimolecular dissociation rates critically *via* quantum-state resolved measurements.

Recent Progress

Spectroscopy and Unimolecular Dissociation Dynamics of HN_3

In the last year we have been applying infrared-optical double resonance to investigate the unimolecular dissociation dynamics of hydrazoic acid (HN_3). Our goal has been to probe the topology of the potential surface and provide stringent test of *ab initio* calculations. Figure 1 shows a schematic of the reaction coordinate for HN_3 dissociation.

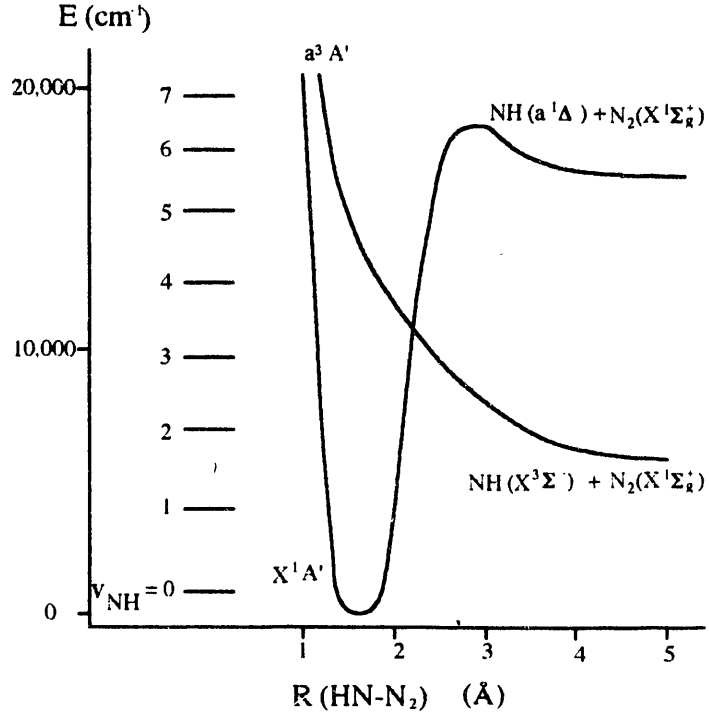

Figure 1. Schematic of Reaction Coordinate for HN_3 dissociation.

A curve crossing between the ground state and a low lying dissociative excited state can lead to dissociation via a spin forbidden channel to produce NH ($^3\Sigma$) + N_2. At sufficiently high energies there is a competition between dissociation on the spin allowed singlet surface and spin forbidden triplet surface, and this competition is sharply dependent upon the reactant energy. Moreover, the topology of the exit channel on the singlet surface is not well characterized. There appears to be a barrier along the coordinate to produce NH($^1\Delta$) + N_2, however estimates of this barrier range from 450 to 1740 cm^{-1}.

Our infrared-optical double resonance studies of this molecule have been aimed at determining: 1) the precise threshold for producing NH($^1\Delta$); 2) the height of the barrier on the singlet surface; 3) the geometry of the molecule at the transition state; and 4) the nature of the coupling of the NH stretch vibration to the other vibrational modes of the molecule. All of this information can be extracted from infrared-optical double resonance photofragment excitation spectra of HN_3 and LIF spectra of the resulting NH fragments. The first step in this process, which we have recently completed, involves assigning the double resonance overtone spectra. The assigned spectra in Fig 2 demonstrate our ability to prepare HN_3 molecules in selected rotational states of the the $6\nu_{NH}$ level.

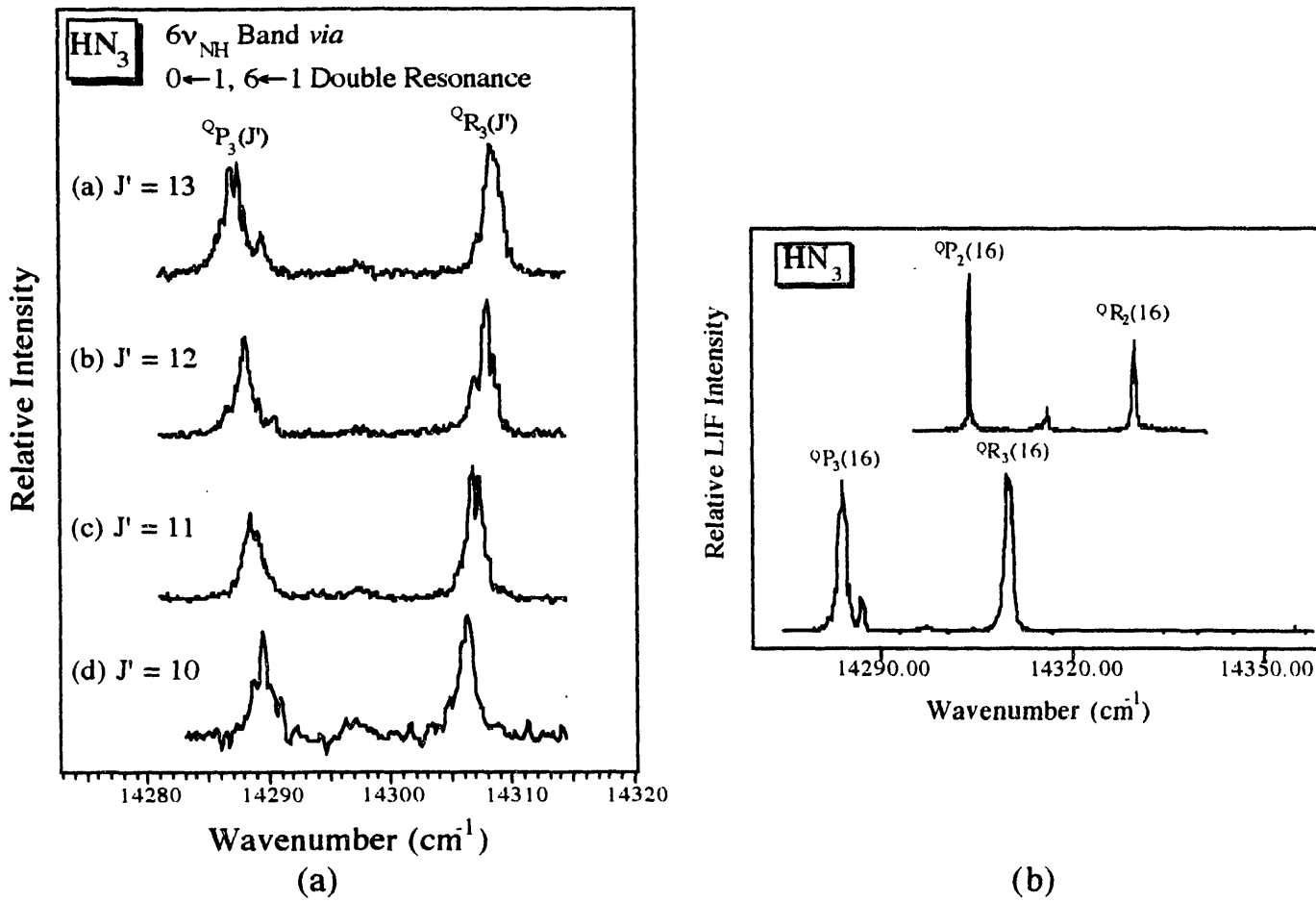

Figure 2. Series of $6\nu_{NH}$ vibrational overtone excitation spectra of HN_3 recorded by infrared-optical double resonance photofragment spectroscopy. An infrared pulse from an optical parametric oscillator prepares HN_3 molecules in v=1 of the OH stretch with a well defined value of J' and K', and a high energy pulse from a tunable dye laser is scanned across the 6←1 vibrational overtone band. Detection of the second photon is accomplished by monitoring the NH fragments *via* laser induced fluorescence. (a) Transitions to states in $6\nu_{NH}$ with K=3 and J=9-14; (b) Comparison of transitions to states with K=2 and K=3 in $6\nu_{NH}$. (Unprimed quantum numbers pertain to the molecule in ν_{NH}=6).

We are in the process of determining the singlet *threshold* by observing how high in J and K we must excite the reactant before dissociation occurs on the singlet surface. This procedure also provides information on the HN_3 rotational constants at the transition state. We will determine the *barrier* on the singlet surface by combining our knowledge of the reaction threshold with measured rotational state distributions of the singlet NH products.

Future Plans

In the coming year we plan to complete our work on HN_3 and apply infrared-optical double resonance spectroscopy to examine the dissociation dynamics of HONO. The HONO molecule can exist in cis- and trans- forms and is a prototype system for isomerization reactions. We plan to use infrared optical double resonance to probe the dynamics of unimolecular isomerization at the v=1 and v=2 levels of the OH stretch.

We are also currently developing the ability to monitor atomic dissociation fragments *via* LIF in the VUV region of the spectrum. VUV light will be generated by frequency tripling in low pressure xenon. Monitoring atomic dissociation fragments such as H atoms will both extend the generality of our spectroscopic techniques and increase their sensitivity. We plan to use this increased sensitivity to measure double resonance photofragment spectra of photogenerated free radicals.

Publications from DOE Supported Work 1991-93

1. X. Luo and T. R. Rizzo. "Unimolecular Dissociation of Hydrogen Peroxide from Single Rovibrational States Near Threshold." J. Chem. Phys. **94**, 889 (1991).

2. P. R. Fleming, M. Li and T. R. Rizzo. "Infrared Spectroscopy of Vibrationally Excited $HONO_2$: Shedding Light on the Dark States of IVR." J. Chem. Phys. **94**, 2425 (1991).

3. "Local Modes of HOOH Probed by Optical-Infrared Double Resonance", P. R. Fleming, M. Li, and T. R. Rizzo, J. Chem. Phys. **95**, 865 (1991).

4. P. R. Fleming and T. R. Rizzo. "Infrared spectrum of t-butyl hydroperoxide excited to the $4\nu_{OH}$ vibrational overtone level." J. Chem. Phys. **95**, 1461 (1991).

5. P. R. Fleming, X. Luo, and T. R. Rizzo,"Multiple Laser Probes of Intramolecular Dynamics at Chemically Significant Energies", in *Mode Selective Chemistry*, B. Pullman and J. Jortner, eds., (Kluwer, Dordrecht, 1991).

6. "Product Energy Partitioning in the Unimolecular Decomposition of Vibrationally and Rotationally State Selected Hydrogen Peroxide", X. Luo and T. R. Rizzo, J. Chem. Phys. **96**, 5129 (1992).

7. "Vibrational overtone spectroscopy of the $4\nu_{OH}+\nu_{OH'}$ combination band of HOOH via sequential local mode-local mode excitation", X. Luo and T. R. Rizzo, J. Chem. Phys. **96**, 5659 (1992).

8. "CO_2 Laser Assisted Vibrational Overtone Spectroscopy", R. D. F. Settle and T. R. Rizzo, J. Chem. Phys. **97**, 2823 (1992).

Applications of Laser-Induced Gratings to Spectroscopy and Dynamics

Eric A. Rohlfing
Combustion Research Facility
Sandia National Laboratories
Livermore, CA 94551

Program Scope:

This program has traditionally emphasized two principal areas of research. The first is the spectroscopic characterization of large-amplitude motion on the ground-state potential surface of small, transient molecules. The second is the reactivity of carbonaceous clusters and its relevance to soot and fullerene formation in combustion. Motivated initially by the desire to find improved methods of obtaining stimulated emission pumping (SEP) spectra of transients, most of our recent work has centered on the use of laser-induced gratings or resonant four-wave mixing in free-jet expansions. These techniques show great promise for several chemical applications, including molecular spectroscopy and photodissociation dynamics. In this abstract I describe our applications of two-color laser-induced grating spectroscopy (LIGS) to obtain background-free SEP spectra of transients and double-resonance spectra of nonfluorescing species, and the use of photofragment transient gratings to probe photodissociation dynamics.

Recent Progress:

Two-color LIGS is a class of resonant four-wave mixing (RFWM) processes that, because of the frequency and (possible) temporal separation of the two input fields, is particularly easy to describe via induced gratings. In our experiments, two laser beams at ω_1 are crossed at a shallow angle in a free-jet expansion; the interference between these two beams forms a spatially modulated intensity pattern. If ω_1 is tuned to a molecular transition, absorption creates a spatial modulation (grating) in the populations in the ground and excited states connected by the transition. If the probe laser frequency, ω_2, is resonant with a transition from either of the levels involved in the grating transition, then the probe beam "sees" a spatially modulated absorption and diffracts off the ground- or excited-state population grating. When the probe laser diffracts off the excited-state grating via downward transitions to higher ground-state rovibrational levels, the two-color LIGS spectrum yields the same spectral information as an SEP spectrum detected by the conventional method of fluorescence depletion. We have recently used this approach to generate background-free SEP spectra of jet-cooled SiC_2. The zero-background nature of LIGS-SEP provides a tremendous advantage over fluorescence depletion, in which small depletions from a large (and fluctuating) fluorescence background must be detected.

One of the great promises of four-wave mixing techniques is that signal generation depends on molecular absorption; thus these approaches should be applicable to non-fluorescing molecules. We have recently applied two-color LIGS to obtain absorption-like spectra of jet-cooled NO_2 both below and above its threshold for predissociation into NO+O. In these experiments, the grating-forming beams are tuned through the dissociation threshold while the probe laser frequency is fixed to a specific rotational line of an isolated, cold vibronic band well below threshold. The probe beam diffracts off the population depletion grating that occurs when ω_1 excites a transition out of the ground-state

rotational level (K"=0, N") that is selected by the probe laser. The resulting spectrum is a true double resonance spectrum that maps the absorption spectrum out of the selected rotational level. In Fig. 1, we compare a two-color LIGS spectrum (N"=0) with an LIF spectrum in the near-threshold region. As anticipated, the LIGS spectrum persists above threshold where the quantum yield of fluorescence is negligible. Under the collision-free conditions of a fully expanded free jet, this type of LIGS spectrum maps the square of the absorption spectrum. Thus, by fitting the lineshapes of isolated spectral lines above threshold to the square of a Lorentzian, we obtain the predissociation lifetimes of NO_2 in the near-threshold region; two examples are shown in Fig. 1.

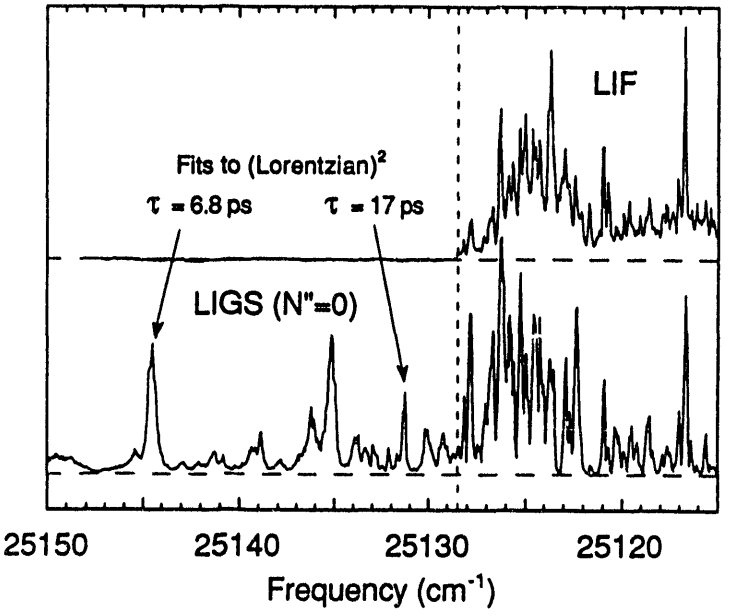

FIG. 1. A comparison of the LIF and two-color LIGS spectra of jet-cooled NO_2 near the dissociation threshold at 25 128.5 cm^{-1} (indicated by the dotted vertical line). The LIGS spectrum is recorded with the probe laser tuned to the $^qR_0(0)$ line and thus selects only the N"=0 level; the LIF spectrum samples all N" levels populated in the jet (N"=0 and N"=2 in roughly equal abundance). The horizontal dashed lines indicate the true signal zeroes for each spectrum. Predissociation lifetimes for two isolated vibronic lines are shown.

In a variation of two-color LIGS, we have used photofragment transient gratings to measure populations, velocities, and translational anisotropies of nascent, state-selected photofragments. In these experiments on jet-cooled NO_2, we make use of the fact that the spatial modulation in the electronically excited state is rapidly transformed via predissociation into spatial modulations in the NO and O photofragments. We probe the NO photofragment grating on the (0,0) band of the $A^2\Sigma^+$–$X^2\Pi$ system at 226 nm. Scanning the probe laser gives spectra that reveal fragment-state populations and scanning the grating laser, with the probe laser monitoring a specific fragment state, produces photofragment excitation (PHOFEX) spectra. For photolysis at 126 cm^{-1} above threshold, the NO rotational distribution obtained from the probe spectrum is in excellent agreement with that determined from an LIF spectrum recorded simultaneously. From the grating PHOFEX spectrum we determine a revised value of the threshold for production of $NO(^2\Pi_{1/2}, v"=0, J"=0.5, e)+O(^3P_2)$ from NO_2 (N"=0) as 25 128.5±0.2 cm^{-1}.

In the photofragment transient grating experiment, both the photolysis and the probe laser frequencies are fixed, and the signal diffracted from the photofragment grating is measured as a function of the time delay between the photolysis and probe pulses. The photodissociation produces translationally excited photofragments whose angular distribution relative to the polarization vector of the photolysis laser, ε_p, is determined by the anisotropy parameter, β. When $\beta=2$ and ε_p is perpendicular to the grating fringes the fragments travel predominantly in the direction perpendicular to the grating fringes (z). In

effect, there are two counterpropagating population gratings: one traveling in the positive z direction and one traveling in the negative z direction. After a time interval that corresponds approximately to traveling a quarter of a fringe spacing, the peaks of one grating overlap with the nulls of the other grating, and the net population grating vanishes. As time increases, the two counterpropagating gratings "rephase" and the net population grating reappears. This phenomenon causes oscillations in the grating decays that carry information on the speed and angular distributions of the fragments.

In Fig. 2 we display the photofragment grating decays for NO fragments in three rotational states produced by photolysis at 126 cm^{-1} above threshold. The left and right panels are results for ε_p perpendicular and parallel to the grating fringes, respectively. The signal oscillations are most pronounced for the former since β is large and positive and thus the fragments are moving predominantly perpendicular to the fringes. Conversely, when ε_p is parallel to the fringes the fragments move mostly along the fringes and few oscillations are observed. The photofragment grating decay is related to the Fourier transform of the velocity distribution of the fragments perpendicular to the fringes.[1] Using this relationship we fit our data to a model that incorporates the standard velocity distribution for photofragments along a space-fixed axis and includes convolutions with the grating and probe laser pulse widths and the velocity distribution of the parent molecule. We determine both fragment speeds and anisotropies; the speeds are in excellent agreement with the known values, even for fragments with as little as 7.3 cm^{-1} of translational energy (J"=7.5 in Fig. 2).

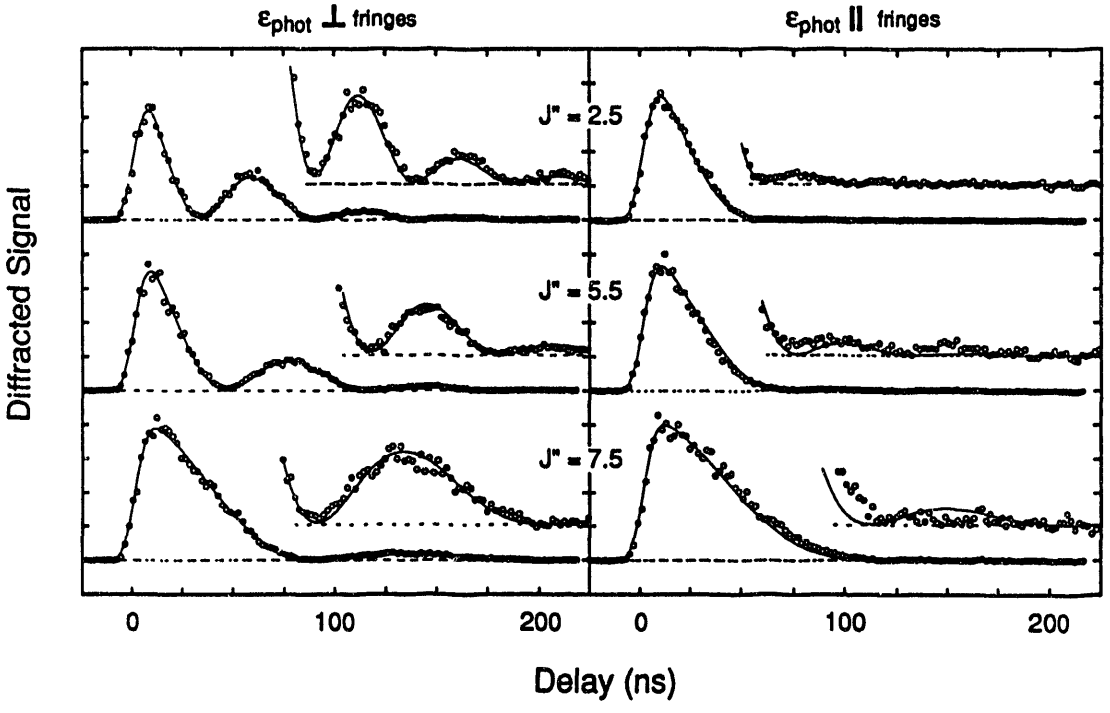

FIG. 2. Photofragment transient grating signals for NO($^2\Pi_{1/2}$, v"=0, e) in J"=2.5, 5.5, and 7.5 produced from the photolysis of jet-cooled NO_2 at an excess energy of 125.9 cm^{-1}. The left and right panels are results for polarization of the photolysis laser (ε_p) perpendicular and parallel to the grating fringes. The lines are the simultaneous least-squares fits of both data sets to a model for the time evolution of the photofragment. Each decay is normalized to one and the insets are 10X magnifications that are vertically offset for clarity.

The photofragment transient grating approach is essentially a time-domain analog of Doppler lineshape measurements made in the frequency domain. The crucial difference in the applicability of these two techniques has to do with the range of product velocities that can be measured using standard pulsed lasers (bandwidth~0.1 cm^{-1} and pulsewidth~10 ns). With such lasers, Doppler spectroscopy can be applied only to fast-moving fragments, typically light fragments produced by photolysis well above threshold. Conversely, the photofragment transient grating technique is ideally suited to slow-moving fragments, such as heavy fragments or light fragments produced by near-threshold photolysis.

References

1. T.S. Rose, W.L. Wilson, G. Wäckerle and M.D. Fayer, J. Chem. Phys. **86**, 5370 (1987).

Future Work:

We shall continue to develop and apply two-color LIGS as a spectroscopic tool for nonfluorescing species, including large molecules that undergo rapid nonradiative decay. The photofragment grating technique will be applied to other near-threshold photodissociations. We shall continue to characterize large-amplitude vibrational motion in SiC_2 through further SEP studies, using LIGS or RFWM; SEP data will be analyzed with a semirigid bender model to extract the large-amplitude potential function. The chemical reactions of carbon and carbonaceous clusters will be pursued using the fast flow reactor/TOF MS apparatus, with an emphasis on reactions of carbonaceous clusters with hydrocarbons as prototypes for reactions that lead to fullerenes or soot in combustion.

Publications: 1991-present

T. J. Butenhoff and E. A. Rohlfing, "Laser-Induced Gratings in Free Jets I. Spectroscopy of Predissociating NO_2," J. Chem. Phys., in press (1993).

T. J. Butenhoff and E. A. Rohlfing, "Laser-Induced Gratings in Free Jets II. Photodissociation Dynamics via Photofragment Transient Gratings," J. Chem. Phys., in press (1993).

T. J. Butenhoff and E. A. Rohlfing, "Resonant Four-Wave Mixing of Transient Molecules in Free Jets," J. Chem. Phys. **97**, 1595 (1992).

"Hydrogenation Reactions of Neutral Carbon Clusters: C_n (n=6-75) + D_2," T. J. Butenhoff and E. A. Rohlfing, Twenty-Fourth Symposium (International) on Combustion, The Combustion Institute, Pittsburgh, PA, p. 947 (1992).

T. J. Butenhoff and E. A. Rohlfing, "The C $^3\Pi$ - X $^3\Pi$ Band System of the SiC Radical," J. Chem. Phys. **95**, 3939(1991).

T. J. Butenhoff and E. A. Rohlfing, "Laser-Induced Fluorescence Spectroscopy of Jet-Cooled SiC_2," J. Chem. Phys. **95**, 1(1991).

F. J. Northrup, T. J. Sears, and E. A. Rohlfing, "A Semirigid Bender Analysis of an Extensive Set of Rotation-Vibration Levels in $\tilde{X}\,^1\Sigma_g^+$ C_3," J. Mol. Spectrosc. **145**, 74 (1991).

Electronic Structure, Molecular Bonding and Potential Energy Surfaces

Klaus Ruedenberg
Ames Laboratory USDOE, Iowa State University, Ames, Iowa 50011

Program Scope

By virtue of the universal validity of the generalized Born-Oppenheimer separation, potential energy surfaces (PES') represent the central conceptual as well as quantitative entities of chemical physics and provide the unifying basis for the understanding of most physico-chemical phenomena in many diverse fields. The research in this group deals with the elucidation of general properties of PES' as well as with the quantitative determination of PES' for concrete systems, in particular pertaining to reactions involving carbon, oxygen, nitrogen and hydrogen molecules.

Recent Progress

We are in the process of determining the global characteristics as well as the critical features of the PES' of the singlet and triplet valence states of ozone. The examination of the $1^1A'$ and the $2^1A'$ states in the entire three-dimensional internal coordinate space has been completed. The $1^1A'$ state has three open minima and one ring minimum, the $2^1A'$ state has only three open minima. In both states, dissociation occurs by abstraction of one end atom at an approximate constant open apex angle. Isomerization between the three open minima is a possibility in the $2^1A'$ state but not in the $1^1A'$ state. The two states approach each other quite closely along an extended two-dimensional surface in the three-dimensional coordinate space and, in fact, intersect along a one-dimensional seam consisting of four loops connected by three nodes as shown in Figure 1. The investigation of the other states is in progress.

In addition, a number of general problems have been addressed.

The aforementioned intersection poses a fundamental problem since the two states are both closed-shell singlets of like symmetry. Intersections between such states had not been previously known. This is understandable because, typically, each of the two states is dominated by *one* closed-shell determinant and the hamiltonian matrix element between two such determinants, by virtue of being a simple exchange integral, cannot change sign. We established that the present case is different in that the two diabatic states, from which the two adiabatic states are formed, both contain two dominant determinants so that, altogether, four closed-shell determinants of like symmetry are involved. *The conclusion is that strong shifts in diabatic correlations can cause conical intersection between closed-shell adiabatic singlets of like symmetry.*

In connection with this work a new, simple and effective method has been developed for the resolution of adiabatic states ψ_1, ψ_2 in terms of diabatic states ϕ_1, ϕ_2:

$$\psi_n = \sum_i T_{ni}\,\phi_i\,, \qquad \psi_n = \sum_\alpha \chi_\alpha\, C_{\alpha n}\,, \qquad \phi_i = \sum_\alpha \chi_\alpha\, (CT)_{\alpha i}$$

$\mathbf{T}$ = orthogonal, χ_α = configuration state wave functions.

If the dominant configurations are such that

Dominant Configurations	Adiabatic States	
	Region I	Region II
$\chi_1 \cdots \chi_a$	dominant in ψ_1	dominant in ψ_2
$\chi_{a+1} \cdots \chi_{a+b}$	dominant in ψ_2	dominant in ψ_1

then the transformation matrix T is determined by maximizing $\sum_{\alpha=1}^{a} (CT)_{\alpha 1}^2 + \sum_{\beta=\alpha+1}^{a+b} (CT)_{\beta 2}^2$, which leads to the eigenvalue problem of a matrix constructed from partial inner products of the columns of C. Figure 2 exhibits the PES of the adiabatic 1^1A_1 and 2^1A_1 states of O_3 in C_{2v} symmetry and the corresponding diabatic states obtained by this method. It also applies to the resolution of N adiabatic states in terms of diabatic states.

A novel method was developed for determining an intersection. It is based on the Herzberg-Longuet-Higgins-Berry phase change theorem and on the fact that, on any path in coordinate space looping around an intersection, one encounters two places where $(H_{11} - H_{22})$ changes sign and two places where H_{12} changes sign. Both induce a characteristic behavior change in the coefficients of the configurations χ_k which allows iteration towards the intersection by successive interpolations.

Since only little quantitative information is available on conical intersections, we analyzed the shapes of two POS of the same symmetry in the vicinity of their conical intersection on the basis of general principles. Aside from minor distinctions, nine types of such intersections were found to exist and their characteristically different energy contours in the two-dimensional branching space were determined. Examples are shown in Figure 3.

As a tool for the global examination of POS', we have developed a new method for following reaction paths, i.e. steepest descent lines (in mass weighted coordinates) on POS'. It is a quadratic generalization of Euler's method, using analytic gradients with or without analytic hessians, and compares favorably with existing methods. It has also proven superior to conventional quasi-Newton methods for minima searching. It is illustrated in Figure 4.

Certain reaction paths follow "streambeds" on potential energy surfaces. Such streambeds are characterized by *gradient extremals*, introduced by us several years ago. We have now shown that gradient extremals are those curves on POS' which connect the points where steepest descent lines have zero curvature, as shown in Figure 5.

The discussed elucidations complement the classification of bifurcating reaction paths on potential energy surfaces which we derived in a previous analysis.

Planned Work

The determination of the valence state potential energy surfaces of ozone will be continued. The stable structures, transition states, reaction paths, intersections etc. will be identified. These features and the concomitant energy changes will be elucidated through an analysis of the electronic structure. To this end, an analysis of molecular energies in terms of interactions between atoms-in-molecular will be developed.

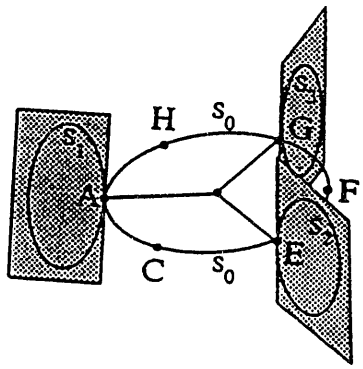

Fig. 1. Intersection seam between $1^1A'$ and $2^1A'$ POS' of O_3.

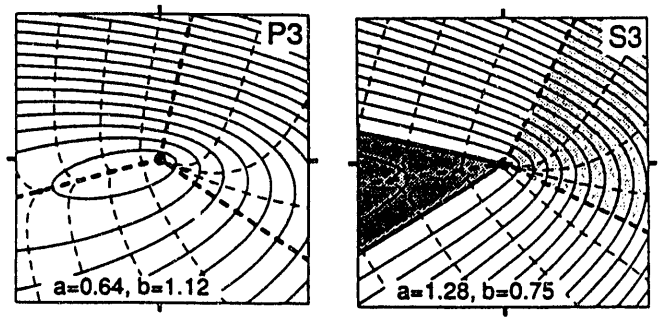

Fig. 3. Possible POS contour maps near a conical intersection.

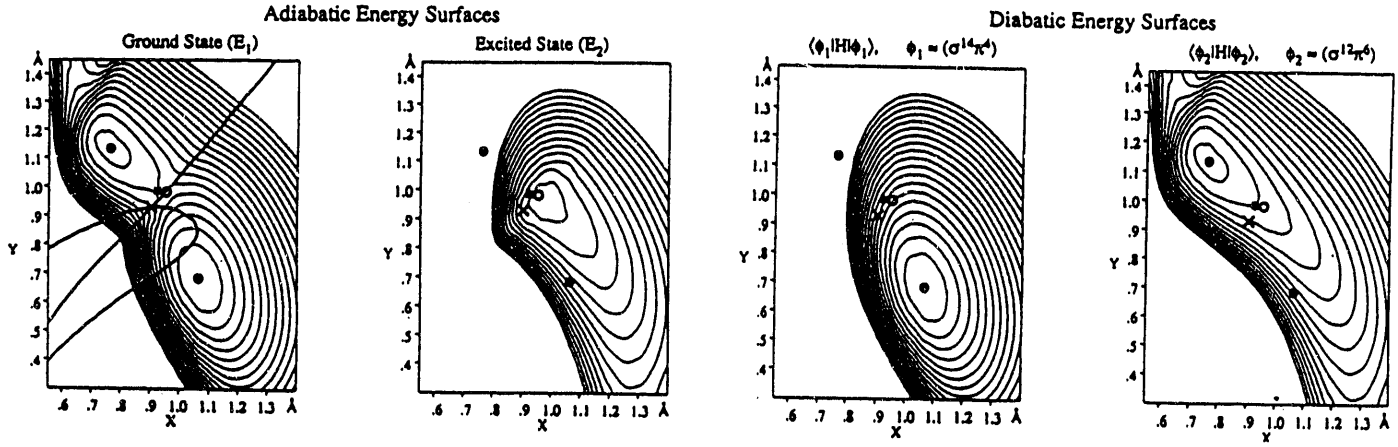

Fig. 2. Diabatic resolution of adiabatic 1^1A_1 and 2^1A_1 states of ozone.

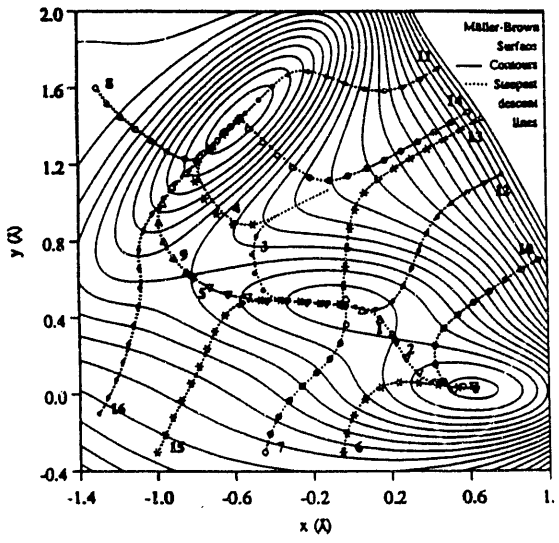

Fig. 4. Steepest descent algorithm on Müller-Brown POS.

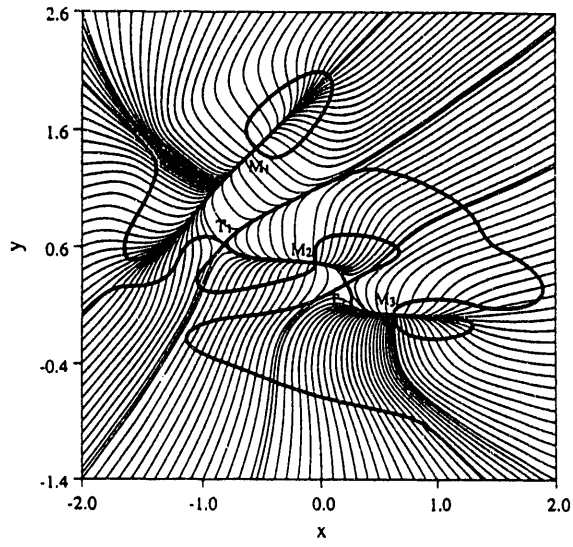

Fig. 5.Steepest descent field and gradient extremals (bold) on Müller Brown POS.

Publications 1991, 1992, 1993

The Ring Opening of Cyclopropylidene to Allene: Global Features of the Reaction Surface. P. Valtazanos, S. T. Elbert, S. Xantheas, K. Ruedenberg, Theor. Chim. Acta, 78, 287 (1991).

The Ring Opening of Cyclopropylidene to Allene and the Isomerization of Allene: Ab-Initio Interpretation of the Electronic Rearrangements in terms of Quasiatomic Orbitals. S. Xantheas, P. Valtazanos, K. Ruedenberg, Theor. Chim. Acta, 78, 327 (1991).

The Ring Opening of Cyclopropylidene to Allene: Key Features of the Accurate Reaction Surface. P. Valtazanos, S. Xantheas, S. T. Elbert, K. Ruedenberg, Theor. Chim. Acta, 78, 365 (1991).

The Ring Opening of Substituted Cyclopropylidene to Substituted Allene: The Effect of Steric and Long Range Electrostatic Interactions. P. Valtazanos and K. Ruedenberg, Theor. Chim. Acta, 78, 397 (1991).

Potential Energy Surfaces of Ozone. S. Xantheas, G. J. Atchity, S. T. Elbert, K. Ruedenberg, J. Chem. Phys., 94, 8054 (1991).

Potential Energy Surfaces Near Intersections. G. J. Atchity, S. Xantheas, and K. Ruedenberg, J. Chem. Phys. 95, 1862 (1991).

Efficient Use of Jacobi Rotations for Orbital Optimization and Localization. R. C. Raffenetti, K. Ruedenberg, C. L. Janssen, H. F. Schaefer, Theor. Chim. Acta, in press (1993).

Gradient Extremals and Steepest Descent Lines on Potential Energy Surfaces. J. Q. Sun and K. Ruedenberg, J. Chem. Phys, in press (1993).

Quadratic Steepest Descent on Potential Energy Surfaces. J. Q. Sun and K. Ruedenberg, J. Chem. Phys., submitted.

A Quantum Chemical Determination of Adiabatic States. K. Ruedenberg and G. J. Atchity, J. Chem. Phys., submitted.

Electronic Structure Basis for the Conical Intersection between the Lowest Two $^1A_1$ States of Ozone. G. J. Atchity and K. Ruedenberg, J. Chem. Phys., submitted.

Oriented Atoms Least Squares.

I. Methodology;

II. Application to 9-tertbutylanthracene, tetrafluoroterephthalodinitrile, and 1,2,3 triazine. L. L. Miller, J. E. Niu, W. H. E. Schwarz, K. Ruedenberg, R. A. Jacobson, Acta Crystallographica B, submitted.

The Attractive Quartet Potential Energy Surface for the $CH(a^4\Sigma^-)$ + CO Reaction : A Role for the a $^4A''$ State of the Ketenyl Radical in Combustion?

Henry F. Schaefer III
Center for Computational Quantum Chemistry
University of Georgia
Athens, Georgia 30602

Fenimore and Jones first suggested in 1963 that the reaction of oxygen atoms with acetylene might form the ketenyl radical, HCCO, in addition to other products :

$$O(^3P) + C_2H_2 \longrightarrow HCCO + H \quad (1a)$$

$$\longrightarrow CH_2 + CO \quad (1b)$$

There has been considerable controversy about whether channel (1a) or (1b) is more important; recent experimental work concludes that for the homogeneous thermal reaction, channel (1a) accounts for about 70% of this reaction. Since acetylene is formed as an intermediate in most hydrocarbon combustion processes, and since the dominant loss of C_2H_2 is by reaction with oxygen atoms, HCCO must be a common radical in hydrocarbon flames. Although important, the ketenyl radical HCCO is difficult to detect and so has received less attention than other combustion related radicals. HCCO was first observed in the gas phase by mass spectrometry in 1972. Only recently has it been possible to identify HCCO by microwave spectrometry and by infrared absorption. No electronic spectrum of HCCO is known, although one of the most intriguing features of this molecule is the possibility of a low-lying quartet state.

The metastable quartet state of methyne, $CH(a\,^4\Sigma^-)$, is a related combustion intermediate that has been neglected because it is difficult to detect. $CH(a\,^4\Sigma^-)$ was predicted in 1973 by Lie, Hinze and Liu to lie 0.62~0.76 eV above the ground $CH(X\,^2\Pi)$ state. Electron photodetachment experiments by CH^- by Kasdan, Herbst and Lineberger led to the conclusion that the energy difference between these two states is 0.74 eV, agreeing well with the theoretical result of Liu. $CH(a\,^4\Sigma^-)$ has also been identified by laser magnetic resonance in the reaction of oxygen atoms with acetylene, and its concentration can be

monitored by chemi-ionization. Some rate constants for chemical reactions of CH(a $^4\Sigma^-$) are now becoming available.

The kinetic behavior of CH(a $^4\Sigma^-$) is different from that of the ground state, CH(X $^2\Pi$). Metastable CH(a $^4\Sigma^-$) is quite unreactive toward most closed shell molecules. One exception is reaction (2), which has a slow but measurable rate.

$$CH(a\ ^4\Sigma^-) + CO(X\ ^1\Sigma^+) \longrightarrow \text{products} \qquad (2)$$

Since there is no spin-allowed channel for this exoergic reaction, it was suggested by Bayes this year that there might be an attractive quartet surface leading to a metastable quartet state of HCCO. This could allow sufficient interaction time for an intersystem crossing to occur, resulting in electronic deactivation of the CH(a $^4\Sigma^-$) state. Our theoretical work was initiated in order to explore the possibility of a quartet state of HCCO playing a significant role in this chemistry.

A*b initio* quantum mechanical techniques, including the self-consistent field (SCF), single and double excitation configuration interaction (CISD), single and double excitation coupled cluster (CCSD), and the single, double and perturbative triple excitation coupled cluster [CCSD(T)] methods have been applied to study the HCCO(a ^{4}A") energy hypersurface. Rate constant measurements suggest an attractive potential for the reaction of CH(a $^4\Sigma^-$) with CO, and a vanishingly small energy barrier is predicted here in the CH(a $^4\Sigma^-$) + CO reaction channel. The $^4A''$ state of HCCO is predicted to be bound by about 30 kcal/mole with respect to separated CH(a $^4\Sigma^-$) + CO. We propose that a spin-forbidden electronic deactivation of CH(a $^4\Sigma^-$) might occur through an intersystem crossing involving the a ^{4}A" state of HCCO. The energetics and the geometries of the reactants and products on both quartet and doublet energy surfaces are presented. The relationship between this research and experimental combustion chemistry has been explored.

Future Plans

We appear to be approaching the completion of a lengthy study of the mechanisms of the $C_2H_5 + O_2$ reaction. Assuming good progress, $C_2H_5 + O_2$ is expected to be the subject of my presentation at the Split Rock Conference Center.

Research Supported by the U.S. Department of Energy 1991, 1992, 1993

1 J. R. Thomas, G. E. Quelch, and H. F. Schaefer, "The Unknown Unsubstituted Tetrazines: 1,2,3,4-Tetrazine and 1,2,3,5-Tetrazine", *J. Org. Chem.* **56**, 539 (1991).

2 M. M. Gallo, T. P. Hamilton, and H. F. Schaefer, "Vinylidene–The Final Chapter?", *J. Amer. Chem. Soc.* **112**, 8714 (1991).

3 K. S. Kim, H. S. Kim, J. H. Jang, B.-J. Mhin, Y. Xie, and H. F. Schaefer, "Hydrogen Bonding Between the Water Molecule and the Hydroxyl Radical (H_2O-OH): The $^2A''$ and $^2A'$ Minima", *J. Chem. Phys.* **94**, 2057 (1991).

4 C. Liang, Y. Xie, H. F. Schaefer, K. S. Kim, and H. S. Kim, "The Vibrational Spectra of Butatriene (C_4H_4) and Pentatetraene (C_5H_4): Is Pentatetraene Bent?" *J. Amer. Chem. Soc.* **113**, 2452 (1991).

5 B. F. Yates, Y. Yamaguchi, and H. F. Schaefer, "The Dissociation Mechanism of Triplet Formaldehyde", *J. Chem. Phys.* **93**, 8798 (1990).

6 C. Meredith, G. E. Quelch, and H. F. Schaefer, "Open-Chain and Cyclic Protonated Ozone: The Ground State Potential Energy Hypersurface", *J. Amer. Chem. Soc.* **113**, 1186 (1991).

7 G. Vacek, B. T. Colegrove, and H. F. Schaefer, "Does Oxirene Exist? A Theoretical Inquiry Involving the Coupled Cluster Method", *Chem. Phys. Lett.* **171**, 468 (1991).

8 A. C. Scheiner and H. F. Schaefer, "Higher Level Theoretical Evidence for the Weak Triple Bond in Benzyne", *Chem. Phys. Lett.* **177**, 471 (1991).

9 T. P. Hamilton and H. F. Schaefer, "Do the Vinyl Isomers of $C_2H_2Cl^+$ and $C_2H_2Br^+$ Exist?", *J. Amer. Chem. Soc.* **113**, 7147 (1991).

10 S. Q. Jin, Y. Xie, and H. F. Schaefer, "The Description of Elementary Organoaluminum Fragments: $AlCH_x$ (x=1,2,3)", *J. Chem. Phys.* **95**, 1834 (1991).

11 I. M. B. Nielsen, C. L. Janssen, N. A. Burton, and H. F. Schaefer, "(1,2)-Hydrogen Shift in Monovalent Carbon Compounds: The Methylcarbyne-Vinyl Radical Isomerization", *J. Phys. Chem.* **96**, 2490 (1992).

12 H. A. Carlson, G. E. Quelch, and H. F. Schaefer, "How Stable is Cyclobutyne? The Activation Energy for the Unimolecular Rearrangement to Butatriene", *J. Amer. Chem. Soc.* **114**, 5344 (1992).

13 J. D. Goddard, Y. Yamaguchi, and H. F. Schaefer, "The Decarboxylation and Dehydration Reactions of Monomeric Formic Acid", *J. Chem. Phys.* **96**, 1158 (1992).

14 D. A. Horner, W. D. Allen, A. G. Csaszar, and H. F. Schaefer, "Sodium Superoxide Radical: $\tilde{X}\ ^2A_2$ and $\tilde{A}\ ^2B_2$ Potential Energy Surfaces", *Chem. Phys. Lett.* **186**, 346 (1991).

15 A. C. Scheiner and H. F. Schaefer, "Cyclopentadienylideneketene: Theoretical Consideration of An Infrared Spectrum Frequently Mistaken for Benzyne", *J. Amer. Chem. Soc.* **114**, 4758 (1992).

16 M. M. Gallo and H. F. Schaefer, "Methylcarbene: The Singlet-Triplet Energy Separation", *J. Phys. Chem.* **96**, 1515 (1992).

17 T. P. Hamilton and H. F. Schaefer, "The Prototypical Zinc Carbene and Zinc Carbyne Molecules $ZnCH_2$ and HZnCH: Triplet Electronic Ground States", *J. Chem. Soc. (London) Chem. Communications* 621 (1991).

18 B. J. DeLeeuw, R. S. Grev, and H. F. Schaefer, "A Comparison and Contrast of Selected Saturated and Unsaturated Hydrides of Group 14 Elements: C_2H_6, Si_2H_6, Ge_2H_6, and C_2H_2, Si_2H_2, Ge_2H_2", *J. Chem. Ed.* **69**, 441 (1992).

19 J. R. Thomas, G. E. Quelch, E. T. Seidl, and H. F. Schaefer, "The Titane Molecule (TiH_4): Equilibrium Geometry, Infrared and Raman Spectra of the First Spectrosopically Characterized Transition Metal Tetrahydride", *J. Chem. Phys.* **96**, 6857 (1992).

20 B. Ma, Y. Xie, and H. F. Schaefer, "Tetraethynylethylene, A Molecule with Four Very Short C-C Single Bonds. Interpretation of the Infrared Spectrum", *Chem. Phys. Lett.* **191**, 521 (1992).

21 G. E. Quelch, M. M. Gallo, and H. F. Schaefer, "Aspects of the Reaction Mechanism of Ethane Combustion. Conformations of the Ethylperoxy Radical", *J. Amer. Chem. Soc.* **114**, 8239 (1992).

22 E. E. Bolton, B. J. DeLeeuw, J. E. Fowler, R. S. Grev, and H. F. Schaefer, "The Silicon-Carbon Symmetric Stretching Fundamental ν_1 of Si_2C: Nonintuitive Theoretical Behavior", *J. Chem. Phys.* **97**, 5586 (1992).

23 C. L. Collins, C. Meredith, Y. Yamaguchi, and H. F. Schaefer, "Advancing the Search for Cyclopropenylidene Carbene, The Exocyclic Ring Isomer of Diacetylene", *J. Amer. Chem. Soc.* **114**, 8694 (1992).

24 C. Meredith, T. P. Hamilton, and H. F. Schaefer, "Oxywater (Water Oxide): New Evidence for the Existence of a Structural Isomer of Hydrogen Peroxide," *J. Phys. Chem.* **96**, 9250 (1992).

25 M. Shen , H. F. Schaefer, and H. Partridge, "Tungsten Hexahydride (WH_6). An Equilibrium Geometry Far From Octahedral," *J. Chem. Phys.* **98**, 508 (1993).

26 B. J. DeLeeuw, J. T. Fermann, Y. Xie, and H. F. Schaefer, "Substitution Effects on the Properties of Unsaturated Carbenes: Fluorovinylidene (HFC=C:)," *J. Amer. Chem. Soc.* **155**, 1039 (1993).

27 Y. Yamaguchi, G. Vacek, and H. F. Schaefer, "Low-Lying Triplet Electronic States of Acetylene: *Cis* $^3B_2$ and $^3A_2$, *Trans* ^3B_u and ^3A_u," Per-Olov Löwdin Issue, *Theoretica Chimica Acta.*

28 G. Vacek, J. R. Thomas, B. J. DeLeeuw, Y. Yamaguchi, and H. F. Schaefer, "Isomerization Reactions on the Lowest Potential Energy Hypersurface of Triplet Vinylidene and Triplet Acetylene," *J. Chem. Phys.*

29 Y. Xie and H. F. Schaefer, "Hydrogen Bonding Between the Water Molecule and the Hydroxyl Radical (H_2O-OH): The Global Minimum", *J. Chem. Phys.*

30 J. K. Lundberg, R. W. Field, C. D. Sherrill, E. T. Seidl, Y. Xie, and H. F. Schaefer, "Acetylene: Synergy Between Theory and Experiment," *J. Chem. Phys.*

31 Y. Yamaguchi, H. F. Schaefer, and I. L. Alberts, "A Mechanistic Study of the Ring Opening Reaction of Singlet Oxirane", *J. Amer. Chem. Soc.*

Theoretical Studies of Chemical Reaction Dynamics

George C. Schatz

Theoretical Chemistry Group, Argonne National Laboratory, Argonne IL 60439
Mailing Address: Department of Chemistry, Northwestern University, Evanston IL 60208-3113

Program Scope: This collaborative program with the Theoretical Chemistry Group at Argonne involves theoretical studies of gas phase chemical reactions and related energy transfer and photodissociation processes. Many of the reactions studied are of direct relevance to combustion; others are selected because they provide important examples of special dynamical processes, or are of relevance to experimental measurements. Both classical trajectory and quantum reactive scattering methods are used for these studies, and the types of information determined range from thermal rate constants to state to state differential cross sections.

Recent Progress:

1. **CH + H and C + H_2 Reaction Kinetics.** We have used the methylene potential energy surface developed by Harding to calculate thermal rate constants for the reactions

$$CH + H \rightarrow C + H_2 \qquad (1)$$

$$C + H_2 \rightarrow CH_2 \qquad (2)$$

Reaction (1) is important in soot production in the pyrolysis of hydrocarbons. Experimental studies of this reaction are in conflict, with one measurement indicating no temperature dependence above 1500K, and another indicating substantial temperature dependence at lower temperatures down to 300K. Our results, which are based on quasiclassical trajectory calculations, indicate no significant temperature dependence over the entire range 300-2000K, and the magnitudes of the rate constants are in good agreement with two previous high-temperature measurements.

Reaction (2) has been the subject of just one kinetics study, and our trajectory results are consistent with this one study. However, the trajectory method is suspect in this particular application, because tunnelling and zero point effects are important as a result of a shallow outer well in the C-H_2 potential that is traversed prior to entry into the deep methylene well. This outer well can trap trajectories long enough both to scramble energy between vibrational and translational motions, and to enhance tunnelling through the small barrier that must be surmounted to form methylene.

2. **Reactions of atomic radicals with hydrogen halides.** We have continued to study several prototype hydrogen atom transfer reactions, including

$$Cl' + HCl \rightarrow Cl'H + Cl \qquad (3)$$

and

$$O + HCl \rightarrow OH + Cl \qquad (4)$$

For both reactions we are especially interested in understanding how quantum mechanical resonance effects influence the reaction dynamics, and in addition, we want to understand transition state photodetachment spectra that have recently been measured by Neumark and coworkers. Both of these reactions are simple enough that it is possible to determine accurate quantum cross sections, rate constants and other information, so in one study that was completed this year, reaction (3) was used as a benchmark for testing the quasiclassical trajectory method under conditions where there are important resonance effects in differential and integral cross sections. In a second study, the potential surface for reaction (1) was calculated using several accurate *ab initio* methods.

A global surface is still being developed, but based on transition state properties, it appears that rate constants in agreement with experiment will result from the best surfaces that we have generated.

3. **Fine structure effects in chemical reactions.** We have continued to develop coupled channel scattering methods which make it possible to solve the Schrodinger equation for reactions of open shell atoms with closed shell diatomic molecules, including for the multiple potential surfaces involved, and spin-orbit coupling. During the last year we have demonstrated full convergence of the calculations for reaction (3) (where three potential surfaces are involved), and we have used the results of the calculations to study the influence of spin-orbit splitting on the overall reaction probability. We find that only a very small splitting (less than 60 cm^{-1}) is needed to switch from dynamics which is statistical in the electronic state index, to one which is nearly adiabatic in this index. This information will be used to develop an improved understanding of how best to choose electronic statistical factors in chemical reactions.

Future Plans

1. **Transition State Photodetachment Spectroscopy of O + HCl Reaction.** We have recently perfected a L^2 method for calculating transition state photodetachment spectra for reactions which involve the transfer of hydrogen atoms between heavy partners. Applications to reaction (4) are currently underway, and we plan to analyze the results in collaboration with Mike Davis through the calculation of tree structures and smoothed states. Comparisons with the measured results from Neumark are currently underway.

2. **Fine structure transitions in O + Ar collisions.** We have developed codes to simulate Liu's recent experimental study of the differential cross sections for fine structure transitions in O + Ar collisions. Both quantum and semiclassical methods are being implemented, and the calculations use high quality *ab initio* surfaces that have been calculated by Harding. Of particular interest will be the mechanistic link between features of the potential curves (espcially the difference potentials) and structure in the differential cross sections. Preliminary results suggest very strong sensitivity of the differential cross sections to the van der Waals well regions of the interaction potentials. This means that the differential cross sections for fine structure changing collisions provide a valuable tool for characterizing potential curves for the interaction of open shell atoms with closed shell molecules.

3. **Hydrogen Atom Transfer Reactions.** Our single-surface studies of Cl + HCl will include the following projects: (a) Comparison of reaction dynamics on LEPS and newly developed *ab initio* potential surfaces; (b) Calculation of fully converged coupled-channel scattering information for nonzero total angular momentum, and the development of angular momentum decoupling approximations that can be used in place of the coupled-channel calculations, and (c) Tests of a new nearside-farside decomposition method that we have developed for determining the origin of complex structures in reactive differential cross sections.

DOE Supported Publications

1. Influence of Transition State Resonances on Integral Cross Sections and Product Rovibrational Distributions for the Cl + HCl → ClH + Cl Reaction, G. C. Schatz, D. Sokolovski, and J. N. L. Connor, J. Chem. Phys., **94**, 4311-19 (1991).

2. Resonances in Heavy + Light-Heavy Atom Reactions: Influence on Differential and Integral Cross Sections and on Transition State Photodetachment Spectra, G. C. Schatz, D. Sokolovski, and J. N. L. Connor, Far. Disc. Chem. Soc., **91**, 17-30 (1991).

3. A Quasiclassical Trajectory Study of the OH + CO Reaction, K. Kudla, G. C. Schatz, and A. F. Wagner, J. Chem. Phys., **95**, 1635-47 (1991).

4. An Analytical Representation of the Lowest Potential Energy Surface for the Reaction $O(^3P)$ + $HCl(X^1\Sigma) \rightarrow OH(X^2\Pi)$ + $Cl(^2P)$, H. Koizumi, G. C. Schatz, and M. S. Gordon, J. Chem. Phys. **95**, 6421-28 (1991).

5. A Quasiclassical Trajectory Study of OH Rotational Excitation in OH + CO Collisions Using *Ab Initio* Potential Surfaces, K. Kudla, A. G. Koures, L. B. Harding and G. C. Schatz, J. Chem. Phys., **96**, 7465-73 (1992).

6. Comparison of Quasiclassical and Quantum Dynamics for Resonance Scattering in the Cl + HCl → ClH + Cl Reaction, W. Jakubetz, D. Sokolovski, J. N. L. Connor and G. C. Schatz, J. Chem. Phys., **97**, 6451-9 (1992).

7. *Ab Initio* Electronic Structure Calculations of Stationary Points and Barrier Heights for the ClHCl and HCl_2 Systems, M. A. Vincent, J. N. L. Connor, M. S. Gordon and G. C. Schatz, *Chem. Phys. Lett.*, in press.

8. Theoretical Studies of the Reactions H + CH → C + H_2 and C + H_2 → CH_2 Using an *Ab Initio* Global Ground State Potential Surface for CH_2, L. B. Harding, R. Guadagnini and G. C. Schatz, *J. Phys. Chem.*, in press.

NO CONCENTRATION IMAGING IN TURBULENT NONPREMIXED FLAMES†

R. W. Schefer

Combustion Research Facility
Sandia National Laboratories, Livermore, CA. 94551

The importance of NO as a pollutant species is well known. An understanding of the formation characteristics of NO in turbulent hydrocarbon flames is important to both the desired reduction of pollutant emissions and the validation of proposed models for turbulent reacting flows. Of particular interest is the relationship between NO formation and the local flame zone, in which the fuel is oxidized and primary heat release occurs. Planar imaging of NO provides the multipoint statistics needed to relate NO formation to the both the flame zone and the local turbulence characteristics. Planar imaging of NO has been demonstrated in turbulent flames where NO was seeded into the flow at high concentrations (2000 ppm) to determine the gas temperature distribution.[1] The NO concentrations in these experiments were significantly higher than those expected in typical hydrocarbon-air flames, which require a much lower detectability limit for NO measurements. An imaging technique based on laser-induced fluorescence with sufficient sensitivity to study the NO formation mechanism in the stabilization region of turbulent lifted-jet methane flames.

The ultraviolet laser light for the fluorescence excitation of the NO molecule was provided by a Nd:YAG-pumped dye laser system. Here the frequency-doubled output of a Nd:YAG laser (6-ns pulse, 500 mJ pulse) was used to pump a pulsed-dye laser with LDS 698 dye. The output of the dye laser (678 nm) was subsequently frequency doubled and mixed with the dye beam in a BBO crystal. With this configuration, about 1 mJ of laser energy was obtained at 226.2 nm, which was used to pump the NO $A^2\Sigma^+$ (v"=0) ← $X^2\Pi$ (v'=0) electronic band. The beam was formed into a 0.2-mm thick sheet of light by a multipass cell consisting of two cylindrical reflectors coated for high reflectivity (>99 %) at 226 nm. The fluorescence signal was collected with an f/0.8 lens system and detected at 240 nm (25-nm bandwidth) using an intensified vidicon camera. The increased sheet intensity provided by the multipass cell and efficient light collection allowed detection of 0.2 ppm of NO, which was confirmed in single-shot experiments in a nonreacting turbulent jet consisting of 5 ppm NO in air.

For the turbulent flame measurements, the burner consisted of a 5.4-mm diameter fuel jet located in the center of a plate. Methane was injected through a central fuel tube into surrounding still air at a velocity of 21 m/s, corresponding to a fuel-jet Reynolds number of 7,000. At this flow condition, the visible flame was stabilized at an axial position approximately 25 mm downstream of the burner face. The lower part of the flame was blue and was connected to an irregular yellow flame that began at about 100 mm downstream.

Shown in Fig. 1 is a single-shot image of the NO concentration distribution in a lifted, turbulent CH_4-jet flame. The maximum NO level is 25 ppm and is located in the mixing region that forms adjacent to the fuel jet on both sides of the centerline. Comparisons with previous CH-CH_4 imaging data in which CH was used as a marker for the flame zone[2,3] show that the high NO region closely coincides with the turbulent flame zone where fuel oxidation occurs. The flame is lifted and NO is not observed below the liftoff height. The flame on the left side of the jet is lifted

† Work supported by the Department of Energy, Office of Basic Energy Sciences, Division of Chemical Sciences.

to an axial location of about 25 mm, while the flame on the right side is stabilized below the field of view. Examination of other images shows that the location and height of the high NO region varies from shot to shot, reflecting the time-varying characteristics of this flame. The previous CH measurements, and more recent temperature imaging data show that no reaction occurs in the central region of the jet and that the mixture is relatively cold at the axial distances shown. These observations are reflected in the absence of any NO in this central region at upstream locations. Farther downstream, the NO extends into the central region of the jet due to convective transport of NO produced in the outer flame zone.

Chemical kinetic modeling calculations show that, depending on flame conditions, both the thermal and so- called "prompt" NO formation pathways may be important.[4] What the relative contribution of each pathway is to total NO production in turbulent flames has not been established. Residence-time estimates in the upstream flame stabilization region corresponding to the images of Fig. 1 indicate insufficient time is available for thermal NO formation to be significant. It therefore appears that the majority of NO in the present flame is formed via the "prompt" NO pathway, in which the reaction $CH + N_2 = HCN + N$ is of primary importance. Further evidence for this conclusion is provided by Fig. 2 in which the time-averaged radial profile of NO (calculated from 300 images) is shown at an axial location of 30 mm downstream. Plotted for comparison are the time-averaged CH, CH_4 and temperature profiles obtained previously. It can be seen that the maximum temperature of 1300 K at this location is well below the temperature needed for significant thermal NO and that a close correspondence exists between the peak NO and CH. The latter observation is consistent with modeling calculations and further indicates that the majority of the NO at the flame base is "prompt" NO.

Future work will combine the NO laser-induced fluorescence technique with Rayleigh scattering to simultaneously measure the instantaneous planar distributions of NO and temperature in nonpremixed turbulent methane flames. This measurement will allow the relationship between the instantaneous temperature and NO fields to be determined. In addition, the NO imaging will be combined with a previously developed CH imaging technique to better determine the role of the CH radial in "prompt" NO formation. These results should lead to valuable insights into the NO formation mechanism in turbulent hydrocarbon flames.

References

1. Kychakoff, G., Knapp, K., Howe, R. D. and Hanson, R. K., *AIAA J.* 22, 153 (1984).

2. Namazian, M., Schefer, R. W. and Kelly, J., *Twenty-Second Symposium (International) on Combustion* (The Combustion Institute, Pittsburgh, PA, 1988), p. 627.

3. Schefer, R. W., Namazian, M. and Kelly, J., *Twenty-Third Symposium (International) on Combustion* (The Combustion Institute, Pittsburgh, PA, 1991), in press.

4. Drake, M. C. and Blint, R. J., *Combust. Flame* 76, 151 (1989).

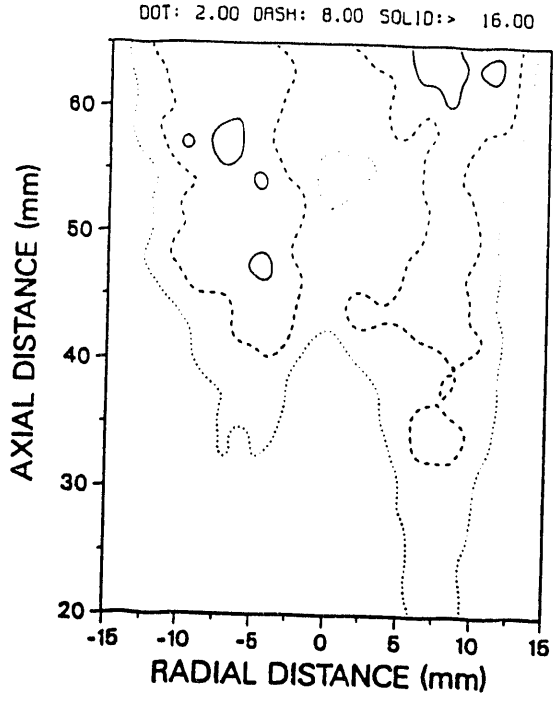

Figure 1. Two-dimensional image shown as instantaneous contours of NO concentration in a lifted, turbulent CH_4-jet flame. The flow direction is from bottom to top of image. Contour levels shown are 2 ppm (dotted line), 8 ppm (dashed line) and 16 ppm (solid line). Fuel jet velocity =21 m/s.

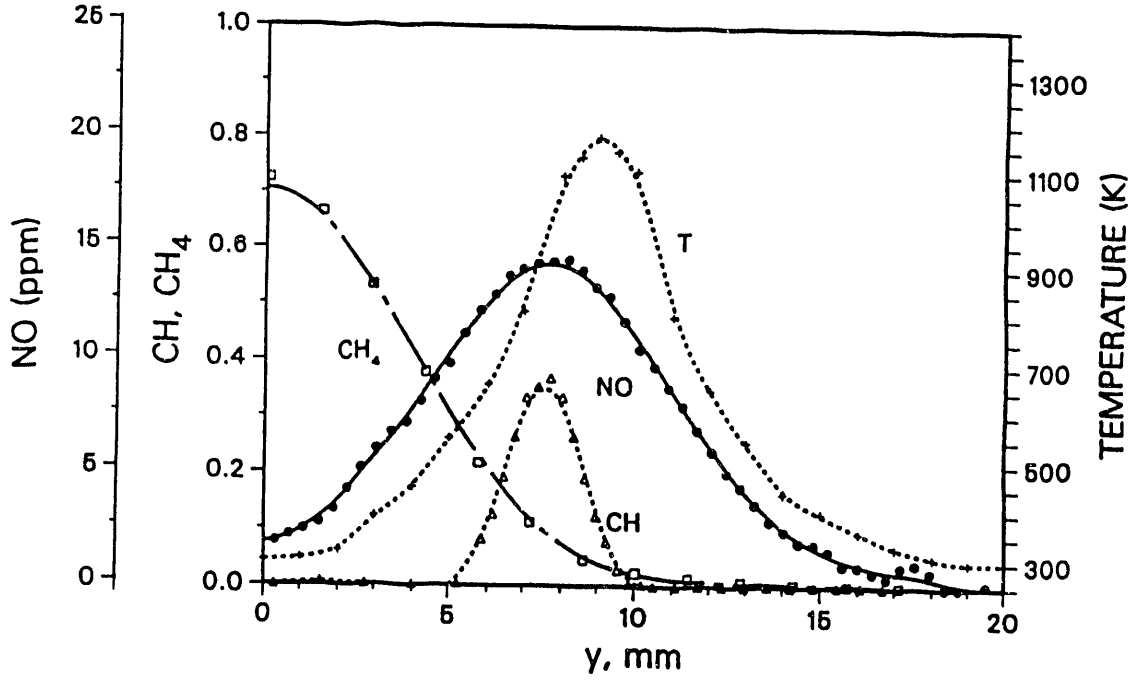

Figure 2. Radial profiles of the time-averaged NO, CH, OH concentrations and temperature in a lifted, turbulent CH_4-jet flame. Profiles are for an axial location of 30 mm downstream.

R. W. Schefer: Journal Publications Supported by This Program 1991-1993

Schefer, R. W., Namazian, M. and Kelly, J., "Stabilization of Lifted Turbulent-Jet Flames," *Combust. Flame*, accepted, 1993.

Schefer, R. W., Kerstein, A. R., Namazian, M. and Kelly, "Role of Large-Scale Structures in a Nonreacting Turbulent CH4 Jet," *Phys. Fluids*, accepted, 1993.

Schefer, R. W., Namazian, M. and Kelly, "Velocity Measurements in Turbulent Bluff-Body Stabilized Flows," *AIAA J.*, accepted, 1993.

Namazian, M., Schefer, R. W. and Kelly, J., Concentration Imaging Measurements in Turbulent Concentric-Jet Flows," *AIAA J.* **30**, 384 (1992).

Schefer, R. W., Namazian, M. and Kelly, J., "Simultaneous Raman Scattering and Laser-Induced Fluorescence for Multi-Species Imaging in Turbulent Flames," *Opt. Lett.* **16**, 858 (1991).

Schefer, R. W., Namazian, M. and Kelly, J., "CO, OH and CH_4 Concentration Measurements in a Lifted Turbulent-Jet Flame," *Twenty Third Symposium (International) on Combustion* (The Combustion Institute, Pittsburgh, PA), p. 669, 1991.

Theoretical Studies of Potential Energy Surfaces and Computational Methods

Ron Shepard
Chemistry Division
Argonne National Laboratory
Argonne, IL 60439
[email: shepard@tcg.anl.gov]

This project involves the development, implementation, and application of theoretical methods for the calculation and characterization of potential energy surfaces involving molecular species that occur in hydrocarbon combustion. These potential energy surfaces require an accurate and balanced treatment of reactants, intermediates, and products. This difficult challenge is met with general multiconfiguration self-consistent-field (MCSCF) and multireference single- and double-excitation configuration interaction (MRSDCI) methods. In contrast to the more common single-reference electronic structure methods, this approach is capable of describing accurately molecular systems that are highly distorted away from their equilibrium geometries, including reactant, fragment, and transition-state geometries, and of describing regions of the potential surface that are associated with electronic wave functions of widely varying nature. The MCSCF reference wave functions are designed to be sufficiently flexible to describe qualitatively the changes in the electronic structure over the broad range of geometries of interest. The necessary mixing of ionic, covalent, and Rydberg contributions, along with the appropriate treatment of the different electron-spin components (e.g. closed shell, high-spin open-shell, low-spin open shell, radical, diradical, etc.) of the wave functions, are treated correctly at this level. Further treatment of electron correlation effects is included using large scale multireference CI wave functions, particularly including the single and double excitations relative to the MCSCF reference space. This leads to the most flexible and accurate large-scale MRSDCI wave functions that have been used to date in global PES studies.

Electronic Structure Code Maintenance and Development: A major component of this project is the development and maintenance of the COLUMBUS Program System. The COLUMBUS Program System is maintained and developed collaboratively with several researchers including Isaiah Shavitt and Russell M. Pitzer (Ohio State University), and Hans Lischka (University of Vienna, Austria). During the past year, the COLUMBUS Program System of electronic structure codes has been maintained on the various machines used by the Argonne Theoretical Chemistry Group, including the Sun workstations, the Stardent Titans, the Alliant FX/2812 , and the Cray Y-MP at SCRI at Florida State University and the Cray-2 at NERSC at Livermore National Laboratory. Additionally, the codes have been ported to the new Cray C90 at NERSC and to IBM RS6000 workstations.

The parallel version of the CI diagonalization program has been ported to several machines, including the Alliant FX/2812. This version is based on a partitioning of the Hamiltonian matrix, trial vector, and matrix-vector product and uses a distributed-memory, single program multiple data (SPMD) programming model based on the TCGMSG library developed by R. J. Harrison. This approach leads to a portable implementation that runs efficiently on both shared-memory and distributed-memory computers, including heterogeneous networks of workstations. Within a single hamiltonian matrix-vector

product, each CPU is responsible for only a subset of the possible combinations of segment pairs. In the original implementation, each CPU processed the entire list of coupling coefficients over the internal orbitals and the complete set of integrals each iteration. In more recent versions, only the required coupling coefficients are now being generated by each CPU as needed during the diagonalization procedure, eliminating the associated I/O and increasing the efficiency significantly in highly-segmented cases. This allows more flexibility in the choice of task size, and eliminates many of the load-balancing problems that occurred in the initial version. The elimination of the shared integral files, and the associated I/O bottleneck, for the three- and four-external integrals has also progressed over the past year. In collaboration with Hans Lischka, the first step of this process involves computing these molecular integral contributions in the atomic orbital basis; the second step will involve the optional recomputation of these integrals upon demand, similar to "direct-SCF" procedures, thereby eliminating the associated I/O completely. This is the first successful attempt to parallelize a production-level MRSDCI code, and this effort represents a major step forward toward using effectively the large-scale parallel supercomputers that are becoming available to scientists (such as the Intel Touchstone Delta).

A general multireference configuration interaction energy gradient code, CIGRD, has been developed. In addition to allowing frozen core orbitals, the program also includes density matrix and Fock matrix resolution of invariant active orbital subspaces and Fock matrix resolution of the virtual orbitals. Analytic energy gradients may also be computed for multireference coupled-pair-functional energies. In addition to the computation of analytic energy gradients, the new formalism lends itself to the computation of other general energy response properties. These are properties that may be written in the form $\frac{dE^{ci}}{d\lambda}$ where λ is a measure of a perturbation to the standard electronic hamiltonian operator. These properties include the dipole moment of a molecule (e.g. $\mu_x=\frac{dE^{ci}}{d\varepsilon_x}$ where ε_x is the strength of the x component of an external electric field $\boldsymbol{\varepsilon}$) and the dipole moment derivatives (e.g. $\frac{d\mu_x}{dR}$ where R is some internal coordinate). Examples of both of these properties have been demonstrated with the new method. Calculations of analytic energy gradients for large-scale MRSDCI wave functions using program CIGRD demonstrate, for the first time, that the effort required for the energy gradient is a small fraction of that required for the energy, even for larger molecules with many degrees of freedom. This property is due to a new formulation of the energy gradient, based on successive orbital transformations, and to a strict adherence to the principle of eliminating any displacement dependence from any of the intermediate quantities computed and/or stored during the computational procedure. The method also exploits the natural advantage of variational energies, such as MRSDCI and MR-ACPF, over nonvariational energy methods such as perturbation theory or coupled-cluster expansions. Future effort will be directed at the elimination of several practical limitations of the current implementation. These include the extension to higher angular-momentum basis functions, the efficient treatment of generally-contracted basis sets, and the efficient treatment of molecular point-group symmetry.

Electronic Structure Method Development: A new method of MCSCF wave function optimization has been developed and analyzed. This method, called Trigonometric Interpolation, is based on a nonlinear transformation of the wave function

variation coordinates along with the construction of a global interpolating function. This interpolating function is constructed for each MCSCF iteration in such a way that it reproduces certain known behavior of the exact energy function. It reproduces exactly the energy, gradient, and hessian at the expansion point, at an infinite number of isolated points, and at points on the surfaces of an infinite number of nested multidimensional balls within the wave function variational space. The optimization of the wave function correction parameters on this interpolating function does not require integral transformations or density matrix constructions, although one-index transformation and transition density matrix techniques may be used if desired. The nonlinear coordinate transformations, along with the necessary derivatives, are computed with simple matrix operations, and require only $O(N_{orb}^3)$ effort. The new method differs from previous optimization methods in several respects. (1) It reproduces certain behavior of the exact energy function that is not displayed by previous approaches. (2) The orbital-state coupling is included explicitly via the partitioned orbital hessian matrix. (3) The minimization of the approximate energy function is simpler than with previous similar approaches. (4) The treatment of redundant orbital rotations is straightforward, since the exact and approximate energy functions display the same qualitative behavior with respect to these wave function variations. (5) Finally, the new method may be implemented as a simple extension to essentially any existing second-order MCSCF code, the required changes being localized within a rather small part of the overall iterative procedure. This new wave function optimization method is being included into the production-level MCSCF code used by the group, and eventually into the COLUMBUS Program System.

In the implementation of Direct-SCF procedures on parallel computers with many computational nodes, it is observed that the time required for diagonalization of the Fock matrix over the atomic orbital basis set often dominates the overall computational procedure. This occurs despite the fact that the diagonalization effort scales only as $O(N_{orb}^3)$ whereas the effort for the Fock matrix construction scales formally as $O(N_{orb}^4)$, a much larger quantity. There are two reasons for this disparity. First, for larger molecular systems, a combination of numerical thresholds and efficient integral approximations leads to an actual total effort that scales as much less than $O(N_{orb}^4)$. Empirically, this step scales only as $O(N_{orb}^{2.2})$ to $O(N_{orb}^3)$. Secondly, the matrix diagonalization step itself does not scale well for small ratios of N_{orb} to N_{cpu}. For N_{orb}/N_{cpu} ~10 or less, the speedup for matrix diagonalization is only in the range of 10 to 20, regardless of the number of CPUs available. In contrast, the Fock matrix construction scales remarkably well, with speedups being close to optimal even for large N_{cpu}. These two features cause the diagonalization step, which is usually inconsequential in sequential calculations, to overshadow the other parts of the calculation in parallel calculations using the traditional SCF optimization approach. A solution to this computational bottleneck has been found in a reformulation of the SCF procedure. This alternative approach uses formal methodology usually associated with MCSCF wave function optimization. Instead of treating the problem as a fixed-point procedure for finding a self-consistent Fock operator, it is treated instead directly as a minimization problem of the energy expectation value within the space of orbital variations. This alternative procedure leads to the same wave function, but not with exactly the same orbitals, as the traditional procedure, but it may be formulated such that it does not involve a Fock matrix diagonalization step each iteration. If desired, the canonical orbitals

associated with the traditional method may be obtained at the end of the optimization procedure with an additional noniterative step involving a single Fock matrix diagonalization, but even this is often unnecessary. It is expected that this method will be most useful for large molecular systems consisting of ~10^3 atoms and ~10^4 basis functions on parallel machines consisting of ~10^3 CPUs.

Public Distribution of the COLUMBUS Program System: The COLUMBUS Program System is now available using the *anonymous ftp* facility of internet from the server `ftp.tcg.anl.gov`. In addition to the source code, the complete online documentation, installation scripts, example calculations, and numerous other utilities are included in the distribution. The entire program system can be downloaded in compressed *tar* format, or individual files may be obtained from within the directory structure. There are currently over 50 sites registered to receive COLUMBUS email announcements. Statistics from the *ftp* server show that almost 4000 individual COLUMBUS files have been accessed in the past year, of which about 150 have been copies of the entire program system. Initial response from the users of the COLUMBUS Program System has been both positive and constructive.

Publications:

"An *Ab Initio* Theoretical Study of the CH_2+H $\rightleftharpoons$ CH_3 $\rightleftharpoons$ CH+H_2 Reactions", M. Aoyagi, R. Shepard, A. F. Wagner, *International Journal of Supercomputing Applications* **5**, 72-89 (1991).

Proceedings of the Argonne Integral Evaluation Workshop, Int. J. Quantum Chem. **40**, (1991) edited by J. Almlöf, R. Shepard, and R. J. Harrison.

"The COLUMBUS Standard Integral File Structure: A Proposed Interchange Format", R. Shepard, *Int. J. Quantum Chem.* **40**, 865-887 (1991).

"A General MRCI Gradient Program", R. Shepard, H. Lischka, P. G. Szalay, T. Kovar, and M. Ernzerhof, *J. Chem. Phys.* **96**, 2085-2098 (1992).

"A Proposal for Generic BLAS, LINPACK, and LAPACK: A Step Towards Portability", R. Shepard, *Fortran Journal* **4** (2), 6-12 (1992).

"On the Global Convergence of MCSCF Wave Function Optimization: The Method of Trigonometric Interpolation", R. Shepard, *Theoretica Chimica Acta* **84**, 55-83 (1992).

"Elimination of the Diagonalization Bottleneck in Parallel Direct-SCF Calculations", R. Shepard, *Theoretica Chimica Acta* **84**, 343-351 (1993).

"A Parallel Implementation of the COLUMBUS Multireference Configuration Interaction Program", M. Schüler, T. Kovar, H. Lischka, R. Shepard, R. J. Harrison, *Theoretica Chimica Acta (in press).*

"A Discussion of Some Aspects of the MCSCF Method", R. Shepard, NATO ASI *(in press).*

Computational and Experimental Study of Laminar Flames

M. D. Smooke and M. B. Long
Department of Mechanical Engineering
Yale University
New Haven, CT
(203) 432-4344

1. Project Overview

Our research has centered on an investigation of the effects of complex chemistry and detailed transport on the structure and extinction of hydrocarbon flames in counterflow, cylindrical and coflowing axisymmetric configurations. We have pursued both computational and experimental aspects of the research in parallel. The computational work has focused on the application of accurate and efficient numerical methods for the solution of the one and two-dimensional nonlinear boundary value problems describing the various reacting systems. Detailed experimental measurements were performed on axisymmetric coflow flames using two-dimensional imaging techniques. In particular, spontaneous Raman scattering and laser induced fluorescence were used to measure the temperature, major and minor species profiles.

2. Recent Progress

Our computational research has focused on both one and two-dimensional systems. In one dimension we have developed models for counterflow premixed flames in a cold-reactant/hot product configuration and for cylindrical premixed flames in which a fuel-air mixture is injected radially inward into an open tube. Since both systems admit similarity solutions of the two-dimensional conservation equations, the governing equations in each case can be reduced to a system of one-dimensional two-point boundary value problems. In two dimensions we have concentrated our efforts on the modeling of axisymmetric laminar diffusion flames in which a fuel jet discharges into a coflowing air stream. The fully elliptic form of the conservation equations were solved in cylindrical coordinates. Spontaneous Raman spectroscopy and laser induced fluorescence have been used to measure major and minor species in a methane-air diffusion flame that was designed to match the conditions of the computed flame. The emphasis of the experimental work was on providing the best quantitative information possible on the flow configurations studied. The information obtained in these experiments will help improve the accuracy of measurements in turbulent flames and it will provide better data on the relative applicability of different scattering mechanisms.

3. Future Plans

During the next three years we hope to expand our research in three main areas. First,

we intend to develop a flamelet model for turbulent nonpremixed combustion based upon three different flamelet libraries–the nonpremixed counterflow system, the nonpremixed cylindrical system and the axisymmetric nonpremixed coflow system. Second, we plan on continuing our studies of methane-air coflow flames. In particular, we want to continue our measurements of minor species in the flame and the comparison of these measurements with the computational results. Finally, the model will be modified to include NO_x chemistry and we will investigate (both computationally and experimentally) the reduction of NO_x by modifications to the inlet velocity field.

Publications

1. M. D. Smooke, R. E. Mitchell and D. E. Keyes, "Numerical Solution of Axisymmetric Laminar Diffusion Flames," *Comb. Sci. and Tech.*, **67**, (1989).

2. M. D. Smooke, P. Lin, J. Lam and M. B. Long, "Computational and Experimental Study of a Laminar Axisymmetric Methane-Air Diffusion Flame," *Twenty-Third Symposium International on Combustion*, (1991).

3. M. D. Smooke and V. Giovangigli, "Extinction of Tubular Premixed Laminar Flames with Complex Chemistry," *Twenty-Third Symposium International on Combustion*, (1991).

4. M. D. Smooke, J. Crump, K. Seshadri and V. Giovangigli, "Comparison Between Numerical Calculations and Experimental Measurements of the Structure of Diluted Methane-Air Premixed Flames," *Twenty-Third Symposium International on Combustion*, (1991).

5. M. D. Smooke and V. Giovangigli, "Numerical Modeling of Axisymmetric Laminar Diffusion Flames," *Impact of Computing in Sci. and Eng.*, (1992).

TURBULENT COMBUSTION

L. Talbot and R. K. Cheng
Lawrence Berkeley Laboratory
Berkeley, CA 94720

Scope

Turbulent combustion is the dominant process in heat and power generating systems. Its most significant aspect is to enhance the burning rate and volumetric power density. Turbulent mixing, however, also influences the chemical rates and has a direct effect on the formation of pollutants, flame ignition and extinction. Therefore, research and development of modern combustion systems for power generation, waste incineration and material synthesis must rely on a fundamental understanding of the physical effect of turbulence on combustion to develop theoretical models that can be used as design tools.

The overall objective of our program is to investigate, primarily experimentally, the interaction and coupling between turbulence and combustion. These processes are complex and are characterized by scalar and velocity fluctuations with time and length scales spanning several orders of magnitude. They are also influenced by the so-called "field" effects associated with the characteristics of the flow and burner geometries. Our approach is to gain a fundamental understanding by investigating idealized laboratory flames. Laboratory flames are amenable to detailed interrogation by laser diagnostics and their flow geometries are chosen to simplify numerical modeling and simulations and to facilitate comparison between experiments and theory.

Our current goal is to obtain a physical understanding of the effects of combustion heat release on turbulence characteristics, and to quantify the relationship between turbulence intensity and the burning rate. The experiments are concentrated on flames with moderate turbulence intensity where chemical reaction rates are not significantly affected by turbulence mixing. The turbulent burning rate can be determined from the flame front topology (i.e. the flamelet geometry) which can be compared to the turbulence characteristics. The flamelet geometry and turbulence statistics are analyzed to elucidate the flame propagation processes and to validate numerical turbulent combustion models.

Recognizing that both the flowfield and local turbulence affect turbulent flame characteristics, our experimental program has emphasized investigating flame propagation under a variety of flow geometries. Typical turbulence intensities studies in these flame configurations are from 5 to 10%. The turbulence Reynolds number, Re_l, is in the range of about 100. These turbulent flames are characterized as wrinkled laminar flamelets because the chemical time scales are small compared to those of turbulence.

Several well-established laser diagnostic techniques with high spatial and temporal resolutions are used to measure statistical moments and correlations of velocity and scalars (i.e. gas density, reaction progress variable). These techniques include laser Doppler anemometry (LDA) for simultaneous measurement of two velocity components and Rayleigh scattering from a focused laser beam for density measurements. Another scalar diagnostics include laser-induced Mie scattering from silicone-oil aerosol (MSOD) for measuring the reaction progress variable and

flame crossing frequencies. Mie scattering is also used for laser sheet imaging of the flame geometry by high-speed tomography.

Recent Progress

We have focused our experimental efforts on using a weak-swirl burner to investigate premixed turbulent flame propagation. This novel weak-swirl burner was discovered in 1991 and has shown to provide a flame that is a close approximation to the 1-D planar flames described in the model of Bray-Moss and Libby. The flames are not in contact with any physical surfaces or objects and can be considered as adiabatic. Another attribute is that the flame zone gives free access to laser diagnostics for detailed measurements. The experimental conditions have been extended to cover a wide range to infer the dependency of the flame speed, S_t with turbulence kinetic energy, q'. The results show S_t correlates linearly with q' and compare well with those obtained previously using the stagnation plate stabilized flames. Because the weak-swirl burner has the potential of stabilizing highly turbulent flames, it is an ideal configuration for investigating turbulent flame speed and flame quenching.

In addition to its scientific significance, the weak swirl burner is a prime candidate for technology transfer. The burner operates under a much broader range of mixture conditions than any of our laboratory burners. In particular, it supports stable combustion in very fuel lean conditions. This feature can be exploited in designing a low NO_x emission furnace. The development of reliable lean-burn systems to replace current models will contribute to the improvement of regional and indoor air quality. Our laboratory burner has about the same power rating as residential air and water heaters. Therefore application of the weak swirl burner to these furnaces seems appropriate. Several approaches to implement this new technique can be sought. One is to retrofit existing furnaces with the swirl burner. Another is to design new furnaces to take full advantage of the unique flame shape produced by this burner. In either case, the operating principle is understood. Scaling the design to different power ratings would be relatively straight forward using the flame speed data we have obtained for a wide range of turbulence conditions. A patent is being sought for the weak-swirl burner and potential licensees and co-developers are being pursued through the Technology Transfer Office at LBL.

Our theoretical study of premixed turbulent flames involves the development of deterministic models of turbulent combustion employing Chorin's vortex dynamics method. The vortex dynamics model is capable of predicting these changes and other flame phenomena, in particular, the flamelet geometry. In simulating the flamelets, one needs to follow the evolution of the flamelets whose speed depends on the local curvature The algorithms approximate the equations of motion of propagating fronts with curvature-dependent speed, which are called PSC schemes, for Propagation of Surfaces under Curvature. These algorithms are coupled to a vortex dynamics approach to describe both the turbulence in the oncoming stream and turbulence production by the flame itself, and a volume production model to represent combustion heat release. Various statistical data including conditioned and unconditioned mean and RMS values of the two velocity components and the Reynolds stress can be deduced form the numerical results and compared with experimental data.

We have developed a two dimensional premixed turbulent flame model which focuses on the structure of v-shaped free-burning anchored flames, including the effects of advection, volume expansion, flame generated vorticity, and curvature effects on the laminar flamelet propagation speed. Except for the restriction to two-dimensionality, this model is a fairly complete numerical representation of our previous experimental work, under the assumptions inherent in the wrinkled laminar flamelet model, where the flame can be treated as a vanishingly thin interface separating

reactants and products. The calculation is a time dependent one; an initial flame configuration is assumed, and the calculation proceeds in time steps until a statistically stationary limit is achieved.

The results obtained bear a striking resemblance to the tomographic data we have obtained previously on turbulent v-flame structure. The numerical results for each time-step have been transferred to a video disk and can be viewed at various speeds to infer the development of the flame wrinkles and their dynamic interaction with the turbulent flow in the reactants ahead and in the products behind. One of the numerical predictions is that the included angle of the v-flame is determined more by volumetric expansion than by enhancement of the burning velocity due to turbulence. This is a feature we observed in our experiments. Our numerical results also show that vorticity production by baroclinicity at the flame front alters the mean angle of the flame. The thickness of the flame brush due to oscillations produced by the incoming turbulence appears to be consistent with what we observe experimentally. In addition, the numerical results can be analyzed to obtain detailed velocity statistics for direct comparison with our LDA data. These quantities include the vorticity, integral scale and Reynolds stresses in the burnt gas. We have experimental data on the integral scale and Reynolds stresses, with which our numerical results can be compared.

Future Plan

Our next goal is to investigate flames with high turbulence intensity to provide a closer simulation of the combustion processes in practical systems. The effect of turbulence on chemical reaction rates can be significant and may lead to the reduction of burning rate and intermittent flame quenching and re-ignition. This study requires in situ measurement of the local burning rate of the flamelets. The steep scalar gradients across the flamelets coupled with rapid flamelet motion makes the task quite challenging even with the application of advanced laser diagnostics. Our current study of flames with moderate turbulence forms the necessary scientific and theoretical background for this work.

Turbulent flame propagation and flame quenching in very fuel lean conditions will be investigated using the swirl burner. The flamelet geometry under stable and near quenching conditions will be interrogated by planar laser imaging techniques, and a series of experiments will be conducted to determine the burning rate, the flamelet geometry and processes leading to flame extinction. The use of Laser Induced Fluorescence (LIF) technique is expected to make a significant contribution to this work. In addition, development of a laminar version for combustion chemistry research is also planned. Also under consideration is the development of a high speed burner with higher turbulence approaching conditions typical of practical systems.

The development of deterministic vortex dynamic models of premixed turbulent flames will focus on predicting the flame phenomena observed by the experiments. We plan to apply our model to problems of v-flames stabilized by large diameter rods. The main goal is to investigating the relative effects of shear turbulence generated by the rod and isotropic turbulence in the free-stream to flamelet structures. Other flame configuration that we can model include stagnation flow turbulent flames stabilized by a plate or by two opposed streams. Both configurations are axi-symmetric and considered to be most suitable for investigating fundamental processes of turbulence-flame interactions.

Recent Publications

1. Kostiuk, L. W., Bray, K. N. C, and Cheng, R. K. "Premixed Turbulent Combustion in Opposed Streams, Part I Non-reacting Flowfield," *Combustion and Flame* , 92, 4, p. 377-395 (1993).
2. Kostiuk, L. W., Bray, K. N. C, and Cheng, R. K. "Premixed Turbulent Combustion in Opposed Streams, Part II Reacting Flowfield and Extinction," *Combustion and Flame*, 92, 4, p. 396-409 (1993)
3. Deschamps, B., Boukhalfa, A., Chauveau, C., Gokalp, I., Shepherd, I. G., and Cheng, R. K., "A Experimental Estimation of Flamelet Surface Density and Mean Reaction in Turbulent Premixed Flames," *24th International Symposium on Combustion,* The Combustion Institute, Pittsburgh, PA., p. 469-475 (1992).
4. Tamai, R., Maxson, J. A., Shepherd, I. G., Cheng, R. K., and Oppenheim, A. K., "Rayleigh Scattering Density Measurements of Combustion in an Enclosure" *24th International Symposium on Combustion*, The Combustion Institute, Pittsburgh, PA., p. 1433-1439 (1992).
5. Chan, C. K., Lau, K. S., Chin, W. K., and Cheng, R. K., "Freely Propagating Open Premixed Turbulent Flames Stabilized by Swirl" *24th International Symposium on Combustion,* The Combustion Institute, Pittsburgh, PA, p. 551-518 (1992). Also LBL Report 31581
6. Shepherd, I. G., Ashurst, Wm. T. "Flame Front Geometry in Premixed Turbulent Flames," *24th International Symposium on Combustion*, The Combustion Institute, Pittsburgh, PA, p. 485-491 (1992).
7. Shepherd, I. G., Cheng, R. K, and Talbot, L. "Experimental Criteria for the Determination of Fractal Parameters of Premixed Turbulent Flames," *Experiments in Fluids,* 13, 386 - 392 (1992).
8. Goix, P. J., Leonard, K. R., Talbot, L., and Chen, J. Y. "Direct Measurement of Mixture Fractions in Reacting Flow Using Rayleigh Scattering" *Experiments in Fluids, (*1993) to appear

Other Publications:

1. Rhee, C-W, "Dynamic Behavior of a Premixed Open V-Flame with Exothermicity and Baroclinicity", Ph. D. Thesis, Department of Mechanical Engineering, University of California at Berkeley, Nov. 9 1992.

Measuring Ultrashort Pulses Using Frequency-Resolved Optical Gating

Rick Trebino

Combustion Research Facility
Sandia National Laboratories
Livermore, California 94551
(510)294-2893

Program Scope

The purpose of this program is the development of techniques for the measurement of ultrafast events important in gas-phase combustion chemistry. Specifically, goals of this program include the development of fundamental concepts and spectroscopic techniques that will augment the information currently available with ultrafast laser techniques. Of equal importance is the development of technology for ultrafast spectroscopy. For example, methods for the production and measurement of ultrashort pulses at wavelengths important for these studies is an important goal. Because the specific vibrational motion excited in a molecule depends sensitively on the intensity, I(t), and the phase, $\varphi(t)$, of the ultrashort pulse used to excite the motion, it is critical to measure both of these quantities for an individual pulse. Unfortunately, this has remained an unsolved problem for many years. Fortunately, this year, we present a technique that achieves this goal.

Recent Progress

We have developed a simple, intuitive, self-contained, and general technique for measuring the intensity and phase of a single arbitrary femtosecond pulse. We use a novel arrangement and reduce the mathematics of the problem to a two-dimensional phase-retrieval problem—a well-known, solved problem from image science.

Our technique, Frequency-Resolved Optical Gating (FROG),[1] requires splitting the pulse [with field E(t)] into two variably delayed replicas, which then cross in any instantaneously responding nonlinear-optical medium. A single-shot optical-gate arrangement is ideal (See Fig. 1), yielding a signal-pulse electric field, $E_{sig}(t, \tau)$:

$$E_{sig}(t, \tau) \propto E(t)\,|E(t-\tau)|^2 \qquad (1)$$

The signal-pulse spectrum is then measured vs. the delay, τ, between the two input pulses. The measured signal trace, I_{FROG}, is thus a function of τ and frequency, ω:

$$I_{FROG}(\omega, \tau) \propto \left| \int_{-\infty}^{\infty} E_{sig}(t, \tau)\, \exp(-i\,\omega t)\, dt \right|^2 \qquad (2)$$

The FROG trace can be considered as a spectrogram, an extremely intuitive mathematical method for *displaying* a pulse (with essentially no ambiguity), showing the spectrum of a temporal slice of the pulse vs. time.[2] It is a mathematically rigorous form of the musical score, and is frequently used in acoustics problems. Thus, the easily measured FROG trace is a similarly intuitive method for displaying an ultrashort laser pulse (See Fig. 2).

The full pulse field is essentially uniquely determined by the FROG trace, even for pathological pulse shapes and/or phases. To see this, first note that E(t) results easily from $E_{sig}(t, \Omega)$, the Fourier transform of $E_{sig}(t, \tau)$ with respect to τ. Thus, we must find $E_{sig}(t, \Omega)$, which is given by:

$$I_{FROG}(\omega, \tau) \propto \left| \int_{-\infty}^{\infty} \int_{-\infty}^{\infty} E_{sig}(t, \Omega) \exp(-i\,\omega t - i\,\Omega\tau)\, dt\, d\Omega \right|^2 \qquad (3)$$

This is a *two-dimensional phase-retrieval problem*, known[3] to yield essentially unique results. In addition, algorithms[4] have been developed to find these solutions. We have implemented an iterative Fourier-transform algorithm analogous to algorithms used in image science.[5]

An amplified, Rhodamine 6G, colliding-pulse-mode-locked dye laser, produced ~ 100-fsec pulses. Spatial filtering, beam splitting, and attenuating yielded two pulses of 6 μJ each. A cylindrical lens focused the two beams, which crossed at a 20° angle, yielding a delay range of 1.2 psec. The electronic Kerr effect in a 3-mm-thick BK-7 window provided signal light with ~ 10^{-4} efficiency. The signal beam was attenuated and focused into an imaging spectrometer. A CCD camera collected the dispersed light, providing intensity vs. ω and τ in a single shot.

Figure 2 shows the experimental FROG trace for a slightly positively chirped pulse. The slightly upward-sloped trace visually indicates the chirp. More quantitatively, use of the algorithm on the 125 x 125 array of data points yields a pulse about 110 fsec in length with an inverted parabolic phase evolution (see Fig. 3), indicative of a positive linear chirp. Noise was used as the initial guess for this iteration, and convergence occurred in 50 iterations. A check of these results is provided by a comparison of the experimentally measured and the numerically derived third-order intensity autocorrelations for this pulse, which was found to be excellent.

Future Plans

A number of improvements to this method may be made in order to increase its generality. For example, the phase-retrieval algorithm we use occasionally does not converge. We have considered a number of methods for improving its reliability, and we plan to implement them. Fortunately, the current algorithm that we use is quite simple, so many new features may be added without impairing its speed.

We also believe that we may be able to measure two different pulses on a single shot. This problem is analogous to "blind deconvolution," in which two 2D functions can be determined if only their convolution is known. Such a development would be useful because measuring a pulse intensity and phase both before and after propagating through a medium would yield the medium's absorption spectrum and refractive-index variation vs. wavelength—on a single shot! We are also investigating a number of other applications of this new-found ability to measure the intensity and phase of a pulse.

Another effort that we are pursuing is an efficient method to produce the second harmonic of an ultrashort pulse. The second harmonic is important because ultraviolet light is critical for gas-phase chemistry studies. Currently, a trade-off exists between efficiency and maintaining a short pulse. We have developed a method, which we plan to demonstrate, that, in principle, maintains the ultrashort pulse length of the input pulse and also yields significantly improved efficiency over current methods. It involves only prisms, which are lossless and easy to work with. It also achieves simultaneous pulse compression.

References

1. D.J. Kane and R. Trebino, "Using Phase Retrieval to Measure the Intensity and Phase of Ultrashort Pulses: Frequency-Resolved Optical Gating," J. Opt. Soc. Am. A, *in press* (1992).
2. R.A. Altes, "Detection, Estimation, and Classification with Spectrograms," J. Acoust. Soc. Am., vol. 67, pp. 1232-1246, (1980).
3. R. Barakat and G. Newsam, "Necessary Conditions for a Unique Solution to Two-Dimensional Phase Recovery," J. Math. Phys., vol. 25, pp. 3190-3193 (1984).
4. J.R. Fienup, "Phase Retrieval Algorithms: A Comparison," Appl. Opt., vol. 21, pp. 2758-2769 (1982).
5. J.R. Fienup, "Reconstruction of a Complex-Valued Object from the Modulus of its Fourier Transform Using a Support Constraint," J. Opt. Soc. Am. A, vol. 4, pp. 118-123 (1987).

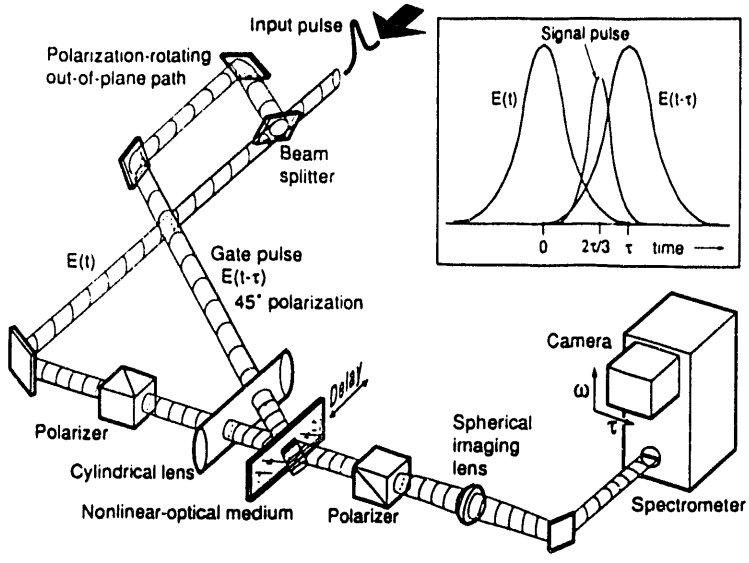

Figure 1. Frequency-Resolved Optical Gating (FROG) involves splitting the pulse and overlapping the two resulting pulse replicas, E(t) and E(t-τ), in an instantaneously responding nonlinear-optical medium. The signal pulse is then spectrally resolved, and its intensity measured vs. frequency, ω, and delay, τ. A single-shot beam geometry is shown here: each replica of the pulse is focused with a cylindrical lens to a line in the sample medium. Inset: overlapping pulses and the signal pulse.

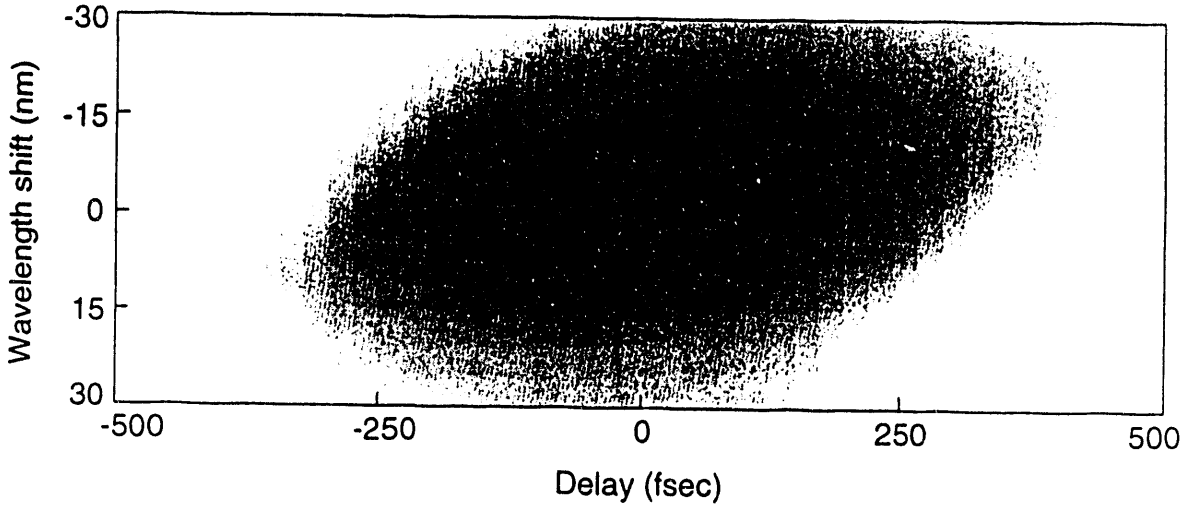

Figure 2. An experimental single-shot FROG trace for a slightly linearly chirped pulse.

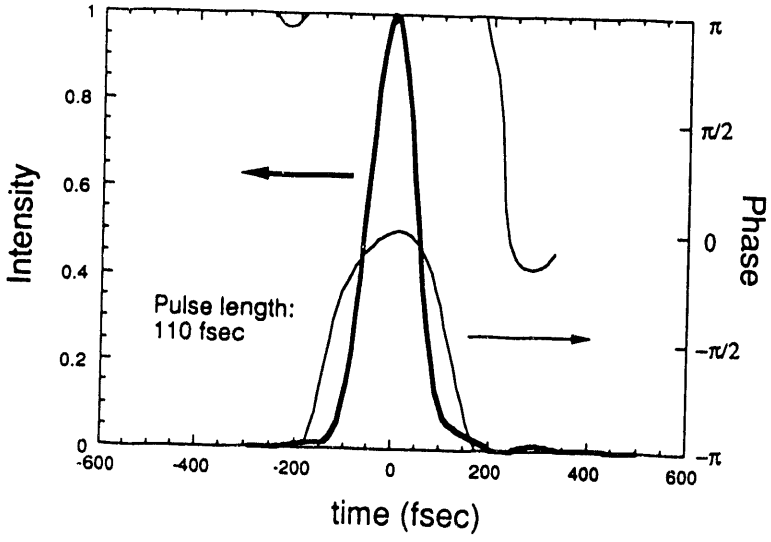

Figure 3. The derived intensity (thick curve) and phase (thin curve) evolution for the pulse whose FROG trace is shown in Fig. 2. The inverted parabolic shape of the phase evolution indicates positive chirp, that is, linearly increasing frequency vs. time ($\omega(t) = -d\varphi/dt$). (Phase behavior for large positive and large negative times is indeterminate because the intensity at these times is zero.)

Publications 1991-93

D. J. Kane and R. Trebino, "Measurement of the Intensity and Phase of Femtosecond Pulses Using Frequency-Resolved Optical Gating," IEEE J. Quant. Electron., *in press* (1993).

D. J. Kane and R. Trebino, "Single-Shot Measurement of the Intensity and Phase of a Femtosecond Pulse," in *The Generation and Measurement of Ultrashort Pulses*, ed. A. J. Taylor and T. Gosnell, (SPIE Press, Bellingham, 1993) *in press*.

D. J. Kane and R. Trebino, "Single-Shot Measurement of the Intensity and Phase of an Arbitrary Femtosecond Pulse Using Frequency-Resolved Optical Gating," Opt. Lett., *in press* (1993).

R. Trebino and D. J. Kane, "Using Phase Retrieval to Measure the Intensity and Phase of Ultrashort Pulses: Frequency-Resolved Optical Gating," J. Opt. Soc. Amer. A, *in press* (1993).

D. J. Kane and R. Trebino, "Single-Shot Measurement of the Intensity and Phase of a Femtosecond Pulse," in *Ultrafast Phenomena VIII, in press* (1993).

J. T. Fourkas, R. Trebino, M. A. Dugan, and M. D. Fayer, "Extra Resonances in Time-Domain Four-Wave-Mixing Experiments," Opt. Lett., *in press* (1993).

R. P. Lucht, R. Trebino, and L. A. Rahn, "Resonant Multiwave-Mixing Spectra of Gas Phase Sodium: Nonperturbative Calculations," Phys. Rev. A, vol. 45, p. 8209 (1992).

J. T. Fourkas, R. Trebino, and M. D. Fayer, "The Grating Decomposition Method: A New Approach for Understanding Polarization-Selective Transient Grating Experiments II. Applications," J. Chem. Phys., vol. 92, p. 78 (1992).

J. T. Fourkas, R. Trebino, and M. D. Fayer, "The Grating Decomposition Method: A New Approach for Understanding Polarization-Selective Transient Grating Experiments I. Theory," J. Chem. Phys., vol. 92, p. 69 (1992).

R. P. Lucht, R. L. Farrow, R. Trebino, and L. A. Rahn, "Nonperturbative Calculations of High-Intensity Effects in Nonlinear Wave-Mixing Processes," in *Laser Spectroscopy X*, ed. M. Ducloy, E. Giacobino, and G. Camy, 1992) p. 320.

A. M. Levine, E. Ozizmir, R. Trebino, and C. C. Hayden, "New Developments in Autocorrelation Measurements of Ultrashort Pulses," in *Laser Spectroscopy X*, ed. M. Ducloy, E. Giacobino, and G. Camy, 1992) p. 384.

R. Trebino, "Unusual Lineshapes in Higher-Order Dephasing-Induced Wave-Mixing," in *Laser Spectroscopy X*, ed. M. Ducloy, E. Giacobino, and G. Camy, 1992) p. 318.

R. Trebino and C. C. Hayden, "Antiresonant-Ring Transient Spectroscopy," Opt. Lett., vol. 16, p. 493 (1991).

VARIATIONAL TRANSITION STATE THEORY

Principal investigator and mailing address

Donald G. Truhlar
Department of Chemistry
University of Minnesota
Minneapolis, MN 55455

Program scope

This research program involves the development of variational transition state theory (VTST) and semiclassical tunneling methods for the calculation of gas-phase reaction rates and selected applications. The applications are selected for their fundamental interest and/or their relevance to combustion.

Recent progress

We have made progress in methodology, in the development of two general computer programs, and in applications.

Methodological progress includes (i) a study of the effect of the definition of the reaction coordinate on computed rates, (ii) optimization of methods for calculating reaction paths, (iii) development and implementation of projection operator techniques for enforcing internal-coordinate constraints in variational transition state theory calculations, (iv) development and implementation of a practical, efficient method for including one-dimensional hindered-internal-rotation anharmonicity all along a polyatomic reaction path, (v) testing and implementation of second-order perturbation theory for mode-mode coupling anharmonic effects along a reaction path, (vi) development and implementation of the centrifugal-dominant small-curvature semiclassical adiabatic ground-state (CD-SCSAG) method for small-curvature tunneling calculations on polyatomics, (vii) full implementation of the large-curvature ground-state, version 3 tunneling method for polyatomics, including tunneling into quasiadiabatic vibrational excited states, (viii) development and implementation of two versions of the semiclassical optimized multidimensional tunneling (OMT) approximation, (ix) development and implementation of the neglect-of-diatomic-differential-overlap with specific reaction parameters (NDDO-SRP) method for using semiempirical molecular orbital theory as an implicit interpolating function for electronic structure information in reaction-path calculations, and (x) development, testing, and implementation of several levels of interpolated variational transition state for interfacing electronic structure calculations with variational transition state theory and small-curvature tunneling calculations.

We have made two computer programs that incorporate most of these methods available to the rest of the community. These programs are called POLYRATE and MORATE. The former is for calculations based on a global potential energy function or a series of electronic calculations at points along a reaction path. The latter is for direct dynamics calculations in which the potential energy function is defined implicitly by semiempirical molecular theory and the intermediate-neglect-of-differential-overlap or neglect-of-diatomic-differential-overlap level.

Recent applications of these methods include (i) a series of studies on gas-phase S_N2 reactions, including $Cl^- + CH_3Cl$, $Cl^-(H_2O) + CH_3Cl$, $Cl^-(H_2O)_2 + CH_3Cl$, and $Cl^- + CH_3Br$, employing several different global analytic potential energy functions, including one developed especially for these studies, and also employing the NDDO-SRP method, (ii) VTST/CD-SCSAG calculations at the NDDO level on the sigmatropic rearrangement of *cis*-1,3-pentadiene and kinetic isotope effects thereon, (iii) IVTST/CD-SCSAG calculations on $OH + CH_4$ and kinetic isotope effects in this system using large-basis-set ab initio calculations at the level of Møller-Plesset second-order perturbation theory, scaling all correlation energy, (iv) application of VTST with an NDDO-SRP potential, hindered-internal-rotation anharmonicity, and the OMT approximation to the reactions $CF_3 + CH_4$ and $CF_3 + CD_4$.

Future plans

We have begun to develop another method of interfacing electronic structure calculations with dynamics. This new method will be complementary to the NDDO-SRP and IVTST approaches. It is called variational transition state theory with interpolated corrections (VTST-IC). In this method, rather than interpolating the reaction path functions globally by analytic functions (IVTST approach) or implicitly by semiempirical molecular orbital theory (NDDO-SRP approach), they are interpolated by a combination of NDDO-SRP for the basic shape of the reaction path function and analytic functions for the correction, where the correction is the amount required to bring the NDDO-SRP calculation into agreement with high-level ab initio calculations at selected points along the reaction path. This new method has already been added to POLYRATE, and it will be added to MORATE in the near future. Since the analytic functions are used for small corrections rather than for the whole reaction-path property, the sensitivity to the choice of functional form is expected to be greatly diminished. We expect that each of the three methods of interpolation, NDDO-SRP, IVTST, and VTST-IC, will be useful under different circumstances.

We will apply the VTST-IC method to reactions of OH radicals with various substrates.

We will also make additional applications of the recently developed methods to a variety of combustion reactions, organic reactions, and reactions of clusters.

We will continue to improve and extend the methods when required for higher accuracy and/or applications to new systems or new kinds of systems and also to make the interface with electronic structure theory more powerful.

Bibliography of DOE-supported work: 1991–present

Journal articles and book chapter

1. "Variational Transition State Theory with Multidimensional Semiclassical Ground-State Transmission Coefficients: Applications to Secondary Deuterium Kinetic Isotope Effects in Reactions Involving Methane and Chloromethane," D. G. Truhlar, D.-h. Lu, S. C. Tucker, X. G. Zhao, A. Gonzalez-Lafont, T. N. Truong, D. Maurice, Y-.P. Liu, and G. C. Lynch, in *Isotope Effects in Chemical Reactions and Photodissociation Processes*, by J. A. Kaye (American Chemical Society Symposium Series, Washington, DC, 1991), pp. 16-36.

2. "Global Control of Suprathreshold Reactivity by Quantized Transition States," D. C. Chatfield, R. S. Friedman, D. G. Truhlar, B. C. Garrett, and D. W. Schwenke, Journal of the American Chemical Society **113**, 486-494 (1991).

3. "Projection Operator Method for Geometry Optimization with Constraints," D.-h. Lu, M. Zhao, and D. G. Truhlar, Journal of Computational Chemistry **12**, 376-384 (1991).

4. "Solvent and Secondary Kinetic Isotope Effects for the Microhydrated S_N2 Reaction of $Cl^-(H_2O)_n$ with CH_3Cl," X. G. Zhao, S. C. Tucker, and D. G. Truhlar, Journal of the American Chemical Society **113**, 826-832 (1991).

5. "A Simple Approximation for the Vibrational Partition Function of a Hindered Internal Rotation," D. G. Truhlar, Journal of Computational Chemistry **12**, 266-270 (1991).

6. "Simple Perturbation Theory Estimates of Equilibrium Constants from Force Fields," D. G. Truhlar and A. D. Isaacson, Journal of Chemical Physics **94**, 357-359 (1991).

7. "Direct Dynamics Calculations with Neglect of Diatomic Differential Overlap Molecular Orbital Theory with Specific Reaction Parameters," A. Gonzalez-Lafont, T. N. Truong, and D. G. Truhlar, Journal of Physical Chemistry **95**, 4618-4627 (1991).

8. "The Definition of Reaction Coordinates for Reaction-Path Dynamics," G. A. Natanson, B. C. Garrett, T. N. Truong, T. Joseph, and D. G. Truhlar, Journal of Chemical Physics **94**, 7875-7892 (1991).

9. "Use of Scaled External Correlation, a Double Many-Body Expansion, and Variational Transition State Theory to Calibrate a Potential Energy Surface for FH_2," G. C. Lynch, R. Steckler, D. W. Schwenke, A. J. C. Varandas, D. G. Truhlar, and B. C. Garrett, Journal of Chemical Physics **94**, 7136-7149 (1991).

10. "Critical Tests of Variational Transition State Theory and Semiclassical Tunneling Methods for Hydrogen and Deuterium Atom Transfer Reactions and Use of the Semiclassical Calculations to Interpret the Overbarrier and Tunneling Dynamics," B. C. Garrett and D. G. Truhlar, Journal of Physical Chemistry **95**, 10374-10379 (1991).

11. "Interpolated Variational Transition State Theory: Practical Methods for Estimating Variational Transition State Properties and Tunneling Contributions to Chemical Reaction Rates from Electronic Structure Calculations," A. Gonzalez-Lafont, T. N. Truong, and D. G. Truhlar, Journal of Chemical Physics **95**, 8875-8894 (1991).

12. "Temperature Dependence of the Kinetic Isotope Effect for a Gas-Phase S_N2 Reaction: $Cl^- + CH_3Br$," A. A. Viggiano, J. Paschkewitz, R. A. Morris, J. F. Paulson, A. Gonzalez-Lafont, and D. G. Truhlar, Journal of the American Chemical Society **113**, 9404-9405 (1991).

13. "Quantized Transition State Structure in the Cumulative Reaction Probabilities for the Cl + HCl, I + HI, and I + DI Reactions," D. C. Chatfield, R. S. Friedman, G. C. Lynch, and D. G. Truhlar, Journal of Physical Chemistry **96**, 57-63 (1992).

14. "The Control of Chemical Reactivity by Quantized Transition States," D. C. Chatfield, R. S. Friedman, D. W. Schwenke, and D. G. Truhlar, Journal of Physical Chemistry **96**, 2414-2421 (1992).

15. "Optimized Calculations of Reaction Paths and Reaction-Path Functions for Chemical Reactions," V. S. Melissas, D. G. Truhlar, and B. C. Garrett, Journal of Chemical Physics **96**, 5758-5772 (1992).

16. "POLYRATE 4: A New Version of a Computer Program for the Calculation of Chemical Reaction Rates for Polyatomics," D.-h. Lu, T. N. Truong, V. S. Melissas, G. C. Lynch, Y.-P. Liu, B. C. Garrett, R. Steckler, A. D. Isaacson, S. N. Rai, G. C. Hancock, J. G. Lauderdale, T. Joseph, and D. G. Truhlar, Computer Physics Communications **71**, 235-262 (1992).

17. "Resonance State Approach to Quantum Mechanical Variational Transition State Theory," D. G. Truhlar and B. C. Garrett, Journal of Physical Chemistry **96**, 6515-6518 (1992).

18. "Use of an Improved Ion-Solvent Potential Energy Function to Calculate the Reaction Rate and α-Deuterium and Microsolvation Kinetic Isotope Effects for the Gas-Phase S_N2 Reaction of $Cl^-(H_2O)$ with CH_3Cl," X. G. Zhao, D.-h. Lu, Y.-P. Liu, G. C. Lynch, and D. G. Truhlar, Journal of Chemical Physics **97**, 6369-6383 (1992).

19. "MORATE: A Program for Direct Dynamics Calculations of Chemical Reaction Rates by Semiempirical Molecular Orbital Theory," T. N. Truong, D.-h. Lu, G. C. Lynch, Y.-P. Liu, V. S. Melissas, J. J. P. Stewart, R. Steckler, B. C. Garrett, A. D. Isaacson, A. Gonzalez-Lafont, S. N. Rai, G. C. Hancock, T. Joseph, and D. G. Truhlar, Computer Physics Communications, in press.

20. "Inclusion of Nonequilibrium Continuum Solvation Effects in Variational Transition State Theory," D. G. Truhlar, G. K. Schenter, and B. C. Garrett, Journal of Chemical Physics, in press.

21. "Molecular Modeling of the Kinetic Isotope Effect for the [1,5]-Sigmatropic Rearrangement of *cis*-1,3-Pentadiene," Y.-P. Liu, G. C. Lynch, T. N. Truong, D.-h. Lu, D. G. Truhlar, and B. C. Garrett, Journal of the American Chemical Society, in press.

22. "Interpolated Variational Transition State Theory and Tunneling Calculations of the Rate Constant of the Reaction OH + CH4 at 223–2400 K," V. S. Melissas and D. G. Truhlar, Journal of Chemical Physics, to be published.

Computer program in international program libraries

"POLYRATE–version 4..0.1," D.-h. Lu, T. N. Truong, V. S. Melissas, G. C. Lynch, Y.-P. Liu, B. C. Garrett, R. Steckler, A. D. Isaacson, S. N. Rai, G. C. Hancock, J. G. Lauderdale, T. Joseph, and D. G. Truhlar:

(i) Computer Physics Communications International Program Library in Physics and Physical Chemistry catalogue no. ACJC.

(ii) Quantum Chemistry Program Exchange program no. 601–version 4.0.1.

KINETIC DATA BASE FOR COMBUSTION MODELING

Wing Tsang and John T. Herron
Chemical Kinetics and Thermodynamics Division
National Institute of Standards and Technology
Gaithersburg, Maryland 20899

Program Scope

The aim of this work is to develop a set of evaluated rate constants for use in the simulation of hydrocarbon combustion. The approach has been to begin with the small molecules and then introduce larger species with the various structural elements that can be found in all hydrocarbon fuels and decomposition products. Currently, the data base contains most of the species present in combustion systems with up to four carbon atoms. Thus, practically all the structural grouping found in aliphatic compounds have now been captured. The direction of future work is the addition of aromatic compounds to the data base.

Recent Progress

The focus of recent work continues to be on the reactions of unsaturated compounds. In the following we discuss a number of the technical issues that have arisen during the past year. Two of these, radical attack on unsaturated compounds and the unimolecular isomerization of large radicals are the natural consequences of going to more complex molecules. The final subject, the treatment of chemical activation processes represents an upgrading of our capability for the treatment of more complex systems. Unfortunately, there are very few experimental data bearing on all these questions. Our approach is to examine the limited data and then generalize results so as to use them as a basis for making recommendations. It is hoped that some of these can be verified in future experimental work.

a. Radical Attack on Unsaturated Compounds: The small radicals that are the active agents in combustion reactions attack unsaturated compounds via abstraction of hydrogen or addition. During the past year the addition of the reactions of allene and propyne to the data base has led to further consideration of the treatment of such systems.

We had shown previously that existing kinetic data on the abstraction of resonance stabilized hydrogens are very similar to those for abstraction of secondary hydrogens[1]. On that basis we assume that rate constants for hydrogen abstraction from allene are similar to those for a methyl substituted vinylic system. Since the propargyl resonance energy is very similar to that for allyl, our recommendation is for the abstraction of a propargyl hydrogen to be equal to that for an allylic hydrogen.

A more uncertain problem is the position of addition. It is generally assumed that at room temperature, terminal addition is favored. For the olefins there is good

evidence for this in the case of hydrogen and methyl. The effect is attributed to the stability of the radicals that are formed (anti-Markovnikoff). We have found that this is actually quantitative, for methyl and hydrogen addition[1,2]. That is, the differences in rate constants for addition correspond very closely to those derived from the differences in bond energies. This also means that non-terminal addition will become increasingly important as the temperature is increased. For propyne, terminal addition is also preferred[3], although the ratio for terminal to non-terminal in the case of hydrogen atoms is a factor of 4 smaller than that for propene. It is tempting to interpret this in terms of a more stable primary vinyl radical. In the case of allene, terminal hydrogen addition is again favored[4]. However, in this case it is non-terminal addition that leads to the much more stable radical (as a result of resonance effects). Thus the simple model that was successful earlier must be used with some caution.

Of particular importance is the prediction of the site of OH addition on allene and propyne. Unlike the case for OH addition to olefins, where the reversibility of the process makes it unimportant at high temperature, for these cases there is the possibility of isomerization processes leading to distinct products. These include

$$OH+H_2C=C=CH_2 \rightarrow H_2C=C(OH)-CH_2^* \rightarrow CH_3COCH_2^*$$

$$OH+HC\equiv C-CH_3 \rightarrow HC=C(OH)-CH_3^* \rightarrow CH_3COCH_2^*$$

$$OH+H_2C=C=CH_2 \leftrightarrow (OH)H_2C-C=CH_2$$

$$OH+HC\equiv C-CH_3 \rightarrow (OH)HC=C-CH_3 \rightarrow HCOCH-CH_3 \rightarrow O=C=CHCH_3+H$$

Most interestingly, OH addition to the terminal position in allene would have led to a radical which should readily decompose as the temperature is increased with the turnover in the same region as that for the olefins. Failure to observe this would suggest that the attack on allene must be on the central carbon atom. This is in accord with the observation[5] the F and Br atom attack on allene is also at this site.

In the course of examining data on OH addition to unsaturated compounds, we were surprised at the lack of direct experimental determination; the monograph of Atkinson[6] containing only one reference, the report by Cvetanovic at the 12th Photochemistry Symposium where it was concluded that at room temperature 65% of the addition was at the terminal position. Thus, non-terminal addition must be quite important. We have also determined the relative stability of the hydroxy-alkyl radicals that are formed as a result of OH addition to propene assuming that C-H bonds strengths are unchanged by beta OH substitution. The order of radical stability is in fact the reverse of that for the alkyl radicals. In other words, if the stability of the newly formed radical is a proper criteria then addition of OH should be at the non-terminal site at room temperature.

b. Large Aliphatic Radicals: Many fuels are made up of large organic molecules, and large organic radicals are formed during the decomposition process. Radical addition and combination generate even larger species. The treatment of such species has become an important problem. Unless they are thermally stable it

would be unrealistic to have these species build up in a simulation. This problem does not appear with smaller systems since the decomposition pathway is usually the reverse of formation and can be taken care of by a simple note in the commentaries. In the present case the radicals not only can decompose but also isomerize. This leads to a very complicated situation and we had decided to use the traditional approach in treating such situations. This assumes that isomerization by hydrogen atom migration involving transfer from the 1->n positions where $n \geq 4$ are so fast that the radicals are equilibrated prior to subsequent reactions.

From a recent examination of the limited literature[7,8] we concluded that at temperatures above 1000 K rate constants for 1-4 hydrogen transfer are not as fast as that for beta C-C bond cleavage, and the equilibrium hypothesis cannot possibly hold. For 1-5 and 1-6 hydrogen transfer, temperatures in excess of 1800 K are needed before the processes have comparable rate constants. In the present treatment equilibrium distributions arising from 1-5 or 1-6 hydrogen transfer are assumed and the contributions from 1-4 hydrogen isomerization are scaled to the contribution from beta bond cleavage. By this means we avoid making detailed RRKM calculations. Finally, for each radical we recommend rate constants for decomposition along the various reaction pathways.

c. Treatment of Chemical Activation Processes: At any given pressure, chemical activation processes become more important as the temperature is raised since the thermal energy content of the molecule is increased and their RRKM lifetimes shortened. In the case of resonance stabilized radicals the effects are of particular importance since their greater thermal stability and lessened reactivity means that at high temperatures they will have much longer lifetimes and greater chance of reaction with other radicals.

Calculation of these effects on the assumption of strong collisions are straightforward[9]. We have now begun to treat weak collision effects on the basis of a step ladder model of the transition probabilities. The earlier reporting format has been retained. That is tables of k(dec)/(k(dec)+k(stab)), where (dec) and (stab) refers to the decomposition and stabilization channels, as a function of temperature and pressure and collision efficiencies as a function of step-size down are presented. This then permits the interpolation for k(dec)/(k(dec)+k(stab)) at any temperature and pressure given a selected step-size down. However, the collision efficiency is now determined from the solution of the steady state master equation. We have found that at any given temperature a single value for the collisional efficiency as applied to the strong collision equation can in fact reproduce the pressure dependence as derived from more detailed calculations.

d. Data compilation: We continue to compile all published data on combustion related reactions and the evaluations of the present work as part of the NIST Chemical Kinetics Database[10], for use on personal computers. The PC data base includes data on over 6600 reaction pairs, and new data are being added continuously.

Plans

The direction of future work is to add to the data base a number of aromatic compounds. In the coming year we will add to the data base kinetic data dealing with phenyl and toluene. This will involve the reactions of these two species with all the compounds that are already in the data base.

References

1. Tsang, W., J. Phys. Chem. Ref. Data., 20, 221, 1991.
2. Slagle, I. R., Batt, L. Gmurczyk, Gutman, D. and Tsang, W., J. Phys. Chem., 95, 7732, 1991.
3. Wagner, H. Gg. and Zellner, E. Ber. Bunsenges. Phys. Chem., 76, 518, 1972.
4. Wagner, H. Gg. and Zellner, E. Ber. Bunsenges. Phys. Chem., 76, 667, 1972.
5. Abell, P. I., "Addition to Multiple Bonds" in "Free Radicals, Vol II" (J. Kochi, ed.) John Wiley and Sons, New York, NY , 1976.
6. Atkinson, R., "Kinetics and Mechanisms of the Gas Phase Reactions of the Hydroxyl Radical with Organic Compounds" J. Phys. Chem. Ref. Data., Monograph #1, 1989.
7. Larson, C. W., Chua, P. T. and Rabinovitch, B. S., J. Phys. Chem., 76, 2507, 1972.
8. Watkins, K. W., and Lawson, D. R., J. Phys. Chem., 73, 1632, 1971.
9. Robinson, P. J., and Holbrook, K. A., "Unimolecular Reactions" Wiley Interscience, New York, 1972.
10. "NIST Standard Reference Database 17; NIST Chemical Kinetics Database", Version 4.0, Standard Reference Data, National Institute of Standards and Technology, Gaithersburg, MD, April, 1992.

Publications - 1991-1993

1. Tsang, W., "Chemical Kinetic Data Base for Combustion Modeling: V. Propene", J. Phys. Chem. Ref. Data., 20, 221, 1991.
2. Slagle, I. R., Batt, L. Gmurczyk, Gutman, D. and Tsang, W., J. Phys. Chem., 95, 7732, 1991.
3. Tsang, W., Chemical Kinetic Data Base for Hydrocarbon Pyrolysis", Ind. Eng. Chem. Res., 31, 3, 1992.
4. Bencsura, A., Knyazev, V. D., Slagle, .I. R., Gutman, D., and Tsang, W. "Weak Collision Effects in the Reaction $CH_3CO=CH_3+CO$", Ber. Bunsenges. Phys. Chem., 1338, 1992.
5. Feng, Y., Niiranen, J. T., Bencsura. A., Knyazev, V. D., Gutman, D. and Tsang, W., "Weak Collision Effects in the reaction $C_2H_5 \rightleftarrows C_2H_4+H$", J. Phys. Chem., 97, 871, 1993.

Kinetic and Mechanistic Studies of Free-Radical Reactions in Combustion

Frank P. Tully
Combustion Research Facility
Sandia National Laboratories
Livermore, CA 94551-0969

Program Scope:

Combustion is driven by energy-releasing chemical reactions. Free radicals that participate in chain reactions carry the combustion process from reactants to products. Research in chemical kinetics enables us to understand the microscopic mechanisms involved in individual chemical reactions as well as to determine the rates at which they proceed. Both types of information are required for an understanding of how flames burn, why engines knock, how to minimize the production of pollutants, and many other important questions in combustion. In this program we emphasize accurate measurements over wide temperature ranges of the rates at which ubiquitous free radicals react with stable molecules. We investigate a variety of OH, CN, and CH + stable molecule reactions important to fuel conversion, emphasizing application of the extraordinarily precise technique of laser photolysis / continuous-wave laser-induced fluorescence (LP/cwLIF). This precision enables kinetic measurements to serve as mechanistic probes; we consider merely supplying rate coefficients to be too modest a goal. Since considerable effort is required to study each individual reaction, prudent selection is critical. Two factors encourage selection of a specific reaction: (1) the rates and mechanisms of the subject reaction are required input to a combustion model; and (2) the reaction is a chemical prototype which, upon characterization, will provide fundamental insight into chemical reactivity, facilitate estimation of kinetic parameters for similar reactions, and constrain and test the computational limits of reaction-rate theory. Most studies performed in this project satisfy both conditions.

Recent Progress:

Reactions of OH and CH radicals with fuel and oxidant molecules constitute critical steps in combustion processes. During the past year, we investigated the kinetics of the reactions of (1) OH with CH_4 and CD_4, (2) OH with $(H_3C)_2CHOH$, and (3) CH with H_2 and D_2. Pulsed-laser photolysis of the radical precursor initiates chemical reaction within a heated cell; cw, laser-induced fluorescence detection quantifies the evolution of the reaction in time.

The reaction between the hydroxyl radical and methane has been studied many times previously. Recently, Vaghjiani and Ravishankara[1] measured rate coefficients (k_1) for $OH + CH_4 \rightarrow H_2O + CH_3$ from $223 \leq T \leq 420$ K that are ~25% slower than previous recommendations. Also, Melissas and Truhlar[2] utilized interpolated canonical variational transition-state theory to compute rate coefficients, k_1, over the temperature range 223-2400 K. We undertook the $OH + CH_4$ study to test the lower k_1 values and extend the temperature range of measurement. The $OH + CD_4 \rightarrow HOD + CD_3$ study provides an experimental benchmark against which Truhlar and coworkers may compare future cal-

culations on isotopic variants. Our results, which are in excellent agreement with those of Vaghjiani and Ravishankara, are displayed in Figs. 1 and 2.

We completed our study of the reaction OH + $(H_3C)_2CHOH \rightarrow$ products during the past year. The rate coefficient for H-atom abstraction by OH is best fit by the expression $k(T) = 1.04 \times 10^{-17} T^{1.86} \exp(736/T)$ cm^3 molecule^{-1} s^{-1}. Chain-catalytic dehydration of 2-propanol by OH is an important component of the reaction mechanism. We characterized the dissociation kinetics of the $H_2CCH(OH)CH_3$ intermediate by fitting biexponential [OH] decays to a reaction model. From these results and previously established kinetic and thermodynamic data, we estimate BDE(H-$CH_2CH(OH)CH_3$) = (102.4 ± 1.6) kcal mol^{-1}. Measurements above T = 600 K demonstrate a role for two minor reaction channels.

We performed time-resolved RRKM/Master Equation calculations to model our experimental data on the reaction

$$\begin{array}{c} CH + H_2 \Leftrightarrow CH_3^* \Leftrightarrow CH_2 + H. \\ \Downarrow M \\ CH_3 \end{array}$$

We had measured previously the pressure dependence of the reaction at 295 K and the temperature dependence of the reaction at P = 8.2 and 750 torr of helium. Only two quantities are varied in global fitting of the data, yielding ΔE_{down} = 80 cm^{-1} and ΔE_{prod}, the energy gap between the CH + H_2 and CH_2 + H channels, = 3.3 kcal mol^{-1}. As shown in Fig. 3, these fixed transition-state calculations agree well with the experimental measurements, but future variational calculations may be expected to be better.

Many important combustion intermediates do not fluoresce, and therefore their kinetics cannot be studied by our well-developed laser photolysis/laser-induced fluorescence technique. Infrared technologies, which permit detection of specific vibrational modes in molecules, have great promise for these systems. During the past year, we built a laser photolysis / cw, infrared-laser, long-path absorption kinetics experiment. Initial studies involved detection of HCl formed by the reactions of Cl-atom with hydrocarbons and chloromethanes. A representative (single-pass) trace is displayed in Fig. 4. Table 1 lists room-temperature rate coefficients measured in this work for several reactant molecules.

Future Directions:

Future work on this project should include (1) completion of OH + alkene and OH + alcohol kinetic studies; (2) extension of CH-radical kinetic studies to higher temperatures and additional reactants, e.g., O_2, N_2, CO, NO, and CH_4; and (3) optimization of the sensitivity of the LP/cwIRLPA experiment and its application to the kinetics of polyatomic species.

[1] G. L. Vaghjiani and A. R. Ravishankara, Nature 350, 406 (1991).
[2] V. S. Melissas and D. G. Truhlar, J. Chem. Phys., in press (1993).

DOE/BES-sponsored publications during the past two years:

1. A. McIlroy and F. P. Tully, "Kinetic Study of OH Reactions with Perfluoropropene and Perfluorobenzene," J. Phys. Chem., 97, 610 (1993).
2. J. R. Dunlop and F. P. Tully, "Catalytic Dehydration of Alcohols by OH. 2-Propanol: An Intermediate Case," J. Phys. Chem., in press (1993).
3. A. McIlroy and F. P. Tully, "CH + H_2 Reaction Kinetics: Temperature and Pressure Dependence and RRKM-Master-Equation Calculation," J. Chem. Phys., in press (1993).

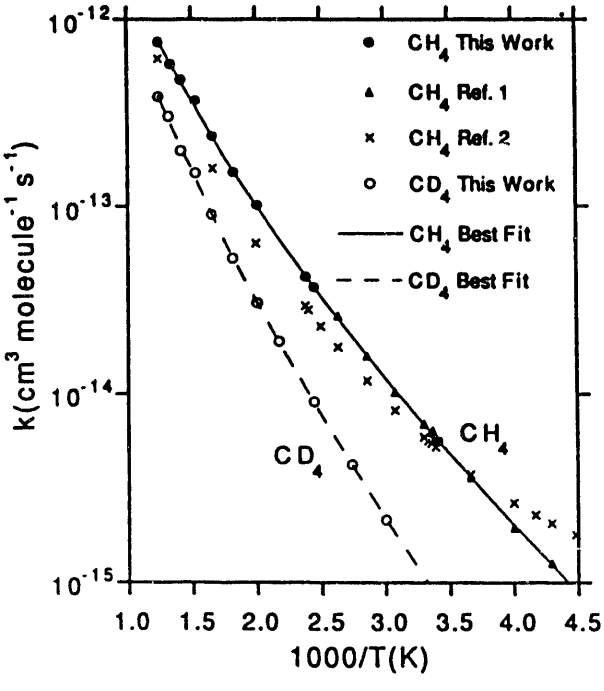

Fig. 1 Arrhenius plot of "slower" experimental data for the reaction OH + CH_4 → H_2O + CH_3, along with IVTST rate-coefficient calculations. Rate-coefficient data for the reaction OH + CD_4 → HOD + CD_3 provides benchmark for future theoretical investigations.

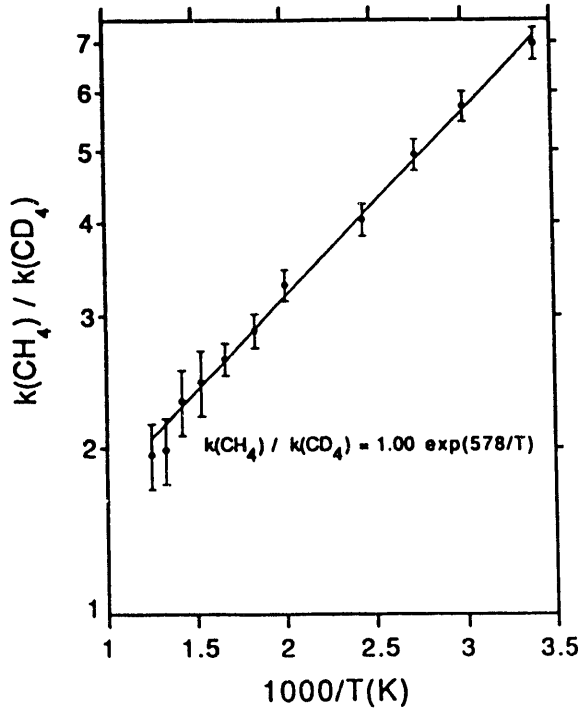

Fig. 2 Kinetic isotope effect for the reactions of OH with CH_4 and CD_4. The KIE is large as expected for abstraction from a strong C-H(D) bond.

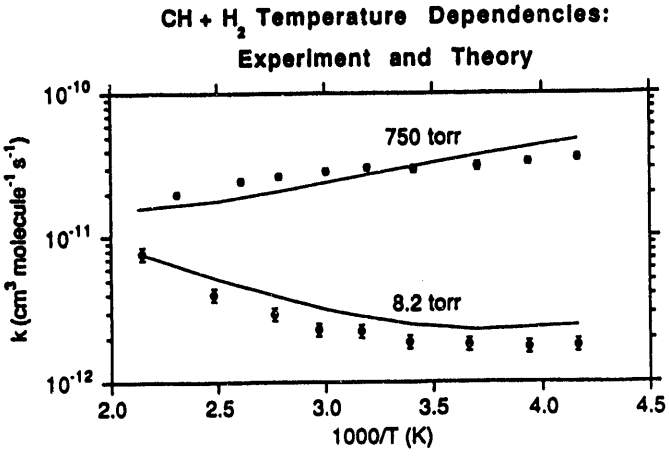

Fig. 3 Experimental and calculated temperature dependence of the reaction-rate coefficient for CH + H_2 → products at pressures of 8.2 and 750 torr of helium bath-gas. The error bars represent two standard deviations and include both systematic and random contributions. The solid lines are the results of RRKM-Master-Equation calculations using ΔE_{down}=80 cm^{-1} and ΔE_{prod}=3.3 kcal mol^{-1}.

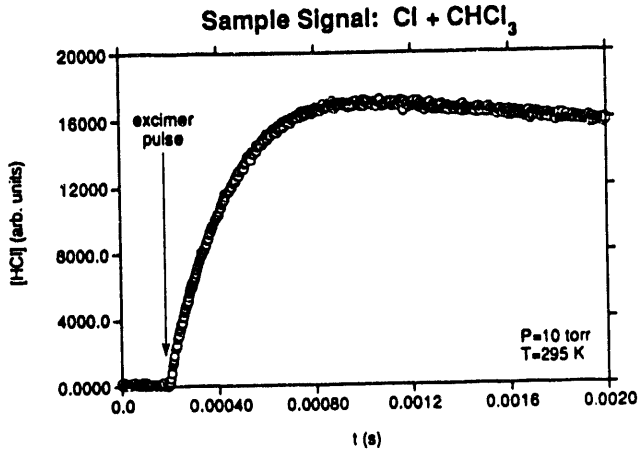

Fig. 4 Sample transient infrared HCl absorption signal for the reaction Cl + chloroform at T=295 K and P=10 torr of bath-gas. The decline at long times is due to HCl diffusion out of the spatial region monitored by the probe beam.

Table 1: Cl-atom hydrogen abstraction rate constants at T=295 K, P=10.0 torr.

RH	this work[a] k (cm^3 $molecule^{-1}$ s^{-1}) ×10^{13}	literature[b] k (cm^3 $molecule^{-1}$ s^{-1}) ×10^{13}
methane	0.999 (±0.014)	0.99
ethane	602 (±15)	569
propane	1380 (±80)	1490
butane	2030 (±80)	1800, 1970, 2230
isobutane	1400 (±30)	1370, 1410, 1510
methylchloride	3.87 (±0.07)	4.75
methylenechloride	3.56 (±0.08)	3.06, 3.8, 5.5
chloroform	15.9 (±0.2)	60

[a]Values in parentheses are two standard deviations of the parameters.

[b]We tabulate the recommended literature value where one exists, otherwise all available data are listed.

SINGLE-COLLISION STUDIES OF ENERGY TRANSFER AND CHEMICAL REACTION

James J. Valentini
Department of Chemistry
Columbia University
New York, NY 10027

PROGRAM SCOPE

Our research focus is state-to-state dynamics of reaction and energy transfer in collisions of free radicals such as H, OH, and CH_3 with H_2, alkanes, alcohols, and other hydrogen-containing molecules. The motivation for the work is the desire to provide a detailed understanding of the chemical dynamics of prototype reactions that are important in the production and utilization of energy sources, most importantly in combustion. The work is primarily experimental, but with an important and growing theoretical/computational component. The focus of this research program is now on reactions in which at least one of the reactants and one of the products is polyatomic. Our objective is to determine how the high dimensionality of the reactants and products differentiates such reactions from atom + diatom reactions of the same kinematics and energetics.

The experiments use highly time-resolved laser spectroscopic methods to prepare reactant states and analyze the states of the products on a single-collision time scale. The primary spectroscopic tool for product state analysis is coherent anti-Stokes Raman scattering (CARS) spectroscopy. CARS is used because of its generality and because the extraction of quantum state populations from CARS spectra is straightforward. The combination of the generality and easy analysis of CARS makes possible absolute cross section measurements (both state-to-state and total), a particularly valuable capability for characterizing reactive and inelastic collisions. Reactant free radicals are produced by laser photolysis of appropriate precursors. For reactant vibrational excitation stimulated Raman techniques are being developed and implemented.

The theoretical component of our research has two important facets. First, we are developing global potential energy surfaces for those reactions involving polyatomic reactants and products that we are studying experimentally, for example the 12-dimensional potential energy hypersurface for $H + CH_4 \rightarrow H_2 + CH_3$. Using these potential energy hypersurfaces we carry out quasiclassical trajectory calculations of the state-to-state dynamics of the reactions. The theoretical calculations provide the detailed analysis and interpretation of the experimental results needed to extract the full value of the laboratory measurements. Much of our current theoretical work is being done in collaboration with Jim Muckerman at Brookhaven.

RECENT PROGRESS

In 1992 we published the complete results from our extensive experimental study of the dynamics of the H + RH → H_2 + R (RH = CH_4, C_2H_6, and C_3H_8) abstraction reactions. We reported absolute partial and total cross sections for the H_2 product as a function of rotational and vibrational state. The $H_2(v',j')$ product state distributions show an anomalous positive correlation of rotational and vibrational energy. We believe that this behavior (unprecedented for a "simple" bimolecular reaction) is an important and characteristic signature of the high dimensionality of the reaction coordinate in these polyatomic reactions, but we do not yet understand the physical source or significance of these observations. Trying to understand this unusual behavior has been the motivation for the experiments and calculations we have undertaken in the last few months.

On the computational side we have extended our quasiclassical trajectory studies to many-atom systems. Of immediate interest to us is the H + CH_4 → H_2 + CH_3 reaction, for which we have already completed the experimental studies, and the H + $CHCl_3$ → H_2 + CCl_3 reaction for which experiments are now under way. We have constructed a global 12-dimensional potential energy hypersurface for the H + CH_4 reaction. This surface is based on limited ab initio calculations of the system energy as a function of all 12 coordinates along the minimum energy path, provided to us by Steve Walch of NASA Ames. We have built a truly global surface by combining these ab initio calculations with semi-empirical data. For our trajectory calculations we have adapted an adiabatic switching approach to correctly conserve the vibrational energy in each of the normal modes of the polyatomic reactant. Many production runs of the trajectory calculations have already been completed. Some of these calculations show the same positive correlation of H_2 product rotational and vibrational energies that we observe experimentally, and we are now trying to establish the physical basis of this effect by detailed analysis of the trajectories.

Experimentally we have extended our investigation of the dynamics of the H + polyatom → H_2 + polyatomic radical reactions through a study of the $H_2(v',j')$ distributions from the H + $CHCl_3$ → H_2 + CCl_3 reaction. We view this reaction as a "reduced dimensionality" analogue of the H + CH_4 reaction. In the H + CH_4 reaction the reaction coordinate is very complicated. The motion of all five H atoms are involved in the reaction coordinate, because the geometry of the CH_3 radical (planar) differs from that of the CH_3 in methane (pyramidal) and all five of these atoms are moving on the same time scale. The reaction coordinate for the H + $CHCl_3$ reaction should be much simpler. On the time scale of the abstraction reaction the motions of the heavy Cl atoms are frozen, and the geometry of the CCl_3 radical product is the same as the geometry of the CCl_3 part of $CHCl_3$. This reaction should look more like an atom + diatom reaction than the methane reaction. In fact, our initial results for H + $CHCl_3$ seem to indicate this, as the H_2 product state distribution is more like that from H + HCl than that from H + CH_4.

It seems clear to us that we need more than just the $H_2(v',j')$ distributions for the H + polyatom reactions in order to fully characterize the dynamics in these high dimensionality systems. What we need is information about the internal state distribution of the polyatomic product. We can get this information in two ways. For simple polyatomic radical products like CH_3 we can measure the CARS spectra and directly extract the rotational and vibrational distributions. For larger polyatomic radical products the Raman spectra are too complicated to allow this. However, we can determine the average internal energy of the polyatomic radical product that accompanies each $H_2(v',j')$ state by Doppler resolving the $H_2(v',j')$ CARS signal. The spectral resolution required to resolve the polyatomic CARS spectra and to make the Doppler profile measurements requires a near-transform-limited - bandwidth pulsed dye laser for the CARS Stokes beam. This year we completed design and construction of such a dye laser, based on a short-cavity dye oscillator and a narrow-band tunable amplifier. The linewidth of this dye laser is no more than a factor of two greater than the transform limit, and the pulse-to-pulse amplitude and frequency stability are very good. Pulse energies up to several tens of mJ have been obtained.

FUTURE PLANS

We will continue our trajectory studies of the H + CH_4 reaction dynamics. This will include investigation of the dynamics of reactions of vibrationally excited CH_4, in anticipation of planned experiments with vibrationally excited reactant. We are developing the capability to produce video portrayals of the trajectories. The trajectory calculations will be extended to the H + $CHCl_3$ reaction for which we now have experimental results. We will develop a semi-empirical potential energy hypersurface for this system by making reasonable adjustments to our H + CH_4 surface to accommodate the different energetics of this reaction. This H + $CHCl_3$ surface will not be as accurate as the ab initio based one we have developed for H + CH_4, but it should be adequate for our purposes.

We plan to investigate the dynamics of the H + $CHCl_3$ and H + CH_4 reactions with vibrationally excited reactants, using stimulated Raman excitation to prepare selected excited states of the $CHCl_3$ and CH_4. For the H + $CHCl_3$ reaction we will also investigate the HCl + $CHCl_2$ reaction channel. We will begin using our new transform-limited bandwidth pulsed dye laser for rotationally resolved CARS spectra of the CH_3 and CCl_3 products of the H + CH_4 and H + $CHCl_3$ reactions, and will carry out Doppler resolved CARS spectra of the H_2 product of such reactions.

RESEARCH PUBLICATIONS 1991-1993

1. G.J. Germann, Y-D. Huh, and J.J. Valentini, "Observation of Anomalous Energy Partitioning to the HD Product of the H + $CD_4 \rightarrow$ HD + CD_3 Reaction," Chem. Phys. Lett. 183, 353 (1991).

2. J.J. Valentini, P.M. Aker, G.J. Germann, and Y-D. Huh, "Transition State Control of Product Rotational Distributions in H + RH → H_2 + R Reactions (RH = HCl, HBr, HI, CH_4, C_2H_6, C_3H_8)" J. Chem. Soc. Faraday Discuss. 91, 173 (1991).
3. G.J. Germann, Y-D. Huh, and J.J. Valentini, "State-to-State Dynamics of Atom + Polyatom Abstraction Reactions. I. The H + CD_4 → HD(v',J') + CD_3 Reaction," J. Chem. Phys. 96, 1957 (1992).
4. N.E. Triggs, M. Zahedi, J.W. Nibler, P. DeBarber, and J.J. Valentini, "High Resolution Study of the ν_1 Vibration of CH_3 by CARS Photofragment Spectroscopy," J. Chem. Phys., 96, 1822 (1992).
5. P.M. Aker, G.J. Germann, and J.J. Valentini, "Experimental and Theoretical Study of H + HI → H_2 + I Reaction Dynamics at 1.3 eV Collision Energy," J. Chem. Phys., 96, 2756 (1992).
6. G.J. Germann, Y-D. Huh, and J.J. Valentini, "State-to-State Dynamics of Atom + Polyatom Abstraction Reactions. II. The H + C_2H_6/C_3H_8 → H_2 (v',J') + C_2H_5/C_3H_7 Reactions," J. Chem. Phys. 96, 5746 (1992).
7. P.M. Aker and J.J. Valentini, "QCT Studies of H + HI → HI(v',j') + H Energy Transfer and Exchange Reaction at High Collision Energy," J. Phys. Chem. 97, 2078 (1993).
8. "CARS and SRE Techniques for Product State Analysis and Reactant State Preparation in Reaction Dynamics, Proc. SPIE 1858, xxx (1993).

Theoretical Studies of the Dynamics of Chemical Reactions

Albert F. Wagner

Theoretical Chemistry Group, Chemistry Division
Argonne National Laboratory, Argonne, IL 60439

Reactions involving the formyl radical. The reaction

$$H + CO \rightleftharpoons HCO^* \xrightarrow{M} HCO \qquad (1)$$

is of long-standing interest as a prototype of a simple addition reaction. In studies on the ground state potential energy surface in collaboration with J. Bowman (U. of Emory), a nearly complete survey of the 27 lowest isolated resonances for total angular momentum J = 1 has been completed using the LBH potential energy surface calculated in our group several years ago. These 27 resonances are composed on 9 families of three resonances that emerge out of the 9 lowest resonances for J=0. Like the case for J=0, the J=1 resonances have been characterized by the stabilization calculations and time-independent scattering calculations described in previous years. Results indicate that HCO resonances have a largely a symmetric top pattern with modest, but measurable, distortions in the pattern occurring for resonances with large amount of HCO bend. All the resonances were found to have lifetimes lower than, but within a factor of two of, the lifetimes for the corresponding J=0 resonances. For each family of three resonances, there is a pair of very closely separated resonances that can be assigned by K=±1, where K is the projection of J on the symmetric top axis. Despite their similar widths and locations, the product distributions of these pairs of resonances are found to be clearly distinct.

The time-independent log-derivative scattering method has been used to calculate the above results on serial machines. A parallel algorithm for this method is being developed that distributes the computational work for the scattering wavefunction propagation with respect to both the scattering coordinate grid and the energy grid. The code minimizes intra-processor communications and external I/O communications and emphasizes vector operations in the calculation of the potential matrix. Future scattering calculations on Reaction (1) will be extended to higher values of J and to higher energies using this parallel code on both modestly and massively parallel computers.

Recombination reactions to form partially halogenated methane. The first step in the pyrolysis of partially halogenated methane is C-Y bond cleavage:

$$CX_3Y \rightarrow CX_3 + Y \qquad (2)$$

where Y is a halogen. Such reactions are under experimental study by Michael in our group. When viewed in reverse, a critical factor in the recombination is the X_3C-Y interaction potential. Studies of H_3C-H be Wardlaw et al. have shown that a fully dimensional flexible transition state theory model of the rate constant for CX_3+Y can be replaced by an approximate model that assumes CX_3 is a disk, uses the calculated X_3C-Y interaction potential, and interpolates the unconserved frequencies along the reaction path. This model can be made less approximate by treating CX_3 as a three-pointed star and calculating three X_3C-Y interaction potentials: one for approach perpendicular to the CX_3 plane and two for approaches within the CX_3 plane along or between the C-X axes. Such calculations are being done by Harding in our group for X and Y = H(or D), F, and Cl. Preliminary kinetics results with the disk model show large variations in the

high pressure recombination rate constants depending on the identity of Y. The theory for the three pointed star model is being developed in collaboration with Wardlaw (Queens University).

Thermal dissociation of HCN and HCCH. A standard derivation of the bond energy from the measured thermal dissociation rate constant of HCN:

$$HCN \xrightarrow{M} H + CN \qquad (3)$$

is more than 5 kcal/mole lower than the known thermodynamic value. Last year, in collaboration with Kiefer (University of Illinois at Chicago), we showed that this difference could be accounted for if the bending degree of freedom is treated as a hindered rotor using moments of inertia and hindered rotor barrier heights that adiabatically varied with the vibrational states of the H-CN and C-N stretches. Our treatment explicitly involved calculating all the bending vibrational levels of the two dimensional hindered rotor for every combination of the pair of stretching quantum numbers. These levels were then used to compute the density of states required in the low pressure limit of the dissociation rate constant.

The thermal dissociation of HCCH:

$$HCCH \xrightarrow{M} H + CCH \qquad (4)$$

displays the same kind of differences in bond energies derived from kinetics or from other more direct approaches. Here also the hindered rotor barrier is approximately 40 kcal/mole but the hindered rotation is quite complicated, involving the chasing of the two hydrogens after each other through the vinylidene structure. Furthermore, calculations by Schaefer et al. have shown the vinylidene can display large (120°) rocking angle variations with no substantial variation in energy, making the hindered rotor potential have a profile more like a mesa than a hill. In a simplified geometry, the hindered rotations can be view as three dimensional in two spherical angles and one dihedral angle. Rather than solve for all the levels of a three dimensional rotor for all combinations of the remaining three stretch quantum numbers, we have reformulated this problem semiclassically to derive a direct expression for the density of states that involves the derivative of a phase space volume integral on a total energy shell. The calculations of Schaefer et al on the vinylidene structure, the calculations of Harding in our group on the approach of H to CCH, and the experimental frequencies of HCCH and CCH are being incorporated into an approximate fit of the potential energy surface in the reduced dimensions of the angles governing the hindered rotation. With this fitted potential and with a purely harmonic representation of the potential, the density of states will be calculated semiclassically. The ratio of the harmonic to hindered rotor results will indicate if the derived bond strength from the kinetics experiment using the harmonic model is in error. The same semiclassical procedure is also being applied to HCN to verify the accuracy of the semiclassical approximation.

Inelastic collisions of NCO with He. As measured by Liu and Macdonald in our group, the inelastic process

$$NCO(^2\Pi,N,F_i,\lambda)+He \rightarrow NCO(^2\Pi,N',F_{i'},\lambda')+He \qquad (5)$$

has dramatically different rotational state distributions ($N \rightarrow N'$) depending on the conservation ($F_i=F_{i'}$) or change ($F_i \neq F_{i'}$) of the spin-orbit state in the collision. NCO is a Hund's case a molecule and it is known that spin-orbit changing collisions can only come about through the difference potential energy surface formed by subtracting the A' and A" surfaces that are sampled by the collision. In the case of NCO, this difference surface should be of much smaller range than that for the average surface formed by averaging the A' and A'' surfaces. A simplifying

hypothesis to describe the overall rotational scattering would be that the average surface controls the overall rotational distribution while the difference surface controls the branching of the distribution into different spin-orbit manifolds. The first part of this model was tested by: (1) constructing a simple parameterized average surface from the known surface for $He+CO_2$, (2) calculating the rotationally inelastic cross section within the Infinite Order Sudden approximation to closed shell quantum dynamics on the average surface, and (3) comparing the results to the experimental rotational distribution (with the distributions from different spin orbit manifolds combined). Excellent agreement between theory and experiment at five different collision energies was obtained with modest modifications in the initial $He+CO_2$ surface. The most important modification was to off set the center of mass of the molecule from the center of symmetry by the experimental amount found in NCO.

Theoretical Studies of the Reactivity and Spectroscopy of H+CO⇌HCO. I. Stabilizaton and Scattering Studies of Resonances for J=0 on the LBH Ab Initio Surface
S-W. Cho, A. F. Wagner, B. Gazdy, and J. M. Bowman, J. Chem. Phys. **96**, 2799 (1992).

Isolated Resonance Decompositon of a Multi-Channle S Matrix: a Test from the Scattering of H+CO⇌HCO
S-W. Cho, A. F. Wagner, B. Gazdy, and J. M. Bowman, J. Chem. Phys. **96**, 2812 (1992).

Isotope Effects in Addition Reactons of Importance in Combustion: Theoretical Studies of the Reactions CH + H_2 ⇌ CH_3* ⇌ CH_2+H
A.F. Wagner and L.B. Harding, ACS Symposium Series **502**, 48 (1992).

The Importance of Hindered Rotations and Other Anharmonic Effects in the Thermal Dissociaton of Small Unsaturated Molecules: Application to HCN
A. F. Wagner, J. H. Kiefer, and S. S. Kumaran, Symp. (Int.) on Comb. **24**, 613 (1992).

Theoretical Studies of He(2S) + CH(X2∏) I. Ab Initio Potential Energy Surfaces
A. F. Wagner, T. H. Dunning, Jr., and R. A. Kok, J. Chem. Phys. (accepted)

Theoretical Studies of He(2S) + CH(X2∏) II. Fully Ab Initio Cross Sections for the Inelastic Scattering and Comparison with Experiment
M. A. Alexander, W. R. Kearney, and A. F. Wagner, J. Chem. Phys. (accepted)

INFRARED SPECTROSCOPY OF ORGANIC FREE RADICALS RELATED TO COMBUSTION PROCESSES

James C. Weisshaar

Department of Chemistry
University of Wisconsin-Madison
Madison, Wisconsin 53706-1396
Internet: WEISSHAAR@CHEM.WISC.EDU

Program Definition

The primary long-term goal of this work is to develop new techniques for measuring vibrational spectra of polyatomic neutral free radicals. We will explore a variation of resonant two-photon ionization (R2PI) in which tunable ω_{IR} excites the radical vibrationally and ω_{UV} selectively ionizes only the vibrationally excited molecules. Development of the IR + UV R2PI experiment is underway. In the meantime, we have used optical R2PI and pulsed field ionization (PFI) detection to obtain new vibrational spectra of species such as the benzyl and phenylsilane cations. In benzyl, we have learned a great deal about the vibronic coupling mechanism in the mixed 1^2A_2-2^2B_2 system near 450 nm by projecting the mixed states onto the manifold of cation vibrational states. In phenylsilane$^+$, we find that the sixfold barrier to internal rotation of the silyl group is small (V_6 = +19 cm^{-1}). We are beginning to understand the mechanisms of coupling of torsional states with vibration, overall rotation, and other electronic states. In addition, we are developing a new model of internal rotation in aromatic compounds based on Prof. Frank Weinhold's natural resonance theory.

Recent Progress

1. Benzyl Radical

We create a skimmed beam of internally cold neutral benzyl radicals by 193 nm photolysis of toluene several mm downstream in a pulsed nozzle expansion.[1] Internally cold benzyl radical is probed by two-color, resonant two-photon ionization (R2PI) through vibronically mixed 1^2A_2-2^2B_2 excited states near 450 nm.[2,3,4] We obtain R2PI spectra of three isotopomers, benzyl$^+$-h_7, benzyl$^+$-αd_2, and benzyl$^+$-d_7. By tuning ω_1 to a particular resonance, scanning ω_2, and detecting electrons produced by delayed, pulsed field ionization (PFI),[5] we obtain vibrational spectra of the corresponding cations primarily in the range 0-650 cm^{-1}. We assign the low frequency bands by comparison with harmonic, normal mode frequencies from *ab initio* calculations of the X^1A_1 state of benzyl$^+$.

The origin bands provide the following adiabatic ionization potentials: 58465 ± 5 cm^{-1} = 7.2487 ± 0.0006 eV for benzyl-h_7; 58410 ± 5 cm^{-1} for benzyl-αd_2; and 58382 ± 5 cm^{-1} for benzyl-d_7. The benzyl-h_7 value refines our previous measurement[6] of 58456 ± 14 cm^{-1} from extrapolation

of cation yield curves to zero field as well as the earlier value[7] of 58100 ± 160 cm^{-1}. The accurate IP is important in thermochemical cycles.

In benzyl$^+$, we observe several low-frequency vibrational states for each isotopomer. Table I collects the measured frequencies for all three isotopomers in the range 0-650 cm^{-1} and compares experiment with *ab initio* calculations of harmonic frequencies. The vibronic mixing in the intermediate states[8,9] allows us to observe benzyl$^+$ vibrational states of both a_1 and b_1 symmetry (C_{2v} point group) in the PFI spectrum. The frequencies of the out-of-plane modes of benzyl$^+$, which we obtain indirectly from combination bands and from *ab initio* calculations, provide a quantitative measure of the bond order between the exocyclic CH_2 group and the benzene ring. The cation clearly has substantially greater double-bond character than the neutral.

In addition, the intensities of the cation bands provide a measure of the vibrational character of the excited states of neutral benzyl, complementing recent dispersed fluorescence measurements.[3a] Our new data indicate that previous models[8,9] of the vibronically mixed 1^2A_2-2^2B_2 system have included unimportant modes and neglected important ones. In particular, certain low frequency *combination* states of overall a_1 or b_1 symmetry induce vibronic mixing efficiently.

Table I. Experimental and Calculated Vibrational Levels of X^1A_1 State of Benzyl Cation.[a]

		benzyl$^+$-h_7		benzyl$^+$-αd_2		benzyl$^+$-d_7	
Level[b]	symm	expt	calc	expt	calc	expt	calc
$\nu_{36}+\nu_{17}$	b_1	487	480	456	452	423	418
$\nu_{36}+\nu_{35}$	a_1	--	552	--	540	488	494
ν_{13}	a_1	526	537	504	524	500	511
ν_{28}	b_1	598	613	596	612	575	588

[a] Calculated harmonic frequencies using Gaussian-90, MP2/6-31G*.

[b] Approximate mode descriptions (op = out-of-plane, ip = in-plane): ν_{36} = ring and CH_2 op wag; ν_{35} = op CH ring wag; ν_{28} = ip ring deform; ν_{17} = op ring + CH_2 torsion; ν_{13} = ip CCC bend.

2. Phenylsilane

Resonant two-photon ionization (R2PI) and pulsed field ionization (PFI) were used to measure S_1-S_0 and cation-S_1 spectra of phenylsilane cooled in a pulsed nozzle expansion.[12] We obtain the adiabatic ionization potentials IP(phenylsilane) = 73680 ± 5 cm^{-1}, IP(phenylsilane·Ar) = 73517 ± 5 cm^{-1} and IP(phenylsilane·Ar_2) = 73359 ± 5 cm^{-1}. We also resolve and assign many low lying torsion-vibration levels of the S_1 (X^1A_1) state of phenylsilane and of the X^2B_1 state of phenylsilane$^+$. In both states, the pure torsional transitions are well fit by a simple sixfold hindered rotor Hamiltonian. The results for the rotor inertial constant B and internal rotation potential barrier V_6 are: in S_1, B = 2.7 ± 0.2 cm^{-1} and V_6 = -44 ± 4 cm^{-1}; in the cation, B = 2.7 ± 0.2 cm^{-1} and V_6 = +19 ± 3 cm^{-1}. The sign of V_6 and the conformation of minimum energy are inferred from spectral intensities of bands terminating at the $3a_1''$ and $3a_2''$ torsional levels.[10,11] In S_1 the staggered conformation is most stable, while in the cation ground state the eclipsed conformation is most stable.

In phenylsilane$^+$ we find experimental evidence of coupling between torsion and vibration.[12] For small V_6, the term $P_\alpha P_a$ in the rigid-frame model Hamiltonian strongly mixes the $6a_1'$ and $6a_2'$ torsional states, which mediates further torsion-vibrational coupling. In addition, the cation X^2B_1 vibrational structure is badly perturbed, apparently by strong vibronic coupling with the low-lying A^2A_2 state. Accordingly, our *ab initio* calculations find a substantial in-plane distortion of the equilibrium geometry of the X^2B_1 state, while the A^2A_2 state is planar and symmetric.

For all sixfold potentials whose absolute phase is known experimentally, the most stable conformer is staggered in the neutral states (S_0 and S_1 *p*-fluorotoluene, S_1 toluene, S_1 *p*-fluorotoluene)[10] and eclipsed in the cationic states (ground state toluene$^+$ [11] and phenylsilane$^+$ [12]). We find that *ab initio* calculations correctly predict the lowest energy conformer for S_0 states and for cation ground states. In addition, we adapt the natural resonance theory (NRT) of Glendening and Weinhold[13] to explain why sixfold barriers for methyl and silyl rotors are uniformly small, while some threefold barriers are quite large. The phase of the sixfold potential is apparently determined by a subtle competition between two types of rotor-ring potential terms: attractive donor-acceptor interactions and repulsive van der Waals interactions (steric effects).[14]

Future Plans

We have obtained high quality PFI spectra of the cations toluene$^+$·Ar, *p*-fluorotoluene$^+$, *p*-fluorotoluene$^+$·Ar, and phenylsilane$^+$·Ar. Analysis of the data will provide a detailed picture of the interaction between the two low frequency motions: van der Waals bending and internal rotation of the methyl or silyl group.

In collaboration with Prof. Frank Weinhold, we have carried out high quality *ab initio* calculations of the equilibrium geometries and vibrational frequencies of toluene (S_0), toluene$^+$, and many related molecules with sixfold and threefold symmetric torsional potentials. We plan to use the

natural resonance theory to try to understand the underlying electronic factors that dictate the widely varying magnitudes of threefold potentials.

References

[1] G.C. Eiden, F. Weinhold, and J.C. Weisshaar, J. Chem. Phys. **95**, 8665 (1991); **G.C. Eiden and J.C. Weisshaar, manuscript in preparation.

[2] C. Cossart-Magos and S. Leach, J. Chem. Phys. **54**, 1534 (1972); C. Cossart-Magos and W. Goetz, J. Mol. Spectrosc. **115**, 366 (1986).

[3] a) M. Fukushima and K. Obi, J. Chem. Phys. **93**, 8488 (1990). b) J. I. Selco and P. G. Carrick, J. Mol. Spectrosc. **137**, 13 (1989).

[4] M. Heaven, L. Dimauro, and T. A. Miller, Chem. Phys. Lett. **95**, 347 (1983).

[5] K. Müller-Dethlefs, and E.W. Schlag, Ann. Rev. Phys. Chem. **42**, 109 (1991), and references therein.

[6] G.C. Eiden and J.C. Weisshaar, J. Phys. Chem. **95**, 6194 (1991).

[7] F. A. Houle and J. L. Beauchamp, J. Am. Chem. Soc. **100**, 3290 (1978).

[8] C. Cossart-Magos and S. Leach, J. Chem. Phys. **64**, 4006 (1976).

[9] F. Negri, G. Orlandi, F. Zerbetto, and M. Z. Zgierski, J. Chem. Phys. **93**, 600 (1990).

[10] A.-Q. Zhao, C.S. Parmenter, D.B. Moss, A.J. Bradley, A.E.W. Knight, and K.G. Owens, J. Chem. Phys. **96**, 6362 (1992). Tables VI and VII summarize experimental knowledge of sixfold and threefold barriers to methyl group internal rotation.

[11] K.-T. Lu, G.C. Eiden, and J.C. Weisshaar, J. Phys. Chem. **96**, 9742 (1992).

[12] **K.-T. Lu and J.C. Weisshaar, J. Chem. Phys., submitted.

[13] E. Glendening, Ph.D. thesis, Dept. of Chemistry, Univ. of Wisconsin-Madison (1991); E. Glendening and F. A. Weinhold, work in progress.

[14] D.B. Moss, C.S. Parmenter, and G.E. Ewing, J. Chem. Phys. **86**, 51 (1987); C.C. Martens and W.P., Reinhardt, J. Chem. Phys. **93**, 5621 (1990).

** Work supported by DOE.

CHEMICAL KINETICS MODELING

Charles K. Westbrook
William J. Pitz

Lawrence Livermore National Laboratory
P. O. Box 808, Livermore, California 94550

This project emphasizes numerical modeling of chemical kinetics of combustion, including applications in both practical combustion systems and in controlled laboratory experiments. Elementary reaction rate parameters are combined into mechanisms which then describe the overall reaction of the fuels being studied. Detailed sensitivity analyses are used to identify those reaction rates and product species distributions to which the results are most sensitive and therefore warrant the greatest attention from other experimental and theoretical research programs. Experimental data from a variety of environments are combined together to validate the reaction mechanisms, including results from laminar flames, shock tubes, flow systems, detonations, and even internal combustion engines.

Our research has focused on the development and application of detailed chemical kinetic models for analysis of combustion in practical systems. During the past year our emphasis has been on combustion in internal combusion engines, pulse combustors, and other practical systems. Our emphasis has been on hydrocarbon fuels, since they provide the great majority of the fuels for practical systems, although other types of fuels have also been considered. In particular, we have devoted some attention to chlorinated hydrocarbon fuels which are a major component in toxic chemical species combustion and emissions.

A large fraction of our research focused on the problem of knock in internal combustion engines. Knock represents a particularly serious limit to improvements in fuel economy and efficiency which might otherwise result from increases in engine compression ratio. Better understanding of the factors leading to engine knock could produce strategies for reduction of knock by chemical modification of the fuel-air mixtures or physical modification of the combustion process in the engine. Our contribution to this subject emphasized the development of chemical kinetic reaction mechanisms to simulate the autoignition of fuel-air mixtures in the engine chamber.

During the past year our contributions to the problem of engine knock chemistry were recognized by the Society of Automotive Engineers with their 1991 Horning Award, given each year for the contribution that best links engines and fuels. The citation for this award recognized our many years of research into the fundamentals of fuel chemistry and the insights our modeling work provided into fuel ignition, antiknock additives, and knock. This is a prestigious award, and DOE has in fact been responsible for the support of most of the recent Horning Award research, including work from Princeton University and Sandia National Laboratory, in addition to our work at LLNL. Since this award comes from the major industrial research organization

in the automotive and petroleum industries, these awards are a tangible indication and confirmation of the relevance of this work to current industrial needs and concerns.

We have continued to study kinetic features of combustion in other types of experimental environments, including shock tubes and laminar flames, where the fluid mechanics and other experimental features can be carefully controlled. Collaborations with programs in Ireland, Israel, and France provided data which were used to develop reaction mechanisms for ethanol, isobutene, methyl tert-butyl ether (mtbe), n-butane, and various isomers of hexane and octane. The results of these studies were then used to improve our ability to model combustion in automotive engines and engine knock problems in particular. We expect this type of collaborative effort to continue with experimental researchers in this country as well as with foreign colleagues.

Previous work in extending modeling capabilities to chlorinated hydrocarbon species was continued. This work has potential application to a wide range of issues, mostly pertaining to destruction of toxic chemical wastes. Our work in the past year emphasized reactions under stirred reactor conditions, with fuels including methyl chloride, ethyl chloride, and hydrochloric acid. This class of species is covered by the Clean Air Act provisions and emissions of these species will be limited drastically in the coming years. The reaction mechanisms which we are developing will be useful in analyzing performance characteristics and emissions from such systems and incinerators, pulse combustors, supercritical water oxidation systems, and stirred reactors. This work will continue in the present and coming years.

One of the features of low and intermediate temperature chemistry related to ignition and engine knock is the addition of molecular oxygen to radical species. This process yields the negative temperature coefficient behavior that impacts knocking behavior of paraffinic components in fuels. None of the rate constants involved in these addition reactions have been measured at temperatures and pressures relevant to engine knock. Recently, QRRK (Quantum Kassel) analysis has become available and can be used to calculate pressure and temperature dependencies of these reactions. We will use QRRK analysis to calculate rate constants of these reactions including the addition of oxygen to alkyl radicals, their isomerization and reaction to products such as olefins, cyclic ethers and di-hydroperoxides.

Together with Sandia National Laboratories, we have initiated a collaborative effort intended to address emissions controls from industrial facilities which are covered by the Clean Air Act. This Act includes a long list of chemical species whose emissions must be controlled or eliminated in coming years. Many species are normal products of hydrocarbon combustion, while others are produced by incomplete hydrocarbon oxidation. Another large number of toxic chemical emissions consist of chlorinated hydrocarbon species, and many of the remaining species are heavy metals and their oxides. We were approached by Chevron Research in Richmond, California, working with Sandia and LLNL to develop a proposal to the Petroleum Environmental Research Forum (PERF). This led to a consortium of seven petroleum company research organizations including Mobil, Unocal, Chevron, Phillips, Arco, Amoco, and

Shell, who agreed to work with us to understand and predict Clean Air Act emissions from industrial combustors. During the present year, we have used stirred reactor and computational fluid dynamics (CFD) models to address the specific problems of this group. This group is currently developing an integrated research plan for the coming several years, and the LLNL capabilities will be an important element in this program.

Of particular concern to the PERF team are reactive intermediate species such as formaldehyde, 1,3-butadiene, and carbon monoxide, all included in our current models of conventional hydrocarbon kinetics. We have been employing various physical models of oxidation to relate these kinetic factors to operational parameters which can be controlled in actual experiments. Several reports and technical presentations have been presented in the past few months, and this work will continue in the coming year.

We are continuing to work on reaction mechanisms for chlorinated hydrocarbon species, which combine theoretical problems of reaction kinetics with practical problems involving the interaction of the oxidation problem with the relevant initial and boundary conditions controlling the flow system. We have begun to understand the separate roles that bond energies, atomic weight, and thermochemistry play in determining kinetic oxidation rates and product distributions. We are currently developing ways of applying this elementary kinetic data to practical systems, including flame structure, reactor configurations, and high pressure reactors including supercritical water oxidation systems. This work will continue into the coming year.

Finally, we are continuing to refine our detailed chemical kinetic reaction mechanisms, using carefully selected laboratory experimental data under controlled conditions in which elementary reaction rate data can be extracted. We have used shock tube data and laminar flame data to improve our treatments of reaction rates for isobutene, ethanol, and propane, and we have used other experimental data to improve other mechanism features. This process is absolutely essential in mechanism refinement, and this activity will also continue in the coming year.

Work on engine knock will be continued, emphasizing the role of mixtures and interactions between fuel elements in determining onset of engine knock. This work has been recognized as the most significant in the entire field, and the connections and collaborations with the U. S. automotive industry make it of great economic impact. There are many scientific questions remaining in this work, including problems with impact on the petroleum industry as well as the automotive industry. The potential of this work to impact the problem of petroleum refinement has only been briefly touched to date, and the future possibilities of this work will be examined in detail.

We also expect to begin to apply developing technologies for oxidation of aromatic hydrocarbon species to applied problems. These species form an important class of hydrocarbon fuel components that have not previously been adequately represented in fuel oxidation studies. Interactions between aromatic and conventional aliphatic hydrocarbon fuel species will be examined and the implications for a variety of practical problems will be pursued. Finally, we will continue to provide technical

guidance for a variety of applied tasks of importance to DOE. The newly developing role that the national laboratories will need to play in assisting American industries to improve their competitive performance will be positively impacted by this work.

We contributed to review journals and other publications, summarizing our expertise in chemical kinetics modeling and application to practical combustion devices. We contributed a chapter on Combustion to the reference books entitled The Encyclopedia of Applied Physics, coordinated by the American Institute of Physics.

Publications

1. Curran, H. J., Dunphy, M. P., Simmie, J. M., Westbrook, C. K., and Pitz, W. J., "Shock Tube Ignition of Ethanol, Isobutene and MTBE: Experiments and Modeling," Twenty-Fourth Symposium (International) on Combustion, pp. 769-776, The Combustion Institute, Pittsburgh, 1992.
2. Chevalier, C., Pitz, W. J., Warnatz, J., Westbrook, C. K., and Melenk, H., "Hydrocarbon Ignition: Automatic Generation of Reaction Mechanisms and Applications to Modeling of Engine Knock," Twenty-Fourth Symposium (International) on Combustion, pp. 93-101, The Combustion Institute, Pittsburgh, 1992.
3. Corre, C., Dryer, F. L., Pitz, W. J., and Westbrook, C. K., "Two-Stage Flame n-Butane Flame: A Comparison between Experimental Measurements and Modeling Results," Twenty-Fourth Symposium (International) on Combustion, pp. 843-851, The Combustion Institute, Pittsburgh, 1992.
4. Mallinson, R. G., Braun, R. L., Westbrook, C. K., and Burnham, A. K., "Detailed Chemical Kinetics Study of the Role of Pressure in Butane Pyrolysis," Industrial and Engineering Chemistry Research 31, 37-45 (1992).
5. Burcat, A., Pitz, W. J., and Westbrook, C. K., "Comparative Ignition of Hexane and Octane Isomers in a Shock Tube, Proceedings of the 18th International Conference on shock Waves and Shock Tubes, 1992.
6. Cowart, J. S., Haghgooie, M., Newman, C. E., Davis, G. C., Pitz, W. J., and Westbrook, C. K., "The Intensity of Knock in an Internal Combustion Engine: An Experimental and Modeling Study," Society of Automotive Engineers SAE-922327 (1992).
7. Westbrook, C. K., Pitz, W. J., and Leppard, W. R., "Autoignition Chemistry of Paraffinic Fuels and Pro-Knock and Anti-Knock Additives: A detailed Chemical Kinetic Study," Society of Automotive Engineers SAE-912314 (1991). Awarded the 1991 Horning Memorial Award by the Society of Automotive Engineers as the best publication of the year relating engines and fuels.
8. Westbrook, C. K., "Combustion," Encyclopedia of Applied Physics, pp. 1-16, VCH Publishers, Inc., New York, 1992.
9. Westbrook, C. K., "The Chemistry Behind Engine Knock," Chemistry and Industry, pp. 562-566, 1992.
10. Koda, S., and Westbrook, "Kinetics,", ch. 4 in Advanced Combustion Science, Springer-Verlag, Tokyo, 1993.

PROBING FLAME CHEMISTRY WITH ' 1BMS, THEORY, AND MODELING

Phillip R. Westmoreland
Department of Chemical Engineering — Phone 413-545-1750 [301-975-2602 until 9/1/93]
University of Massachusetts at Amherst — FAX 413-545-1647 [301-869-5924 until 9/1/93]
159 Goessmann Laboratory; Amherst, Massachusetts 01003 — E-mail: "westm@ecs.umass.edu"

Program Scope

The objective is to establish kinetics of combustion and molecular-weight growth in C_3 hydrocarbon flames as part of an ongoing study of flame chemistry. Specific reactions being studied are (1) the growth reactions of C_3H_5 and C_3H_3 with themselves and with unsaturated hydrocarbons and (2) the oxidation reactions of O and OH with C_3's. Our approach combines molecular-beam mass spectrometry (MBMS) experiments on low-pressure flat flames; theoretical predictions of rate constants by thermochemical kinetics, Bimolecular Quantum-RRK, RRKM, and master-equation theory; and whole-flame modeling using full mechanisms of elementary reactions.

Recent Progress

Work in the first year and a half has focused on propene flame chemistry. Flame structures of fuel-lean and fuel-rich propene flat flames at low pressures have been measured and used as tests of proposed reaction sets using Chemkin-based models. To go beyond literature reports of allyl kinetics, reaction theory has been used to predict rate constants and product channels.

Flame measurements. Concentrations, temperatures, and area expansion ratios have been mapped in two premixed flat flames of propene and O_2:

- Fuel-lean with ϕ=0.229 (4.715 mole % C_3H_6, 92.701 mole % O_2, 2.584 mole % Ar); pressure of 0.03947 atm (30.00 Torr); and a mass flux of $3.031 \cdot 10^{-3}$ g·cm^{-3}·s^{-1} (v_o = 57 cm/s at 298 K); and
- Fuel-rich at ϕ=1.64 (24.88 mole % C_3H_6, 68.41 mole % O_2, 6.71 mole % Ar); 0.04605 atm (35.00 Torr); and a mass flux of $1.797 \cdot 10^{-3}$g·cm^{-3}·s^{-1} (v_o = 57 cm/s at 298 K).

Axial profiles of mole fractions have been measured (Table 1) in the flat-flame/MBMS apparatus built originally by Biordi[1,2] and modernized by us. Microprobe measurements with GC and GC/MS analyses supplemented the MBMS data, specifically to resolve C_6 and heavier species. At 4.5 mm in the fuel-rich flame, concentrations were measured for nine peaks from benzene to naphthalene.

Data on flow cross section and temperatures were measured for use in mole-fraction data analysis and for flame modeling. Area expansion ratio was measured by hot-wire anemometry in a cold flow of gas, and temperatures were measured with Y_2O_3-BeO-coated, 76-μm-diameter, Pt/Pt-13%Rh thermocouples, experimentally corrected for convective and radiative cooling.

Modeling of the propene flames. A C_1-C_3 reaction set was constructed, and its predictions were compared against data for radicals and stable species in the two propene flames. The predictions are generally good, but too-rapid destruction of propene and a resulting shift of all profiles toward the burner; overprediction of H_2, H, OH, and OH; the unmodeled presence of C_3H_xO species; and poor prediction of the initial intermediate, allyl, point to the needs for better kinetics. Reaction theory and literature data are being used to improve the reaction set, as opposed to adjusting parameters to best fit.

A set of 323 reversible reactions and 57 species was constructed from: (1) the C_1 and C_2 reaction mechanism of Miller and Bowman,[3] (2) C_3 and C_4 reactions in the mechanism of Dagaut *et al..*,[4] (3) modifications in the C_2H_2 mechanism of Miller *et al.*,[5] (4) improvements to the Miller and Bowman mechanism by Michaud *et al.*,[6] and (5) calculations at a Bimolecular Quantum-RRK level for H + allyl → C_3H_6 or CH_3 + C_2H_3 and for allyl recombination to C_6H_{10}. Flame structures were calculated using the PREMIX/Chemkin codes of Sandia on a DECstation 5000 Model 200 workstation.

Profiles for allyl and CH_3 are shown in Figure 1. First, note that the maxima of these profiles, like

---

[1]Biordi, J. C., Lazzara, C. P., Papp, J. F. *Combustion and Flame* **1974**, *23*, 73.
[2]Biordi, J. C. *Prog. Energy Comb. Sci.* **1977**, *3*, 151.
[3]Miller, J. A.; Bowman, C. T. *Prog. Energy Combust. Sci.* **1989**, *15*, 287.
[4]Dagaut, P.; Cathonnet, M.; Boettner, J. C. *Combust. Sci. and Tech.* **1990**, *71*, 111.
[5]Miller, J. A. *et al. 23rd Symp. (Intl.) on Combustion* **1990**, 187.
[6]Michaud, M.G.; Westmoreland, P.R.; Feitelberg, A.S. *24th Symp. (Intl.) on Combustion* **1992**, 879.

Table 1. Species measured in low-pressure flat flames of propene/oxygen/argon at fuel-lean (ϕ = 0.229) and fuel-rich (ϕ = 1.64) conditions. Data for different species and masses include complete profiles by MBMS, point measurements and upper bounds by MBMS, and point measurements by microprobe sampling and GC analyses.

Species	Fuel-lean	Fuel-rich	Species	Fuel-lean	Fuel-rich
H	Profile	Profile	C_4H_3	-	Profile
H_2	Profile	Profile	C_4H_4	-	Profile
CH_2	MBMS point	Profile	C_4H_5	-	Profile
CH_3	Profile	Profile	Mass 54	Profile (C_3H_2O)	Profile (C_4H_6)
Mass 16	Profile (O)	Profile (CH_4)	C_3H_5O	Profile	-
OH	Profile	Profile	Mass 56	Profile (C_3H_4O)	Profile (C_4H_8)
H_2O	Profile	Profile	C_3H_5O	Profile	-
C_2H	-	Profile	Mass 58	Profile (C_3H_6O)	Profile (C_4H_{10})
C_2H_2	Profile	Profile	C_5H_4	-	Profile
C_2H_3	MBMS point	Profile	C_5H_5	-	Profile
C_2H_4	Profile	Profile	C_5H_6	-	Profile
CO	Profile	Profile	C_5H_7	-	Profile
Mass 29	Profile (HCO)	MBMS point	C_6H_2	-	Profile
Mass 30	Profile (H_2CO)	Profile	Mass 75	-	MBMS point
O_2	Profile	Profile	Mass 76	-	MBMS point
HO_2	MBMS point	-	Mass 77	-	MBMS point
H_2O_2	MBMS bound	-	C_6H_6	-	Profile
C_3H_2	-	Profile	Benzene	-	GC point
C_3H_3	MBMS point	Profile	Mass 79	-	MBMS point
C_3H_4	Profile	Profile	Mass 80	-	MBMS point
Propyne	-	MBMS point	Mass 92 (Toluene)	-	MBMS, GC point
Propadiene	-	MBMS point	Phenylacetylene	-	GC point
Ar	Profile	Profile	Styrene	-	GC point
C_3H_5	Profile	Profile	Ethylbenzene	-	GC point
C_3H_6	Profile	Profile	Allylbenzene	-	GC point
CH_3CHO	MBMS point	-	o-Methylstyrene	-	GC point
CO_2	Profile	Profile	Indene	-	GC point
C_4H_2	-	Profile	Naphthalene	-	GC point

many of the rest, are shifted about 2 mm closer to the burner than measured; however, the mole-fraction profiles have already been shifted 2.5 orifice diameters (0.20 mm) to account for the probe-perturbation shifts which have previously been characterized by optical methods in this apparatus.[1] Second, note that the CH_3 maximum is barely within the factor-of-two calibration uncertainty for radicals, but predicted allyl is a factor of three too high in the fuel-rich flame and a factor of twenty too high in the fuel-lean flame of Figure 1. Both differences, plus overprediction of the key oxidation radicals, suggest that the predicted flame chemistry is occurring too close to the burner, possibly due to deficiencies in propene and allyl kinetics. Examining their reactions is ongoing, as described below, but it is useful to examine the key reactions in the initial predictions.

Propene was destroyed primarily by abstraction of allylic hydrogen by H-atom. Kinetics of this reaction are uncertain, and Westbrook and Pitz[7] had required a slower rate constant ($\approx$ x 1/4) to predict flame velocities correctly in atmospheric propene-air combustion. Abstraction by OH and addition of H were other important channels.

Another factor that contributed to overprediction of allyl was lack of rapid destruction channels. Beyond the allyl maximum, the dominant destruction channel was allyl + H $\rightarrow$ CH_3 + C_2H_3, an added reaction that is discussed below. Occurrence of C_3H_xO suggests that missing destruction reactions include allyl + O, OH, and HO_2, discussed below. Kinetics for allyl + O_2 should be improved, as it is represented only by a very slow reaction ($k = 1.32 \cdot 10^7$ $cm^3mol^{-1}s^{-1}$) that produces CH_3CHO + HCO. However, allyl + O_2 channels are probably unimportant because of falloff effects.

Early in the flame, allyl was consumed by combination and, at slightly higher temperatures, it was regenerated by the reverse, decomposition of C_6H_{10}. In the rich flame, this reversible sink resulted in a hump on the low-temperature side of the predicted allyl peak. No such behavior was observed in the

[7]Westbrook, C.K.; Pitz, W. J. *Combust. Sci. Tech.* **1984**, *37*, 177.

data and no destruction channels for C_6H_{10} had been included in the mechanism. This effect is then apparently an artifact of the reaction set, but the amount of allyl combination indicates that C_6H_{10} kinetics must be added because C_6H_{10} will be an oxidation intermediate, even in lean flames.

Theoretical kinetics. The flame calculations show that better allyl and vinyl kinetics are needed, so predictions have been made for allyl + H, O, OH, HO_2, and itself, as well as for vinyl + O_2. Allyl calculations show that the reactions of allyl with the above species may be summarized as:

$C_3H_5 + H$	$\rightleftarrows$	C_3H_6
$C_3H_5 + H$	$\rightleftarrows$	$CH_3 + C_2H_3$
$C_3H_5 + O$	$\leftarrow$	$H + CH_2{=}CH{-}CH{=}O$ (acrolein)
$C_3H_5 + OH$	$\rightleftarrows$	$CH_2{=}CH{-}CH_2{-}OH$ (allyl alcohol)
$C_3H_5 + HO_2$	$\rightleftarrows$	$CH_2{=}CH{-}CH_2{-}O\cdot + OH$
$C_3H_5 + CH_3$	$\rightleftarrows$	$CH_2{=}CH{-}CH_2{-}CH_3$ (1-butene)
$C_3H_5 + C_3H_5$	$\rightleftarrows$	$CH_2{=}CH{-}CH_2{-}CH_2{-}CH{=}CH_2$ (1,5-hexadiene)

The lowest state of the chemically activated adduct from H + allyl combination, $(C_3H_6)^*$, is 86.5 kcal/mol above thermal C_3H_6. This energized adduct may be stabilized by third-body collisions to thermal C_3H_6, revert to reactants, or decompose to methyl+vinyl. At 30 Torr and 1400 K, association/stabilization to C_3H_6 is predicted to have fallen off to half of $k_{\infty,a/s}$, and the addition/decomposition channel to $CH_3+C_2H_3$ begins to dominate. By 2000 K, the $CH_3+C_2H_3$ channel is more than an order of magnitude faster than the stabilization channel and is approximately equal to $k_{\infty,a/s}$. Because of the importance of this transition, higher-level calculations (RRKM and Master Equation) will be performed on the chemically activated reaction.

Reaction of allyl with O-atom produces acrolein (2-propenal, $CH_2{=}CH{-}CH{=}O$) with a rate constant equal to the high-pressure limit of association, much as for CH_3+O. The chemically activated adduct $(CH_2{=}CH{-}CH_2{-}O\cdot)^*$ may also decompose to $C_2H_3 + H_2CO$, but predictions indicate that the acrolein channel dominates. The association rate constant was initially chosen by analogy to $k_\infty(O+CH_3 \rightarrow CH_3O^* \rightarrow H+H_2CO) = 8.0\cdot10^{13}$. The present calculations make the low-temperature, low-pressure $k(O+allyl \rightarrow H+C_3H_4O)$ measured by Slagle *et al.*[8] a better choice, valid for 300-2100 K and all reasonable pressures providing that the radical-combination $k_{\infty,a/s}$ is assumed to be temperature-independent. No calculations on $C_3H_5 + O$ at a higher level of theory appear necessary.

From allyl + OH, the association/stabilization product allyl alcohol is the dominant product. The entrance channel is barrierless and loose, so $A_\infty(C_3H_5OH \rightarrow C_3H_5 + OH)$ is high, and the relative weakness of the allylic OH bonds makes E_∞ low relative to the chemically activated decomposition channels from $(C_3H_5OH)^*$. Those channels are all loose and barrierless from their association sides, but all are endothermic relative to $C_3H_5 + OH$: $H + \dot{C}H_2CHCH_2{-}OH$ by 5.7 kcal/mol, $C_2H_3 + CH_2OH$ by 10.5, $CH_2{=}CH{-}CH_2{-}O\cdot + H$ by 28, and $H + \cdot CH{=}CH{-}CH_2{-}OH$ by 33. Only at the lowest pressure (30 Torr) and the highest temperature (2100 K) does the lowest-energy channel reach the C_3H_5OH rate constant, and at those conditions the latter has fallen off to $9\cdot10^{11}$ $cm^3mol^{-1}s^{-1}$. No RRKM calculations are then required for the other channels — only for the thermal decomposition of C_3H_5OH.

Allyl + HO_2 forms products by chemically activated decomposition with a rate constant equal to $k_{a/s,\infty}$, much like allyl + O. Hot allyl peroxide may decompose either to $CH_2{=}CH{-}CH_2{-}O\cdot + OH$ or to the allylic radical of the hydroperoxide. The O–O peroxide bond is so weak that it breaks easily and, in $C_3H_5OOH^*$, so quickly that no other fate of the hot adduct is possible. The key parameter is then $k_{a/s,\infty} = 1.0\cdot10^{13}$, estimated as a geometric mean of rate constants for ethyl and allyl recombinations.

The allyl + CH_3 case gives very similar results to the isoelectronic allyl + OH case in that only the association product 1-butene is important, even with falloff. At 2000 K and 1 atm, $k_{a/s}$ has fallen off by an order of magnitude, and at 30 Torr, it is down by two orders of magnitude.

---

[8]Slagle, I. R.; Bernhardt, J. R.; Gutman, D.; Hanning-Lee, M. A.; Pilling, M. J. *J. Phys. Chem.* **1990**, *94*, 3652.

Allyl combination leads primarily to 1,5-hexadiene, but falloff is significant above about 1000 K: at 30 Torr, the recombination rate was predicted to begin to drop below k_∞ ($8.5 \cdot 10^{12}$) at 1000 K, and by 2000 K, k/k_∞ was 0.02. A 1,3,5-hexatriene + H_2 channel is also predicted to contribute, having implications in molecular-weight growth in fuel-rich flames. This channel still plays little part in allyl combination, reaching a maximum rate constant of $6 \cdot 10^{10}$ at 2000 K.

Finally, $C_2H_3 + O_2$ plays an important role in the flame, so it has been studied to examine whether an $O + C_2H_3O$ channel opens at high temperatures. Earlier experimental[9] and theoretical[10] work paint a consistent picture that $HCO + H_2CO$ forms with a negative activation energy at low temperatures and pressures. The flame calculations above use the experimental rate constant. However, theory[4] indicated that the rate constant is in fact downward curving on the Arrhenius plot, dropping much lower than extrapolation from the low-temperature fit. Chemically activated decomposition of the hot adduct to $O + C_2H_3O$ was shown possibly to contribute, depending on present uncertainty in the high-pressure-limit rate constant for the reverse, $\cdot CH_2CHO + O$ association. Calculations using local density functional theory (double numerical plus polarization basis sets) indicate that this association has a barrier sufficient to prevent the O-atom channel from contributing.

Future Plans

Work in the next year will extend the measurements to propene flames with 0.1% propadiene added, allowing more direct study of C_3H_4 and C_3H_3 kinetics. Predicted kinetics for allyl, vinyl, and C_3H_xO species will be added to the flame calculations, making initial predictions using Quantum-RRK methods and refining predictions where necessary with RRKM and Master Equation calculations. To that end, an RRKM code is being developed for chemically activated multiple isomerizations by extending the Q-formalism which had been developed for Bimolecular Quantum-RRK theory.

Presentations and Publications of DOE-sponsored Research

1. P.R. Westmoreland, "Getting Reactions and Mechanisms from Experiments Integrated with Computational Chemistry," Fourth Engineering Foundation Conference on Chemical Reaction Engineering, Palm Coast FL, February 21-26, 1993.
2. P.R. Westmoreland, "Kinetics of Allyl Radical," Paper 54e, 1992 Annual Meeting of AIChE, Miami Beach FL, November 1-6, 1992.
3. P.R. Westmoreland, "Kinetics of the Vinyl + Oxygen Reaction," Poster P55, 24th International Symposium on Combustion, Sydney, Australia, July 5-10, 1992.
4. M.G. Michaud and P.R. Westmoreland, "Testing an Improved Flame Mechanism for Oxidation and NO_x Kinetics," Poster P184, 24th International Symposium on Combustion, Sydney, Australia, July 5-10, 1992.

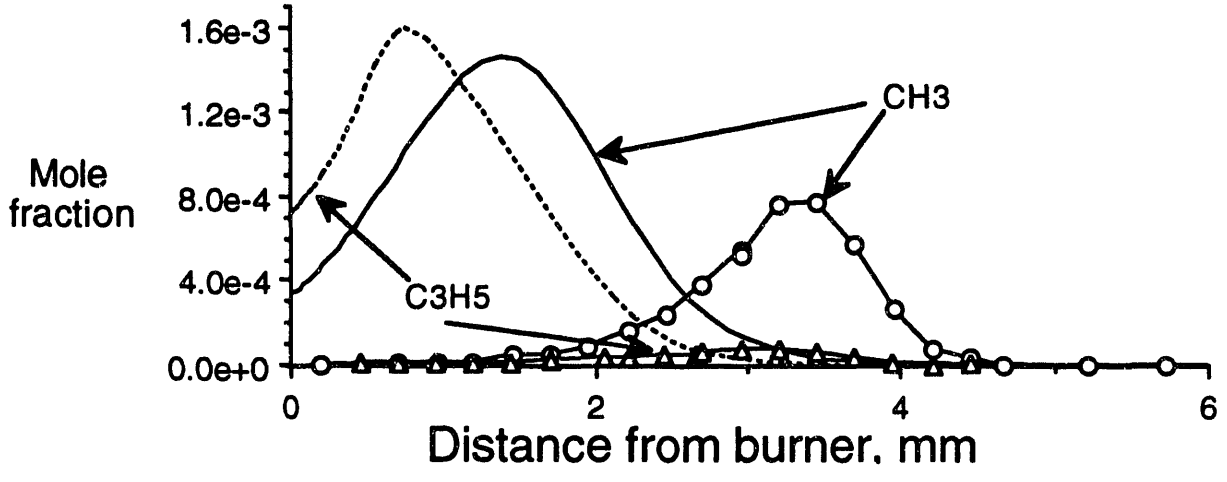

Figure 1. Data and predicted profiles for CH_3 and C_3H_5 from a fuel-lean propene flame.

[9]Slagle, I. R.; Park, J.-Y.; Heaven, M. C.; Gutman, D. *J. Am. Chem. Soc.* **1984**, *106*, 4356.
[10]Westmoreland, P. R. *Combust. Sci. and Tech.* **1992**, *82*, 151.

Gas-Phase Chemical Dynamics

Ralph E. Weston, Jr, Trevor J. Sears and Jack M. Preses.
Chemistry Department, Brookhaven National Laboratory, Upton, NY 11973

Program Scope

Research in this program is directed towards the spectroscopy of small free radicals and reactive molecules and the state-to-state dynamics of gas phase collision, energy transfer, and photodissociation phenomena. Two projects from this group, from G. E. Hall and J. T. Muckerman, are highlighted separately in this year's abstracts; other work is summarized here.

Infrared Absorption Spectroscopy of Radicals

Last year, we reported the observation and analysis of infrared and millimeter wave spectra of the HOCO and DOCO radicals. This species is crucially important as the intermediate in the reaction between hydroxyl radical and carbon monoxide. We have extended our investigations to determine more accurately electronic and structural parameters for this species. While our earlier work established that HOCO exists in the *trans-* configuration in its ground state, the observed infrared and millimeter wave spectra consisted only of *a*-dipole (parallel) transitions and the precision to which the A rotational constant could be determined was limited. To rectify this and also to characterize the fine and hyperfine splittings in HOCO reliably, we measured components of 12 rotational transitions using far infrared laser magnetic resonance (FIR LMR) spectroscopy. This technique is very sensitive although it can be difficult to analyze spectra obtained without prior knowledge of the molecular species under study.

For HOCO, data obtained at 9 different FIR laser frequencies were analyzed in conjunction with the zero field sub-millimeter rotational spectra previously obtained in collaboration with Prof. H. E. Radford (Center for Astrophysics, Harvard). All the assigned FIR LMR spectra were *b*-dipole in character; hence, the two sets of data were complementary. A least-squares fit to a standard effective Hamiltonian resulted in a very reliable set of molecular parameters that describe the ground state of the radical, and the experimental measurements were fitted to within their expected uncertainties. In addition, a much more precise determination of the A rotational constant, and several K_a dependent centrifugal distortion parameters was made and the hyperfine splitting was reliably measured for the first time. All the evidence points towards an electronic structure in which the unpaired electron predominantly resides on the carbon atom in an in-plane sp^2-like orbital. The rotational structure in the ground state shows no evidence for large amplitude motion associated with facile *cis- trans-* isomerization and the inertial defect, $\Delta_0 = 0.07719$ amu Å^2, is quite consistent with a rigid planar molecule.

Photolysis of Pyruvic Acid at 193 nm

At the Combustion Research Conference last year, our group reported on time-resolved FTIR studies of the photolysis of pyruvic acid. We observed IR emission that we assigned to CO_2 produced in the reaction:

$$CH_3COCOOH + h\nu\ (193\ nm) \rightarrow CH_3CHO + CO_2,\ \Delta H = -147\ kcal/mol.$$

In the ensuing discussion, Y. T. Lee suggested the possibility of another channel; the "triple whammy:"

$$CH_3COCOOH + h\nu\ (193\ nm) \rightarrow CH_2CO + CO_2 + H_2,\ \Delta H = -125\ kcal/mol.$$

We have searched for this possible channel, using gas chromatographic analysis of the reaction products after extensive photolysis at 193 nm. We do indeed find hydrogen as a product, in an amount corresponding to a product ratio $H_2/CO_2 = 0.36\pm0.03$. The absolute quantum yield of CO_2 was 0.7 ± 0.1, determined by comparison with the known quantum yield of the N_2O photolysis. However, we also observe significant amounts of other products. These products and their yields relative to the yield of CO_2 are as follows: CO (2.0 ± 0.1), CH_4 (0.21 ± 0.03), C_2H_4 (0.09 ± 0.01), C_2H_6 (0.46 ± 0.04), $(CH_3CO)_2$ (~0.05). These products are indicative of another channel that has already been observed by C. B. Moore and co-workers:

$$CH_3COCOOH + h\nu\ (193\ nm) \rightarrow CH_3CO + HOCO,\ \Delta H = -68\ kcal/mol.$$

The observed CO and other products may be produced by secondary fragmentation reactions of vibrationally excited photoproducts, followed by radical abstraction and recombination:

$$CH_3CHO \rightarrow CH_4 + CO \qquad CH_2CO \rightarrow CH_2 + CO$$

$$CH_3CO \rightarrow CH_3 + CO \qquad HOCO \rightarrow OH + CO \text{ or } H + CO_2\ .$$

Determination of the relative quantum yields of the three photofragmentation channels proposed here would require the use of a more universal detection method than our FTIR, such as time-of-flight mass spectrometry.

Diode Laser Studies of Energy Transfer

Collisional deactivation of highly vibrationally excited molecules is a crucial step in the mechanism of unimolecular reactions. We use time-resolved infrared diode laser absorption spectroscopy to determine the translational, rotational, and vibrational excitation of the acceptor molecule after collisions with the excited donor. So far, our experiments have used carbon dioxide as the acceptor species, and the excited species has been benzene, benzene-d_6, or hexafluorobenzene. Excitation to a higher singlet state by pulsed radiation from an excimer laser (KrF, 248 nm) is followed by very rapid internal conversion, which is instantaneous on the time scale of the collision processes under investigation.

Last year we reported the results of experiments designed to probe the antisymmetric stretching mode (ν_3) of CO_2. We found that the cross section for excitation of this mode is two to three orders of magnitude smaller than the gas kinetic collision cross section. In addition, the rotational and translational temperatures are found to be only slightly above the ambient temperature. In contrast to this result, the vibrationless ground state molecules are found to be excited to high rotational levels, and the Doppler line widths indicate that the molecules are translationally hot.

For the past year, we have been refining our initial measurements of the rotational population distribution, in order to determine the total rotational energy transferred per collision, and to calculate the total rate constant for this process. These experiments are now being carried out following significant improvements in the diode laser apparatus. A new microprocessor-based controller for the diode laser improves the temperature stability of the diode by an order of magnitude compared with the old controller; this increases the stability and reproducibility

of the laser wavelength. In addition, we have acquired a liquid nitrogen cryostat (77 K) designed for the new generation of "high temperature" diodes. This mode of operation eliminates the noise on the signal contributed by the mechanical motion in the low temperature cryostat ($\sim$ 10 K) required for the older diodes. We are also developing new methods which will essentially convert the experimental arrangement from a single-beam to a double-beam configuration. This will lead to a significant cancellation in noise from the diode laser, and will also compensate for long-term drifts in either diode or excimer laser output. Improvements to the scan control of the etalon used to determine line shapes have been implemented. We have updated the PC used for the diode laser experiments to a current model using an i486 microprocessor, and much of the control software has been rewritten.

Stimulated Emission Pumping of Radicals

We have continued our study of NCO formed in a supersonic free jet expansion by the reaction between CN radical and O_2. The NCO radicals so formed have a rotational temperature of approximately 15 K and relatively very small population in excited vibrational levels in the collision-free region of the expansion where they are probed. In the stimulated emission pumping (SEP) experiment, the pump laser excites the molecule to specific rovibrational levels in the excited $\tilde{A}^2\Sigma^+$ state, and the dump laser promotes transitions out of this prepared level to the vibrationally excited rovibronic levels of interest on the ground state, $\tilde{X}^2\Pi$, surface.

Interest in the NCO radical comes from the fact that it is subject to a Renner-Teller (RT) breakdown of the Born-Oppenheimer approximation in its ground state. The RT effect (RTE) results in a lifting of the degeneracies normally associated with the bending vibration (ν_2) in a linear triatomic. In NCO, this leads to a complex pattern of bending vibronic levels which is further complicated by the presence of a Fermi resonance ($2\nu_2 \approx \nu_1$, where ν_1 is the lower frequency stretching vibration in the radical) and the spin-orbit coupling. We have concentrated on $^2\Pi$ vibronic levels with $2 \leq v_2 \leq 4$ and $1 \leq v_1 \leq 2$ and have recorded SEP spectra that access all such levels in the ground state of NCO. In addition, we have recorded spectra of levels of $^2\Sigma$ symmetry associated with $v_1 = 1$, $v_2 = 1$ and $v_1 = 0$, $v_2 = 3$. These measurements constitute the first rotationally resolved spectra of such levels in any of the NCO-like radicals. Together with earlier spectroscopic measurements reported by many workers, the available data for NCO represent a large body of information with which to test current models of the RTE in this type of radical. We have developed a computational model that includes all of the major interactions involving ν_1 and ν_2 and the spin-orbit interaction. For the first time, end-over-end rotation was also accurately included.

The new model reproduces all the currently available rotationally resolved spectroscopic data for $J \leq 11/2$ to an accuracy that is comparable to the experimental uncertainty. The molecular parameters resulting from a fit to these data include harmonic and anharmonic vibrational contributions as well as the RT contributions. Predictions of the positions of vibronic levels that have been observed using low resolution techniques appear very reliable and for the first time, anharmonic corrections to the RTE have been estimated accurately. The derived parameters can be related to the physical characteristics of the potential energy surface and work along these lines is currently in progress.

In other work, some preliminary laser induced fluorescence (LIF) excitation and emission experiments were carried out on HNCN. This species is related to NCO. However the off-axis hydrogen atom lifts the orbital degeneracy and therefore, the degeneracy of the ground electronic state. Activity in an out-of-plane vibrational mode in the emission spectra was

identified and interpreted as evidence for a RT-like interaction between the low-lying electronic states of the radical. Experiments designed to use resonant four wave mixing in order to detect SEP signals in our experimental apparatus were not successful.

Time-Resolved FTIR Studies

During the past year we have concentrated on the reaction

$$CF_2CH_2 + h\nu(193nm) \rightarrow FCCH + HF.$$

where HF (and perhaps FCCH) are produced in vibrationally excited states. We have observed rotationally resolved HF fluorescence from transitions as high as $v=5 \rightarrow v=4$. We have investigated the rotational and vibrational distributions of HF products under conditions ranging from 10 mTorr CF_2CH_2+10 mTorr Ar to 60 mTorr CF_2CH_2+50 mTorr Ar+4.8 Torr He. At the highest pressures, collisional relaxation by rare gas produces HF rotational distributions that appear essentially thermal near ambient temperature, with a modest excess population above $J \sim 10$ that represents HF molecules rotationally relaxing slowly from high-J states with only large energy gap transitions available to them. The ratios of the vibrational populations of each state to that of $v=1$ plotted *vs.* time show the higher states relaxing most rapidly, and intermediate states relaxing more slowly, perhaps reflecting their population dropping to lower states while these states receive population from states above. Vibrational distributions fit a linear surprisal model. Recent data suggest that emission from highly vibrationally excited FCCH may have been detected near 2700 cm^{-1}.

R. Bersohn has investigated the dynamics of the photodecomposition of ethylene sulfide (thiirane)

$$C_2H_4S + h\nu(193nm) \rightarrow C_2H_4 + S(^1D) \qquad \Delta E = 84 \text{ kcal/mol}$$

by observing lineshapes of Doppler-broadened S-atom fluorescence, induced by a two-photon absorption of polarized laser radiation. Results indicated that the only products were ethylene and ^1D S-atoms and that considerable energy is available to be deposited in the internal degrees of freedom of the ethylene product. We have performed an initial survey experiment on this system using our FTIR. Our objective is to determine the energy deposition in the internal degrees of freedom of ethylene, a molecule important in hydrocarbon combustion. Initial experiments indicate that the total fluorescence intensity from pressures as low as 5 mTorr ethylene sulfide in 100 mTorr Ar is extremely strong. However, when interferograms are transformed, noisy spectra are obtained. Possibilities to explain this result are as follows. Ethylene, a 6-atom polyatomic molecule, has a large number of nondegenerate internal degrees of freedom that give rise to many rovibrational transitions. Even strong excitation distributed over a very large number of transitions may produce individual lines barely above background. This bears further investigation, and we are planning an intensive inquiry. Second, we may need to increase the collection efficiency of the optical system that couples infrared radiation from our sample cell to the interferometer so that we can better distinguish the forest of lines from the background. We have begun the improvement of the optical system. Currently, fluorescence from a small volume in the middle of our sample cell is imaged into the interferometer using a series of flats, spheres, and off-axis paraboloids. The volume of space occupied by fluorescing molecules is much larger than the region imaged. We are replacing the

collection optics with an integrating sphere and associated optics.

Future Plans

We are presently designing a new absorption cell for the infrared absorption experiments based on a collisional cooling technique demonstrated at sub-millimeter wavelengths. In this experiment, a bath gas is maintained at cryogenic temperatures (77 K or 4 K) by collisions with the cold walls of the container. The sample gas is introduced to this environment and is itself cooled by collisions with the background gas at a rate that is much faster than loss by diffusion to the walls and condensation. In our modification, the sample gas will be photolyzed and the radical products cooled before being probed by the infrared laser in the normal way. This experimental apparatus will also be used with the Ti:sapphire based spectrometer described in the separate abstract by G. Hall from our group.

Current experimental effort is centered on the detection of the *cis-* isomer of HOCO. Theoretical predictions place it some 500 to 1000 cm^{-1} above the *trans-* isomer and there is evidence from the matrix infrared spectrum that its ν_2 mode is some 50 cm^{-1} lower. A liquid nitrogen cooled variant of our standard absorption cell will be used in an attempt to obtain a rotationally cooled spectrum of C_2H_5. High quality spectra of ethyl around 20 μm were obtained some years ago but have so far resisted analysis.

In our discussions of the excitation of the antisymmetric stretching mode of CO_2, we have tacitly assumed that it is typical of the other two vibrational modes. However, in experiments we carried out a few years ago with azulene as the excited donor, we found that the probability for exciting the ν_2 bending mode was much higher than that for the antisymmetric stretch. Furthermore, Toselli and Barker have developed a model for aromatic-CO_2 interactions that predicts 30-100 times as much energy transferred from benzene to the bending mode as to the antisymmetric stretch of carbon dioxide. For these reasons, we are now attempting to determine the relative excitation of these two modes. These experiments are complicated by the fact that at room temperature almost 10% of the CO_2 molecules are in the 01^10 level. An observed increase in population of the 01^10, J′ state can result from either rotational-vibrational excitation or pure rotational excitation. To control the ambient population of the 01^10 state, we will use a temperature-controlled absorption cell. The vapor pressure of C_6F_6 determines the lowest useful temperature, which will be ~220 K.

Our current time resolved FTIR emission apparatus can be used to detect ethylene C-H stretch transitions near 3000 cm^{-1}. Addition of a HgCdTe or, better, HgMnTe detector will extend the range of sensitivity down to ~1200 cm^{-1}, so that the strong C-H ν_{12} bending mode will also be accessible. The v-v coupling rates between the C-H stretches, the C-H bends, and the overtones of the C-H bends in ethylene are known, so that simultaneous observation of the initial excitation of these states and their subsequent relaxation should be informative.

$X+Y_2$ reaction systems are excellent prototype models for more complex combustion reactions. Calculations and experiments to determine cross sections and product distributions for the reactions

$$F+H_2 \rightarrow HF+H \quad \text{and}$$
$$H+F_2 \rightarrow HF+F$$

can yet reveal new details about potentials controlling these reactions. Surprisingly, nascent rotational distributions for HF produced from the first reaction have not been measured with modern techniques. We will undertake such measurements. A likely source of F-atoms is XeF_2 excited by 193-nm radiation. For the second reaction, hot H-atoms will be obtained from 193-

nm photolysis of H_2S.

Knowledge of the branching ratio for the production of NH_2 and NH from the photolysis of ammonia can be useful in the clarification of reaction mechanisms related to problems in practical combustion. Therefore, we will attempt to measure this branching ratio.

The reaction

$$OH + H_2 \rightarrow H_2O + H$$

is important in many combustion mechanisms. The OH reactant can be generated by photolysis of H_2O_2, and the H_2O product ought to be produced with considerable vibrational excitation. Using our FTIR apparatus we should be able to characterize energy deposition into H_2O produced by this reaction.

Recent Publications

A semi-rigid Bender Analysis of an Extensive set of Rotation-Vibration Levels in $\tilde{X}^1\Sigma^+$ C_3
F. J. Northrup, T. J. Sears and E. A. Rohlfing
J. Molec. Spectrosc. **145**, 74-88 (1991)

Photodissociation of Acetone at 193 nm: Rotational and Vibrational State Distributions of Methyl Fragments by Diode Laser Absorption/Gain Spectroscopy
G. E. Hall, D. Vanden Bout and T. J. Sears
J. Chem. Phys. **94**, 4182-4188 (1991)

The FIR LMR Spectrum of FO_2: Some Classic Examples of Level Anticrossing Resonances
U. Bley, P. B. Davies, M. Grantz, T. J. Sears and F. Temps
Chem. Phys. **152**, 281-292 (1991)

Avoided Crossings in the FIR LMR Spectrum of HCO
J. M. Brown, H. E. Radford and T. J. Sears
J. Molec. Spectrosc. **148**, 20-37 (1991)

Far Infrared Laser Frequencies of CH_3OD and N_2H_4
H. E. Radford, K. M. Evenson, F. Matushima, L. R. Zink, G. P. Galvao and T. J. Sears
Int. J. IR and MM Waves **12**, 1161-1166 (1991)

Interrogating the Vibrational Relaxation of Highly Excited Polyatomics with Time-Resolved Diode Laser Spectroscopy: C_6H_6, C_6D_6, and C_6F_6 + CO_2
A. J. Sedlacek, R. E. Weston, Jr., and G. W. Flynn
J. Chem. Phys. **94**, 6483-6490 (1991)

High Resolution Fourier Transform Spectroscopy Using Infrared Synchrotron Radiation. I. Instrumentation.
K. D. Moeller, D. Scardino, T. Sears, D. Carlson, C. J. Hirschmugl, G. P. Williams, E. Chang and H. T. Liu
Int. J. IR and MM Waves **13**, 275-287 (1992)

Stimulated Emission Pumping: Applications to Highly Vibrationally Excited Transient Molecules
F. J. Northrup and T. J. Sears
Ann. Rev. Phys. Chem. **43**, 127-152 (1992)

Measurement of $(00v_3)$ Levels in $\tilde{X}^2\Pi$ NCO by Stimulated Emission Pumping Spectroscopy
F. J. Northrup, M. Wu and T. J. Sears
J. Chem. Phys. **96**, 7218-7228 (1992)

The Rotational Spectrum of *trans*- HOCO and DOCO
H. E. Radford, W. Wei and T. J. Sears
J. Chem. Phys. **97**, 3989-3995 (1992)

Transient Diode Laser Absorption Spectroscopy of the ν_2 Fundamental of *trans*- HOCO and DOCO
T. J. Sears, W. M. Fawzy and P. M. Johnson
J. Chem. Phys. **97**, 3996-4007 (1992)

Study of Renner-Teller, Spin-Orbit and Fermi-Resonance in $\tilde{X}^2\Pi$ (v_1v_20) Levels of NCO by Stimulated Emission Pumping Spectroscopy

M. Wu, F. J. Northrup and T. J. Sears

J. Chem. Phys. **97**, 4583-4595 (1992)

Chemical Reactions

R. E. Weston, Jr.

In *Encyclopedia of Applied Physics*; Trigg, G. L., Ed.; VCH Publishers, New York, NY, 1992; Vol. 3, pp. 377-411

Relaxation of Molecules with Chemically Significant Amounts of Vibrational Energy: The Dawn of the Quantum State Resolved Era

R. E. Weston, Jr. and G. W. Flynn

In *Annual Review of Physical Chemistry*; Strauss, H. L., Ed.; Annual Reviews, Inc., Palo Alto, CA, 1992; Vol. 43, pp. 559-589

Time-Resolved FTIR Studies of the Photodissociation of Pyruvic Acid at 193 nm

G. E. Hall, J. T. Muckerman, J. M. Preses, R. E. Weston, Jr. and G. W. Flynn

Chem. Phys. Letts. **193**, 77-83 (1992)

Laser Spectroscopy of Transient Species

M. Wu and T. J. Sears

SPIE Conference No. 1858, Laser Techniques for State Selected and State-to-State Chemistry, Los Angeles CA, January 16-23 (1993)

Stimulated Emission Pumping Spectroscopy of CH_3O ($\tilde{X}^2E$, ν_6); New Observations on the Jahn-Teller Effect

A. Geers, J. Kappert, F. Temps and T. J. Sears

J. Chem. Phys. **98**, 4297-4300 (1993)

A Fourier-Transform Spectrophotometer for Time-Resolved Emission Measurements using a 100-Point Transient Digitizer

J. M. Preses, G. E. Hall, J. T. Muckerman, T. J. Sears, R. E. Weston, Jr., C. Guyot, J. C. Hanson, G. W. Flynn, and H. J. Bernstein

Rev. Sci. Instrum. **64**, 95-102 (1993)

b-Dipole Transitions in *trans*- HOCO Observed by Far Infrared Laser Magnetic Resonance

T. J. Sears, H. E. Radford and M. A. Moore

J. Chem. Phys. (in press)

Laser Induced Fluorescence Spectroscopy of the Jet Cooled HNCN Radical

M. Wu, G. E. Hall and T. J. Sears

J. Chem. Soc. Farad. Trans. **89**, 615-621 (1993)

Studies of the Renner-Teller Effect in NCO by SEP Spectroscopy

M. Wu and T. J. Sears

in Molecular Dynamics and Spectroscopy by Stimulated Emission Pumping, H. L. Dai and R. W. Field Eds. World Scientific Press (submitted)

The LET Dependence of Excited Singlet State Lifetimes of Hydrocarbon Liquids Exposed to X-rays

R.A. Holroyd, J.M. Preses, and J.C. Hanson

Radiation Research (submitted)

VUV Studies of Molecular Photofragmentation Dynamics

Michael G. White

Chemistry Department, Brookhaven National Laboratory, Upton NY 11973

Project Scope

State-resolved, photoion and photoelectron methods are used to study the neutral fragmentation and ionization dynamics of small molecules relevant to atmospheric and combustion chemistry. Photodissociation and ionization are initiated by coherent VUV radiation and the fragmentation dynamics are extracted from measurements of product rovibronic state distributions, kinetic energies and angular distributions. The general aim of these studies is to investigate the multichannel interactions between the electronic and nuclear motions which determine the evolution of the photoexcited "complex" into the observed asymptotic channels.

Recent Progress

Rotationally-resolved threshold photoelectron spectra were obtained for nitric oxide (NO), formaldehyde (H_2CO) and the methyl radical (CH_3) by the pulsed field ionization technique (PFI) in conjunction with coherent VUV radiation. These experiments build on our earlier measurements of several diatomic (O_2, OH, HCl) and triatomic (N_2O, H_2O, H_2S) molecules and explore angular momentum balance and symmetry selection rules in molecular photoionization. In addition to probing the photoionization dynamics, the high resolution capabilities of the VUV/PFI measurements also resulted in the first accurate ionization potentials (± 2 cm^{-1}) for H_2CO^+ and CH_3^+ and rotational constants for H_2CO^+. Furthermore, the the CH_3 threshold photoelectron spectrum represents the first rotationally resolved photoionization measurement for a polyatomic radical.

Threshold photoionization of NO. The cation rotational state distributions for threshold photoionization of the $v^+ = 0$ and $v^+ = 1$ vibrational levels of the $X\,^1\Sigma^+$ ground state of NO^+ exhibit only small changes in core angular momentum ($|\Delta J| \leq 5/2$). An *ab initio* calculation by Wang and McKoy also predicts small angular momentum transfers for NO photoionization and is in near quantitative agreement with the data. Surprisingly, the theoretically calculated partial wave distribution predicts that photoelectron channels with high orbital angular momentum ($l \geq 2$) have relatively large transition amplitudes. From angular momentum conservation, this result would suggest that photoelectron ejection by NO should be accompanied by large changes in NO^+ angular momentum with $\Delta J \geq 7/2$. These seemingly contradictory results are rationalized in terms of a "spectator" model of ionization in which angular momentum transfers between the escaping photoelectron and ion core are small. In this case, the ion core acts as a spectator to the photoionization process and the angular momentum of the photon(s) is transfered primarily to the

photoexcited electron.

Photoionization of H_2CO and CH_3. Our earlier studies on the bent triatomics H_2O and H_2S were the first to investigate the symmetry properties of allowed rotational photoionization transitions in non-linear molecules. The rotationally-resolved H_2X (X ≡ O, S) PFI spectra could be readily assigned to two types of rotational photoionization transitions corresponding to specific changes in the asymmetric top angular momentum projection quantum numbers, $|JK_{a,b,c}\rangle$. The utility of this classification stems from the fact that these transition types are associated with only one photoelectron symmetry, i.e. $l \equiv$ *even* with type *C* and $l \equiv$ *odd* with type *A*. To further our investigation of photoionization selection rules in non-linear polyatomics, we recently obtained rotationally-resolved PFI data for formaldehyde (CH_2O) and methyl radical (CH_3). Both systems are related to the H_2X molecules but represent different limiting rotational top cases; the H_2X (H_2X^+) molecules are prolate tops in C_{2v} symmetry while H_2CO (H_2CO^+) is an oblate top in C_{2v} symmetry and CH_3 (CH_3^+) is a symmetric top with even higher symmetry, D_{3h}. This variation in top case is important as different types of rotational photoionization transitions, e.g. type A or type C, correspond to different photoelectron symmetries in the three classes of molecules.

Measurement of the PFI spectrum of CH_3 was made possible through a collaboration with Dr. Peter Chen at Harvard, who has developed a supersonic-jet, flash pyrolysis technique for the production of reactive species. The methyl radical was produced by flash pyrolysis of a 2% mix of azomethane (CH_3NNCH_3) in argon at an expansion pressure of 900 Torr. A highly structured and well resolved rotational photoionization spectrum was obtained which could be readily assigned to simple *P*, *Q*, and *R* branches ($\Delta J = -1, 0, +1$) with individual ΔJ lines composed of many closely spaced $\Delta K = 0$ sub-band lines. The latter results from the close similarity of the neutral and cation geometries. The surprising feature of the spectrum is the complete lack of transitions with $\Delta K = \pm 1$. From bound state spectroscopy, electronic transitions with $\Delta K = 0$ and $\Delta K = \pm 1$ are associated with parallel and perpendicular transition moments (relative to the top axis) and our data strongly suggested that the latter are "forbidden." In fact, a symmetry analysis of CH_3 photoionization predicts that for *both* parallel and perpendicular bound-to-continum transitions, only $\Delta K \equiv$ *even* transitions are allowed. Although this prediction is not consistent with observations in bound-to-bound spectroscopy, it is a natural consequence of the uncoupling of the angular momentum of the photoexcited electron from the cation core at large distances. As the electron escapes from molecular ion, the quantization of the orbital angular momentum in the molecular frame is lost and it is no longer appropriate to ascribe a particular point group symmetry to the photoexcited electron. The selection rules on ΔK remain, however, since the overall angular momentum and its projections are strictly conserved.

In analyzing the rotationally-resolved PFI spectra for H_2CO^+ and CH_3^+ we naturally obtain band origins which correspond to the adiabatic ionization energies. For H_2CO the spectral assignment was hampered by the lack of accurate rotational constants and it was necessary to derive them from spectral simulations. In this way we were able to obtain

the three H_2CO^+ rotational constants to an accuracy of ± 0.05 cm^{-1}as well as an accurate determination of the ionization potential (87,837.3 ± 2 cm^{-1}). The extracted ionization potential for CH_3 (79,349 ± 3 cm) is more accurate than previous measurements by a factor of 20 and should be useful for deriving or refining thermochemical properties of the methy radical and its gas phase reactions.

Future Plans

Future studies will be directed towards small molecular radicals and molecular complexes. A number of different radical sources will be employed including free-jet laser photolysis and supersonic-jet, flash pyrolysis of polyatomic precursor systems or fast radical reactions in a discharge flow tube source. Both the flow tube and flash pyrolysis sources have been used successfully in our previous studies of the hydroxyl (OH/OD) and methyl (CH_3) radicals, respectively. Of particular interest are the second row radical hydrides BH_n, CH, CH_2, NH, NH_2, C_2H, HCO and CH_3O which are extremely important as reactive intermediates in combustion or atmospheric chemistry, yet are tractable for study by high resolution spectroscopic techniques and fully *ab initio* theoretical methods. Using a combination of mass analyzed photoionization and threshold photoelectron spectroscopy, we hope to obtain rotationally-resolved photoionization spectra for a number of second row hydrides with particular emphasis on examining the ionization dynamics and determining very accurate ionization potentials. The latter are extremely useful for obtaining accurate heats of formation used in reaction rate kinetics. The spectroscopic data is also pertinent to small hydrocarbon radicals such as HCO^+ which are produced via chemi-ionization reactions in flames. Currently, our pulsed ionization technique coupled with a laser-based VUV radiation source can be used to determine ionization potentials to ≤ 2 cm^{-1}, which is at least an order of magnitude better than conventional photoelectron spectroscopy. These small molecules are also readily ammenable to theoretical calculations, e.g. Schwinger variational methods and multichannel quantum defect theory, which treat dynamical interactions between discrete (superexcited neutral states) and continuum channels (dissociation and ionization) realistically.

Research Publications 1991–1993

1. High Resolution Threshold Photoionization of N_2O, R. T. Weidmann, E. R. Grant, R. G. Tonkyn and M. G. White, *J. Chem. Phys.*, **95**, 746 (1991).

2. Proposed UV-FEL User Facility at Brookhaven National Laboratory, I. Ben-Zvi, L. F. DiMauro, S. Krinsky, M. G. White and L. H. Yu, *Nuclear Instrum. Meth.*, **A304**, 181 (1991).

3. Rotationally Resolved Photoionization of H_2O, R. G. Tonkyn, R. T. Wiedmann E. R. Grant and M. G. White, *J. Chem. Phys.*, **95**, 7033 (1991).

4. Vibrational Spectroscopy of Xe_2^+ by Pulsed Field Ionization, R. G. Tonkyn and M. G. White, *J. Chem. Phys.*, **95**, 5582 (1991).

5. ZEKE Threshold Photoelectron Spectroscopy: Photoionization Dynamics and the Level Structure of Molecular Cations, E. R. Grant and M. G. White, *Nature*, **354**, 249 (1991).

6. Rotationally Resolved Threshold Photoionization of H_2S, R. T. Wiedmann and M. G. White, *SPIE Proceedings, Conf. 1638 - Optical Methods for Time- and State- Resolved Chemistry, Los Angeles, CA, January 19-25, 1992.*

7. Anomalous Branch Intensities in the Threshold Photoionization of HCl, R. G. Tonkyn, R. T. Wiedmann and M. G. White, *J. Chem. Phys.*, **96**, 3696 (1992).

8. Rotational Ion Distributions for Near Threshold Photoionization of H_2O, M. T. Lee, K. Wang, V. McKoy, R. G. Tonkyn, R. T. Wiedmann, E. R. Grant and M. G. White, *J. Chem. Phys. Commun.*, **96**, 7848 (1992).

9. Rotationally Resolved Threshold Photoelectron Spectra of OH and OD, R. T. Wiedmann, R. G. Tonkyn, M. G. White, K. Wang and V. McKoy, *J. Chem. Phys.*, **97**, 768 (1992).

10. Photoionization Dynamics and Cation Spectroscopy with Coherent VUV Radiation, R. T. Wiedmann, R. G. Tonkyn, E. R. Grant and M. G. White, *Inst. Phys. Conf. Ser. No. 128*, Sect. 5, 161 (1992) (Proc. of the Sixth Int. Conf. Resonance Ionization Spectrosc., Santa Fe NM, 1992).

11. Rotationally Resolved Threshold Photoelectron Spectrum of the Methyl Radical, J. A. Blush, P. Chen, R. T. Wiedmann and M. G. White, *J. Chem. Phys. Commun.*, **98**, 3557 (1993).

12. Single Photon Threshold Photoionization of NO, R. T. Wiedmann, M. G. White, K. Wang and V. McKoy, *J. Chem. Phys.* in press.

13. The VUV Photodissociation of the Chlorofluorocarbons: Photolyis of CF_3Cl, CF_2Cl_2 and $CFCl_3$ at 187 nm, 125 nm and 118 nm, M.-W. Yen, P. M. Johnson and M. G. White, *J. Chem. Phys.* accepted for publication.

Reactions of Small Molecular Systems

Curt Wittig, Department of Chemistry, USC, Los Angeles, CA 90089

Scope and Overview

Our DOE program remains focused on small molecular systems relevant to combustion. Though a number of experimental approaches and machines are available for this research, our activities are centered around the high-n Rydberg time-of-flight (HRTOF) apparatus in our laboratory. One student and one postdoc carry out experiments with this machine and also engage in small intra-group collaborations involving shared equipment. This past year was more productive than the previous two, due to the uninterrupted operation of our HRTOF apparatus. Results were obtained with CH_3OH, CH_3SH, Rg-HX complexes, HCOOH, and their deuterated analogs where appropriate. One paper is in print, three have been accepted for publication, and one is under review. Many preliminary results that augur well for the future were obtained with other systems such as HNO_3, HBr-HI complexes, toluene, etc. Highlights from the past year are presented below that display some of the features of our program.

Vibrationally Resolved HRTOF Spectra: CH_3SH and CH_3OH

The photochemistry of CH_3SH has been studied extensively, in part because it is produced in various industrial processes and released into the atmosphere. Early studies covering the range 185-254 nm established that the dominant process leads to breaking the S-H bond, though the C-S bond is weaker. This suggests that dissociation occurs on an excited PES, repulsive in the S-H coordinate. Indeed, electronic structure calculations show an accessible singlet PES repulsive in the S-H coordinate. Recent studies have measured the overall energetics, as well as details of the C-S bond breaking channel, which becomes significant below ~ 222 nm. Butler and coworkers demonstrated the increased importance of C-S bond fission at shorter wavelengths, which is attributable to a higher singlet PES bound in both S-H and C-S coordinates. Calculations of this PES, along with resonance Raman spectra observed following excitation to this PES, indicate that the equilibrium C-S distance is greater than on the ground PES. Excitation to this higher PES, they reason, leads to elongation of the C-S bond and thus increases the relative CH_3 + SH probability after the system crosses to the lower excited surface on which dissociation proceeds. Thus, excitation to this bound surface can yield a dramatically different internal state distribution of CH_3S compared to exciting the dissociative lower surface directly.

The translational energy distribution for 193 nm photolysis is shown in fig. 1. At the highest energies, there are two peaks, roughly 800 cm^{-1} apart, which we refer to as the fast component. This is followed by approximately 15 poorly resolved features, also approximately 700-800 cm^{-1} apart: the slow component. As with the fast component, the features of this slow component spectrum can be attributed to a C-S stretch progression. The main part of the progression peaks ~ 5500 cm^{-1} from the origin at v=8; levels as high as v=17 can be seen. The width of the features, roughly 500 cm^{-1}, exceeds the experimental resolution of ~ 200 cm^{-1}.

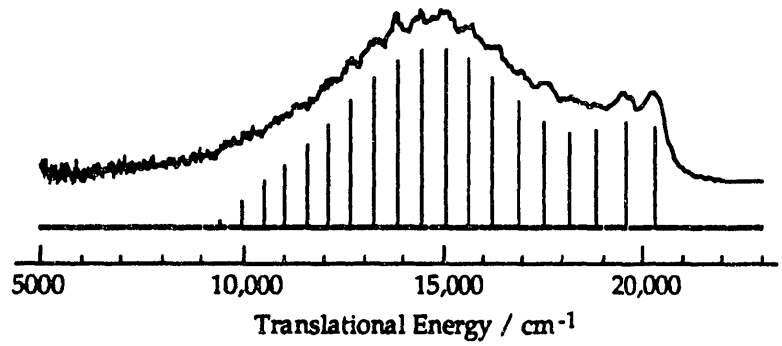

Figure 1. Translational energy release (experiment and fit) from 193 nm CH_3SH photodissociation.

One way to rationalize these observations is to assume that a part of the wavepacket initially excited to the $2^1A''$ surface accesses the $1^1A''$ surface rapidly, perhaps a part of the Franck-Condon region closest to the avoided crossing between the two surfaces. The rest of the packet remains on $2^1A''$ for a longer period, during which time the C-S bond is extended, before crossing to the lower surface and dissociating. Such a combination of a direct and delayed dissociation caused by a splitting of the initially excited wavepacket has been proposed before, *cf.* FNO.

The case of CH_3OH is similar in many respects to that of CH_3SH. Experiments were carried out with deuterated samples (CH_3OD and CD_3OH), confirming that the primary process is O—H bond rupture. Moreover, it has been possible to see directly the consequence of the impulsive kick given by the departing hydrogen, producing rotation in the other fragment. These results are shown in Fig. 2; a large manuscript is in preparation.

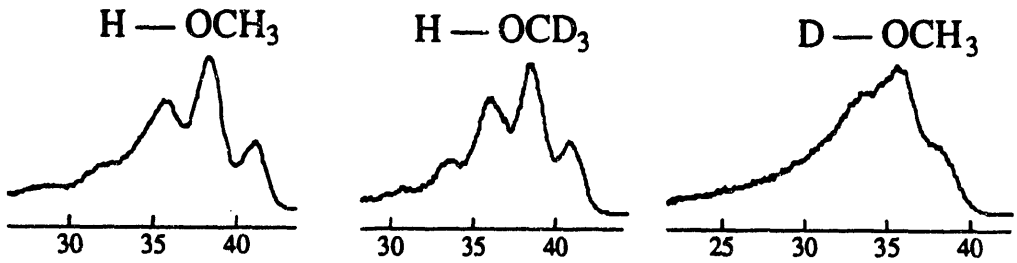

Figure 2. c.m. translational energy distributions (kcal/mol) for deuterated methanol. Note the enhanced broadening for D—OCH_3, as expected when doubling the impulsive force.

Photoexcitation of Ar-HBr Complexes

There has been interest in recent years in the dynamics of photoinitiated chemical reactions in weakly bound clusters. One of the interesting aspects of these systems is the restricted relative geometries of the reactants imposed by the structure of the cluster. Forces between molecules bound together in a cluster may constrain to some extent their mutual orientations and consequently the angles and impact parameters of a photoinitiated reaction, thereby allowing a higher degree of control over the initial conditions of the reaction than under gas phase conditions. The

study of reactivity in weakly bound clusters also offers new possibilities for exploring the effect of the weak interactions, or solvation bonds, on a reaction. These systems thus provide a useful guide to a better understanding of solvation effects on chemical reactions, with simplifications due to the small number of degrees of freedom involved in the case of clusters. Several analogous systems are under study in our lab and it appears likely that a number of bimolecular reactions can be studied. Additionally, we have shown that photolytic stripping of hydrogen from complexes is an efficient means of preparing radical-molecule complexes.

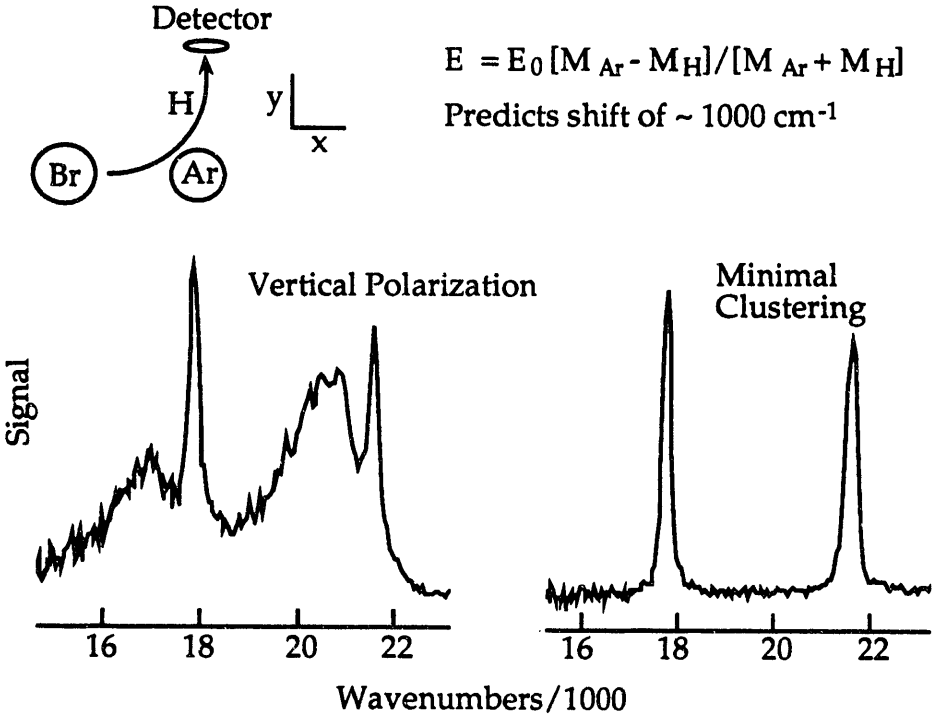

Figure 3. Translational energy distributions for HBr/Ar samples. With minimal clustering the signal is small and the peaks correspond to Br and Br*. With clustering, hydrogen can be scattered toward the detector (see text).

Polarized photolysis radiation can be used to align transition dipoles of dissociating molecules, and for HX, parallel and perpendicular transitions are known to display strong halogen atom spin orbit preferences. For 193 nm HBr excitation, the transition moment is predominatly perpendicular, yielding mainly ground state Br. Because fragmentation is rapid, the hydrogen distribution is spatially anisotropic. Since the experiment is sensitive only to a certain laboratory solid angle, a differential cross section at a fixed laboratory final scattering angle is obtained.

The spatial anisotropies can be exploited. For example, hydrogen scattered from the nearby moiety in a complex can lead to large signal enhancements in cases where the hydrogen would not reach the detector *unless* it scatters from the nearby species. This can be seen in fig. 3, which shows kinetic energy distributions for cases of significant and minimal clustering. Since photodissociation at 193 nm occurs primarily via a perpendicular transition, signals deriving from uncomplexed material are largest with the photolysis E-field horizontal, *i.e.*, in the plane formed by the molecular and photolysis beams. With the field vertical, the monomer signal

is relatively small, and the percentage of the signal that derives from clustered material is much higher than for the case of horizontal polarization.

An important feature is that the energy distribution for the scattered hydrogen atoms peaks ~ 1000 cm^{-1} below the peak for atoms that derive from the photolysis of uncomplexed HBr. This is because only strongly scattered hydrogen atoms reach the detector. The distribution of photoexcited HBr axes peaks in the plane containing the photolysis beam and the molecular beam, and this plane is perpendicular to the line between the interaction region and the detector. Thus, a hydrogen atom initially moving in this plane must have its trajectory turned by ~ 90° in order for it to reach the detector The classical equations of motion for an initial hydrogen velocity in the x direction that is deflected into the y direction in a single collision yields: $E = E_0[M_{Ar}-M_H]/[M_{Ar}+M_H]$, where $E_0 = 21{,}600$ cm^{-1} is the hydrogen kinetic energy for 193 nm HBr photolysis. Therefore, $E_0 - E$ is approximately 1000 cm^{-1}, in good agreement with the data. Were Ar_n-HBr with $n > 1$ playing a dominant role, such agreement would be surprising.

Plans for the future

These items listed below are taken directly from our renewal proposal, which was submitted early this year.

- Advances in the HRTOF machine: improved resolution; improved photolysis source; use of a parametric oscillator and Ti:sapphire laser; four-wave mixing for Lyman-α generation
- The HOCO system: overtone spectra; resonances above reaction threshold; k(E); D_0(HO-CO); CO_2 vibrational distributions versus E; H-OCO transition state and barrier height.
- Unimolecular decomposition of CH_3O and C_2H_5.
- Ultraviolet photodissociation, including OPO/Ti:S excitation.

Publications Since Last Meeting

1. Photoinitiated Hydrogen and Deuterium Atom Reactions with N_2O in the Gas Phase and in N_2O-HI and N_2O-DI Complexes, E. Böhmer, S.K. Shin, Y. Chen and C. Wittig, J. Chem. Phys. 97, 2536 (1992).
2. Evidence for a Cage Effect in the Ultraviolet Photolysis of HBr in the Ar-HBr: Theoretical and Experimental ResultsJ. Segall, Y. Wen, R. Singer, C. Wittig, A. Garcia-Vela, and R.B. Gerber, Chem. Phys. Letters, in press (1993).
3. Photoinitiated Processes in Complexes: Subpicosecond Studies of CO_2-HI and Stereospecificity in Ar-HX, C. Jaques, L. Valachovic, S. Ionov, E. Böhmer, Y. Wen, J. Segall and C. Wittig, J. Chem. Soc. Faraday Transactions II, in press (1993).
4. Vibrationally Resolved Translational Energy Release Spectrum from the UV Photodissociation of Methyl Mercaptan, J. Segall, Y. Wen, R. Singer, M. Dulligan and C. Wittig, J. Chem. Phys., in press (1993).
5. Reactions of Hot Deuterium Atoms with OCS in the Gas Phase and in OCS-DI Complexes, E. Böhmer, K. Mikhaylichenko and C. Wittig, J. Chem. Phys., submitted (1993).

Theoretical Studies of Nonadiabatic and Spin-Forbidden Processes: Investigations of the Reactions and Spectroscopy of Radical Species Relevant to Combustion Reactions and Diagnostics

David R. Yarkony
Department of Chemistry, Johns Hopkins University, Baltimore, MD 21218

Our research program focusses on studies of spin-forbidden and electronically nonadiabatic processes involving radical species relevant to combustion reactions and combustion diagnostics. To study the electronic structure aspects of these processes a unique and powerful system of electronic structure programs, developed over the past nine years, the BROOKLYN codes, is employed. These programs enable us to address questions basic to the understanding of elementary combustion processes not tractable using more standard quantum chemistry codes. Particularly relevant to this research program are the capabilities to

(i) treat the spin-orbit interaction within the context of the full microscopic Breit-Pauli approximation,

(ii) determine the interstate derivative couplings $f_\alpha^{IJ}(\mathbf{R}) = \langle \Psi_I(\mathbf{r};\mathbf{R}) | \partial/\partial R_\alpha | \Psi_J(\mathbf{r};\mathbf{R}) \rangle$ that result in the breakdown of the single surface Born–Oppenheimer approximation,

(iii) locate surfaces of (actual/avoided) intersection of potential energy surfaces of the same symmetry, and

(iv) locate the minimum energy point on the surface of intersection of two potential energy surfaces of different spin-multiplicity.

During the current performance period we have developed

An Algorithm for the Systematic Determination of Points on the Surface of Intersection of Two Potential Energy Surfaces of Distinct Spin–Multiplicity

Two nonrelativistic Born-Oppenheimer potential energy surfaces of distinct space–spin symmetry intersect on a surface of dimension N^I-1 where N^I is the number of internal nuclear degrees of freedom. Characterization of this entire surface can be quite costly. In many circumstances it suffices to determine only the minimum energy point on the surface of intersection in question. Such a situation is illustrated in the figure below.

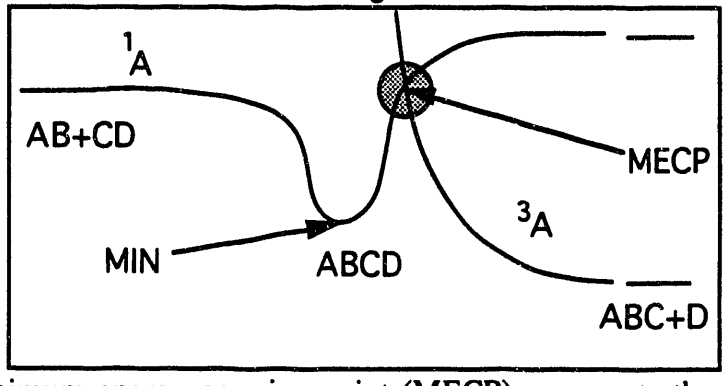

In this case the minimum energy crossing point (MECP) represents the barrier to the spin–forbidden process. However favorable situations such as this are not uniformly the case. The figure below depicts a spin-forbidden bimolecular reaction in which much more of the crossing surface is energetically accessible.

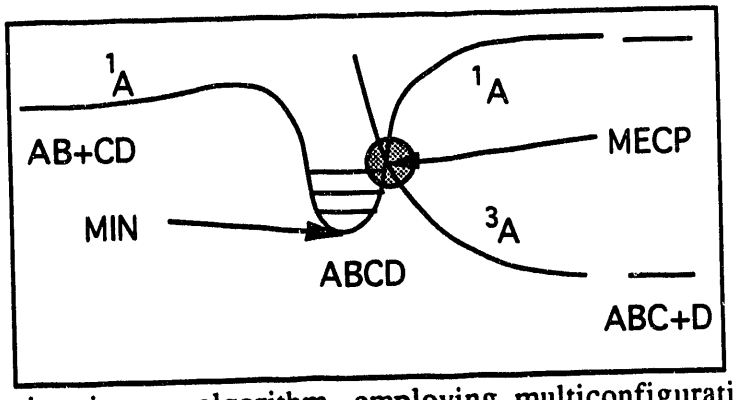

Motivated by this situation an algorithm, employing multiconfiguration self-consistent-field(MCSCF) / configuration interaction(CI) wavefunctions and analytic gradient techniques, has been developed which avoids the determination of the full N^I–1 dimensional surface, while directly locating portions of the crossing surface that are energetically important. The algorithm represents an extension of our previously introduced method[1, 2] for determining the minimum energy point on the surface of intersection of two states of distinct spin-multiplicity. The algorithm is based on the minimization of the Lagrangian function $L^{IJ}(\mathbf{R},\lambda_0,\boldsymbol{\lambda}) = E_I(\mathbf{R}) + \lambda_0[E_I(\mathbf{R})-E_J(\mathbf{R})] + \sum_k \lambda_k C_k(\mathbf{R})$ where $C_k(\mathbf{R})$ is any geometrical equality constraint such as $R_{KL}^2 - a_{KL}^2 = 0$, or $R_{KL}^2 - R_{MN}^2 = 0$, with $R_{KL} = |\mathbf{R}_K - \mathbf{R}_L|$, and the λ_0, $\boldsymbol{\lambda}$ are Lagrange multipliers.[3]

The key aspects of the algorithm are:(i) it is *direct*, in the sense that the desired constrained minima on the surface of intersection are determined *without prior determination* of the individual potential energy surfaces themselves and (ii) the requisite energy gradients are evaluated using analytic gradient techniques. The details of the formalism can be found in Ref. 3.

The situation illustrated in the later figure above is expected to be encountered in the spin-forbidden reaction $CH(X^2\Pi) + N_2(X^1\Sigma_g^+) \rightarrow HCN(X^1\Sigma^+) + N(^4S)$. Consequently this system was used to demonstrate the efficacy of this new algorithm using a simple MCSCF/first order CI description of that reaction.

The methods discussed above have been used to consider:

(a) Spin-forbidden processes involving N_2O

Motivated by conversations with Dr. Bruce Klemm at the Brookhaven National Laboratory concerning the spin-forbidden predissociation

$$N_2O(X^1\Sigma^+) \rightarrow N_2(X^1\Sigma_g^+) + O(^3P)$$

and our longstanding interest in the atmospheric quenching reaction

$$N_2(X^1\Sigma_g^+) + O(^1D) \rightarrow N_2(X^1\Sigma_g^+) + O(^3P)$$

we have largely completed a study of the crossing surfaces, denoted ($1^1A'$, $1^3A'$), ($1^1A'$, $1^3A''$), and ($1^1A'$, $2^3A''$), corresponding to the intersection of the lowest singlet surface of N_2O ($1^1A'$) with of the three triplet surfaces correlating with $N_2 + O(^3P)$ ($1^3A'$, $1,2^3A''$), using multireference CI wavefunctions comprised of 400,000 – 600,000 terms. These crossing surfaces were characterized in the vicinity of their minimum energy crossing points. The minimum energy crossing structures are all linear and thus correspond to $C_{\infty v}$ ($X^1\Sigma^+$, $^3\Pi$) and ($X^1\Sigma^+$, $^3\Sigma^-$) intersections. The minimum energy point on the ($X^1\Sigma^+$, $^3\Pi$) crossing surface, was found to be 57kcal/mol above the $N_2O(X^1\Sigma^+)$ minimum. The minimum energy point on the ($X^1\Sigma^+$, $^3\Sigma^-$) crossing surface was found to be 68kcal/mol above the $N_2O(X^1\Sigma^+)$ minimum. The N–N bond distance is similar at the ($X^1\Sigma^+$, $^3\Pi$) and ($X^1\Sigma^+$, $^3\Sigma^-$) minimum energy crossing structures, being 1.116Å and 1.113Å respectively, and approximately equal to that in isolated $N_2(X^1\Sigma_g^+)$. The N-O

bond is 1.72Å and 1.96Å at the ($X^1\Sigma^+$, $^3\Pi$) and ($X^1\Sigma^+$, $^3\Sigma^-$) minimum energy crossing points respectively and is significantly stretched, by over 0.5Å, when compared with its value, 1.184Å, at the equilibrium geometry of $N_2O(X^1\Sigma^+)$.

The spin-orbit couplings were also evaluated on each of the ($1^1A'$, $1^3A'$), ($1^1A'$, $1^3A''$), and ($1^1A'$, $2^3A''$) crossing surfaces. For collinear geometries the ($X^1\Sigma^+$, $^3\Pi$) and ($X^1\Sigma^+$, $^3\Sigma^-$) spin-orbit induced couplings are found to be significantly different. The ($X^1\Sigma^+$, $^3\Pi$) spin-orbit interaction was found to be ~90cm^{-1} at the minimum energy crossing point for the ($X^1\Sigma^+$, $^3\Pi$) intersection while the ($X^1\Sigma^+$, $^3\Sigma^-$) spin-orbit interaction interaction is only ~8cm^{-1} at the minimum energy crossing point for the ($X^1\Sigma^+$, $^3\Sigma^-$) intersection. Similar observations apply for noncollinear geometries.

(b) State Specific Photodissociation of OH($X^2\Pi$) via OH($A^2\Sigma^+$)

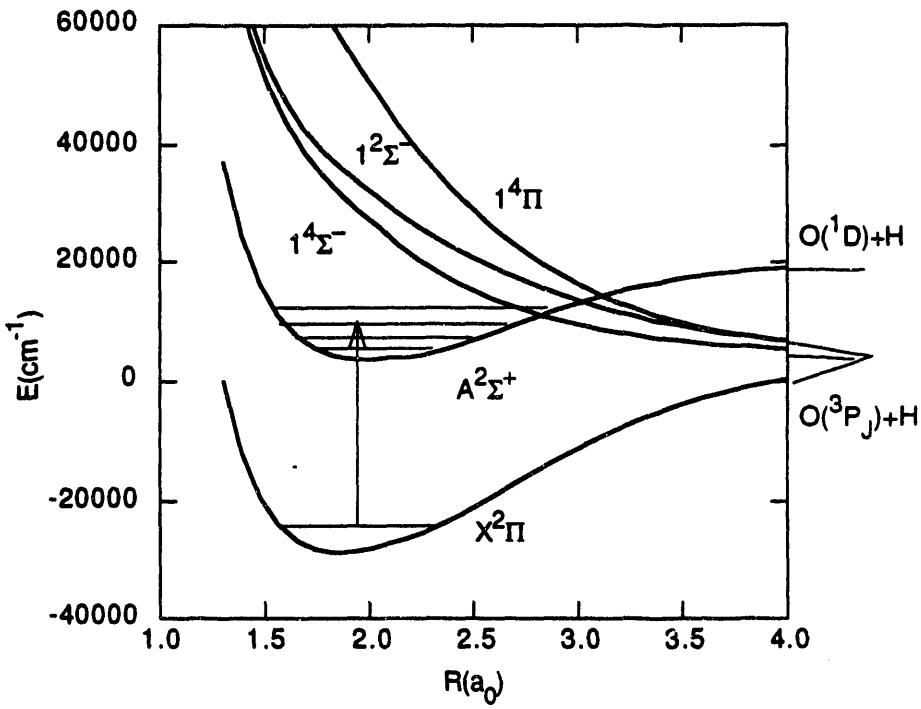

In situ detection of nascent OH is an important problem in studies of combustion processes. Recently several groups,[4, 5, 6] including Gray and Farrow at the Sandia Combustion Research Facility[5] and Crosley and co-workers are SRI International,[6] have considered using the strongly predissociated OH($A^2\Sigma^+$,v=3) state in a laser fluorescence detection scheme. In a complementary study we considered the predissociation of the OH($A^2\Sigma^+$, v=3).[7] During the current performance period we have extended our studies to consider the fine–structure state product distribution for the overall process OH($X^2\Pi$, v=0) + hν → OH($A^2\Sigma^+$, v) → O(^3P_J) + H(^{2}S).

To study this process in a realistic manner it was necessary to determine all the intersurface –nonadiabatic– interactions (11 unique spin-orbit interactions and 3 coriolus couplings) among the five electronic states in question, $X^2\Pi$, $1^4\Pi$, $1^4\Sigma^-$, $1^2\Sigma^-$, and $A^2\Sigma^+$. This was accomplished using the same large scale configuration interaction wavefunctions employed in our previous treatment of OH($A^2\Sigma^+$, v=3) predissociation[7] and represents the first study in which all the relevant nonadiabatic interactions have been determined with such accurate electronic wavefunctions. The photodissociation process was treated using a fully quantum mechanical

scattering procedure. Although state specific photodissociation of OH has been studied in the past[8] our results permit, for the first time, definitive conclusions concerning the influence of the geometry dependence of the nonadiabatic interactions on the $O(^3P_J)$ branching ratios. It was found that the $O(^3P_J)$ distributions resulting from photodissociation involving $OH(A^2\Sigma^+, v=4,5)$ exhibit the most significant quantum interference effects. $O(^3P_J)$ distributions for the remaining vibrational levels studied could be determined semiquantitatively using branching ratios obtained from the Fermi Golden Rule. The Golden Rule values for the *total* decay rates were found to be in good agreement with the exact quantum values even for levels with lifetimes on the order of picoseconds.

FUTURE PLANS

The potential energy surfaces for the reaction $CH(X^2\Pi) + N_2 \rightarrow HCN(X^1\Sigma^+) + N(^4S)$ reaction are currently the object of study in several research groups. We intend to complement these studies with a characterization of the doublet-quartet crossing surface based on the algorithm discussed above and determine the spin-orbit interaction between these states on the surface of crossings. This electronic structure data is crucial for any reliable treatment of this spin-forbidden reaction. We will also be considering the CO analogue of the N_2+O system discussed above, studying from a similar perspective both $CO+O(^1D)$ quenching and CO_2 photodissociation. The later aspect of this investigation is motivated by the recent work of Stolow and Lee.[9]

We are currently considering nonadiabatic effects in excited states of the HCO molecule focussing on the mechanism of predissociation in the $\tilde{B}^2A'$ system. Both spin–allowed and spin–forbidden predissociations will be considered. Our initial studies have for example located crossing of the $1^2A'$ and $2^2A'$ potential energy surfaces for general C_s geometries. These crossings of two states of the same symmetry, which turn out not to effect predissociation of the low vibrational levels of the $\tilde{B}^2A'$ state, had not been reported in previous theoretical studies of this system. Our treatment of nonadiabatic effects in this system will complement (largely DOE supported) experimental work[10, 11, 12, 13] on this system.

REFERENCES

References with index in bold/italic are funded by the DOE Office of Basic Energy Sciences

1. D. R. Yarkony, J. Chem. Phys. **92**, 2457 (1990).
2. D. R. Yarkony, J. Amer. Chem. Soc. **114**, 5406 (1992).
3. D. R. Yarkony, J. Phys. Chem (1993), to appear.
4. P. Andresen, A. Bath, W. Groger, H. W. Lulf, G. Meijer, and J. J. t. Meulen, Appl. Opt. **27**, 365 (1988).
5. J. A. Gray and R. L. Farrow, J. Chem. Phys. **95**, 7054 (1991).
6. D. E. Heard, D. R. Crosley, J. B. Jeffries, G. P. Smith, and A. Hirano, J. Chem. Phys. **96**, 4366 (1992).
7. D. R. Yarkony, J. Chem. Phys. **97**, 1838 (1992).
8. S. Lee and K. F. Freed, J. Chem. Phys. **87**, 5772 (1987).
9. A. Stolow and Y. T. Lee, J. Chem. Phys. **98**, 2066 (1993).
10. A. Sappey and D. R. Crosley, J. Chem. Phys. **93**, 7601 (1990).
11. U. E. Meier, L. E. Hunziker, and D. R. Crosley, J. Phys. Chem. **95**, 5163 (1991).
12. T. Cool and X.-M. Song, J. Chem. Phys. **96**, 8675 (1992).
13. G. W. Adamson, X. Zhao, and R. W. Field, J. Mol. Spectr. (1993), to appear.

Work performed under the auspices of
U. S. Department of Energy.

LIST OF INVITEES AND PARTICIPANTS

Dr. William T. Ashurst
Combustion Research Facility
Sandia National Laboratory
Livermore, California 94551-0609

Professor Tomas Baer
Department of Chemistry
University of North Carolina
Chapel Hill, North Carolina 27599-3290

Professor John R. Barker
Department of Atmospheric,
Oceanic, & Space Sciences
1520 Space Research Building
University of Michigan
2455 Hayward St.
Ann Arbor, Michigan 48109-2143

Dr. Robert S. Barlow
Combustion Research Facility
Sandia National Laboratory
Livermore, California 94551-0609

Professor Robert A. Beaudet
Department of Chemistry
University of Southern California
Los Angeles, California 90089-0482

Dr. Joseph Berkowitz
Chemistry Division
Argonne National Laboratory
9700 South Cass Avenue
Argonne, Illinois 60439

Professor Richard Bersohn
Department of Chemistry
Columbia University
959 Havemeyer Hall
New York, New York 10027

Dr. J. Stephen Binkley
Sandia National Laboratories
1401 Wilson Blvd.
Suite 1050
Arlington, Virginia 22209

Dr. Kenneth Brezinsky
Department of Mechanical
& Aerospace Engineering
Princeton University
Princeton, New Jersey 08544

Professor Joel M. Bowman
Department of Chemistry
Emory University
1515 Pierce Drive
Atlanta, Georgia 30322

Professor C. Thomas Bowman
Department of Mechanical Engineering
Stanford University
Stanford, California 94305

Dr. Nancy J. Brown
Applied Science Division
Lawrence Berkeley Laboratory
University of California
Berkeley, California 94720

Professor Laurie J. Butler
The James Franck Institute
The University of Chicago
5640 S. Ellis Avenue
Chicago, Illinois 60637

Dr. Elton J. Cairns
Applied Science Division
University of California
Lawrence Berkeley Laboratory
One Cyclotron Road
Berkeley, California 94720

Dr. David W. Chandler
Combustion Research Facility
Sandia National Laboratory
Livermore, California 94551-0609

Dr. Jacqueline H. Chen
Combustion Research Facility
Sandia National Laboratory
Livermore, California 94551-0609

Professor Peter Chen
Department of Chemistry
Harvard University
12 Oxford Street
Cambridge, Massachusetts 02138

Dr. Robert K. Cheng
Applied Sciences Division
Lawrence Berkeley Laboratory
University of California
Berkeley, California 94720

Professor Dennis J. Clouthier
Department of Chemistry
University of Kentucky
Lexington, Kentucky 40506-0055

Dr. Norman Cohen
The Aerospace Corporation
Post Office Box 92957
Los Angeles, California 90009-2957

Prof. Philip Colella
Department of Mechanical Engineering
University of California, Berkeley
Berkeley, California 97420

Dr. Meredith B. Colket, III
United Technologies Research Center
East Hartford, Connecticut 06108

Professor Terrill A. Cool
Department of Applied
& Engineering Physics
Cornell University
Ithaca, New York 14853-1301

Professor F. Fleming Crim
Department of Chemistry
University of Wisconsin
Madison, Wisconsin 53706

Professor Robert F. Curl, Jr.
Department of Chemistry
Rice University
6100 South Main Street
Houston, Texas 77251

Professor Hai-Lung Dai
Department of Chemistry
University of Pennsylvania
Philadelphia, Pennsylvania 19104

Dr. Michael J. Davis
Chemistry Division
Argonne National Laboratory
9700 South Cass Avenue
Argonne, Illinois 60439

Dr. Anthony M. Dean
Exxon Research & Engineering Co.
Clinton Township, Route 22 East
Annandale, New Jersey 08801

Dr. Andrew DePristo
Chemistry Department
Iowa State University
Ames, Iowa 50011

Professor Frederick L. Dryer
Department of Mechanical
& Aerospace Engineering
Princeton University
Princeton, New Jersey 08544

Dr. Joseph L. Durant
Combustion Research Facility
Sandia National Laboratory
Livermore, California 94551-0609

Dr. Alan Eckbreth
Assistant Director of Research,
Propulsion & Flight Systems
United Technologies Research Center
East Hartford, Connecticut 06108

Professor G. Barney Ellison
Department of Chemistry & Biochemistry
University of Colorado
Boulder, Colorado 80309-0215

Professor James M. Farrar
Department of Chemistry
University of Rochester
Rochester, New York 14627

Dr. Roger L. Farrow
Combustion Research Facility
Sandia National Laboratory
Livermore, California 94551-0609

Professor Peter M. Felker
Department of Chemistry & Biochemistry
University of California at Los Angeles
405 Hilgard Avenue
Los Angeles, California 90024-1406

Professor Robert W. Field
Department of Chemistry
Massachusetts Institute of Technology
Cambridge, Massachusetts 02139

Dr. George A. Fisk
Combustion Research Facility
Sandia National Laboratory
Livermore, California 94551-0609

Professor George W. Flynn
Department of Chemistry
Box 315, Havemeyer Hall
Columbia University
New York, New York 10027

Professor Arthur Fontijn
Department of Chemical
and Environmental Engineering
Rensselaer Polytechnic Institute
Troy, New York 12180-3590

Mr. Charles W. Garrett
FE-14 B-129/GTN
Office of Fossil Energy
U. S. Department of Energy
Washington, D.C. 20545

Professor W. Ronald Gentry
Department of Chemistry
University of Minnesota
207 Pleasant St., S.E.
Minneapolis, Minnesota 55455

Professor Clayton F. Giese
Department of Chemistry
University of Minnesota
207 Pleasant St., S.E.
Minneapolis, Minnesota 55455

Professor Graham P. Glass
Department of Chemistry
Rice University
6100 South Main Street
Houston, Texas 77251

Professor Irvin Glassman
Department of Mechanical
& Aerospace Engineering
Princeton University
Princeton, New Jersey 08544

Dr. Carl A. Gottlieb
Division of Applied Sciences
Pierce Hall 107C
Harvard University
Cambridge, Massachusetts 02138

Dr. Jeffrey A. Gray
Combustion Research Facility
Sandia National Laboratory
Livermore, California 94551-0609

Dr. Stephen Gray
Chemistry Division
Argonne National Laboratory
9700 South Cass Ave.
Argonne, Illinois 60439

Dr. J. Robb Grover
Chemistry Department
Brookhaven National Laboratory
Upton, New York 11973

Professor David Gutman
Department of Chemistry
The Catholic University of America
Michigan Avenue at 7th Street, N.E.
Washington, D.C. 20064

Dr. Gregory Hall
Chemistry Department
Brookhaven National Laboratory
Upton, New York 11973

Professor Ronald K. Hanson
Department of Mechanical Engineering
Stanford University
Stanford, California 94305

Dr. Lawrence B. Harding
JILA
Campus Box 440
University of Colorado
Boulder, Colorado 80309-0440

Dr. Stephen J. Harris
Physical Chemistry Department
General Motors Research Laboratories
Box 9055
Warren, Michigan 48090-9055

Prof. Charles B. Harris
Chemical Sciences Division
Lawrence Berkeley Laboratory
University of California
Berkeley, California 94720

Dr. Carl C. Hayden
Combustion Research Facility
Sandia National Laboratory
Livermore, California 94551-0609

Dr. John Herron
Chemical Sciences
& Technology Laboratory
Natl. Inst. of Standards & Technology
Gaithersburg, Maryland 20899

Dr. Jan R. Hessler
Chemistry Division
Argonne National Laboratory
9700 South Cass Ave.
Argonne, Illinois 60439

Dr. Jon T. Hougen
Molecular Physics Division
Natl. Inst. of Standards & Technology
Gaithersburg, Maryland 20899

Professor Paul L. Houston
Department of Chemistry
Baker Laboratory
Cornell University
Ithaca, New York 14853-1301

Professor Jack B. Howard
Department of Chemical Engineering
Massachusetts Institute of Technology
Cambridge, Massachusetts 02139

Professor Philip M. Johnson
Department of Chemistry
State University of New York at Stony Brook
Stony Brook, New York 11794

Professor Harold Johnston
Materials & Chemical Sciences Division
Lawrence Berkeley Laboratory
University of California
Berkeley, California 94720

Professor Michael E. Kellman
Department of Chemistry
University of Oregon
Eugene, Oregon 97403

Professor Ralph D. Kern, Jr.
Department of Chemistry
Lakefront Campus
University of New Orleans
New Orleans, Louisiana 70148

Dr. Alan R. Kerstein
Combustion Research Facility
Sandia National Laboratory
Livermore, California 94551-0609

Professor John H. Kiefer
Department of Chemical Engineering
University of Illinois at Chicago
Chicago, Illinois 60680

Dr. R. Bruce Klemm
Applied Sciences Department
Brookhaven National Laboratory
Upton, New York 11973

Dr. Michael L. Koszykowski
Combustion Research Facility
Sandia National Laboratory
Livermore, California 94551-0609

Dr. Andrew Kung
Materials & Chemical Sciences Division
Lawrence Berkeley Laboratory
University of California
Berkeley, California 94720

Dr. Allan H. Laufer
Fundamental Interactions Branch
Chemical Sciences Division
Office of Basic Energy Sciences
Department of Energy, ER-141, G-340/GTN
Washington, DC 20585

Professor C. K. Law
Department of Mechanical
& Aerospace Engineering
Princeton University
Princeton, New Jersey 08544

Professor Yuan T. Lee
Materials & Chemical Sciences Division
Lawrence Berkeley Laboratory
University of California
Berkeley, California 94720

Professor Stephen R. Leone
Department of Chemistry
University of Colorado
Campus Box 215
Boulder, Colorado 80309

Professor William A. Lester, Jr.
Materials & Chemical Sciences Division
Lawrence Berkeley Laboratory
University of California
Berkeley, California 94720

Professor Marsha I. Lester
Department of Chemistry
University of Pennsylvania
231 South 34th Street
Philadelphia, Pennsylvania 19104-6323

Professor Paul A. Libby
Department of Applied Mechanics
and Engineering Sciences
University of California, San Diego
La Jolla, California 92093-0023

Professor John C. Light
The James Franck Institute
University of Chicago
5640 Ellis Avenue
Chicago, Illinois 60637

Professor Ming-Chang Lin
Department of Chemistry
Emory University
1515 Pierce Drive
Atlanta, Georgia 30322

Dr. Kopin Liu
Chemistry Division
Argonne National Laboratory
9700 South Cass Avenue
Argonne, Illinois 60439

Professor Marshall B. Long
Department of Mechanical Engineering
Yale University
P.O. Box 1504A Yale Station
New Haven, Connecticut 06511

Dr. R. Glen Macdonald
Chemistry Division
Argonne National Laboratory
9700 South Cass Avenue
Argonne, Illinois 60439

Dr. David Mann
Army Research Office
Research Triangle Park,
North Carolina 27709-2211

Dr. J. R. McDonald
Code 6110
Naval Research Laboratory
Washington, D.C. 20375-5000

Dr. William J. McLean, Director,
Combustion Research
& Technology Center
Sandia National Laboratories
Livermore, California 94551-0969

Dr. Joseph V. Michael
Chemistry Division
Argonne National Laboratory
9700 South Cass Avenue
Argonne, Illinois 60439

Dr. Richard Miller
Power Branch
Office of Naval Research
800 N. Quincy St.
Arlington, Virginia 22217-5000

Professor William H. Miller
Materials & Chemical Sciences Division
Lawrence Berkeley Laboratory
University of California
Berkeley, California 94720

Dr. James A. Miller
Combustion Research Facility
Sandia National Laboratory
Livermore, California 94551-0609

Dr. Louis Monchik
Milton S. Eisenhower Research Center
Applied Physics Laboratory
The Johns Hopkins University
Johns Hopkins Road
Laurel, Maryland 20723-6099

Professor C. Bradley Moore
Materials & Chemical Sciences Division
Lawrence Berkeley Laboratory
University of California
Berkeley, California 94720

Dr. James Muckerman
Chemistry Department
Brookhaven National Laboratory
Upton, New York 11973

Dr. Herbert H. Nelson
Code 6111
Naval Research Laboratory
Washington, D.C. 20375-5000

Professor Daniel M. Neumark
Materials & Chemical Sciences Division
Lawrence Berkeley Laboratory
University of California
Berkeley, California 94720

Prof. Cheuk-Yiu Ng
Institute for Physical Research &
Technology
Ames Laboratory
Iowa State University
Ames, Iowa 50011-3020

Dr. Phillip H. Paul
Combustion Research Facility
Sandia National Laboratory
Livermore, California 94551-0609

Professor David S. Perry
Department of Chemistry
University of Akron
Akron, Ohio 44325

Dr. Leon Petrakis
Department of Applied Science
Brookhaven National Laboratory
Upton, New York 11973

Dr. William J. Pitz
L-298
Lawrence Livermore National Laboratory
P.O. Box 808
Livermore, California 94550

Professor Stephen B. Pope
Department of Mechanical
and Aerospace Engineering
Cornell University
106 Upson Hall
Ithaca, New York 14853

Dr. Jack M. Preses
Chemistry Department
Brookhaven National Laboratory
Upton, New York 11973

Professor Herschel A. Rabitz
Department of Chemistry
Princeton University
Princeton, New Jersey 08544

Dr. Larry A. Rahn
Combustion Research Facility
Sandia National Laboratory
Livermore, California 94551-0609

Dr. A. R. Ravishankara
R/E/AL2
National Oceanic & Atmospheric Admin.
325 Broadway
Boulder, Colorado 80303

Professor Hanna Reisler
Department of Chemistry
University of Southern California
Los Angeles, California 90089-0482

Professor Thomas R. Rizzo
Department of Chemistry
University of Rochester
River Station
Rochester, New York 14627

Dr. Eric A. Rohlfing
Combustion Research Facility
Sandia National Laboratory
Livermore, California 94551-0609

Dr. Thomas R. Roose
Physical Sciences Department
Gas Research Institute
8600 W. Bryn Mawr Avenue
Chicago, Illinois 60631

Mr. Neil P. Rossmeissl
Advanced Industrial Concepts Division
CE-232 5F-043/FORS
U. S. Department of Energy
Washington, D.C. 20585

Prof. Klaus Ruedenberg
Institute for Physical Research
& Technology
Ames Laboratory
Iowa State University
Ames, Iowa 50011-3020

Dr. Branko Ruscic
Chemistry Division
Argonne National Laboratory
9700 South Cass Avenue
Argonne, Illinois 60439

Professor Henry F. Schaefer III
Department of Chemistry
University of Georgia
Athens, Georgia 30602

Professor George C. Schatz
Department of Chemistry
Northwestern University
2145 Sheridan Road
Evanston, Illinois 60201

Dr. Robert W. Schefer
Combustion Research Facility
Sandia National Laboratory
Livermore, California 94551-0609

Dr. Trevor Sears
Chemistry Department
Brookhaven National Laboratory
Upton, New York 11973

Mr. Thomas M. Sebestyen
Advanced Propulsion Division, CE-322
Office of Transportation Technologies
Conservation & Renewable Energy
U.S. Department of Energy
Washington, D.C. 20585

Dr. Daniel J. Seery
Manager, Combustion Science
United Technologies Research Center
Silver Lane
Hartford, Connecticut 06108

Dr. Robert V. Serauskas
Gas Research Institute
8600 W. Bryn Mawr
Chicago, Illinois 60631

Dr. Robert Shaw
Army Research Office
Research Triangle Park, North Carolina
27709-2211

Dr. Ron Shepard
Chemistry Division
Argonne National Laboratory
9700 South Cass Ave.
Argonne, Illinois 60439

Professor Robert Silbey
Department of Chemistry
Massachusetts Institute of Technology
Cambridge, Massachusetts 02139

Dr. Thompson M. Sloane
Physical Chemistry Department
General Motors Research Laboratories
Warren, Michigan 48090-9055

Professor Mitchell Smooke
Department of Mechanical Engineering
Yale University
P.O. Box 1504A Yale Station
New Haven, Connecticut 06511

Dr. Kermit Smyth
Center for Fire Research
B258 Polymers Building
Natl. Inst. of Standards & Technology
Gaithersburg, Maryland 20899

Dr. Leon M. Stock, Director
Chemistry Division
Argonne National Laboratory
9700 South Cass Avenue
Argonne, Illinois 60439

Dr. James Sutherland
Applied Sciences Department
Brookhaven National Laboratory
Upton, New York 11973

Dr. Norman Sutin
Chemistry Department
Brookhaven National Laboratory
Upton, New York 11973

Dr. Donald W. Sweeney
Combustion Research Facility
Sandia National Laboratory
Livermore, California 94551-0609

Professor Lawrence Talbot
Applied Sciences Division
Lawrence Berkeley Laboratory
University of California
Berkeley, California 94720

Professor Patrick Thaddeus
Division of Applied Sciences
Pierce Hall 107C
Harvard University
Cambridge, Massachusetts 02138

Dr. Julian M. Tishkoff
Aerospace Sciences
Air Force Office of Scientific Research
Bolling Air Force Base, DC 20332-6448

Dr. Frederick P. Trebino
Combustion Research Facility
Sandia National Laboratory
Livermore, California 94551-0609

Prof. Jurgen Troe
Institut fur Physikalische Chemie
Universitat Gottingen
Tammannstrasse 6
D-3400 Gottingen, West Germany

Professor Donald G. Truhlar
Department of Chemistry
University of Minnesota
Minneapolis, Minnesota 55455

Dr. Wing Tsang
Chemical Sciences
& Technology Laboratory
Natl. Inst. of Standards & Technology
Gaithersburg, Maryland 20899

Dr. Frank P. Tully
Combustion Research Facility
Sandia National Laboratory
Livermore, California 94551-0609

Professor James J. Valentini
Department of Chemistry
Columbia University
116th Street & Broadway
New York, New York 10027

Mr. Gideon M. Varga, Jr.
Industrial Energy Efficiency Division
CE-221 5F-035/FORS
U. S. Department of Energy
Washington, D.C. 20585

Dr. Albert F. Wagner
Chemistry Division
Argonne National Laboratory
9700 South Cass Ave.
Argonne, Illinois 60439

Professor James C. Weisshaar
Department of Chemistry
University of Wisconsin
1101 University Avenue
Madison, Wisconsin 53706

Dr. Charles Westbrook
L-298
Lawrence Livermore National Laboratory
P.O. Box 808
Livermore, California 94550

Professor Phillip R. Westmoreland
Bldg. 221, Room B312
Natl. Inst. of Standards & Technology
Gaithersburg, MD 20899

Dr. Ralph E. Weston
Chemistry Department
Brookhaven National Laboratory
Upton, Long Island, New York 11973

Dr. Michael G. White
Chemistry Department
Brookhaven National Laboratory
Upton, New York 11973

Professor Curt Wittig
Department of Chemistry
University of Southern California
Los Angeles, California 90089-0484

Dr. Francis J. Wodarczyk
Chemistry Division
Experimental Physical
Chemistry Program
National Science Foundation
Washington, D.C. 20550

Prof. Jurgen Wolfrum
Physikalisch-Chemisches Institut
Universitat Heidelberg
Im Neuenheimer Feld 253
D-6900 Heidelberg
Fed. Rep. of Germany

Professor David R. Yarkony
Department of Chemistry
Johns Hopkins University
34th & Charles Streets
Baltimore, Maryland 21218

END

DATE FILMED

8/3/93